frontiers | Research Topics

# Novel technologies targeting the rehabilitation of neurological disorders

**Edited by**
Jie Jia, Jingchun Guo, Lin Yao and Dingguo Zhang

**Published in**
Frontiers in Neuroscience

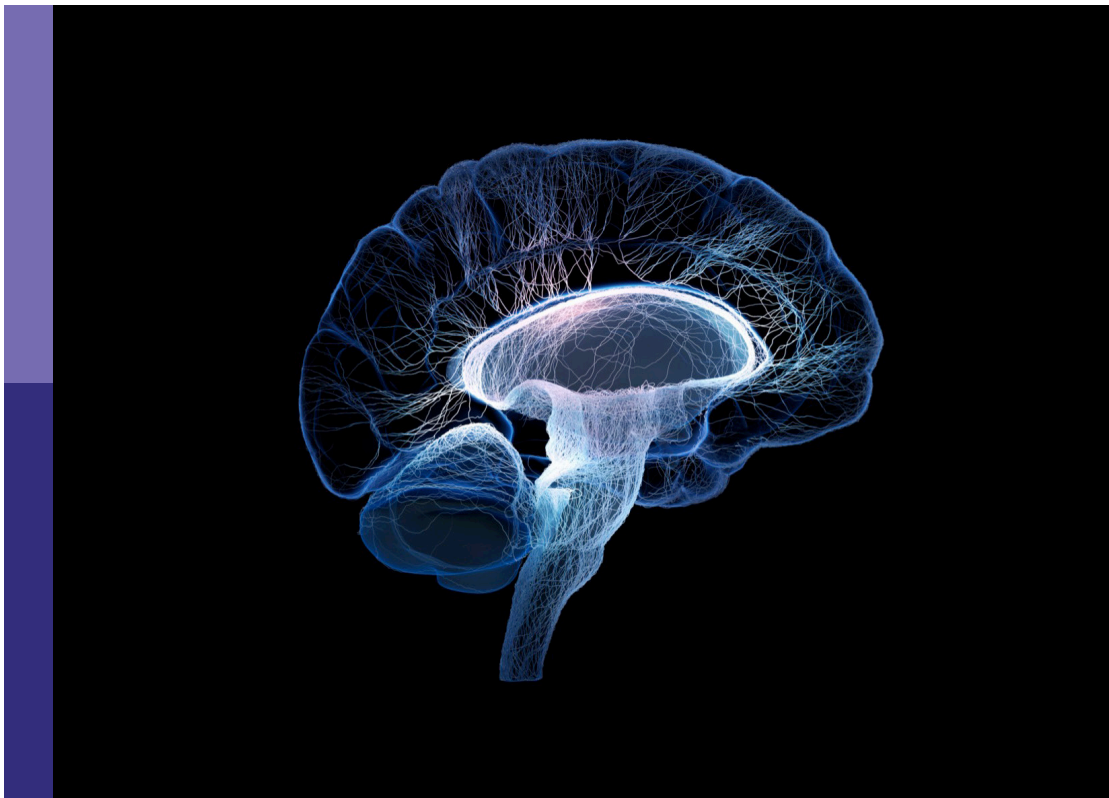

ISSN 1664-8714
ISBN 978-2-8325-4724-3
DOI 10.3389/978-2-8325-4724-3

## About Frontiers

Frontiers is more than just an open access publisher of scholarly articles: it is a pioneering approach to the world of academia, radically improving the way scholarly research is managed. The grand vision of Frontiers is a world where all people have an equal opportunity to seek, share and generate knowledge. Frontiers provides immediate and permanent online open access to all its publications, but this alone is not enough to realize our grand goals.

## Frontiers journal series

The Frontiers journal series is a multi-tier and interdisciplinary set of open-access, online journals, promising a paradigm shift from the current review, selection and dissemination processes in academic publishing. All Frontiers journals are driven by researchers for researchers; therefore, they constitute a service to the scholarly community. At the same time, the *Frontiers journal series* operates on a revolutionary invention, the tiered publishing system, initially addressing specific communities of scholars, and gradually climbing up to broader public understanding, thus serving the interests of the lay society, too.

## Dedication to quality

Each Frontiers article is a landmark of the highest quality, thanks to genuinely collaborative interactions between authors and review editors, who include some of the world's best academicians. Research must be certified by peers before entering a stream of knowledge that may eventually reach the public - and shape society; therefore, Frontiers only applies the most rigorous and unbiased reviews. Frontiers revolutionizes research publishing by freely delivering the most outstanding research, evaluated with no bias from both the academic and social point of view. By applying the most advanced information technologies, Frontiers is catapulting scholarly publishing into a new generation.

## What are Frontiers Research Topics?

Frontiers Research Topics are very popular trademarks of the *Frontiers journals series*: they are collections of at least ten articles, all centered on a particular subject. With their unique mix of varied contributions from Original Research to Review Articles, Frontiers Research Topics unify the most influential researchers, the latest key findings and historical advances in a hot research area.

Find out more on how to host your own Frontiers Research Topic or contribute to one as an author by contacting the Frontiers editorial office: frontiersin.org/about/contact

# Novel technologies targeting the rehabilitation of neurological disorders

**Topic editors**
Jie Jia — Fudan University, China
Jingchun Guo — Fudan University, China
Lin Yao — Zhejiang University, China
Dingguo Zhang — University of Bath, United Kingdom

**Citation**
Jia, J., Guo, J., Yao, L., Zhang, D., eds. (2024). *Novel technologies targeting the rehabilitation of neurological disorders*. Lausanne: Frontiers Media SA.
doi: 10.3389/978-2-8325-4724-3

# Table of contents

frontiers | Frontiers in Neuroscience

TYPE Editorial
PUBLISHED 26 March 2024
DOI 10.3389/fnins.2024.1367286



OPEN ACCESS

EDITED BY
Guo-Yuan Yang,
Shanghai Jiao Tong University, China

REVIEWED BY
Angelo Pascarella,
University of Magna Graecia, Italy

*CORRESPONDENCE
Jie Jia
✉ shannonjj@126.com

†These authors share first authorship

RECEIVED 08 January 2024
ACCEPTED 13 March 2024
PUBLISHED 26 March 2024

CITATION
Jia J, Guo J, Yao L and Zhang D (2024) Editorial: Novel technologies targeting the rehabilitation of neurological disorders. *Front. Neurosci.* 18:1367286. doi: 10.3389/fnins.2024.1367286



# Editorial: Novel technologies targeting the rehabilitation of neurological disorders

Jie Jia[1,2,3*†], Jingchun Guo[4†], Lin Yao[5†] and Dingguo Zhang[6†]

[1]Department of Rehabilitation Medicine, Huashan Hospital, Fudan University, Shanghai, China, [2]National Clinical Research Center for Aging and Medicine, Huashan Hospital, Fudan University, Shanghai, China, [3]National Center for Neurological Disorders, Shanghai, China, [4]State Key Laboratory of Medical Neurobiology, MOE Frontier Center for Brain Science, Department of Translational Neuroscience of Shanghai Jing'an District Centre Hospital, Institutes of Brain Science, Fudan University, Shanghai, China, [5]College of Computer Science, College of Biomedical Engineering and Instrument Science, Zhejiang University, Hangzhou, China, [6]Department of Electronic and Electrical Engineering, University of Bath, Bath, United Kingdom

KEYWORDS

**neurological disorders, stroke, TMS, close-loop, novel technologies**

Editorial on the Research Topic
Novel technologies targeting the rehabilitation of neurological disorders

## 1 Background

The Research Topic—Novel technologies targeting the rehabilitation of neurological disorders was launched to collect the latest research and progress of new rehabilitation technologies for neurological diseases. Finally, 20 papers were included, comprising 14 original articles, four reviews, and two research protocols. They cover many new technologies for the assessment and treatment of neurological diseases. The evaluation techniques include motor-evoked potential (MEP), magnetic resonance imaging (MRI), electroencephalogram (EEG), sensory-evoked potential (SEP), and functional near-infrared spectroscopy (fNIRS). Regarding treatment techniques, they are mainly divided into non-invasive brain stimulation techniques, such as transcranial magnetic stimulation (TMS), transcranial direct current/alternating current technology (tDCS/tACS), ultrasound technology, and mirror therapy (MT). In contrast, invasive brain stimulation techniques include the brain-computer interface (BCI), vagus nerve stimulation (VNS), deep brain stimulation (DBS), and Contralateral Seventh Cervical Nerve Transfer (CC7). However, the papers included in this Research Topic did not involve new techniques of invasive brain stimulation. In this editorial, we will provide a summary of the papers included in our Research Topic from three perspectives. We will also expand on some of the content that our Research Topic lacks.

## 2 Novel assessment methods

With the progress of brain science and technology, innovative techniques have been promoted and applied based on new detection principles, and more accurate assessment methods have promoted the rehabilitation of functional disorders caused by neurological diseases. This part covers the exploration of a variety of new assessment techniques in neurological rehabilitation.

### 2.1 fNIRS

As a relatively new imaging method, fNIRS is a non-invasive optical imaging technology based on the principle of neurovascular coupling. Wang et al. used fNIRS as a monitoring and evaluation basis to monitor the degree of increased metabolic activity in the prefrontal cortex of stroke patients, and meta-analysis showed the value of PFC research in exploring the double-task effect of stroke. Chen H. et al. collected the topological structure of the frontal functional network during resting state for analysis using fNIRS. The study aimed to explore changes present in the frontal functional network region of patients in the lowest conscious state. In addition, Lacerenza et al. used fNIRS as a detection method to measure the functional activation of the motor cortex during arm lifting.

### 2.2 TMS-EEG

The physiological mechanism of TMS is to generate a brief magnetic field by placing an electromagnetic coil on the scalp, which stimulates the activity of neurons in the cerebral cortex. EEG provides a non-invasive way of recording electrical activity in the brain. It measures the electrical activity of neurons in the cerebral cortex by placing multiple electrodes on the scalp. The technique of TMS with EEG can observe the cortical reactivity and connectivity, and record the changes of cortical excitability and connectivity evoked by TMS (Hernandez-Pavon et al., 2023).

### 2.3 fMRI

fMRI is one of the most widely used non-invasive functional imaging techniques in observing the efficacy of new technologies in the rehabilitation of neurological diseases (Feng et al., 2021). It can indirectly characterize the function of brain neurons by capturing changes in blood oxygen levels. Its greatest advantage is its high spatial resolution, which allows us to observe deep brain structures, which fNIRS and EEG do not possess (Varley et al., 2020). It can help us analyze and understand the way the human brain works in basic cognitive processes (such as attention, memory, sensation, and perception) and higher cognitive processes (such as language, problem-solving, reasoning, etc.), and explore the psychophysiological mechanisms of various brain diseases (Kim et al., 2017).

### 2.4 Respiratory ultrasound

Respiratory ultrasound is widely used, feasible, non-invasive, and convenient for clinical application. In terms of rehabilitation treatment, in addition to the observation of the lungs by ultrasound, it can also evaluate the activity and morphological measurement of the respiratory muscle of patients through ultrasound visualization, improve the information about the structure and function of the respiratory muscle, and have good reproducibility. Sufficient sensitivity to detect clinically important changes. Under our Research Topic, Liu, Yang et al. summarized and described the application of ultrasonic measurement of respiratory muscle, and summarizes the function of respiratory muscle in stroke patients.

### 2.5 SEP

SEP is a commonly used neurophysiological test in clinical practice, and it is the most objective method to evaluate sensory pathways. The latent waveform of somatosensory evoked potentials may indicate the source of neurogenesis and is a highly sensitive neurophysiological indicator. Liu Y. et al. is based on somatosensory evoked potentials to explore the correlation between light touch and two-point discrimination measurements in the assessment of upper limb function.

## 3 Non-invasive brain stimulation techniques

### 3.1 TMS

Transcranial magnetic stimulation (TMS) is an adjunctive treatment for neurological recovery in disorders like stroke. It aids post-stroke recovery through neurogenesis, vascular regeneration, and anti-inflammatory actions (Zhou et al.). Clinically, TMS is used for improving motor functions, speech, swallowing, cognition, mood, spasticity, and pain in stroke patients (Zhou et al.). For post-stroke cognitive impairment (PSCI), excitatory TMS on the left hemisphere's DLPFC improves cognition, attention, and memory (Han K. et al.). Intermittent theta burst stimulation (iTBS), a novel mode of TMS, might be a more advantageous and convenient treatment than the classic rTMS for patients with PSCI (Han M. et al.). Recent research focuses on optimizing TMS efficacy. iTBS increases motor cortical excitability and enhances performance in task-specific activities (Goldenkoff et al.). A study on rTMS intensity revealed its impact on treatment efficacy, with high-frequency (25 Hz) rTMS demonstrating bidirectional effects on hippocampal plasticity, offering potential benefits for memory loss (Chen S. et al.).

### 3.2 tDCS/tACS

Transcranial direct current stimulation (tDCS) is a convenient and low-cost option for treatment, which modulates the neuronal activity in the cerebral cortex using constant, low-intensity direct current. For the first time, a recent study has confirmed that bilateral tDCS was a boost for the recovery of those suffering from Parkinsonian tremor (Zhang et al.). A network meta-analysis study found that cathodal tDCS was the most promising treatment option to improve ADL capacity in people with stroke (Elsner et al., 2017). Iodice et al. (2017) reviewed that motor (i.e., hand dexterity) and cognitive performances (i.e., attention and working memory) can be improved by applying rTMS or tDCS alone or in association with motor/cognitive training, for pain's treatment by using tDCS. However, it's also necessary to study the effects of tDCS in patients with disorders of consciousness (Estraneo et al., 2017). Compared

with the direct current stimulation of tDCS, transcranial alternating current stimulation (tACS) synchronizes and modulates brainwave oscillations via the bidirectional current. It has been observed that patients with cerebellar ataxia (CA) benefited from this alternative treatment, suggesting that tACS is a promising NIBS technique for CA (Liu, Lin et al.).

### 3.3 TUS

Focused transcranial ultrasound stimulation (TUS) is a highly accurate NIBS modality, which can straightly focus low-intensity sound waves to deeper cerebral areas (Folloni, 2022). With the potential of a short and offline therapeutic program, TUS based on its advantages can be a prospective treatment for neurological diseases, like stroke and Parkinson's (Wang et al., 2020; Folloni, 2022; Wang Y. et al., 2022). Presently, it's still in the initial exploratory phase, whose mechanisms are yet to be explored for extensible application.

### 3.4 MT

Mirror visual feedback (MVF), also known as mirror therapy (MT), has been widely applied in clinical neurorehabilitation. However, the underlying neuro-mechanisms of MVF are still unclear. It was believed to encourage cortical reorganization in the brain, which plays a crucial role in functional recovery after stroke. Recently, a study has verified that embodiment via MVF could bring denser functional brain connectivity to healthy people, digging deeper into these unknown mechanisms. In addition, an intervention combining mirror visual with vibrotactile stimulus is developed as a prospective rehabilitation strategy, which can enhance the embodiment perception (Ding et al.).

### 3.5 BCI

Brain-computer interface (BCI) is a communication channel by delivers the signals from the central nervous system (CNS) to external computers or machines. At present, this advanced technique has been used in various fields, including clinical rehabilitation training programs, typing communication systems, robotics, etc (Wang et al., 2023). For meeting the users with different training requirements and functional states, a personalized BCI paradigm has been established and optimized in terms of design, development, evaluation, and application (Ma et al., 2023).

### 3.6 Closed-loop

Developed based on the central-peripheral-central concept, closed-loop rehabilitation is a therapeutic strategy that integrates the application of central and peripheral interventions (see Figure 1) (Jia, 2022). On behalf of the central intervention, non-invasive brain stimulation plays an important role in enhancing the links of corresponding brain networks and neuroplasticity (Yamamura et al., 2018). However, peripheral interventions like neurophysiological therapy reinforce the correct movement patterns through continuous sensory feedback. A novel closed-loop rehabilitation program, combining melodic intonation therapy (MIT) with tDCS verified its positive effects for post-stroke aphasia (Yan et al.). An Individualized closed-loop TMS system coordinated with an exoskeleton was developed to recover the patients with different spasticity states (Singh et al.).

## 4 Invasive techniques

Invasive brain stimulation has shown promising prospects in improving the dysfunction caused by organic or non-organic neurological diseases such as stroke, Parkinson's disease, and Alzheimer's disease. Invasive brain stimulation technology can have various options according to the stimulation depth, stimulation location, stimulation tools, and so on. At present, in the rehabilitation of neurological diseases, invasive brain stimulation technology has been widely concerned with invasive brain-computer interface technology (invasive BCI), deep brain stimulation technology (DBS), vagus nerve electrical stimulation technology (VNS), as well as the contralateral seventh cervical nerve transfer (CC7) surgery.

### 4.1 Invasive brain-computer interface (invasive BCI)

Invasive BCI records information about brain activity by surgically implanting electrodes in the brain that are placed very close to or directly on target neurons in targeted cortical regions or subcortical structures, allowing for neural signals with higher spatial resolution (Zhao et al., 2023). The effectiveness of invasive BCI has been extensively tested in animals like macaques, and in 2007, invasive BCI was found to help restore motor function in a paralyzed patient (Donoghue et al., 2007). Since then, human research on invasive BCI has been gradually carried out, replacing impaired motor functions with robotic arms (Hochberg et al., 2012). In addition, with the help of invasive BCI, it can also compensate for functional deficiencies such as walking and speech (Dawson et al., 2016; Willett et al., 2021). The safety of invasive BCI under minimally invasive surgical operations has also been verified, providing stronger evidence for further promoting the application of invasive BCI (Mitchell et al., 2023).

### 4.2 Deep brain stimulation

Deep brain stimulation, which generally covers a large number of neurons, currently plays an important role in the treatment of neurological diseases and neuropsychiatric disorders. Boraud found that high-frequency DBS can alleviate hand and foot convulsions and other motor symptoms of Parkinson's patients, and there are also studies showing that DBS can improve the sleeping quality of Parkinson's patients (Boraud et al., 1996; Castillo et al., 2020). The effectiveness of DBS for Parkinson's patients

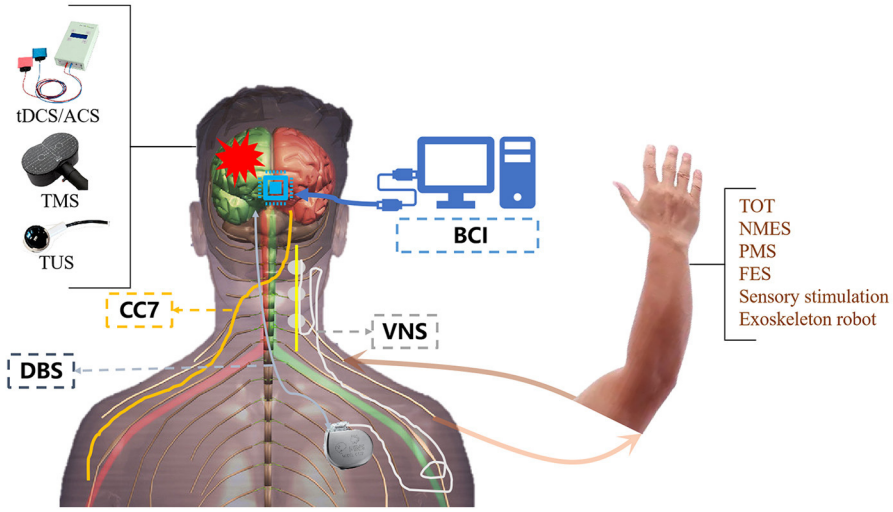


FIGURE 1
Central combined with peripheral stimulation techniques. TOT, task-oriented therapy; NMES, neuromuscular electrical stimulation; PMS, peripheral magnetic stimulation; FES, functional electrical stimulation.

has not only been demonstrated in patients with different disease courses but it has also been shown not to fade over time (Malek, 2019).

## 4.3 Vagus nerve stimulation

The first human installation of an electrical vagus nerve stimulator was in 1988, and since then several studies have been conducted to observe the effectiveness, safety, and tolerability of this technology as a treatment, as well as the selection of stimulation frequency. Dawson et al. (2016) used VNS to treat upper limb function in patients with chronic stroke and found that after 6 weeks of intervention, patients in the experimental group showed significant improvement in FMA-UE score compared with the control group, proving that VNS is a feasible and effective stroke rehabilitation method. Five years later, Dawson et al. (2021) continued to supplement the research findings and conducted more rigorous studies with larger sample sizes to further verify it. VNS technology has also been shown to be an effective means to treat cognitive disorders, epilepsy, depression, and so on (Fisher et al., 2015; Reif-Leonhard et al., 2022; Wang L. et al., 2022).

## 4.4 Contralateral seventh cervical nerve transfer (CC7)

In 1986, Gu et al. (2002) pioneered the contralateral seventh cervical nerve transfer operation, which connects the cervical seventh nerve root in the healthy brachial plexus nerve with the nerve controlling the paralytic hand, and has been used to treat the patients with total brachial plexus nerve injury and has achieved remarkable results. So far, this technology has been applied for nearly 40 years, and has played an important role in promoting the recovery of upper limb hand function in stroke patients (Hong et al., 2019). In 2018, Zheng et al. used CC7 surgery to treat patients with chronic stroke and found that it can improve patients' upper limb motor function and relieve spasms (Zheng et al., 2018). The efficacy has been further verified through a multi-center, large-scale research in 2022, and a standardized guidance reference will be provided for the promotion and application of this technology (Feng et al., 2022).

# 5 Limitations

For research on innovation assessment methods, most sample sizes are small due to constraints on assessment sites and equipment. Small sample sizes and the limited information available made it difficult to analyze other confounding factors, such as injury types, injury regions, and different age groups. In particular, the clinical prediction Models require more sample sizes and multiple medical institutions for better clinical generalizing (Yu et al.). Some brain imaging assessment methods (e.g., EEG, fNIRS) use specific-channel caps, that might limit further exploration of sub-network alterations (Ding et al.). For clinical research of non-invasive brain stimulation techniques and invasive techniques, considering patients' limited hospital days and the difficulty of post-discharge follow-up, some researchers just focus on the short-term effect and pay less attention to the long-term effect (Zhang et al.; Liu, Lin et al.) (Dawson et al., 2021). Most clinical studies are performed in a single center, and they may not represent the results from other regions (Liu, Lin et al.), also cannot generalize the findings to people who do not meet trial eligibility criteria or to people with other types of stroke or other neurological disorders (Dawson et al., 2021). There are different conditions of one neurological disorder (e.g., different types, disease urgency, duration), so stimulation parameters used for the same neurological disorder may also vary from different

studies, which makes the optimal treatment protocol difficult to find.

## 6 Conclusion

Nowadays, increasing research focuses on the use of new technologies in the rehabilitation of neurological disorders. The innovative assessment methods can complement existing assessment methods and provide in-depth functional assessments from neurophysiological or brain imaging perspectives, which may aid in better understanding the mechanism of neurological disorders. The innovative treatment methods show significant treatment effects in many studies. In the future, researchers involved in novel technologies targeting the rehabilitation of neurological disorders should recruit more samples from different institutions and regions to verify the stability and repeatability of the data. Additionally, more randomized controlled trials with large samples, high quality, and follow-up are needed to explore a usable protocol.

## Author contributions

JJ: Writing – original draft, Writing – review & editing, Supervision. JG: Supervision, Writing – review & editing. LY: Supervision, Writing – review & editing. DZ: Writing – review & editing.

## Funding

The author(s) declare that no financial support was received for the research, authorship, and/or publication of this article.

## Conflict of interest

The authors declare that the research was conducted in the absence of any commercial or financial relationships that could be construed as a potential conflict of interest.

## Publisher's note

All claims expressed in this article are solely those of the authors and do not necessarily represent those of their affiliated organizations, or those of the publisher, the editors and the reviewers. Any product that may be evaluated in this article, or claim that may be made by its manufacturer, is not guaranteed or endorsed by the publisher.

## References

Boraud, T., Bezard, E., Bioulac, B., and Gross, C. (1996). High frequency stimulation of the internal globus pallidus (GPi) simultaneously improves parkinsonian symptoms and reduces the firing frequency of GPi neurons in the MPTP-treated monkey. *Neurosci. Lett.* 215, 17–20. doi: 10.1016/S0304-3940(96)12943-8

Castillo, P. R., Middlebrooks, E. H., Grewal, S. S., Okromelidze, L., Meschia, J. F., Quinones-Hinojosa, A., et al. (2020). Globus pallidus externus deep brain stimulation treats insomnia in a patient with parkinson disease. *Mayo Clin. Proc.* 95, 419–422. doi: 10.1016/j.mayocp.2019.11.020

Dawson, J., Liu, C. Y., Francisco, G. E., Cramer, S. C., Wolf, S. L., Dixit, A., et al. (2021). Vagus nerve stimulation paired with rehabilitation for upper limb motor function after ischaemic stroke (VNS-rehab): a randomised, blinded, pivotal, device trial. *Lancet* 397, 1545–1553. doi: 10.1016/S0140-6736(21)00475-X

Dawson, J., Pierce, D., Dixit, A., Kimberley, T. J., Robertson, M., Tarver, B., et al. (2016). Safety, feasibility, and efficacy of vagus nerve stimulation paired with upper-limb rehabilitation after ischemic stroke. *Stroke* 47, 143–150. doi: 10.1161/STROKEAHA.115.010477

Donoghue, J. P., Nurmikko, A., Black, M., and Hochberg, L. R. (2007). Assistive technology and robotic control using motor cortex ensemble-based neural interface systems in humans with tetraplegia. *J. Physiol.* 579, 603–611. doi: 10.1113/jphysiol.2006.127209

Elsner, B., Kwakkel, G., Kugler, J., and Mehrholz, J. (2017). Transcranial direct current stimulation (TDCS) for improving capacity in activities and arm function after stroke: a network meta-analysis of randomised controlled trials. *J. Neuroeng. Rehabil.* 14:95. doi: 10.1186/s12984-017-0301-7

Estraneo, A., Pascarella, A., Moretta, P., Masotta, O., Fiorenza, S., Chirico, G., et al. (2017). Repeated transcranial direct current stimulation in prolonged disorders of consciousness: a double-blind cross-over study. *J. Neurol. Sci.* 375, 464–470. doi: 10.1016/j.jns.2017.02.036

Feng, J., Li, T., Lv, M., Kim, S., Shin, J. H., Zhao, N., et al. (2022). Reconstruction of paralyzed arm function in patients with hemiplegia through contralateral seventh cervical nerve cross transfer: a multicenter study and real-world practice guidance. *EClinicalMedicine* 43:101258. doi: 10.1016/j.eclinm.2021.101258

Feng, M., Wen, H., Xin, H., Zhang, N., Liang, C., Guo, L., et al. (2021). Altered spontaneous brain activity related to neurologic dysfunction in patients with cerebral small vessel disease. *Front. Aging Neurosci.* 13:731585. doi: 10.3389/fnagi.2021.731585

Fisher, R. S., Eggleston, K. S., and Wright, C. W. (2015). Vagus nerve stimulation magnet activation for seizures: a critical review. *Acta Neurol. Scand.* 131, 1–8. doi: 10.1111/ane.12288

Folloni, D. (2022). Ultrasound neuromodulation of the deep brain. *Science* 377:589. doi: 10.1126/science.add4836

Gu, Y., Xu, J., Chen, L., Wang, H., and Hu, S. (2002). Long term outcome of contralateral C7 transfer: a report of 32 cases. *Chin. Med. J.* 115, 866–868.

Hernandez-Pavon, J. C., Veniero, D., Bergmann, T. O., Belardinelli, P., Bortoletto, M., Casarotto, S., et al. (2023). TMS combined with EEG: recommendations and open issues for data collection and analysis. *Brain Stimul.* 16, 567–593. doi: 10.1016/j.brs.2023.02.009

Hochberg, L. R., Bacher, D., Jarosiewicz, B., Masse, N. Y., Simeral, J. D., Vogel, J., et al. (2012). Reach and grasp by people with tetraplegia using a neurally controlled robotic arm. *Nature* 485, 372–375. doi: 10.1038/nature11076

Hong, G., Liu, J., Liu, Y., Gao, K., Zhao, X., Lao, J., et al. (2019). Modified contralateral C7 nerve transfer: the possibility of permitting ulnar nerve recovery is confirmed by 10 cases of autopsy. *Neural Regen. Res.* 14, 1449–1454. doi: 10.4103/1673-5374.253530

Iodice, R., Manganelli, F., and Dubbioso, R. (2017). The therapeutic use of non-invasive brain stimulation in multiple sclerosis – a review. *Restor. Neurol. Neurosci.* 35, 497–509. doi: 10.3233/RNN-170735

Jia, J. (2022). Exploration on neurobiological mechanisms of the central-peripheral-central closed-loop rehabilitation. *Front. Cell. Neurosci.* 16:982881. doi: 10.3389/fncel.2022.982881

Kim, J. H., Yu, D., Huh, Y. H., Lee, E. H., Kim, H., Kim, H. R., et al. (2017). Long-term exposure to 835 MHZ RF-EMF induces hyperactivity, autophagy and demyelination in the cortical neurons of mice. *Sci. Rep.* 7:41129. doi: 10.1038/srep41129

Ma, Y., Gong, A., Nan, W., Ding, P., Wang, F., Fu, Y., et al. (2023). Personalized brain–computer interface and its applications. *J. Pers. Med.* 13:46. doi: 10.3390/jpm13010046

Malek, N. (2019). Deep brain stimulation in parkinson's disease. *Neurol. India* 67, 968–978. doi: 10.4103/0028-3886.266268

Mitchell, P., Lee, S. C. M., Yoo, P. E., Morokoff, A., Sharma, R. P., Williams, D. L., et al. (2023). Assessment of safety of a fully implanted endovascular brain-computer

interface for severe paralysis in 4 patients: the stentrode with thought-controlled digital switch (switch) study. *JAMA Neurol.* 80, 270–278. doi: 10.1001/jamaneurol.2022.4847

Reif-Leonhard, C., Reif, A., Baune, B. T., and Kavakbasi, E. (2022). [Vagus nerve stimulation for difficult to treat depression]. *Nervenarzt* 93, 921–930. doi: 10.1007/s00115-022-01282-6

Varley, T. F., Luppi, A. I., Pappas, I., Naci, L., Adapa, R., Owen, A. M., et al. (2020). Consciousness and brain functional complexity in propofol anaesthesia. *Sci. Rep*. 10:1018. doi: 10.1038/s41598-020-57695-3

Wang, L., Zhang, J., Guo, C., He, J., Zhang, S., Wang, Y., et al. (2022). The efficacy and safety of transcutaneous auricular vagus nerve stimulation in patients with mild cognitive impairment: a double blinded randomized clinical trial. *Brain Stimul.* 15, 1405–1414. doi: 10.1016/j.brs.2022.09.003

Wang, P., Cao, X., Zhou, Y., Gong, P., Yousefnezhad, M., Shao, W., et al. (2023). A comprehensive review on motion trajectory reconstruction for EEG-based brain-computer interface. *Front Neurosci*. 17:1138406. doi: 10.3389/fnins.2023.1138406

Wang, Y., Li, F., He, M., and Chen, S. (2022). The effects and mechanisms of transcranial ultrasound stimulation combined with cognitive rehabilitation on post-stroke cognitive impairment. *Neurol. Sci*. 43, 4315–4321. doi: 10.1007/s10072-022-05906-2

Wang, Z., Yan, J., Wang, X., Yuan, Y., and Li, X. (2020). Transcranial ultrasound stimulation directly influences the cortical excitability of the motor cortex in parkinsonian mice. *Mov. Disord*. 35, 693–698. doi: 10.1002/mds.27952

Willett, F. R., Avansino, D. T., Hochberg, L. R., Henderson, J. M., and Shenoy, K. V. (2021). High-performance brain-to-text communication via handwriting. *Nature* 593, 249–254. doi: 10.1038/s41586-021-03506-2

Yamamura, K., Kurose, M., and Okamoto, K. (2018). Guide to enhancing swallowing initiation: insights from findings in healthy subjects and dysphagic patients. *Curr. Phys. Med. Rehabil. Rep*. 6, 178–185. doi: 10.1007/s40141-018-0192-y

Zhao, Z. P., Nie, C., Jiang, C. T., Cao, S. H., Tian, K. X., Yu, S., et al. (2023). Modulating brain activity with invasive brain-computer interface: a narrative review. *Brain Sci*. 13:134. doi: 10.3390/brainsci13010134

Zheng, M. X., Hua, X. Y., Feng, J. T., Li, T., Lu, Y. C., Shen, Y. D., et al. (2018). Trial of contralateral seventh cervical nerve transfer for spastic arm paralysis. *N. Engl. J. Med.* 378, 22–34. doi: 10.1056/NEJMoa1615208

frontiers | Frontiers in Neuroscience

TYPE Original Research
PUBLISHED 11 January 2023
DOI 10.3389/fnins.2022.1065629



OPEN ACCESS

EDITED BY
Jie Jia,
Fudan University, China

REVIEWED BY
Syoichi Tashiro,
Keio University School of Medicine, Japan
Ranran Wang,
Binzhou Medical University, China

*CORRESPONDENCE
Jiang Ma
✉ majiangtutor@sina.com

†These authors share first authorship

SPECIALTY SECTION
This article was submitted to Translational Neuroscience, a section of the journal Frontiers in Neuroscience

RECEIVED 10 October 2022
ACCEPTED 07 December 2022
PUBLISHED 11 January 2023

CITATION
Liu Y, Ma J, Li H, Shi W-y, Xiao Z-h, Yang Q, Zhao Q-q, Wang F, Tao X-l and Bai Y-f (2023) Which sites better represent the sensory function of hands in convalescent stroke patients? A study based on electrophysiological examination. *Front. Neurosci.* 16:1065629. doi: 10.3389/fnins.2022.1065629



# Which sites better represent the sensory function of hands in convalescent stroke patients? A study based on electrophysiological examination

Yu Liu[1†], Jiang Ma[1*†], Hong Li[1,2], Wan-ying Shi[1], Zheng-hua Xiao[2], Qian Yang[3], Qing-qing Zhao[4], Fang Wang[2], Xiao-lin Tao[1] and Yun-fei Bai[1]

[1]Department of Rehabilitation Medicine, Shijiazhuang People's Hospital, Shijiazhuang, China, [2]Physical Education College, Hebei Normal University, Shijiazhuang, China, [3]Department of Electrophysiology, Shijiazhuang People's Hospital, Shijiazhuang, Hebei, China, [4]School of Nursing and Rehabilitation, North China University of Science and Technology, Tangshan, Hebei, China

**Background:** Assessing hand sensation in stroke patients is necessary; however, current clinical assessments are time-consuming and inaccurate.

**Objective:** This study aimed to explore the nature of light touch sensation and two-point discrimination (2-PD) of different hand sites in convalescent stroke patients based on somatosensory evoked potentials (SEP).

**Methods:** Light touch sensation and 2-PD of the thumb, the index finger, the little finger, thenar, and hypothenar were measured ($n$ = 112) using sensory measurement tools. Sensory differences among the hand sites were then compared. The correlation analysis between SEP and the hemiplegic hand function was made. Sensory functions were divided into three levels: sensory intactness, sensory impairment, and sensory loss.

**Results:** Light touch sensations were mainly associated with sensory impairment in the finger and palm region. The 2-PD of the finger region was mainly sensory loss and that of the palm region was mainly sensory impairment. There was no statistical difference in the light touch sensation among the sites of the hand. The correlation coefficients between the 2-PD and SEP N20 amplitudes

differed. The correlation coefficients of the thenar and hypothenar were the smallest, and that of the finger was the largest. Light touch sensation and 2-PD in patients with stroke were related to the hemiplegic hand function.

**Conclusion:** Any site on the hand could be selected as the measurement site for light touch sensation. The little finger and hypothenar may be appropriate sites when screening for 2-PD. To improve the patient's recovery they could receive more sensory stimulation of the hand.

KEYWORDS

**stroke, sensory, SEP, light touch sensation, 2-PD**

## 1. Introduction

Nearly 85% of patients with stroke reportedly have sensory dysfunction (Wang et al., 2017; GBD 2017 Mortality Collaborators, 2018). Sensory dysfunction can affect the motor function, activities of daily living, and social participation of patients with stroke (Kessner et al., 2016; Chen et al., 2018). Increasing clinical attention has been paid to the recovery of motor function in patients with stroke, and less attention has been given to the recovery of sensory function. The reason for this may be that motor dysfunction is more easily observed than sensory dysfunction, and the impact of sensory dysfunction on patients' activities of daily living and participation is often overlooked when motor impairment is more severe. Doctors perform sensory assessments cursorily and do not have a full picture of how the patient is feeling. As motor function improves, sensory problems become more pronounced, which affects the patient's fine movement and motor control (Carey et al., 2018). Sensory assessment scales, which are less commonly used, do not have sufficient reliability and require a certain level of cognitive ability. Physical examinations provide a quick overview of the patient's overall sensory function but lack objectivity. Therefore, a comprehensive, objective, and clinically efficient assessment method is needed. In addition, there is evidence that sensory retraining helps the recovery of sensory and modulated sensorimotor integration in convalescent stroke patients and improves activities of daily living and motor function in the upper limbs and hands, with different sensory stimulation sites have different effects (Diego et al., 2013; Brown et al., 2018; Lim, 2019). Therefore, selecting the right area for sensory stimulation is important for improving the efficiency of clinical rehabilitation.

The upper limbs and hands play a key role in precise gripping, motor control, and the manipulation of objects (Tonak et al., 2021) and have a significant impact on patients' activities of daily living (Tashiro et al., 2021). The upper limb and palm of the hand have high sensory thresholds. Most sensory receptors located in the fingers and palm play different processing roles in sensory coding. Merkel cells, mainly located in the tips of the thumb, the index and middle fingers, and thenar, perceive the material of objects in contact with the skin, and Merkel cells contain the receptors that are important for monofilament touch and two-point discrimination (2-PD) (Feng et al., 2018). The large pachytene microsomal receptor area senses which part of the hand is being stimulated and then localizes the sensation (Germann et al., 2020). Normal touch in mammals requires the function of brain sodium channels in receptors, which may have implications for touch and potentially compound sensory functions when damaged (Price et al., 2000). There was no significant difference in light touch sensation in the two sides of the forearms of patients with stroke, and sensory dysfunction sites were mainly in the fingers (Peng et al., 2018). Stroke lesions are located in the central nervous system, and measurement points are generally not selected according to the distribution of the peripheral nervous system. Current measurement points for sensory assessment are mainly selected in the areas of the hand and upper limb where the function is achieved, such as the thumb and the index finger. Patients with stroke have been shown to have different sensory thresholds among the five fingers on the affected side (Enders and Seo, 2016). Suda et al. (2021) suggested that the light touch sensations of the thumb and the index finger were similar. Thus, different parts of the fingers have different receptors, thresholds, and types of sensations. Post-stroke sensory dysfunction is caused by a variety of factors, including damage to the focal brain areas that can affect hand function (Tyson et al., 2008; Umeki et al., 2018).

Somatosensory evoked potentials (SEP) are objective electrophysiological examinations that reflect proprioceptive and fine tactile conduction pathways, evaluate the sensory function, and predict prognosis. Compared to CT and MRI, SEP is less affected by aphasia, consciousness, and cognitive function and is more sensitive to stroke diagnosis (Sridharan et al., 2016; Macerollo et al., 2018). Feng et al. (2018) showed that more than half of patients with stroke had tactile abnormalities, which may be related to the loss or reduction of the higher central processing of sensory signals

and changes in the somatosensory network of the brain in patients with stroke. Different waveforms of SEP represent different sources of neurogenesis, and N20 is one of the indexes that originates from the primary somatosensory cortex, which processes proprioception and fine touch. N20 is an objective, accurate, and sensitive index to examine the sensory function of patients with stroke (Macerollo et al., 2018). The prolonged latency and decreased amplitude of N20 on the affected side compared to the healthy side after stroke suggest that demyelination and axonal damage, respectively, may occur in early patients with stroke (Keren et al., 1993; Song et al., 2016). In addition, there are few studies on convalescent patients, and the parameters remain controversial. SEP can be affected by different factors; although it may be used as an auxiliary diagnostic tool, it should be used in conjunction with the patient's clinical manifestations to make an objective and comprehensive assessment (Horn and Tjepkema-Cloostermans, 2017).

The main objective of this study was to investigate the characteristics and significance of light touch sensation and 2-PD in different parts of the hand in patients with stroke based on SEP analysis. To investigate the correlation between sensation and hemiplegic hand function, we aimed to identify more appropriate hand sensory measurement points with clinical significance and provide guidance for clinical sensory assessment and treatment.

## 2. Materials and methods

### 2.1. Participants

Patients with stroke treated in the third ward of the Department of Rehabilitation Medicine, Shijiazhuang People's Hospital from June 2021 to August 2022, who met the diagnostic criteria for cerebrovascular disease, were selected for the study.

The inclusion criteria were as follows: (1) an age of 30–75 years; (2) first stroke with unilateral hemispheric lesions, including cerebral hemorrhage and infarction [criteria of the revised 4th National Cerebrovascular Disease Conference, 1995 (Neuroscience, and Surgery, 1997)]; (3) a disease course of 2 weeks–6 months; (4) sensory dysfunction defined as a degree of light touch sensation below grade 6 according to the Semmes–Weinstein Monofilaments (SWMs) test (Tyson et al., 2008) of at least one part of the hand, having a shortest 2-PD of $>$ 5 mm for at least one part of the hand, or an abnormal SEP; (5) an ability to complete examinations; and (6) right-handedness evaluated by Edinburg handedness scale (Oldfield, 1971).

The exclusion criteria were as follows: (1) history of peripheral nerve damage, such as cervical spondylosis, trauma to the hands or upper limbs, and diabetic peripheral neuropathy; (2) Mini-Mental State Examination score of $<$ 26, hemi-spatial neglect, body agony, mental, visual, hearing, and speech impairment; (3) sensory and motor dysfunction caused by other reasons; and (4) long-term use of drugs that provide nutrition for nerve or affect sensory function.

Sample size calculation. The formula for the sample size was $N = \frac{z^2_{1-\alpha/2}(1-p)}{\varepsilon^2 p}$, where $z_{1-\alpha/2}$ is the percentage corresponding to an area of 1-α/2 under the standard normal distribution; $p$ is the expected incidence rate; and ε is the percentage of the expected incidence rate. Using α = 0.05, ε = 0.1, $p$ = 0.9 [according to the incidence of sensory dysfunction (Carlsson et al., 2018a), and realistic clinical situations], and $z_{1-\alpha/2}$ = 1.96, we calculated $N$ = 43. Because this study used whole-group sampling, the actual sample size was multiplied by the design efficiency value, which was assumed to be 2 for $N$ = 43. Thus, 86 cases were required; this study included 112 patients.

TABLE 1 Patients' characteristics.

| Characteristics | |
|---|---|
| Sex, *n* | |
| Female | 79 |
| Male | 33 |
| Age, years, mean ± SD | 54.13 ± 11.87 |
| Physical labor intensity, *n* | |
| Light physical labor | 63 |
| Moderate physical labor | 35 |
| Heavy physical labor | 14 |
| Hemiplegic side, *n* | |
| Left | 59 |
| Right | 53 |
| Type of stroke, *n* | |
| Ischemic | 48 |
| Hemorrhagic | 64 |
| Location | |
| Cortical | 6 |
| Subcortical | 71 |
| Mixture of cortical and subcortical lesions | 35 |
| Course of the stroke, days, median ($P_{25}$–$P_{75}$) | 30 (19–60) |
| VAS, median ($P_{25}$–$P_{75}$) | 0 (0–2) |
| Fugl-Meyer score, median ($P_{25}$–$P_{75}$) | 22 (8, 46) |
| Brunnstrom stage, median ($P_{25}$–$P_{75}$) | |
| Hand | 3 (1–4) |
| Upper extremities | 3 (2–4) |

SD, standard deviation; VAS, visual analog scale.

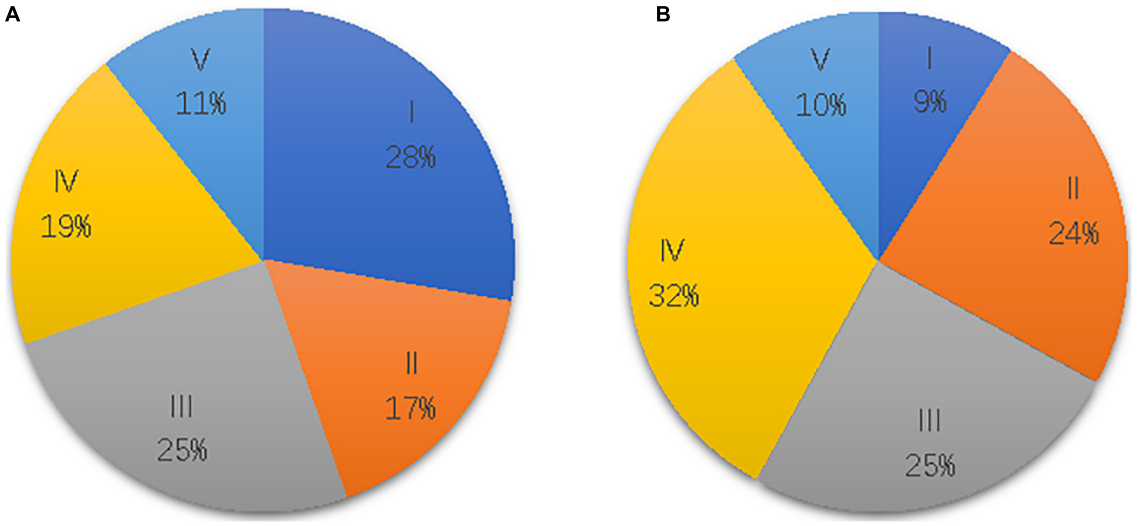


FIGURE 1
Brunnstrom stage distributions in the hand **(A)** and upper limb **(B)** of 112 patients.

## 2.2. Procedure

The characteristics of the patients with stroke were recorded, including sex, age, physical labor intensity (Zhongliang, 1995), hemiplegic side, stroke type and location, disease course, Visual Analog Score (VAS), and Brunnstrom stage of the upper limbs and hands. Brunnstrom stage of motor function is as follows: flaccid without voluntary movement, stage I; causes joint movement of voluntary muscle contraction with the presence of spasticity, stage II; voluntary control of the movement with an intensified spasticity, stage III; spasticity starts to decline with more selective activation of muscles, stage IV; spasticity gradually recovers with a fine movement, stage V; presents individual joint movements and well-coordinated movement with normal muscle tone, stage VI (Brunnstrom, 1966). In addition, the following assessments were performed.

### 2.2.1. Nerve electrophysiology

The test required a quiet room at 25°C and the patient's skin at 32–34°C. The patient was quiet and had a clean skin surface. A Dandy Keypoint 4 EMG-evoked potential device (Denmark Alpine bioMed ApS Company) was used for testing. Median nerve stimulation of SEP involved placing the stimulating electrode 2–3 cm above the transverse wrist, using square wave stimulation with a duration of 0.2 ms, a frequency of 5 Hz, and slight thumb movement. Two SEP examinations were performed for each lateral cortical recording, each stacked 100 times. The placement of the recording electrodes was marked using the EEG International 10–20 system. The contralateral C3′ and C4′ were taken as recording points, and the reference electrode was placed at the FPz point and ipsilateral earlobe. After all electrodes are installed, resistance testing is performed. SEP can be recorded only when the electrode recording impedance is between 1 and 5 kΩ. The computer superimposed the signals generated by each stimulus in the center and traced the individual potentials. The N20 latency and wave amplitude were recorded. N20 waveforms without good repeatability, prolonged N20 latency, or decreased N20 amplitude were regarded as abnormal.

### 2.2.2. Sensory function assessment

#### 2.2.2.1. Semmes–Weinstein monofilament testing

Semmes–Weinstein monofilaments testing (SMWT) were selected for light-touch sensory testing (Touch Test®Complete Hand Kit, North Coast Medical Inc., USA). SWMT was performed with a constant length and different diameters of six light levels of nylon monofilaments: 0.07, 0.2, 2, 4, 10, and 300 g, representing grades 6, 5, 4, 3, 2, and 1, respectively. If the heaviest monofilament could not be measured by touch, a score of 0 was recorded. The test was performed with the patient's eyes closed. Starting with the smallest value, the patient informed the examiner immediately when they felt a touch sensation. When using the 0.07 and 0.2 g wires, each wire was used three times by applying the wire to the skin for 1–1.5 s and then lifting it for 1–1.5 s. Each filament from 2 to 300 g was applied once only. When the nylon monofilament was bent, and the patient was still unable to feel it, the wire was changed to a heavier wire and retested. If the patient felt it two times in a row, the researcher recorded the number for the result. Five measurement sites innervated by the median and ulnar nerves were assessed, including the palmar aspect of the thumb, the index finger, the little finger, thenar, and hypothenar (Fedorczyk, 2002). The interval for each measurement site was at least 5 s. Grade 6 was considered sensory intactness; grades

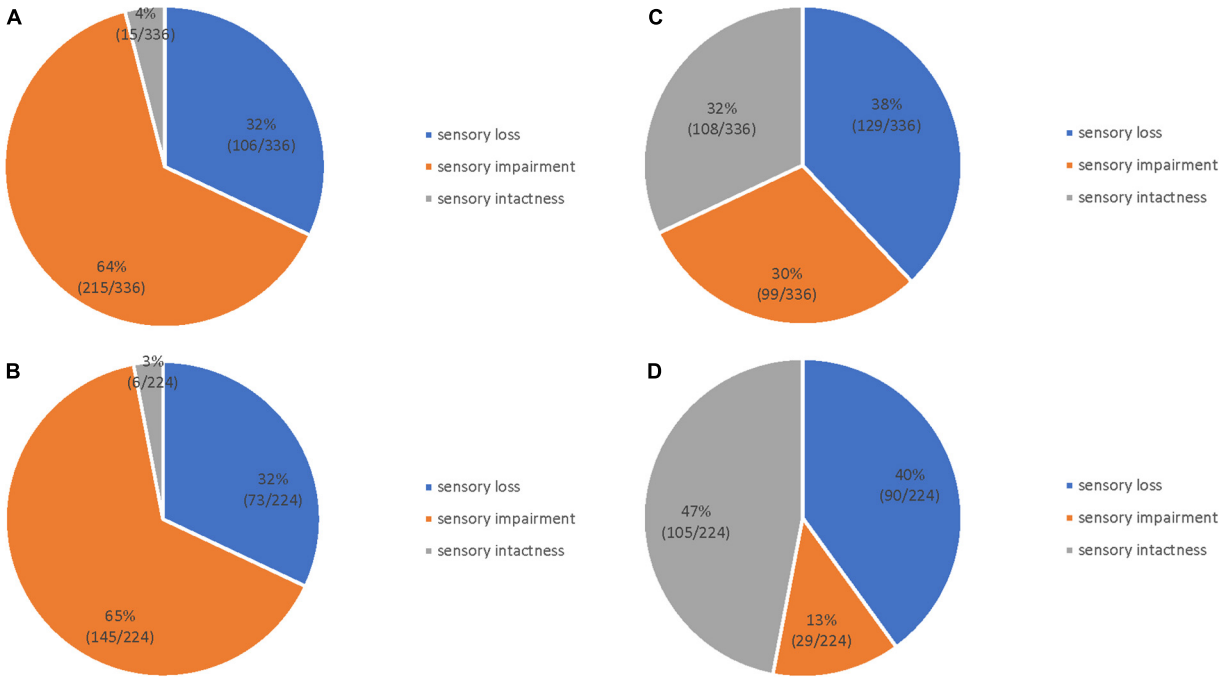


FIGURE 2
Sensory dysfunction distribution in 112 patients with stroke. Light touch sensation in the finger **(A)** and palm **(B)** regions; 2-PD in the finger **(C)** and palm **(D)** regions.

2–5 were considered sensory impairment; and grades 0–1 were considered a sensory loss. Whereby at least two of the five sites on the affected side were considered to have a poor light touch sensation if the result was = 2. In addition, if one or none of the five sites got a grade of = 2, we considered it to have a good light touch sensation (Tyson et al., 2008; Peng et al., 2018). The thumb, the index finger, and the little finger were classified as the finger group. The thenar and hypothenar were classified as the palm group. The same is as the following 2-PD.

#### 2.2.2.2. 2-PD

The 2-PD test tool (Touch Test® Complete Hand Kit, Two-Point Discriminator, North Coast Medical Inc., USA) was used to evaluate 2-PD. With the patient's eyes closed, the examiner recorded the smallest distance that could be felt between two points. The measurement range was 2–15 mm, and measurements > 15 mm were out of range. The test site was the same as that used for light touch sensation testing. The interval for each measurement site was at least 5 s. Patients' fingers with a 2-PD of 2–5, 6–15, and > 15 mm were considered to have sensory intactness, sensory impairment, and sensory loss, respectively (Peng et al., 2018). The standard of the patients' palms was that < 12 mm was regarded as sensory intactness, 12–15 mm was regarded as sensory impairment, and > 15 mm was regarded as sensory loss (Dawei et al., 2018). We defined > 15 mm as 16 mm. If two of the five sites' results on the affected side were > 15 mm, the hand was considered to have lost 2-PD (Tyson et al., 2008; Peng et al., 2018).

#### 2.2.2.3. Motor function assessment

Hemiplegic hand function was used to assess the hand function of patients with stroke. Patients were required to gradually complete five kinds of movements. If they could not complete all the tasks, the grade was recorded as I. If they could complete 1, 2, 3, 4, or 5 kinds of movement, then the grades were recorded as II, III, IV, V, and VI, respectively (Zhao et al., 2022).

## 2.3. Data analysis

Statistical software (SPSS 26.0; IBM, Chicago, Illinois, USA) was used to analyze the data. Measurement data that conformed to a normal distribution are expressed as ($\bar{x} \pm$ SD), while data that did not conform to a normal distribution are expressed as median (*P25–P75*). Differences were considered statistically significant at $p < 0.05$. The light touch impairment level of the thumb, the index finger, and the little finger was aggregated for each patient as the impairment level for the finger group. The final distribution of light touch sensation in the finger group was obtained by summing all included patients. The distribution of light touch sensation in the palm group was obtained by summing the impairment grades of the thenar and hypothenar for all patients. 2-PD was calculated in the

TABLE 2 The level of sensory in the finger and the palm region.

| | | Finger region | Palm region |
|---|---|---|---|
| The level of light touch sensation | Sensory loss | 106 | 73 |
| | Sensory impairment | 215 | 145 |
| | Sensory intactness | 15 | 6 |
| | *z* | 0.404 | 0.407 |
| | *p*-value | <0.001 | <0.001 |
| The level of 2-PD | Sensory loss | 129 | 90 |
| | Sensory impairment | 99 | 29 |
| | Sensory intactness | 108 | 105 |
| | z | 0.279 | 0.385 |
| | *p*-value | <0.001 | <0.001 |

same way. The Pearson correlation required the two sample data distributions to be normal. If there were variables that did not conform to a normal distribution, Spearman's correlation was used. We make the correlation between the grade of light touch sensation and N20 parameters. The correlation between the distance of 2-PD and N20 parameters was also made. Wilcoxon signed-ranks tests were used to compare the light touch sensation, 2-PD, and N20 amplitude and latency between the unaffected and affected sides of patients with stroke. The mean levels of light touch sensation and 2-PD in the fingers (including the thumb, the index finger, and the little finger) and palm (including the thenar and hypothenar) were counted separately, and the percentage of their corresponding numbers was calculated. Within- and between-group comparisons were performed using the Mann–Whitney, Kruskal–Wallis, and chi-square tests, and multiple comparisons were performed using the S-N-K method if the data distribution locations were not the same between groups. The Spearman correlation was performed between the light touch sensation and the N20 wave amplitude, latency, and hemiplegic hand function for all testing sites in the included patients. 2-PD was performed with the same Spearman correlation as the light touch sensation.

# 3. Results

A total of 112 patients with stroke, age (54.13 ± 11.87) years, were included in this trial. There were 48 cases of cerebral hemorrhage and 64 cases of cerebral infarction; 79 patients were male and 33 were female. All participants were right-handed before the stroke. Detailed clinical patient characteristics are presented in Table 1, and the Brunnstrom stage data are presented in Figure 1.

## 3.1. Comparison of light touch sensation and 2-PD in patients with stroke

The distribution of light touch sensation and 2-PD in the finger and palm regions of patients with stroke is shown in Figure 2. Figures 2A, B show the level of light touch sensation in the finger and palm regions, respectively. The light touch sensation level was dominated by sensory impairments in both the finger and palm regions. The 2-PD level of the finger region was dominated by sensory loss (Figure 2C), and the palm region was mainly sensory intactness (Figure 2D). The degree of 2-PD dysfunction was worse in the palm region than in the finger region. There were significant differences in the levels of light touch sensation and 2-PD impairment in both finger and palm regions (Table 2).

## 3.2. Distribution of patients with stroke and the corresponding degree of light touch sensation dysfunction in five hand regions

There was no significant difference in the number of patients corresponding to the degree of sensory dysfunction among the various parts of the fingers ($x^2$ = 1.344, $p$ = 0.511), and the distribution of the degrees of sensory intactness, impairment, and loss in the different locations was not significant ($x^2$ = 0.556, $p$ = 0.757) (Table 3).

## 3.3. Distribution of participants corresponding to the degree of 2-PD dysfunction in five hand regions

There was a statistically significant difference in 2-PD among the five parts. Multiple comparisons showed a statistically significant difference among the thenar and thumb, the index finger, and the little finger ($p < 0.001$). There was also a statistically significant difference between the hypothenar and thumb, the index finger, and the little finger ($p < 0.001$). However, there was no statistical difference between the fingers (the thumb, the index finger, and the little finger) or between the thenar and hypothenar regions.

The three degrees of 2-PD impairment were statistically different at different locations ($p$ = 0.525), with most 2-PD graded as sensory loss (39.1%) (Table 4).

TABLE 3 Degree of light touch sensation dysfunction.

| | Thumb | Index finger | Little finger | Thenar | Hypothenar | $x^2$ | *P*-value |
|---|---|---|---|---|---|---|---|
| Sensory loss | 33 | 36 | 37 | 36 | 37 | 0.556 | 0.757 |
| Sensory impairment | 76 | 67 | 72 | 72 | 73 | | |
| Sensory intactness | 3 | 9 | 3 | 4 | 2 | | |
| $x^2$ | 1.344 | | | | | | |
| *p*-value | 0.511 | | | | | | |

TABLE 4 Degree of 2-PD dysfunction.

| | Thumb | Index finger | Little finger | Thenar | Hypothenar | $x^2$ | *P*-value |
|---|---|---|---|---|---|---|---|
| Sensory loss | 43 | 42 | 44 | 45 | 45 | 3.200 | 0.525 |
| Sensory impairment | 34 | 31 | 34 | 13 | 16 | | |
| Sensory intactness | 35 | 39 | 34 | 54 | 51 | | |
| $x^2$ | 16.658 | | | | | | |
| *p*-value | <0.001 | | | | | | |

2-PD, two-point discrimination.

## 3.4. Correlation of light touch sensation and 2-PD

The two sides of the patients with stroke had significant differences in light touch sensation and 2-PD ($p < 0.001$). In a total of 112 patients, 44 patients had good light touch sensation and 36 patients had a 2-PD sensory loss. There were 8 patients without good light touch sensation and having 2-PD sensory.

## 3.5. Correlation of SEP with light touch sensation and 2-PD

The included patients had an elicitation rate of 93.75%; seven patients did not elicit N20 waveforms with good repeatability. Of the included patients, 65 had a decreased N20 amplitude and/or prolonged latency, with an abnormal rate of 61.32%. The two sides of the patients with stroke demonstrated a significant difference in the N20 latency and amplitude (latency: $z = -3.752$, $p < 0.001$; amplitude: $z = -4.428$, $p < 0.001$). The N20 amplitude was positively correlated with 2-PD and light touch sensation in each part of the hand, and all were statistically different. The correlation coefficient between the N20 amplitude and 2-PD in the little finger was the largest ($r = -0.409$, $p < 0.001$) (**Table 5**).

## 3.6. Correlation of hemiplegic hand function with sensation

The grade of hemiplegic hand function in patients with stroke was positively correlated with the light touch sensation of each part of the affected side and negatively correlated with 2-PD. The correlation coefficient between the 2-PD of the little finger and hemiplegic hand function ($r = -0.359$, $p < 0.001$) was the largest (**Table 6**).

# 4. Discussion

Post-stroke sensory dysfunction not only affects patients' perception of pins, needles, temperature, and pain (Goodin et al., 2018) but also affects motor function and activities of daily living (Carlsson et al., 2018a). The current clinical procedures for sensory assessment are complex, and the criteria are unclear; therefore, more comprehensive and accurate assessments are needed to provide a basis for training. This study evaluated 112 patients with stroke with at least one type of sensory dysfunction and found that light touch sensation was dominated by sensory impairment, and the distribution of light touch sensation was different in both the finger and palm regions, with no significant difference. Both finger and palm regions experienced sensory impairment (65%), and sensory intactness was the least experienced. One study using the same assessment method and criteria calculated a rate of light touch sensory loss of approximately 25.5% (Tyson et al., 2008), compared to 32% in this study. This may be because our study included convalescent stroke patients with sensory dysfunction but did not include patients with stroke with normal sensations (Tyson et al., 2008). The 2-PD distribution in the palm and finger regions was different; the finger region experienced predominantly sensory loss (38%) and the palm region experienced predominantly sensory loss (39%). The hands have fine motor skills, and the sensory cortex occupies a large proportion of the functional areas of the brain

TABLE 5 The relationship between sensation and N20.

| | N20 amplitude | | | | N20 latency | | | |
|---|---|---|---|---|---|---|---|---|
| | Light touch sensation | | 2-PD | | Light touch sensation | | 2-PD | |
| | *r* | *P*-value | *r* | *P*-value | *r* | *P*-value | *r* | *P*-value |
| Thumb | 0.243 | 0.012 | −0.368 | <0.001 | −0.105 | 0.288 | −0.107 | 0.278 |
| Index finger | 0.276 | 0.004 | −0.338 | <0.001 | −0.103 | 0.297 | −0.127 | 0.196 |
| Little finger | 0.253 | 0.009 | −0.409 | <0.001 | −0.158 | 0.107 | −0.158 | 0.107 |
| Thenar | 0.279 | 0.004 | −0.277 | 0.004 | −0.147 | 0.134 | −0.153 | 0.118 |
| Hypothenar | 0.257 | 0.008 | −0.315 | <0.001 | −0.136 | 0.166 | −0.136 | 0.166 |

2-PD, two-point discrimination; N20, negative peak at 20 ms.

TABLE 6 The relationship between hemiplegic hand function and sensation.

| | Light tough sensation | | 2-PD | |
|---|---|---|---|---|
| | *r* | *P*-value | *r* | *P*-value |
| Thumb | 0.272 | 0.004 | −0.342 | <0.001 |
| Index finger | 0.259 | 0.006 | −0.340 | <0.001 |
| Little finger | 0.258 | 0.006 | −0.359 | <0.001 |
| Thenar | 0.222 | 0.019 | −0.245 | 0.011 |
| Hypothenar | 0.251 | 0.008 | −0.235 | 0.015 |

2-PD, two-point discrimination.

(Williams and Warwick, 1973). Hand sensory impairment is one of the common manifestations of hemiplegia, which affects the flexibility of hand movements (Kitai et al., 2021). We found that the impairment of 2-PD was worse than that of light touch sensation in patients with stroke, which is consistent with Lima et al. (2015) and Wolny et al. (2017). However, Tyson et al. (2008) found no significant difference in light touch sensation and 2-PD among the elbow, the wrist, and the thumb. This may be because they included patients with stroke at 2–4 weeks who were more severe and had poorer motor functions. In addition, anxiety, depression, and cognitive impairment affect patient perceptions (Paolucci, 2017).

Light touch sensation and 2-PD differed in patients with stroke at different measurement points, and the site of choice may reflect different functional levels. Peng et al. (2018) found that 2-PD in the index finger was negatively correlated with the Fugl-Meyer Assessment of the upper extremities (FMA-UE) in elderly patients with stroke, whereas 2-PD in the thenar was not correlated with FMA-UE. There was a significant difference in sensory function between the unaffected and affected sides of the thumbs and the index fingers in patients with stroke but not in the thenars (Peng et al., 2018). Enders and Seo (2016) found that stroke patients with sensory impairment had greater deviations from the normal strength measured in each finger than those without sensory impairment, suggesting that differences in the pinch grip control in each finger may be related to hyperalgesia in each finger. Similar results were found in the present study; there was no significant difference in light touch sensation among all parts of the hand, and there was a significant difference in 2-PD among all parts of the hand, providing a basis for clinical evaluations. Carlsson et al. (2018b) studied the effect of sensorimotor training in patients with stroke and more thoroughly examined the effect of treatment by performing a sensory analysis of digits I, II, and V in the thenar and hypothenar regions. Although such an evaluation method improves the accuracy of the objective examination, it is time-consuming. Whether this represents the true nature of sensory impairment is worth investigating.

The SEP, a neurophysiological detection method commonly used in clinical practice, is stimulated mainly by the Ia fiber at the end of the limb, reflecting the conductive proprioceptive and fine tactile sensations, such as 2-PD and the tactile sensation of discriminating the texture of objects, of the posterior cord medial tegmental system. Currently, it is the most objective method for evaluating sensory pathways (Karnaze et al., 1987). The waveforms of the SEP latency could indicate the source of neurogenesis; N20 is generally considered to represent the cortical activity of the postcentral gyrus recorded during the stimulation of the median nerve (Tamura et al., 2009). We found that the N20 amplitude was mostly reduced and correlated with the level of sensory function in patients with stroke. Some studies found that early patients with stroke had predominantly axonal damage, manifested by a decreased N20 amplitude. The reason why the N20 latency was not correlated with the sensory function was that there were fewer stroke patients with demyelinating changes (Wang et al., 2012; Chen et al., 2021; Yoon et al., 2021). Al-Rawi et al. (2009) showed that the N20 amplitude correlated with the Medical Research Council

score and could represent the level of function in patients with stroke, which was consistent with the results of this study. We found that light touch sensation and 2-PD had no relationship with the N20 latency. Tzvetanov and Rousseff (2005) found no correlation between the N20 latency and limb function in patients with acute stroke, which is consistent with our results. Keren et al. (1993) found that the median nerve SEP with a prolonged latency and shortened amplitude was also associated with poor motor function. It may be related to the fact that the SEP component studied by Keren et al. (1993) was not N20. Few studies have examined the correlation between SEP and sensory function in patients with stroke. The variations in these studies may be related to the duration of the disease, age, and other factors.

In this study, we found that both light touch sensation and 2-PD were correlated with the N20 amplitude. Light touch sensation was not significantly different among all parts of the hand and was weakly correlated with the N20 amplitude. The correlation coefficients between the light touch sensation of the hand and the N20 amplitude were different, with smaller correlation coefficients for the palm of the hand (thenar and hypothenar) and larger correlation coefficients for the fingers (with the little finger > thumb > index finger). Therefore, it is recommended that when screening the sensation of patients with stroke, any part of the fingers or palm should be selected to assess light touch sensation. For 2-PD, the finger and palm regions represented different sensory states; we could select the little finger for the fingers and any part of the palm. Suda et al. (2021) found that the light touch sensation between the thumb and the index finger was not significant and was consistent with the results of our study. In contrast, 2-PD is a complex sensation that requires not only a complete medial thalamus sensory transmission pathway but also a deficit in cognitive function that could affect the discrimination of general sensations during the assessments (Harvey, 2019). It was reported that there was a correlation between sensory and cognitive function in a normal aging sample (Tay et al., 2006). Lin and Jia (2020) demonstrated that cognitive function recovery is important in the areas of sensory, memory, attention, and emotion. Sensory training is inseparable from good attention and thinking and memory skills and influences cognitive behaviors such as attention and perception (Lin and Jia, 2020). The accuracy and authenticity remain to be verified.

Most studies have shown that sensory and motor functions are closely related to patients with stroke. Meyer et al. (2014) performed a meta-analysis of six articles to examine the relationship between proprioceptive deficits and function in patients with stroke and found that light touch sensation combined with proprioception was significantly associated with upper limb motor function and activities of daily living. To study the effect of intensive sensorimotor training in patients with stroke, Diego et al. (2013) divided patients into two groups: a control group undergoing conventional rehabilitation and an experimental group undergoing additional intensive sensorimotor training. The results showed that the latter was more statistically significant in the Fugl-Meyer test. The results of our study showed that the hemiplegic hand function was positively correlated with the light touch sensation of the hand and negatively correlated with 2-PD, which is more consistent with the results of Diego et al. (2013) and Meyer et al. (2014). Sensory function decreases after stroke and correlates with hemiplegic hand function, with the highest correlation coefficient observed in the thumb. To improve disabilities in patients with stroke, more sensory stimulation of the thumb can be provided. In addition, this study also found 10 patients with a normal light touch sensation but with 2-PD loss, 35 patients presenting with both light touch sensation and 2-PD loss, and only 1 patient presenting with a light touch sensation with normal 2-PD. This was generally consistent with the majority of studies that demonstrate that light touch sensation could be exempted from the 2-PD test if it was lost (Barnett, 1998; Carlsson et al., 2018a). However, our study also found that light touch sensation was poor, whereas 2-PD may not be poor, and 2-PD is related to the ability to perform daily activities. Therefore, assessing 2-PD in the sensory assessment was necessary if the light touch sensation was poor. The little finger and hypothenar may also better represent the function of 2-PD.

However, this study had some limitations. First, the difference between two adjacent monofilaments is not very large so that it may lead to the limited use of SWMT. Furthermore, light touch sensation and 2-PD may not be simple examinations of superficial and compound sensory sensations. The formation of light touch sensation and 2-PD was complex, and the assessment process was influenced by the patient's injury location and subjective consciousness, which may influence the accuracy. The education level, occupation, living habits, etc., may be factors that affect the epidermal thickness, which may affect sensation (Zimmerman et al., 2014; Fu et al., 2016). It is worth exploring whether they represent superficial and compound sensory stimuli. In this study, when the patient could not feel the touch of the heaviest monofilament, they got a score of 0. However, for example, patients may feel a monofilament weighing 448 g, a score of 0 was still credited according to the criteria of this study. It may confuse the level of this patient's light touch sensation. The weight span of the monofilament selected in this study is large, which limits its use in the evaluation. Second, SEP is a highly sensitive neurophysiological index that may be influenced by noise as well as physiological factors such as height and weight. In addition, the disease duration may be a factor that influences N20, which may explain the lack of a statistical difference between the sensory function and N20 latency. Besides that, we just exclude the patients with a history of cervical spondylosis,

which had an effect on their daily living through their CT or MRI of the cervical spine. Those patients who did not undergo a relative examination presenting mild symptoms were not completely excluded. Furthermore, tremors or spasms are a source of noise in patients after stroke, which in turn affects SEP. The sweep number of SEP was only 100 accumulation in this study. In the next study, we will consider the noise of SEP and expand the sweep number of SEP to 500 accumulate (Tashiro et al., 2019). Therefore, further research will involve examining shorter disease durations. Finally, this study only evaluated light touch sensation and 2-PD without screening for deep sensation; therefore, more in-depth and comprehensive studies are needed on the dysfunction of sensory function in patients with stroke.

## Data availability statement

The original contributions presented in this study are included in the article/supplementary material, further inquiries can be directed to the corresponding author.

## Ethics statement

The studies involving human participants were reviewed and approved by the North China University of Science and Technology. The patients/participants provided their written informed consent to participate in this study.

## Author contributions

YL: project conception, writing the original manuscript, data analysis, and investigation. JM: project administration, methodology, and modifying the manuscript. HL: data curation and review and editing the manuscript. W-YS: patients' interview and methodology. Z-HX: data analysis and investigation. QY: evaluation of the patients and data analysis. Q-QZ: evaluation of the patients. FW: data analysis. X-LT: patients' interview. Y-FB: quality control. All authors contributed to the article and approved the submitted version.

## Acknowledgments

We are very grateful to Zhibo Wang and Mengsi Zhang from the Department of Electrophysiology, Shijiazhuang People's Hospital for their contributions to the data collection of this experiment. In addition, we would also like to thank Editage (www.editage.cn) for English language editing.

## Conflict of interest

The authors declare that the research was conducted in the absence of any commercial or financial relationships that could be construed as a potential conflict of interest.

## Publisher's note

All claims expressed in this article are solely those of the authors and do not necessarily represent those of their affiliated organizations, or those of the publisher, the editors and the reviewers. Any product that may be evaluated in this article, or claim that may be made by its manufacturer, is not guaranteed or endorsed by the publisher.

## References

Al-Rawi, M. A., Hamdan, F. B., and Abdul-Muttalib, A. K. (2009). Somatosensory evoked potentials as a predictor for functional recovery of the upper limb in patients with stroke. *J. Stroke Cerebrovasc. Dis.* 18, 262–268.

Barnett, H. (1998). *Stroke: Pathophysiology, Diagnosis, and Management*. London: Churchill Livingstone.

Brown, K. E., Neva, J. L., Feldman, S. J., Staines, W. R., and Boyd, L. A. (2018). Sensorimotor integration in chronic stroke: baseline differences and response to sensory training. *Restor. Neurol. Neurosci.* 36, 245–259. doi: 10.3233/RNN-170790

Brunnstrom, S. (1966). Motor testing procedures in hemiplegia: based on sequential recovery stages. *Phys. Ther.* 46, 357–375. doi: 10.1093/ptj/46.4.357

Carey, L. M., Matyas, T. A., and Baum, C. (2018). Effects of somatosensory impairment on participation after stroke. *Am. J. Occup. Ther.* 72, 7203205100p1–7203205100p10.

Carlsson, H., Gard, G., and Brogårdh, C. (2018a). Upper-limb sensory impairments after stroke: self-reported experiences of daily life and rehabilitation. *J. Rehabil. Med.* 50, 45–51. doi: 10.2340/16501977-2282

Carlsson, H., Rosén, B., Pessah-Rasmussen, H., Björkman, A., and Brogårdh, C. (2018b). SENSory re-learning of the UPPer limb after stroke (SENSUPP): study protocol for a pilot randomized controlled trial. *Trials* 19:229. doi: 10.1186/s13063-018-2628-1

Chen, L., Li, W., Cheng, S., Liang, S., Huang, M., Lei, T., et al. (2021). Correlation of N30 somatosensory evoked potentials with spasticity and neurological function after stroke: a cross-sectional study. *J. Rehabil. Med.* 53:jrm00223. doi: 10.2340/16501977-2867

Chen, X., Liu, F., Yan, Z., Cheng, S., Liu, X., Li, H., et al. (2018). Therapeutic effects of sensory input training on motor function rehabilitation after stroke. *Medicine* 97:e13387. doi: 10.1097/md.0000000000013387

Dawei, Z., Hui, Z., Buguo, C., Weiya, Q., Rongjian, S., and Kuishui, S. (2018). Measurement of two-point discrimination of the extremities in healthy adults. *Chinese Med. J.* 98, 3212–3214.

Diego, C. D., Puig, S., and Navarro, X. (2013). A sensorimotor stimulation program for rehabilitation of chronic stroke patients. *Restor. Neurol. Neurosci.* 31, 361–371.

Enders, L. R., and Seo, N. J. (2016). Effects of sensory deficit on phalanx force deviation during power grip post stroke. *J. Mot. Behav.* 49, 55–66. doi: 10.1080/00222895.2016.1191416

Fedorczyk, J. (2002). Rehabilitation of the hand and upper extremity. *J. Hand Therapy* 15, 380–380.

Feng, J., Luo, J., Yang, P., Du, J., Kim, B. S., and Hu, H. (2018). Piezo2 channel-Merkel cell signaling modulates the conversion of touch to itch. *Science* 360, 530–533. doi: 10.1126/science.aar5703

Fu, Y., Zhang, Q., Yu, C., Zhang, J., Wang, N., Zuo, S., et al. (2016). Longitudinal assessment of motor recovery of contralateral hand after basal ganglia infarction using functional magnetic resonance imaging. *Biomed. Res. Int.* 2016:7403795. doi: 10.1155/2016/7403795

GBD 2017 Mortality Collaborators (2018). Global, regional, and national disability-adjusted life-years (DALYs) for 359 diseases and injuries and healthy life expectancy (HALE) for 195 countries and territories, 1990–2017: a systematic analysis for the Global Burden of Disease Study 2017. *Lancet* 392, 1859–1922. doi: 10.1016/S0140-6736(18)32335-3

Germann, C., Sutter, R., and Nanz, D. (2020). Novel observations of Pacinian corpuscle distribution in the hands and feet based on high-resolution 7-T MRI in healthy volunteers. *Skeletal. Radiol.* 50, 1249–1255. doi: 10.1007/s00256-020-03667-7

Goodin, P., Lamp, G., Vidyasagar, R., McArdle, D., Seitz, R. J., and Carey, L. M. (2018). Altered functional connectivity differs in stroke survivors with impaired touch sensation following left and right hemisphere lesions. *Neuroimage Clin.* 18, 342–355. doi: 10.1016/j.nicl.2018.02.012

Harvey, P. D. (2019). Domains of cognition and their assessment. *Dial. Clin. Neurosci.* 21, 227–237.

Horn, J., and Tjepkema-Cloostermans, M. (2017). Somatosensory evoked potentials in patients with hypoxic-ischemic brain injury. *J. Sem. Neurol.* 37, 60–65.

Karnaze, D., Fisher, M., Ahmadi, J., and Gott, P. (1987). Short-latency somatosensory evoked potentials correlate with the severity of the neurological deficit and sensory abnormalities following cerebral ischemia. *Electroencephalogr. Clin. Neurophysiol.* 67, 147–150. doi: 10.1016/0013-4694(87)90037-x

Keren, O., Ring, H., Solzi, P., Pratt, H., and Groswasser, Z. (1993). Upper limb somatosensory evoked potentials as a predictor of rehabilitation progress in dominant hemisphere stroke patients. *J. Stroke J. Cereb. Circulat.* 24:1789. doi: 10.1161/01.str.24.12.1789

Kessner, S. S., Bingel, U., and Thomalla, G. (2016). Somatosensory deficits after stroke: a scoping review. *Top. Stroke Rehabil.* 23, 136–146. doi: 10.1080/10749357.2015.1116822

Kitai, K., Odagiri, M., Yamauchi, R., and Kodama, T. (2021). Evaluation of intervention effectiveness of sensory compensatory training with tactile discrimination feedback on sensorimotor dysfunction of the hand after stroke. *Brain Sci.* 11:1314. doi: 10.3390/brainsci11101314

Lim, C. (2019). Multi-Sensorimotor training improves proprioception and balance in subacute stroke patients: a randomized controlled pilot trial. *Front. Neurol.* 10:157. doi: 10.3389/fneur.2019.00157

Lima, N. M., Menegatti, K. C., Yu, É., Sacomoto, N. Y., Scalha, T. B., Lima, I.N., et al. (2015). Sensory deficits in ipsilesional upper-extremity in chronic stroke patients. *Arq. Neuropsiquiatr.* 73, 834–839. doi: 10.1590/0004-282x20150128.

Lin, J., and Jia, J. (2020). Progress of post-stroke sensory training in upper limb and hand function rehabilitation Chinese. *J. Rehabil. Med.* 35, 488–492.

Macerollo, A., Brown, M. J. N., Kilner, J. M., and Chen, R. (2018). Neurophysiological changes measured using somatosensory evoked potentials. *Trends Neurosci.* 41, 294–310.

Meyer, S., Karttunen, A. H., Thijs, V., Feys, H., and Verheyden, G. (2014). How do somatosensory deficits in the arm and hand relate to upper limb impairment, activity, and participation problems after stroke? a systematic review. *Phys. Ther.* 94, 1220–1231. doi: 10.2522/ptj.20130271

Neuroscience, and Surgery (1997). Diagnostic points of various cerebrovascular diseases. *Chinese J. Neurol.* 29, 379–380.

Oldfield, R. C. (1971). The assessment and analysis of handedness: the Edinburgh inventory. *Neuropsychologia* 9, 97–113. doi: 10.1016/0028-3932(71)90067-4

Paolucci, S. (2017). Advances in antidepressants for treating post-stroke depression. *Expert Opin. Pharmacother.* 18, 1011–1017. doi: 10.1080/14656566.2017.1334765

Peng, S., Ying, X., Li, D., Wei, S., Yanyun, J., Haifeng, L., et al. (2018). Changes in tactile sensation and two-point discrimination of hands and upper limbs and the correlation with upper limb motor function in the elderly after stroke. *Geriatr. Health Care* 24:5.

Price, M. P., Lewin, G. R., McIlwrath, S. L., Cheng, C., Xie, J., Heppenstall, P. A., et al. (2000). The mammalian sodium channel BNC1 is required for normal touch sensation. *Nature* 407, 1007–1011. doi: 10.1038/35039512

Song, Y., Prakash, R., and Reddy, J. (2016). Prognostic value of somatosensory-evoked potentials in neurology: a critical review in hypoxic encephalopathy. *J. Neurol. India* 64:396. doi: 10.4103/0028-3886.181555

Sridharan, N. D., Chaer, R. A., Thirumala, P. D., Balzer, J., Long, B., Tzeng, E., et al. (2016). Somatosensory evoked potentials and electroencephalography during carotid endarterectomy predict late stroke but not death. *Ann. Vascular Surg.* 38, 18–19. doi: 10.1016/j.avsg.2016.07.064

Suda, M., Kawakami, M., Okuyama, K., Ishii, R., and Liu, M. (2021). Validity and reliability of the semmes-weinstein monofilament test and the thumb localizing test in patients with stroke. *Front. Neurol.* 11:625917. doi: 10.3389/fneur.2020.625917

Tamura, Y., Ueki, Y., Lin, P., Vorbach, S., Mima, T., Kakigi, R., et al. (2009). Disordered plasticity in the primary somatosensory cortex in focal hand dystonia. *Brain* 132(Pt 3), 749–755. doi: 10.1093/brain/awn348

Tashiro, S., Kuroki, M., Okuyama, K., Oshima, O., Ogura, M., Hijikata, N., et al. (2021). Factors related to daily use of the paretic upper limb in patients with chronic hemiparetic stroke-a retrospective cross-sectional study. *PLoS One* 16:e0247998. doi: 10.1371/journal.pone.0247998

Tashiro, S., Mizuno, K., Kawakami, M., Takahashi, O., Nakamura, T., Suda, M., et al. (2019). Neuromuscular electrical stimulation-enhanced rehabilitation is associated with not only motor but also somatosensory cortical plasticity in chronic stroke patients: an interventional study. *Ther. Adv. Chronic. Dis.* 10:2040622319889259. doi: 10.1177/2040622319889259

Tay, T., Wang, J. J., Kifley, A., Lindley, R., Newall, P., and Mitchell, P. (2006). Sensory and cognitive association in older persons: findings from an older Australian population. *Gerontology* 52, 386–394. doi: 10.1159/000095129

Tonak, H. A., Kaya Kara, O., and Sahin, S. (2021). Correlation of hand functionality and grip strengths with anthropometric measurements. *Work* 69, 187–195. doi: 10.3233/wor-213468

Tyson, S. F., Hanley, M., Chillala, J., Selley, A .B., and Tallis, R. C. (2008). Sensory loss in hospital-admitted people with stroke: characteristics, associated factors, and relationship with function. *Neurorehabil. Neural Repair.* 22, 166–172. doi: 10.1177/1545968307305523

Tzvetanov, P., and Rousseff, R. T. (2005). Predictive value of median-SSEP in early phase of stroke: a comparison in supratentorial infarction and hemorrhage. *Clin. Neurol. Neurosurg.* 107, 475–481. doi: 10.1016/j.clineuro.2004.12.008

Umeki, N., Murata, J., Kubota, S., Kogo, H., Yamaguchi, T., and Higashijima, M. (2018). Relationship between motor paralysis and impairments in tactile sensitivity in elderly stroke patients. *Int. J. Gerontol.* 12, 310–313. doi: 10.1161/01.str.32.7.1627

Wang, Q., Song, Z., Zhou, Y., Dong, Y., and Liang, H. (2012). [Fractional anisotropy and somatosensory evoked potentials in the postcentral gyrus subcortex after acute infarction of the posterior limb of the internal capsule]. *Nan Fang Yi Ke Da Xue Xue Bao* 32, 1004–1007.

Wang, W., Jiang, B., Sun, H., Ru, X., Sun, D., Wang, L., et al. (2017). Prevalence, incidence, and mortality of stroke in China clinical perspective: results from a nationwide population-based survey of 480687 adults. *Circulation* 135:759.

Williams, P. L., and Warwick, R. (1973). *Gray's Anatomy. the Anatomical Basis of Medicine and Surgery*. New York, NY: Churchill Livingstone.

Wolny, T., Linek, P., and Michalski, P. (2017). Inter-rater reliability of two-point discrimination in acute stroke patients. *Neuro Rehabil.* 41, 127–134. doi: 10.3233/nre-171464

Yoon, H., Park, C., Park, I., Kim, K., and Cha, Y. (2021). A precision neurorehabilitation using SSEP for early detection of sensory deficit and restoration of the motor recovery in balance, gait and activities of daily living in acute stroke. *Technol. Health Care* 29, 377–383. doi: 10.3233/thc-218036.

Zhao, L., Liu, Z., Sun, Q., and Li, H. (2022). Effect of transcranial direct current stimulation combined with a smart hand joint training device on hand dysfunction in patients with early stroke. *Folia Neuropathol.* 60, 177–184. doi: 10.5114/fn.2022.117534

Zhongliang, L. (1995). Physical labor intensity classification and basis. *Occup. Health* 6.

Zimmerman, A., Bai, L., and Ginty, D. D. (2014). The gentle touch receptors of mammalian skin. *Science* 346, 950–954. doi: 10.1126/science.1254229

frontiers | Frontiers in Neuroscience

TYPE Original Research
PUBLISHED 16 January 2023
DOI 10.3389/fnins.2022.1107688



OPEN ACCESS

EDITED BY
Jie Jia,
Fudan University, China

REVIEWED BY
Ningbo Yu,
Nankai University, China
Hewei Wang,
Fudan University, China
Beiyao Gao,
China-Japan Friendship Hospital, China
Anjing Zhang,
Shanghai First Rehabilitation Hospital, China

*CORRESPONDENCE
Da-wei Zang
✉ zangdawei@bjtth.org

SPECIALTY SECTION
This article was submitted to Translational Neuroscience, a section of the journal Frontiers in Neuroscience

RECEIVED 25 November 2022
ACCEPTED 28 December 2022
PUBLISHED 16 January 2023

CITATION
Yu H-x, Liu S-h, Wang Z-x, Liu C-b, Dai P and Zang D-w (2023) Efficacy on gait and posture control after botulinum toxin A injection for lower-limb spasticity treatment after stroke: A randomized controlled trial.
*Front. Neurosci.* 16:1107688.
doi: 10.3389/fnins.2022.1107688



# Efficacy on gait and posture control after botulinum toxin A injection for lower-limb spasticity treatment after stroke: A randomized controlled trial

Hui-xian Yu, Si-hao Liu, Zhao-xia Wang, Chang-bin Liu, Pei Dai and Da-wei Zang*

Department of Rehabilitation Medicine, Beijing Tiantan Hospital, Capital Medical University, Beijing, China

**Objectives:** To observe the efficacy of botulinum toxin type A (BoNT-A) for the spasticity of the lower-limb post-stroke on gait and posture control.

**Methods:** A total of 46 patients with hemiplegia gait were randomly divided into the experimental group (23 patients) and the control group (23 patients). In patients in the experimental group received injections of BoNT-A by electrical stimulation-guided. At the same time, patients of the two groups received routine physical therapy. Gait analysis, plantar pressure analysis, lower-limb Fugl–Meyer assessment (L-FMA), 10 meter walking test (10MWT), timed "Up and Go" test (TUGT), and modified Ashworth Scale assess (MAS) of the lower limbs were performed at 0, 1, 4, and 12 weeks after treatment.

**Results:** At 1, 4, and 12 weeks after treatment, the L-FMA, stride length, speed, and TUGT significantly improved than 0 week in both groups. The L-FMA and peak of forefoot pressure, and MAS results in the experimental group were better than those in the control group at 4 and 12 weeks. The TUGT, speed, and stride length in experimental group was significantly shortened than that in control group at 1, 4, and 12 weeks.

**Conclusion:** Botulinum toxin type A injection can improve motor functions of the lower limb, gait, spasticity, forefoot pressure, and posture control of patients after stroke.

KEYWORDS

**stroke, botulinum toxin A, gait, spasticity, posture control**

## Introduction

Stroke is one of the leading causes of death and adult disability globally (Wang, 2022). A total of 75% of patients who sustain a stroke have limitations in walking (Abilleira et al., 2005), and the most common pattern of walking impairment post-stroke

is hemiparetic gait. Patients with post-stroke hemiparesis may experience classic changes in spatiotemporal, kinematic, and kinetic parameters. A hemiplegic gait is often described as insufficient knee flexion or knee hyperextension, hip lifting, external rotation, ankle varus, and plantarflexion of the affected side limb (Sheffler and Chae, 2015; Nikamp et al., 2019). Most of this gait pattern is caused by spasticity. The spasticity after central nervous system injury is the main cause of this typical abnormal pattern. Spasticity is a common complication in upper motor neuron syndrome after neurological diseases, which is characterized clinically by a velocity-dependent increase in muscle tone and the stretch reflex. In the single hemiplegic side limb-supporting phase, the foot is in the abnormal position. This equinovarus foot posture affects gait, standing, and weight transfer (Tao et al., 2015). Furthermore, spasticity of the lower limb can impair the function of daily activities and increase the risk of falls (Thibaut et al., 2013).

The spasticity should be treated in time, triceps spasm in calves causes forefoot landing and knee hyperextension (Sankaranarayan et al., 2016). Spasms of the posterior tibialis muscle and flexor digitorum longus (FDL) muscle can cause strephenopodia and toe flexion (like **Figure 1**). This abnormal movement pattern leads to a decrease in walking speed and falls (Paula et al., 2019a).

Botulinum toxin type A injections are effective in treatments available for spasticity (Baker and Pereira, 2016). BoNT-A is used to reduce the excessive activity of the focal muscles of upper motor neuron injured syndrome (Pandyan et al., 2005). BoNT-A can induce weakness, relax the target muscles temporarily, and make them easier to be extended. This can alleviate neurogenic and biomechanical factors that contribute to the spasticity.

Studies have shown that Botox injection can significantly reduce lower limb muscle tone (Kaňovsk et al., 2021), improve walking speed (Marciniak et al., 2019), and improve ankle motion (Marciniak et al., 2019). However, there is insufficient evidence to support the improvement of lower limb gait and postural control. There are fewer data reporting the efficacy of BoNT in well-designed clinical trials in adults with lower-limb spasticity (Santamato et al., 2019). In this study, we used a plantar pressure system and performed gait analysis to evaluate the effect of BoNT-A injection on the lower limb, gait, and posture control function.

# Materials and methods

## Study design

The study was performed as a randomized controlled trial with single-blinded assessments. The assessors and statisticians were blinded to the group assignment. That was approved by the Ethics Committee of Beijing Tiantan Hospital, Capital Medical University (KY2020-069-01). The registration number of this clinical trial was ChiCTR2000037479.

## Study participants

A total of 46 patients with hemiplegia gait after stroke localized to the corticospinal tract were included in the Department of Rehabilitation Medicine of Beijing Tiantan Hospital from 1st January, 2021 to 31st July, 2022. This study used nets sample size calculator. The patients were randomly divided into treatment and control groups using random number table[1] (23 patients in each group). Randomization was performed by one doctor who was not involved in other work of this study. The inclusion criteria were as follows: (1) first-ever stroke; (2) age of 35–65 years; (3) $\leq$6 months post-stroke; (4) they had slight spasticity at resting state of the triceps surae as defined by a score of 1−1+ on the MAS or ankle clonus (+); (5) at Brunnstrom recovery stage III–IV; (6) walking with hyperextension or foot drop or toe flexion deformity. (7) no obvious effect after oral anti-spasticity medications for at least 1 month. (8) Mini-mental state examination (MMSE) score $>$ 25. The exclusion criteria were as follows: (1) other cerebrovascular diseases; (2) sensory impairment; (3) other osteoarticular system diseases; (4) history of BoNT injection; (5) severe allergic constitution.

All participants signed informed consent.

## Study protocol

### Intervention

In the control group, patients received routine rehabilitation treatment, including oral anti-spasticity medications and the use of ankle-foot orthotics. In this study, we did not intervene in the choice of medication, method of rehabilitation, and brace type. In the experimental group, patients received BoNT-A (Allergan) injection and routine rehabilitation treatment without oral anti-spasticity medications. The injection was administered by the same physician using electrical stimulation-guided injection. The injection dose and target sites were selected by the physician after individual assessment, referring to Chinese guidelines for the treatment of adult limb spasm with BoNT (Li et al., 2015). The main target muscles were selected mainly depending on gait patterns including quadriceps femoris (QF), gastrocnemius (GS), tibialis posterior (TP), flexor hallucis longus (FHL), FDL, FD brevis (FDB), and FH brevis (FHB) [specific operations followed table (**Table 1**)].

1 http://www.calculator.net/sample-size-calculator.html

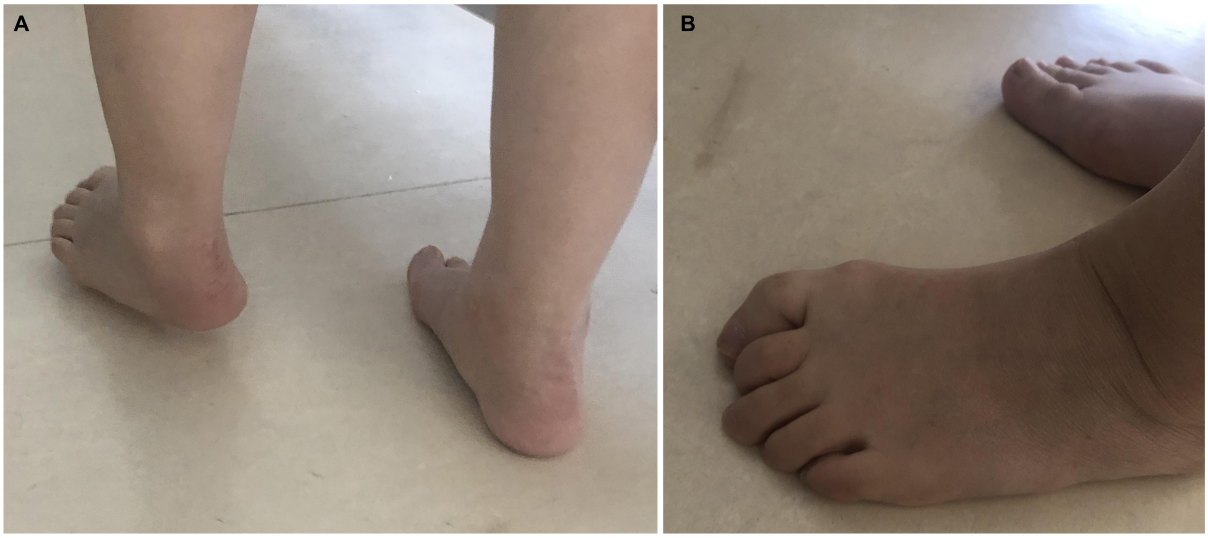


FIGURE 1
Common patterns of varus and toe flexion after stroke. **(A)** Foot drop; the heel can not land first replaced by the anterolateral edge of the foot. **(B)** In the weight-bearing phase, the spasm of the flexion muscle of the toes increases with the increase of the weight of the affected limb, the arch of the feet cannot support the weight stably. In the off-ground, the toes cannot be lifted off the ground by dorsiflexion.

### Outcome measures

All patients were evaluated using a modified Ashworth Scale assess (MAS), Fugl–Meyer assessment (FMA) of the lower limbs, gait analysis, dynamic plantar pressure analysis, and timed "Up and Go" test (TUGT) at 0, 1, 4, and 12 weeks. These assessments were performed by another physician.

Modified Ashworth Scale assess was used to evaluate the spasticity of the GS muscle, and the score ranged from 0 to 5 grades (instead of 0, 1, 1+, 2, 3, and 4).

The motor function of the lower limb was assessed using the lower-limb FMA (L-FMA) motor score (from 0 to 34 grades). The walk and balance functions were assessed using a gait analysis and plantar pressure analysis system (zebris FDM 1.12).

### 10 meter walking test

Patients were asked to walk 12 m forward in a state of natural speed, assessor recorded the time they spent between 1 and 11 m (Yeung et al., 2018).

TABLE 1 BoNT-A injection scheme protocol.

| Target muscles | Number | Dose (IU) |
|---|---|---|
| QF + GS + TP | 3 | 150 + 150 + 70 |
| GS + TP + FDL + FHL | 8 | 150 + 70 + 70 + 50 |
| GS + TP + FDL + FHL + FDB + FHB | 7 | 150 + 70 + 70 + 50 + 20 + 10 |
| GS + TP | 3 | 150 + 70 |

QF, quadriceps femoris; GS, gastrocnemius; TP, tibialis posterior; FHL, flexor hallucis longus; FDL, flexor digitorum longus; FDB, flexor digitorum brevis; FHB, flexor hallucis brevis.

### TUGT

The patients were required to sit on the chair after which the researcher began to record with a stopwatch from the moment the patient got up, walked for 3 m, turned around the cone, and returned to sit down (Dong et al., 2021).

Zebris gait analysis and plantar pressure measurement system (zebris FDM 1.12) was used in this study. The patients were required to take off the shoes on the platform. The participant was asked to release the railings, turn on the evaluation device, and then stop the device after walking for the 30 s. The device mainly recorded the data of both lower limbs while walking, including the peak plantar pressure ($N/cm^2$) of the forefoot and heel, and the gait parameters.

Follow-up was performed at 1, 4, and 12 weeks after injection.

## Statistical analysis

Statistical analyses were performed using GraphPad Prism 8.0 (GraphPad Software, Inc., San Diego, CA, USA). All data sets were tested for normality. Descriptive summary statistics for differences between the two groups of baseline data are presented using the Kruskal–Wallis test. Continuous variables are expressed as the mean ± standard deviation. Differences within the groups before and after treatment were analyzed using one-way analysis of variance (ANOVA). Differences between the two groups were analyzed using unpaired $T$ test. A $p$-value of $< 0.05$ was considered statistically significant.

## Results

During the follow-up, three patients did not complete the study (two from the experimental group and one from the control group). Among these, one from the experimental group had a second stroke during follow-up, whereas the other from the experimental group patient could not reach the hospital on time to complete the evaluation. The one from the control group patient had a hip fracture because of a fall. Thus, 43 patients completed the follow-up (21 from the experimental group and 22 from the control group). No side effects were reported. The flow diagram for enrollment and outcomes like Figure 2.

The statistical results can be shown in Table 2. In the control group, the scores of MAS were increased for the three patients at 1 and 4 weeks. A total of 8 patients showed no changes in MAS, and 11 patients had improved muscular tone. In the experimental group, all the scores of MAS decreased after injection and until 12 weeks.

At 1, 4, and 12 weeks after treatment, L-FMA significantly improved compared with that before treatment in both the groups (control group: $P = 0.000$; experimental group: $P = 0.000$). Analysis between the two groups showed significant improvement in L-FMA in the experimental group compared with the control group at 4 and 12 weeks ($P = 0.000$), there was no significant difference between the two groups at 1 week ($P = 0.0736$; Figure 3).

At 1, 4, and 12 weeks after treatment, TUGT significantly decreased compared with that before treatment in both the groups (control group: $P = 0.000$; experimental group: $P = 0.000$). Analysis between the two groups showed significant improvement in TUGT in the experimental group compared with the control group ($P = 0.000$; Figure 4).

The stride length was significantly improved compared with that before treatment in both the groups at 4 and 12 weeks after treatment (control group: 4 weeks $P = 0.010$ and 12 weeks $P = 0.000$; experimental group: $P = 0.000$). Analysis between the two groups showed significant improvement in stride length in the experimental group compared with the control group ($P = 0.000$). At 1 week, no significant difference was observed compared with that before treatment in the control group ($P = 0.8118$). In the experimental group, a significant difference was observed at 1 week compared with that before treatment ($P = 0.000$; Figure 5).

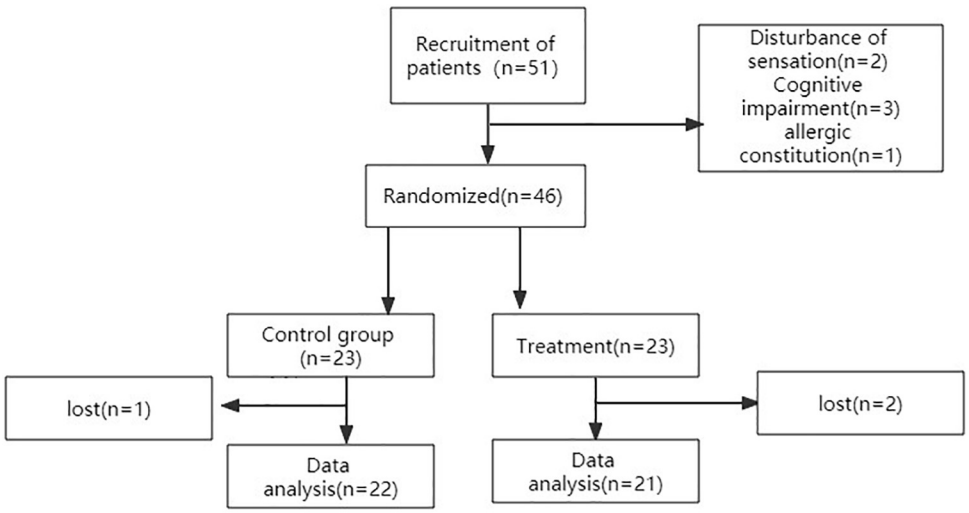


FIGURE 2
The flow diagram of the study.

TABLE 2 Baseline characteristics of active and sham groups.

| Group | Age (years) | Gender (*n*) | Hemiplegia side (*n*) | Time (*m*) | Disorders (*n*) | Focal site |
|---|---|---|---|---|---|---|
| Control group | 54.37 ± 9.78 | F 8 | L 12 | 3.4 ± 0.16 | CH 7 | BG 16 |
| | | M 14 | R 10 | | CI 15 | BS 6 |
| Experimental group | 56.47 ± 6.82 | F 5 | L 13 | 4.2 ± 0.09 | CH 4 | BG 14 |
| | | M16 | R 8 | | CI 17 | BS 7 |

CI, cerebral Infarct; CH, cerebral hemorrhage; BG, basal ganglia; BS, brain stem.

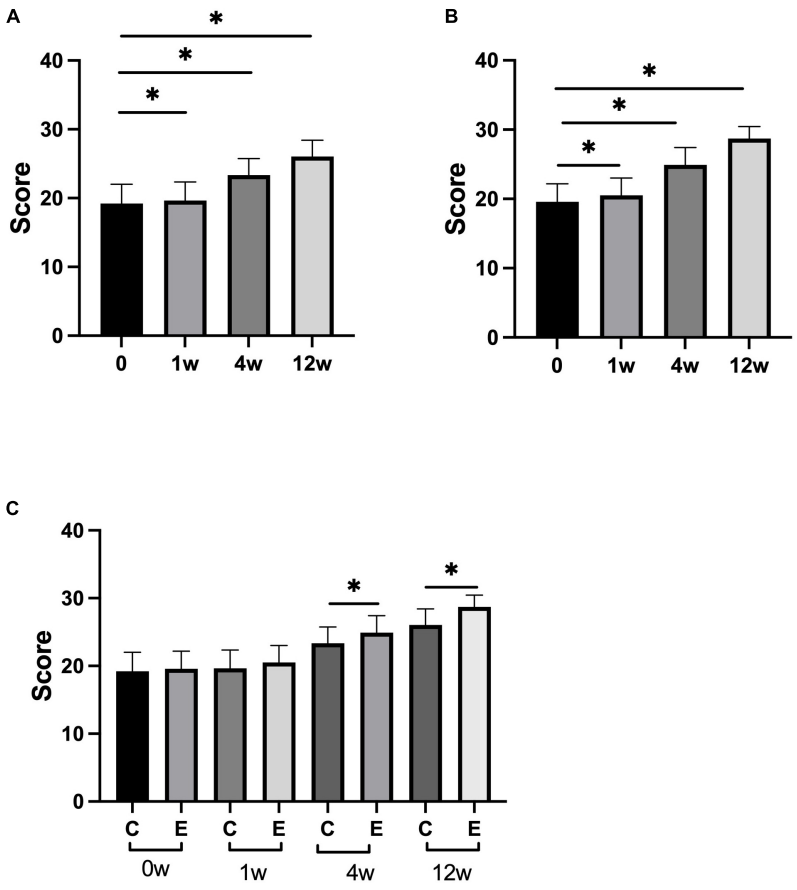


FIGURE 3
Changes in lower-limb Fugl–Meyer assessment (L-FMA) scores. **(A)** Scores of L-FMA at 1, 4, 12 weeks compared with that at 0 week in control group; **(B)** scores of L-FMA at 1, 4, 12 weeks compared with that at 0 week in experimental group; **(C)** scores of L-FMA at 0, 1, 4, and 12 weeks in experimental group compared with control group; $^{*}p < 0.05$.

The speed of 10 meter walking test (10MWT) in the experimental group was higher than that of the control group (control group at 1 week $P = 0.027$, the others and experimental group $P = 0.000$). In the experimental group, the speed significantly improved at 1, 4, and 12 weeks compared with 0 week ($P = 0.000$). Analysis between the two groups showed significant improvement in speed of walking in the experimental group compared with the control group ($P = 0.000$; **Figure 6**).

The peak of forefoot pressure in the experimental group was significantly higher than that in the control group ($P = 0.000$). No significant change was observed after 1 week compared with that after 0 week in the control group ($P = 0.967$). At 4 and 12 weeks after treatment, forefoot pressure was significantly increased compared with that at 0 week ($P = 0.000$). In the experimental group, it significantly improved at 1, 4, and 12 weeks compared with 0 week ($P = 0.000$; **Figure 7**). No significant difference was observed in the peak of rear foot pressure between the two groups (0 week: control group and experimental group $P = 0.993$; 1 week: control group and experimental group $P = 0.543$; 4 weeks: control group and experimental group $P = 0.323$; and 12 weeks: control group and experimental group $P = 0.145$). The peak of rear foot pressure did not significantly change at 1, 4, or 12 weeks compared with 0 week in the control group after treatment (1 week: $P = 0.956$, 4 weeks: $P = 0.550$, and 12 weeks: $P = 0.265$). After injection, forefoot pressure significantly increased at 4 and 12 weeks compared with 0 week in the experimental group (4 weeks: $P = 0.017$ and 12 weeks: $P = 0.035$; **Figure 8**).

## Discussion

In this study, we studied whether a lower-limb injection of BoNT-A in the spastic muscle of patients with stroke could improve their walking ability. BoNT-A injection could significantly improve motor function of the lower limb, gait, spasticity, forefoot pressure, and posture control of patients.

A common incapacitating disease in adults is stroke (Araujo et al., 2018). Motor function is the primary treatment strategy that is most essential for the ability to perform daily activities

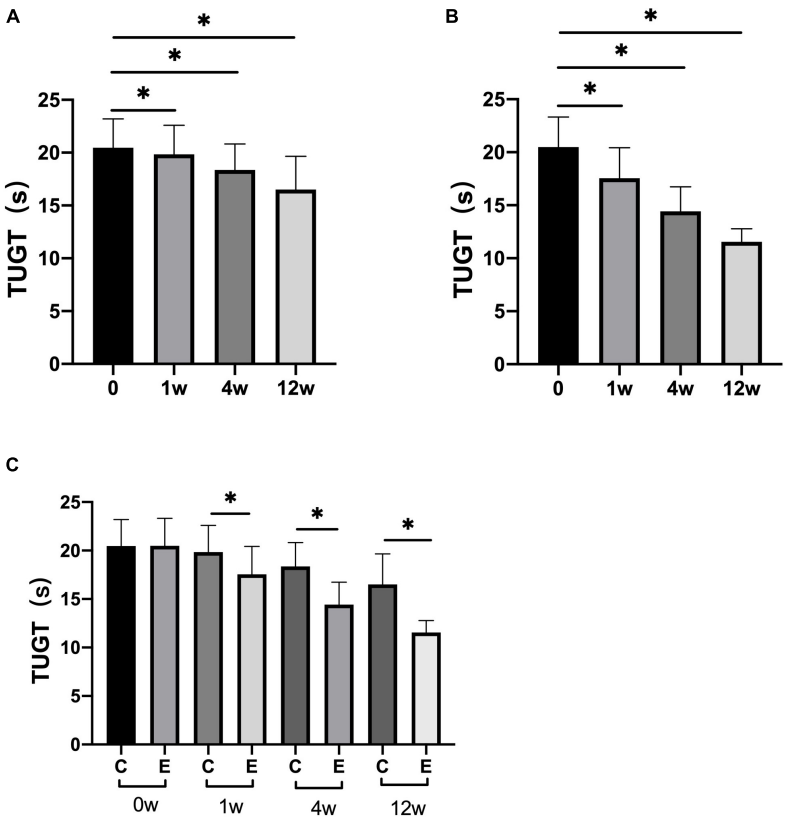


FIGURE 4
Changes in timed "Up and Go" tests (TUGTs). **(A)** TUGT at 1, 4, and 12 weeks compared with that at 0 week in control group; **(B)** TUGT at 1, 4, and 12 weeks compared with that at 0 week in experimental group; **(C)** TUGT at 0, 1, 4, and 12 weeks in experimental group compared with control group; $*p < 0.05$.

independently for patients and families (Tyson and Kent, 2013). After a stroke, most of the abnormal movement patterns are caused by spasticity. Gracies et al. (2017) reported that BoNT-A injection for lower-limb treatment significantly reduced the MAS of the triceps calf after 4 weeks of injection, and they also proved that in the case of repeated injection, patients could have continuous improvement in muscle tone. Fietzek et al. (2014) reported that BoNT-A reduced the MAS scores over all follow-up data after 24 weeks after injection. In this study, the MAS of some patients in the control group was worsened, and some patients showed no change. Upper limb treatment for spasticity reportedly improves muscle tone after stroke; however, treatment outcome after lower limb or pes equinovarus has not been reported (Wissel et al., 2017). Therefore, the ability of BoNT-A to improve lower-limb spasticity and its benefits in treating lower-limb spasticity and spastic equinus foot cannot be ignored. In the experimental group, the MAS of all patients was better than that before injection.

Rousseaux et al. (2014) reported that after BoNT-A injection, the spasticity, passive range of motion, limb positioning, and pain were improved, but the motor function remained unchanged. Controversy exists about improvements in motor function after BoNT-A treatment, Wu et al. (2016) demonstrated the improvement of FMA, but the gait speed was not improved in a systematic review and meta-analysis. Tao et al. (2015) reported BoNT-A injection can increase a FMA at 4 and 8 weeks after treatment. In this study, rehabilitation could improve L-FMA, and the motor function was better after BoNT-A injection than in the control group.

Tao et al. (2015) also reported that BoNT-A injection can increase a patient's stride length, speed at 4 and 8 weeks. Bensmail et al. (2021) reported that BoNT-A injection can improve functional ambulation classification scale scores after 2 weeks and improve independent walking. Gracies et al. (2015) reported that walking speed of patients improvement at 12 weeks after injection. This study showed significant improvement in speed of walking in the experimental group compared with the control group.

The most common synkinesis motion pattern of lower extremity extensor muscles, a fundamental principle of motor control, is the alternating contraction of antagonistic flexor and extensor muscles, which is required for all motor behaviors, including locomotion (Ausborn et al., 2018). Spastic equinus foot is caused by spasms of calf triceps, FDL, or FHL and reduces

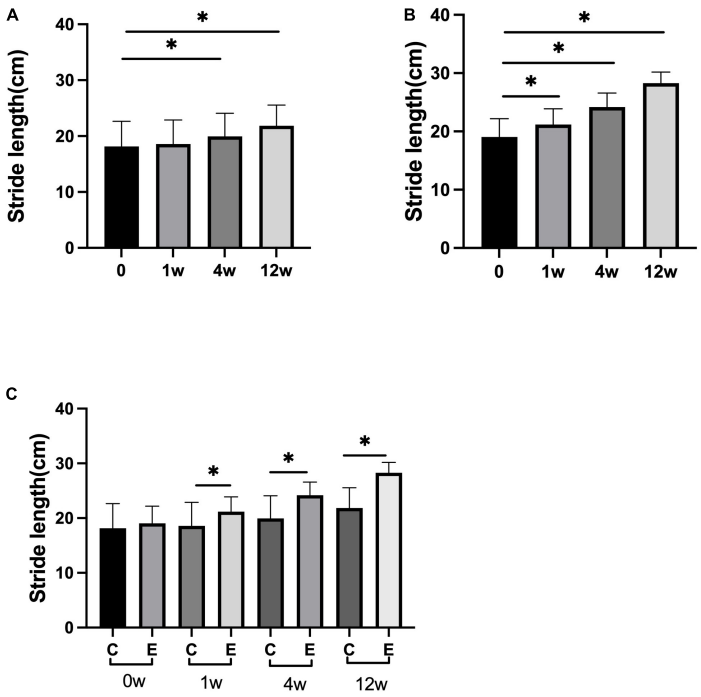


FIGURE 5
Changes in stride length (cm). **(A)** Stride length at 1, 4, and 12 weeks compared with that at 0 week in control group; **(B)** stride length at 1, 4, and 12 weeks compared with that at 0 week in experimental group; **(C)** stride length at 0, 1, 4, and 12 weeks in experimental group compared with control group; $*p < 0.05$.

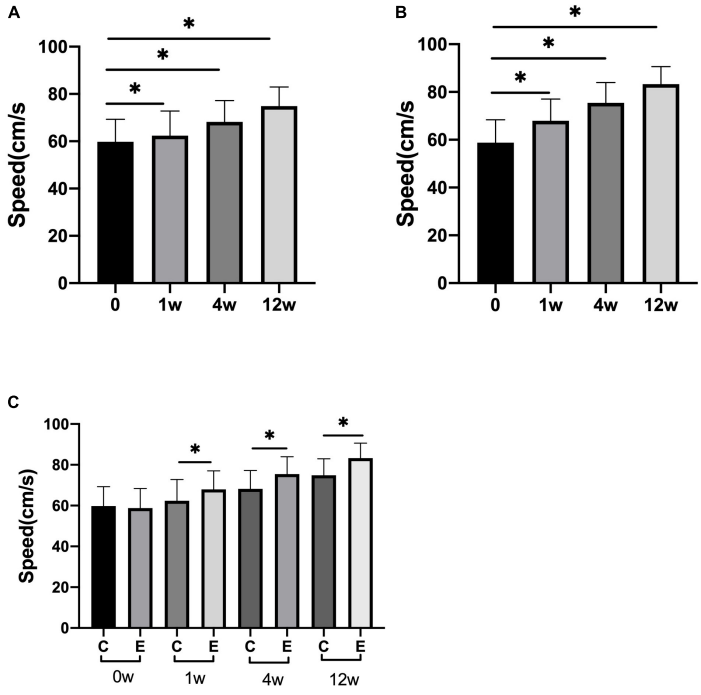


FIGURE 6
Changes in speed of 10 meter walking test (10MWT) (cm/s). **(A)** The speed at 1, 4, and 12 weeks compared with that at 0 week in control group; **(B)** speed at 1, 4, and 12 weeks compared with that at 0 week in experimental group; **(C)** speed at 0, 1, 4, and 12 weeks in experimental group compared with control group; $*p < 0.05$.

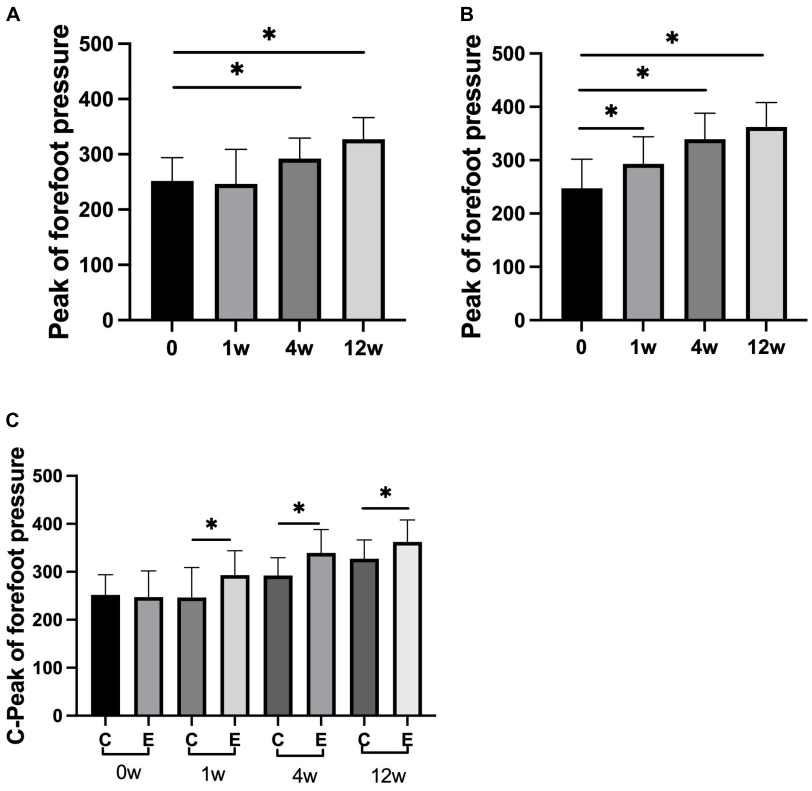


FIGURE 7
Changes in peak of forefoot pressure (*N*). **(A)** Forefoot pressure in control group at 1, 4, and 12 weeks compared with that at 0 week; **(B)** forefoot pressure at 1, 4, and 12 weeks compared with that at 0 week in experimental group; **(C)** forefoot pressure at 0, 1, 4, and 12 weeks in experimental group compared with control group; $^{*}p < 0.05$.

the lower limb stability and affects walking and hemiplegic lower limb weight bearing (Ferreira et al., 2013). Thus, the pressure of the center of gravity in the weight-bearing phase cannot be transferred forward to the medial side. Spasticity can exacerbate asymmetrical hemiplegia gait that includes equinus foot. Gait analysis after BoNT-A injection has been performed in a few studies, but analysis of plantar pressure after BoNT-A injection has not been reported. Manipulative treatment and bracing treatment are commonly used for treating foot drop (Ibuki et al., 2010; Paula et al., 2019b). Clinical observations in our study have shown that the patients were often accompanied by obvious foot varus and spasms of the toe muscles (Yu, 2021). After a stroke, treating foot varus is more difficult than treating foot drop. In a walking cycle, the lateral edge of the foot lands, and in the support phase, plantar pressure cannot sufficiently be transferred from the hindfoot to the medial side of the forefoot (Tao et al., 2015; Yu, 2021).

In this study, although stride length improved significantly in both the groups, the improvement was greater in the injection group and BoNT-A injection could increase the pressure on the forefoot more significantly than that in the control group. The gait control of patients after BoNT-A injection was better than that of patients in from the control group. BoNT-A injection can improve the extensibility of lower limb and plantar muscles, which can transfer plantar pressure from the lateral edge to the anterior side of the foot, and improve load-bearing capacity and gait stability.

Timed "Up and Go" test can be used to detect the risk of falls in stroke patients. Based on the results of this study, the improved TUGT test can record postural control ability in more detail under different motor modes (Yu et al., 2021). This study showed that rehabilitation could improve TUGT, and the motor function was better after BoNT-A injection than in the control group, which means BoNT-A injection can improve postural control more effectively and reduce the risk of falling. Few research about the plantar pressure and TUGT after injection of BoNT-A was reported, so more research is needed.

## Limitation

This study was a small sample, single center study, results, and data were not comprehensive. The design of the experiment may not be very rigorous. At the same time, due to the limited conditions, our evaluation equipment is unadvanced and lacks more objective indicators. It is hoped that a multi-center study will be carried out in future studies, and more

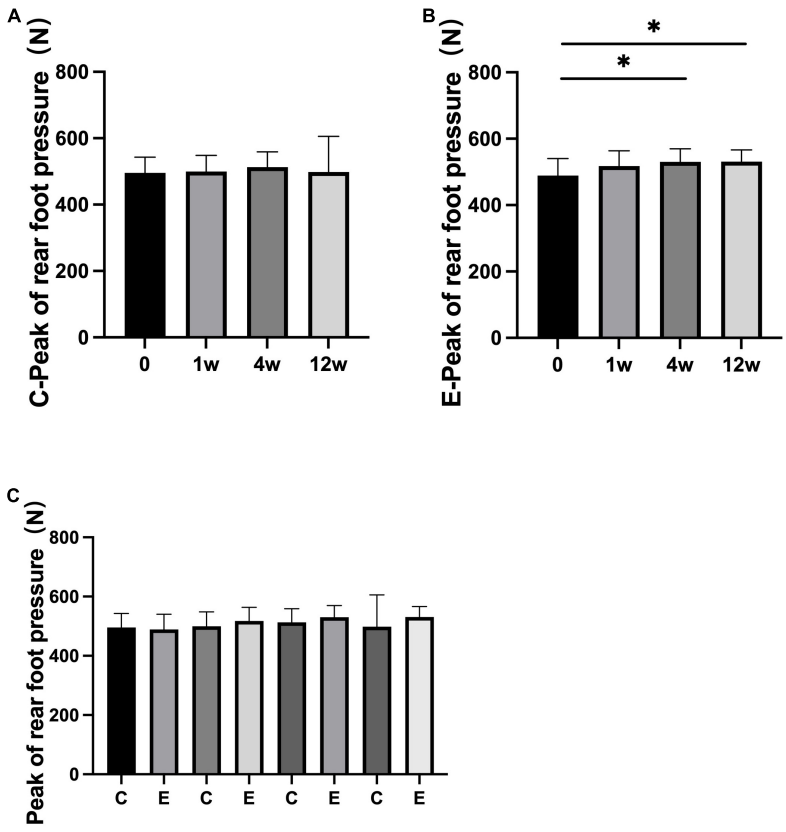


FIGURE 8
Changes in peak of rear foot pressure (*N*). **(A)** Rear foot pressure in control group at 1, 4, and 12 weeks compared with that at 0 week; **(B)** rear foot pressure at 1, 4, and 12 weeks compared with that at 0 week in experimental group; **(C)** rear foot pressure at 0, 1, 4, and 12 weeks in experimental group compared with control group; $^{*}p < 0.05$.

objective indicators such as electromyography and ultrasound will be collected.

## Conclusion

Botulinum toxin type A injection can improve gait and postural control and reduce the risk of falls for patients with pes equinovarus due to triceps surae and toe muscle spasm and other patterns of lower-limb post-stroke spasticity.

## Data availability statement

The raw data supporting the conclusions of this article will be made available by the authors, without undue reservation.

## Ethics statement

The studies involving human participants were reviewed and approved by the Ethics Committee of Tiantan Hospital. The patients/participants provided their written informed consent to participate in this study.

## Author contributions

D-WZ and H-XY: conceptualization. H-XY: methodology, investigation, writing—original draft preparation, visualization, and project administration. C-BL: software. D-WZ, S-HL, and H-XY: validation. Z-XW: formal analysis and data curation. H-XY and PD: resources. H-XY and S-HL: writing—review and editing. PD: supervision. D-WZ: funding acquisition. All authors have read and agreed to the published version of the manuscript.

## Funding

This work was supported by grants from the National Natural Science Foundation of China (Grant Numbers: 82072532 and 82000723) and National Natural Science

Foundation of Capital Medical University (Grant Number: XZR2021-114).

## Conflict of interest

The authors declare that the research was conducted in the absence of any commercial or financial relationships that could be construed as a potential conflict of interest.

## Publisher's note

All claims expressed in this article are solely those of the authors and do not necessarily represent those of their affiliated organizations, or those of the publisher, the editors and the reviewers. Any product that may be evaluated in this article, or claim that may be made by its manufacturer, is not guaranteed or endorsed by the publisher.

## References

Wang, C. (2022). The role of neuromodulation to drive neural plasticity in stroke recovery: a narrative review. *Brain Netw. Modul.* 1, 2–8. doi: 10.4103/2773-2398.339171

Abilleira, S., Ribera, A., Sánchez, E., Roquer, J., Duarte, E., Tresserras, R., et al. (2005). Management of adult stroke rehabilitation care: a clinical practice guideline. *Stroke* 36, e100–e143.

Sheffler, L., and Chae, J. (2015). Hemiparetic gait physical medicine & rehabilitation clinics of North America, 2015. *Phys. Med. Rehabil. Clin. N. Am.* 26, 611–623. doi: 10.1016/j.pmr.2015.06.006

Nikamp, C., Hobbelink, M., Job, V., Hermens, H. J., Rietman, J. S., and Buurke, J. H. (2019). The effect of ankle-foot orthoses on fall/near fall incidence in patients with (sub-)acute stroke: A randomized controlled trial. *PLoS One* 14:e0213538. doi: 10.1371/journal.pone.0213538

Tao, W., Yan, D., Li, J. H., and Shi, Z. H. (2015). Gait improvement by low-dose botulinum toxin A injection treatment of the lower limbs in subacute stroke patients. *J. Phys. Ther. Sci.* 27, 759–762. doi: 10.1589/jpts.27.759

Thibaut, A., Chatelle, C., Ziegler, E., Bruno, M., Laureys, S., and Gosseries, O. (2013). Spasticity after stroke: Physiology, assessment and treatment. *Brain Inj.* 27, 1093–1105.

Sankaranarayan, H., Gupta, A., Khanna, M., Taly, A. B., and Thennarasu, K. (2016). Role of ankle foot orthosis in improving locomotion and functional recovery in patients with stroke: A prospective rehabilitation study. *J. Neurosci. Rural Pract.* 7, 544–549. doi: 10.4103/0976-3147.185507

Paula, G. V., Silva, T. R., Souza, J. T., Luvizutto, G. J., Bazan, S. G., Modolo, G. P., et al. (2019a). Effect of ankle-foot orthosis on functional mobility and dynamic balance of patients after stroke: Study protocol for a randomized controlled clinical trial. *Medicine* 98, e17317. doi: 10.1097/MD.0000000000017317

Baker, J., and Pereira, G. (2016). The efcacy of Botulinum Toxin A for limb spasticity on improving activity restriction and quality of life: a systematic review and meta-analysis using the GRADE approach. *Clin. Rehabil.* 30, 549–558. doi: 10.1177/0269215515593609

Pandyan, A., Gregoric, M., Barnes, M., Wood, D., Wijck, F Van, and Burridge, J. (2005). Spasticity: clinical perceptions, neurological realities and meaningful measurement. *Disabil. Rehabil.* 27, 2–6. doi: 10.1080/09638280400014576

Kaňovsk, P., Elovic, E. P., Hanschmann, A., Pulte, I., Althaus, M., Hiersemenzel, R., et al. (2021). Duration of treatment effect using incobotulinumtoxina for upper-limb spasticity: a post-hoc analysis. *Front. Neurol.* 11, 1887–1895. doi: 10.3389/fneur.2020.615706

Marciniak, C., McAllister, P., Walker, H., Brashear, A., Edgley, S., Deltombe, T., et al. (2019). Efficacy and safety of abobotulinumtoxina (dysport) for the treatment of hemiparesis in adults with upper limb spasticity previously treated with botulinum toxin: Subanalysis from a phase 3 randomized controlled trial. *PMR* 9, 1181–1190. doi: 10.1016/j.pmrj.2017.06.007

Bensmail, D., Wissel, J., Laffont, I., Simon, O., Scheschonka, A., Flatau-Baqué, B., et al. (2021). Efficacy of incobotulinumtoxinA for the treatment of adult lower-limb post-stroke spasticity, including pes equinovarus. *Ann. Phys. Rehabil. Med.* 64:101376. doi: 10.1016/j.rehab.2020.03.005

Santamato, A., Cinone, N., Panza, F., Letizia, S., Santoro, L., and Lozupone, M. (2019). Botulinum toxin type a for the treatment of lower limb spasticity after Stroke. *Springer Nat. Switzerl. AG* 79, 143–160.

Li, J., Zhu, X., and Aao, J. (2015). Guidelines for the treatment of adult limb spasm with botulinum toxin. *J. Chin. Med.* 30, 80–110.

Yeung, L., Ockenfeld, C., Pang, M., Wai, H., Soo, O., Li, S., et al. (2018). Randomized controlled trial of robot-assisted gait training with dorsiflexion assistance on chronic stroke patients wearing ankle-foot-orthosis. *J. Neuro.Eng. Rehabil.* 15:51. doi: 10.1186/s12984-018-0394-7

Dong, K., Meng, S., Guo, Z., Zhang, R., Xu, P., Yuan, E., et al. (2021). The Effects of transcranial direct current stimulation on balance and gait in stroke patients: A Systematic Review and Meta-Analysis. *Front. Neurol.* 12:650925. doi: 10.3389/fneur.2021.650925

Araujo, J., Darcis, J., and Tomas, A. (2018). Tendência de mortalidade por acidente vascular encefálico na cidade de maringá, paraná, entre os anos de 2005 a 2015. *Int. J. Cardiovasc. Sci.* 31, 56–62.

Tyson, S., and Kent, R. (2013). Effects of na ankle-foot orthosis on balance and walking after stroke: a systematic review and pooled meta-analysis. *Arch. Phys. Med. Rehabil.* 9, 1377–1385. doi: 10.1016/j.apmr.2012.12.025

Gracies, J., Esquenazi, A., Brashear, A., Banach, M., Kocer, S., Jech, R., et al. (2017). Efficacy and safety of abobotulinumtoxinA in spastic lower limb: randomized trial and extension. *Neurology* 89, 2245–2253.

Fietzek, U. M., Kossmehl, P., Schelosky, L., Ebersbach, G., and Wissel, J. (2014). Early botulinum toxin treatment for spastic pes equinovarus a randomized double-blind placebo-controlled study. European journal of neurology the official journal of the european federation of neurological societies, 2014. *Eur. J. Neurol.* 21, 1089–1095. doi: 10.1111/ene.12381

Wissel, J., Bensmail, D., Ferreira, J. J., Molteni, F., Satkunam, L., Moraleda, S., et al. (2017). Safety and efficacy of incobotulinumtoxin A doses up to 800 U in limb spasticity: The TOWER study. *Neurology* 88:1321. doi: 10.1212/WNL.0000000000003789

Rousseaux, M., Daveluy, W., Kozlowski, O., and Allart, E. (2014). Onabotulinumtoxin-A injection for disabling lower limb fexion in hemiplegic patients. *Neuro Rehabil.* 35, 2–30. doi: 10.3233/NRE-141093

Wu, T., Li, J., Song, H., and Dong, Y. (2016). Efectiveness of botulinum toxin for lower limbs spasticity after stroke: a systematic review and meta-analysis. *Top Stroke Rehabil.* 23, 217–223. doi: 10.1080/10749357.2016.1139294

Gracies, J., Brashear, A., Jech, R., McAllister, P., Banach, M., Valkovic, P., et al. (2015). Safety and efficacy of abobotulinumtoxinA for hemiparesis in adults with upper limb spasticity after stroke or traumatic brain injury: a double-blind randomised controlled trial. *Lancet Neurol* 14, 992–1001. doi: 10.1016/S1474-4422(15)00216-1

Ausborn, J., Snyder, A. C., Shevtsova, N. A., Rybak, I. A., and Rubin, J. E. (2018). State-dependent rhythmogenesis and frequency control in a half-center locomotor CPG. *J. Neurophysiol.* 119, 96–117. doi: 10.1152/jn.00550.2017

Ferreira, L. A., Neto, H. P., Grecco, L. A., Christovão, T. C., Duarte, N. A., Lazzari, R. D., et al. (2013). Effect of ankle-foot orthosis on gait velocity and cadence of stroke patients: a systematic review. *J. Phys. Ther. Sci.* 25, 1503–1508. doi: 10.1589/jpts.25.1503

Ibuki, A., Bach, T., Rogers, D., and Bernhardt, J. (2010). An investigation of the neurophysiologic effect of tone-reducing AFOs on reflex excitability in subjects

with spasticity following stroke while standing. *Prosthet. Orthot. Int.* 34, 154–165. doi: 10.3109/03093641003649405

Paula, G. V., Silva, T. R., Souza, J. T., Luvizutto, G. J., Bazan, S. G., Modolo, G. P., et al. (2019b). Effect of ankle-foot orthosis on functional mobility and dynamic balance of patients after stroke: Study protocol for a randomized controlled clinical trial. *Medicine* 98, e17317. doi: 10.1097/MD.0000000000017317

Yu, H. (2021). Observation of the therapeutic effect of correcting foot varus on improving knee hyperextension and gait in patients after stroke. *Curr. Neurovasc. Res.* 18, 314–317. doi: 10.2174/1567202618666210923150711

Yu, H., Wang, Z., Liu, C., Dai, P., Lan, Y., and Xu, G. (2021). Effect of cognitive function on balance and posture control after stroke. *Neural Plasticity* 10:6636999. doi: 10.1155/2021/6636999

frontiers | Frontiers in Neuroscience

TYPE Original Research
PUBLISHED 10 February 2023
DOI 10.3389/fnins.2023.1118395



OPEN ACCESS

EDITED BY
Jie Jia,
Fudan University, China

REVIEWED BY
Qiuyou Xie,
Southern Medical University, China
Liudmila Legostaeva,
Research Center of Neurology, Russia

*CORRESPONDENCE
Yu Gong
✉ gongyu@whu.edu.cn
Weijing Liao
✉ weijingliao@whu.edu.cn

†These authors have contributed equally to this work and share first authorship

SPECIALTY SECTION
This article was submitted to Translational Neuroscience, a section of the journal Frontiers in Neuroscience

RECEIVED 07 December 2022
ACCEPTED 30 January 2023
PUBLISHED 10 February 2023

CITATION
Chen H, Miao G, Wang S, Zheng J, Zhang X, Lin J, Hao C, Huang H, Jiang T, Gong Y and Liao W (2023) Disturbed functional connectivity and topological properties of the frontal lobe in minimally conscious state based on resting-state fNIRS. *Front. Neurosci.* 17:1118395. doi: 10.3389/fnins.2023.1118395



# Disturbed functional connectivity and topological properties of the frontal lobe in minimally conscious state based on resting-state fNIRS

Hui Chen†, Guofu Miao†, Sirui Wang, Jun Zheng, Xin Zhang, Junbin Lin, Chizi Hao, Hailong Huang, Ting Jiang, Yu Gong* and Weijing Liao*

Department of Rehabilitation Medicine, Zhongnan Hospital of Wuhan University, Wuhan, Hubei, China

**Background:** Patients in minimally conscious state (MCS) exist measurable evidence of consciousness. The frontal lobe is a crucial part of the brain that encodes abstract information and is closely related to the conscious state. We hypothesized that the disturbance of the frontal functional network exists in MCS patients.

**Methods:** We collected the resting-state functional near-infrared spectroscopy (fNIRS) data of fifteen MCS patients and sixteen age- and gender-matched healthy controls (HC). The Coma Recovery Scale-Revised (CRS-R) scale of MCS patients was also composed. The topology of the frontal functional network was analyzed in two groups.

**Results:** Compared with HC, the MCS patients showed widely disrupted functional connectivity in the frontal lobe, especially in the frontopolar area and right dorsolateral prefrontal cortex. Moreover, the MCS patients displayed lower clustering coefficient, global efficiency, local efficiency, and higher characteristic path length. In addition, the nodal clustering coefficient and nodal local efficiency in the left frontopolar area and right dorsolateral prefrontal cortex were significantly reduced in MCS patients. Furthermore, the nodal clustering coefficient and nodal local efficiency in the right dorsolateral prefrontal cortex were positively correlated to auditory subscale scores.

**Conclusion:** This study reveals that MCS patients' frontal functional network is synergistically dysfunctional. And the balance between information separation and integration in the frontal lobe is broken, especially the local information transmission in the prefrontal cortex. These findings help us to understand the pathological mechanism of MCS patients better.

KEYWORDS

**minimally conscious state, functional near-infrared spectroscopy, frontal lobe, functional connectivity, graph theory**

# 1. Introduction

Disorders of consciousness (DOC) caused by acquired severe brain injury from various causes are several states that include coma, unresponsive wakefulness syndrome (UWS), and minimally conscious state (MCS) (Owen, 2019). Prolonged DOC is defined as losing consciousness for more than 28 days (Kondziella et al., 2020). The survival time of patients with prolonged DOC is generally 2–5 years (Hirschberg and Giacino, 2011). It is called MCS when the patient appears to have any conscious perception of the surrounding environment with repetitive behavior, such as visual tracking or gazing at targets, pain localization, etc. (Giacino et al., 2002). Compared to UWS, patients in MCS have developed definite signs of consciousness and may have better aware potential (Song et al., 2020). The MCS may be the final state of consciousness in some DOC patients, or it may be a transitional state to further clear consciousness. Patients in MCS are bedridden for a long time and require specialized care, which increases the financial burden on the family (Owen, 2008). However, the neuropathological mechanism of MCS patients is still unclear.

As a relatively new imaging method, functional near-infrared spectroscopy (fNIRS) measures the changed concentration of oxyhemoglobin (HbO) and deoxyhemoglobin (HbR) in the cerebral cortex by emitting near-infrared light (Boas et al., 2014; Rupawala et al., 2018). Compared with functional magnetic resonance imaging (fMRI) and other functional neuroimaging technology, fNIRS is more portable, easier to wear, has lower detection cost, and is safer to scan in a natural environment for MCS patients in bed. Currently, fNIRS can monitor real-time physiological responses to quantify the stimulation parameters for different neuroregulatory techniques. Zhang et al. (2018) found increased local cerebral blood flow in the prefrontal cortex during spinal cord stimulation in patients with prolonged DOC. Moreover, some studies have monitored the residual consciousness of DOC patients while performing mental arithmetic (Kurz et al., 2018) and motor imagery tasks based on fNIRS (Molteni et al., 2013). However, judging whether a DOC patient completes the task paradigm is difficult because their attention and awareness may fluctuate over time (Abdalmalak et al., 2021). Resting-state fNIRS is measured when subjects are quiet, relaxed, and not performing specific cognitive tasks, which can reflect the cooperative and spontaneous activity between different brain regions. Compared with task state, resting-state data acquisition is easier to implement, and the results are more stable.

Functional connectivity refers to the temporal correlation of neuronal activity, and the strength of functional connectivity is measured by the correlation coefficient (Fingelkurts et al., 2005). Studies found that the functional connectivity strength in the resting-state brain networks decreased in patients with DOC compared with healthy people (Sinitsyn et al., 2018; Martinez et al., 2020). Another study found that the default mode network, frontoparietal network, sensorimotor network, and other resting-state functional networks of patients with DOC were extensively disrupted (Demertzi et al., 2015). Many studies consider the human brain as a complex brain network, and the brain network is a set of nodes and edges (functional connectivity between brain regions) (Bullmore and Sporns, 2009; Avena-Koenigsberger et al., 2017). The brain network often exhibits the balance of spontaneous integration and separation in function, which can be quantified by graph-theoretic topological analysis based on resting-state data (Bullmore and Sporns, 2012). Some studies found that the alterations of the brain's network topology tended to occur in many disorders, such as depressive disorder (Zhang et al., 2011), Alzheimer's disease (Stam et al., 2007), and post-stroke cognitive impairment (Miao et al., 2022).

To date, a few studies have used functional neuroimaging technology to explore the topological properties of patients with DOC and have identified changes in the frontal regions. Liu et al. (2023) found that the intraconnections within Brodmann area 10 and interhemispheric connections between Brodmann area 10 and Brodmann area 46 were helpful in distinguishing between MCS and UWS based on fNIRS study. One fMRI study found that the patients in MCS had increased nodal degree in the left superior frontal and decreased in the right orbital frontal (Crone et al., 2014). Another electroencephalography (EEG) study found that UWS patients showed decreased nodal degree and betweenness centrality in the frontal regions in β1 band (13–20 Hz) compared to MCS patients (Cacciola et al., 2019). The frontal lobe receives extensive neural projection connections from other cortical and subcortical regions. The complex pattern of fiber connections determines the functional complexity of the frontal lobe, a key brain region associated with many higher cognitive functions (Cusack et al., 2016). Several leading theories of consciousness suggest that the prefrontal cortex is inextricably linked to consciousness (Seth and Bayne, 2022), like higher-order theories (HOTs) (Cleeremans et al., 2020; Fleming, 2020), and global workspace theories (Dehaene and Changeux, 2011; Mashour et al., 2020). However, no studies have specifically explored the topological properties of the frontal lobe in MCS patients. We still do not know how the consciousness impairment caused by pathological injury affects the frontal network topology.

In this study, we hypothesized the disturbance in the functional connectivity and topology of the frontal lobe in MCS patients. We used complex network analysis to investigate the spontaneous integration and separation of information in the frontal lobe of MCS patients based on resting-state fNIRS data. Moreover, we explored the potential correlation between network topology that changed significantly between-group differences and the Coma Recovery Scale-Revised (CRS-R) scores.

# 2. Materials and methods

## 2.1. Participants

Sixteen patients in MCS and sixteen age- and gender-matched healthy controls (HC) were included in this study. Among them, sixteen HC were recruited from the community, and all the MCS patients were from the Department of Rehabilitation in Zhongnan Hospital of Wuhan University between November 2021 and June 2022. All patients were diagnosed as MCS based on continuously repeated (≥5) CRS-R assessed by a professional therapist (Giacino et al., 2004). The exclusion criteria were as follows, (1) The course of disease <28 days (Giacino et al., 2018); (2) Skull defect or after cranioplasty; and (3) History of psychiatric or neurological illness, such as Alzheimer's disease, Parkinson or depression. This study was conducted in Zhongnan Hospital of Wuhan University, approved by the Medical Research Ethics Committee and Institutional Review

Board of Zhongnan Hospital (2021126), and written informed consent was signed by the legal surrogate of each subject.

The CRS-R scale consists of six functional subscales addressing auditory, visual, motor, oro-motor, communication, and arousal level, totaling 23 hierarchically organized items (Giacino et al., 2004; Di et al., 2017). In addition to the total score, the single score of this scale was important to diagnose DOC patients.

The demographic and clinical data of all MCS patients are summarized in **Table 1**.

## 2.2. Data acquisition

The data were collected by a multichannel continuous wave near-infrared optical imaging system (BS-3000, Wuhan Znion Medical Technology Co., Wuhan, China). This system can emit two wavelengths of 690 and 830 nm at each source optic fiber with a sampling rate of 20 Hz and measure the changes in concentration of HbO, and HbR through optical attenuation. To normalize the fNIRS channels, we applied a 3D digitizer to record the exact spatial coordinates of 4 reference points (Nz, Cz, AL, and RL) and 32 probes (16 sources and 16 detectors with 3 cm source-detector-distance). Then the 53 channels were converted to an estimated Montreal Neurological Institute (MNI) space (Singh et al., 2005) by NIRS-SPM (Ye et al., 2009). Based on the Brodmann probabilistic atlas, all 53 channels were divided into the following five cortical regions: Premotor and supplementary motor area (PreM and SMA), frontal eye fields (FEF), Broca's area, frontopolar area (FPA), and dorsolateral prefrontal cortex (DLPFC) (**Figure 1**). The lowest row of probes was aligned along the subject's eyebrow arch, and the middle row of probes was parallel to the midsagittal line of the nasal root-occipital tuberosity. The subjects underwent a 5-min resting-state session of fNIRS measurement in a quiet evaluation room. They were required to keep still and relax the mind with their eyes opened (Yang and Hong, 2021).

## 2.3. Data pre-processing

Data processing was performed by Homer2 toolbox in the MATLAB environment (Huppert et al., 2009). Pre-processing procedures were as following: (1) Converting raw data to the optical density (OD) (Scholkmann and Wolf, 2013); (2) Trimming the first and the last 60 s; (3) Correcting motion artifacts by spline interpolation algorithm (Scholkmann et al., 2010); (4) 0.01–0.1 Hz bandpass filtering to minimize the physiological interference and produce the data with the best signal-to-noise ratio, such as blood pressure (Mayer) waves (∼0.1 Hz), respiration (∼0.4 Hz) and heart pulsation (1∼1.5 Hz) (White et al., 2009; Mesquita et al., 2010); and (5) Converting optical density to relative HbO/HbR concentration through the modified Beer-Lambert law.

Only HbO signals were analyzed in this study since they have a better signal-to-noise ratio than HBR and are more sensitive to monitoring regional cerebral blood flow (Fu et al., 2014).

## 2.4. Functional connectivity calculation and network construction

The three midline channels (channels 25, 28, and 29) were removed from the analysis because they did not belong to either side of the brain. The time series' correlation coefficients (r) for each pair of nodes were calculated using Pearson correlation analysis. Fisher's r-to-z transformation was used to normalize the correlation coefficients to *z*-values. The nodes were defined as channels, and the edges were defined as correlation coefficients between pairs of nodes. Thus, a 50 × 50 functional connectivity matrix was calculated for each subject. Our network analysis was confined to positive correlations. Negative correlation coefficients were set as zero because the biological explanation of negative correlations was ambiguous and equivocal in the correlation matrix (Murphy et al., 2009;

TABLE 1 Demographic and clinical data of MCS patients.

| Index | Patient | Gender/age (years) | Etiology | Duration (months) | CRS-R |
|---|---|---|---|---|---|
| 1 | MCS- | F/49 | Traumatic brain injury | 7 | 10 (1/1/5/1/0/2) |
| 2 | MCS- | F/79 | Intracerebral infarction | 1.5 | 13 (1/3/5/2/0/2) |
| 3 | MCS- | M/31 | Traumatic brain injury | 12 | 11 (2/3/2/2/0/2) |
| 4 | MCS + | M/70 | Intracerebral infarction | 1 | 15 (3/1/5/3/1/2) |
| 5 | MCS + | M/53 | Intracerebral hemorrhage | 1 | 11 (3/1/5/1/0/1) |
| 6 | MCS- | F/85 | Traumatic brain injury | 1.5 | 9 (2/3/3/0/0/1) |
| 7 | MCS- | F/69 | Intracerebral hemorrhage | 1.5 | 8 (1/3/2/1/0/1) |
| 8 | MCS- | M/70 | Intracerebral infarction | 1 | 8 (2/3/2/1/0/1) |
| 9 | MCS- | M/53 | Traumatic brain injury | 11 | 12 (2/3/5/1/0/1) |
| 10 | MCS- | M/86 | Traumatic brain injury | 3.5 | 4 (0/0/3/0/0/1) |
| 11 | MCS- | F/82 | Intracerebral hemorrhage | 1 | 9 (1/1/3/2/0/2) |
| 12 | MCS- | M/65 | Intracerebral hemorrhage | 1 | 4 (0/0/3/0/0/1) |
| 13 | MCS- | F/54 | Intracerebral hemorrhage | 1 | 10 (1/3/5/0/0/1) |
| 14 | MCS- | M/83 | Intracerebral infarction | 3 | 11 (0/3/5/2/0/1) |
| 15 | MCS- | F/84 | Intracerebral infarction | 1.5 | 8 (0/3/2/2/0/1) |

MCS, minimally conscious state; CRS-R, coma recovery scale-revised.

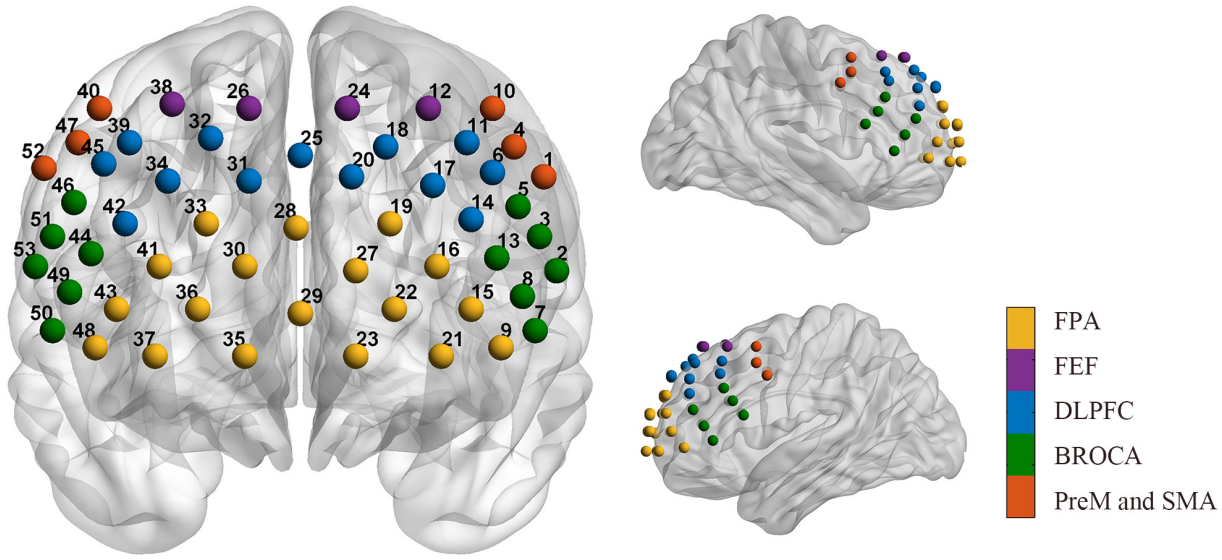


FIGURE 1
Arrangement of the 53 channels covering the frontal lobe. Including the PreM and SMA (red, Premotor, and supplementary motor area), FEF (purple, frontal eye fields), BROCA (green, Broca's area), FPA (yellow, frontopolar area), and DLPFC (blue, dorsolateral prefrontal cortex).

Carbonell et al., 2014). Before using graph theory to quantify the network topology, we applied thresholds to retain only connections above a set threshold (0.4–0.9, 0.05 interval).

Since the 50 channels can be divided into ten regions of interest (ROIs) according to the Brodmann probabilistic atlas, we calculated the average nodal topological properties for all channels in each ROI, including the left PreM and SMA, left Broca's area, left FEF, left FPA, left DLPFC, right PreM and SMA, right Broca's area, right FEF, right FPA, right DLPFC.

## 2.5. Network analysis

The topological properties of functional network can be quantified by graph theoretic methods to reflect the functional integration and separation of the brain network, including global and nodal network metrics. All network metrics were computed in the GRETNA toolbox (Wang et al., 2015). We calculated several typical global topological properties: small-worldness (σ), clustering coefficient (Cp), characteristic path length (Lp), global efficiency (Eg), and local efficiency (Eloc). The node topological properties included nodal clustering coefficient (NCp) and nodal local efficiency (NLe). NCp refers to the likelihood that its neighbor nodes are also connected, and the Cp is defined as the average of the cluster coefficients of all nodes in the network. NLe refers to the communication efficiency between adjacent nodes after a node is removed, and the Eloc is the average of all NLe. Lp is the average of the shortest path lengths of any pair of nodes in the network. The Eg of a network is the inverse of the harmonic mean of the shortest path between any two nodes. The small-worldness of the network means that the network has a shorter Lp and greater Cp (Watts and Strogatz, 1998).

TABLE 2 Baseline of demographic and clinical data.

| Characteristics | HC | MCS | *p*-value |
|---|---|---|---|
| Gender (male/female) | 9/7 | 8/7 | $p > 0.05$ |
| Age (years) | 58.63 ± 14.51 | 67.53 ± 16.48 | $p > 0.05$ |
| Duration (months) | – | 3.23 ± 3.72 | – |
| CRS-R scores | – | 9.60 ± 2.95 | – |

HC, healthy controls; MCS, minimally conscious state; CRS-R, coma recovery scale-revised.

## 2.6. Statistical analysis

All statistical analyses were performed by SPSS 23.0. We used mean ± standard deviation to represent the numerical variables and Shapiro-Wilk (S-W) test to analyze the normal distribution. The chi-square test examined gender differences between groups. Two-sample *t*-tests were used to compare the group differences in age and the area under the curve (AUC) of global topological properties. Two-sample *t*-tests with false discovery rate (FDR) correction were performed for multiple comparisons in functional connectivity and the AUC of nodal topological properties (Storey, 2002). Pearson correlation analysis was performed between network metrics that changed significantly between-group differences and the CRS-R scale scores. $P < 0.05$ means a statistically significant difference.

# 3. Results

## 3.1. Demographic and clinical results

Fifteen MCS patients met the inclusion criteria, and one patient was excluded due to head movement. The clinical data of the recruited MCS patients are shown in Table 1. Fifteen MCS patients (eight males, age 67.53 ± 16.48 years) and sixteen HC (nine males, age 58.63 ± 14.51 years) were finally included in this study. There were no significant between-group differences in age and gender between HC and MCS groups ($p > 0.05$) (Table 2).

## 3.2. Between-group differences in functional connectivity

Figures 2A, B show the group-averaged functional connectivity metrics of HC and MCS groups. It can be observed that the averaged correlation coefficient was significantly lower in the MCS group. Among them, 118 connections were still significantly different ($p < 0.01$, FDR correction), and most of these connections were located in the channels of the frontopolar area and DLPFC (Figure 2C).

Figure 3A shows the number of edges at different thresholds (0.4–0.9, 0.05 interval) for the HC and MCS groups (Supplementary Tables 1, 2). The average number of edges at different thresholds was taken as each subject's total number of edges, and the total number of edges in the MCS group was significantly less than in the HC group (Figure 3B).

## 3.3. Between-group differences in network topological properties

For global topological properties, the AUC of Cp, Eg, and Eloc in the MCS group was significantly lower than in the HC group, and the AUC of Lp in the MCS group was higher than in the HC group. There was no difference in the AUC of σ (Figure 4 and Supplementary Table 3).

For nodal topological properties, the MCS group showed lower NCp and NLe after FDR correction than the HC group. Lower NCp were located in L_FPA ($p = 0.020$), R_DLPFC ($p = 0.047$), R_FEF ($p = 0.035$) (Table 3 and Supplementary Table 4), and lower NLe were located in L_FPA ($p = 0.020$), R_DLPFC ($p = 0.035$) (Table 4 and Supplementary Table 5).

## 3.4. Correlation between topological properties and CRS-R scale

Correlation analysis was performed between the topological properties with group differences and the CRS-R scale scores of the MCS group. No significant correlation was found between the global topological properties and the total and subscale score of CRS-R. Moreover, we found that two nodal topological properties of right DLPFC, averaged NCp ($r = 0.742$, $p = 0.002$) and NLe ($r = 0.714$, $p = 0.003$), was positively correlated with the auditory subscale scores (Figure 5).

# 4. Discussion

This study explored the topological changes of the functional network in the frontal lobe of MCS patients based on resting-state fNIRS. The study results were as follows: (1) MCS patients had significantly reduced functional connectivity in the frontal lobe, especially in the frontopolar area and DLPFC. (2) MCS patients displayed lower Cp, Eg, Eloc, and higher Lp than the HC group, revealing that frontal network topology changed with the conscious

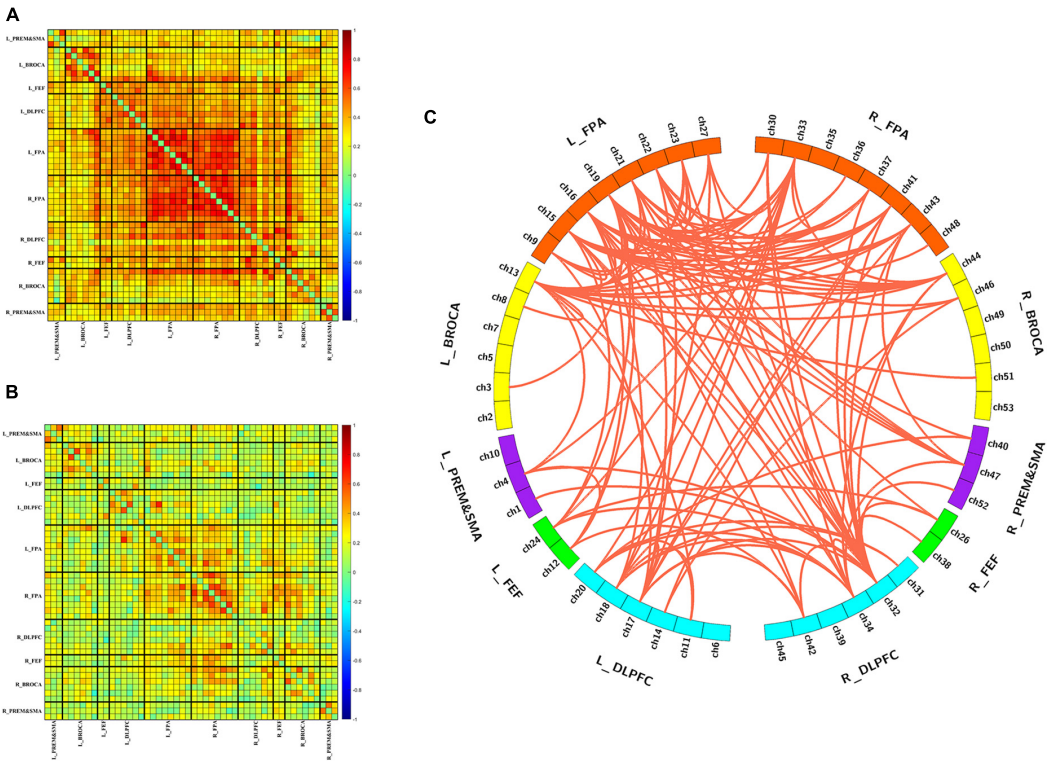


FIGURE 2
Differences in functional connectivity between HC and MCS groups. **(A)** Group-averaged functional connectivity metrics in HC; **(B)** group-averaged functional connectivity metrics in MCS; **(C)** 118 functional connectivity that changed significantly between-group differences. L, left; R, right; PreM and SMA, premotor and supplementary motor area; BROCA, Broca's area; FEF, frontal eye fields; DLPFC, dorsolateral prefrontal cortex; FPA, frontopolar area.

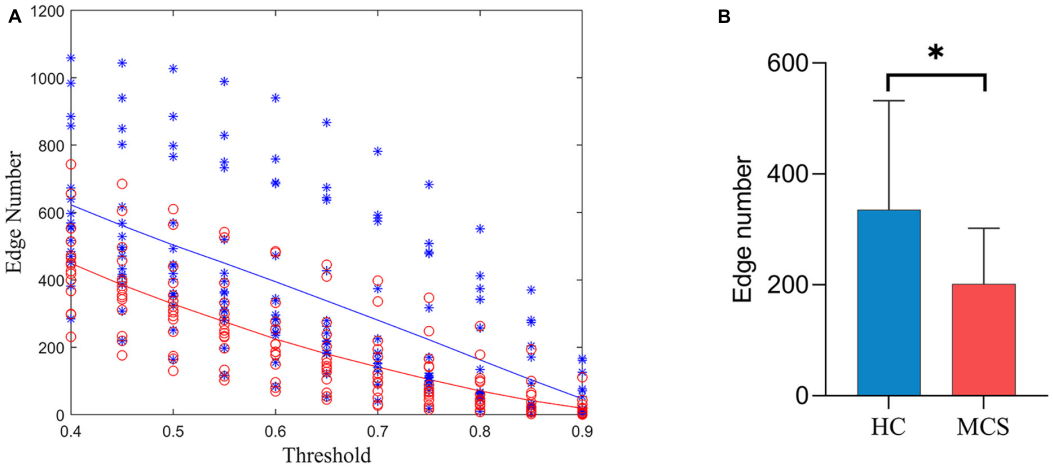


FIGURE 3
Differences in the number of edges between HC and MCS groups. **(A)** Scatter plot: distribution of edges with different thresholds (0.4–0.9, 0.05 interval). Functional connectivity strength larger than the threshold was defined as edge. HC (blue), MCS (red); **(B)** group differences in the total number of edges. HC, healthy controls; MCS, minimally conscious state. *$p < 0.05$.

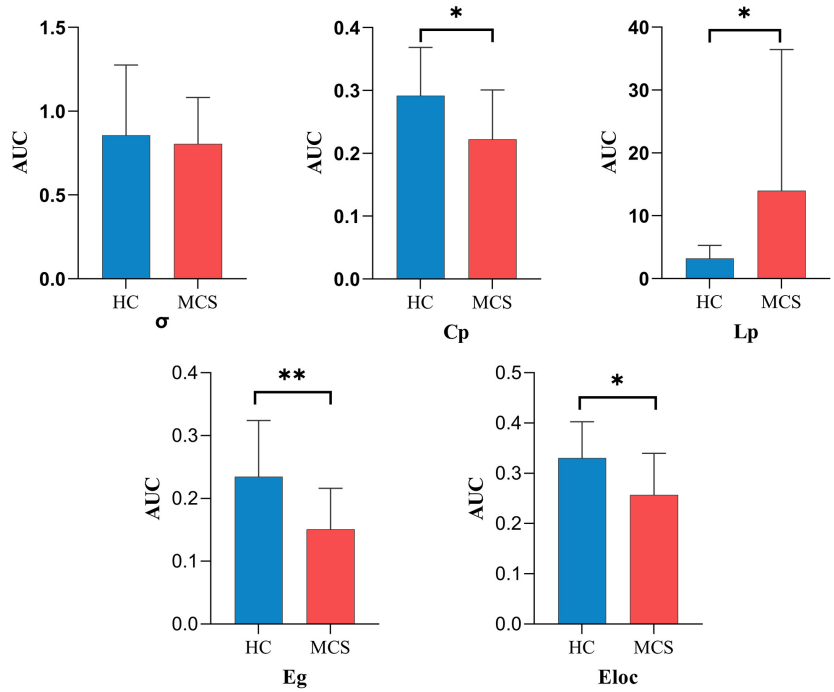


FIGURE 4
The global topological properties between HC and MCS groups. AUC, area under the curve; σ, small-worldness; Cp, clustering coefficient; Lp, characteristic path length; Eg, global efficiency; Eloc, local efficiency; HC, healthy controls; MCS, minimally conscious state. *$p < 0.05$, **$p < 0.01$.

state. (3) NCp and NLe all showed lower in different ROIs, and nodal topological properties in the right DLPFC were correlated with the auditory subscale scores.

## 4.1. Widely disrupted functional connectivity

In this study, we found that resting-state functional connectivity of the whole frontal lobe had severely reduced in MCS patients. Functional connectivity refers to the temporal correlation of neural activity between different brain regions, reflecting the synergistic cooperation of neural activity between brain regions to integrate information (Fingelkurts et al., 2005; Geng et al., 2017). In particular, weakened functional connectivity occurred mainly in the frontopolar area and DLPFC. The frontopolar area and DLPFC are important components of the prefrontal cortex. As the brain's core, the prefrontal cortex receives and integrates information from many cortical and subcortical areas and participates in conscious perception and cognitive processing (Block, 2020). According to the claim in HOTs theory of consciousness, mental states are conscious by being the target of specific kinds of meta-representation

TABLE 3 Comparison of NCp between HC and MCS groups.

| Regions | NCp | | *t*-value | *p*-value (FDR correction) |
|---|---|---|---|---|
| | HC | MCS | | |
| L_FPA | 0.322 ± 0.080 | 0.225 ± 0.080 | 3.349 | 0.020 |
| R_DLPFC | 0.288 ± 0.098 | 0.197 ± 0.097 | 2.605 | 0.047 |
| R_FEF | 0.319 ± 0.085 | 0.219 ± 0.107 | 2.888 | 0.035 |

NCp, nodal clustering coefficient; HC, healthy controls; MCS, minimally conscious state; L_FPA, left frontopolar area; R_DLPFC, right dorsolateral prefrontal cortex; R_FEF, right frontal eye field; FDR, false discovery rate.

TABLE 4 Comparison of NLe between HC and MCS groups.

| Regions | NLe | | *t*-value | *p*-value (FDR correction) |
|---|---|---|---|---|
| | HC | MCS | | |
| L_FPA | 0.369 ± 0.071 | 0.264 ± 0.087 | 3.677 | 0.020 |
| R_DLPFC | 0.325 ± 0.099 | 0.224 ± 0.103 | 2.788 | 0.035 |

NLe, nodal local efficiency; HC, healthy controls; MCS, minimally conscious state; L_FPA, left frontopolar area; R_DLPFC, right dorsolateral prefrontal cortex; FDR, false discovery rate.

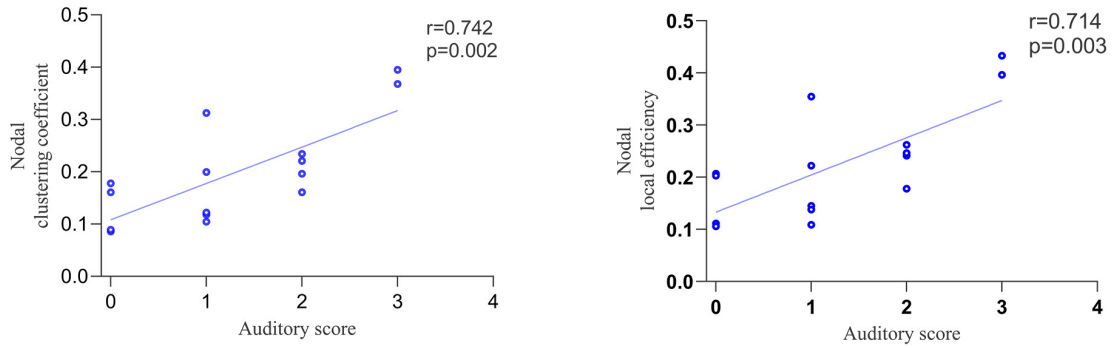


FIGURE 5
The correlation between nodal topological properties in right dorsolateral prefrontal cortex (DLPFC) and auditory subscale scores.

(Seth and Bayne, 2022). Specifically, lower-order representations of auditory signals in posterior cortex would support conscious auditory perception when targeted by the right kind of higher-order meta-representation (especially the prefrontal cortex) (Lau and Rosenthal, 2011; Fleming, 2020). Demertzi et al. also found that functional connectivity was widely declined in DOC patients in the default mode network, frontoparietal network, sensorimotor network, and other resting-state functional networks (Demertzi et al., 2014, 2015). Our study implies a widely disrupted functional connectivity in the frontal lobe of MCS patients, especially in the frontopolar area and DLPFC, further confirming that the changes in the functional connectivity of the frontal lobe may be associated with the altered conscious state (Demertzi et al., 2015; Liu et al., 2017; Moriya and Sakatani, 2018). The functional cooperation of multiple brain regions in the prefrontal cortex played a role in consciousness. Widely disrupted prefrontal functional connectivity means that the prefrontal functional network is synergistically dysfunctional, and the efficiency of conscious processing naturally decreases.

## 4.2. The damage of global topological properties

The results showed that the MCS patients had lower Cp, Eg, Eloc, and higher Lp in the frontal lobe than HC. Cp and Eloc measure the local information transmission capability of the network and represent the functional separation, while Lp and Eg measure the global information transmission capability of the network and represent the functional integration (Bassett and Bullmore, 2017). Weng et al. (2017) found the same changes in Cp and Lp with our results in the whole brain structural network of patients with DOC. Changes in these topological properties in MCS patients not only imply a reduction in global and local information transmission efficiency but also indicate the disturbance in the optimal balance configuration of functional integration and separation in the frontal lobe.

The small-worldness did not show significant differences in MCS and HC groups, which was consistent with previous studies (Tan et al., 2019). The Small-world network can be quantified as shorter Lp and larger Cp. In other words, the Lp and Cp of the small-world network lie between the regular network and the random network (Bassett and Bullmore, 2017). It is found that the brain network of healthy adults satisfies the characteristics of the small-world network, which can consume low-cost neuron resources and efficiently complete information transmission due to the brain function in a dynamic balance between network separation and integration (Bassett and Bullmore, 2006; Samu et al., 2014). This dynamic balance has the inherent ability to support different levels of consciousness and cognitive functions (Wang et al., 2021). A small-world network is an economic network that achieves efficient information transmission with the lowest wiring cost (Samu et al., 2014). Small-worldness is a comprehensive topological property to

measure the brain's functional network. Although there was no significant difference in small-worldness between HC and MCS groups, changes in other network topological properties (Cp, Lp, Eg, and Eloc) indicated that the frontal network configuration of MCS patients tended to have a lower capacity for functional integration and separation. This network state deviates from the optimal critical state, which is not conducive to conscious processing and may consume more neuronal resources. The altered topology caused by pathological injury leads to increased wiring costs and metabolic demands in the frontal lobe. Thus, the frontal network of MCS patients does not belong to the economic network.

### 4.3. Between-group differences in nodal topology properties

We found reduced averaged NCp and averaged NLe of the prefrontal cortex in MCS patients (left frontopolar area and right DLPFC). Previous study had found that the MCS patients showed decreased NCp in the posterior cingulate cortex and right insula cortex and decreased NLe in the right precuneus (Crone et al., 2014). Our findings supplement the existing results and further demonstrate that the activation of the frontoparietal network is related to the conscious state (Crone et al., 2014; Cavinato et al., 2015). One fMRI study showed that higher-level control networks (mainly referring to the frontal and parietal cortex) begin to encode predictive information long before the individual has made a conscious decision (Soon et al., 2008). The prefrontal cortex is also associated with storing conscious decisions and strategy shifts following negative feedback (Soon et al., 2008).

In addition, we found that two nodal topological properties of the right DLPFC, averaged NCp and NLe, were positively correlated with auditory subscale scores. The evaluation of the auditory subscale mainly reflects auditory perception, language comprehension, and executive control of DOC patients (Giacino et al., 2018). The dorsal pathway projects from the primary auditory cortex through the temporal plane across the parietal cortex to the DLPFC, supporting the transmission of auditory perception-motor signals (Hertrich et al., 2021). The DLPFC is involved in auditory information attention, evaluation, and working memory processing (Nakai et al., 2005; Rämä and Courtney, 2005; Chen et al., 2008). It is also a core area of the control network, which is closely related to executive control function (Panikratova et al., 2020). Witt et al. (2010) found that patients with mild traumatic brain injury had significantly reduced activity in the right DLPFC during auditory oddball tasks. NCp and NLe reflect local information transmission capacity. The results of correlation analysis showed that the worse auditory functions, the less efficient local information transmission in the right DLPFC.

## 5. Limitations

Several limitations of this study should be considered. First, the sample size is too small. We should recruit more samples to verify the stability and repeatability of the data. When the sample size is large enough, the MCS group can be subdivided into MCS- and MCS + groups to explore the functional network of different levels of consciousness, which may lead to more accurate results. Secondly, the etiology of consciousness impairment may be a crucial factor in the disturbance of the functional network. We should group different etiology, such as stroke, hypoxic-ischemic encephalopathy (HIE), traumatic brain injury, intracranial surgery, etc. Finally, this study is a non-longitudinal design, and dynamic follow-up is needed in the future to observe whether the correlation results of this study can be further verified with the improvement of patients' consciousness levels.

## 6. Conclusion

Using resting-state fNIRS to explore the topology of the functional network in the frontal lobe in MCS patients, we found these metrics were widely disrupted in the frontal lobe. Moreover, the functional separation and integration of the frontal network were seriously unbalanced, especially the local information transmission in the prefrontal cortex. We also found that nodal topological properties in the right DLPFC were positively correlated with auditory behavior scores. Our results reveal the disturbance in frontal functional network caused by pathological injury, which may be conducive to understanding the pathological mechanism of MCS patients better.

## Data availability statement

The original contributions presented in this study are included in the article/**Supplementary material**, further inquiries can be directed to the corresponding authors.

## Ethics statement

This study was conducted in Zhongnan Hospital of Wuhan University, approved by the Medical Research Ethics Committee and Institutional Review Board of Zhongnan Hospital (2021126), and written informed consent was signed by the legal surrogate of each patient. The patients/participants provided their written informed consent to participate in this study.

## Author contributions

HC, GM, YG, and WL: study contributions included study design and conception. GM, YG, SW, JZ, XZ, JL, CH, HH, and TJ: data collection. HC and GM: statistical analysis and interpretation of results. All authors contributed to the article and approved the submitted version.

## Funding

This study was supported by the National Key Technology Research and Development Program of China (2018YFC2002300).

## Acknowledgments

We thank Xia Lirong, Zhang Peiwen, and Ren Bin (Wuhan Znion Medical Technology Company) for solving the problems of data analysis in this study.

## Conflict of interest

The authors declare that the research was conducted in the absence of any commercial or financial relationships that could be construed as a potential conflict of interest.

## Publisher's note

All claims expressed in this article are solely those of the authors and do not necessarily represent those of their affiliated organizations, or those of the publisher, the editors and the reviewers. Any product that may be evaluated in this article, or claim that may be made by its manufacturer, is not guaranteed or endorsed by the publisher.

## Supplementary material

The Supplementary Material for this article can be found online at: https://www.frontiersin.org/articles/10.3389/fnins.2023.1118395/full#supplementary-material

## References


Abdalmalak, A., Milej, D., Norton, L., Debicki, D. B., Owen, A. M., and Lawrence, K. S. (2021). The potential role of fnirs in evaluating levels of consciousness. *Front. Hum. Neurosci.* 15:703405. doi: 10.3389/fnhum.2021.703405

Avena-Koenigsberger, A., Misic, B., and Sporns, O. (2017). Communication dynamics in complex brain networks. *Nat. Rev. Neurosci.* 19, 17–33. doi: 10.1038/nrn.2017.149

Bassett, D. S., and Bullmore, E. (2006). Small-world brain networks. *Neurosci.* 12, 512–523. doi: 10.1177/1073858406293182

Bassett, D. S., and Bullmore, E. T. (2017). Small-world brain networks revisited. *Neurosci.* 23, 499–516. doi: 10.1177/1073858416667720

Block, N. (2020). Finessing the bored monkey problem. *Trends Cogn. Sci.* 24, 167–168. doi: 10.1016/j.tics.2019.12.012

Boas, D. A., Elwell, C. E., Ferrari, M., and Taga, G. (2014). Twenty years of functional near-infrared spectroscopy: introduction for the special issue. *Neuroimage* 85, 1–5. doi: 10.1016/j.neuroimage.2013.11.033

Bullmore, E., and Sporns, O. (2009). Complex brain networks: graph theoretical analysis of structural and functional systems. *Nat. Rev. Neurosci.* 10, 186–198. doi: 10.1038/nrn2575

Bullmore, E., and Sporns, O. (2012). The economy of brain network organization. *Nat. Rev. Neurosci.* 13, 336–349. doi: 10.1038/nrn3214

Cacciola, A., Naro, A., Milardi, D., Bramanti, A., Malatacca, L., Spitaleri, M., et al. (2019). Functional brain network topology discriminates between patients with minimally conscious state and unresponsive wakefulness syndrome. *J. Clin. Med.* 8:306. doi: 10.3390/jcm8030306

Carbonell, F., Bellec, P., and Shmuel, A. (2014). Quantification of the impact of a confounding variable on functional connectivity confirms anti-correlated networks in the resting-state. *Neuroimage* 86, 343–353. doi: 10.1016/j.neuroimage.2013.10.013

Cavinato, M., Genna, C., Manganotti, P., Formaggio, E., Storti, S. F., Campostrini, S., et al. (2015). Coherence and consciousness: study of fronto-parietal gamma synchrony in patients with disorders of consciousness. *Brain Topogr.* 28, 570–579. doi: 10.1007/s10548-014-0383-5

Chen, J. L., Penhune, V. B., and Zatorre, R. J. (2008). Moving on time: brain network for auditory-motor synchronization is modulated by rhythm complexity and musical training. *J. Cogn. Neurosci.* 20, 226–239. doi: 10.1162/jocn.2008.20018

Cleeremans, A., Achoui, D., Beauny, A., Keuninckx, L., Martin, J., Muñoz-Moldes, S., et al. (2020). Learning to be conscious. *Trends Cogn. Sci.* 24, 112–123. doi: 10.1016/j.tics.2019.11.011

Crone, J. S., Soddu, A., Höller, Y., Vanhaudenhuyse, A., Schurz, M., Bergmann, J., et al. (2014). Altered network properties of the fronto-parietal network and the thalamus in impaired consciousness. *Neuroimage Clin.* 4, 240–248. doi: 10.1016/j.nicl.2013.12.005

Cusack, R., Ball, G., Smyser, C. D., and Dehaene-Lambertz, G. (2016). A neural window on the emergence of cognition. *Ann. N. Y. Acad. Sci.* 1369, 7–23. doi: 10.1111/nyas.13036

Dehaene, S., and Changeux, J. P. (2011). Experimental and theoretical approaches to conscious processing. *Neuron* 70, 200–227. doi: 10.1016/j.neuron.2011.03.018

Demertzi, A., Antonopoulos, G., Heine, L., Voss, H. U., Crone, J. S., de Los Angeles, C., et al. (2015). Intrinsic functional connectivity differentiates minimally conscious from unresponsive patients. *Brain* 138, 2619–2631. doi: 10.1093/brain/awv169

Demertzi, A., Gómez, F., Crone, J. S., Vanhaudenhuyse, A., Tshibanda, L., Noirhomme, Q., et al. (2014). Multiple fmri system-level baseline connectivity is disrupted in patients with consciousness alterations. *Cortex* 52, 35–46. doi: 10.1016/j.cortex.2013.11.005

Di, H., He, M., Zhang, Y., Cheng, L., Wang, F., Nie, Y., et al. (2017). Chinese translation of the coma recovery scale-revised. *Brain Inj.* 31, 363–365. doi: 10.1080/02699052.2016.1255780

Fingelkurts, A. A., Fingelkurts, A. A., and Kähkönen, S. (2005). Functional connectivity in the brain—is it an elusive concept? *Neurosci. Biobehav. Rev.* 28, 827–836. doi: 10.1016/j.neubiorev.2004.10.009

Fleming, S. M. (2020). Awareness as inference in a higher-order state space. *Neurosci. Conscious.* 2020:niz020. doi: 10.1093/nc/niz020

Fu, G., Mondloch, C. J., Ding, X. P., Short, A., Sun, L., and Lee, K. (2014). The neural correlates of the face attractiveness aftereffect: a functional near-infrared spectroscopy (fnirs) study. *Neuroimage* 85, 363–371. doi: 10.1016/j.neuroimage.2013.04.092

Geng, S., Liu, X., Biswal, B. B., and Niu, H. (2017). Effect of resting-state fnirs scanning duration on functional brain connectivity and graph theory metrics of brain network. *Front. Neurosci.* 11:392. doi: 10.3389/fnins.2017.00392

Giacino, J. T., Ashwal, S., Childs, N., Cranford, R., Jennett, B., Katz, D. I., et al. (2002). The minimally conscious state: definition and diagnostic criteria. *Neurology* 58, 349–353. doi: 10.1212/WNL.58.3.349

Giacino, J. T., Kalmar, K., and Whyte, J. (2004). The jfk coma recovery scale-revised: measurement characteristics and diagnostic utility11no commercial party having a direct financial interest in the results of the research supporting this article has or will confer a benefit upon the authors or upon any organization with which the authors are associated. *Arch. Phys. Med. Rehabil.* 85, 2020–2029. doi: 10.1016/j.apmr.2004.02.033

Giacino, J. T., Katz, D. I., Schiff, N. D., Whyte, J., Ashman, E. J., Ashwal, S., et al. (2018). Practice guideline update recommendations summary: disorders of consciousness. *Neurology* 91, 450–460. doi: 10.1212/WNL.0000000000005926

Hertrich, I., Dietrich, S., Blum, C., and Ackermann, H. (2021). The role of the dorsolateral prefrontal cortex for speech and language processing. *Front. Hum. Neurosci.* 15:645209. doi: 10.3389/fnhum.2021.645209

Hirschberg, R., and Giacino, J. T. (2011). The vegetative and minimally conscious states: diagnosis, prognosis and treatment. *Neurol. Clin.* 29, 773–786. doi: 10.1016/j.ncl.2011.07.009

Huppert, T. J., Diamond, S. G., Franceschini, M. A., and Boas, D. A. (2009). Homer: a review of time-series analysis methods for near-infrared spectroscopy of the brain. *Appl. Opt.* 48:D280. doi: 10.1364/ao.48.00d280

Kondziella, D., Bender, A., Diserens, K., Erp, W. V., Estraneo, A., Formisano, R., et al. (2020). European academy of neurology guideline on the diagnosis of coma and other disorders of consciousness. *Eur. J. Neurol.* 27, 741–756. doi: 10.1111/ene.14151

Kurz, E., Wood, G., Kober, S. E., Schippinger, W., Pichler, G., Müller-Putz, G., et al. (2018). Towards using fnirs recordings of mental arithmetic for the detection of residual cognitive activity in patients with disorders of consciousness (doc). *Brain Cogn.* 125, 78–87. doi: 10.1016/j.bandc.2018.06.002

Lau, H., and Rosenthal, D. (2011). Empirical support for higher-order theories of conscious awareness. *Trends Cogn. Sci.* 15, 365–373. doi: 10.1016/j.tics.2011.05.009

Liu, X., Li, J., Gao, J., Zhou, Z., Meng, F., Pan, G., et al. (2017). Association of medial prefrontal cortex connectivity with consciousness level and its outcome in patients with acquired brain injury. *J. Clin. Neurosci.* 42, 160–166. doi: 10.1016/j.jocn.2017.04.015

Liu, Y., Kang, X. G., Chen, B. B., Song, C. G., Liu, Y., Hao, J. M., et al. (2023). Detecting residual brain networks in disorders of consciousness: a resting-state fnirs study. *Brain Res.* 1798:148162. doi: 10.1016/j.brainres.2022.148162

Martinez, D. E., Rudas, J., Demertzi, A., Charland-Verville, V., Soddu, A., Laureys, S., et al. (2020). Reconfiguration of large-scale functional connectivity in patients with disorders of consciousness. *Brain Behav.* 10:e1476. doi: 10.1002/brb3.1476

Mashour, G. A., Roelfsema, P., Changeux, J., and Dehaene, S. (2020). Conscious processing and the global neuronal workspace hypothesis. *Neuron* 105, 776–798. doi: 10.1016/j.neuron.2020.01.026

Mesquita, R. C., Franceschini, M. A., and Boas, D. A. (2010). Resting state functional connectivity of the whole head with near-infrared spectroscopy. *Biomed. Opt. Express* 1, 324–336. doi: 10.1364/BOE.1.000324

Miao, G., Rao, B., Wang, S., Fang, P., Chen, Z., Chen, L., et al. (2022). Decreased functional connectivities of low-degree level rich club organization and caudate in post-stroke cognitive impairment based on resting-state fmri and radiomics features. *Front. Neurosci.* 15:796530. doi: 10.3389/fnins.2021.796530

Molteni, E., Arrigoni, F., Bardoni, A., Galbiati, S., Villa, F., Colombo, K., et al. (2013). Bedside assessment of residual functional activation in minimally conscious state using nirs and general linear models. *Annu. Int. Conf. IEEE Eng. Med. Biol. Soc.* 2013, 3551–3554. doi: 10.1109/EMBC.2013.6610309

Moriya, M., and Sakatani, K. (2018). Relation between asymmetry of prefrontal activity and autonomic nervous system in post-stroke patients with a disorder of consciousness. *Adv. Exp. Med. Biol.* 1072, 53–58. doi: 10.1007/978-3-319-91287-5_9

Murphy, K., Birn, R. M., Handwerker, D. A., Jones, T. B., and Bandettini, P. A. (2009). The impact of global signal regression on resting state correlations: are anti-correlated networks introduced? *Neuroimage* 44, 893–905. doi: 10.1016/j.neuroimage.2008.09.036

Nakai, T., Kato, C., and Matsuo, K. (2005). An fmri study to investigate auditory attention: a model of the cocktail party phenomenon. *Magn. Reson. Med. Sci.* 4, 75–82. doi: 10.2463/mrms.4.75

Owen, A. M. (2008). Disorders of consciousness. *Ann. N. Y. Acad. Sci.* 1124, 225–238. doi: 10.1196/annals.1440.013

Owen, A. M. (2019). The search for consciousness. *Neuron* 102, 526–528. doi: 10.1016/j.neuron.2019.03.024

Panikratova, Y. R., Vlasova, R. M., Akhutina, T. V., Korneev, A. A., Sinitsyn, V. E., and Pechenkova, E. V. (2020). Functional connectivity of the dorsolateral prefrontal cortex contributes to different components of executive functions. *Int. J. Psychophysiol.* 151, 70–79. doi: 10.1016/j.ijpsycho.2020.02.013

Rämä, P., and Courtney, S. M. (2005). Functional topography of working memory for face or voice identity. *Neuroimage* 24, 224–234. doi: 10.1016/j.neuroimage.2004.08.024

Rupawala, M., Dehghani, H., Lucas, S. J. E., Tino, P., and Cruse, D. (2018). Shining a light on awareness: a review of functional near-infrared spectroscopy for prolonged disorders of consciousness. *Front. Neurol.* 9:350. doi: 10.3389/fneur.2018.00350

Samu, D., Seth, A. K., and Nowotny, T. (2014). Influence of wiring cost on the large-scale architecture of human cortical connectivity. *PLoS Comput. Biol.* 10:e1003557. doi: 10.1371/journal.pcbi.1003557

Scholkmann, F., Spichtig, S., Muehlemann, T., and Wolf, M. (2010). How to detect and reduce movement artifacts in near-infrared imaging using moving standard deviation and spline interpolation. *Physiol. Meas.* 31, 649–662. doi: 10.1088/0967-3334/31/5/004

Scholkmann, F., and Wolf, M. (2013). General equation for the differential pathlength factor of the frontal human head depending on wavelength and age. *J. Biomed. Opt.* 18:105004. doi: 10.1117/1.JBO.18.10.105004

Seth, A. K., and Bayne, T. (2022). Theories of consciousness. *Nat. Rev. Neurosci.* 23, 439–452. doi: 10.1038/s41583-022-00587-4

Singh, A. K., Okamoto, M., Dan, H., Jurcak, V., and Dan, I. (2005). Spatial registration of multichannel multi-subject fnirs data to mni space without mri. *Neuroimage* 27, 842–851. doi: 10.1016/j.neuroimage.2005.05.019

Sinitsyn, D. O., Legostaeva, L. A., Kremneva, E. I., Morozova, S. N., Poydasheva, A. G., Mochalova, E. G., et al. (2018). Degrees of functional connectome abnormality in disorders of consciousness. *Hum. Brain Mapp.* 39, 2929–2940. doi: 10.1002/hbm.24050

Song, M., Yang, Y., Yang, Z., Cui, Y., Yu, S., He, J., et al. (2020). Prognostic models for prolonged disorders of consciousness: an integrative review. *Cell. Mol. Life Sci.* 77, 3945–3961. doi: 10.1007/s00018-020-03512-z

Soon, C. S., Brass, M., Heinze, H., and Haynes, J. (2008). Unconscious determinants of free decisions in the human brain. *Nat. Neurosci.* 11, 543–545. doi: 10.1038/nn.2112

Stam, C. J., Jones, B. F., Nolte, G., Breakspear, M., and Scheltens, P. (2007). Small-world networks and functional connectivity in alzheimer's disease. *Cereb. Cortex* 17, 92–99. doi: 10.1093/cercor/bhj127

Storey, J. D. (2002). A direct approach to false discovery rates. *J. R. Stat. Soc. Ser. B Stat. Methodol.* 64, 479–498. doi: 10.1111/1467-9868.00346

Tan, X., Zhou, Z., Gao, J., Meng, F., Yu, Y., Zhang, J., et al. (2019). Structural connectome alterations in patients with disorders of consciousness revealed by 7-tesla magnetic resonance imaging. *Neuroimage: Clin.* 22:101702. doi: 10.1016/j.nicl.2019.101702

Wang, J., Wang, X., Xia, M., Liao, X., Evans, A., and He, Y. (2015). Corrigendum: gretna: a graph theoretical network analysis toolbox for imaging connectomics. *Front. Hum. Neurosci.* 9:458. doi: 10.3389/fnhum.2015.00458

Wang, R., Liu, M., Cheng, X., Wu, Y., Hildebrandt, A., and Zhou, C. (2021). Segregation, integration, and balance of large-scale resting brain networks configure different cognitive abilities. *Proc. Natl. Acad. Sci. U.S.A.* 118:e2022288118. doi: 10.1073/pnas.2022288118

Watts, D. J., and Strogatz, S. H. (1998). Collective dynamics of 'small-world' networks. *Nature* 393, 440–442. doi: 10.1038/30918

Weng, L., Xie, Q., Zhao, L., Zhang, R., Ma, Q., Wang, J., et al. (2017). Abnormal structural connectivity between the basal ganglia, thalamus, and frontal cortex in patients with disorders of consciousness. *Cortex* 90, 71–87. doi: 10.1016/j.cortex.2017.02.011

White, B. R., Snyder, A. Z., Cohen, A. L., Petersen, S. E., Raichle, M. E., Schlaggar, B. L., et al. (2009). Resting-state functional connectivity in the human brain revealed with diffuse optical tomography. *Neuroimage* 47, 148–156. doi: 10.1016/j.neuroimage.2009.03.058

Witt, S. T., Lovejoy, D. W., Pearlson, G. D., and Stevens, M. C. (2010). Decreased prefrontal cortex activity in mild traumatic brain injury during performance of an auditory oddball task. *Brain Imaging Behav.* 4, 232–247. doi: 10.1007/s11682-010-9102-3

Yang, D., and Hong, K. (2021). Quantitative assessment of resting-state for mild cognitive impairment detection: a functional near-infrared spectroscopy and deep learning approach. *J. Alzheimer's Dis.* 80, 647–663. doi: 10.3233/JAD-201163

Ye, J., Tak, S., Jang, K., Jung, J., and Jang, J. (2009). Nirs-spm: statistical parametric mapping for near-infrared spectroscopy. *Neuroimage* 44, 428–447. doi: 10.1016/j.neuroimage.2008.08.036

Zhang, J., Wang, J., Wu, Q., Kuang, W., Huang, X., He, Y., et al. (2011). Disrupted brain connectivity networks in drug-naive, first-episode major depressive disorder. *Biol. Psychiatry* 70, 334–342. doi: 10.1016/j.biopsych.2011.05.018

Zhang, Y., Yang, Y., Si, J., Xia, X., He, J., and Jiang, T. (2018). Influence of inter-stimulus interval of spinal cord stimulation in patients with disorders of consciousness: a preliminary functional near-infrared spectroscopy study. *Neuroimage Clin.* 17, 1–9. doi: 10.1016/j.nicl.2017.09.017

frontiers | Frontiers in Neuroscience

TYPE Original Research
PUBLISHED 15 February 2023
DOI 10.3389/fnins.2023.1100681



OPEN ACCESS

EDITED BY
Jie Jia,
Fudan University, China

REVIEWED BY
Yuzhen Xu,
Tongji University, China
Simin Deng,
Southern Medical University, China

*CORRESPONDENCE
Yiming Xu
✉ yui5@163.com
Yanhong Ma
✉ myhmyh2006@126.com

†These authors have contributed equally to this work and share last authorship

SPECIALTY SECTION
This article was submitted to Translational Neuroscience, a section of the journal Frontiers in Neuroscience

RECEIVED 17 November 2022
ACCEPTED 30 January 2023
PUBLISHED 15 February 2023

CITATION
Huang L, Jiang L, Xu Y and Ma Y (2023) Design and implementation of informatization for unified management of stroke rehabilitation in urban multi-level hospitals. *Front. Neurosci.* 17:1100681. doi: 10.3389/fnins.2023.1100681



# Design and implementation of informatization for unified management of stroke rehabilitation in urban multi-level hospitals

Lihua Huang, Lan Jiang, Yiming Xu*† and Yanhong Ma*†

Shanghai Sixth People's Hospital, Shanghai Jiao Tong University School of Medicine, Shanghai, China

**Background:** With the aging of the population, the prevalence and incidence of stroke in China are increasing every year. China advocates the establishment of a three-level medical service system for stroke rehabilitation, but it lacks uniform information management among all levels of medical institutions.

**Objective:** To achieve unified management of stroke patient rehabilitation in multilevel hospitals in the region through informatization construction.

**Methods:** The need for informatization of three-level stroke rehabilitation management was analyzed. Then, network connections were established, and a common rehabilitation information management system (RIMS) was developed for all levels of hospitals to enable daily stroke rehabilitation management, inter-hospitals referral, and remote video consultation. Finally, the impact on the efficiency of daily rehabilitation work, the functioning and satisfaction of stroke patients were investigated after implementing the three-level rehabilitation network.

**Results:** One year after implementation, 338 two-way referrals and 56 remote consultations were completed using RIMS. The stroke RIMS improved the efficiency of doctors' orders, reduced therapists' time to write medical documents, simplified statistical analysis of data and made referrals and remote consultations more convenient compared to the traditional model. The curative effect of stroke patients managed by RIMS is better than that of traditional management. Patient satisfaction with rehabilitation services in the region has increased.

**Conclusion:** The three-level stroke rehabilitation informatization has enabled the unified management of stroke rehabilitation in multilevel hospitals in the region. The developed RIMS improved the efficiency of daily work, improved the clinical outcomes of stroke patients, and increased patient satisfaction.

KEYWORDS

**stroke rehabilitation, three-level rehabilitation, unified management, informatization, hierarchical diagnosis and treatment**

# 1. Introduction

Stroke is the second leading cause of death worldwide, accounting for 1 in 10 deaths (Kim and Johnston, 2013), and the prevalence, incidence, and mortality rates are higher in developing countries than in developed countries (Mehndiratta et al., 2014). According to the Report on National Health Commission (2020), stroke remains the number one cause of disability and mortality in China (Chao et al., 2021a). The National Epidemiological Stroke Survey of China (NESS-China) estimated 11 million cases of stroke, 2.4 million new strokes, and 1.1 million stroke-related deaths in China each year (Wang et al., 2017), causing a huge economic burden on families and society (Zhao et al., 2022).

Stroke rehabilitation is a critical measure to reduce disability and improve the quality of life, which is an integral part of the treatment system for cerebrovascular disease (Langhorne et al., 2011). In China, the Ministry of Health China Stroke Prevention Project Committee (CSPPC) was established in 2011 (Chao et al., 2021a). The officials advocate the establishment of a three-level stroke rehabilitation service system (Chen et al., 2010), with primary rehabilitation for acute and sub-acute stroke rehabilitation in tertiary hospitals or tertiary rehabilitation hospitals, secondary rehabilitation for convalescent phase of stroke in secondary hospitals or secondary rehabilitation hospitals, and tertiary rehabilitation for chronic phase of stroke in community health service centers or township health centers or families. Although the three-level stroke rehabilitation system has established recommended referral criteria and treatment protocols (Xu et al., 2021), the lack of uniform management practices across all levels of care may delay the treatment due to poor referral, indicating that coordinating the treatment of stroke patients between the acute, convalescent, and chronic phases is essential (Kinoshita et al., 2021).

The development of information technology facilitates uniform stroke rehabilitation management in hospitals at all levels in the region. Xuhui District in Shanghai has seized the opportunity of smart city construction to connect all levels of hospitals in the region through network- and design-dedicated rehabilitation management software. Also, tertiary rehabilitation referral criteria and recommended rehabilitation treatment protocols applicable to the region were developed. This study aimed to analyze the need for the informatization of a three-level rehabilitation network for stroke and present the hardware and software's design, implementation, and efficiency.

# 2. Materials and methods

## 2.1. Analysis of the informatization needs of three-level stroke rehabilitation management

First, an information management system for stroke rehabilitation that can be used in primary, secondary, and tertiary hospitals needs to be developed. A total of 16 hospitals were involved in this project in Xuhui District, Shanghai. Among these, 13 were primary hospitals (i.e., Community Health Service Centers), including Xujiahui Street, Hunan Street, Tianping Street, Xietu Street, Longhua Street, Fenglin Street, Tianlin Street, Caohejing Street, Kangjian Street, and Hongmei Street, two were secondary hospitals, including Xuhui Central Hospital, and Xuhui Dahua Hospital, and one was a tertiary hospital, Shanghai Sixth People's Hospital. In the three-level rehabilitation management of stroke, hospitals at different levels treating stroke in different phases lead to variations in the types and difficulties with respect to rehabilitation equipment, rehabilitation technicians, and rehabilitation treatment technologies. Therefore, during the software design, the rehabilitation evaluation and treatment technology in the system should be customized according to the actual situation.

Second, the diagnosis and treatment information of stroke patients need to be shared among different hospitals, such that when stroke patients are referred between hospitals at different levels in the region, historical information on rehabilitation can be shared through downloads. This avoids duplication of tests, examinations, and assessments and provides a basis for the next stage of treatment.

Third, remote video consultation is required. It is common for primary hospitals to request consultations from secondary and tertiary hospitals. Teleconsultations through web-based video conferencing can improve the efficiency of consultations in a time-effective manner.

## 2.2. Design and implementation of a three-level stroke rehabilitation network in the region

### 2.2.1. Design thinking

Based on the above requirement analysis, in terms of hardware, a data center and multiple subcenters are established using a distributed architecture. All data centers are connected. Each data center does not rely on the general data center to operate independently. In the case of a data request (such as referral and consultation), data exchange can be generated. If one of the network members (Unit A) needs to refer a patient to another network member (Unit B), the patient's data are uploaded from Unit A to the data center, and Unit B downloads the patient's data, thus avoiding network congestion caused by frequent synchronization. In terms of software, a common stroke rehabilitation management system for primary, secondary, and tertiary hospitals will be developed, with integrated data synchronization and remote video consultation modules.

### 2.2.2. Hardware and network connectivity

As shown in **Figure 1**, the data center is located in the tertiary hospital, which is connected to the client of the rehabilitation medicine department through the hospital's internal network and the Hospital-Hospital Network of Xuhui District through an optical fiber. The Hospital-Hospital Network connects 13 primary hospitals (Community Health Service Centers) and two secondary hospitals in Xuhui District.

### 2.2.3. Software main modules and functions

The same rehabilitation information management system (RIMS) is used in all levels of hospitals. The software is a B/S (browser/server) architecture, wherein the client interacts with the server *via* a web page for data interaction. C# and Net are used for the data center, application service, and client. The server operating system is Windows Server 2008 R2 Enterprise, and the database is Windows SQL Server 2008 + MySQL. The functional modules of the software are as follows.

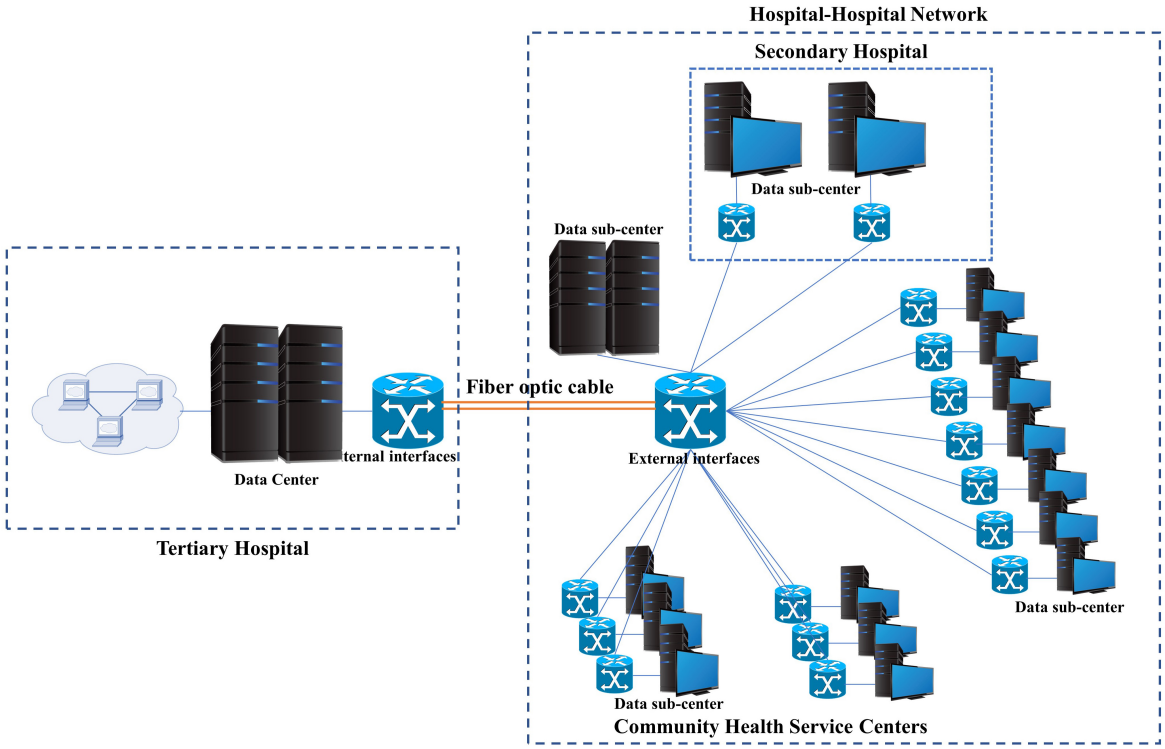


FIGURE 1
Topology of the three-level stroke rehabilitation network.

#### 2.2.3.1. User management

The system divides users into five roles: Doctor, nurse, therapist, administrator, and super-administrator, with each role assigned after appropriate permissions. The doctor's role is to issue and amend medical orders; the nurse views and bills the orders; the therapist views the medical orders and submits the treatment records; the head of the department and the leader of health administration review the operational data as administrators; the super administration is effectuated by the software designer to make changes or delete the software function modules.

#### 2.2.3.2. Medical records management

The system manages the medical history of all stroke patients in both outpatient and inpatient settings. When a patient needs rehabilitation treatment, medical record information is entered as required, including basic patient and medical history information. The former includes name, gender, age, hospitalization number, and ward and bed number, while the latter includes the patient's chief complaint, medical history, physical examination, auxiliary tests, and diagnosis.

#### 2.2.3.3. Rehabilitation medical order management

The system categorizes all the rehabilitation technology items carried out in the treatment room. Each rehabilitation technology item contains five sub-items: Technology name, dose, time, site, and frequency, and the items have been set to default values so that doctors can easily issue medical orders. After the doctor submits the orders, the therapist can view the detailed list of orders in the rehabilitation treatment interface and initiate the treatment according to the orders. The system can automatically record the relevant parameters of the rehabilitation treatment, such as the operator, operation time, and actual dose. The previous medical orders could be copied automatically when the patient re-visited or modified and submitted according to the situation, which greatly improves the efficiency of the re-visit.

#### 2.2.3.4. Rehabilitation assessment management

The system provides mandatory and optional assessments for stroke, which can be completed by both doctors and therapists. The assessment results can be viewed in the same interface, such that the patient's condition can be understood and follow-up treatment can be planned.

#### 2.2.3.5. Staging referrals

Referrals are made between hospitals in accordance with the criteria listed in Table 1. When a referral is made, the system uploads the treatment information of the patient to the data center, and the receiving hospital downloads the patient information. The downloaded treatment information is presented as a report.

#### 2.2.3.6. Teleconsultation

This module initiates a remote video conference when activated. In addition to video and voice communication, a separate window displays the patient's medical history, history of examination, and treatment for the remote specialist's reference in the video conference, which helps the specialist to make an accurate diagnosis and give treatment advice (Figure 2).

#### 2.2.3.7. Customization of rehabilitation service items of hospitals at all levels

For the system to be used in the rehabilitation medicine departments of all levels of hospitals, the rehabilitation items need

TABLE 1 Staged stroke referral criteria.

| Stages of stroke | Acute and sub-acute phases | Convalescent phases | Chronic phases |
|---|---|---|---|
| Referral Hospitals | Department of Rehabilitation Medicine in a tertiary hospital or a tertiary rehabilitation hospital | Department of Rehabilitation Medicine in a secondary hospital or a secondary rehabilitation hospital | Community Health Center or Home |
| Referral criteria | Either of the following appears:<br>• Stroke recurrence.<br>• The presence of progressive cerebral edema, severe lung infection, urinary tract infection, sepsis or severe pressure sores.<br>• Impaired consciousness or increased functional impairment.<br>• Multiple organ failure occurs. | The following conditions are all met:<br>• Vital signs are stable.<br>• Neurospecialist treatment finished.<br>• Stroke-related clinical laboratory tests are generally normal or stable.<br>•After receiving early rehabilitation diagnosis and treatment, there are still serious dysfunctions or complications, such as consciousness or cognitive impairment, tracheotomy, acute myocardial infarction, dysphagia, etc. | The following conditions are all met:<br>• Vital signs are stable.<br>• Stroke-related clinical laboratory tests are generally normal.<br>• No serious complications or comorbidities.<br>• Mild functional impairment is present. |

to be personalized. Under super administrator privileges, hospitals at all levels can configure the number of treatment rooms, and the rehabilitation technology programs were included according to their actual needs (Figure 3) or set default values for the dose, time, and site of each rehabilitation technology item.

#### 2.2.3.8. Research support

The unified patient information data facilitates the collection of data. The researchers can use the system for retrospective analysis and also for the evaluation of the efficacy of new technologies.

### 2.2.4. Network information security

Each hospital has a Department of Information Management responsible for network information security. Clients in the Department of Rehabilitation Medicine are prohibited from connecting to external storage devices for possible information leakage, and communication between sub-centers in each hospital is protected by hardware firewalls.

## 2.3. Evaluation of the effectiveness of a three-level stroke rehabilitation network in the region

After 1 year, we evaluated the effectiveness of the three-level stroke RIMS in terms of daily work efficiency, the function of stroke patients and patient satisfaction. The impact of RIMS on daily work efficiency was studied through face-to-face interviews. The face-to-face interviews were conducted to collect information on the experience of using RIMS, including the time taken to give medical orders at the initial consultation, the time taken to give medical orders at follow-up consultations, the time taken by the therapist to write the medical document, the convenience of statistical analysis of treatment data, the convenience of referral, the convenience of teleconsultation (7-point Likert scales were used for convenience, with 7-points representing very good convenience) and the problems that needed improvement. The impact of RIMS on the function of stroke patients and patients' satisfaction has been published in Chinese journals (Yuan et al., 2016; Li et al., 2019) and the findings are cited and presented below.

FIGURE 2
The expert was using the system for remote consultation.

## 2.4. Statistical analysis

All data were analyzed using SPSS 22(SPSS, IBM Corp., USA)The data of time and grade obtained from face-to-face interviews were reported as the mean and standard deviation, and analyzed by paired *t*-test. The satisfaction of patients before and after the project was compared using Ridit analysis. *P*-value $< 0.05$ and 95% confidence interval were used to indicate statistical significance.

# 3. Results

A total of 46 clients in one tertiary hospital, two secondary hospitals, and 13 primary hospitals have installed RIMS and accessed the network, and the rehabilitation treatment of both outpatients and inpatients with stroke was managed using RIMS. One year after the implementation, 338 two-way referrals and 56 remote consultations were completed with the software. A total of 32 people were interviewed. The results show that after the use of stroke RIMS, the efficiency of doctors' orders is improved ($P < 0.05$), the time for therapists to write medical documents is reduced ($P < 0.05$) (Figure 4), statistical analysis of data is simplified ($P < 0.05$), and the referral and remote consultation are convenient compared to the traditional work mode ($P < 0.05$) (Figure 5).

To understand the impact of a regional three-level rehabilitation network on the self-care ability and quality of survival of stroke patients, Yuan et al. (2016) from one of the network member units conducted a retrospective clinical study. The study divided 90 stroke

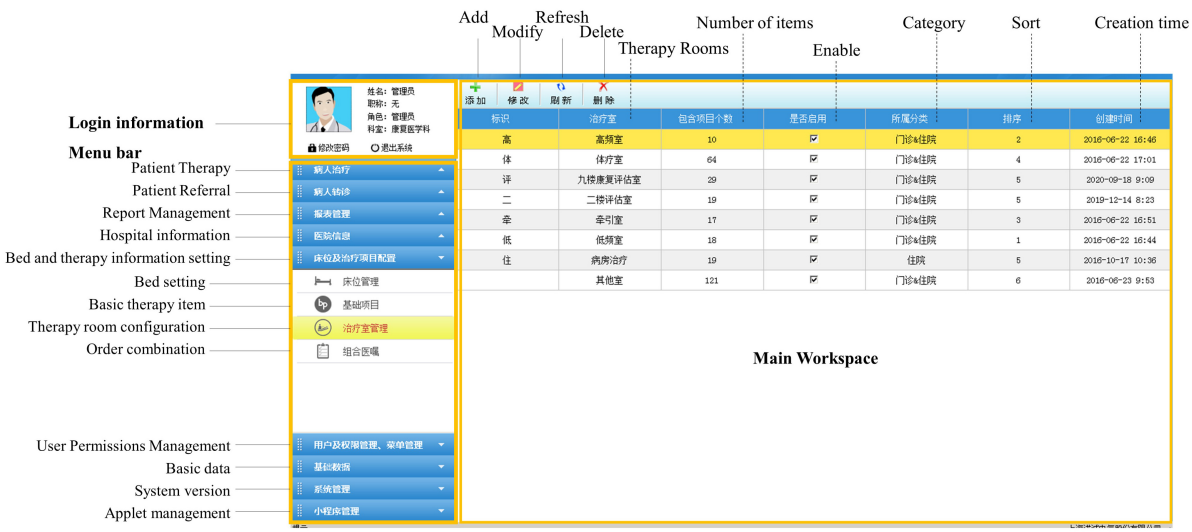


FIGURE 3
Customized therapy items in rooms.

patients into the network and conventional groups, respectively. A total of 60 patients in the network group were treated according to the three-level stroke rehabilitation program, while 30 patients in the conventional group were rehabilitated according to the conventional methods. The results showed that after 6 weeks of intervention, the scores of Modified Barthel Index and Stroke-Specific Quality of life in both groups were significantly higher than those before the treatment ($P < 0.05$), and those in the network group were significantly higher than those in the conventional group ($P < 0.05$). This finding showed that the information management of the three-level rehabilitation network for stroke can improve the rehabilitation effect.

To understand the satisfaction of residents in Xuhui District with three-level stroke rehabilitation, we conducted a questionnaire survey on a sample of six streets in Xuhui District (Li et al., 2019). The results of the research analysis by the independent third-party management consulting organization (ZERO Power Intelligence Group) showed that the overall satisfaction of residents with community rehabilitation services increased from 79.44 to 98.31% ($P < 0.01$) (**Figure 6**; Li et al., 2019).

# 4. Discussion

The three-level stroke RIMS introduced in this article enabled the unified management of stroke rehabilitation patients in 16 hospitals at different levels in the Xuhui District of Shanghai. Finally, efficient daily work, referral and remote consultation were realized, which improved patients' satisfaction with rehabilitation services, as well as the clinical outcomes of rehabilitation treatment.

## 4.1. Three-level stroke rehabilitation

With increasing life expectancy, the population ages and living standards are also improved, and the prevalence and incidence of stroke are increasing (Zhao et al., 2022). The development of Stroke Network, Stroke Map, and Stroke Green Channel has reduced stroke mortality (Chao et al., 2021b), but the increase in prevalence has elevated the absolute number of stroke patients and the subsequent cost of stroke care year by year. Health managers have been trying to achieve cost savings *via* clinical pathways without reducing the effectiveness of care.

Previous studies have shown that clinical pathways can significantly reduce the length of hospital stay and the cost of stroke care for patients (Deng et al., 2014; Pilato et al., 2021). The three-level rehabilitation, also known as the regional clinical pathway (Fujino et al., 2014), is a seamless integration of the acute stroke clinical pathway (Stroke Unit), the convalescent clinical pathway, and the chronic clinical pathway (Xu et al., 2021). This facilitates the discharge of stroke patients with significant burdens and allows the tertiary hospitals to accept patients with severe conditions (Van der Cruyssen et al., 2015) and refer discharged patients to the next level of the hospital for appropriate treatment according to their condition, thus saving treatment costs without reducing the treatment effect. Another reason why three-level rehabilitation is possible in China is related to the hierarchy of hospitals. Unlike Western countries, such as the

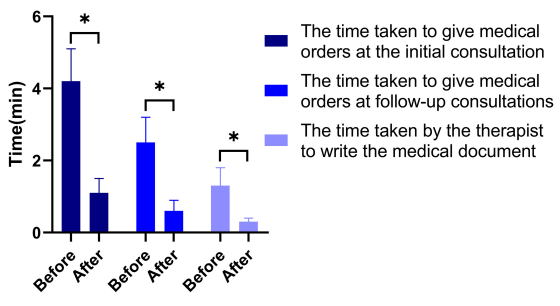


FIGURE 4
Comparison of the time spent by doctors and therapists on daily medical records before and after project implementation. *$P < 0.05$.

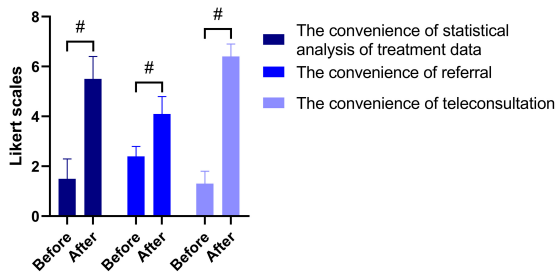


FIGURE 5
Comparison of the convenience of daily work before and after project implementation. $^{\#}P < 0.05$.

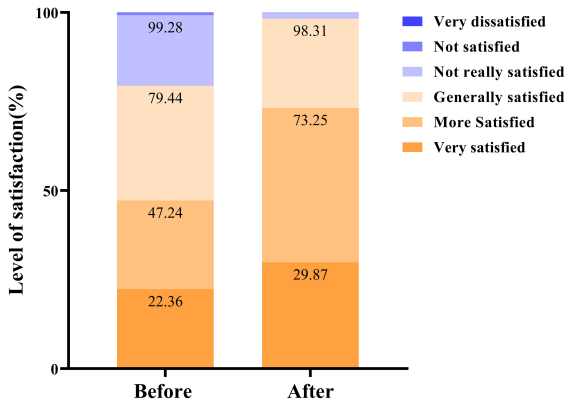


FIGURE 6
Comparison of resident satisfaction before and after project implementation.

USA and Europe, most cities in China have primary, secondary, and tertiary hospitals corresponding to the acute, convalescent, and chronic phases of stroke. Some Asian countries refer to the second level of three-level rehabilitation as transitional rehabilitation (Leigh et al., 2022), which does not change the fact that they also practice three-level rehabilitation (Kinoshita et al., 2021). In China, many studies have confirmed that the three-level stroke rehabilitation network is beneficial for rehabilitation of stroke patients, and was recommended by the Chinese Stroke Association guidelines for clinical management of cerebrovascular disorders (Zhang et al., 2020).

## 4.2. Informatics-assisted three-level stroke rehabilitation

China's hospital informatization is the earliest area of medical informatization development and is now widespread in the country. However, one hospital's informatization is only an information island (Liang et al., 2019), while the regional medical consortium based on the information network is the direction of future development to promote hierarchical diagnosis and treatment. Currently, the construction of regional medical informatization has become the hot spot of medical informatization in China (Zhang et al., 2022).

A key component of regional medical informatics is the collaborative management of common and chronic diseases, such as stroke. However, the current focus of regional medical informatics is on the establishment of pre-hospital stroke networks, which have been established in different countries and regions, such as the Cardiovascular Health and Stroke Strategic Clinical Network (CvHS SCN) in Canada (McIntosh et al., 2019), Emergency Medical Services (EMS) in Korea (Park et al., 2016), the Neurovascular Network of Southwest Bavaria (NEVAS) in Germany (Feil et al., 2021) and the Distributive Stroke Network (DSN) in USA (Holder et al., 2021). In China, although CSPPC has led a Stroke Network that has shown initial success in stroke prevention and emergency care (Chao et al., 2021a), post-stroke three-level rehabilitation informatics is still underdeveloped.

Currently, fewer studies have focused on the role of post-stroke rehabilitation network informatics, and post-stroke rehabilitation informatics has only been mentioned when investigating data such as healthcare costs and length of stay. In the study of the role of regional clinical pathways, Japanese researcher Fujino (Fujino et al., 2014) described the Diagnosis Procedure Combination (DPC) database system they used. The DPC system was a national case-mix patient classification system and consisted of clinical data from 82 university hospitals, which played an important role in the statistical correlation of regional clinical pathways and length of stay. The Korean researcher Leigh (Leigh et al., 2022) referred to the National Health Insurance (NHI) claims database in their review of the Korean stroke transitional and long-term rehabilitation care system. Through this database, researchers were able to investigate information such as inpatient rehabilitation and outpatient rehabilitation patients, and the length of time patients received rehabilitation services, which assisted with statistics such as the cost of rehabilitation. The three-level stroke RIMS developed in this project is not the same as the DPC and NHI. Recording information on the cost of rehabilitation is only one of its functions and the more important function is to record rehabilitation process while providing referral and teleconsultation functions similar to those of the pre-hospital stroke network. This study found that the three-level stroke RIMS not only improved the efficiency of daily stroke management but also improved the satisfaction and clinical outcomes of stroke patients. This observation was consistent with the findings of Xu et al. (2021).

## 4.3. Challenges of informatization

The process of stroke three-level rehabilitation informatization may also encounter some problems. Firstly, the Hospital Information System (HIS) varies across hospitals, and establishing a standard format is difficult. This could be ascribed to the need to manually enter the basic information of stroke patients in the RIMS. Secondly, the network connection may encounter interface restrictions and security restrictions, resulting in the inability to connect to the network. Thus, several meetings were undertaken to communicate and purchase new gateway equipment before it was resolved. Thirdly, the willingness to use the software was low. Some doctors and therapists were accustomed to the original treatment process, thereby using the software less frequently. These users should be informed of "Thorndike's law," which is a learning curve for the software, and that although the work efficiency is low in the beginning, it increases significantly when they become proficient.

### 4.4. Deficiencies of the project

Nevertheless, this stroke three-level rehabilitation informatization has some shortcomings. Firstly, there are still flaws in the software design. The software was not designed to gather all the requirements for use at the beginning; for example, some doctors only raised the issue after the project was completed and wanted to add a stroke knowledge database and work reminder functions. Secondly, the RIMS could not be synchronized with the HIS systems of different hospitals. This increased the manual input workload, which seemed to be a problem that could not be solved even at a later stage. Finally, the assessment methods for using RIMS were not established, discouraging the doctors from including all stroke patients.

## 5. Conclusion

The three-level stroke rehabilitation informatization has enabled the unified management of stroke rehabilitation in multilevel hospitals in the region. The developed RIMS can improve the efficiency of daily work and the clinical outcomes of stroke patients, thereby increasing patient satisfaction. This project provides a reference for other regions to establish a unified regional management of chronic diseases.

## Data availability statement

The original contributions presented in this study are included in this article/supplementary material, further inquiries can be directed to the corresponding authors.

## Author contributions

YX: conceptualization, software, and writing – review and editing. YM: methodology and supervision. LH and LJ: investigation. LH and YX: data curation. LJ: resources. LH: writing – original draft preparation. All authors have read and agreed to the published version of the manuscript.

## Funding

This study was funded by the Science and Technology Commission of Shanghai Municipality (No. 13231202600).

## Acknowledgments

We thank the doctors, therapists, nurses, and administrative staff of our Medical Services Section, Department of Information Service, Xuhui Municipal Health Commission, Xuhui Central Hospital, Xuhui Dahua Hospital, and the thirteen Community Health Service Centers that participated in this project.

## Conflict of interest

The authors declare that the research was conducted in the absence of any commercial or financial relationships that could be construed as a potential conflict of interest.

## Publisher's note



## References

Chao, B.-H., Tu, W.-J., and Wang, L.-D. (2021a). Initial establishment of a stroke management model in China: 10 years (2011-2020) of stroke prevention project committee, national health commission. *Chin. Med. J.* 134, 2418–2420. doi: 10.1097/CM9.0000000000001856

Chao, B.-H., Yan, F., Hua, Y., Liu, J.-M., Yang, Y., Ji, X.-M., et al. (2021b). Stroke prevention and control system in China: CSPPC-stroke program. *Int. J. Stroke.* 16, 265–272. doi: 10.1177/1747493020913557

Chen, Z., Yu, J., Song, Y., and Chui, D. (2010). Aging Beijing: Challenges and strategies of health care for the elderly. *Ageing Res. Rev.* 9(Suppl. 1), S2–S5. doi: 10.1016/j.arr.2010.07.001

Deng, Y., Jiao, Y., Hu, R., Wang, Y., Wang, Y., and Zhao, X. (2014). Reduction of length of stay and costs through the implementation of clinical pathways for stroke management in China. *Stroke* 45, e81–e83. doi: 10.1161/STROKEAHA.114.004729

Feil, K., Rémi, J., Küpper, C., Herzberg, M., Dorn, F., Kunz, W. G., et al. (2021). Inter-hospital transfer for mechanical thrombectomy within the supraregional stroke network NEVAS. *J. Neurol.* 268, 623–631. doi: 10.1007/s00415-020-10165-2

Fujino, Y., Kubo, T., Muramatsu, K., Murata, A., Hayashida, K., Tomioka, S., et al. (2014). Impact of regional clinical pathways on the length of stay in hospital among stroke patients in Japan. *Med. Care* 52, 634–640. doi: 10.1097/MLR.0000000000000146

Holder, D., Leeseberg, K., Giles, J. A., Lee, J.-M., Namazie, S., and Ford, A. L. (2021). Central triage of acute stroke patients across a distributive stroke network is safe and reduces transfer denials. *Stroke* 52, 2671–2675. doi: 10.1161/STROKEAHA.120.033018

Kim, A. S., and Johnston, S. C. (2013). Temporal and geographic trends in the global stroke epidemic. *Stroke* 44, S123–S125. doi: 10.1161/STROKEAHA.111.000067

Kinoshita, S., Abo, M., Okamoto, T., and Miyamura, K. (2021). Transitional and long-term care system in Japan and current challenges for stroke patient rehabilitation. *Front. Neurol.* 12:711470. doi: 10.3389/fneur.2021.711470

Langhorne, P., Bernhardt, J., and Kwakkel, G. (2011). Stroke rehabilitation. *Lancet* 377, 1693–1702. doi: 10.1016/S0140-6736(11)60325-5

Leigh, J.-H., Kim, W.-S., Sohn, D.-G., Chang, W. K., and Paik, N.-J. (2022). Transitional and long-term rehabilitation care system after stroke in Korea. *Front. Neurol.* 13:786648. doi: 10.3389/fneur.2022.786648

Li, B., Bai, Y., Yang, J., Zhang, J., Liu, G., and Xu, Y. (2019). Demand and satisfaction with rehabilitation knowledge and services in community residents. *Rehabil. Med.* 29, 13–18. doi: 10.3724/SP.J.1329.2019.04013

Liang, J., Zheng, X., Chen, Z., Dai, S., Xu, J., Ye, H., et al. (2019). The experience and challenges of healthcare-reform-driven medical consortia and regional health information technologies in China: A longitudinal study. *Int. J. Med. Inform.* 131:103954. doi: 10.1016/j.ijmedinf.2019.103954

McIntosh, C. J., Valaire, S., and Norris, C. M. (2019). Cardiovascular health and stroke strategic clinical network: Healthy hearts and brains for all Albertans. *CMAJ* 191, S15–S16. doi: 10.1503/cmaj.190592

Mehndiratta, M. M., Khan, M., Mehndiratta, P., and Wasay, M. (2014). Stroke in Asia: Geographical variations and temporal trends. *J. Neurol. Neurosurg. Psychiatry* 85, 1308–1312. doi: 10.1136/jnnp-2013-306992

National Health Commission (2020). *Report on nutrition and chronic disease status of Chinese residents*. Beijing: People's Medical Publishing House.

Park, H. A., Ahn, K. O., Shin, S. D., Cha, W. C., and Ro, Y. S. (2016). The effect of emergency medical service use and inter-hospital transfer on prehospital delay among ischemic stroke patients: A multicenter observational study. *J. Korean Med. Sci.* 31, 139–146. doi: 10.3346/jkms.2016.31.1.139

Pilato, F., Calandrelli, R., Capone, F., Alessiani, M., Ferrante, M., Iaccarino, G., et al. (2021). New perspectives in stroke management: Old issues and new pathways. *Brain Sci.* 11:767. doi: 10.3390/brainsci11060767

Van der Cruyssen, K., Vereeck, L., Saeys, W., and Remmen, R. (2015). Prognostic factors for discharge destination after acute stroke: A comprehensive literature review. *Disabil. Rehabil.* 37, 1214–1227. doi: 10.3109/09638288.2014.961655

Wang, W., Jiang, B., Sun, H., Ru, X., Sun, D., Wang, L., et al. (2017). Prevalence, incidence, and mortality of stroke in China: Results from a nationwide population-based survey of 480 687 adults. *Circulation* 135, 759–771. doi: 10.1161/CIRCULATIONAHA.116.025250

Xu, W., Liu, L., and Zhang, J. (2021). Application analysis based on big data technology in stroke rehabilitation nursing. *J. Healthc. Eng.* 2021:3081549. doi: 10.1155/2021/3081549

Yuan, W., Zhang, Y., Yang, J., Qiao, L., Bai, Y., Xu, Y., et al. (2016). The impact of a regional three-level rehabilitation network service system on the self-care ability and quality of life of stroke patients. *Zhong Guo Kang Fu* 31, 290–291. doi: 10.3870/zgkf.2016.04.016

Zhang, T., Zhao, J., Li, X., Bai, Y., Wang, B., Qu, Y., et al. (2020). Chinese Stroke Association guidelines for clinical management of cerebrovascular disorders: Executive summary and 2019 update of clinical management of stroke rehabilitation. *Stroke Vasc. Neurol.* 5, 250–259. doi: 10.1136/svn-2019-000321

Zhang, Z., Zheng, X., An, K., He, Y., Wang, T., Zhou, R., et al. (2022). Current status of the health information technology industry in China from the China hospital information network conference: Cross-sectional study of participating companies. *JMIR Med. Inform.* 10:e33600. doi: 10.2196/33600

Zhao, W. Y., Hua, X., Ren, X., Ouyang, M., Chen, C., Li, Y., et al. (2022). Increasing burden of stroke in China: A systematic review and meta-analysis of prevalence, incidence, mortality, and case fatality. *Int. J. Stroke*. doi: 10.1177/17474930221135983 [Epub ahead of print].

frontiers | Frontiers in Neuroscience

TYPE Systematic Review
PUBLISHED 16 February 2023
DOI 10.3389/fnins.2023.1111274



OPEN ACCESS

EDITED BY
Jie Jia,
Fudan University, China

REVIEWED BY
Fang Li,
Capital Medical University, China
Xing Wang,
Chongqing University, China

*CORRESPONDENCE
Tong Wang
✉ wangtong60621@163.com
Chuan Guo
✉ guochuanrehab@126.com
Yi Zhu
✉ lucky.zyx@163.com

†These authors have contributed equally to this work and share first authorship

SPECIALTY SECTION
This article was submitted to Translational Neuroscience, a section of the journal Frontiers in Neuroscience

RECEIVED 29 November 2022
ACCEPTED 30 January 2023
PUBLISHED 16 February 2023

CITATION
Wang Q, Dai W, Xu S, Zhu S, Sui Y, Kan C, Shen Y, Zhu Y, Guo C and Wang T (2023) Brain activation of the PFC during dual-task walking in stroke patients: A systematic review and meta-analysis of functional near-infrared spectroscopy studies.
*Front. Neurosci.* 17:1111274.
doi: 10.3389/fnins.2023.1111274



# Brain activation of the PFC during dual-task walking in stroke patients: A systematic review and meta-analysis of functional near-infrared spectroscopy studies

Qinglei Wang[1,2†], Wenjun Dai[1†], Sheng Xu[3†], Shizhe Zhu[1,2], Youxin Sui[1,2], Chaojie Kan[2,3], Ying Shen[1], Yi Zhu[1*], Chuan Guo[1*] and Tong Wang[1*]

[1]Department of Rehabilitation, The First Affiliated Hospital of Nanjing Medical University, Nanjing, China, [2]School of Rehabilitation Medicine, Nanjing Medical University, Nanjing, China, [3]Department of Rehabilitation, Changzhou Dean Hospital, Changzhou, China

**Background:** Dual-task walking is a good paradigm to measure the walking ability of stroke patients in daily life. It allows for a better observation of brain activation under dual-task walking to assess the impact of the different tasks on the patient when combining with functional near-infrared spectroscopy (fNIRS). This review aims to summarize the cortical change of the prefrontal cortex (PFC) detected in single-task and dual-task walking in stroke patients.

**Methods:** Six databases (Medline, Embase, PubMed, Web of Science, CINAHL, and Cochrane Library) were systematically searched for relevant studies, from inception to August 2022. Studies that measured the brain activation of single-task and dual-task walking in stroke patients were included. The main outcome of the study was PFC activity measured using fNIRS. In addition, a subgroup analysis was also performed for study characteristics based on HbO to analyze the different effects of disease duration and the type of dual task.

**Results:** Ten articles were included in the final review, and nine articles were included in the quantitative meta-analysis. The primary analysis showed more significant PFC activation in stroke patients performing dual-task walking than single-task walking ($SMD = 0.340$, $P = 0.02$, $I^2 = 7.853\%$, 95% $CI = 0.054–0.626$). The secondary analysis showed a significant difference in PFC activation when performing dual-task walking and single-task walking in chronic patients ($SMD = 0.369$, $P = 0.038$, $I^2 = 13.692\%$, 95% $CI = 0.020–0.717$), but not in subacute patients ($SMD = 0.203$, $P = 0.419$, $I^2 = 0\%$, 95% $CI = -0.289–0.696$). In addition, performing walking combining serial subtraction ($SMD = 0.516$, $P < 0.001$, $I^2 = 0\%$, 95% $CI = 0.239–0.794$), obstacle crossing ($SMD = 0.564$, $P = 0.002$, $I^2 = 0\%$, 95% $CI = 0.205–0.903$), or a verbal task ($SMD = 0.654$, $P = 0.009$, $I^2 = 0\%$, 95% $CI = 0.164–1.137$) had more PFC activation than single-task walking, while performing the n-back task did not show significant differentiation ($SMD = 0.203$, $P = 0.419$, $I^2 = 0\%$, 95% $CI = -0.289–0.696$).

**Conclusions:** Different dual-task paradigms produce different levels of dual-task interference in stroke patients with different disease durations, and it is important to choose the matching dual-task type in relation to the walking ability and cognitive ability of the patient, in order to better improve the assessment and training effects.

**Systematic review registration:** https://www.crd.york.ac.uk/prospero/, identifier: CRD42022356699.

KEYWORDS

**prefrontal cortex (PFC), dual task (DT), walking, functional near-infrared spectroscopy (fNIRS), ischemic stroke, hemorrhagic stroke**

# 1. Introduction

Stroke is the second leading cause of death and disability worldwide (Saini et al., 2021). Many surviving post-stroke patients have residual cognitive impairment and long-term disability that severely affect their normal lives (Delavaran et al., 2017; Young et al., 2020). Studies have shown that more than 50% of patients are unable to walk independently in the community (Blennerhassett et al., 2018). This community ambulation of immersion in daily life requires getting out of the therapeutic environment and interacting with a variety of information (Lord et al., 2004). It goes beyond mere walking and involves motor, sensory and cognitive functions interacting with each other to cope with obstacles and disturbances that may arise during walking to accomplish this multitasking (Caetano et al., 2017). Stroke patients have reduced brain processing capacity due to brain damage, making it difficult for them to multitask (Veldkamp et al., 2021).

Dual-task paradigm is defined as the concurrent performance of two distinct tasks by an individual, and it has been proven that dual-task (DT) walking is a good and valuable paradigm for exploring the walking abilities of stroke patients in daily life (Liu et al., 2018; Bishnoi et al., 2021). As compared to processing one task alone, the performance of one or even both tasks can be degraded when processing two tasks at the same time. This common situation is called dual-task interference (DTI; Tsang et al., 2022). This is manifested in stroke patients by slowed gait speed and increased gait variability (Chatterjee et al., 2019; Hermand et al., 2019). Many theories can be used to explain this occurrence, such as the Capacity theory, Bottleneck theory, or Multiple resource theory (Pashler, 1994; Handy, 2000; Wickens, 2002). However, they have been constructed based on assumed behavioral manifestations and brain capacity. The former has been observed and estimated through many studies on gait parameters. The favorable evidence for the latter needs to be further explored. The study of the neural mechanisms of dual-task is essential for furthering our understanding of how stroke populations cope with DTI.

Brain injury studies have found that patients with prefrontal injury have impaired dual-task execution, but that single-task (ST) processing is not affected (Baddeley et al., 1997). fMRI, PET, and other imaging tools further indicate that specific cortical areas that are associated with dual-task processing include the dorsolateral prefrontal cortex (Kondo et al., 2004; Collette et al., 2005; Low et al., 2009). Elevated metabolic activity in the prefrontal cortex (PFC) has proven that it is strongly associated with increased planning and attention in motor and cognitive tasks, which can verify the changes of brain capacity in theories of DTI (Hamacher et al., 2015). This all points to the value of studying PFC for exploring the effects of dual task in stroke.

Recent neuroimaging techniques have been able to objectively measure the contribution of PFC involvement in human activity (Parris et al., 2019; Udina et al., 2019; Min et al., 2021). Traditional brain imaging techniques such as functional magnetic resonance imaging (fMRI) has a high spatial resolution to detect cerebral blood flow signals. But fMRI has contraindicates of metal implants and they require a more restrictive environment (Mehagnoul-Schipper et al., 2002). EEG has high temporal resolution. But it is less resistant to motion interference and has a lower spatial resolution. It has difficulty in providing a better observation role during a walk. Functional near-infrared spectroscopy (fNIRS) is a new non-invasive optical imaging technique based on the principle of neuro-vascular coupling. When cortical neurons are excited, the oxyhemoglobin (HbO) concentration increases and the deoxyhemoglobin (HbR) concentration decreases, which can indirectly reflects neural activity in the brain (Gramigna et al., 2017). fNIRS has a temporal resolution superior compared to fMRI and can be used in a naturalistic environment. It has better spatial resolution and tolerance to motion artifacts than EEG. fNIRS enables the real-time monitoring of cerebral hemodynamic changes during walking and is not restricted by the freedom to walk (Pinti et al., 2020). So, it can provide a suitable measure of the PFC contribution to walking control (Perrey, 2014). However, fNIRS had limited clinical use due to the lack of anatomic specificity, suboptimal temporal resolution, variable signal-to-noise ratio, and low intra-subject reproducibility for individual analysis (Chen et al., 2020). First, there may be a bias in the anatomical localization of the PFC during the procedure of measuring. Second, it only reflects the overall degree of PFC activation during dual task and cannot detect whether individual neural events occur in the PFC during dual task (Pinti et al., 2020). Third, the hemodynamic response has a delay of 2 s after the occurrence of the event (Jasdzewski et al., 2003). So, it was not temporally synchronized with the occurrence of the event. Fourth, fNIRS has shallow imaging depth. The imaging depth of fNIRS is generally limited to the surface of the cortex in the case of humans (Kim et al., 2017).

Despite the growing body of studies on dual tasks, most of the existing studies performed various types of dual-task paradigms, including motor dual-task, computational dual-task, memory dual-task, and verbal dual-task (Al-Yahya et al., 2016; Hawkins et al., 2018; Hermand et al., 2020). Even for the same pattern, the specific tasks chosen varied across studies. It is not clear whether there are similarities and differences in the degree of PFC activation brought about by these different paradigms in stroke patients. There is a lack of basis for suggestions what dual task should be selected in future clinics. Secondly, with the recovery of the disease duration, the walking activation patterns will be different in different stroke patients (Beyaert et al., 2015). There are no studies directly observing the differences in brain area activation between patients in the subacute and chronic phases while performing dual tasks, which should be explored further. The relevant reviews are mostly qualitative descriptions of the activation of brain regions and the type of tasks (Lim et al., 2021; Veldkamp et al., 2021). The quantitative analysis of the dual task was also about spatiotemopral gait parameters such as walking speed and walking distance, with few fNIRS metrics (Tsang et al., 2022). In addition to that, many studies are currently conducted on dual-task training (Pang et al., 2018; Iqbal et al., 2020; Collett et al., 2021). Brain imaging evidence still to be explored whether it is an appropriate matching of the patient's abilities to the dual-task paradigm for assessment and effective training. The published meta-analysis related to the relationship between PFC and dual task has mainly focused on the elderly and Parkinson's patients, with insufficient inclusion of studies on stroke. It does not reveal well the situation of stroke as a group. We aimed to explore the above questions by analyzing related studies through meta-analysis.

The primary objective of this meta-analysis was to identify the difference of brain activation in PFC between single-task walking and dual-task walking in stroke patients. In addition, the secondary

objective was to use subgroup analyses to assess the effects of different dual-task types and disease durations on the differences in activation between stroke patients performing single task and dual task.

## 2. Materials and methods

The results of this systematic review and meta-analysis are reported in accordance with the Preferred Reporting Items for Systematic Reviews and Meta-Analysis (PRISMA) guidelines (Moher et al., 2009). In addition, it was registered on the International Prospective Register of Systematic Reviews (PROSPERO; registration number: CRD42022356699).

### 2.1. Study selection criteria

We used the PICOS framework to formulate the inclusion criteria. Studies that met the following criteria were included in the review: (1) Population: adult participants with stroke. (2) Intervention: Participants in the studies performing dual-task walking (walking whilst performing a cognitive task or another type of motor task). (3) Comparison: The control group was a single walking task. Other tasks were not mixed during the walking. (4) Outcome: Studies used fNIRS to quantify the concentration changes of oxygenated hemoglobin (HbO) in PFC during single-task or dual-task walking. (5) Studies: The study design and the time of publication were not limited. The following types of articles were excluded: (1) conference proceedings, (2) review articles, (3) case reports, (4) retrospective studies, or (5) not written in English.

### 2.2. Search strategy

Keyword searches were performed in Medline, Embase, PubMed, Web of Science, CINAHL, and Cochrane Library from inception to August 2022. The search algorithm included all possible combinations of keywords from the following three groups: (1) stroke; (2) dual task, walking, gait, locomotion, mobility, ambulation, lower limb movement, lower limb motor; and (3) fNIRS, functional near infrared spectroscopy, functional near-infrared spectroscopy, NIRS, near-infrared spectroscopy, near infrared spectroscopy. Keywords and medical subject headings (MeSH) terms were used in the search. Relevant professional journals were searched manually when necessary. The specific search algorithm for each database is provided in Supplementary material.

### 2.3. Data extraction

A standardized data extraction form was used to collect the following methodological and outcome variables from each included study: author(s), year of publication, study design, type of pathology, sample size, participant characteristics (i.e., age, type of stroke, and disease duration), type of dual-task, and fNIRS outcome. Single-task walking was defined as the control group, while dual-task walking was defined as the experimental group. The subacute phase is defined as the range between 7 and 180 days after initial stroke. Chronic stroke is defined as the open-ended time period starting 180 days after initial stroke (Bernhardt et al., 2017). Most data were entered as mean with standard deviation (SD) for both groups at the baseline and when performing the task. When the authors analyzed patients according to gender or functional status categories, we combined the data for patients performing the same task type using the following formula:

$$Combined\ mean = \frac{N1^{*}M1 + N2^{*}M2}{N1 + N2} \quad (1)$$

$$Combined\ Standard\ Deviation = \sqrt{\frac{(N1-1)^{*}S1^{2} + (N2-1)^{*}S2^{2}}{N1+N2-2}} \quad (2)$$

$N$, the size of sample; $M$, the mean of sample, $S$, the standard deviation of sample.

For the missing data, we tried to contact the authors to obtain the original data. HbO has been reported to be more sensitive to changes in cortical activity associated with walking, while HbR is more susceptible to contamination by factors affecting optical path length and crosstalk than HbO (Leff et al., 2011). For these reasons, HbO was generally chosen as the primary outcome of prefrontal recruitment (Hoshi et al., 2001). Therefore, we only extracted HbO but not HbR to explore the activation of PFC. For randomized controlled trial (RCT) designed studies, only pre-test data were extracted in order to avoid the influence of intervention on PFC (Moon et al., 2016). To avoid the effect of the intervention on the pattern of stroke processing dual task, post-intervention HbO data were not extracted.

### 2.4. Quantitative data synthesis

Meta-analysis was used to determine the pooled effect size of PFC activation comparing single tasks and dual tasks, to measure activation differences between single tasks and dual tasks in stroke patients (ST-DT diff). For each trial in the articles, we used Comprehensive Meta-Analysis (CMA) software version 2.0 (Biostat, Inc., Englewood, NJ, USA) to synthesize an effect size. The overall effect of group comparisons was assessed using the standardized difference in means (SMD) and 95% confidence intervals (CI).

$$SMD = \frac{M1i - M2i}{\sqrt{\frac{[(N1i-1)^{*}S1i^{2}+(N2i-1)^{*}S2i^{2}]}{(N1i+N2i-2)}}} \quad (3)$$

The effect sizes were interpreted as 0.2 for a small effect, 0.5 for a moderate effect, and 0.8 or greater for a large effect (Pei and Wu, 2019). We used a random effects model to correct for variable effect sizes due to the heterogeneity in included studies (e.g., characteristics of patients, walking environment, time, or outcome measures). The $I^2$ index was used to assess the study heterogeneity. In addition, we performed subgroup analyses for study characteristics (disease duration, type of dual-task, or hemispheres) to complete secondary analyses on the impacts of different factors. Publication bias was assessed using a visual inspection of funnel plots. Studies that fell outside the funnel shape had a high risk of bias.

## 2.5. Study quality assessment

The National Institutes of Health (NIH) Research Quality Assessment tool was used to assess the quality of each included study by two reviewers (QL and WJ). The "Quality Assessment Tool for Observational Cohort and Cross-Sectional Studies" was used for cross-sectional studies. The "Quality Assessment of Controlled Intervention Studies" was used for RCT. Each tool consisted of 14 questions. The study quality assessment helped to measure the strength of scientific evidence, but it was not used to determine the inclusion of studies. The GRADEPro (McMaster University, 2020, Ontario, Canada) was used for assessing the quality of the evidence. When two reviewers had a disagreement, a third person (SX) was consulted to resolve it.

# 3. Results

## 3.1. Selection process

A total of 377 articles were retrieved in the database from six databases, and three articles were identified through other sources. After removing duplicates, 189 eligible records were retrieved. In total, 174 articles were excluded from the title and abstract screening. After full-text reading, five articles were excluded because they did not meet the criteria. Finally, 10 articles were included in the review, and nine articles were included in the meta-quantitative analysis. One paper was excluded from the meta-analysis because it only performed the difference value between HbO and HbR without reporting the HbO data separately. The detailed process is shown in Figure 1.

## 3.2. Basic characteristics of the included studies

Tables 1, 2 summarize the information extracted from the 10 included articles. Eight articles were cross-sectional studies and two articles were RCTs. A total of 224 stroke patients were involved, including 32 patients in the subacute stage and 192 patients in the chronic stage. Five articles adopted the dual-task walking involving serial subtraction. Two articles adopted walking whilst obstacle crossing (Hawkins et al., 2018; Clark et al., 2021). Two articles adopted walking whilst n-back (Hermand et al., 2019, 2020). Two articles adopted walking whilst a verbal task (Hawkins et al., 2018; Lim et al., 2022). Only one paper adopted walking whilst picture-planning or stroop (Collett et al., 2021).

## 3.3. Meta-analysis

### 3.3.1. Primary and secondary analyses

#### 3.3.1.1. Activation of PFC: ST vs. DT

Figure 2 shows the overall meta-analysis of comparing the PFC activation between ST and DT. We found that there was more PFC activation when performing dual-task walking than when performing single-task walking. The total number of studies included in the random effect model was nine. Compared with the ST group, the overall effect size of HbO increase in the DT group was significant ($SMD = 0.340$, $P = 0.02$, $I^2 = 7.853\%$, 95% $CI = 0.054$–$0.626$).

#### 3.3.1.2. Variations of ST-DT diff: Comparing different disease durations

Subgroup analyses according to disease duration are shown in Figure 3. The ST-DT diff is significant for stroke patients in the chronic phase ($SMD = 0.369$, $P = 0.038$, $I^2 = 13.692\%$, 95%$CI = 0.020$–$0.717$), while no significant ST-DT diff was found in patients with subacute stroke ($SMD = 0.203$, $P = 0.419$, $I^2 = 0\%$, 95% $CI = -0.289$–$0.696$).

#### 3.3.1.3. Variations of ST-DT diff: Comparing different types of dual-task

Subgroup analyses according to the type of dual-task are shown in Figure 4. We separated the meta-analysis for serial subtraction, obstacle walking, and verbal and n-back tasks. We found that stroke patients who performed the dual-task walking combined with serial subtraction ($SMD = 0.516$, $P < 0.001$, $I^2 = 0\%$, 95% $CI = 0.239$–$0.794$), obstacle crossing ($SMD = 0.564$, $P = 0.002$, $I^2 = 0\%$, 95% $CI = 0.205$–$0.903$), or verbal task ($SMD = 0.654$, $P = 0.009$, $I^2 = 0\%$, 95% $CI = 0.164$–$1.137$) had greater PFC activation than performing single-task walking. Combined with the n-back task, it did not show a significant differentiation of activation compared with single-task walking ($SMD = 0.203$, $P = 0.419$, $I^2 = 0\%$, 95% $CI = -0.289$–$0.696$).

### 3.3.2. Sensitivity analyses

To further explore the effect of each article on the total effect size and the accuracy of the results, we performed a sensitivity analysis by sequentially excluding one of the studies, and then repeating the analysis. The results are shown in Figure 5. We found that the significance of the overall effect size changed when some studies were removed. But the results did not change direction. When study by Collett et al. was removed, the heterogeneity index $I^2$ of the combined results decreased to 0. We considered this study to have a large heterogeneity due to differences in design and equipment. Our results were robust when we included other studies with less heterogeneity.

### 3.3.3. Publication bias analyses

Figure 6 shows the funnel plot of the nine studies. We performed a publication bias analysis on the standard difference in means between ST and DT. We found that one article fell outside the funnel plot and had a large bias (Collett et al., 2021). The other articles were more evenly distributed and showed no hint of publication bias.

## 3.4. Study quality assessment

Table 3 reports the results of our study quality assessment. All of the eight cross-sectional studies clearly described the research question or purpose, and they followed the inclusion and exclusion criteria of the study. Their outcome measures were also clearly defined and adjusted for the effect of the relationship between exposure and outcome. Five studies examined different levels of the exposure as related to the outcome (Liu et al., 2018; Chatterjee et al., 2019; Hermand et al., 2019, 2020; Lim et al., 2022). Two studies did

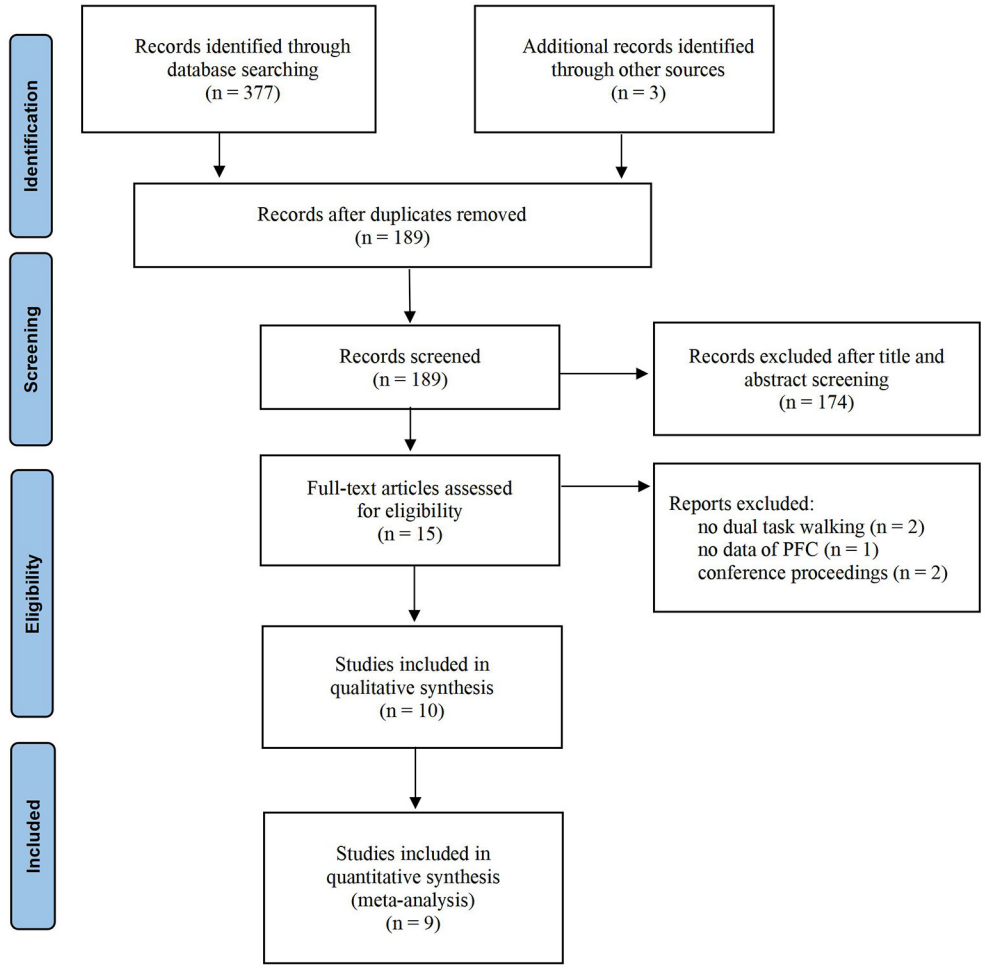


FIGURE 1
Systematic review, PRISMA flow diagram.

**TABLE 1** Study and participant characteristics.

| Study name | Study design | Participant characteristics | | | *N* |
|---|---|---|---|---|---|
| | | Age | Type of stroke | Disease duration | |
| Al-Yahya et al. (2016) | Cross-sectional | 59.61 ± 15.03 | Ischemic; Hemorrhagic | 26.5 ± 27.46[a] | 19 |
| Hawkins et al. (2018) | Cross-sectional | 58.0 ± 9.3 | Ischemic; Hemorrhagic | 18.3 ± 9.3[a] | 24 |
| Liu et al. (2018) | Cross-sectional | 51.5 | Ischemic; Hemorrhagic | 41.5[a] | 23 |
| Mori et al. (2018) | Cross-sectional | 61.1 ± 9.3 | Ischemic; Hemorrhagic | NR | 14 |
| Chatterjee et al. (2019) | Cross-sectional | 59.6 ± 9.7 | Ischemic; Hemorrhagic | 19.2 ± 10.4[a] | 33 |
| Hermand et al. (2019) | Cross-sectional | 71.4 ± 10.1 | Ischemic; Hemorrhagic | 45.5 ± 34.5[b] | 11 |
| Hermand et al. (2020) | Cross-sectional | 68.1 ± 9.4 | Ischemic; Hemorrhagic | 62.92 ± 32.61[b] | 21 |
| Clark et al. (2021) | RCT | 59.6 ± 9.15 | Ischemic; Hemorrhagic | 18.00 ± 10.48[a] | 38 |
| Collett et al. (2021) | RCT | 62 ± 14 | Ischemic; Hemorrhagic | 51 ± 59[a] | 21 |
| Lim et al. (2022) | Cross-sectional | 64 ± 7.6 | Ischemic; Hemorrhagic | 82 ± 67.4[a] | 20 |

[a]Represents the units are months.
[b]Represents the units are days.
RCT, randomized controlled trial; N, the size of sample; NR, not reported.

TABLE 2 Dual-task type and HbO data extraction.

| Study name | Type of dual task | Representative area | ST | | DT | | Unit | *N* |
|---|---|---|---|---|---|---|---|---|
| | | | Mean | SD | Mean | SD | | |
| Al-Yahya et al. (2016) | ①SS7 | Average L and R | 0.69 | 0.96 | 1.02 | 1.22 | μmol/L | 19 |
| Chatterjee et al. (2019) | ①SS7 | Average L and R | 0.26 | 0.52 | 0.92 | 0.98 | μmol/L | 33 |
| Clark et al. (2021) | ①SS7<br>②Obstacles | Average L and R | 0.34 | 0.89 | 0.84<br>0.8 | 0.95<br>1 | μmol/L | 38<br>38 |
| Hawkins et al. (2018) | ①Verbal<br>②Obstacles | Average L and R | 0.2 | 0.58 | 0.68<br>0.72 | 0.98<br>0.59 | μmol/L | 24<br>24 |
| Hermand et al. (2019) | ①1-back<br>②2-back | Average L and R | 2.42 | 1.93 | 2<br>2.69 | 2.24<br>2.22 | μmol/L | 11<br>11 |
| Hermand et al. (2020) | ②2-back | Affected | NR | NR | NR | NR | μmol/L | 21 |
| | ②2-back | Un-affected | 1.04 | 1.02 | 1.49 | 1.65 | μmol/L | 21 |
| Collett et al. (2021) | ①Stroop<br>②Planning | Affected | 0.67 | 0.26 | 0.33<br>0.42 | 0.38<br>0.36 | mmol/L | 15<br>15 |
| | ①Stroop<br>②Planning | Unaffected | 0.64 | 0.3 | 0.49<br>0.34 | 0.32<br>0.39 | mmol/L | 13<br>13 |
| Lim et al. (2022) | ①Easy verbal<br>②Hard verbal | Affected | 0.14 | 0.33 | 0.24<br>0.25 | 0.31<br>0.33 | μmol/L | 20<br>20 |
| | ①Easy verbal<br>②Hard verbal | Unaffected | 0.06 | 0.29 | 0.21<br>0.18 | 0.3<br>0.29 | μmol/L | 20<br>20 |
| Mori et al. (2018) | ①SS3 | Average L and R | −0.3 | 1.73 | −0.073 | 0.41 | AU | 14 |

ST, single-task; DT, dual-task; N, the size of sample; SD, standard deviation; SS7, serial-7 subtraction during walking; Obstacles, walking across obstacles; Stroop, auditory stroop task whilst walking; Planning, picture-planning whilst walking; SS3, serial-3 subtraction during walking; NR, not reported; L, left hemisphere; R, right hemisphere; affected, affected hemisphere; unaffected, unaffected hemisphere.

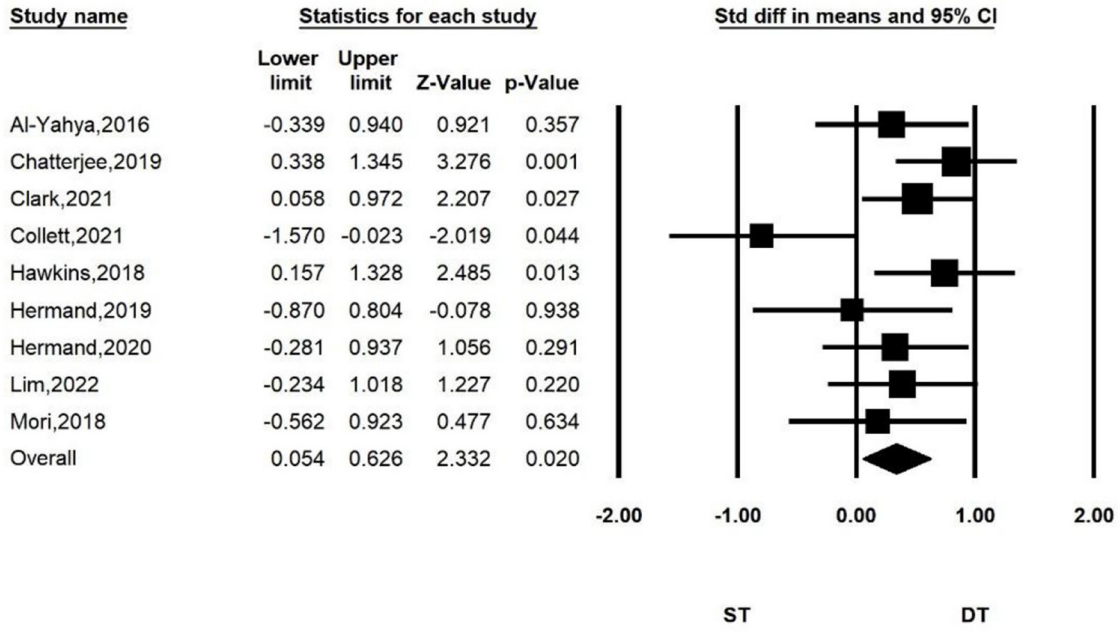


FIGURE 2
Forest plot for the PFC activation of DT group compared with ST group.

not implement consistently across all study participants (Hermand et al., 2019, 2020). Only one study provided a clear definition of the study population and reported that the participation rate of eligible persons was at least 50% (Liu et al., 2018). No study provided a sample size justification. Two RCTs used random sequence generation. Participants and assessments were blinded in only one study (Clark

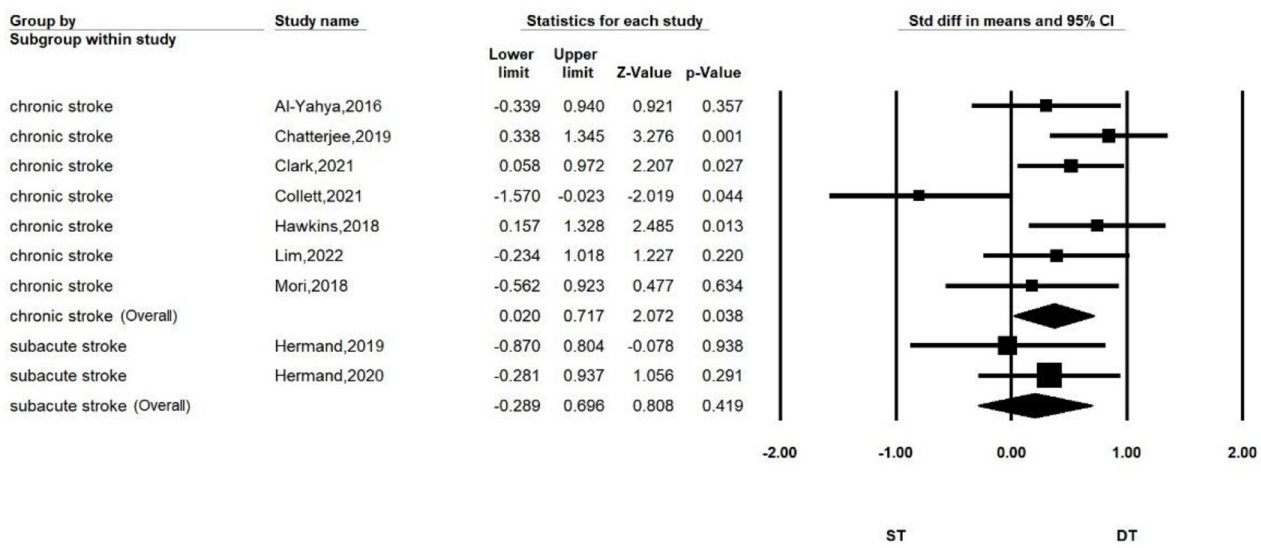


FIGURE 3
Forest plot for comparing PFC activation of ST and DT in subacute and chronic patients.

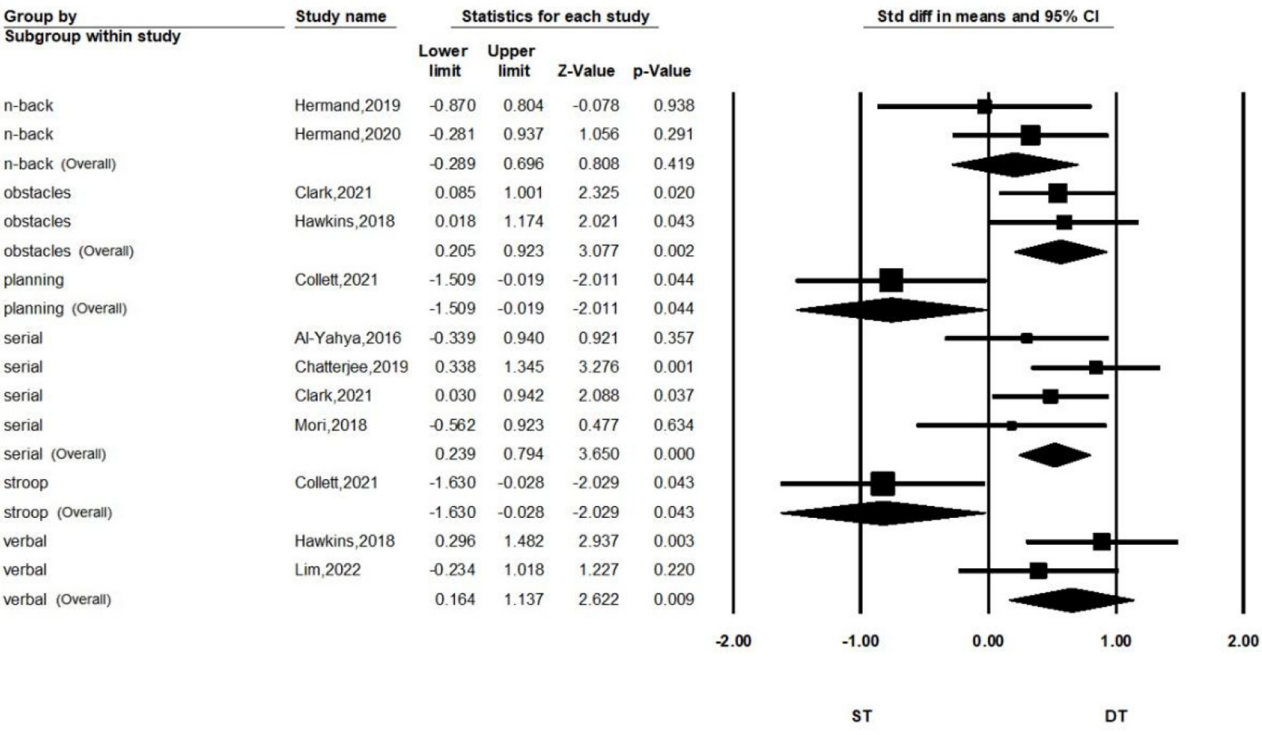


FIGURE 4
Forest plot for comparing PFC activation of ST and DT in different types of dual task.

et al., 2021). In the other study, only participants were blinded (Collett et al., 2021). All studies included had good study quality. Table 4 shows the quality of the evidence by GRADE criteria. Dual-task had higher PFC activation than single-task, with low certainty of evidence.

## 4. Discussion

This study systematically reviews and quantifies the differences in PFC activation between stroke patients performing single-task walking and dual-task walking. Our meta-analysis

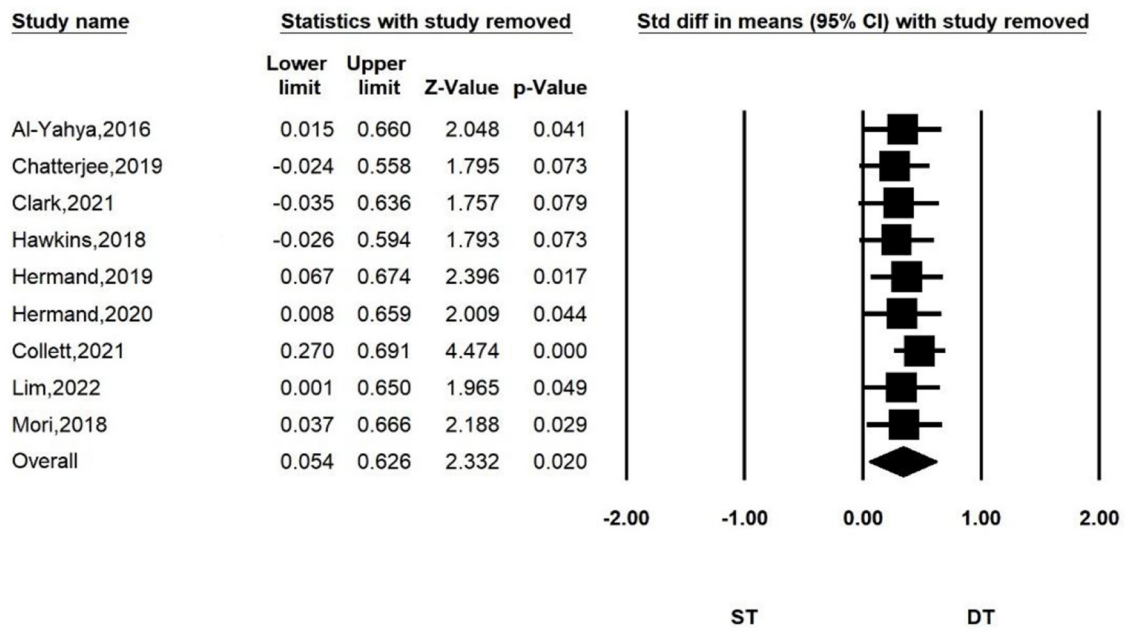


FIGURE 5
Sensitivity analysis for comparing PFC activation of ST and DT. When the following studies were excluded, the heterogeneity of the combined results was as follows: $I^2 = 9.878\%$ (Al-Yahya et al., 2016); $I^2 = 6.688\%$ (Chatterjee et al., 2019); $I^2 = 3.832\%$ (Clark et al., 2021); $I^2 = 5.709\%$ (Hawkins et al., 2018); $I^2 = 11.319\%$ (Hermand et al., 2019); $I^2 = 9.19\%$ (Hermand et al., 2020); $I^2 = 0\%$ (Collett et al., 2021); $I^2 = 9.03\%$ (Lim et al., 2022); $I^2 = 11.411\%$ (Mori et al., 2018).

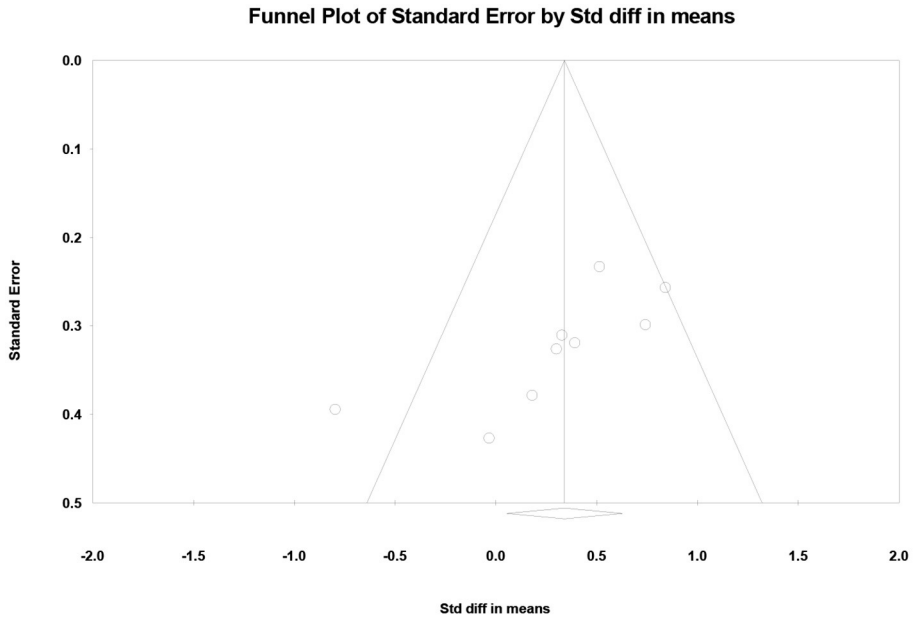


FIGURE 6
Funnel plots used to examine publication bias in dual task-single task differences in PFC activation.

shows that PFC activation is higher in stroke patients performing dual-task walking than single-task walking. This differences in this PFC activation also vary according to the different types of dual-task and different disease durations in stroke groups.

## 4.1. Activation of PFC: ST vs. DT

Our meta-analysis showed that there was a significant difference in PFC activation between stroke patients performing single-task walking and dual-task walking, which was mainly manifested by an

TABLE 3 Quality assessment.

| Study name | Q1 | Q2 | Q3 | Q4 | Q5 | Q6 | Q7 | Q8 | Q9 | Q10 | Q11 | Q12 | Q13 | Q14 | Total score |
|---|---|---|---|---|---|---|---|---|---|---|---|---|---|---|---|
| Cross-sectional studies | | | | | | | | | | | | | | | |
| Al-Yahya et al. (2016) | 1 | 0 | CD | 1 | 0 | 0 | 0 | NA | 1 | NA | 1 | NA | NA | 1 | 5/10 |
| Hawkins et al. (2018) | 1 | 0 | CD | 1 | 0 | 0 | 0 | NA | 1 | NA | 1 | NA | NA | 1 | 5/10 |
| Liu et al. (2018) | 1 | 1 | 1 | 1 | 0 | 0 | 0 | 1 | 1 | NA | 1 | NA | NA | 1 | 8/11 |
| Mori et al. (2018) | 1 | 0 | CD | 1 | 0 | 0 | 0 | NA | 1 | NA | 1 | NA | NA | 1 | 5/10 |
| Chatterjee et al. (2019) | 1 | 0 | CD | 1 | 0 | 0 | 0 | 1 | 1 | NA | 1 | NA | NA | 1 | 6/11 |
| Hermand et al. (2019) | 1 | 0 | CD | 1 | 0 | 0 | 0 | 1 | 0 | NA | 1 | NA | NA | 1 | 5/11 |
| Hermand et al. (2020) | 1 | 0 | CD | 1 | 0 | 0 | 0 | 1 | 0 | NA | 1 | NA | NA | 1 | 5/11 |
| Lim et al. (2022) | 1 | 0 | CD | 1 | 0 | 0 | 0 | 1 | 1 | NA | 1 | NA | NA | 1 | 6/11 |
| Controlled intervention studies | | | | | | | | | | | | | | | |
| Clark et al. (2021) | 1 | 1 | 1 | 1 | 1 | 1 | 1 | 1 | CD | 0 | 1 | 0 | 1 | 1 | 11/14 |
| Collett et al. (2021) | 1 | 0 | 1 | 1 | CD | 1 | 1 | 1 | 1 | 1 | 1 | 0 | 1 | 1 | 11/14 |

CD, cannot determine; NA, not applicable.

activation degree that was significantly increased during dual-task walking. The following are possible explanations for the results. First, compared with single-task processing, dual-task processing requires additional executive functions to resolve the interference between tasks. Previous studies indicated that the PFC is the main brain region responsible for executive functions in dual-task processing. The PFC has three subregions. The frontopolar cortex is mainly related to coordinating independent tasks processing. The medial frontal cortex forms reward expectations for task setting, based on motivational cues. The lateral prefrontal cortex is mainly responsible for the selection and characterization of task setting rules (Koechlin et al., 2003; Koechlin and Hyafil, 2007). When additional tasks are added, these relevant regions and networks will be mobilized further to complete the dual-task processing. Secondly, this may be the result of the loss of walking automaticity in stroke patients. Healthy individuals can switch intrinsically between automatic and executive control strategies (Clark, 2015). They can reduce the cognitive demands of walking when they perform dual-task walking and use remaining prefrontal resources to complete additional cognitive tasks. The presence of neurological damage in stroke patients exposes dual-task neurocompensatory mechanisms that resulting in a shift in motor strategy from normal automaticity to compensatory. The cognitive control of walking has to be enhanced when automated walking ability is diminished (Ehgoetz Martens et al., 2020). Thirdly, the confidence of patients in their own balance can affect walking performance (Danks et al., 2016). Patients with stroke have deficits in physical functioning, including motor and balance. So they become involuntarily nervous and concentrated when challenged with complex tasks. The fear of falling may massively increase their focus to cope with unfamiliar or unpredictable situations (Aihara et al., 2021). Eventually the patient exhibits a cautious gait and an increase in the control of walking (Rosén et al., 2005; Schinkel-Ivy et al., 2016).

However, a study showed the opposite result. Collett et al. showed that dual task brought lower PFC activity than single task (Collett et al., 2021). We consider that this heterogeneity stems from their different dual-task type. Stroop testing involves the handling of conflicts. Participants are required to perform a less automated task while simultaneously inhibiting a more automated task (Scarpina and Tagini, 2017). The picture planning task involves sequential planning of actions. We presume that the auditory stroop task and picture-planning task in their experiments made it impossible for the subjects to maintain their level of task performance when they reached the upper limits of their available neural resources, and their performances may have declined rapidly (Cabeza et al., 2002). This was similar to the results of an article observing older adults (Salzman et al., 2021). Moreover, one study argued from the concept of resource competition that reduced activation is consistent with the resource allocation model of dual-task processing (Low et al., 2009).

## 4.2. Variations of ST-DT diff: Comparing different disease durations

In our meta-analysis, chronic patients showed small effect sizes, but there were no significant effect sizes in patients in the subacute phase. We interpret that the source of the difference is existence of a "ceiling" phenomenon and can be explained by models of limited capacity. Additional cognitive tasks make it difficult to activate PFC more when the patients already perform single task at or near maximum prefrontal replenishment capacity. This phenomenon has been found in multiple studies (Chatterjee et al., 2019; Hermand et al., 2020). Subacute patients followed the "posture first" strategy to prioritize walking (Ohzuno and Usuda, 2019; Chan and Tsang, 2021). Then, they could only use a small portion of their remaining capacity for additional cognitive tasks, which was limited by a smaller reserve of cognitive resources. A study showed significant cognitive improvement in stroke patients at 3 and 12 months compared to baseline (Buvarp et al., 2021). In the subacute subgroup, the disease duration of the patients in the two included studies was <3 months, which was in the early subacute phase. At this time, it is still in the stage of motor and cognitive recovery. Another study also found that PFC activation was enhanced in stroke patients after prolonged rehabilitation (Miyai et al., 2003). Therefore, chronic patients may have better cognitive reserves and executive functioning after a period of recovery than those in the subacute phase. They were able to allocate more cognitive resources to cognitive tasks (Hermand et al.,

TABLE 4 The certainty of evidence by GRADE.

| No.of studies | Certainty assessment | | | | | | No.of patients | | Effect | | Certainty |
|---|---|---|---|---|---|---|---|---|---|---|---|
| | Study design | Risk of bias | Inconsistency | Indirectness | Imprecision | Other considerations | Dual task | Single task | Relative (95% CI) | Absolute (95% CI) | |
| 10 | Observational studies | Not serious[a] | Not serious[b] | Not serious[c] | Serious[d] | All plausible residual confounding would reduce the demonstrated effect[e,f,g,h] | 224 | 224 | - | SMD 0.34 (0.054 to 0.626) | ⊕⊕◯◯ Low |

CI, confidence interval; SMD, standardized mean difference.

[a]No studies with high risk of bias were identified.

[b]Three studies showed inconsistent results, but the heterogeneity test $I^2$ was < 10%.

[c]All studies explored-the association directly.

[d]The sample size of some studies was small and the confidence intervals were wide.

[e]The funnel plot showed that there was no significant publication bias.

[f]The effect sizes were interpreted as 0.2 for a small effect, 0.5 for a moderate effect, and 0.8 or greater for a large effect. This effect size was defined as small.

[g]The two tasks were performed by the same subject to avoid the interference of factors such as the course of the disease, the degree of cognition and the degree of movement.

[h]No study found a dose response gradient.

Study design represents the types of study designs, including randomized trial, observational study and any other evidence. Risk of bias represents the possible deviation between the results of a study and the real situation due to methodological problems. Inconsistency represents whether there are large differences in outcomes between studies.

Indirectness represents whether to compare the efficacy of two interventions directly and indirectly. Imprecision represents effect of the width of the confidence interval on the accuracy of the results. Certainty of evidence reflects the extent to which our confidence in an estimate of the effect is adequate to support a particular recommendation.

⊕⊕⊕ represents "High"; ⊕⊕◯◯ represents "Moderate"; ⊕◯◯◯ represents "Low"; ◯◯◯◯ represents "Very low".

2019). In addition, the subacute patients included in this study mainly underwent the n-back paradigm. This was too difficult to accomplish for subacute patients, who are inherently limited in their abilities. Hermand et al. also found a sharp decrease in the correct response rate when subjects performed the 2-back task, compared to the 1-back task (Hermand et al., 2019). This suggests that patients may drop out of cognitive tasks due to complexity, leading to a not significant ST-DT diff.

## 4.3. Variations of ST-DT diff: Comparing different types of dual-task

Another finding of our study is the different ST-DT diff when stroke patients perform different dual-task types. In our study, serial subtraction, crossing obstacles, and verbal dual tasks all showed moderate effect sizes. The largest effect size of ST-DT diff was found in the verbal task. This is consistent with the results reported by Bishnoi et al. (2021). Verbal tasks involve language-related channels in the frontal lobe. The inferior frontal junction (IFJ) in PFC as the language-related subregion has strong connectivity with known language-related subregions (Hwang et al., 2022). This combined cognitive and linguistic functional demand makes prefrontal activation more pronounced. For the other two dual-task types, a study reported that PFC activation is greater for the cognitive dual-task than for the motor dual-task (Lu et al., 2015). However, our analysis did not show a greater ST-DT diff for the serial subtraction task whilst walking than for the crossing obstacle task. Serial subtraction involves the formation of working memory and concept formation in executive functions while crossing obstacles involves decision planning and the monitoring of actions in executive functions (Darekar et al., 2017; Yang et al., 2018). No matter which dual-task paradigm is used, the brain needs the executive function of the PFC to coordinate and to complete the processing of the two tasks smoothly. Therefore, this caused a similar increase in ST-DT diff.

The n-back task while walking did not show significant ST-DT diff, which is consistent with the results reported by Hermand et al. (2019). This phenomenon may be related to its excessive difficulty. The n-back paradigm involves a mass of working memory. Subjects need to match the stimuli and make specific responses to the information (Li et al., 2021). This is a great challenge for the cognitively impaired stroke patients. They are at increased risk by focusing too much on cognition, so they will prioritize posture control to reduce fall risk (Yogev-Seligmann et al., 2012). At this time, the blood is diverted to other areas that are important for movement, and the transmission of HbO to the PFC is reduced (Beurskens et al., 2014). On the other hand, the inclusion of subacute patients may also have an impact, as mentioned earlier. The results of the more difficult auditory stroop task and the picture-planning task were also explained before.

## 4.4. Clinical implications

It was previously thought that the unique features of the dual-task were allowed to assess the risk of falling and the potential of patients to return to their homes and communities (Hyndman and Ashburn, 2004; Feld et al., 2018; Tsang and Pang, 2020). When patients perform

dual task, a poorer performance suggests an increased risk of falls (Wollesen et al., 2019). fNIRS brings more information as another tool. PFC overactivation during dual-task walking often suggests neural inefficiency and is accompanied by a decline in performance ability (Kahya et al., 2019). This indication also signals that the patient is still finding difficulty in walking independently and safely during daily life. Moreover, the variability of ST-DT diff between the dual-task paradigms also implies that different combinations of tasks should be considered during assessment. This will provide a more comprehensive understanding of the deficits in dual-task ability for different stroke patients.

The result may also inform the creation of future intervention programs for the rehabilitation of stroke patients. Many current dual-task trainings aim to use the dual-task practice to improve walking ability and executive function in stroke patients (Liu et al., 2017; Pang et al., 2018; Meester et al., 2019; Strobach, 2020). However, we need to be careful when choosing the cognitive task. We suggest that the intensity of DTI given should increase PFC activation without a significant deterioration in walking performance, in order to achieve the effect of promoting the functional recovery of brain regions and increased dual-task processing capacity. When the activation is too little, one can consider that the cognitive load is too small to achieve the purpose of training, and the other is that the cognitive load is too large, exceeding the upper limit of the patient's ability. This standardized dual-task combination can be used to observe the functional capacity of indicators in more challenging situations than conventional clinical testing, and to individually tailor corresponding interventions for stroke patients.

On the other hand, we do not recommend starting dual-task training in subacute patients, which not only increases the risk during training, but also, the training effect may not meet expectations. One study found that dual-task walking speed increased after dual-task training in patients with better walking abilities, but this was not effective in those with poorer abilities (Collett et al., 2021). We suggest that subacute patients with poorer function should focus more on improving the automation of walking, while chronic patients with better function increase the complexity of cognitive tasks.

### 4.5. Limitations

Our study also had certain limitations. Not only did stroke patients have activity changes in PFC during the performance of dual-task, but other brain regions such as SMA and PMC also underwent characteristic and regular changes in response to increased cognitive tasks. However, these messages were not included in our review, due to the fewer studies analyzing the activations in these brain regions. Additionally, the number of included studies in each of our subgroups varied, which may have biased the review. For example, when we compared the activation differences between subacute and chronic patients, the types of dual-task included in two subgroups included were different. Secondly, we found that most of the included studies used the combined HbO values of the left and right PFC, or compared the difference between the left and right hemispheres. Differences in PFC between the healthy and affected sides were less frequently reported. In general, strokes mostly involve unilateral damage. It is inconclusive as to whether this neural tissue damage makes the results of dual-task response different on the affected side of the brain. Moreover, the number of studies and the limited information available made it difficult to analyze other confounding factors, such as ischemic stroke vs. hemorrhagic stroke, different age groups of the stroke population, and treadmill vs. ground walking. The impacts of these factors should continue to be explored in the future.

## 5. Conclusions

Our meta-analysis shows differences in PFC activation after stroke between the performance of single and dual tasks, based on fNIRS measurements. It varies with the task type and disease duration. The results provide informative suggestions for the future clinical use of the dual-task paradigm to assess the extent of patient walking recovery and training effectiveness, and to predict community walking ability. This also provides a theoretical basis for a better understanding of post-stroke walking behavior deficits and the development of strategies to optimize safe mobility after stroke.

## Data availability statement

The original contributions presented in the study are included in the article, further inquiries can be directed to the corresponding authors.

## Author contributions

QW, SX, WD, and CG chose the topic. QW, SZ, and YSu searched and assessed the studies. WD and SX extracted and analyzed the data. QW, WD, YSh, and CK participated in the writing process. TW, CG, and YZ supervised in the whole process and made the final decision. All authors listed have made a substantial and direct contribution to the work.

## Funding

This work was supported by the National Key R&D Program of China (Grant Nos. 2018YFC2001600 and 2018YFC2001603).

## Acknowledgments

We genuinely thank the authors of the primary study who provided the data and each of the researchers who participated in this study.

## Conflict of interest

The authors declare that the research was conducted in the absence of any commercial or financial relationships that could be construed as a potential conflict of interest.

## Publisher's note

All claims expressed in this article are solely those of the authors and do not necessarily represent those of

their affiliated organizations, or those of the publisher, the editors and the reviewers. Any product that may be evaluated in this article, or claim that may be made by its manufacturer, is not guaranteed or endorsed by the publisher.

## Supplementary material

The Supplementary Material for this article can be found online at: https://www.frontiersin.org/articles/10.3389/fnins.2023.1111274/full#supplementary-material

## References


Aihara, S., Kitamura, S., Dogan, M., Sakata, S., Kondo, K., and Otaka, Y. (2021). Patients' thoughts on their falls in a rehabilitation hospital: A qualitative study of patients with stroke. *BMC Geriatr.* 21, 713. doi: 10.1186/s12877-021-02649-1

Al-Yahya, E., Johansen-Berg, H., Kischka, U., Zarei, M., Cockburn, J., and Dawes, H. (2016). Prefrontal cortex activation while walking under dual-task conditions in stroke: A multimodal imaging study. *Neurorehabil. Neural Repair* 30, 591–599. doi: 10.1177/1545968315613864

Baddeley, A., Della Sala, S., Papagno, C., and Spinnler, H. (1997). Dual-task performance in dysexecutive and nondysexecutive patients with a frontal lesion. *Neuropsychology* 11, 187–194. doi: 10.1037/0894-4105.11.2.187

Bernhardt, J., Hayward, K. S., Kwakkel, G., Ward, N. S., Wolf, S. L., Borschmann, K., et al. (2017). Agreed definitions and a shared vision for new standards in stroke recovery research: The Stroke Recovery and Rehabilitation Roundtable taskforce. *Int. J. Stroke* 12, 444–450. doi: 10.1177/1747493017711816

Beurskens, R., Helmich, I., Rein, R., and Bock, O. (2014). Age-related changes in prefrontal activity during walking in dual-task situations: A fNIRS study. *Int. J. Psychophysiol.* 92, 122–128. doi: 10.1016/j.ijpsycho.2014.03.005

Beyaert, C., Vasa, R., and Frykberg, G. E. (2015). Gait post-stroke: Pathophysiology and rehabilitation strategies. *Neurophysiol. Clin.* 45, 335–355. doi: 10.1016/j.neucli.2015.09.005

Bishnoi, A., Holtzer, R., and Hernandez, M. E. (2021). Brain activation changes while walking in adults with and without neurological disease: Systematic review and meta-analysis of functional near-infrared spectroscopy studies. *Brain Sci.* 11, 30291. doi: 10.3390/brainsci11030291

Blennerhassett, J. M., Levy, C. E., Mackintosh, A., Yong, A., and McGinley, J. L. (2018). One-quarter of people leave inpatient stroke rehabilitation with physical capacity for community ambulation. *J. Stroke Cerebrovasc. Dis.* 27, 3404–3410. doi: 10.1016/j.jstrokecerebrovasdis.2018.08.004

Buvarp, D., Rafsten, L., Abzhandadze, T., and Sunnerhagen, K. S. (2021). A prospective cohort study on longitudinal trajectories of cognitive function after stroke. *Sci. Rep.* 11, 17271. doi: 10.1038/s41598-021-96347-y

Cabeza, R., Anderson, N. D., Locantore, J. K., and McIntosh, A. R. (2002). Aging gracefully: Compensatory brain activity in high-performing older adults. *Neuroimage* 17, 1394–1402. doi: 10.1006/nimg.2002.1280

Caetano, M. J. D., Menant, J. C., Schoene, D., Pelicioni, P. H. S., Sturnieks, D. L., and Lord, S. R. (2017). Sensorimotor and cognitive predictors of impaired gait adaptability in older people. *J. Gerontol. A Biol. Sci. Med. Sci.* 72, 1257–1263. doi: 10.1093/gerona/glw171

Chan, W. N., and Tsang, W. W. N. (2021). Compromised cognition, but not stepping-down performance, when dual-tasking in stroke survivors. *J. Mot. Behav.* 2021, 1–10. doi: 10.1080/00222895.2021.1918054

Chatterjee, S. A., Fox, E. J., Daly, J. J., Rose, D. K., Wu, S. S., Christou, E. A., et al. (2019). Interpreting prefrontal recruitment during walking after stroke: Influence of individual differences in mobility and cognitive function. *Front. Hum. Neurosci.* 13, 194. doi: 10.3389/fnhum.2019.00194

Chen, W. L., Wagner, J., Heugel, N., Sugar, J., Lee, Y. W., Conant, L., et al. (2020). Functional near-infrared spectroscopy and its clinical application in the field of neuroscience: Advances and future directions. *Front. Neurosci.* 14, 724. doi: 10.3389/fnins.2020.00724

Clark, D. J. (2015). Automaticity of walking: Functional significance, mechanisms, measurement and rehabilitation strategies. *Front. Hum. Neurosci.* 9, 246. doi: 10.3389/fnhum.2015.00246

Clark, D. J., Rose, D. K., Butera, K. A., Hoisington, B., DeMark, L., Chatterjee, S. A., et al. (2021). Rehabilitation with accurate adaptability walking tasks or steady state walking: A randomized clinical trial in adults post-stroke. *Clin. Rehabil.* 35, 1196–1206. doi: 10.1177/02692155211001682

Collett, J., Fleming, M. K., Meester, D., Al-Yahya, E., Wade, D. T., Dennis, A., et al. (2021). Dual-task walking and automaticity after stroke: Insights from a secondary analysis and imaging sub-study of a randomised controlled trial. *Clin. Rehabil.* 35, 1599–1610. doi: 10.1177/02692155211017360

Collette, F., Olivier, L., Van der Linden, M., Laureys, S., Delfiore, G., Luxen, A., et al. (2005). Involvement of both prefrontal and inferior parietal cortex in dual-task performance. *Brain Res. Cogn. Brain Res.* 24, 237–251. doi: 10.1016/j.cogbrainres.2005.01.023

Danks, K. A., Pohlig, R. T., Roos, M., Wright, T. R., and Reisman, D. S. (2016). Relationship between walking capacity, biopsychosocial factors, self-efficacy, and walking activity in persons poststroke. *J. Neurol Phys. Ther.* 40, 232–238. doi: 10.1097/NPT.0000000000000143

Darekar, A., Lamontagne, A., and Fung, J. (2017). Locomotor circumvention strategies are altered by stroke: I. Obstacle clearance. *J. Neuroeng. Rehabil.* 14, 56. doi: 10.1186/s12984-017-0264-8

Delavaran, H., Jönsson, A. C., Lövkvist, H., Iwarsson, S., Elmståhl, S., Norrving, B., et al. (2017). Cognitive function in stroke survivors: A 10-year follow-up study. *Acta Neurol. Scand.* 136, 187–194. doi: 10.1111/ane.12709

Ehgoetz Martens, K. A., Matar, E., Shine, J. M., Phillips, J. R., Georgiades, M. J., Grunstein, R. R., et al. (2020). The neural signature of impaired dual-tasking in idiopathic rapid eye movement sleep behavior disorder patients. *Mov. Disord.* 35, 1596–1606. doi: 10.1002/mds.28114

Feld, J. A., Zukowski, L. A., Howard, A. G., Giuliani, C. A., Altmann, L. J. P., Najafi, B., et al. (2018). Relationship between dual-task gait speed and walking activity poststroke. *Stroke* 49, 1296–1298. doi: 10.1161/STROKEAHA.117.019694

Gramigna, V., Pellegrino, G., Cerasa, A., Cutini, S., Vasta, R., Olivadese, G., et al. (2017). Near-infrared spectroscopy in gait disorders: Is it time to begin? *Neurorehabil. Neural Repair* 31, 402–412. doi: 10.1177/1545968317693304

Hamacher, D., Herold, F., Wiegel, P., Hamacher, D., and Schega, L. (2015). Brain activity during walking: A systematic review. *Neurosci. Biobehav. Rev.* 57, 310–327. doi: 10.1016/j.neubiorev.2015.08.002

Handy, T. C. (2000). Capacity theory as a model of cortical behavior. *J. Cogn. Neurosci.* 12, 1066–1069. doi: 10.1162/08989290051137576

Hawkins, K. A., Fox, E. J., Daly, J. J., Rose, D. K., Christou, E. A., McGuirk, T. E., et al. (2018). Prefrontal over-activation during walking in people with mobility deficits: Interpretation and functional implications. *Hum. Mov. Sci.* 59, 46–55. doi: 10.1016/j.humov.2018.03.010

Hermand, E., Compagnat, M., Dupuy, O., Salle, J. Y., Daviet, J. C., and Perrochon, A. (2020). Functional status is associated with prefrontal cortex activation in gait in subacute stroke patients: A functional near-infrared spectroscopy study. *Front. Neurol.* 11, 559227. doi: 10.3389/fneur.2020.559227

Hermand, E., Tapie, B., Dupuy, O., Fraser, S., Compagnat, M., Salle, J. Y., et al. (2019). Prefrontal cortex activation during dual task with increasing cognitive load in subacute stroke patients: A pilot study. *Front. Aging Neurosci.* 11, 160. doi: 10.3389/fnagi.2019.00160

Hoshi, Y., Kobayashi, N., and Tamura, M. (2001). Interpretation of near-infrared spectroscopy signals: A study with a newly developed perfused rat brain model. *J. Appl. Physiol.* 90, 1657–1662. doi: 10.1152/jappl.2001.90.5.1657

Hwang, Y. E., Kim, Y. B., and Son, Y. D. (2022). Finding cortical subregions regarding the dorsal language pathway based on the structural connectivity. *Front. Hum. Neurosci.* 16, 784340. doi: 10.3389/fnhum.2022.784340

Hyndman, D., and Ashburn, A. (2004). Stops walking when talking as a predictor of falls in people with stroke living in the community. *J. Neurol Neurosurg. Psychiatry* 75, 994–997. doi: 10.1136/jnnp.2003.016014

Iqbal, M., Arsh, A., Hammad, S. M., Haq, I. U., and Darain, H. (2020). Comparison of dual task specific training and conventional physical therapy in ambulation of hemiplegic stroke patients: A randomized controlled trial. *J. Pak. Med. Assoc.* 70, 7–10. doi: 10.5455/J.P.M.A.10443

Jasdzewski, G., Strangman, G., Wagner, J., Kwong, K. K., Poldrack, R. A., and Boas, D. A. (2003). Differences in the hemodynamic response to event-related motor and visual paradigms as measured by near-infrared spectroscopy. *Neuroimage* 20, 479–488. doi: 10.1016/S1053-8119(03)00311-2

Kahya, M., Moon, S., Ranchet, M., Vukas, R. R., Lyons, K. E., Pahwa, R., et al. (2019). Brain activity during dual task gait and balance in aging and age-related neurodegenerative conditions: A systematic review. *Exp. Gerontol.* 128, 110756. doi: 10.1016/j.exger.2019.110756

Kim, H. Y., Seo, K., Jeon, H. J., Lee, U., and Lee, H. (2017). Application of functional near-infrared spectroscopy to the study of brain function in humans and animal models. *Mol. Cells* 40, 523–532. doi: 10.14348/molcells.2017.0153

Koechlin, E., and Hyafil, A. (2007). Anterior prefrontal function and the limits of human decision-making. *Science* 318, 594–598. doi: 10.1126/science.1142995

Koechlin, E., Ody, C., and Kouneiher, F. (2003). The architecture of cognitive control in the human prefrontal cortex. *Science* 302, 1181–1185. doi: 10.1126/science.1088545

Kondo, H., Osaka, N., and Osaka, M. (2004). Cooperation of the anterior cingulate cortex and dorsolateral prefrontal cortex for attention shifting. *Neuroimage* 23, 670–679. doi: 10.1016/j.neuroimage.2004.06.014

Leff, D. R., Orihuela-Espina, F., Elwell, C. E., Athanasiou, T., Delpy, D. T., Darzi, A. W., et al. (2011). Assessment of the cerebral cortex during motor task behaviours in adults: A systematic review of functional near infrared spectroscopy (fNIRS) studies. *Neuroimage* 54, 2922–2936. doi: 10.1016/j.neuroimage.2010.10.058

Li, W., Zhang, Q., Qiao, H., Jin, D., Ngetich, R. K., Zhang, J., et al. (2021). Dual n-back working memory training evinces superior transfer effects compared to the method of loci. *Sci. Rep.* 11, 3072. doi: 10.1038/s41598-021-82663-w

Lim, S. B., Louie, D. R., Peters, S., Liu-Ambrose, T., Boyd, L. A., and Eng, J. J. (2021). Brain activity during real-time walking and with walking interventions after stroke: A systematic review. *J. Neuroeng. Rehabil.* 18, 8. doi: 10.1186/s12984-020-00797-w

Lim, S. B., Peters, S., Yang, C. L., Boyd, L. A., Liu-Ambrose, T., and Eng, J. J. (2022). Frontal, sensorimotor, and posterior parietal regions are involved in dual-task walking after stroke. *Front. Neurol.* 13, 904145. doi: 10.3389/fneur.2022.904145

Liu, Y. C., Yang, Y. R., Tsai, Y. A., and Wang, R. Y. (2017). Cognitive and motor dual task gait training improve dual task gait performance after stroke—A randomized controlled pilot trial. *Sci. Rep.* 7, 4070. doi: 10.1038/s41598-017-04165-y

Liu, Y. C., Yang, Y. R., Tsai, Y. A., Wang, R. Y., and Lu, C. F. (2018). Brain activation and gait alteration during cognitive and motor dual task walking in stroke—A functional near-infrared spectroscopy study. *IEEE Trans. Neural Syst. Rehabil. Eng.* 26, 2416–2423. doi: 10.1109/TNSRE.2018.2878045

Lord, S. E., McPherson, K., McNaughton, H. K., Rochester, L., and Weatherall, M. (2004). Community ambulation after stroke: How important and obtainable is it and what measures appear predictive? *Arch. Phys. Med. Rehabil.* 85, 234–239. doi: 10.1016/j.apmr.2003.05.002

Low, K. A., Leaver, E. E., Kramer, A. F., Fabiani, M., and Gratton, G. (2009). Share or compete? Load-dependent recruitment of prefrontal cortex during dual-task performance. *Psychophysiology* 46, 1069–1079. doi: 10.1111/j.1469-8986.2009.00854.x

Lu, C. F., Liu, Y. C., Yang, Y. R., Wu, Y. T., and Wang, R. Y. (2015). Maintaining gait performance by cortical activation during dual-task interference: A functional near-infrared spectroscopy study. *PLoS ONE* 10, e0129390. doi: 10.1145/2818302

Meester, D., Al-Yahya, E., Dennis, A., Collett, J., Wade, D. T., Ovington, M., et al. (2019). A randomized controlled trial of a walking training with simultaneous cognitive demand (dual-task) in chronic stroke. *Eur. J. Neurol.* 26, 435–441. doi: 10.1111/ene.13833

Mehagnoul-Schipper, D. J., van der Kallen, B. F., Colier, W. N., van der Sluijs, M. C., van Erning, L. J., Thijssen, H. O., et al. (2002). Simultaneous measurements of cerebral oxygenation changes during brain activation by near-infrared spectroscopy and functional magnetic resonance imaging in healthy young and elderly subjects. *Hum. Brain Mapp.* 16, 14–23. doi: 10.1002/hbm.10026

Min, B. K., Kim, H. S., Ko, W., Ahn, M. H., Suk, H. I., Pantazis, D., et al. (2021). Electrophysiological decoding of spatial and color processing in human prefrontal cortex. *Neuroimage* 237, 118165. doi: 10.1016/j.neuroimage.2021.118165

Miyai, I., Yagura, H., Hatakenaka, M., Oda, I., Konishi, I., and Kubota, K. (2003). Longitudinal optical imaging study for locomotor recovery after stroke. *Stroke* 34, 2866–2870. doi: 10.1161/01.STR.0000100166.81077.8A

Moher, D., Liberati, A., Tetzlaff, J., and Altman, D. G. (2009). Preferred reporting items for systematic reviews and meta-analyses: The PRISMA statement. *Br. Med. J.* 339, b2535. doi: 10.1136/bmj.b2535

Moon, Y., Sung, J., An, R., Hernandez, M. E., and Sosnoff, J. J. (2016). Gait variability in people with neurological disorders: A systematic review and meta-analysis. *Hum. Mov. Sci.* 47, 197–208. doi: 10.1016/j.humov.2016.03.010

Mori, T., Takeuchi, N., and Izumi, S. I. (2018). Prefrontal cortex activation during a dual task in patients with stroke. *Gait Posture* 59, 193–198. doi: 10.1016/j.gaitpost.2017.09.032

Ohzuno, T., and Usuda, S. (2019). Cognitive-motor interference in post-stroke individuals and healthy adults under different cognitive load and task prioritization conditions. *J. Phys. Ther. Sci.* 31, 255–260. doi: 10.1589/jpts.31.255

Pang, M. Y. C., Yang, L., Ouyang, H., Lam, F. M. H., Huang, M., and Jehu, D. A. (2018). Dual-task exercise reduces cognitive-motor interference in walking and falls after stroke. *Stroke* 49, 2990–2998. doi: 10.1161/STROKEAHA.118.022157

Parris, B. A., Wadsley, M. G., Hasshim, N., Benattayallah, A., Augustinova, M., and Ferrand, L. (2019). An fMRI study of response and semantic conflict in the stroop task. *Front. Psychol.* 10, 2426. doi: 10.3389/fpsyg.2019.02426

Pashler, H. (1994). Dual-task interference in simple tasks: Data and theory. *Psychol. Bull.* 116, 220–244. doi: 10.1037/0033-2909.116.2.220

Pei, L., and Wu, H. (2019). Does online learning work better than offline learning in undergraduate medical education? A systematic review and meta-analysis. *Med. Educ. Onl.* 24, 1666538. doi: 10.1080/10872981.2019.1666538

Perrey, S. (2014). Possibilities for examining the neural control of gait in humans with fNIRS. *Front. Physiol.* 5, 204. doi: 10.3389/fphys.2014.00204

Pinti, P., Tachtsidis, I., Hamilton, A., Hirsch, J., Aichelburg, C., Gilbert, S., et al. (2020). The present and future use of functional near-infrared spectroscopy (fNIRS) for cognitive neuroscience. *Ann. N. Y. Acad. Sci.* 1464, 5–29. doi: 10.1111/nyas.13948

Rosén, E., Sunnerhagen, K. S., and Kreuter, M. (2005). Fear of falling, balance, and gait velocity in patients with stroke. *Physiother. Theory Pract.* 21, 113–120. doi: 10.1080/09593980590922299

Saini, V., Guada, L., and Yavagal, D. R. (2021). Global epidemiology of stroke and access to acute ischemic stroke interventions. *Neurology* 97(20 Suppl.2), S6–s16. doi: 10.1212/WNL.0000000000012781

Salzman, T., Tobón Vallejo, D., Polskaia, N., Michaud, L., St-Amant, G., Lajoie, Y., et al. (2021). Hemodynamic and behavioral changes in older adults during cognitively demanding dual tasks. *Brain Behav.* 11, e02021. doi: 10.1002/brb3.2021

Scarpina, F., and Tagini, S. (2017). The stroop color and word test. *Front. Psychol.* 8, 557. doi: 10.3389/fpsyg.2017.00557

Schinkel-Ivy, A., Inness, E. L., and Mansfield, A. (2016). *Relationships Between Fear of Falling, Balance Confidence, and Control of Balance, Gait, and Reactive Stepping in Individuals With Sub-acute Stroke. [1879-2219 (Electronic)].*

Strobach, T. (2020). The dual-task practice advantage: Empirical evidence and cognitive mechanisms. *Psychon. Bull. Rev.* 27, 3–14. doi: 10.3758/s13423-019-01619-4

Tsang, C. S., Wang, S., Miller, T., and Pang, M. Y. (2022). Degree and pattern of dual-task interference during walking vary with component tasks in people after stroke: A systematic review. *J. Physiother.* 68, 26–36. doi: 10.1016/j.jphys.2021.12.009

Tsang, C. S. L., and Pang, M. Y. C. (2020). Association of subsequent falls with evidence of dual-task interference while walking in community-dwelling individuals after stroke. *Clin. Rehabil.* 34, 971–980. doi: 10.1177/0269215520923700

Udina, C., Avtzi, S., Durduran, T., Holtzer, R., Rosso, A. L., Castellano-Tejedor, C., et al. (2019). Functional near-infrared spectroscopy to study cerebral hemodynamics in older adults during cognitive and motor tasks: A review. *Front. Aging Neurosci.* 11, 367. doi: 10.3389/fnagi.2019.00367

Veldkamp, R., Goetschalckx, M., Hulst, H. E., Nieuwboer, A., Grieten, K., Baert, I., et al. (2021). Cognitive-motor interference in individuals with a neurologic disorder: A systematic review of neural correlates. *Cogn. Behav. Neurol.* 34, 79–95. doi: 10.1097/WNN.0000000000000269

Wickens, C. D. (2002). Multiple resources and performance prediction. *Theoret. Iss. Erg. Sci.* 3, 159–177. doi: 10.1080/14639220210123806

Wollesen, B., Wanstrath, M., van Schooten, K. S., and Delbaere, K. (2019). A taxonomy of cognitive tasks to evaluate cognitive-motor interference on spatiotemoporal gait parameters in older people: A systematic review and meta-analysis. *Eur. Rev. Aging Phys. Act.* 16, 12. doi: 10.1186/s11556-019-0218-1

Yang, L., Lam, F. M., Huang, M., He, C., and Pang, M. Y. (2018). Dual-task mobility among individuals with chronic stroke: Changes in cognitive-motor interference patterns and relationship to difficulty level of mobility and cognitive tasks. *Eur. J. Phys. Rehabil. Med.* 54, 526–535. doi: 10.23736/S1973-9087.17.04773-6

Yogev-Seligmann, G., Hausdorff, J. M., and Giladi, N. (2012). Do we always prioritize balance when walking? Towards an integrated model of task prioritization. *Mov. Disord.* 27, 765–770. doi: 10.1002/mds.24963

Young, M. J., Regenhardt, R. W., Leslie-Mazwi, T. M., and Stein, M. A. (2020). Disabling stroke in persons already with a disability: Ethical dimensions and directives. *Neurology* 94, 306–310. doi: 10.1212/WNL.0000000000008964

frontiers | Frontiers in Neuroscience

TYPE Clinical Trial
PUBLISHED 24 February 2023
DOI 10.3389/fnins.2023.1101751



OPEN ACCESS

EDITED BY
Yong Hu,
The University of Hong Kong,
Hong Kong SAR, China

REVIEWED BY
Ningbo Yu,
Nankai University, China
Yaohua Liu,
Shanghai First People's Hospital, China

*CORRESPONDENCE
Dingguo Zhang
✉ d.zhang@bath.ac.uk

†These authors have contributed equally to this work

SPECIALTY SECTION
This article was submitted to Translational Neuroscience, a section of the journal Frontiers in Neuroscience

RECEIVED 18 November 2022
ACCEPTED 31 January 2023
PUBLISHED 24 February 2023

CITATION
Zhang B, Huang F, Liu J and Zhang D (2023) Bilateral transcranial direct current stimulation may be a feasible treatment of Parkinsonian tremor. *Front. Neurosci.* 17:1101751. doi: 10.3389/fnins.2023.1101751



# Bilateral transcranial direct current stimulation may be a feasible treatment of Parkinsonian tremor

Bin Zhang[1†], Feifei Huang[2†], Jun Liu[2] and Dingguo Zhang[3*]

[1]State Key Laboratory of Mechanical Systems and Vibrations, Robotics Institute, Shanghai Jiao Tong University, Shanghai, China, [2]Department of Neurology, Rui Jin Hospital, School of Medicine, Shanghai Jiao Tong University, Shanghai, China, [3]Department of Electronic and Electrical Engineering, University of Bath, Bath, United Kingdom

**Background:** Parkinsonian tremor is a common pathological tremor that affects over 6 million people worldwide. It lowers patients' quality of life and threatens their career development, especially when patients' occupation requires dexterous manipulation. In spite of current available treatments in clinics, there is a lack of low-cost, low side-effect, effective solutions for Parkinsonian tremor. Transcranial direct current stimulation (tDCS) may be an alternative treatment.

**Objective:** In this research, we explored the immediate effect of tDCS with a novel bilateral electrode setup over Parkinsonian tremor. In such a bilateral setup, the cathode was placed over the primary cortex contralateral to the more affected side of Parkinsonian tremor while the anode symmetrically over the other hemisphere. It was designed as a modification to the traditional cathodal setup. The performance of this bilateral setup was compared with three other setups including anodal setup, cathodal setup, and sham (control).

**Methods:** A randomized, sham-controlled, double-blind, crossover experiment was carried out over 13 qualified patients diagnosed with idiopathic Parkinson's disease (PD). Before and after the stimulus of each tDCS setup, subjects were tested before and after tDCS with four measures, including the Unified Parkinson's Disease Rating Scale (UPDRS), Fahn-Tolosa-Marin Tremor Rating Scale (FTMTRS), Purdue Pegboard Test (PPT) and a self-design Continuous Tremor Signal Assessment (CTSA). Tremor intensity calculated from CTSA data were regarded as the primary outcome of the experiment.

**Results:** Statistical results of CTSA, FTMTRS and PPT showed both bilateral tDCS and cathodal tDCS effectively suppressed Parkinsonian tremor. A quantitative comparison of the effect in tremor suppression indicated the optimal suppressive effect was obtained with bilateral tDCS. Based on the results of UPDRS, anodal tDCS was found to benefit subjects' overall performance the most, however, it had little effect in improving Parkinsonian tremor, as revealed by the results of other evaluations.

**Conclusion:** Our study suggests a beneficial immediate effect of bilateral tDCS in Parkinsonian tremor suppression. In addition, we assume there may be an underlying interhemispheric unbalance of cortical excitability which contributes to Parkinsonian tremor genesis.

**Clinical trial registration:** Identifier: ChiCTR2100054804.

KEYWORDS

**transcranial direct current stimulation, Parkinson's disease, Parkinsonian tremor, tremor suppression, electrode setups**

## 1. Introduction

Pathological tremor is the most common movement disorder that manifests as an involuntary, large-amplitude, rhythmic oscillation in human body (Helmich et al., 2013). It lowers patients' quality of life by affecting their daily behaviors (Berk et al., 2002). Particularly by weakening limb control ability (especially fine movements), tremor can threaten patients' career development especially when patients' occupation requires dexterous manipulation (Dick et al., 2000; Lee et al., 2014). Parkinsonian tremor is an early unfatal symptom originated from Parkinson's disease (PD) (Deuschl et al., 1998). However, as time moves, it will deteriorate in intensity alongside with other complications (Weintraub and Stern, 2005; Tinazzi et al., 2006) and finally lead to subsequent fatal accidents, such as falls (Gray and Hildebrand, 2000). As indicated by a recent investigation related with PD patients, Parkinsonian tremor tremendously reduced patients' life satisfactory level (Rosqvist et al., 2017). To tackle this, a timely effective treatment is needed once Parkinsonian tremor takes place.

The most fundamental therapy targeting Parkinsonian tremor is pharmaceutical treatment. Although easy to access (levodopa, dopamine agonists etc.), it has been constantly reported with unsatisfactory side-effects as well as the weakening treatment effect post honeymoon (Rinne, 1983; Borovac, 2016; Nonnekes et al., 2016). Moreover, there is significant drug action difference between individuals, which may lead to suboptimal clinical prescription (Pavese et al., 2006; Tomlinson et al., 2010). Regardless of pharmaceutical treatments, deep brain stimulation (DBS) (Benabid, 2003), representative of relevant surgical operations, is mainly considered for the levodopa-responsive patients with intermediate symptoms of PD (Bronstein et al., 2011). It facilitates a reduction of dopamine absorption amount (Kleiner-Fisman et al., 2006) and substantially improve the quality of life with Parkinsonian tremor by decreasing the tremor intensity (Diamond and Jankovic, 2005). However, patients have to bear high cost for the surgical operation along with high risks of major surgery (hemorrhage, infection, hallucination, severe depression etc.) (Doshi, 2011). With regard to other available surgical treatments, pallidotomy and thalamotomy are little considered because of their irreversible lesion to the brain (Lee et al., 2018). Other novel attempts to offset Parkinsonian tremor with antagonist muscles includes methods applying functional electrical stimulation (FES) (Maneski et al., 2011; Zhang et al., 2011). However, it was withheld from practical use due to electric safety concern where electricity was applied directly to human skin surface.

Considering neuromodulation, there have been some promising, non-invasive neuromodulation techniques. One of them is transcranial direct current stimulation (tDCS) which elicits sustained cortical excitability alterations by inducing low-intensity direct currents onto the scalp (Nitsche et al., 2008). Compared to other neuromodulation techniques such as transcranial magnetic stimulation (TMS) that requires bulky and expensive device, tDCS requires much lower cost device and is more portable to be home-used (Hallett, 2007). Therefore, considering practical conditions, tDCS may better suit the vast and urgent need of patients suffering from Parkinsonian tremor. A quantity of studies investigating tDCS have been carried out and confirmed the efficacy of tDCS in various applications, including cognitive enhancement (Coffman et al., 2014), and disease treatments, such as depression treatment (Fregni et al., 2006a). Targeting incurable neurologic disorders, tDCS was first used in stroke. A study by Fregni et al. (2005) found out tDCS could significantly improve the motor functions of stroke patients with either anodal stimulus over their affected primary cortex or cathodal stimulus over their unaffected primary cortex. The effect of tDCS was also proven by other studies combining tDCS with other methods, such as tDCS + occupational therapy (Nair et al., 2011), tDCS + FES (Shaheiwola et al., 2018) etc. Additionally, the motor functions of stroke patients were found to improve better with combined methods than with either technique alone. Fundamental studies demonstrated the effect of tDCS is polarity-dependent: in general, anodal tDCS (a-tDCS) facilitates cortical excitability while cathodal tDCS (c-tDCS) inhibits (Nitsche and Paulus, 2000, 2001). A study by Mahmoudi et al. (2011) proposed a novel setup of electrode placement named bilateral tDCS, where two pairs of electrodes were used together. Their results showed bilateral tDCS induced more motor improvement in stroke patients than traditional setups. The effect of bilateral tDCS in motor cortex excitability alteration was proven by another study by Di Lazzaro et al. (2014) with motor evoked potentials (MEP).

The application of tDCS in Parkinson's disease was initiated by Fregni et al. (2006b). According to their MEP results, both anodal tDCS and cathodal tDCS elicited an immediate motor cortex excitability alteration after stimulus; however, UPDRS results showed only anodal tDCS facilitated a significant improvement in PD patients' comprehensive motor function. The lasting effect of tDCS in PD was demonstrated by Benninger et al. (2010) who conducted an 8-session anodal tDCS over a cohort of qualified PD patients. Their results showed long-term tDCS treatment could especially improve PD symptoms of bradykinesia and mobility. In addition, tDCS treatment was found to affect PD patients in working memory (Boggio et al., 2006), functional mobility (Manenti et al., 2014), freezing of gait (Valentino et al., 2014), executive function (Doruk et al., 2014) etc. Attempts to enhance the effect of tDCS were made by combining tDCS with other methods, such as gait training (Costa-Ribeiro et al., 2017; Fernández-Lago et al., 2017), dancing (Kaski et al., 2014) and cognitive training (Manenti et al., 2018). While most studies evaluated the effect of tDCS with scales targeting the comprehensive motor function behaviors of PD, few has focused on Parkinsonian tremor.

In our research, we investigated the immediate effect of tDCS with different electrode placement setups and focused on Parkinsonian tremor which occurs in upper limbs. A novel bilateral electrode setup was considered (bilateral tDCS, b-tDCS) where a pair of anode and cathode was placed over the scalp symmetrically. It was designed as a modification of anodal setup. We expected b-tDCS could produce a similar or better effect in suppressing Parkinsonian tremor. This bilateral setup was never used for PD, however has been tested to be safe in studies of stroke treatment. Related to PD, we found only one study investigating balance and fear of fall, where bilateral anodal tDCS was applied and two pairs of electrodes were used (Hadoush et al., 2018). Thus, to our knowledge, the bilateral setup used in our research was the first

time to be applied in the topic of PD. As comparison, traditional anodal and cathodal setup (a-tDCS and c-tDCS), along with sham tDCS (s-tDCS) as control, were considered in the experiment. In addition, primary motor cortex (M1) was chosen as the target area for stimulation in accordance with previous studies (Fregni et al., 2006b; Benninger et al., 2010).

# 2. Methods

## 2.1. Subjects

The research has been approved by the Chinese Clinical Trial Registry (Registration No.: ChiCTR2100054804) and the local Ethics Committee of Shanghai Jiao Tong University, China (Approved No. of Ethic Committee: 2019 Clinical Trial No. 136). All subjects provided written consent after being informed of the purpose and the procedures of the experiment. The overall experiment was strictly performed in accordance with all relevant guidelines and regulations of the institutional review board and the Declaration of Helsinki. Patients were recruited by the department of neurology of Rui Jin Hospital (Shanghai, China). All of them were out-patients with upper limb tremor resulted from Parkinson's disease (Excluded $N = 11$; Not meeting the inclusion criteria $N = 7$; Declined to participate $N = 4$) (Figure 1).

The inclusion criteria for subjects were: (1) age between 50 and 80 years old, (2) confirmed diagnosis of idiopathic Parkinson's disease according to the MDS clinical diagnostic criteria for PD (Postuma et al., 2015), (3) symptom of upper limb tremor (rest tremor or postural tremor) resulted from PD, and (4) modified Hoen & Yahr (H&Y) Stage 1 to 3 (Hoehn and Yahr, 1967). The exclusion criteria included: (1) history of other diseases that may lead to pathological tremor, such as essential tremor (Deuschl et al., 1998), (2) under the treatment of other neuromodulation therapy, such as DBS, within recent 1 month, (3) history of mental problems, including anxiety, dementia, hallucination or delusion etc., (4) strong reliance on anti-Parkinson medications, or (5) history of cognitive disorder [Mini-mental State Examination (MMSE) score $\leq 16$] (Tombaugh and McIntyre, 1992).

The average disease duration of PD among all subjects [7M/6F, all right-handed, aged 67.5 $\pm$ 4.9 (mean $\pm$ SD)] were 4.38 $\pm$ 1.86 (mean $\pm$ SD) years. The Unified Parkinson's Disease Rating Scale (UPDRS) score ranged from 20 to 78 [31.7 $\pm$ 15.4 (mean $\pm$ SD)] while the modified H&Y stage ranged from 1.0 to 3.0 [1.8 $\pm$ 0.8 (mean $\pm$ SD)]. The tremor was found to be lateralized in all subjects. Throughout the manuscript, we refer to the more-affected side (MAS) as the side of body exhibiting more severe tremor, which was determined visually by an experienced physician, while the less-affected side (LAS)was defined as the other. Of all subjects, about half ($n = 7$) were found to be more-affected by tremor on the left side with the other half ($n = 6$) on the right side. The average levodopa-equivalent daily dose (LEDD) among all subjects was 278.8 $\pm$ 203.3 (mean $\pm$ SD) mg according to the calculation protocol provided by Tomlinson et al. (2010). In order to exclude drug effects, all subjects were told to discontinue anti-Parkinson medications on the day of the experiment, which ensured a withdrawal period of more than 12 h. Anti-Parkinson medications were resumed immediately after the experiment session of the day.

## 2.2. Study design

The experiment followed a randomized, sham-controlled, double-blind, crossover design (Schulz et al., 2010). It was designed based on the baseline stability assumption that the subjects could maintain a constant tremor manifestation if left unaffected. The aim of this experiment is to investigate the short-term (immediate) effect over Parkinsonian tremor, with three different active tDCS setups, namely the anodal, cathodal and bilateral setup. In order to exclude placebo effects, a control setup with sham tDCS was considered for comparison. Therefore, the complete experiment consisted of four different setups, with each corresponding to a session in the experiment (Figure 2). The sequence of carrying out the four sessions over each subject was generated by a random sequence generator programmed on Matlab R2015b (Mathworks Inc., USA). Each session was conducted around the same time of the day to minimize the circadian influences. It started with the pre-intervention evaluations involving three clinical scales and the continuous tremor signal assessment (CTSA), followed immediately by the tDCS intervention (sham/active) and the post-intervention evaluation. During the experiment, a specific physician served as the evaluator and finished all evaluations, while another experimenter performed the tDCS intervention. All subjects and the physician were blind to the current tDCS setup. Between each session, there was a long enough wash-out period of more than 2 days to clear up the effect of the previous intervention. In subsequent analysis, we evaluated the effect of the current setup of tDCS by comparing the performance of subjects before and after the tDCS intervention.

The three related clinical scales were: (1) UPDRS, (2) Fahn-Tolosa-Marin Tremor Rating Scale (FTMTRS) and (3) Purdue Pegboard Test (PPT). To lessen the time cost of the evaluation, full UPDRS and full FTMTRS were only used as a pre-intervention evaluation and a simplified version of them, namely the simplified version with only Part III of the UPDRS that relates motor function (UPDRS-III) and the modified FTMTRS (mFTMTRS) comprising Part A and Part B in FTMTRS, was used as the post-intervention evaluation. The assessment of the PPT remained the same before and after the intervention. To obtain more accurate and detailed description of tremor, we designed the procedure of CTSA where tremor acceleration and EMG signals were assessed. The sensors used for the CTSA were kept on subjects until the end of the post-intervention CTSA. In case that the accelerometer and EMG sensors might interfere with subjects' performance in chosen scales, we modified the sequence of the measures and arranged CTSA to be the last pre-intervention evaluation and the first post-intervention evaluation.

## 2.3. Intervention

To apply tDCS, a commercial CE-certified device named DC-Stimulator (NeuroConn GmbH, Germany) was used. For each subject, we started by locating the primary motor cortex (M1) on the more-affected side through targeting the abductor pollicis brevis (APB) hot spot at rest with transcranial magnetic stimulation (TMS) with a device called Magstim Rapid 2 (Magstim Co., UK).

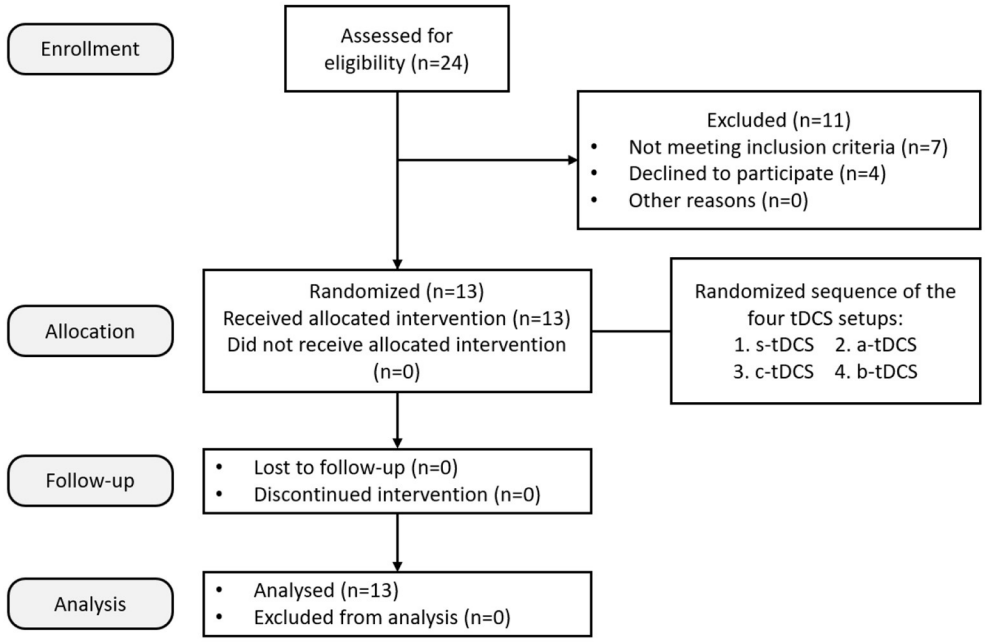


FIGURE 1
CONSORT diagram demonstrating the study recruitment process.

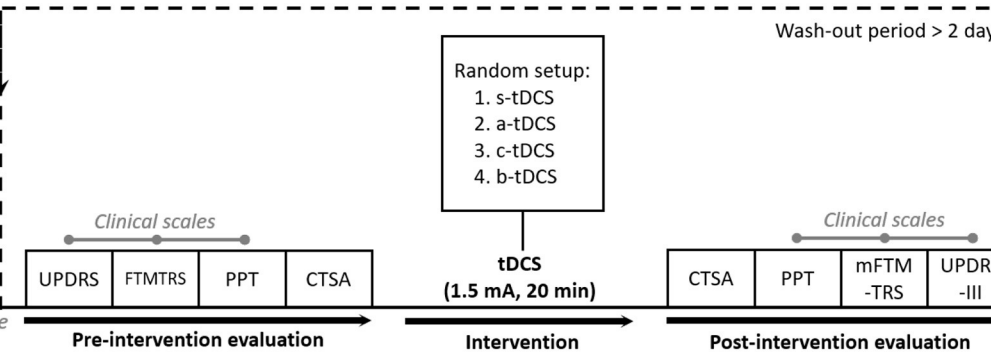


FIGURE 2
Experimental protocol.

A pair of sponge electrodes (6.5 cm*6.5 cm) moistened with 0.9% NaCl solution were placed regarding different tDCS setups, as shown in Figure 3A (assuming the MAS is on subject's left side): in the anodal setup, the anode was placed over the left M1 hotspot and the cathode was placed over the right supraorbital region. An opposite electrode placement setup was used in the cathodal setup. For bilateral setup, we placed the anode and the cathode over the right and the left M1 hotspot symmetrically. In all aforementioned active stimulations, a direct current of 1.5 mA was delivered constantly to the skull over 20 min with a ramp-up and ramp-down of 20 s. The parameters of the active stimulations were chosen in accordance with the most up-to-date safety guidelines for tDCS (Bikson et al., 2016). In sham tDCS, the electrode placement was the same as in the bilateral setup, however, in the 20-min protocol the direct current only lasted for a short time, followed by a serial pulse train of 110 uA (Figure 3B) without any therapeutic effect (Palm et al., 2013). In either active or sham setup of tDCS, the subject was seated comfortably on a chair in a quiet state and waited until the end of the intervention.

## 2.4. Continuous tremor signal assessment

In order to quantify upper limb tremor for comparison, we collected two continuous tremor signals, which were tremor acceleration and EMG signals, respectively. Before experiment, the tremor type (postural tremor/resting tremor) to record of each subject was decided independently by a physician after patient's enrollment. The main principle of choosing the main tremor

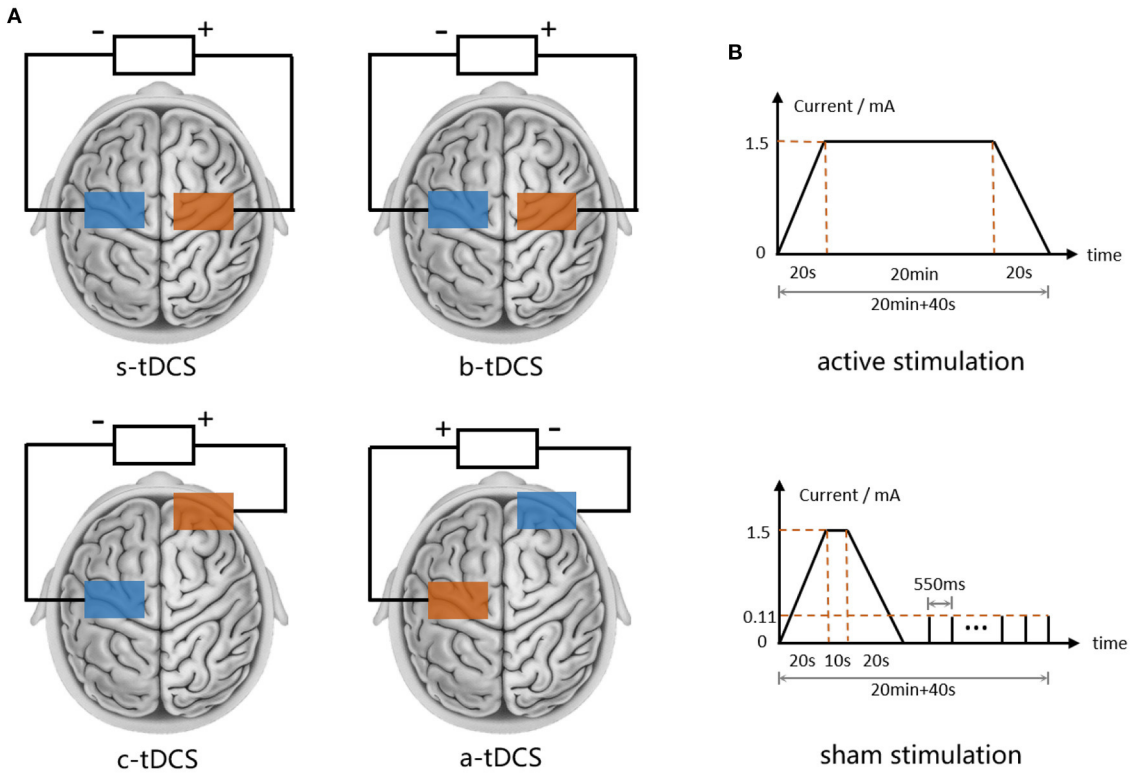


FIGURE 3
tDCS settings. **(A)** Electrode placement of s-tDCS, b-tDCS, c-tDCS and a-tDCS. **(B)** Current waveform of active and sham tDCS.

type is tremor intensity and stability. Intentional tremor was not considered in our research since it is difficult to standardize motion. For subjects whose main tremor type is resting tremor, we had them seated comfortably with arms fully supported on armrests and recorded their tremor. For the others, postural tremor was inspected with seated subject stretching the whole upper limb forward and maintaining the posture for some time (Zhang et al., 2018). Additional requirements in recording postural tremor included: (1) fingers closed, (2) palms facing downward, and (3) seated upright.

All data was recorded through a commercial device system named the Biometrics Datalog (Biometrics Inc., the USA), along with a three-axis accelerometer sensor and four surface EMG (sEMG) sensors. The accelerometer sensor was fixed onto the third knuckle of the middle finger on the more affected side. Four sEMG sensors were attached respectively onto the muscle bellies of the flexor carpi radialis (FCR), the flexor carpi ulnaris (FCU), the extensor carpi radialis (ECR) and the extensor carpi ulnaris (ECU). The data of tremor acceleration and EMG signals were both digitized into 1,000 Hz and simultaneously recorded. From each subject, we obtained a 5-min sequential data package comprising tremor acceleration and EMG signals.

## 2.5. Clinical measures

The full UPDRS is a standardized evaluation test for both motor and non-motor deficits of Parkinson's disease (Goetz et al., 2008) and was utilized in this experiment to assess the baseline of subjects. Since this research mainly focused on the symptom of tremor, a subscale consisting of Part III in UPDRS (UPDRS-III, Motor Examination) was used instead after intervention. The excluded parts were: (Part I) Non-motor Experiences of Daily Living, (Part II) Motor Experiences of Daily Living and (Part IV) Motor Complications, which were less associated with the immediate response of tremor.

FTMTRS is a tool used to evaluate tremor severity in human body (Fahn et al., 1993). The full scale was used in the pre-intervention evaluation to assess baseline. A subscale comprising Part A and Part B in FTMTRS was used as a corresponding post-intervention evaluation. We excluded Part C: Functional Disabilities Resulting from Tremor for it had less relevance with the short-term response in tremor.

PPT is a tool for manipulative dexterity evaluation and requires the subject to place the specific small objects as many as possible in the limited time (Tiffin and Asher, 1948). Since upper limb tremor was one of the factors that affect subject's hand dexterity, we assumed any change in subject's performance in PPT manifested the change in tremor severity. The scale consists of four parts: (1) moving pins with the right hand, (2) moving pins with the left hand, (3) moving pins with both hands and (4) assembling pins, collars and washers with both hands. We followed the standard procedure to implement PPT over subjects. Subjects were instructed to practice the tasks before the evaluation and afterwards underwent a three-trial PPT in both the pre- and post-evaluation.

## 2.6. Data processing

The raw scores of the clinical scales were summarized in Excel (2015, Microsoft Corp., the USA). For UPDRS-III, we computed: (1) the sum score of the UPDRS-III and (2) the sum score of item 20 and item 21 in UPDRS-III (UPDRS-III-tr). Please note that item 20 and item 21 in UPDRS III are the items that evaluates the intensity of upper limb resting tremor and postural tremor. For mFTMTRS, we computed: (1) the sum score of the mFTMTRS, (2) the sum score of the items related to the more-affected-side tremor (mFTMTRS-MAS) and (3) the sum score of the items related to the less-affected-side tremor (mFTMTRS-LAS). Assuming the more affected side was the right side of the body, the items related to mFTMTRS-MAS were item 5, 8, 11-Right, 12-Right, 13-Right, 14-Right, and 15-Right while items related to mFTMTRS-LAS were item 6, 8, 11-Left, 12-Left, 13-Left, 14-Left, and 15-Left. For PPT, the score of each item was first averaged among the 3 trials of PPT. We then computed: (1) the sum score of the PPT, (2) the score related to the more affected hand (PPT-MAS) and (3) the score related to the less affected hand (PPT-LAS). Assuming the more affected side was the right side, the score related to the more affected hand was the score of part 1, and the score related to the less affected hand was that of part 2.

The sequential data of the CTSA was converted into its text format and processed in Matlab (R2017a, MathWorks Inc., the USA). For three-axis tremor acceleration signals, the z-axis data that incorporated the most information of tremor (perpendicular to the ground) was used for analysis. A second-order zero-phase Butterworth bandpass filter with a passband from 0.5 Hz to 10 Hz was applied over the z-axis data to remove the zero-shifting of hardware sampling, the low-frequency voluntary movement components and the high-frequency irrelevant components (e.g., noise). For ease of further calculation, the filtered acceleration signal was then down-sampled to 100 Hz. For EMG signals, we applied a second-order zero-phase Butterworth bandpass filter with a passband from 0.5 Hz to 450 Hz to preserve the significant components of EMG activities (Merletti and Di Torino, 1999). A denoising notch filter was then utilized to remove the 50-Hz power line interference and its higher harmonics. Among the four EMG channels, the one with the largest mean absolute value (MAV) was selected for further analysis.

Both filtered acceleration and EMG signals were subsequently characterized in amplitude, frequency and shape. To feature amplitude, we computed root mean square (RMS) value as the primary outcome (Equation 1).

$$RMS = \sqrt{\frac{1}{N}\sum_{i=1}^{N} x_i^2} \tag{1}$$

where $x_i$ is the $i$-th sample in the data sequence ($i = 1, 2, \ldots, N$).

In addition, the filtered acceleration data of each subject was segmented with a 1-second non-overlap sliding window, after which a set of each subject consisting of 300 acceleration segments could be generated. For each subject, we computed the RMS value of each acceleration segment and generated the set of segmented RMS (sRMS) value (Equation 2).

$$\text{sRMS} = \{\text{RMS}(X_1), \text{RMS}(X_2), \ldots, \text{RMS}(X_{N_X})\} \tag{2}$$

where $X_j \in A$ is the $j$-th segment of set $A$ ($j = 1, 2, 3, \ldots, N_X$).

The sRMS sequence was then sorted from small to large and generated another sequence called sorted sRMS (ssRMS) sequence. The ssRMS sequence manifested the distribution of sub-regional tremor amplitude. For ease of description, the ssRMS values were labeled from 1 to 300 based on their numerical order in the ssRMS sequence. The maximum value in the ssRMS sequence was also marked down as a feature for tremor acceleration.

To characterize the filtered tremor acceleration sequence in frequency, we computed the dominant frequency of its bispectrum. Bispectrum transform was chosen because it is mathematically able to describe non-linear, non-Gaussian, stochastic signals, such as Parkinson's tremor signals. It yields features that are more stable and anti-noise compared to those generated from power spectrum density (PSD) (Zhang et al., 2018). Here in this research, we computed dominant frequency by tracking the peak frequency on the diagonal slice of bispectrum. For EMG signals, we computed the feature called zero-crossing (ZC) to represent frequency, as shown in Equation 3.

$$\text{ZC} = \sum_{i=1}^{N} sgn(-x_i x_{i+1}) \tag{3}$$

where $sgn(x) = \begin{cases} 1 & x > 0 \\ 0 & \text{otherwise} \end{cases}$.

With regard to shape factor, asymmetry between upper and lower waveform is one of the most characteristic features for tremor acceleration data. The third momentum was commonly used to quantify such a feature (Timmer et al., 1993; Jang et al., 2013). However, the third momentum considers time series data samples in an isolated manner and thus leads to the loss of information in time dimension. To solve the problem, we proposed another feature termed upper-lower symmetry (ULS) index inspired by cross-correlation function (Equation 4). The ULS index evaluates the symmetry of a zero-mean sequence by computing the maximum cross-correlation between its upper and lower waveform (Equations 5, 6). Its value ranges between 0 and 1 and is more sensitive in shape factor than the third momentum.

$$\text{ULS} = \max R_{X_U X_L}(\tau) = \max \sum_{n=-\infty}^{\infty} x_U^*(i) x_L(i+\tau) \tag{4}$$

$$x_U(i) = \begin{cases} x(i) & \text{sign}(x(i)) \geq 0 \\ 0 & \text{otherwise} \end{cases} \tag{5}$$

$$x_L(i) = \begin{cases} -x(i) & \text{sign}(x(i)) < 0 \\ 0 & \text{otherwise} \end{cases} \tag{6}$$

where $x_U(i)$ denotes the upper waveform sequence, $x_L(i)$ denotes the lower waveform sequence and $R_{X_U X_L}(\tau)$ denotes the cross-correlation function between the upper and lower waveform with delay $\tau$.

For EMG signal, we computed its approximate entropy (ApEn) with parameters: embedded dimension $m = 2$ and tolerance $r = 0.2$*std. ApEn assessed the shape of the EMG signals by evaluating the regularity and complexity in time domain (Pincus, 1994).

To compare the difference in tremor before and after a certain intervention, we considered two indexes which were: absolute post/pre ratio (Equation 7) and relative post/pre ratio (Equation 8). The absolute post/pre ratio is a basic measure considering mainly the time factor and represents the difference between post-intervention condition and pre-intervention condition. The relative post/pre ratio is a more discreet measure that considers potential confounding factors, such as placebo effect. It was basically calculated as the absolute post/pre ratio of an active tDCS setup subtracted by the absolute post/pre ratio of sham setup. It represented the real difference induced by a certain tDCS setup. Both indexes ranged above 0. A larger post/pre ratio above 1 indicated a more prominent effect of tDCS. On the opposite, a smaller post/pre ratios below 1 indicated a more prominent effect.

$$\text{Absolute post/pre ratio} = \frac{Post_{cur}}{Pre_{cur}} \tag{7}$$

where $Post_{cur}$ and $Pre_{cur}$ denote the value of an index after and before intervention, respectively.

$$\text{Relative post/pre ratio} = \frac{Post_{active}}{Pre_{active}} - \frac{Post_{sham}}{Pre_{sham}} + 1 \tag{8}$$

where $Post_{active}$ and $Pre_{active}$ denote the value of an index after and before a certain active tDCS intervention, and $Post_{sham}$ and $Pre_{sham}$ denote the value of an index after and before sham tDCS.

## 2.7. Statistics

The post/pre ratios of each feature was grouped based on the factor of session (tDCS setup). For absolute post/pre ratios, the data was grouped with four levels (s-tDCS, a-tDCS, c-tDCS, and b-tDCS) while that of the relative post/pre ratios was grouped with three levels (a-tDCS, c-tDCS, and b-tDCS). The Gaussianity of each group and their homogeneity of variance were tested by the Lilliefors test and the Bartlett test. If the null hypothesis of both tests held, namely the groups were both Gaussian and homogeneous in variance, a one-way analysis of variance (ANOVA) with repeated measures was performed, followed by the Tukey-Kramer *post-hoc* analysis. Otherwise, a non-parametric statistical test called the Friedman test was performed, followed by the Nemenyi *post-hoc* analysis. Since the purpose of the analysis over the absolute post/pre ratios was to investigate the effectiveness of the active setups, we considered the performance in the control (s-tDCS) session as a baseline and compared only the pairs between the control (s-tDCS) session and the active tDCS (a-tDCS, c-tDCS, and b-tDCS) sessions in *post-hoc*. In contrast, the relative post/pre ratio was analyzed to investigate the difference between different active tDCS sessions without the baseline effect of the control (s-tDCS) setup. We considered all possible session pairs that were between different active tDCS setups in *post-hoc*.

The baseline stability assumption was verified from two aspects. First, for short-term baseline stability (within one single session), we inspected the pre- and the post-data of each subject and grouped them based on the factor of time with two levels (pre s-tDCS and post s-tDCS). If the null hypothesis of the Lilliefors test and the Bartlett test held, the paired student's t-test was performed. Otherwise, the Wilcoxon signed rank test was performed. Second, for long-term baseline stability (across different sessions), the pre-intervention data of different tDCS setups was targeted and grouped based on the factor of session with 4 levels (pre s-tDCS, pre a-tDCS, pre c-tDCS, and pre b-tDCS). The grouped data was analyzed with the same statistical procedure as in post/pre ratios.

All statistics were performed using Matlab (R2017a, MathWorks Inc., the USA) with the basic level of statistical significance set at $p < 0.05$.

# 3. Results

## 3.1. Baseline stability

A paired student's t-test was performed over the UPDRS-III sum score of the control (s-tDCS) session to evaluate the short-term baseline stability. The result showed there was no significant difference between the pre- and post-data [$t_{(12)} = -0.433, p = 0.672$]. Likewise, no significant difference between the pre- and post-data was found in the result by a Wilcoxon signed rank test over the mFTMTRS sum score ($Z = 0.264, p = 0.792$), the PPT sum score ($Z = -0.786, p = 0.432$), the RMS value of tremor acceleration ($Z = -0.594, p = 0.552$) and the RMS value of EMG signal ($Z = -1.712, p = 0.087$), respectively.

For long-term baseline stability, only the pre-intervention data of each session was targeted. The result of the repeated-measure ANOVA showed there was no significant effect of the factor of session in the UPDRS-III sum score [$F_{(3,22)} = 0.544, p = 0.580$], the RMS value of the tremor acceleration [$F_{(3,33)} = 0.512, p = 0.565$] and the RMS value of the EMG signal [$F_{(3,33)} = 0.873, p = 0.396$], respectively. In addition, no significant effect in session was found in the mFTMTRS sum score [$\chi^2_{(3)} = 3.813, p = 0.282$] and the PPT sum score [$\chi^2_{(3)} = 4.861, p = 0.182$], as revealed by Friedman test.

## 3.2. CTSA

### 3.2.1. Tremor acceleration

For RMS value of tremor acceleration, there was a significant effect of the factor of session in the absolute post/pre ratio [$\chi^2_{(3)} = 32.5, p < 0.001$] and in the relative post/pre ratio [$F_{(2,22)} = 12.3, p < 0.001$]. Compared with the control (s-tDCS) session, we found a significant decrease in the c-tDCS session ($p = 0.0482$) and in the b-tDCS session ($p < 0.001$). The *post-hoc* analysis over the relative post/pre ratio showed the ratio in the b-tDCS was significantly lower than that in the a-tDCS session ($p < 0.001$) and the c-tDCS session ($p = 0.00635$). In addition, the relative post/pre ratio in the c-tDCS session was significantly lower than that in the a-tDCS session ($p = 0.00311$) (Figure 4A).

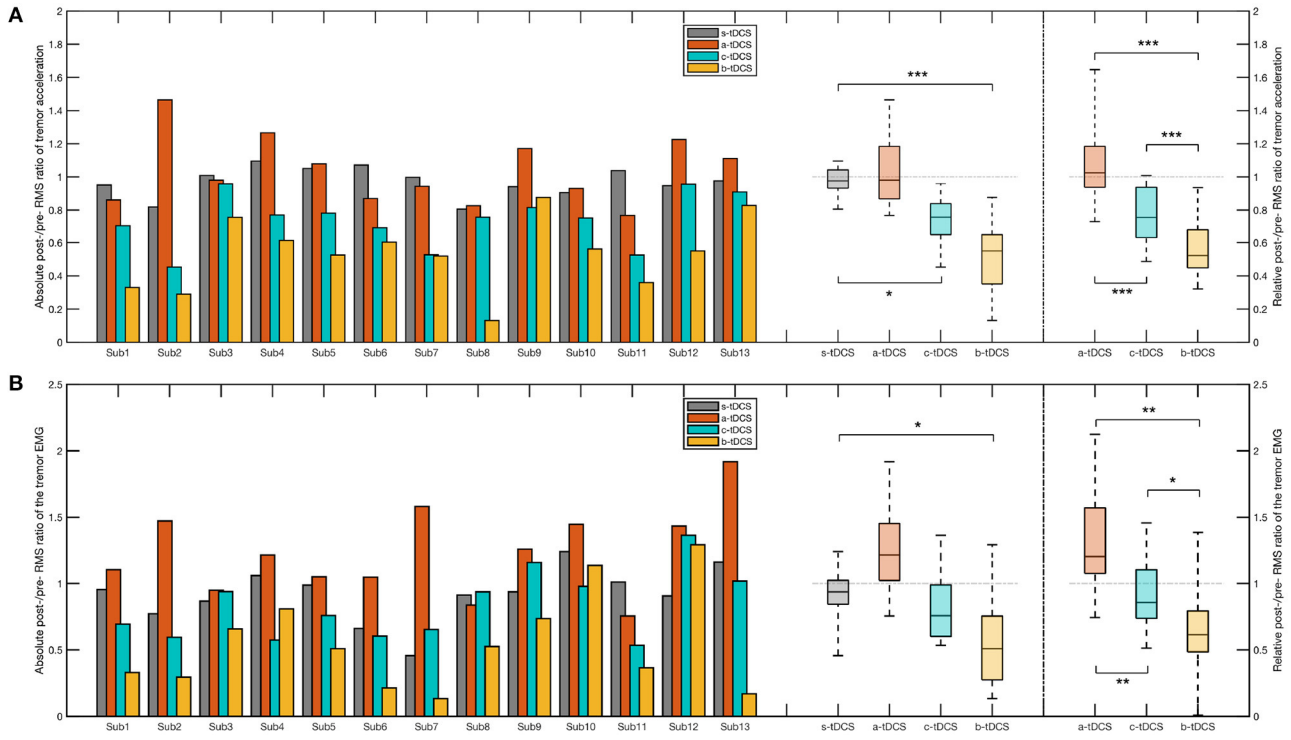


FIGURE 4
Bar plot and box plot of the post/pre ratios in the CTSA. **(A)** Left: The bar plot and the box plot representing the absolute post-/pre-RMS ratio of the tremor acceleration; Right: The box plot representing the relative post-/pre-RMS ratio of the tremor acceleration. **(B)** Left: The bar plot and the box plot representing the absolute post-/pre-RMS ratio of the EMG signal; Right: The box plot representing the relative post-/pre-RMS ratio of the EMG signal. In the *post-hoc* analysis of the absolute post/pre ratio, we considered only the session pairs between the control (s-tDCS) session and the active tDCS (a-tDCS, c-tDCS, and b-tDCS) session. In the *post-hoc* analysis of the relative post/pre ratios, all session pairs were considered. The significance of *post-hoc* analysis was indicated by asterisks ($^{*}p < 0.05$; $^{**}p < 0.01$; $^{***}p < 0.001$).

In order to compare in detail how the tremor amplitude differed across various tDCS setups, we computed the absolute post/pre ratio and the relative post/pre ratio of each value in the ssRMS sequence (Figure 5B). The post/pre ratios of the same kind with the same numerical label in the ssRMS sequence were grouped together based on the factor of session and afterwards statistically managed. The outcomes of the significance in the *post-hoc* analysis are shown in Figure 5A, where a plus sign indicates a significant difference between the current session pair at the current percentile. Based on these, the ratio of significant results for each session pair was computed. The b-tDCS session achieved the highest significance ratio of 45.7% among the three concerned active tDCS sessions, compared with the control (s-tDCS) session. The a-tDCS session achieved the lowest significance ratio of 0.00%, while the c-tDCS session achieved a medium significance ratio of 21.3%. When the relative post/pre ratios of active sessions were compared against each other, the significant results of all session pairs were found to occur densely from the 35th percentile to the 97th percentile (correspondingly, from Label No. 106 to Label No. 293 in the ssRMS sequence), as shown in the lower subfigure of Figure 5A. It's worth noting that no significant effect by session was found in either the absolute post/pre ratio [$F_{(3,33)} = 1.38, p = 0.271$] or the relative post/pre ratio [$F_{(2,22)} = 1.50, p = 0.247$] of the maximum ssRMS value.

With regard to the dominant frequency of bispectrum, no significant effect by session was found in the statistical analysis over the absolute post/pre ratio [$\chi^2_{(3)} = 5.21, p = 0.157$] and the absolute post/pre ratio [$\chi^2_{(2)} = 4.15, p = 0.125$], respectively. Likewise, for the ULS index, there was no significant effect by session found in the absolute post/pre ratio [$\chi^2_{(3)} = 5.95, p = 0.114$] and the absolute post/pre ratio [$F_{(2,22)} = 0.577, p = 0.564$], respectively.

### 3.2.2. EMG signal

In RMS value of EMG signals, we found a significant effect by session in both the absolute post/pre ratio [$F_{(3,33)} = 3.51, p = 0.0466$] and the relative post/pre ratio [$F_{(2,22)} = 4.31, p = 0.0452$], respectively. In the *post-hoc* analysis over the absolute post/pre ratio, a significant difference between the b-tDCS session and the control (s-tDCS) session was found ($p = 0.0113$). There was no significant difference between the a-tDCS session and the control (s-tDCS) session ($p = 0.686$), and between the c-tDCS session and the control (s-tDCS) session ($p = 0.0576$). In comparing between different active tDCS sessions, the *post-hoc* analysis over the relative post/pre ratio revealed both the c-tDCS session ($p = 0.00521$) and the b-tDCS ($p = 0.00152$) has a lower relative post/pre ratio than the a-tDCS session. In addition, the b-tDCS session yielded the lowest relative post/pre

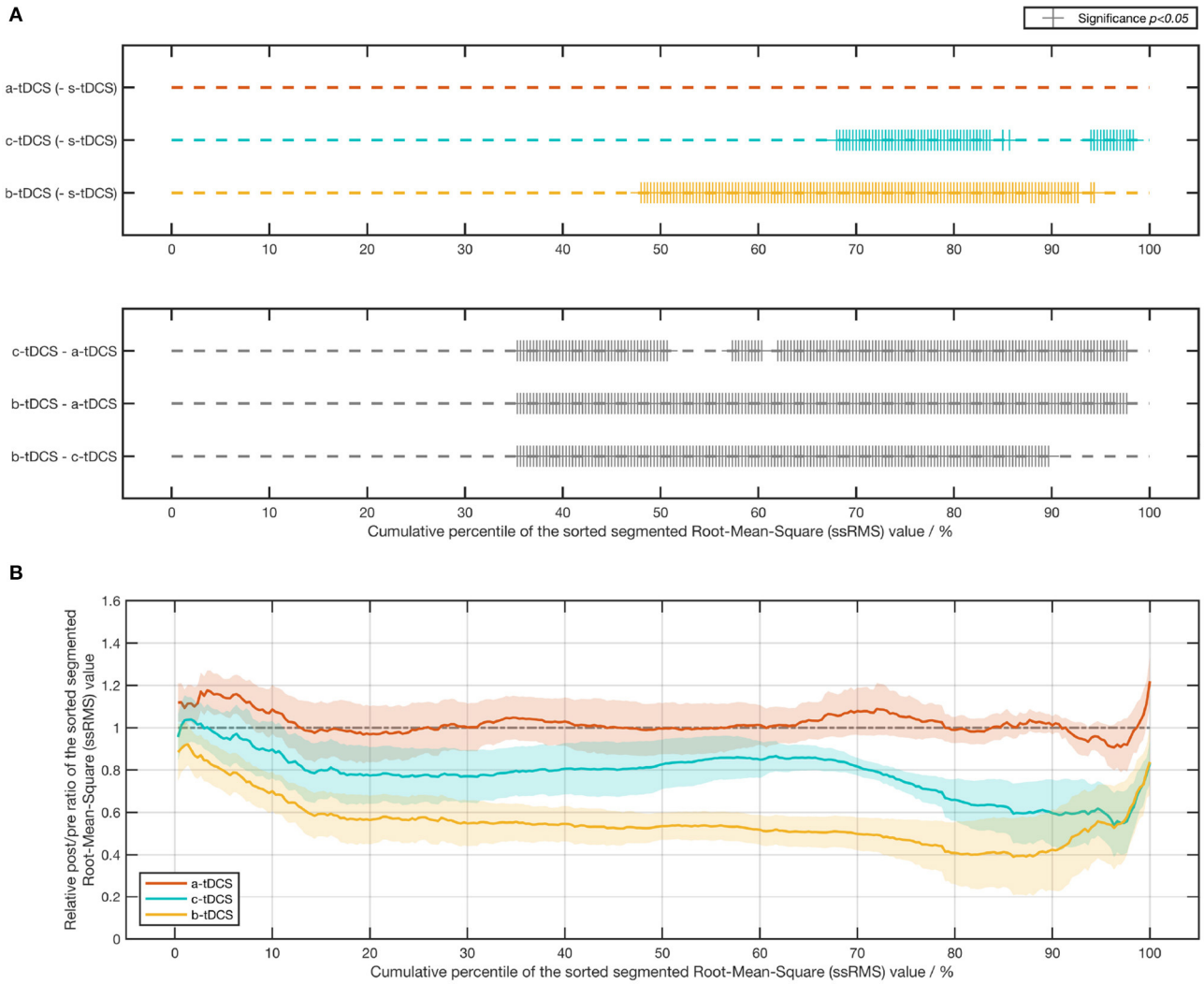


FIGURE 5
Results of the post/pre ratio of the sorted segmented root-mean-square (ssRMS) values in tremor acceleration. **(A)** Statistical significance of the post-/pre-ssRMS value ratio between different tDCS session pairs. **(B)** Line chart (mean ± SE) of the relative post-/pre-ssRMS value ratio of three active tDCS sessions.

ratio, even compared with the c-tDCS session ($p = 0.0136$) (Figure 4B).

No significant effect by session was found in the absolute post/pre ratio and the relative post/pre ratio of ZC [$\chi^2_{(3)} = 3.92, p = 0.270$]. Likewise, there was no significant session effect in the absolute post/pre ratio and the relative post/pre ratio of ApEn [$\chi^2_(3) = 5.77, p = 0.123$].

## 3.3. Clinical scales

### 3.3.1. UPDRS-III

To investigate the effectiveness of the three concerned tDCS setups, a Friedman test was performed over the absolute post/pre ratio of the sum score. The result showed there was a significant effect of the factor of session [$\chi^2_{(3)} = 16.1, p = 0.00110$]. Post-hoc analysis revealed, among the three concerned active setups, only the a-tDCS session resulted in a significant reduction of the absolute post/pre ratio compared with the control (s-tDCS) session ($p = 0.0186$). Likewise, we found a significant effect of session in the relative post/pre ratio [$\chi^2_{(3)} = 11.3, p = 0.00354$] and that the relative post/pre ratio in the a-tDCS session was significantly lower than that in the c-tDCS session in *post-hoc* ($p = 0.0031$) (Figure 6A).

When we only considered the items related to tremor, namely item 20 and item 21 of UPDRS-III (UPDRS-III-tr), a significant reduction of the absolute post/pre ratio was found in the b-tDCS session compared to the control (s-tDCS) session ($p < 0.001$). There was no significant difference between the a-tDCS session and the control (s-tDCS) session ($p = 1.00$) and no significant difference between the c-tDCS session and the control (s-tDCS) session ($p = 0.606$). There was a significant effect of the session factor in the relative post/pre ratio [$\chi^2(3) = 24.3, p < 0.001$]. *Post-hoc* analysis indicated there was a significant decrease in the b-tDCS session compared with the a-tDCS session ($p < 0.001$) and the c-tDCS session ($p = 0.0164$), respectively.

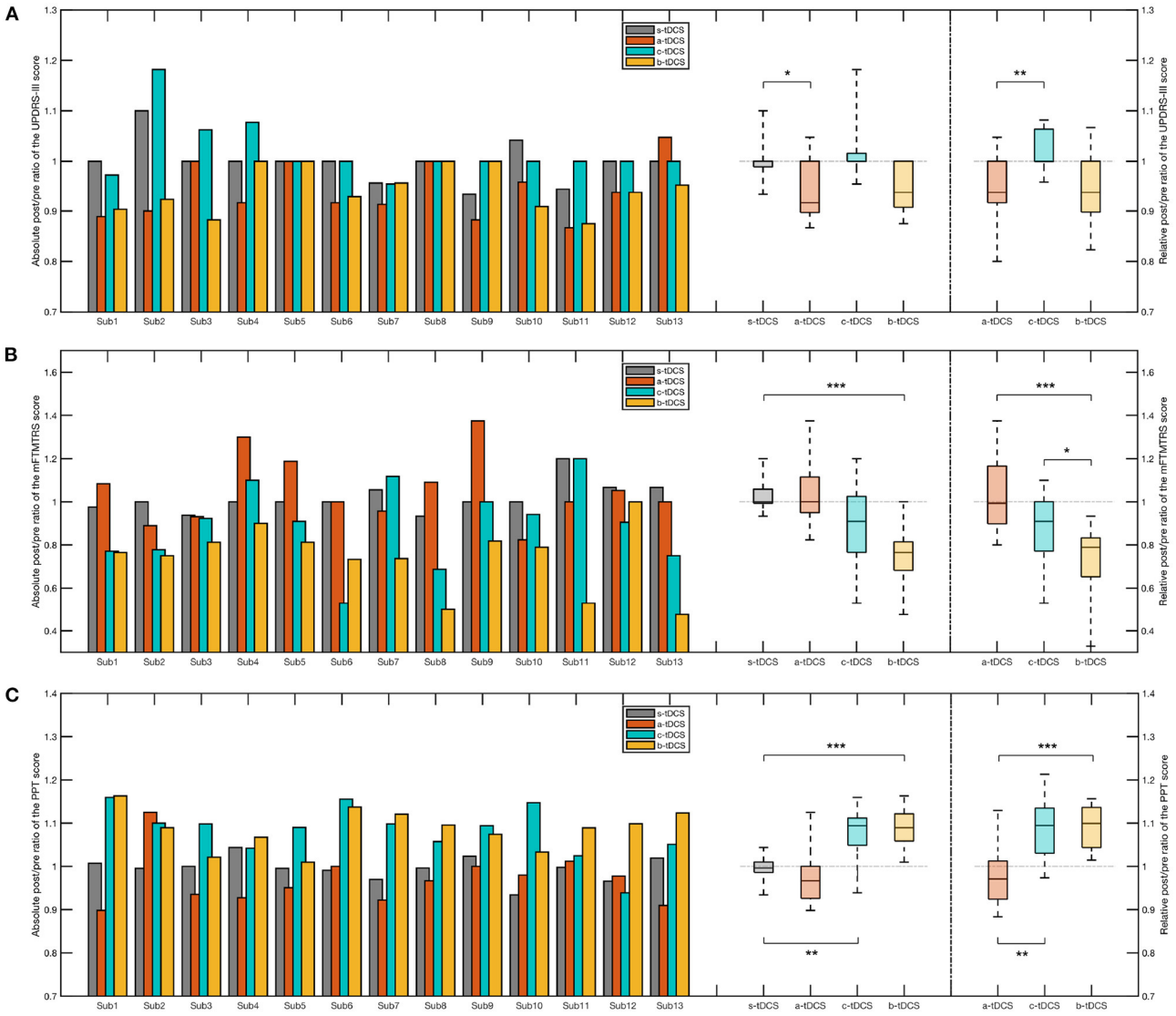


FIGURE 6
Bar plot and box plot of the post/pre ratios in different clinical measures. **(A)** Left: The bar plot and the box plot representing the absolute post/pre ratio of the UPDRS-III sum score; Right: The box plot representing the relative post/pre ratio of the UPDRS-III sum score. **(B)** Left: The bar plot and the box plot representing the absolute post/pre ratio of the mFTMTRS sum score; Right: The box plot representing the relative post/pre ratio of the mFTMTRS sum score. **(C)** Left: The bar plot and the box plot representing the absolute post/pre ratio of the PPT sum score; Right: The box plot representing the relative post/pre ratio of the PPT sum score. In the *post-hoc* analysis of the absolute post/pre ratio, we considered only the session pairs between the control (s-tDCS) session and the active tDCS (a-tDCS, c-tDCS, and b-tDCS) session. In the *post-hoc* analysis of the relative post/pre ratios, all session pairs were considered. The significance of *post-hoc* analysis was indicated by asterisks (*$p < 0.05$; **$p < 0.01$; ***$p < 0.001$).

### 3.3.2. mFTMTRS

Considering the sum score of mFTMTRS, there was a significant effect of the factor of session over the absolute post/pre ratio [$\chi^2_{(3)} = 24.3, p < 0.001$]. Among the three active tDCS sessions, only the b-tDCS session generated a significant difference compared with the control (s-tDCS) session ($p < 0.001$). With regard to the relative post/pre ratio, a significant increase was found in the b-tDCS session, compared with the a-tDCS session ($p < 0.001$) and the c-tDCS session ($p = 0.0488$), respectively (Figure 6B).

In analyzing the sum score of mFTMTRS-MAS, we found a significant effect by the factor of session in the absolute post/pre-ratio [$\chi^2_{(3)} = 18.4, p < 0.001$] and a significant decrease in the b-tDCS session compared with the control (s-tDCS) session ($p < 0.001$). The result of the *post-hoc* analysis over the relative post/pre ratio showed there was a significant decrease in the b-tDCS session compared with the a-tDCS session ($p = 0.0035$). Similar results were found in the analysis over the sum score of mFTMTRS-LAS. In an attempt to investigate whether there was a difference in the effect of tDCS between MAS and LAS, we computed the difference of the relative post/pre ratio between the mFTMTRS-MAS sum score and the mFTMTRS-LAS. A Friedman test was performed over the computed difference. However, no significant effect of session was found [$\chi^2_{(2)} = 0.0426, p = 0.979$].

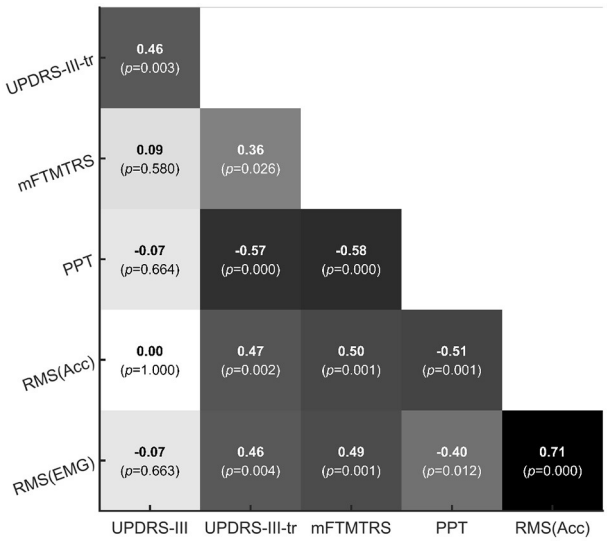


FIGURE 7
Correlation matrix of the relative post/pre ratio in different measures.

### 3.3.3. PPT

A repeated-measure ANOVA was performed over the absolute post/pre ratio of the PPT sum score, where a significant effect of session was found [$F_{(3,33)} = 6.28, p = 0.00323$]. The Tukey-Kramer *post-hoc* analysis showed there was a significant increase respectively in the c-tDCS session ($p = 0.00339$) and in the b-tDCS session ($p < 0.001$), compared with the s-tDCS session. The *post-hoc* analysis over the relative post/pre ratio revealed a significant difference between the c-tDCS session and the a-tDCS session ($p = 0.00541$), and between the b-tDCS session and the a-tDCS session ($p < 0.001$), respectively (Figure 6C).

Considering the sum score of PPT-MAS, we found a significant effect of the session factor in the absolute post/pre ratio [$\chi^2_{(3)} = 27.5, p < 0.001$] and the relative post/pre ratio [$\chi^2_{(3)} = 17.2, p < 0.001$], respectively. The *post hoc* analysis over the absolute post/pre ratio showed there was a significant increase in the c-tDCS session ($p = 0.0096$) and the b-tDCS session ($p < 0.001$) respectively, compared with the control (s-tDCS) session. A significant increase in the c-tDCS session ($p = 0.0048$) and in the b-tDCS session ($p < 0.001$), compared with the a-tDCS session, was found in statistical analysis over the relative post/pre ratio. With regard to the sum score of PPT-LAS, the statistical analysis revealed a result that was similar to that of PPT-MAS. To investigate whether there was a difference between MAS and LAS in the effect of active tDCS setups, a repeated-measure ANOVA was performed over the relative post/pre ratio difference between PPT-MAS and PPT-LAS. However, no significant effect of session was found [$F_{(2,22)} = 2.14, p = 0.147$].

## 3.4. Correlation between different measures

To investigate the correlation between different measures, a Spearman correlation analysis was performed over the relative post/pre ratio of the UPDRS-III sum score, the UPDRS-III-tr sum score, the mFTMTRS sum score, the PPT sum score, the RMS value of tremor acceleration and the RMS value of the EMG signal. The result of the Spearman correlation matrix is shown in Figure 7, where a darker background color indicates a higher Spearman correlation coefficient, and vice versa. The highest Spearman coefficient was found between the RMS value of tremor acceleration and the RMS value of EMG signal ($\rho = 0.71, p < 0.001$), followed by the Spearman coefficient between the PPT sum score and the mFTMTRS sum score ($\rho = -0.58, p < 0.001$). The UPDRS-III sum score had the lowest correlation coefficients with the other measures. However, the UPDRS-III-tr sum score had a much higher correlation coefficient with the other measures than the UPDRS-III sum score did.

# 4. Conclusion and discussion

In the research, we designed a randomized, sham-controlled, double-blind, crossover experiment to investigate the immediate response of Parkinsonian tremor with different tDCS setups. In addition to the control (s-tDCS) setup, there were three active tDCS setups, namely the a-tDCS setup, the c-tDCS setup and the b-tDCS setup, with each corresponding to one of the randomized sessions in the experiment. In each session, our subjects underwent a similar set of evaluation procedure before and after the intervention. The effect of one specific tDCS setup was evaluated by comparing the pre-intervention and post-intervention performance of the subjects. We investigated the effectiveness of a specific active tDCS setup by comparing it with the sham tDCS setup in the absolute post/pre ratio while the difference between different active tDCS setups were evaluated by comparing their relative post/pre ratio where the effect resulted from the sham setup were removed as a baseline.

## 4.1. Effectiveness of different tDCS setups

The baseline stability assumption was verified by inspecting carefully whether subjects could maintain a constant motor performance with different measures in both the control session and before intervention across different sessions. Consistent with the results of the study by Fregni et al. (2006b), we found only the a-tDCS setup resulted in a significant reduction in the sum score of the UPDRS-III compared with the control (s-tDCS) setup, indicating that only the a-tDCS had a positive effect over the motor function related to Parkinson's disease. However, when we looked into the subscale related to tremor severity (item 20 and item 21 of UPDRS-III), our results showed only the b-tDCS setup resulted in a significant reduction of the sum score and outperformed the other active tDCS setups in suppressing tremor, which was contrary to the result of UPDRS-III sum score. In the mFTMTRS assessment, only the b-tDCS setup brought a significant reduction in the sum score of the mFTMTRS compared with the control (s-tDCS), indicating the b-tDCS setup was effective in suppressing the intensity of tremor. The results of the PPT assessment showed the c-tDCS setup and the b-tDCS setup were both effective in improving hand manipulative dexterity, indicating a potential improvement in

the intensity of hand tremor by c-tdCS and b-tDCS. In addition, no significant effect was found in the a-tDCS setup. Differently, a study by Fregni et al. (2006b) showed no significant effect of either a-tDCS or c-tDCS with the measure of PPT. We considered several possible contributing factors: first, the number of subjects [$N$(a-tDCS) = 9, $N$(c-tDCS) = 8] in their study was smaller than that in ours ($N = 13$), which might cause the lack of power in statistics. Second, the current intensity and density transduced through the sponge electrodes in their experiment [$I$(tDCS) = 1.0mA, $J$(tDCS) = 0.0286mA/cm$^2$] were smaller than those in our experiment [$I$(tDCS) = 1.5 mA, $J(tDCS)$ = 0.0355mA/cm$^2$], indicating that our setup might induce stronger effect by reaching the deeper structure of the brain and thus produced a more significant result. In terms of the CTSA, the c-tDCS setup and the b-tDCS setup both resulted in a significant reduction in the intensity of tremor acceleration. In addition, the optimal effect of tremor suppression was obtained under the bilateral setup. For EMG signal, the statistical results showed only the b-tDCS setup among the three concerned active tDCS setups was effective in reducing tremor-related muscle activities, namely, the b-tDCS setup could suppress tremor more effectively than the other tDCS setups. No significant effect of tDCS with regard to tremor frequency and shape was found in either the tremor acceleration or the EMG signal.

Taken together, our results revealed the technique of tDCS was effective in suppressing tremor and that although a-tDCS benefited Parkinson's disease more as revealed by UPDRS-III, the b-tDCS and c-tDCS setup might be more beneficial when targeting the symptom of Parkinsonian tremor solely. Among the three active tDCS setups, the b-tDCS setup outperformed the others in suppressing tremor. Therefore, in treating Parkinsonian tremor, we proposed the use of the c-tDCS or b-tDCS setup, especially the b-tDCS setup, rather than the a-tDCS setup that was widely accepted in tDCS treatment over Parkinson's disease in previous studies. In addition, our research suggested different symptoms of Parkinson's disease might require different tDCS setups to induce an optimal treatment effect.

## 4.2. Crossover design of the experiment

As reported by previous studies, the effect of tDCS over human bodies may be unstable or even contradictive in similar experimental setups (López-Alonso et al., 2014, 2015). We attributed these discrepancies to the mental factors, such as the placebo effect, which originated mentally from the experiment and affected the performance of subjects physically in return. Under consideration of such factors, our experiment followed a crossover design. The aim was to rule out the subject-specific factors by taking the baseline performance of the subjects into consideration. We assessed the net effect of a specific active tDCS setup by first computing its absolute post/pre ratio and then detracting the individual-specific baseline post/pre ratio of the control (s-tDCS). We assumed that the crossover design increased the reliability of our study. The results of the statistical analysis demonstrated our assumption and that the crossover design was indispensable in exploring the explicit effect of tDCS.

One of the disadvantages resulted from a crossover design was its additional physical and mental burden over subjects. To alleviate the problem, we suggested a long enough time interval of over 48 hours between intervention sessions. The feedback from our subjects showed all subjects tolerated the experiment burden well. Another potential problem resulted from a crossover design was the familiarization effect, with which subjects might perform better in the experiment as time elapsed. The involvement of familiarization effect might lead in type-2 error in our statistics. To check whether the familiarization effect is significant, we re-grouped our data with the factor of stimulation order and performed statistical analysis. Results showed no significant effect of stimulation order in UPDRS-III sum score [$\chi^2_{(3)} = 0.735, p = 0.865$], mFTMTRS sum score [$F_{(3,33)} = 0.835, p = 0.466$], PPT sum score [$F_{(3,33)} = 2.22, p = 0.131$], RMS value of tremor acceleration [$F_{(3,33)} = 1.68, p = 0.210$] and RMS value of EMG signal [$F_{(3,33)} = 1.01, p = 0.387$], respectively. Therefore, we concluded the familiarization effect didn't significantly affect our result in our experiment.

## 4.3. Association between different measures

To assess tremor, three different clinical measures and a self-design evaluation related to continuous tremor signals were utilized in the experiment. Among the four measures utilized in the experiment, the CTSA along with its subsequent analysis was theoretically more objective and less operator-dependent since it required only a series of standardized procedure. It could additionally provide more detailed information in depicting tremor. Based on previous studies, the traditional clinical scales that require a specific physician to score each item with a few levels (such as UPDRS, each item of which has five levels: "Normal," "Slight," "Mild," "Moderate" and "Severe") may be more operator-dependent and less specific in setting (Palmer et al., 2010). Therefore, in this research, we computed the correlation between the CTSA and the other measures to provide a feedback to evaluate the objectiveness of the other chosen clinical measures. Among the results of the Spearman correlation analysis, the most correlated result was within the CTSA, namely between the RMS value of the tremor acceleration and the RMS value of the EMG signal ($\rho = 0.71, p < 0.001$). The correlation between the CTSA and the other measures was relatively lower and reached a coefficient of approximately 0.50 with significance, indicating the potential insufficiency of traditional clinical measures in both accuracy and sensitivity while measuring tremor. The correlation coefficient between the three clinical measures reached up to 0.58, which was slightly lower than that within the CTSA. Specifically, between the UPDRS-III sum score and other measures, the correlation coefficient was as low as almost zero, probably because the UPDRS-III considers symptoms more than tremor. Our results suggested that traditional clinical scales might be potentially insufficient in depicting especially the instant response of tremor. The use of less-operator-dependent and more-objective tools, such as CTSA, was more recommended in measuring tremor.

## 4.4. Mechanism underlying tDCS in suppressing Parkinsonian tremor

As two of the most fundamental electrode setups of tDCS, the anodal setup and the cathodal setup were included in the experimental protocol. In general, the effect of tDCS over primary cortex is polarity-dependent, namely, a-tDCS facilitates while c-tDCS inhibits contralateral motor cortex excitability (Nitsche and Paulus, 2000, 2001). However, based on our findings, tremor was found to decrease more in intensity after the c-tDCS session. We considered two possibilities that might explain this:

First, our result may be directly linked to the excitability alteration of sensorimotor cortex which plays a positive correlative modulatory role in tremorgenesis. The study by Fregni et al. (2006b) reported substantial evidence of c-tDCS in lowering PD subjects' motor cortex excitability with MEP assessment. Thus, the suppressed motor cortex with c-tDCS may result in a lower tremor intensity. In contrast, the facilitating effect of a-tDCS in motor cortex excitability may accordingly lead to an uplift in tremor intensity. However, within our results, no significant increase of tremor was found with a-tDCS. We assumed the intensified components of tremor might be offset by the beneficial effect of the increased dopamine concentration induced by a-tDCS (Fonteneau et al., 2018). Therefore, a-tDCS might exert a beneficial and adverse effect over tremor simultaneously. This was in line with the findings by Fregni et al. (2006b), who found the improvement of tremor after a-tDCS was much less than that in either rigidity or bradykinesia.

Second, the function of c-tDCS might be related to the disruption hypothesis of DBS, where abnormal information flow was disrupted. Although, based on the results of simulated models, the stimuli of tDCS might not reach the depth as DBS did (Dannhauer et al., 2012), tDCS might function by involving in the complex transmitter modulation through the motor cortex to disconnect the basal ganglia-thalamo-cortical loop (Jitkritsadakul et al., 2015). Within our results of the ssRMS sequence, we found after c-tDCS there was no significant change in the maximum ssRMS value of tremor acceleration, regardless of the significant reduction in the average RMS value. This was similar to the effect of DBS in tremor, which could be best described as altering the "on/off" state of tremor, that is, increasing the time of the "on" state while reducing that of the "off" state (Hawley et al., 2014), rather than, reducing tremor intensity directly. Substantial evidence has been reported in, such as, a previous study by Beuter and Titcombe (2003), who found little effect of DBS with low-amplitude resting tremor. In addition, another long-term study showed clearly that DBS increased the "on" state time in the day approximately from originally 25% to 75%, that is, for about 25% of the day, patients remained at the "off" state with DBS. With regard to how c-tDCS affected tremor, a most recent study by Bachtiar et al. (2018) investigated the setup of c-tDCS over the more-affected M1 and found a reduction of GABA concentration in the less-affected M1. A recent study by van Nuland et al. (2020) revealed the GABA concentration was negatively correlated with the tremor severity. Thus, the setup of c-tDCS led to a reduction of tremor severity.

The setup of b-tDCS might have a different mechanism to interact with tremor. Some relevant evidence has been reported: first, with b-tDCS, the cortical currents were found to transduce in a more lateral to medial orientation, compared to the setup of either a-tDCS or c-tDCS, where the currents were transduced in a more dorsal to ventral direction (Wagner et al., 2007). The difference in current flows could lead to the activation in different cerebral structure that contributed to different pathways of tremor suppression. Second, Bachtiar et al. (2018) have reported a reduction of GABA concentration in the more-affected M1 after b-tDCS, which was different from that after c-tDCS where the GABA concentration reduction was found in the contralateral M1. Besides, a study comparing b-tDCS and a-tDCS found an ongoing increase in intracortical functional connectivity only after b-tDCS rather than a-tDCS (Sehm et al., 2013). Another study by Mordillo-Mateos et al. (2012) assessed the cortical excitability using motor-evoked potential and proved b-tDCS could induced a combined effect of a-tDCS and c-tDCS in shifting cortical excitability. A clinical study related to stroke combined with b-tDCS as well as unilateral tDCS showed the effect b-tDCS outperformed that of either a-tDCS or c-tDCS, and proposed b-tDCS for rectifying interhemispheric imbalances in stroke (Mahmoudi et al., 2011). This might also be the case in Parkinsonian tremor, whose onset and progress in general are unilateral and unbalanced. Additionally, according to our results, no bilateral difference (difference between MAS and LAS) of the effect of tDCS was found in terms of FTMTRS and PPT, respectively. Thus, our results in return might reveal an underlying interhemispheric unbalance of cortical excitability induced by Parkinsonian tremor, which could be rectified with tDCS. However, to further prove this, more substantial evidence and research are needed.

## 4.5. Highlights, limitations and future work

To the best of our knowledge, this is the first randomized, sham-controlled, double-blind, crossover research that compared the immediate effect of different tDCS setups targeting Parkinsonian tremor solely. In addition, this is the first time the bilateral tDCS setup, with the cathode over the more affected M1 and the anode over the contralateral M1, was introduced to the treatment of Parkinson's disease. A self-design assessment termed the CTSA was specifically designed for a more accurate and detailed evaluation of the continuous tremor signals. A few novel features, such as the ULS index and the ssRMS sequence to quantify tremor shape and sub-regional tremor amplitude, and the index of the significance ratio for comparison between session pairs were proposed in the paper. With regard to the limitation of the research, a limited number of subjects participated in the experiment because of the time and effort cost due to the crossover design. More cases of qualified subjects are needed to fully verify the efficiency of different tDCS setups in the future. Another limitation of the experiment is the lack of the involvement of cerebral monitoring techniques, such as electroencephalography (EEG) or functional magnetic resonance imaging (fMRI), which may provide information on cortical excitability alteration and help reveal the mechanism of tDCS better. In the future, we may systematically investigate both the short-term and long-term effect of different bilateral

tDCS setups over Parkinson's disease as a continuation of the current research.

## Data availability statement

The raw data supporting the conclusions of this article will be made available by the authors, without undue reservation.

## Ethics statement

The studies involving human participants were reviewed and approved by Ethics Committee of Shanghai Jiao Tong University. The patients/participants provided their written informed consent to participate in this study.

## Author contributions

BZ contributed in carrying out the experiment, data analysis, and drafting the manuscript. FH contributed in carrying out the experiment and coordinating the process of patient recruitment and participation. JL contributed in coordinating the process of patient recruitment and participation. DZ conceived of the study and gave instructions on experimental design. All authors contributed to the article and approved the submitted version.

## Funding

This work was supported by the National Key R&D Program of China (2018YFB1307301) and the National Natural Science Foundation of China (Nos. 61761166006 and 91848112).

## Acknowledgments

We would like to thank all subjects for their participation.

## Conflict of interest

The authors declare that the research was conducted in the absence of any commercial or financial relationships that could be construed as a potential conflict of interest.

## Publisher's note



## References

Bachtiar, V., Johnstone, A., Berrington, A., Lemke, C., Johansen-Berg, H., Emir, U., et al. (2018). Modulating regional motor cortical excitability with noninvasive brain stimulation results in neurochemical changes in bilateral motor cortices. *J. Neurosci.* 38, 7327–7336. doi: 10.1523/JNEUROSCI.2853-17.2018

Benabid, A. L. (2003). Deep brain stimulation for Parkinson's disease. *Curr. Opin. Neurobiol.* 13, 696–706. doi: 10.1016/j.conb.2003.11.001

Benninger, D. H., Lomarev, M., Lopez, G., Wassermann, E. M., Li, X., Considine, E., et al. (2010). Transcranial direct current stimulation for the treatment of Parkinson's disease. *J. Neurol. Neurosurg. Psychiatry* 81, 1105–1111. doi: 10.1136/jnnp.2009.202556

Berk, C., Carr, J., Sinden, M., Martzke, J., and Honey, C. R. (2002). Thalamic deep brain stimulation for the treatment of tremor due to multiple sclerosis: a prospective study of tremor and quality of life. *J. Neurosurg.* 97, 815–820. doi: 10.3171/jns.2002.97.4.0815

Beuter, A., and Titcombe, M. S. (2003). Modulation of tremor amplitude during deep brain stimulation at different frequencies. *Brain Cogn.* 53, 190–192. doi: 10.1016/S0278-2626(03)00107-6

Bikson, M., Grossman, P., Thomas, C., Zannou, A. L., Jiang, J., Adnan, T., et al. (2016). Safety of transcranial direct current stimulation: evidence based update 2016. *Brain Stimul.* 9, 641–661. doi: 10.1016/j.brs.2016.06.004

Boggio, P. S., Ferrucci, R., Rigonatti, S. P., Covre, P., Nitsche, M., Pascual-Leone, A., et al. (2006). Effects of transcranial direct current stimulation on working memory in patients with Parkinson's disease. *J. Neurol. Sci.* 249, 31–38. doi: 10.1016/j.jns.2006.05.062

Borovac, J. A. (2016). Side effects of a dopamine agonist therapy for Parkinson's disease: a mini-review of clinical pharmacology. *Yale J. Biol. Med.* 89, 37–47.

Bronstein, J. M., Tagliati, M., Alterman, R. L., Lozano, A. M., Volkmann, J., Stefani, A., et al. (2011). Deep brain stimulation for Parkinson disease: an expert consensus and review of key issues. *Arch. Neurol.* 68, 165–165. doi: 10.1001/archneurol.2010.260

Coffman, B. A., Clark, V. P., and Parasuraman, R. (2014). Battery powered thought: enhancement of attention, learning, and memory in healthy adults using transcranial direct current stimulation. *Neuroimage* 85, 895–908. doi: 10.1016/j.neuroimage.2013.07.083

Costa-Ribeiro, A., Maux, A., Bosford, T., Aoki, Y., Castro, R., Baltar, A., et al. (2017). Transcranial direct current stimulation associated with gait training in Parkinson's disease: a pilot randomized clinical trial. *Develop. Neurorehabil.* 20, 121–128. doi: 10.3109/17518423.2015.1131755

Dannhauer, M., Brooks, D., Tucker, D., and MacLeod, R. (2012). "A pipeline for the simulation of transcranial direct current stimulation for realistic human head models using SCIRUN/BIOMESH3D," in 2012 Annual International Conference of the IEEE Engineering in Medicine and Biology Society. IEEE, 5486–5489. doi: 10.1109/EMBC.2012.6347236

Deuschl, G., Bain, P., Brin, M., and Committee, A. H. S. (1998). Consensus statement of the movement disorder society on tremor. *Mov. Disord.* 13, 2–23. doi: 10.1002/mds.870131303

Di Lazzaro, V., Dileone, M., Capone, F., Pellegrino, G., Ranieri, F., Musumeci, G., et al. (2014). Immediate and late modulation of interhemipheric imbalance with bilateral transcranial direct current stimulation in acute stroke. *Brain Stimul.* 7, 841–848. doi: 10.1016/j.brs.2014.10.001

Diamond, A., and Jankovic, J. (2005). The effect of deep brain stimulation on quality of life in movement disorders. *J. Neurol. Neurosurg. Psychiatry* 76, 1188–1193. doi: 10.1136/jnnp.2005.065334

Dick, F., Semple, S., Chen, R., and Seaton, A. (2000). Neurological deficits in solvent-exposed painters: a syndrome including impaired colour vision, cognitive defects, tremor and loss of vibration sensation. *QJM* 93, 655–661. doi: 10.1093/qjmed/93.10.655

Doruk, D., Gray, Z., Bravo, G. L., Pascual-Leone, A., and Fregni, F. (2014). Effects of tdcs on executive function in Parkinson's disease. *Neurosci. Lett.* 582, 27–31. doi: 10.1016/j.neulet.2014.08.043

Doshi, P. K. (2011). Long-term surgical and hardware-related complications of deep brain stimulation. *Stereotact. Funct. Neuros.* 89, 89–95. doi: 10.1159/000323372

Fahn, S., Tolosa, E., and Marín, C. (1993). Clinical rating scale for tremor. *Parkinson's Dis. Mov. Disord.* 2, 271–280.

Fernández-Lago, H., Bello, O., Mora-Cerdá, F., Montero-Cámara, J., and Fernández-del Olmo, M. Á. (2017). Treadmill walking combined with anodal transcranial direct current stimulation in Parkinson disease: a pilot study of

kinematic and neurophysiological effects. *Am. J. Phys. Med. Rehabil.* 96, 801–808. doi: 10.1097/PHM.0000000000000751

Fonteneau, C., Redoute, J., Haesebaert, F., Le Bars, D., Costes, N., Suaud-Chagny, M.-F., et al. (2018). Frontal transcranial direct current stimulation induces dopamine release in the ventral striatum in human. *Cereb. Cortex* 28, 2636–2646. doi: 10.1093/cercor/bhy093

Fregni, F., Boggio, P. S., Mansur, C. G., Wagner, T., Ferreira, M. J., Lima, M. C., et al. (2005). Transcranial direct current stimulation of the unaffected hemisphere in stroke patients. *Neuroreport* 16, 1551–1555. doi: 10.1097/01.wnr.0000177010.44602.5e

Fregni, F., Boggio, P. S., Nitsche, M. A., Marcolin, M. A., Rigonatti, S. P., and Pascual-Leone, A. (2006a). Treatment of major depression with transcranial direct current stimulation. *Bipolar Disord.* 8, 203–204. doi: 10.1111/j.1399-5618.2006.00291.x

Fregni, F., Boggio, P. S., Santos, M. C., Lima, M., Vieira, A. L., Rigonatti, S. P., et al. (2006b). Noninvasive cortical stimulation with transcranial direct current stimulation in Parkinson's disease. *Mov. Disord.* 21, 1693–1702. doi: 10.1002/mds.21012

Goetz, C. G., Tilley, B. C., Shaftman, S. R., Stebbins, G. T., Fahn, S., Martinez-Martin, P., et al. (2008). Movement disorder society-sponsored revision of the unified Parkinson's disease rating scale (MDS-UPDRS): scale presentation and clinimetric testing results. *Movement Disord.* 23, 2129–2170. doi: 10.1002/mds.22340

Gray, P., and Hildebrand, K. (2000). Fall risk factors in Parkinson's disease. *J. Neurosci. Nurs.* 32, 222. doi: 10.1097/01376517-200008000-00006

Hadoush, H., Al-Jarrah, M., Khalil, H., Al-Sharman, A., and Al-Ghazawi, S. (2018). Bilateral anodal transcranial direct current stimulation effect on balance and fearing of fall in patient with Parkinson's disease. *NeuroRehabilitation* 42, 63–68. doi: 10.3233/NRE-172212

Hallett, M. (2007). Transcranial magnetic stimulation: a primer. *Neuron* 55, 187–199. doi: 10.1016/j.neuron.2007.06.026

Hawley, J. S., Armstrong, M. J., and Weiner, W. J. (2014). *Parkinson's Disease: Improving Patient Care*. Oxford: Oxford University Press.

Helmich, R. C., Toni, I., Deuschl, G., and Bloem, B. R. (2013). The pathophysiology of essential tremor and Parkinson's tremor. *Curr. Neurol. Neurosci. Rep.* 13, 378. doi: 10.1007/s11910-013-0378-8

Hoehn, M. M., and Yahr, M. D. (1967). Parkinsonism: onset, progression, and mortality. *Neurology* 17, 427–427. doi: 10.1212/WNL.17.5.427

Jang, W., Han, J., Park, J., Kim, J., Cho, J., Koh, S. B., et al. (2013). Waveform analysis of tremor may help to differentiate Parkinson's disease from drug-induced Parkinsonism. *Physiol. Meas.* 34, N15. doi: 10.1088/0967-3334/34/3/N15

Jitkritsadakul, O., Thanawattano, C., Anan, C., and Bhidayasiri, R. (2015). Exploring the effect of electrical muscle stimulation as a novel treatment of intractable tremor in Parkinson's disease. *J. Neurol. Sci.* 358, 146–152. doi: 10.1016/j.jns.2015.08.1527

Kaski, D., Allum, J., Bronstein, A., and Dominguez, R. (2014). Applying anodal tDCS during tango dancing in a patient with Parkinson's disease. *Neurosci. Lett.* 568, 39–43. doi: 10.1016/j.neulet.2014.03.043

Kleiner-Fisman, G., Herzog, J., Fisman, D. N., Tamma, F., Lyons, K. E., Pahwa, R., et al. (2006). Subthalamic nucleus deep brain stimulation: summary and meta-analysis of outcomes. *Mov. Disord.* 21, S290–S304. doi: 10.1002/mds.20962

Lee, A., Furuya, S., and Altenmüller, E. (2014). Epidemiology and treatment of 23 musicians with task specific tremor. *J. Clin. Mov. Disord.* 1, 5. doi: 10.1186/2054-7072-1-5

Lee, D. J., Dallapiazza, R. F., De Vloo, P., and Lozano, A. M. (2018). Current surgical treatments for Parkinson's disease and potential therapeutic targets. *Neural Regenerat. Res.* 13, 1342. doi: 10.4103/1673-5374.235220

López-Alonso, V., Cheeran, B., Río-Rodríguez, D., and Fernández-del Olmo, M. (2014). Inter-individual variability in response to non-invasive brain stimulation paradigms. *Brain Stimul.* 7, 372–380. doi: 10.1016/j.brs.2014.02.004

López-Alonso, V., Fernández-del Olmo, M., Costantini, A., Gonzalez-Henriquez, J. J., and Cheeran, B. (2015). Intra-individual variability in the response to anodal transcranial direct current stimulation. *Clin. Neurophysiol.* 126, 2342–2347. doi: 10.1016/j.clinph.2015.03.022

Mahmoudi, H., Haghighi, A. B., Petramfar, P., Jahanshahi, S., Salehi, Z., and Fregni, F. (2011). Transcranial direct current stimulation: electrode montage in stroke. *Disabil. Rehabil.* 33, 1383–1388. doi: 10.3109/09638288.2010.532283

Manenti, R., Brambilla, M., Rosini, S., Orizio, I., Ferrari, C., Borroni, B., et al. (2014). Time up and go task performance improves after transcranial direct current stimulation in patient affected by Parkinson's disease. *Neurosci. Lett.* 580, 74–77. doi: 10.1016/j.neulet.2014.07.052

Manenti, R., Cotelli, M. S., Cobelli, C., Gobbi, E., Brambilla, M., Rusich, D., et al. (2018). Transcranial direct current stimulation combined with cognitive training for the treatment of Parkinson disease: a randomized, placebo-controlled study. *Brain Stimul.* 11, 1251–1262. doi: 10.1016/j.brs.2018.07.046

Maneski, L. P., Jorgovanović, N., Ilić, V., Došen, S., Keller, T., Popović, M. B., et al. (2011). Electrical stimulation for the suppression of pathological tremor. *Med. Biol. Eng. Comput.* 49, 1187. doi: 10.1007/s11517-011-0803-6

Merletti, R., and Di Torino, P. (1999). Standards for reporting emg data. *J. Electromyogr. Kinesiol.* 9, 3–4.

Mordillo-Mateos, L., Turpin-Fenoll, L., Millán-Pascual, J., Nú nez-Pérez, N., Panyavin, I., Gómez-Argüelles, J. M., et al. (2012). Effects of simultaneous bilateral tDCS of the human motor cortex. *Brain Stimul.* 5, 214–222. doi: 10.1016/j.brs.2011.05.001

Nair, D. G., Renga, V., Lindenberg, R., Zhu, L., and Schlaug, G. (2011). Optimizing recovery potential through simultaneous occupational therapy and non-invasive brain-stimulation using tDCS. *Restorat. Neurol. Neurosci.* 29, 411–420. doi: 10.3233/RNN-2011-0612

Nitsche, M. A., Cohen, L. G., Wassermann, E. M., Priori, A., Lang, N., Antal, A., et al. (2008). Transcranial direct current stimulation: state of the art 2008. *Brain Stimul.* 1, 206–223. doi: 10.1016/j.brs.2008.06.004

Nitsche, M. A., and Paulus, W. (2000). Excitability changes induced in the human motor cortex by weak transcranial direct current stimulation. *J. Physiol.* 527, 633–639. doi: 10.1111/j.1469-7793.2000.t01-1-00633.x

Nitsche, M. A., and Paulus, W. (2001). Sustained excitability elevations induced by transcranial dc motor cortex stimulation in humans. *Neurology* 57, 1899–1901. doi: 10.1212/WNL.57.10.1899

Nonnekes, J., Timmer, M. H., de Vries, N. M., Rascol, O., Helmich, R. C., and Bloem, B. R. (2016). Unmasking levodopa resistance in Parkinson's disease. *Mov. Disord.* 31, 1602–1609. doi: 10.1002/mds.26712

Palm, U., Reisinger, E., Keeser, D., Kuo, M.-F., Pogarell, O., Leicht, G., et al. (2013). Evaluation of sham transcranial direct current stimulation for randomized, placebo-controlled clinical trials. *Brain Stimul.* 6, 690–695. doi: 10.1016/j.brs.2013.01.005

Palmer, J. L., Coats, M. A., Roe, C. M., Hanko, S. M., Xiong, C., and Morris, J. C. (2010). Unified Parkinson's disease rating scale-motor exam: inter-rater reliability of advanced practice nurse and neurologist assessments. *J. Adv. Nurs.* 66, 1382–1387. doi: 10.1111/j.1365-2648.2010.05313.x

Pavese, N., Evans, A., Tai, Y., Hotton, G., Brooks, D., Lees, A., et al. (2006). Clinical correlates of levodopa-induced dopamine release in Parkinson's disease: a pet study. *Neurology* 67, 1612–1617. doi: 10.1212/01.wnl.0000242888.30755.5d

Pincus, S. (1994). Singular stationary measures are not always fractal. *J. Theor. Prob.* 7, 199–208. doi: 10.1007/BF02213368

Postuma, R. B., Berg, D., Stern, M., Poewe, W., Olanow, C. W., Oertel, W., et al. (2015). MDS clinical diagnostic criteria for Parkinson's disease. *Mov. Disord.* 30, 1591–1601. doi: 10.1002/mds.26424

Rinne, U. (1983). Problems associated with long-term levodopa treatment of Parkinson's disease. *Acta Neurol. Scand.* 68, 19–26. doi: 10.1111/j.1600-0404.1983.tb01513.x

Rosqvist, K., Hagell, P., Odin, P., Ekström, H., Iwarsson, S., and Nilsson, M. (2017). Factors associated with life satisfaction in Parkinson's disease. *Acta Neurol. Scand.* 136, 64–71. doi: 10.1111/ane.12695

Schulz, K. F., Altman, D. G., Moher, D., and CONSORT Group. (2010). CONSORT 2010 statement: updated guidelines for reporting parallel group randomised trials. *BMJ.* 340, c332. doi: 10.1136/bmj.c332

Sehm, B., Kipping, J. A., Schäfer, A., Villringer, A., and Ragert, P. (2013). A comparison between uni-and bilateral tDCS effects on functional connectivity of the human motor cortex. *Front. Human Neurosci.* 7, 183. doi: 10.3389/fnhum.2013.00183

Shaheiwola, N., Zhang, B., Jia, J., and Zhang, D. (2018). Using tDCS as an add-on treatment prior to FES therapy in improving upper limb function in severe chronic stroke patients: a randomized controlled study. *Front. Human Neurosci.* 12, 233. doi: 10.3389/fnhum.2018.00233

Tiffin, J., and Asher, E. J. (1948). The purdue pegboard: norms and studies of reliability and validity. *J. Appl. Psychol.* 32, 234. doi: 10.1037/h0061266

Timmer, J., Gantert, C., Deuschl, G., and Honerkamp, J. (1993). Characteristics of hand tremor time series. *Biol. Cybern.* 70, 75–80. doi: 10.1007/BF00202568

Tinazzi, M., Del Vesco, C., Fincati, E., Ottaviani, S., Smania, N., Moretto, G., et al. (2006). Pain and motor complications in Parkinson's disease. *J. Neurol. Neurosurg. Psychiatry* 77, 822–825. doi: 10.1136/jnnp.2005.079053

Tombaugh, T. N., and McIntyre, N. J. (1992). The mini-mental state examination: a comprehensive review. *J. Am. Geriatr. Soc.* 40, 922–935. doi: 10.1111/j.1532-5415.1992.tb01992.x

Tomlinson, C. L., Stowe, R., Patel, S., Rick, C., Gray, R., and Clarke, C. E. (2010). Systematic review of levodopa dose equivalency reporting in Parkinson's disease. *Mov. Disord.* 25, 2649–2653. doi: 10.1002/mds.23429

Valentino, F., Cosentino, G., Brighina, F., Pozzi, N. G., Sandrini, G., Fierro, B., et al. (2014). Transcranial direct current stimulation for treatment of freezing of gait: a cross-over study. *Mov. Disord.* 29, 1064–1069. doi: 10.1002/mds.25897

van Nuland, A. J., den Ouden, H. E., Zach, H., Dirkx, M. F., van Asten, J. J., Scheenen, T. W., et al. (2020). Gabaergic changes in the thalamocortical circuit in Parkinson's disease. *Human Brain Map.* 41, 1017–1029. doi: 10.1002/hbm.24857

Wagner, T., Fregni, F., Fecteau, S., Grodzinsky, A., Zahn, M., and Pascual-Leone, A. (2007). Transcranial direct current stimulation: a computer-based human model study. *Neuroimage* 35, 1113–1124. doi: 10.1016/j.neuroimage.2007.01.027

Weintraub, D., and Stern, M. B. (2005). Psychiatric complications in Parkinson disease. *Am. J. Geriatr. Psychiatry* 13, 844–851. doi: 10.1097/00019442-200510000-00003

Zhang, B., Huang, F., Liu, J., and Zhang, D. (2018). A novel posture for better differentiation between Parkinson's tremor and essential tremor. *Front. Neurosci.* 12, 317. doi: 10.3389/fnins.2018.00317

Zhang, D., Poignet, P., Widjaja, F., and Ang, W. T. (2011). Neural oscillator based control for pathological tremor suppression via functional electrical stimulation. *Control Eng. Pract.* 19, 74–88. doi: 10.1016/j.conengprac.2010.08.009

frontiers | Frontiers in Neuroscience

TYPE Original Research
PUBLISHED 20 March 2023
DOI 10.3389/fnins.2023.1138406



OPEN ACCESS

EDITED BY
Ali Asghar Zarei,
UNEEG Medical A/S, Denmark

REVIEWED BY
Rory O'Keeffe,
Tandon School of Engineering, New York University, United States
Marco Rizzo,
Aalborg University, Denmark

*CORRESPONDENCE
Jie Jia
✉ shannonjj@126.com
Jiayuan He
✉ jiayuan.he@wchscu.cn

†These authors have contributed equally to this work

SPECIALTY SECTION
This article was submitted to Translational Neuroscience, a section of the journal Frontiers in Neuroscience

RECEIVED 05 January 2023
ACCEPTED 28 February 2023
PUBLISHED 20 March 2023

CITATION
Ding L, Sun Q, Jiang N, He J and Jia J (2023) The instant effect of embodiment *via* mirror visual feedback on electroencephalogram-based brain connectivity changes: A pilot study. *Front. Neurosci.* 17:1138406. doi: 10.3389/fnins.2023.1138406



# The instant effect of embodiment *via* mirror visual feedback on electroencephalogram-based brain connectivity changes: A pilot study

Li Ding[1,2†], Qiang Sun[3,4†], Ning Jiang[3,4], Jiayuan He[3,4*] and Jie Jia[1,2*]

[1]Department of Rehabilitation Medicine, Huashan Hospital, Fudan University, Shanghai, China, [2]The National Clinical Research Center for Aging and Medicine, Huashan Hospital, Fudan University, Shanghai, China, [3]National Clinical Research Center for Geriatrics, West China Hospital, Sichuan University, Sichuan, China, [4]Med-X Center for Manufacturing, Sichuan University, Sichuan, China

The therapeutic efficacy of mirror visual feedback (MVF) is attributed to the perception of embodiment. This study intends to investigate the instantaneous effect of embodiment on brain connectivity. Twelve healthy subjects were required to clench and open their non-dominant hands and keep the dominant hands still during two experimental sessions. In the first session, the dominant hand was covered and no MVF was applied, named the sham-MVF condition. Random vibrotactile stimulations were applied to the non-dominant hand with MVF in the subsequent session. Subjects were asked to pedal while having embodiment perception during motor tasks. As suggested by previous findings, trials of no vibration and continuous vibration were selected for this study, named the condition of MVF and vt-MVF. EEG signals were recorded and the alterations in brain connectivity were analyzed. The average node degrees of sham-MVF, MVF, and vt-MVF conditions were largely different in the alpha band (9.94, 11.19, and 17.37, respectively). Further analyses showed the MVF and vt-MVF had more nodes with a significantly large degree, which mainly occurred in the central and the visual stream involved regions. Results of network metrics showed a significant increment of local and global efficiency, and a reduction of characteristic path length for the vt-MVF condition in the alpha and beta bands compared to sham-MVF, and in the alpha band compared to MVF. Similar trends were found for MVF condition in the beta band compared to sham-MVF. Moreover, significant leftward asymmetry of global efficiency and rightward asymmetry of characteristic path length was reported in the vt-MVF condition in the beta band. These results indicated a positive impact of embodiment on network connectivity and neural communication efficiency, which reflected the potential mechanisms of MVF for new insight into neural modulation.

KEYWORDS

**mirror visual feedback, embodiment perception, network, electroencephalogram, rehabilitation, vibrotactile simulation**

# 1. Introduction

Mirror visual feedback (MVF) is a non-invasive priming technique that has been widely adopted in neurorehabilitation. Reviews have demonstrated the therapeutic effects of MVF on improving motor recovery and daily living ability after stroke, especially for upper limb function (Rothgangel et al., 2011; Pollock et al., 2014; Thieme et al., 2018). A plain mirror placed the moving non between the upper limbs reflects -affected hand and the reflection produces the embodiment perception of the affected hand, which has effects on the recovery of motor functions after impairments. To present an optimal use in the clinic, lots of studies have investigated the correlated potential neuro-mechanisms of MVF, including activations of widely distributed brain regions, normalization of hemisphere asymmetry, and brain activity modulation (Michielsen et al., 2011a,b; Saleh et al., 2014; Rossiter et al., 2015; Chang et al., 2017). Observed activation of motor cortical regions *via* EEG and fMRI, such as the primary motor cortex and supplementary motor area (SMA), is one of the direct and instant effects of MVF (Michielsen et al., 2011a; Debnath and Franz, 2016; Ding et al., 2020a). Moreover, increased activities of the postcentral gyrus, frontal-parietal areas, posterior parietal cortex, precuneus, visual cortex, and dorsolateral prefrontal cortex are also observed during MVF (Fink et al., 1999; Matthys et al., 2009; Michielsen et al., 2011b; Arya, 2016; Rizzo et al., 2022), which are responsible for sensorimotor coordination, visuomotor transformation, and visual attention. Regarding the long-term effects of MVF, studies showed facilitating corticospinal outputs and restoring hemispheric balance after MVF intervention (Michielsen et al., 2011a; Lappchen et al., 2012). Brain connectivity is regarded as a primary contributor to brain reorganization, which has been described using graph theory (Caliandro et al., 2017). However, only a few studies investigated the underlying mechanisms of MVF from the perspective of brain connectivity (Hamzei et al., 2012; Rjosk et al., 2017; Saleh et al., 2017; Ding et al., 2019). Hamzei et al. (2012) reported an increased interaction between the premotor region and SMA after MVF training in healthy subjects. Rjosk et al. (2017) investigated the improved performance induced by MVF and concluded that it was the result of enhanced connections between perceptual and motor cortical regions, including the primary sensorimotor cortex, visual cortex, and anterior intraparietal sulcus. Furthermore, a dynamic causal modelling study showed an effective connection between the primary cortex and the contralateral parietal cortex (Saleh et al., 2017), which suggested the MVF-based motor activation was driven by the contralateral parietal cortex. In our previous study, increased network segregations in the visual, somatosensory, and motor areas were observed, which suggested enhanced communication efficiency after MVF intervention in stroke patients (Ding et al., 2019). To the best of our knowledge, rare studies explored the instant effects of MVF on network topology and communication efficiency using EEG for new insight, which outperformed MRI on temporal resolution. Thus, we intended to explore the instantaneous effect of embodiment *via* MVF on network connectivity and the efficiency of information transmission.

Embodiment is a subjective sense of self, comprising body ownership, location, agency, and deafference (Blanke et al., 2015). Studies presented that the therapeutic efficacy of MVF might be attributed to the perception of embodiment, which could affect the sensorimotor activity and multisensory integration (Michielsen et al., 2011b; Medina et al., 2015; Ding et al., 2019). Our previous studies found multisensory inputs could strengthen embodiment perception during MVF and observed correlative enhanced motor cortical activation in healthy subjects (Ding et al., 2020a,b). Moreover, a slightly higher weighted clustering coefficient and shorter weighted path length were obtained in our prior study when receiving MVF with continuous vibrotactile simulation (Ding et al., 2020a). Therefore, we hypothesized a potential influence of embodiment intensity on network topology, which might contribute to further exploring its effect on brain connectivity changes.

In this study, no MVF, pure MVF, and MVF with vibrotactile stimulation were employed to induce different degrees of embodiment perception and the related instant effects on the EEG-based brain network were investigated. As more in-depth analyses of our previous experiment, we aimed to provide more tentative evidence on the potential mechanisms of MVF for new insight from the brain connectivity perspective and further exploration of neural modulation. Moreover, part of the dataset has been used in our previous study and re-analyzed in this present study (Ding et al., 2020a).

# 2. Materials and methods

## 2.1. Subjects

Twelve healthy subjects with an average age of 25 years (four females and eight males) were recruited for the experiment. None of these subjects experienced any MVF experiment before. Prior to the experiment, all subjects were informed, agreed, and signed the consent form approved by the Research Ethics Committee of the University of Waterloo (ORE# 22900).

## 2.2. Experimental paradigm

In the experiment, an acrylic mirror (40 cm by 50 cm) was suspended on a holder and placed over the chest of a lying subject in a sagittal plane, see **Figure 1**. Subjects were required to lie down on a bed, clench their fists, and open their hands using their non-dominant hands (two out of the twelve subjects were left-handed) at the pace of 1 Hz on the reflecting side of the mirror, place the dominant hands in a similar position as the non-dominant side and keep static behind the mirror. Moreover, a pedal was set under the non-dominant foot, and subjects were asked to press on the pedal for a very short time as soon as they experienced the sense of embodiment from the dominant side *via* mirror reflection, such as the feeling that he/she could move the reflection without moving the dominant hand or the reflection was part of his/her body.

This experiment comprised two sessions, which was illustrated in **Figure 2**. In the first session, subjects performed 30 trials of hand motor tasks (non-dominant hand clenching and opening while dominant hand keeping still) without MVF and vibrotactile stimulation, which was defined as the condition of sham-MVF, see

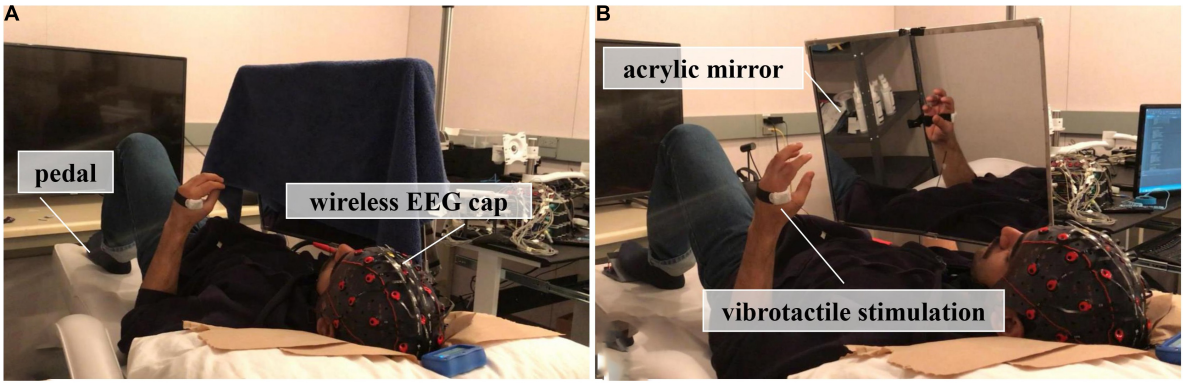


FIGURE 1
Experimental setup, **(A)** The first session, where no mirror visual feedback (MVF) was applied; **(B)** The second session, where subjects received MVF or MVF combined with vibrotactile stimulation.

Figure 1A. In the subsequent session, subjects conducted the same hand motor task with MVF while vibrotactile stimulations were applied randomly, see Figure 1B. The vibrotactile stimulation was provided *via* a liner resonance actuator (type C10–100, Precision Microdrivers Ltd., London, England) at the first interosseous dorsal muscle tendon of the non-dominant hand. In this session, subjects performed 30 trials (as one run) for a total of 180 trials (six runs) and rested between trials. Each run contained 10 trials for each type of vibration that appeared randomly. The sequence of events in each trial for these two sessions was the same as illustrated in our previous study, including a ready phase, motor task phase, and rest phase (see Figure 2). In the previous study, enhanced embodiment was obtained while subjects received MVF combining vibrotactile stimulation (continuous and intermittent), according to the shorter pedal time latency and a higher score on the embodiment questionnaire (Ding et al., 2020a). Moreover, a stronger power desynchronization in the dominant hand area was found in the alpha and beta bands with an enhanced embodiment. However, around the parietal-occipital region, a relatively stronger power desynchronization was observed under MVF and MVF combined with continuous vibrotactile stimulation than the intermittent one in the both frequency bands (Ding et al., 2020a). Thus, trials of no vibration and continuous vibration were selected for the analyses in this study, which were defined as the condition of MVF and vt-MVF, respectively. Moreover, these data have been used in our previous study and re-analyzed in this study for further exploration (Ding et al., 2020a). EEG signals were recorded continuously in the experiment.

## 2.3. EEG signal acquisition and preprocessing

A 32-channel wireless EEG recording equipment (g.Nautilus, g.tec, Austria) was used in the experiment. Electrodes were placed at Fp1, Fp2, AF3, AF4, F7, F3, Fz, F4, F8, FC5, FC1, FC2, FC4, T7, C3, Cz, C4, T8, CP5, CP1, CP2, CP6, P7, P3, Pz, P4, P8, PO7, PO3, PO4, PO8, and Oz with their arrangements followed the extended 10–20 system. The reference and ground electrodes were placed on the right ear lobe and the forehead, respectively. EEG signals were recorded at a 250 Hz sampling rate and notch filtered the power line noise at 60 Hz. Raw data were cleaned offline using MATLAB (MathWorks, Inc., version 2021a) toolbox EEGLAB (Delorme and Makeig, 2004). First, EEG signals were visually inspected and trials with unexpected experimental artifacts, including large drifts and spikes, were removed. After that, independent component analysis (learning rate: 0.001; max number of interactions: 512; the other settings are in default from EEGLAB) was employed in the remaining trials to remove eye movement and ECG, etc., artifacts.

This study analyzed EEG signals of three conditions, including sham-MVF, MVF, and vt-MVF, in four frequency bands, including theta (4–8 Hz), alpha (8–13 Hz), beta (13–30 Hz), and gamma (low gamma band 30–40 Hz). The 4 s data after the subject pedaled (perceiving embodiment) was analyzed for the condition of MVF and vt-MVF. For the sham-MVF condition, as the subject doesn't need to respond to their embodiment feeling, to better reflect their brain activity on account of response latency, we empirically choose the middle 4 s (4–8 s after the "Go" cue) data for analysis. Then, all segmented data were filtered into the frequency band of interest using a Hamming windowed sinc FIR filter (*pop_eegfiltnew()* function in EEGLAB). Note that, after removing noise-contaminated trials, there were an average of 22 trials per subject being remained for analysis of the sham-MVF condition. For the MVF and vt-MVF conditions, only trials with embodiment perception remained, which resulted in an average of 33.1 and 39.2 trials per subject, respectively.

## 2.4. Construction of functional connectivity networks

A brain network consisted of multiple nodes (EEG electrodes) and edges (connectivity strength between two nodes). In this study, a 32-node brain network was constructed with each node representing one specific electrode. To estimate the functional connectivity of pairwise nodes, the phase lag index (PLI), which measures the asymmetry of the distribution of phase differences between two signals while eliminating volume conduction effects (Stam et al., 2007), was applied. Given two signals $x(t)$ and $y(t)$ from pairwise nodes, together with their Hilbert transform $\tilde{x}(t)$ and $\tilde{y}(t)$,

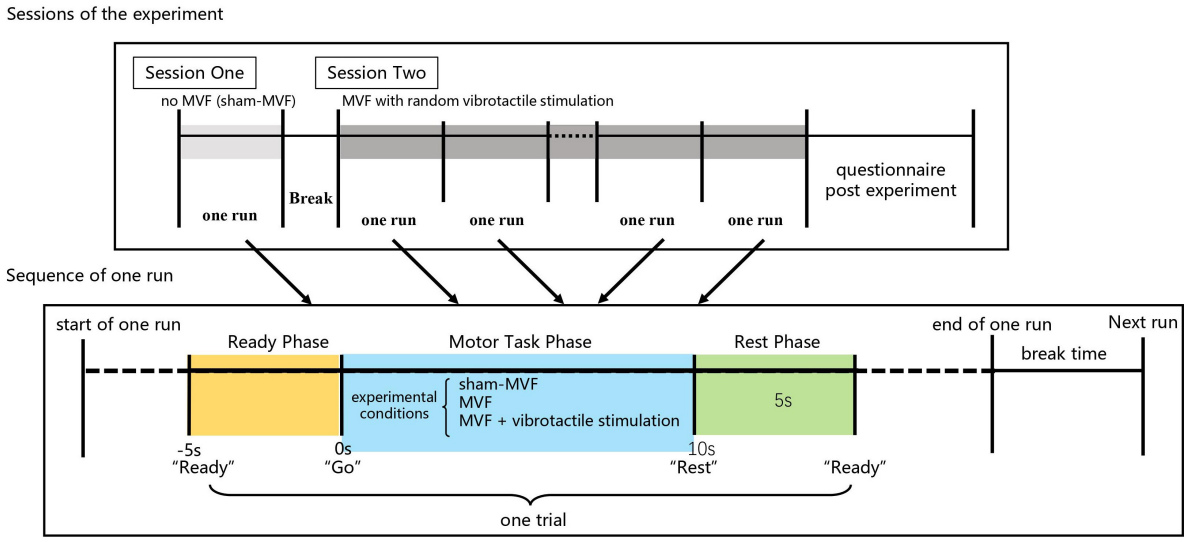


FIGURE 2
Experimental paradigm and sequence of events in each trial.

the analytical signal $z_x(t)$ and $z_y(t)$ can be formulated as:

$$z_x(t) = x(t) + i\tilde{x}(t) \tag{1}$$

$$z_y(t) = y(t) + i\tilde{y}(t) \tag{2}$$

with

$$\tilde{x}(t) = \frac{1}{\pi} PV \int_{-\infty}^{+\infty} \frac{x(\tau)}{t-\tau} d(\tau) \tag{3}$$

$$\tilde{y}(t) = \frac{1}{\pi} PV \int_{-\infty}^{+\infty} \frac{y(\tau)}{t-\tau} d(\tau) \tag{4}$$

where $PV$ refers to the Cauchy principal value.

Then, the instantaneous phases $\Phi_{x(t)}$ and $\Phi_{y(t)}$ of $x(t)$ and $y(t)$ can be calculated as:

$$\Phi_x(t) = arctan\frac{\tilde{x}(t)}{x(t)} \tag{5}$$

$$\Phi_y(t) = arctan\frac{\tilde{y}(t)}{y(t)} \tag{6}$$

Finally, we can obtain the PLI value of the pairwise nodes:

$$PLI = |\frac{1}{N_s} \sum_{k=1}^{N_s} \text{sign}[\sin \Delta\Phi(t_k)]| \tag{7}$$

where $N_s$ denotes the sample number, $\Phi(t_k)$ denotes the phase differences between $\Phi_{x(t)}$ and $\Phi_{y(t)}$ at $t_k$ . Note that the PLI value ranges between 0 and 1 with 0 indicating either no or instantaneous coupling and 1 indicating perfect phase locking (Stam et al., 2007).

After calculating the PLI value of all possible pairwise nodes, a 32 × 32 weighted adjacency matrix was yielded for each trial. In this study, we aimed to analyze brain network differences of different experimental conditions on each frequency band in an individual and grouped fashion. Specifically, the individual functional connectivity matrix of each subject on each frequency band and experimental condition was calculated by averaging the adjacency matrices across all trials, while the grouped functional connectivity matrix was calculated by averaging the individual functional connectivity matrices across subjects.

## 2.5. Network binarization

A critical step in network construction is to exclude the weak and spurious connections within the graph. In this study, we employed the Cluster-Span Threshold (CST) method for unbiased network binarization (Smith et al., 2015, 2016). CST determines the optimal proportional threshold on the condition that the network topology achieves balance in segregation and integration. Given that triples, formed by two neighboring nodes sharing connections with one common node, play a key role in graph analysis, network integration, and segregation can be represented by clustering (or closed) and spanning (or open) triples, respectively. Therefore, the alternative definition of CST selects the proportional threshold for which the ratio of clustering triples to spanning triples is balanced. This situation happens when the global clustering coefficient ($CC_{glob}$, see its definition in the next section) of the binarised network equals 0.5.

In this study, we searched the threshold value across the sparsity level from 10 to 100% with an interval of 1%. Sparsity level is defined as the proportion of remaining edges to all possible edges of a network. Due to the discrete nature of a binarized network, we technically took the CST as the proportional threshold at which the $CC_{glob}$ was closest to 0.5.

## 2.6. Network metrics

Multiple measures can be used to characterize network connectivity, as suggested by the review (Rubinov and Sporns, 2010). Based on grouped functional connectivity matrices, we first computed the degree of each node, which represents

the importance of a node within the network, as it is a commonly used measure of centrality. In such a case, we aimed to investigate the distribution difference of functional connectivity between experimental conditions on different brain regions. Furthermore, we investigated the network segregation and integration differences between experimental conditions *via* individual functional connectivity matrices. Here, the clustering coefficient (*CC*) and local efficiency (*LE*) were adopted as segregation measures, and the characteristic path length (*CPL*) and global efficiency (*GE*) were adopted as integration measures. All these network metrics were calculated based on the brain connectivity toolbox (BCT),[1] and their mathematical definition sees follows.

Assume that a network has $n$ nodes, and all nodes form a set $N$. Moreover, the connection status between node $i$ and $j$ is denoted as $a_{ij}$ ($a_{ij}=1$ if a link exists between $i$ and $j$, otherwise, $a_{ij}=0$), the shortest path length between node $i$ and $j$ is denoted as $d_{ij}$, and the length of the shortest path between node $j$ and $h$ that contains only the neighbors of node $i$ is denoted as $d_{jh}(N_i)$. Then, the degree of a given node $i$ can be obtained as the number of connected links:

$$k_i = \sum_{j \in N} a_{ij} \tag{8}$$

The larger the node degree is, the more important this node is within the network. Besides, *CC*, *LE*, *CPL*, and *GE* of the network are formulated as:

$$CC = \frac{1}{n}\sum_{i \in N} CC_{\text{node},i} = \frac{1}{n}\sum_{i \in N} \frac{\sum_{j,h \in N} a_{ij}a_{ih}a_{jh}}{k_i(k_i-1)} \tag{9}$$

$$LE = \frac{1}{n}\sum_{i \in N} \frac{\sum_{j,h \in N, j \neq i} a_{ij}a_{ih}\left[d_{jh}(N_i)\right]^{-1}}{k_i(k_i-1)} \tag{10}$$

$$CPL = \frac{n(n-1)}{\sum_{i \in N}\sum_{j \in N, j \neq i} d_{ij}^{-1}} \tag{11}$$

$$GE = \frac{\sum_{i \in N}\sum_{j \in N, j \neq i} d_{ij}^{-1}}{n(n-1)} \tag{12}$$

where$CC_{\text{node},i}$ represent the clustering coefficient of node $i$. The upper mentioned $CC_{\text{glob}}$ is defined as the summation of $CC_{\text{node}}$. Note that to avoid infinite value caused by disconnected pairs of nodes, in this study, *CPL* is defined as the harmonic mean of the shortest path length as recommended by Newman (2003), which is also the reciprocal of *GE*. Moreover, as hubs are vital components for network efficient communication and reliance (Hosseini et al., 2012), we consider a node as a hub if its degree is one standard deviation higher than the mean network degree (Bernhardt et al., 2011).

## 2.7. Hemispheric asymmetry analysis

Although many studies reported the ability of MVF on balancing hemisphere asymmetry and modulating hemispheric activation (Rossiter et al., 2015; Bartur et al., 2018; Rohafza et al., 2019; Zhang and Fong, 2019), its effect on shifting network metrics is rarely reported. Thus, as an additional measure, the hemispheric asymmetry in metrics was analyzed for future study. The hemispheric asymmetry of connectivity patterns was analyzed *via* the laterality index (LI) (Hassanin et al., 2021). In this study, the LI value is defined as follows:

$$LI = \frac{NM_r - NM_l}{NM_r + NM_l} \tag{13}$$

where $NM_r$ and $NM_l$ indicate the network metrics of the right and left sub-network, respectively. To be specific, two groups of channels (i.e., right group: FP2, AF4, F8, F4, FC6, FC2, T8, C4, CP6, CP2, P8, P4, PO8, PO4; left group: FP1, AF3, F7, F3, FC5, FC1, T7, C3, CP5, CP1, P7, P3, PO7, PO3) were selected out of the overall recording channels. Then, the sub-network corresponding to each group was constructed and used for the regional clustering coefficient, characteristic path length, local efficiency, and global efficiency estimations. The LI value was finally computed based on these regional network metrics. In the study, the LI values ranged from −1 to 1, with negative values indicating the left hemisphere (representing the dominant hand) and vice versa.

## 2.8. Statistical analysis

We performed one-way repeated measures analysis of variance (ANOVA) to test the effects of experimental conditions on segregation and integration measures. The conditions of sham-MVF, MVF, and vt-MVF were the three levels of the single factor. Post-hoc multiple comparisons were conducted with Bonferroni correction. Besides, paired $t$-test was used to test the significant node degree difference between different experimental conditions, as well as the LI value difference between the left and right brain regions on each experimental condition. Note that the normality of parameter distribution was first determined by Shapiro-Wilk's test, and the homogeneity of parameter variance was checked by Bartlett's test. All tests had a significance level of 0.05. The script used for statistical analysis was developed based on built-in functions in MATLAB.

# 3. Results

## 3.1. Scalp network topology

The scalp network topology of the sham-MVF, MVF, and vt-MVF experimental conditions after CST binarization was shown in **Figure 3**. Besides, the binarization threshold of node degree was also presented in **Table 1**. As can be seen, MVF and vt-MVF conditions enjoyed more prominent connectivity compared to the sham-MVF condition in the alpha and gamma bands. Specifically, the connectivity was largely different in the alpha band, where the average node degrees of the sham-MVF, MVF, and vt-MVF conditions were 9.94, 11.19, and 17.37, respectively. Moreover, only the MVF condition showed more dense connectivity compared to the sham-MVF in the beta band. In the theta band, the sham-MVF condition had more dense connectivity compared to MVF and vt-MVF conditions. To be specific, the average node degree of the sham-MVF condition was 14.87, which outperformed that of the conditions of MVF (9.31) and vt-MVF (9.62). Moreover,

1 https://www.nitrc.org/projects/bct/

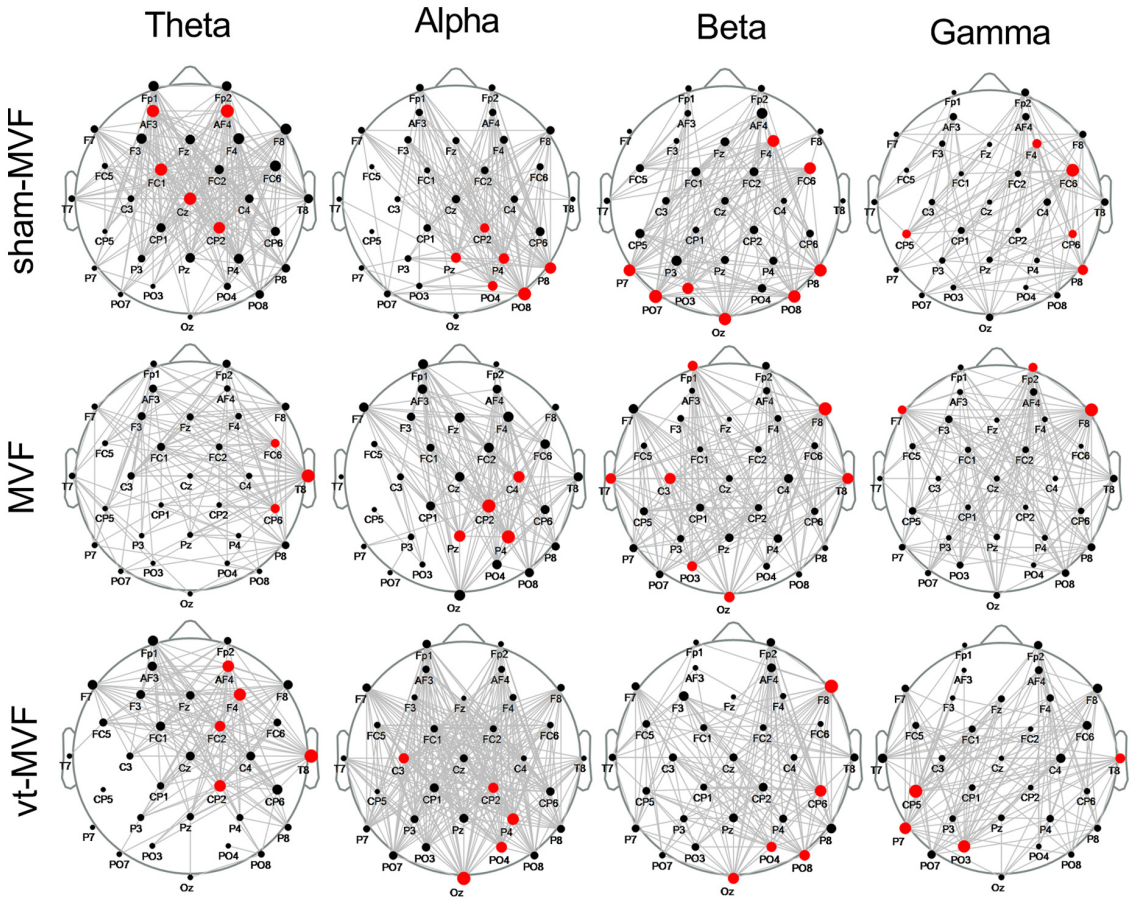


FIGURE 3
Scalp network topology of the sham-mirror visual feedback (MVF), MVF, and vt-MVF experimental condition in theta (4–8 Hz), alpha (8–13 Hz), beta (13–30 Hz), and gamma (30–40 Hz) frequency band. The bigger dot on each node (electrode location) indicates the larger node degree within this network. Note that the hubs are marked in red.

the network hubs were distributed differently under the three experimental conditions in each frequency band without distinct patterns in the meantime.

To further explore the topological differences within the three experimental conditions, the node degree differences between different pairs of conditions were statistically investigated. As shown in Figure 4A, the sham-MVF condition had more nodes with a significantly larger degree than the MVF condition in the theta band on the middle brain regions (Frontal, Central, Central-Parietal, Parietal, and Parietal-Occipital regions), while in the alpha and the beta bands, the number of nodes with a significantly larger degree of the MVF condition increased (mainly distributed around Frontal, Central, Central-Parietal regions). Regarding the comparison between conditions of vt-MVF and sham-MVF (see Figure 4B), the vt-MVF condition had almost all nodes with a significantly larger degree in the alpha and the beta bands, which mainly located in the left Frontal-Central, left Central, Central-Parietal, Parietal, and Parietal-Occipital regions. However, in the theta band, the nodes with a significantly larger degree were shown in the condition of sham-MVF and mainly located in the left Central-Parietal, left Parietal, and right Parietal-Occipital regions. As demonstrated in Figure 4C, the vt-MVF condition had more nodes with a significantly larger degree compared to the MVF condition in the theta, alpha, and beta bands, especially in the alpha band and located in the left Frontal-Central, left Central, left Central-Parietal, left Parietal-Occipital regions. Furthermore, a few nodes with statistical differences were obtained *via* the comparison among three experimental conditions in the gamma band in this study.

## 3.2. Alteration of network metrics

One-way repeated measures ANOVA demonstrated significant interactions of experimental conditions on CPL in the theta [$F(2, 22) = 4.4592$, $p = 0.0237$], alpha [$F(2, 22) = 5.8564$, $p = 0.0055$], and

TABLE 1 Binarization threshold of brain networks in different frequency bands and the corresponding node degree.

| | Theta | Alpha | Beta | Gamma |
|---|---|---|---|---|
| sham-MVF | 14.87 (48%) | 9.93 (32%) | 10.87 (35%) | 7.75 (25%) |
| MVF | 9.31 (30%) | 11.19 (36%) | 12.37 (40%) | 10.25 (33%) |
| vt-MVF | 9.62 (31%) | 17.37 (56%) | 10.56 (34%) | 9.62 (31%) |

Data are formatted as node degree (binarization threshold).

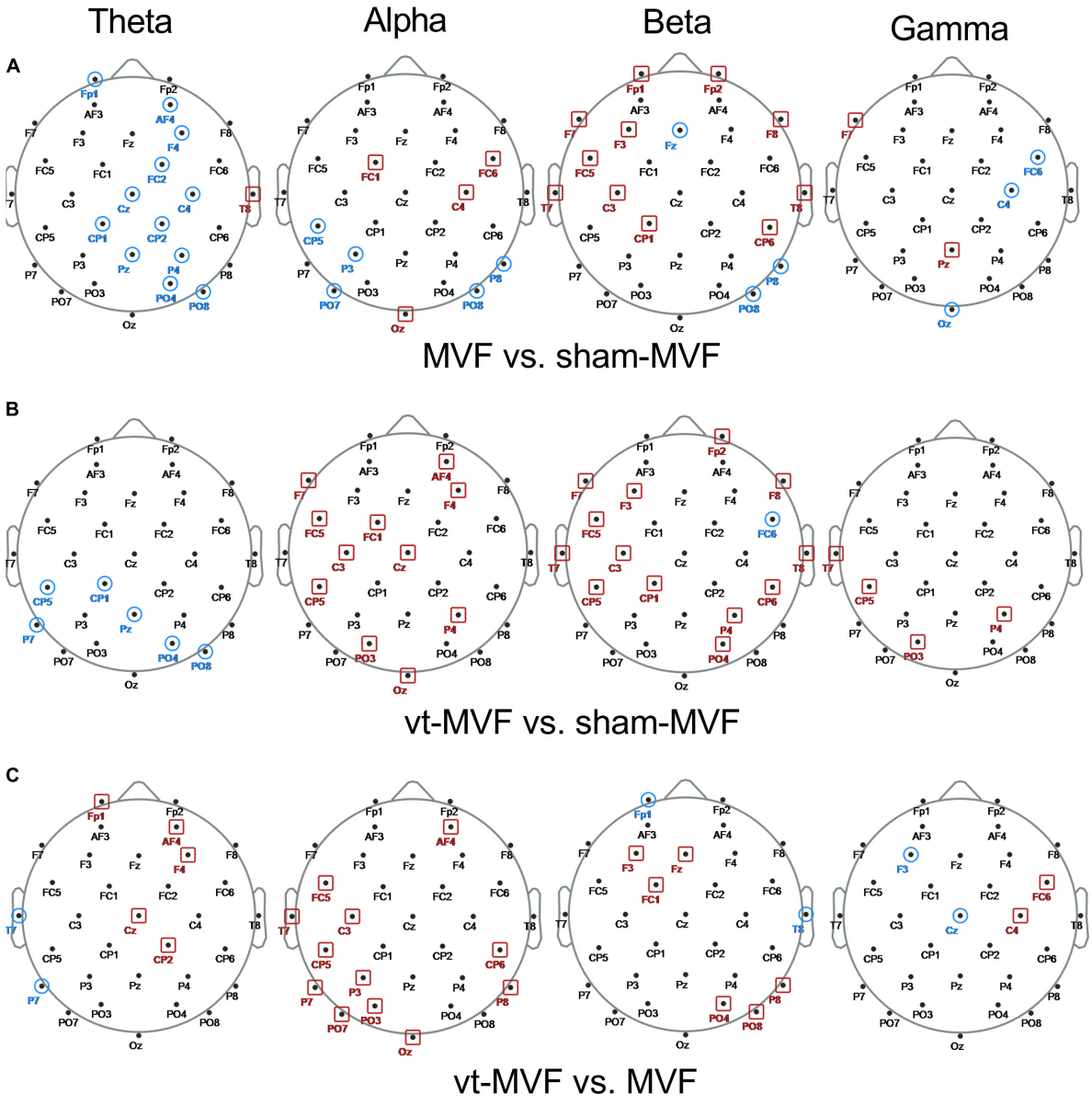


FIGURE 4
Scalp topological differences between **(A)** mirror visual feedback (MVF) and sham-MVF, **(B)** vt-MVF and sham-MVF, and **(C)** vt-MVF and MVF experimental conditions in different frequency bands (from left to right in each row corresponding to theta, alpha, beta, and gamma frequency band, respectively). Taking the condition pair MVF vs. sham-MVF as an example, the node marked with a red square denoted that the node degree of MVF on this location was significantly larger ($p < 0.05$) than that of sham-MVF, while the node marked with a blue circle denoted the opposite case.

beta [$F(2, 22) = 5.9490$, $p = 0.0086$] bands, LE in the alpha [$F(2, 22) = 6.6530$, $p = 0.0021$] and beta [$F(2, 22) = 8.0101$, $p = 0.0024$] bands, GE in the theta [$F(2, 22) = 4.4727$, $p = 0.0234$], alpha [$F(2, 22) = 6.7632$, $p = 0.0051$], and beta [$F(2, 22) = 6.4428$, $p = 0.0063$] bands, respectively.

The results of post-hoc multiple comparisons were shown in Figure 5. According to Figures 5B, D, the vt-MVF condition showed significant increments of LE and GE, and significant reductions of CPL in the alpha band, compared to both the sham-MVF and MVF condition, which indicated an enhanced functional integration and segregation *via* the combination of vibrotactile stimulation. In the beta band, there were a significant reduction of CPL and an increment of LE and GE of the vt-MVF condition compared to that of the sham-MVF condition. Moreover, a similar trend could be found when comparing the MVF to the sham-MVF condition in the beta band, although without significant differences.

## 3.3. Hemispheric asymmetry

Table 2 showed the LI of the CC, CPL, LE, and GE under sham-MVF, MVF, and vt-MVF experimental conditions in different frequency bands. A significant leftward asymmetry of GE and rightward asymmetry of CPL were obtained in the condition of vt-MVF in the beta band, which indicated the improved general efficiency of brain neural communication in the left hemisphere

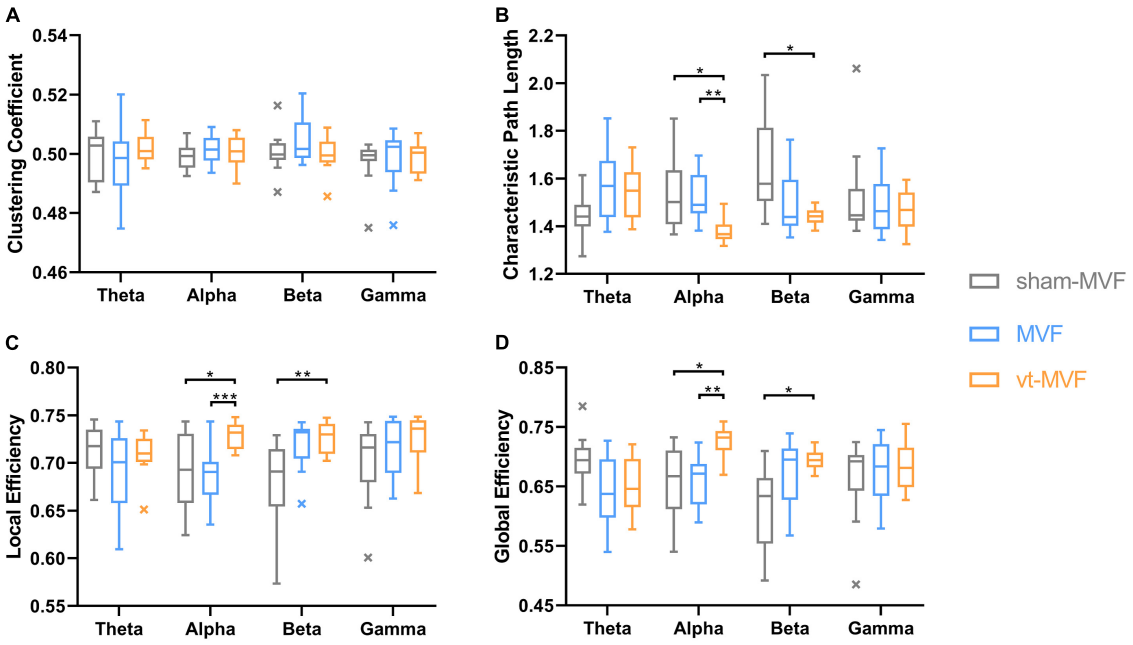


FIGURE 5
Network metrics, including **(A)** clustering coefficient, **(B)** characteristic path length, **(C)** local efficiency, and **(D)** global efficiency, of the three experimental conditions in different frequency bands. The central line in these boxplots indicates the median and the cross markers are the outliers. The asterisk indicates a significant difference between the two conditions (*$0.01 < p < 0.05$, **$0.001 < p < 0.01$, ***$p < 0.001$).

(dominant hand). Besides, CC in the gamma band revealed a significant rightward asymmetry in the condition of vt-MVF, which suggested increased segregation of the right hemisphere. Moreover, a leftward asymmetry of LE in the gamma band was shown in the condition of sham-MVF.

## 4. Discussion

This study reveals a positive impact of the perception of embodiment on network connectivity and neural communication efficiency in healthy subjects. Moreover, the present study also provides tentative evidence that a stronger perception of embodiment induced *via* the combination of mirror visual and vibrotactile stimulus could enhance neural communication efficiency and generate a shift in global brain network efficiency toward the hemisphere of the dominant hand.

The present study explored the instantaneous effect of embodiment perception on the alteration of neural connectivity. Previous studies indicated that visual inputs induced mirror illusion combined with vibrotactile stimulation evoked kinesthesia illusion could promote embodiment perception *via* multisensory integration and presented an enhancement of embodiment with upgrading activation of the motor region (Wittkopf et al., 2017; Ding et al., 2020a,b). As suggested by the average node degree, dense network connectivity was observed in subjects while perceiving embodiment, and large differences in network connectivity were demonstrated among conditions. This observation indicates the centrality of embodiment perception in the EEG-based network and suggested a tendency of more obvious centrality of strengthening embodiment while receiving the combination of MVF and vibrotactile stimulation. Moreover, subsequent observations of node degrees showed centralities of the embodiment perception mainly in the left central area in the alpha and the beta bands. Similar to our observation, studies reported the activation of the motor cortex during MVF, when subjects had mirror illusion/embodiment (Lee et al., 2015; Ding et al., 2020a). Centralities in the left frontal, bilateral occipital-parietal, and bilateral temporal areas were also obtained in the condition of MVF and vt-MVF in our study. This finding is in line with our previous observations and provides tentative evidence for the instant effects of embodiment on mediating the information transmission in the visual stream (Goodale and Milner, 1992; Ding et al., 2019). The ventral-dorsal visual streams comprised the temporal, parietal, and visual cortex, which play an important role in the perceptual identification of objects and sensorimotor transformations (Goodale and Milner, 1992). In addition, this study demonstrates a trend of prominent centralities in visual stream areas from the beta band to the alpha band while embodiment perception is enhanced *via* the combination of vibrotactile stimulation. Thus, we inferred a positive relationship between embodiment perception and network topology, especially in the visual stream-involved regions.

An efficient network would contribute to the enhancement of human brain functions, which relied on suitable properties of the network (Bassett et al., 2006; Laney et al., 2015). A network with a high clustering coefficient (segregation) and short characteristic path length (integration) was regarded as an optimal network, where the efficiency of local and/or global information communication and processing was facilitated (Bassett et al., 2006). Previous studies reported enhanced neural communication after the intervention of MVF, which indicated the long-term effects of

TABLE 2 Laterality index (mean ± standard deviation) of the sham-MVF, MVF, and vt-MVF experimental conditions in different frequency bands.

| Metric | Condition | Frequency band | | | |
|---|---|---|---|---|---|
| | | Theta | Alpha | Beta | Gamma |
| *CC* | sham-MVF | −0.0003 ± 0.0073 | −0.0071 ± 0.0134 | 0.0021 ± 0.0256 | −0.0065 ± 0.0116 |
| | MVF | 0.0043 ± 0.0121 | −0.0097 ± 0.0148 | −0.0019 ± 0.0083 | −0.0007 ± 0.0172 |
| | vt-MVF | −0.0025 ± 0.0209 | −0.0045 ± 0.0154 | 0.0038 ± 0.0099 | **0.0066 ± 0.0095** |
| *CPL* | sham-MVF | −0.0336 ± 0.0886 | −0.0025 ± 0.0638 | −0.0289 ± 0.0962 | −0.0044 ± 0.0357 |
| | MVF | −0.0151 ± 0.1062 | 0.0068 ± 0.1306 | 0.0337 ± 0.0959 | 0.0158 ± 0.0657 |
| | vt-MVF | −0.0198 ± 0.0477 | −0.0133 ± 0.1023 | **0.0399 ± 0.0392** | 0.0069 ± 0.0789 |
| *LE* | sham-MVF | 0.0131 ± 0.0577 | 0 ± 0.0546 | 0.0055 ± 0.0213 | **−0.0261 ± 0.0302** |
| | MVF | 0.0199 ± 0.0532 | −0.0077 ± 0.0506 | −0.0254 ± 0.0622 | −0.0125 ± 0.0503 |
| | vt-MVF | −0.0057 ± 0.044 | −0.0042 ± 0.0615 | −0.0119 ± 0.0325 | 0.0063 ± 0.0483 |
| *GE* | sham-MVF | 0.0336 ± 0.0886 | 0.0025 ± 0.0638 | 0.0289 ± 0.0962 | 0.0044 ± 0.0357 |
| | MVF | 0.0151 ± 0.1062 | −0.0068 ± 0.1306 | −0.0337 ± 0.0959 | −0.0158 ± 0.0657 |
| | vt-MVF | 0.0198 ± 0.0477 | 0.0133 ± 0.1023 | **−0.0399 ± 0.0392** | −0.0069 ± 0.0789 |

Bold values indicated statistically significant ($p < 0.05$) laterality indexes, i.e., left and right sub-networks had a significant difference in network metrics.

embodiment (Hamzei et al., 2012; Saleh et al., 2014; Ding et al., 2019). In the present study, increased global and local neural communication efficiencies were obtained in the condition of vt-MVF as an instant effect of enhanced embodiment, compared to the other two conditions. To our knowledge, our study is the first to demonstrate the prominent segregation and integration of brain networks in healthy subjects during motor tasks while receiving MVF with vibrotactile stimuli. However, significant alterations of neural communications were only observed in the vt-MVF condition. Our previous study supported that the combination of MVF and vibrotactile stimuli could strengthen the embodiment perception and activate motor regions in both alpha and beta bands (Ding et al., 2020a). Thus, we speculated that the enhanced embodiment *via* multi-sensory integration might have more prominent instant effects on neural communication in healthy subjects. In addition, this study also reported that the enhanced embodiment could generate a shift in global neural communication efficiency toward the dominant side, which might contribute to the practice of the vt-MVF in the clinic for hemiplegic paralysis rehabilitation. Although no significant alterations were found in the condition of MVF, a similar trend was still demonstrated in the beta band when compared to the sham-MVF. One possible interpretation might be the alpha oscillations were the dominant rhythm during wakeful relaxation with closed eyes (Lindgren et al., 1999), while the beta oscillations were more involved in active tasks, including cognitive tasks (Jin et al., 2012). In our study, subjects were required to watch the reflection of their non-dominant hand and feel as if his/her dominant hand was moving with the image in the mirror. Thus, the beta band would be more sensitive and predominant. The MVF-induced embodiment might have a long-term effect on shifting brain function toward an efficient pattern, but it might be difficult or insufficient to observe its instant effect in our study. This might be another potential reason.

It should be noted that opposite results were shown in the theta band, where larger connections and enhanced global brain neural communication efficiency were revealed in healthy subjects without MVF stimulation. Theta rhythm appears during a relaxed brain state and is involved in inward-focused concentration (Shenefelt, 2018), which might be one possible reason. Moreover, motor imagery showed increased theta synchronization, which reflected an increased effort, and reduction of visuospatial attention (Lubbe et al., 2021). Thus, the major involvement of motor imagery in the condition of sham-MVF might contribute to the results. Further studies were necessary to investigate these factors.

## 5. Limitation

As an in-depth analysis of our previous experiment, this study suggested potential mechanisms of MVF from the perspective of brain connectivity. Although this was a pilot study, the small sample size still hindered the power of statistical analyses. Second, it might provide more suggestions and directions for the clinic, if the subjects were elderly healthy people or stroke patients. Third, it would be better to use individualized frequency bands, which might eliminate the impact of interindividual differences in EEG frequencies. Furthermore, the data were collected by a 32-channel wireless EEG cap, which might limit further exploration of sub-network alterations.

## 6. Conclusion

This study explored the instant effects of MVF on brain connectivity for new insight, which revealed the capacity of embodiment perception to strengthen network connectivity and facilitate neural communication efficiency in healthy subjects. Moreover, this study also provided tentative evidence that a stronger embodiment sense induced *via* the combination of mirror visual and vibrotactile stimulus could enhance neural communication efficiency and generate a shift toward the hemisphere of the dominant hand. These findings might contribute

to the investigation of the therapeutic effect of MVF and the development of a new rehabilitation strategy.

## Data availability statement

The raw data supporting the conclusion of this article will be made available by the authors, without undue reservation.

## Ethics statement

The studies involving human participants were reviewed and approved by the Research Ethics Committee of the University of Waterloo. The patients/participants provided their written informed consent to participate in this study.

## Author contributions

JJ, JH, and NJ conceived the study. LD performed the experiment. LD and QS analyzed the data and wrote the manuscript. All authors read and approved the final manuscript.

## Funding

This work was supported by the National Natural Science Foundation of China (82002385), the National Key R&D Program of China (2018YFC2002300 and 2018YFC2002301), and the Shanghai Sailing Program (20YF1403400).

## Acknowledgments

We thank the China Scholarship Council for supporting LD studying at the University of Waterloo as a visiting scholar.

## Conflict of interest

The authors declare that the research was conducted in the absence of any commercial or financial relationships that could be construed as a potential conflict of interest.

## Publisher's note



## References

Arya, K. N. (2016). Underlying neural mechanisms of mirror therapy: Implications for motor rehabilitation in stroke. *Neurol. India* 64, 38–44. doi: 10.4103/0028-3886.173622

Bartur, G., Pratt, H., Frenkel-Toledo, S., and Soroker, N. (2018). Neurophysiological effects of mirror visual feedback in stroke patients with unilateral hemispheric damage. *Brain Res.* 1700, 170–180. doi: 10.1016/j.brainres.2018.09.003

Bassett, D. S., Meyer-Lindenberg, A., Achard, S., Duke, T., and Bullmore, E. (2006). Adaptive reconfiguration of fractal small-world human brain functional networks. *Proc. Natl. Acad. Sci. U. S. A.* 103, 19518–19523. doi: 10.1073/pnas.0606005103

Bernhardt, B. C., Chen, Z., He, Y., Evans, A. C., and Bernasconi, N. (2011). Graph-theoretical analysis reveals disrupted small-world organization of cortical thickness correlation networks in temporal lobe epilepsy. *Cereb. Cortex* 21, 2147–2157. doi: 10.1093/cercor/bhq291

Blanke, O., Slater, M., and Serino, A. (2015). Behavioral, neural, and computational principles of bodily self-consciousness. *Neuron* 88, 145–166. doi: 10.1016/j.neuron.2015.09.029

Caliandro, P., Vecchio, F., Miraglia, F., Reale, G., Della, M. G., La, T. G., et al. (2017). Small-World Characteristics of cortical connectivity changes in acute stroke. *Neurorehabil. Neural Repair* 31, 81–94. doi: 10.1177/1545968316662525

Chang, M. Y., Kim, H. H., Kim, K. M., Oh, J. S., Jang, C., and Yoon, T. H. (2017). Effects of observation of hand movements reflected in a mirror on cortical activation in patients with stroke. *J. Phys. Ther. Sci.* 29, 38–42. doi: 10.1589/jpts.29.38

Debnath, R., and Franz, E. A. (2016). Perception of hand movement by mirror reflection evokes brain activation in the motor cortex contralateral to a non-moving hand. *Cortex* 81, 118–125. doi: 10.1016/j.cortex.2016.04.015

Delorme, A., and Makeig, S. (2004). EEGLAB: An open source toolbox for analysis of single-trial EEG dynamics including independent component analysis. *J. Neurosci. Methods* 134, 9–21. doi: 10.1016/j.jneumeth.2003.10.009

Ding, L., He, J., Yao, L., Zhuang, J., Chen, S., Wang, H., et al. (2020a). Mirror visual feedback combining vibrotactile stimulation promotes embodiment perception: An electroencephalogram (EEG) pilot study. *Front. Bioeng. Biotechnol.* 8:553270. doi: 10.3389/fbioe.2020.553270

Ding, L., Li, L., Xu, Z., Tian, J., Chen, S., Wang, H., et al. (2020b). Computer vision technology-based face mirroring system providing mirror therapy for Bell's palsy patients. *Disabil. Rehabil.* 42, 833–840. doi: 10.1080/09638288.2018.1510551

Ding, L., Wang, X., Chen, S., Wang, H., Tian, J., Rong, J., et al. (2019). Camera-based mirror visual input for priming promotes motor recovery, daily function, and brain network segregation in subacute stroke patients. *Neurorehabil. Neural Repair* 33, 307–318. doi: 10.1177/1545968319836207

Fink, G. R., Marshall, J. C., Halligan, P. W., Frith, C. D., Driver, J., Frackowiak, R. S., et al. (1999). The neural consequences of conflict between intention and the senses. *Brain* 122, 497–512. doi: 10.1093/brain/122.3.497

Goodale, M. A., and Milner, A. D. (1992). Separate visual pathways for perception and action. *Trends Neurosci.* 15, 20–25. doi: 10.1016/0166-2236(92)90344-8

Hamzei, F., Lappchen, C. H., Glauche, V., Mader, I., Rijntjes, M., and Weiller, C. (2012). Functional plasticity induced by mirror training: The mirror as the element connecting both hands to one hemisphere. *Neurorehabil. Neural Repair* 26, 484–496. doi: 10.1177/1545968311427917

Hassanin, O., Al-Shargie, F., Tariq, U., and Al-Nashash, H. (2021). Asymmetry of regional phase synchrony cortical networks under cognitive alertness and vigilance decrement states. *IEEE Trans. Neural Syst. Rehabil. Eng.* 29, 2378–2387. doi: 10.1109/TNSRE.2021.3125420

Hosseini, S. M., Hoeft, F., and Kesler, S. R. (2012). GAT: A graph-theoretical analysis toolbox for analyzing between-group differences in large-scale structural and functional brain networks. *PLoS One* 7:e40709. doi: 10.1371/journal.pone.0040709

Jin, S. H., Lin, P., and Hallett, M. (2012). Reorganization of brain functional small-world networks during finger movements. *Hum. Brain Mapp.* 33, 861–872. doi: 10.1002/hbm.21253

Laney, J., Adali, T., Mccombe, S., and Westlake, K. P. (2015). Quantifying motor recovery after stroke using independent vector analysis and graph-theoretical analysis. *Neuroimage Clin.* 8, 298–304. doi: 10.1016/j.nicl.2015.04.014

Lappchen, C. H., Ringer, T., Blessin, J., Seidel, G., Grieshammer, S., Lange, R., et al. (2012). Optical illusion alters M1 excitability after mirror therapy: A TMS study. *J. Neurophysiol.* 108, 2857–2861. doi: 10.1152/jn.00321.2012

Lee, H. M., Li, P. C., and Fan, S. C. (2015). Delayed mirror visual feedback presented using a novel mirror therapy system enhances cortical activation in healthy adults. *J. Neuroeng. Rehabil.* 12:56. doi: 10.1186/s12984-015-0053-1

Lindgren, K. A., Larson, C. L., Schaefer, S. M., Abercrombie, H. C., Ward, R. T., Oakes, T. R., et al. (1999). Thalamic metabolic rate predicts EEG alpha power in healthy control subjects but not in depressed patients. *Biol. Psychiatry* 45, 943–952. doi: 10.1016/S0006-3223(98)00350-3

Lubbe, V. D., Sobierajewicz, J., Jongsma, M. L. A., Verwey, W. B., and Przekoracka-Krawczyk, A. (2021). Frontal brain areas are more involved during motor imagery than during motor execution/preparation of a response sequence. *Int. J. Psychophysiol.* 164, 71–86. doi: 10.1016/j.ijpsycho.2021.02.020

Matthys, K., Smits, M., Van der Geest, J. N., Van der Lugt, A., Seurinck, R., Stam, H. J., et al. (2009). Mirror-induced visual illusion of hand movements: A functional magnetic resonance imaging study. *Arch. Phys. Med. Rehabil.* 90, 675–681. doi: 10.1016/j.apmr.2008.09.571

Medina, J., Khurana, P., and Coslett, H. B. (2015). The influence of embodiment on multisensory integration using the mirror box illusion. *Conscious. Cogn.* 37, 71–82. doi: 10.1016/j.concog.2015.08.011

Michielsen, M. E., Selles, R. W., Van, D. G., Eckhardt, M., Yavuzer, G., Stam, H. J., et al. (2011a). Motor recovery and cortical reorganization after mirror therapy in chronic stroke patients: A phase II randomized controlled trial. *Neurorehabil. Neural Repair* 25, 223–233. doi: 10.1177/1545968310385127

Michielsen, M. E., Smits, M., Ribbers, G. M., Stam, H. J., Van, D. G., Bussmann, J. B., et al. (2011b). The neuronal correlates of mirror therapy: An fMRI study on mirror induced visual illusions in patients with stroke. *J. Neurol. Neurosurg. Psychiatry* 82, 393–398. doi: 10.1136/jnnp.2009.194134

Newman, M. E. J. (2003). The structure and function of complex networks. *Soc. Ind. Appl. Math.* 43, 167–256. doi: 10.1137/S003614450342480

Pollock, A., Farmer, S. E., Brady, M. C., Langhorne, P., Mead, G. E., Mehrholz, J., et al. (2014). Interventions for improving upper limb function after stroke. *Cochrane Database Syst. Rev.* 2014:CD010820. doi: 10.1002/14651858.CD010820.pub2

Rizzo, M., Petrini, L., Del, P. C., Lopez, S., Arendt-Nielsen, L., and Babiloni, C. (2022). Mirror visual feedback during unilateral finger movements is related to the desynchronization of cortical electroencephalographic somatomotor alpha rhythms. *Psychophysiology* 59:e14116. doi: 10.1111/psyp.14116

Rjosk, V., Lepsien, J., Kaminski, E., Hoff, M., Sehm, B., Steele, C. J., et al. (2017). Neural correlates of mirror visual feedback-induced performance improvements: A resting-state fMRI study. *Front. Hum. Neurosci.* 11:54. doi: 10.3389/fnhum.2017.00054

Rohafza, M., Saleh, S., and Adamovich, S. (2019). EEG based analysis of cortical activity during mirror visual feedback target-directed movement. *Annu. Int. Conf. IEEE Eng. Med. Biol. Soc.* 2019, 5156–5159. doi: 10.1109/EMBC.2019.8857945

Rossiter, H. E., Borrelli, M. R., Borchert, R. J., Bradbury, D., and Ward, N. S. (2015). Cortical mechanisms of mirror therapy after stroke. *Neurorehabil. Neural Repair* 29, 444–452. doi: 10.1177/1545968314554622

Rothgangel, A. S., Braun, S. M., Beurskens, A. J., Seitz, R. J., and Wade, D. T. (2011). The clinical aspects of mirror therapy in rehabilitation: A systematic review of the literature. *Int. J. Rehabil. Res.* 34, 1–13. doi: 10.1097/MRR.0b013e3283441e98

Rubinov, M., and Sporns, O. (2010). Complex network measures of brain connectivity: Uses and interpretations. *Neuroimage* 52, 1059–1069. doi: 10.1016/j.neuroimage.2009.10.003

Saleh, S., Adamovich, S. V., and Tunik, E. (2014). Mirrored feedback in chronic stroke: Recruitment and effective connectivity of ipsilesional sensorimotor networks. *Neurorehabil. Neural Repair* 28, 344–354. doi: 10.1177/1545968313513074

Saleh, S., Yarossi, M., Manuweera, T., Adamovich, S., and Tunik, E. (2017). Network interactions underlying mirror feedback in stroke: A dynamic causal modeling study. *Neuroimage Clin.* 13, 46–54. doi: 10.1016/j.nicl.2016.11.012

Shenefelt, P. D. (2018). Mindfulness-based cognitive hypnotherapy and skin disorders. *Am. J. Clin. Hypn.* 61, 34–44. doi: 10.1080/00029157.2017.1419457

Smith, K., Abasolo, D., and Escudero, J. (2016). A comparison of the cluster-span threshold and the union of shortest paths as objective thresholds of EEG functional connectivity networks from Beta activity in Alzheimer's disease. *Annu. Int. Conf. IEEE Eng. Med. Biol. Soc.* 2016, 2826–2829. doi: 10.1109/EMBC.2016.7591318

Smith, K., Azami, H., Parra, M. A., Starr, J. M., and Escudero, J. (2015). Cluster-span threshold: An unbiased threshold for binarising weighted complete networks in functional connectivity analysis. *Annu. Int. Conf. IEEE Eng. Med. Biol. Soc.* 2015, 2840–2843. doi: 10.1109/EMBC.2015.7318983

Stam, C. J., Nolte, G., and Daffertshofer, A. (2007). Phase lag index: Assessment of functional connectivity from multi channel EEG and MEG with diminished bias from common sources. *Hum. Brain Mapp.* 28, 1178–1193. doi: 10.1002/hbm.20346

Thieme, H., Morkisch, N., Mehrholz, J., Pohl, M., Behrens, J., Borgetto, B., et al. (2018). Mirror therapy for improving motor function after stroke. *Cochrane Database Syst. Rev.* 7:CD008449. doi: 10.1002/14651858.CD008449.pub3

Wittkopf, P. G., Lloyd, D. M., and Johnson, M. I. (2017). Changing the size of a mirror-reflected hand moderates the experience of embodiment but not proprioceptive drift: A repeated measures study on healthy human participants. *Exp. Brain Res.* 235, 1933–1944. doi: 10.1007/s00221-017-4930-7

Zhang, J. J., and Fong, K. N. K. (2019). Enhancing mirror visual feedback with intermittent theta burst stimulation in healthy adults. *Restor. Neurol. Neurosci.* 37, 483–495. doi: 10.3233/RNN-190927

frontiers | Frontiers in Neuroscience

TYPE Study Protocol
PUBLISHED 30 March 2023
DOI 10.3389/fnins.2023.1121043



OPEN ACCESS

EDITED BY
Jie Jia,
Fudan University, China

REVIEWED BY
Ying Shen,
The First Affiliated Hospital of Nanjing Medical University, China
Mengyuan Ding,
Harvard University, United States

*CORRESPONDENCE
Kangling Wang
✉ wkangling@126.com

SPECIALTY SECTION
This article was submitted to Translational Neuroscience, a section of the journal Frontiers in Neuroscience

RECEIVED 11 December 2022
ACCEPTED 08 March 2023
PUBLISHED 30 March 2023

CITATION
Han M, He J, Chen N, Gao Y, Wang Z and Wang K (2023) Intermittent theta burst stimulation vs. high-frequency repetitive transcranial magnetic stimulation for post-stroke cognitive impairment: Protocol of a pilot randomized controlled double-blind trial.
*Front. Neurosci.* 17:1121043.
doi: 10.3389/fnins.2023.1121043



# Intermittent theta burst stimulation vs. high-frequency repetitive transcranial magnetic stimulation for post-stroke cognitive impairment: Protocol of a pilot randomized controlled double-blind trial

Menglin Han, Jinyan He, Na Chen, Yulan Gao, Zhiqiang Wang and Kangling Wang*

Department of Rehabilitation, Zhujiang Hospital, Southern Medical University, Guangzhou, China

**Introduction:** Intermittent theta burst stimulation (iTBS), a novel mode of transcranial magnetic stimulation (TMS), has curative effects on patients with post-stroke cognitive impairment (PSCI). However, whether iTBS will be more applicable in clinical use than conventional high-frequency repetitive transcranial magnetic stimulation (rTMS) is unknown. Our study aims to compare the difference in effect between iTBS and rTMS in treating PSCI based on a randomized controlled trial, as well as to determine its safety and tolerability, and to further explore the underlying neural mechanism.

**Methods:** The study protocol is designed as a single-center, double-blind, randomized controlled trial. Forty patients with PSCI will be randomly assigned to two different TMS groups, one with iTBS and the other with 5 Hz rTMS. Neuropsychological evaluation, activities of daily living, and resting electroencephalography will be conducted before treatment, immediately post-treatment, and 1 month after iTBS/rTMS stimulation. The primary outcome is the change in the Montreal Cognitive Assessment Beijing Version (MoCA-BJ) score from baseline to the end of the intervention (D11). The secondary outcomes comprise changes in resting electroencephalogram (EEG) indexes from baseline to the end of the intervention (D11) as well as the Auditory Verbal Learning Test, the symbol digit modality test, the Digital Span Test findings, and the MoCA-BJ scores from baseline to endpoint (W6).

**Discussion:** In this study, the effects of iTBS and rTMS will be evaluated using cognitive function scales in patients with PSCI as well as data from resting EEG, which allows for an in-depth exploration of underlying neural oscillations. In the future, these results may contribute to the application of iTBS for cognitive rehabilitation of patients with PSCI.

KEYWORDS

**post-stroke cognitive impairment (PSCI), high-frequency repetitive transcranial magnetic stimulation (HF-rTMS), intermittent theta burst stimulation (iTBS), electroencephalography, randomized controlled trial**

# 1. Introduction

Post-stroke cognitive impairment (PSCI), one of the most common complications of stroke (Zlokovic et al., 2020), refers to a variety of symptoms ranging from mild cognitive impairment to dementia. Approximately 20–70% of stroke survivors suffer cognitive impairment within 6 months of stroke (Liao et al., 2021; Merriman et al., 2021). Due to impaired attention, memory, language, and visuospatial functions, PSCI impedes recovery from stroke-related sequelae, including sensory impairment, motor dysfunction, and limitations in daily activities (Viktorisson et al., 2021). Currently, evidence-based treatment guidelines for PSCI are lacking, due to the limited pharmacological (donepezil, galantamine, and memantine) and non-pharmacological therapies (cognitive training and physical interventions) (Mijajlovиæ et al., 2017). Hence, the identification of optimal and effective treatment is crucial. Recent studies have shown that neuromodulation techniques help improve cognitive impairment through neuroplasticity (Paolucci et al., 1996; Cicerone et al., 2011; Paolucci, 2013; Di Lazzaro et al., 2021), similar to repetitive transcranial magnetic stimulation (rTMS), which has been proven by several meta-analyses to have promising and positive effects (Lefaucheur et al., 2014, 2020; Hara et al., 2021; Liu et al., 2021; Zhang et al., 2021). Intermittent Theta Burst Stimulation (iTBS) is a novel neuromodulation technique with a unique advantage in treatment time compared to rTMS (Huang et al., 2005) and a reported better facilitation effect on modulating cortical excitability in brain regions (Blumberger et al., 2018; Kaster et al., 2019; Si et al., 2019). ITBS is effective and safe for treating depression, autism, and Parkinson's disease in patients with mild cognitive impairment (Trung et al., 2019). However, evidence for iTBS treatment for patients with PSCI is limited. Some studies on PSCI have demonstrated that iTBS can improve patients' overall cognitive function (Tsai et al., 2020; Li et al., 2022), specifically memory function (Tsai et al., 2020). However, the therapeutic mechanism of iTBS remains unclear, in the absence of sufficient neuroimaging assessments and long-term follow-up (Tsai et al., 2020; Li et al., 2022). In addition, there is inadequate evidence to suggest that iTBS is equally or more effective than traditional rTMS in terms of the treatment outcome. Therefore, we are conducting a randomized, double-blind controlled trial using neurobehavioral assessments combined with a neurobehavioral method, electroencephalogram (EEG), to compare the difference in effect between iTBS and rTMS in treating PSCI, as well as to explore neuroelectrophysiological changes. We hope to provide a theoretical basis for PSCI treatment. The protocol for this trial has been prepared according to the recommendations for interventional trials (SPIRIT) 2013 guidelines (Chan et al., 2013).

# 2. Methods and analysis

## 2.1. Patients

### 2.1.1. Study setting

This study will be conducted at Zhujiang Hospital, Southern Medical University (Guangzhou, China). Forty inpatients with PSCI in the rehabilitation medicine ward will be included between October 2022 and December 2023.

### 2.1.2. Eligibility criteria

Researchers will screen patients based on the inclusion and exclusion criteria. Once participants are confirmed as eligible, they will sign an informed consent form. To maintain safety criteria, we will not enroll patients who are intolerant to TMS. Women who are pregnant, breastfeeding, or intend to have children in the near future will not be eligible for enrolment. In addition, we will not enroll patients who have participated in other clinical trials or have a history of epilepsy. If a patient who has had TMS treatment has not received TMS treatment in more than 3 months, we may consider enrolling them. Finally, by conducting a preliminary exploratory study to compare clinical efficacy between rTMS and iTBS therapy on patients with PSCI, we aim to analyze data within and between the two hemispheres (the healthy and the affected sides) for the dynamic changes of oscillations to mine additional information. In light of the above statistical analysis, we decide to exclude patients with bilateral lesions from this study.

#### 2.1.2.1. Inclusion criteria

- Age 18 to 80 years;
- Stroke patients meeting the diagnostic criteria established at the Fourth National Cerebrovascular Disease Academic Conference in 1995;
- Imaging evidence of stroke confirmed by computed tomography (CT) or magnetic resonance imaging (MRI);
- Montreal Cognitive Assessment Scale (MoCA) score $\leq$24;
- Cognitive impairment should occur within 12 months of the vascular event and last for at least 3 months;
- First-ever stroke;
- Right-handed;
- Normal cognitive function before stroke;
- No severe aphasia (screened by the Chinese Aphasia Battery) and capable of completing cognitive tests;
- Stable vital signs;
- Voluntary participation and signed informed consent (signed by the patient or another authorized representative).

#### 2.1.2.2. Exclusion criteria

- Complete damage to the left prefrontal cortex confirmed by CT/MRI;
- Bilateral brain lesions;
- Defect of the skull;
- Use of antidepressants or psychostimulants;
- Metal or cardiac pacemaker implants near the treatment site;
- Previous brain disorders such as brain tumors, brain trauma, and seizures;
- History of malignant trauma;
- Unstable vital signs or failure of vital organs;
- Any neuropsychiatric comorbidity or affective disorder that could affect the test results;
- Patients with dementia (Clinical Dementia Rating grade $\geq$0.5) who are unable to cooperate with the cognitive assessment and intervention described below.

### 2.1.3. Participant timeline

The study will begin by screening the participants for eligibility. Once the patient's eligibility has been confirmed, an informed consent form will be signed, and the patient will be randomly assigned to one of the two treatment groups. Clinical assessment and resting EEG measurements will be performed at baseline (D0), after 10 TMS treatments (D11), and at the 6-week follow-up (W6). It is possible that some participants will not be able to attend our hospital for their evaluation at W6. Therefore, we will present two situations. Participants who can return to the hospital will have their EEG data collected at W6, while those who are unable to return to the hospital will be evaluated door-to-door. A record will be made if a patient leaves the trial, is excluded, or withdraws at any point, along with the reasons. The visit schedule and study flowchart are presented in **Table 1** and **Figure 1**.

### 2.1.4. Sample size

This will be an exploratory study. The required sample size for this study was estimated using GPower software (version 3.1.9.7) (Faul et al., 2007). Repeated measures analysis of variance (ANOVA) will be used for statistical analysis, with group and time as affecting factors. Accordingly, the *F*-test (repeated-measures ANOVA, between factors) was chosen, with a power of 85%, an alpha value of 0.05, and an effect size of 0.25 (Cunningham and Mccrum-Gardner, 2007). The predicted minimum sample size was 32 (two groups) considering a 20% loss to follow-up. Therefore, we set the sample size at 40 patients in total, with 20 patients in each group.

### 2.1.5. Recruitment

Forty inpatients with PSCI at Zhujiang Hospital, Southern Medical University will be recruited. The participants will be screened by a dedicated individual for those who meet the inclusion and exclusion criteria and are willing to receive TMS treatment. The participants will receive information in both written and verbal formats about the purpose and procedures of the study once their verbal consent has been confirmed. In this study, no biological specimens will be collected for storage, and no severe adverse effects on the participants are expected (Lefaucheur et al., 2020). The study will begin with a baseline assessment followed by random allocation after written informed consent is obtained from the participants.

### 2.1.6. Randomization and blinding

Using a random number sequence generated using SPSS 25.0 software, all eligible patients will be randomly assigned to one of two treatment groups. The allocation and detailed TMS protocol will be known only to the two doctors who will perform TMS stimulation but will be blinded to the patients and other members of the study staff (such as outcome assessors or data analysts). Doctors performing TMS interventions will not be involved in any other aspect of the study, such as patient recruitment, randomization, allocation, outcome assessment, or data analysis.

## 2.2. Interventions

Transcranial magnetic stimulation treatments will be delivered by a magnetic simulator (Magneuro100, VISHEE Medical Technology Co., LTD, Nanjing, China) with a figure-8 coil. Each patient will receive TMS stimulation in the afternoon for 10 consecutive days. The left DLPFC (F3) will be the target site to stimulate the left prefrontal cortex according to the international 10/20 EEG recording system (Kim et al., 2010). The intensity will be set at 80% of the resting motor threshold in both the rTMS and iTBS groups (Shajahan et al., 2002; Kim et al., 2010).

### 2.2.1. rTMS protocol

The 5 Hz rTMS parameters include 2-s trains (10 pulses) at an intertrain interval of 8 s, repeated every 10 s for a total of 10 min and 600 pulses.

### 2.2.2. iTBS protocol

The iTBS parameters include three continuous pulses at 50 Hz, repeated at 5 Hz (2 s on, 8 s off) for a total of 192 s and 600 pulses. After the stimulation is completed, the direction of the coil is turned 90°, and a sham stimulation lasting 408 s is conducted in order to ensure the consistency of treatment time such that all patients are blinded to the experimental protocol.

### 2.2.3. RMT

The resting motor threshold (RMT) refers to the minimum stimulus intensity that can evoke a response at least 50% of the time in a given number of trials (usually 10 trials). The patients will be asked to relax with their eyes open. During the recording process, the coils will be systematically moved (mapped) over the primary motor cortex until the maximal consistent response of the contralateral first dorsal interosseous muscle is detected. The RMT between the first dorsal interosseous bone and the minimum intensity is defined as the ability to elicit motor-evoked potentials of at least 50 mV in 5 out of 10 consecutive treatments (Rossini et al., 2015).

### 2.2.4. Routine medical care

Medical care based on the disease of each patient is permitted.

### 2.2.5. Discontinuation criteria

Patients with worsening symptoms, such as recurrent stroke, decreased muscle strength, or persistent unexplained infections.

Patients who wish to discontinue participation.

Patients who are unable to complete the treatment sessions.

Patients who are unable to participate in the baseline assessment.

## 2.3. Outcomes

Our primary outcome will be the Montreal Cognitive Assessment Beijing Version (MoCA-BJ) score from baseline to the end of the intervention (D11). Secondary outcomes will be resting EEG indexes, the Auditory Verbal Learning Test (AVLT), the symbol digit modality test (SDMT), the Digital Span Test (DST), and adverse events. Indexes of resting EEG include the absolute power and relative power of neural oscillations. Other outcomes include the Hamilton Depression Scale (HAMD) and Activities of Daily Living (ADL). All clinical assessments will be performed thrice: pre-treatment (baseline), post-last treatment, and

TABLE 1 Trial schedule.

| | Trial schedule | | | | |
|---|---|---|---|---|---|
| Timepoint | Enrollment -D1 | Allocation 0 | Post-allocation D1–D10 | Close-out D11 | Follow-up W6 |
| **Enrolment** | | | | | |
| Eligibility screen | × | | | | |
| Informed consent | × | | | | |
| Allocation | | × | | | |
| **Interventions** | | | | | |
| (rTMS) | | | ×——× | | |
| (iTBS) | | | ×——× | | |
| **Assessments** | | | | | |
| Demographics and clinical characteristics | | × | | | |
| MoCA; AVLT; SDMT; DST; HAMD; ADL | | × | | × | × |
| Resting EEG | | × | | × | |

DLPFC, dorsolateral prefrontal cortex; rTMS, repetitive transcranial magnetic stimulation; iTBS, intermittent theta burst transcranial magnetic stimulation; MoCA, Montreal cognitive assessment; AVLT, auditory verbal learning test; SDMT, symbol digit modalities test; DST, digital span test, HAMD: Hamilton depression scale; ADL, activities of daily living; EEG, electroencephalography.

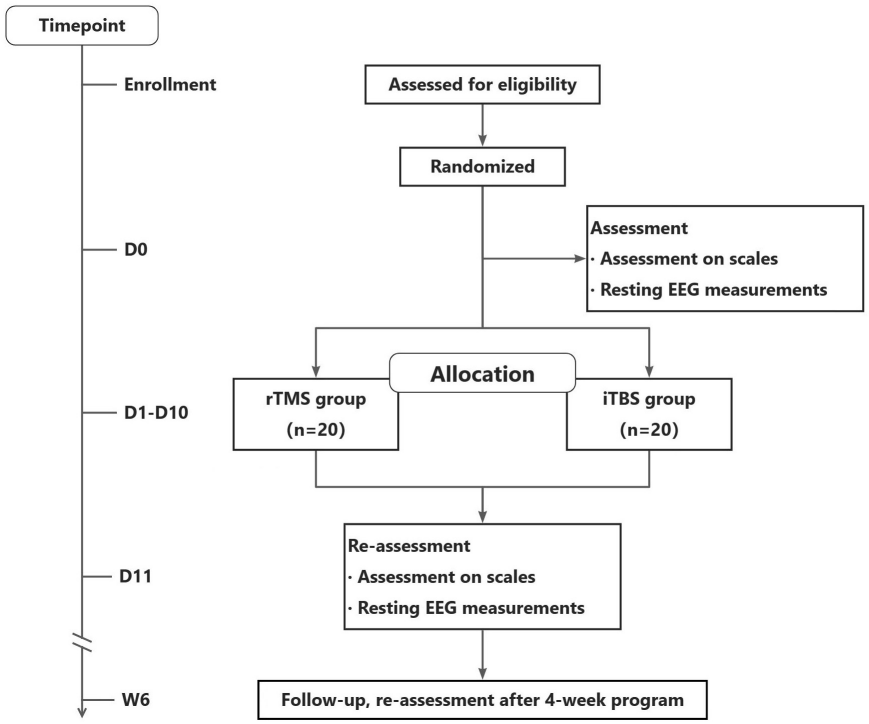


FIGURE 1
Design and flow of participants through the study.

at the 1-month follow-up. An experienced physician will conduct all cognitive assessments throughout the study and will be blinded to the participants' group assignment and trial phases. The resting EEG will be conducted at baseline and at the end of TMS treatment.

### 2.3.1. MoCA-BJ

The MoCA-BJ is a Chinese version of the Montreal Cognitive Assessment that is highly sensitive and specific for screening cognitive impairment in stroke patients (Nasreddine et al., 2005; Yu et al., 2012).

### 2.3.2. Resting EEG measurements

A resting EEG is a graphical representation of the spontaneous electrical activity of a population of brain cells. It is obtained by magnifying and recording spontaneous biopotentials of the brain from the scalp using sophisticated electronic equipment

(Höller and Nardone, 2021). EEG signals will be recorded using an EEG cap equipped with 64 Ag/AgCl electrodes, arranged according to the Extended International 10–20 electrode placement system (Tamburro et al., 2020). A 5-min EEG recording will be conducted with participants seated comfortably in a sound-insulated, dimly lit room with their eyes closed. All channels will be referenced online to the bilateral mastoid and amplified using an amplifier (Compumedics Neuroscan, Neuroscan 8050). Data will be sampled at 2,048 Hz, with impedances kept below 10 kΩ for all channels throughout data collection.

The acquired EEG signals will be analyzed offline using MATLAB2013b. Given previous evidence that oscillatory dynamics are affected by rTMS (Thut et al., 2011; Veniero et al., 2011; Chota et al., 2021) and are closely related to cognitive improvement (Klimesch et al., 1993; Richard Clark et al., 2004; Iliopoulos et al., 2020), we will analyze the power spectrum and functional connectivity of each oscillation within and between hemispheres, between groups, and pre- and post-treatment. Oscillation ratios, such as θ/α ratio, θ/γ ratio, and (α + β)/(θ + δ) ratio will be further analyzed (Coben et al., 1985; Moretti et al., 2013; Sato et al., 2022).

#### 2.3.3. AVLT

In the neuropsychology literature, AVLT is frequently used to assess memory. The test measures immediate and delayed free recall, retroactive and proactive interference, and recognition through verbal learning (Hawkins et al., 2004).

#### 2.3.4. SDMT

Several cognitive operations require the evaluation of information processing speed, which can be achieved through SDMT (Silva et al., 2018).

#### 2.3.5. DST

The scale can be divided into digit span forward (DSF) and digit span backward (DSB), each of which consists of two sets of 2-digit to 10-digit tables. The total score of the DSF and DSB indicates the participant's attentional functioning, with a higher score indicating better function (Jahanshahi et al., 2008).

#### 2.3.6. HAMD

Hamilton Depression Scale has been widely used in psychopharmacological and clinical research since the 1960s (Hamilton, 1967).

#### 2.3.7. ADL

The modified Barthel Index (MBI) is used to assess an individual's ability to perform basic activities of daily living (Mahoney and Barthel, 1965; Shah et al., 1989). In this study, a Chinese version of the MBI that includes ten items (personal hygiene, bathing, feeding, toileting, stair climbing, dressing, bowel control, bladder control, walking or wheelchair transfers, and chair-bed transfers) will be used (Leung et al., 2007). Total independence is indicated by a score of 100.

#### 2.3.8. Adverse events

During the treatment period and within 1 h following each treatment, adverse events, such as headaches, scalp sensations or nociception, temporal and neck muscle pain, and seizures will be recorded.

### 2.4. Statistical analyses

In the case of quantitative data, we will calculate the mean, standard deviation, and confidence interval as well as the minimum, maximum, P25, P50, and P75, as needed. For count data, we will calculate the frequency distributions and corresponding percentages. For rank data, we will provide frequency distributions and percentages, as well as median and mean rankings. Qualitative data will be presented as the positive rate, positive number, and denominator number of cases. Data from MoCA-BJ, AVLT, SDMT, DST, HAMA, and ADL will be analyzed by repeated-measures ANOVA using SPSS software (version 25.0; IBM, Armonk, NY, USA). Repeated-measures ANOVA will be used to analyze the differences between time points and groups. The acquired EEG signals will be analyzed offline using MATLAB2013b. The EEGLAB toolbox (version 13.0.0b) will be used for EEG data preprocessing (Delorme and Makeig, 2004), followed by interest channel selection based on the average level of the two groups and the relative spectral energy extracted from each frequency band. Finally, we will use repeated-measures ANOVA to compare the differences between groups and the relative spectral energy at different times. Statistical significance will be set at $P < 0.05$.

## 3. Discussion

Transcranial magnetic stimulation modulates brain function through neural changes induced by magnetic pulses. Using pulsed magnetic fields, TMS regulates the action potentials of nerve cells by inducing current in the central nervous system. This approach can affect the metabolic and neurophysiological activities of the brain. In recent decades, TMS has been widely used to treat cognitive impairment caused by various neurological, psychiatric, and psychological disorders, including stroke, Alzheimer's disease, Parkinson's disease, and schizophrenia. While iTBS, a new model of TMS, has been proven to be effective in Parkinson's disease with cognitive impairment, its use in patients with PSCI is unclear. Several studies have shown that rTMS is a safe and effective method for improving cognitive function (Chou et al., 2020; Jiang et al., 2020; Alyagon et al., 2021). Regarding neurophysiology, iTBS may have equal or greater excitatory effects than conventional TMS (Di Lazzaro et al., 2011; Bakker et al., 2015). However, previous evidence indicates that conventional high-frequency TMS facilitates neurogenesis in the motor cortex more effectively than iTBS in a rat model (Luo et al., 2017). Another study that applied rTMS to healthy individuals found that rTMS produced a greater response than iTBS (Curtin et al., 2017). In patients with PSCI, there is no consensus regarding whether conventional rTMS or iTBS is more effective.

To assess the effect of the treatment, neurobehavioral scales are often used in studies of PSCI (Tsai et al., 2020). However, scale results are sometimes, to some extent, subjective because of the evaluator's judgment and the state of the patient (Tsai et al., 2020). Therefore, objective means of assessment are urgently needed. EEG is gaining increasing attention because it is a special and complex bioelectrical signal reflecting the functional state of the brain, with the advantages of high temporal resolution, non-invasiveness, and

low cost. A direct effect of rTMS treatment on brain function is altered nerve oscillation, which can have a therapeutic effect by resetting the oscillations of the thalamus and cortex (Thut et al., 2011; Veniero et al., 2011; Chota et al., 2021). Rhythmic patterns of neural oscillations are believed to play a functional role in local processing and communication among neuronal systems (Fries, 2005; Thut et al., 2012). Different regions of the human cortex tend to oscillate at different frequencies. Thus, it is possible to study neural oscillation activity in more detail. Most cognitive processes are associated with a frequency band in the delta, theta, alpha, beta, or gamma range. Several researchers have suggested, based on high-quality correlative EEG data, that brain oscillations are involved in a variety of sensory and cognitive processes (Klimesch, 1999; Lu et al., 2022). However, a causal relationship can only be demonstrated by directly modulating the oscillatory signals. EEG is an effective and dependable tool for detecting neural oscillations in the brain. Thus, this study may be able to investigate the specific relationship between neural oscillations and TMS facilitative effects on cognitive function in more detail.

In conclusion, the goal of this study will be to compare effect differences among various TMS protocols (iTBS and conventional rTMS) on PSCI and analyze whether iTBS is non-inferior or superior to conventional rTMS treatment. Given that iTBS has a shorter treatment time, it is more convenient to use if its therapeutic effect is not inferior to that of rTMS. Thus, iTBS might prove more advantageous and convenient than the classic rTMS for outpatients. Furthermore, we hope to explore the neural activity changes underlying iTBS/rTMS intervention in PSCI and thus, provide a theoretical foundation for clinical applications.

This study has some limitations. It will be a single-center trial with a comparatively small sample size, due to recruitment difficulties associated with the management of coronavirus disease 2019. In addition, the heterogeneity of oral medication in patients with PSCI may also pose potential problems in measuring cortical excitability and therapeutic response (Cantone et al., 2020). Future multi-center studies should be conducted to mitigate these limitations.

## Ethics statement

The studies involving human participants were reviewed and approved by the Medical Ethics Committee of Zhujiang Hospital of Southern Medical University. The patients/participants provided their written informed consent to participate in this study.

## Author contributions

MH designed the study and drafted the manuscript. MH, JH, NC, YG, and ZW collected the clinical data. KW critically revised the manuscript and contributed the most important intellectual content. All authors have read and approved the final manuscript.

## Funding

This study was supported by the National Natural Youth Science Foundation of China (grant no. 82002374).

## Conflict of interest

The authors declare that the research was conducted in the absence of any commercial or financial relationships that could be construed as a potential conflict of interest.

## Publisher's note

All claims expressed in this article are solely those of the authors and do not necessarily represent those of their affiliated organizations, or those of the publisher, the editors and the reviewers. Any product that may be evaluated in this article, or claim that may be made by its manufacturer, is not guaranteed or endorsed by the publisher.

## References

Alyagon, U., Barnea-Ygael, N., Carmi, L., and Zangen, A. (2021). Modifications of cognitive performance in the stroop task following deep rTMS treatment course in OCD patients. *Brain Stimul.* 14, 48–50. doi: 10.1016/j.brs.2020.11.008

Bakker, N., Shahab, S., Giacobbe, P., Blumberger, D. M., Daskalakis, Z. J., Kennedy, S. H., et al. (2015). rTMS of the dorsomedial prefrontal cortex for major depression: Safety, tolerability, effectiveness, and outcome predictors for 10 Hz versus intermittent theta-burst stimulation. *Brain Stimul.* 8, 208–215. doi: 10.1016/j.brs.2014.11.002

Blumberger, D. M., Vila-Rodriguez, F., Thorpe, K. E., Feffer, K., Noda, Y., Giacobbe, P., et al. (2018). Effectiveness of theta burst versus high-frequency repetitive transcranial magnetic stimulation in patients with depression (THREE-D): A randomised non-inferiority trial. *Lancet* 391, 1683–1692. doi: 10.1016/S0140-6736(18)30295-2

Cantone, M., Lanza, G., Fisicaro, F., Pennisi, M., Bella, R., Di Lazzaro, V., et al. (2020). Evaluation and treatment of vascular cognitive impairment by transcranial magnetic stimulation. *Neural Plast.* 2020:8820881. doi: 10.1155/2020/8820881

Chan, A. W., Tetzlaff, J. M., Altman, D. G., Laupacis, A., Gøtzsche, P. C., Krleža-Jerić, K., et al. (2013). SPIRIT 2013 statement: Defining standard protocol items for clinical trials. *Ann. Intern. Med.* 158, 200–207. doi: 10.7326/0003-4819-158-3-201302050-00583

Chota, S., Marque, P., and VanRullen, R. (2021). Occipital alpha-TMS causally modulates temporal order judgements: Evidence for discrete temporal windows in vision. *Neuroimage* 237:118173. doi: 10.1016/j.neuroimage.2021.118173

Chou, Y. H., Ton That, V., and Sundman, M. (2020). A systematic review and meta-analysis of rTMS effects on cognitive enhancement in mild cognitive impairment and Alzheimer's disease. *Neurobiol. Aging* 86, 1–10. doi: 10.1016/j.neurobiolaging.2019.08.020

Cicerone, K. D., Langenbahn, D. M., Braden, C., Malec, J. F., Kalmar, K., Fraas, M., et al. (2011). Evidence-based cognitive rehabilitation: Updated review of the literature from 2003 through 2008. *Arch. Phys. Med. Rehabil.* 92, 519–530. doi: 10.1016/j.apmr.2010.11.015

Coben, L., Danziger, W., and Storandt, M. (1985). A longitudinal EEG study of mild senile dementia of Alzheimer type: Changes at 1 year and at 2.5 years. *Electroencephalogr. Clin. Neurophysiol.* 61, 101–112. doi: 10.1016/0013-4694(85)91048-x

Cunningham, J. B., and Mccrum-Gardner, E. (2007). Power, effect and sample size using gpower: Practical issues for researchers and members of research ethics committees. *Evid. Based Midwifery* 5, 132–136.

Curtin, A., Sun, J., Ayaz, H., Qian, Z., Onaral, B., Wang, J., et al. (2017). Evaluation of evoked responses to pulse-matched high frequency and intermittent theta burst transcranial magnetic stimulation using simultaneous functional near-infrared spectroscopy. *Neurophotonics* 4:041405. doi: 10.1117/1.NPh.4.4.041405

Delorme, A., and Makeig, S. (2004). EEGLAB: An open source toolbox for analysis of single-trial EEG dynamics including independent component analysis. *J. Neurosci. Methods* 134, 9–21. doi: 10.1016/j.jneumeth.2003.10.009

Di Lazzaro, V., Bella, R., Benussi, A., Bologna, M., Borroni, B., Capone, F., et al. (2021). Diagnostic contribution and therapeutic perspectives of transcranial magnetic stimulation in dementia. *Clin. Neurophysiol.* 132, 2568–2607. doi: 10.1016/j.clinph.2021.05.035

Di Lazzaro, V., Dileone, M., Pilato, F., Capone, F., Musumeci, G., Ranieri, F., et al. (2011). Modulation of motor cortex neuronal networks by rTMS: Comparison of local and remote effects of six different protocols of stimulation. *J. Neurophysiol.* 105, 2150–2156. doi: 10.1152/jn.00781.2010

Faul, F., Erdfelder, E., Lang, A. G., and Buchner, A. (2007). G*Power 3: A flexible statistical power analysis program for the social, behavioral, and biomedical sciences. *Behav. Res. Methods* 39, 175–191. doi: 10.3758/bf03193146

Fries, P. (2005). A mechanism for cognitive dynamics: Neuronal communication through neuronal coherence. *Trends Cogn. Sci.* 9, 474–480.

Hamilton, M. (1967). Development of a rating scale for primary depressive illness. *Br. J. Soc. Clin. Psychol.* 6, 278–296. doi: 10.1111/j.2044-8260.1967.tb00530.x

Hara, T., Shanmugalingam, A., McIntyre, A., and Burhan, A. M. (2021). The Effect of non-invasive brain stimulation (NIBS) on attention and memory function in stroke rehabilitation patients: A systematic review and meta-analysis. *Diagnostics* 11:227. doi: 10.3390/diagnostics11020227

Hawkins, K. A., Dean, D., and Pearlson, G. D. (2004). Alternative forms of the rey auditory verbal learning test: A review. *Behav. Neurol.* 15, 99–107. doi: 10.1155/2004/940191

Höller, Y., and Nardone, R. (2021). Quantitative EEG biomarkers for epilepsy and their relation to chemical biomarkers. *Adv. Clin. Chem.* 102, 271–336. doi: 10.1016/bs.acc.2020.08.004

Huang, Y. Z., Edwards, M. J., Rounis, E., Bhatia, K. P., and Rothwell, J. C. (2005). Theta burst stimulation of the human motor cortex. *Neuron* 45, 201–206. doi: 10.1016/j.neuron.2004.12.033

Iliopoulos, F., Taskin, B., Villringer, A., and Nierhaus, T. (2020). Imperceptible somatosensory single pulse and pulse train stimulation oppositely modulate Mu Rhythm Activity and perceptual performance. *Cereb. Cortex* 30, 6284–6295. doi: 10.1093/cercor/bhaa185

Jahanshahi, M., Saleem, T., Ho, A. K., Fuller, R., and Dirnberger, G. (2008). A preliminary investigation of the running digit span as a test of working memory. *Behav. Neurol.* 20, 17–25. doi: 10.3233/BEN-2008-0212

Jiang, Y., Guo, Z., McClure, M. A., He, L., and Mu, Q. (2020). Effect of rTMS on Parkinson's cognitive function: A systematic review and meta-analysis. *BMC Neurol.* 20:377. doi: 10.1186/s12883-020-01953-4

Kaster, T. S., Downar, J., Vila-Rodriguez, F., Thorpe, K. E., Feffer, K., Noda, Y., et al. (2019). Trajectories of response to dorsolateral prefrontal rTMS in major depression: A THREE-D study. *Am. J. Psychiatry* 176, 367–375. doi: 10.1176/appi.ajp.2018.18091096

Kim, B. R., Kim, D. Y., Chun, M. H., Yi, J. H., and Kwon, J. S. (2010). Effect of repetitive transcranial magnetic stimulation on cognition and mood in stroke patients: A double-blind, sham-controlled trial. *Am. J. Phys. Med. Rehabil.* 89, 362–368. doi: 10.1097/PHM.0b013e3181d8a5b1

Klimesch, W. (1999). EEG alpha and theta oscillations reflect cognitive and memory performance: A review and analysis. *Brain Res. Brain Res. Rev.* 29, 169–195. doi: 10.1016/s0165-0173(98)00056-3

Klimesch, W., Schimke, H., and Pfurtscheller, G. (1993). Alpha frequency, cognitive load and memory performance. *Brain Topogr.* 5, 241–251.

Lefaucheur, J., Aleman, A., Baeken, C., Benninger, D., Brunelin, J., Di Lazzaro, V., et al. (2020). Evidence-based guidelines on the therapeutic use of repetitive transcranial magnetic stimulation (rTMS): An update (2014-2018). *Clin. Neurophysiol.* 131, 474–528. doi: 10.1016/j.clinph.2019.11.002

Lefaucheur, J., André-Obadia, N., Antal, A., Ayache, S., Baeken, C., Benninger, D., et al. (2014). Evidence-based guidelines on the therapeutic use of repetitive transcranial magnetic stimulation (rTMS). *Clin. Neurophysiol.* 125, 2150–2206. doi: 10.1016/j.clinph.2014.05.021

Leung, S. O., Chan, C. C., and Shah, S. (2007). Development of a Chinese version of the modified barthel index– validity and reliability. *Clin. Rehabil.* 21, 912–922. doi: 10.1177/0269215507077286

Li, W., Wen, Q., Xie, Y., Hu, A., Wu, Q., and Wang, Y. (2022). Improvement of poststroke cognitive impairment by intermittent theta bursts: A double-blind randomized controlled trial. *Brain Behav.* 12:e2569. doi: 10.1002/brb3.2569

Liao, X., Zuo, L., Pan, Y., Xiang, X., Meng, X., Li, H., et al. (2021). Screening for cognitive impairment with the Montreal cognitive assessment at six months after stroke and transient ischemic attack. *Neurol. Res.* 43, 15–21. doi: 10.1080/01616412.2020.1819070

Liu, M., Bao, G., Bai, L., and Yu, E. (2021). The role of repetitive transcranial magnetic stimulation in the treatment of cognitive impairment in stroke patients: A systematic review and meta-analysis. *Sci. Prog.* 104:368504211004266. doi: 10.1177/00368504211004266

Lu, Z., Wang, H., Gu, J., and Gao, F. (2022). Association between abnormal brain oscillations and cognitive performance in patients with bipolar disorder: Molecular mechanisms and clinical evidence. *Synapse* 76:e22247. doi: 10.1002/syn.22247

Luo, J., Zheng, H., Zhang, L., Zhang, Q., Li, L., Pei, Z., et al. (2017). High-frequency repetitive transcranial magnetic stimulation (rTMS) improves functional recovery by enhancing neurogenesis and activating BDNF/TrkB signaling in ischemic rats. *Int. J. Mol. Sci.* 18:455. doi: 10.3390/ijms18020455

Mahoney, F. I., and Barthel, D. W. (1965). Functional evaluation: The barthel index. *Md. State Med. J.* 14, 61–65.

Merriman, N. A., Gillan, D., Pender, N., Williams, D. J., Horgan, F., Sexton, E., et al. (2021). The StrokeCog study: Development and description of a cognition-focused psychological intervention to address cognitive impairment following stroke. *Psychol. Health* 36, 792–809. doi: 10.1080/08870446.2020.1820009

Mijajloviæ, M. D., Pavloviæ, A., Brainin, M., Heiss, W. D., Quinn, T. J., Ihle-Hansen, H. B., et al. (2017). Post-stroke dementia – a comprehensive review. *BMC Med.* 15:11. doi: 10.1186/s12916-017-0779-7

Moretti, D., Paternicò, D., Binetti, G., Zanetti, O., and Frisoni, G. (2013). Relationship between EEG alpha3/alpha2 ration and the nucleus accumbens in subjects with mild cognitive impairment. *J. Neurol. Neurophysiol.* 4, 1–6.

Nasreddine, Z. S., Phillips, N. A., Bédirian, V., Charbonneau, S., Whitehead, V., Collin, I., et al. (2005). The montreal cognitive assessment, MoCA: A brief screening tool for mild cognitive impairment. *J. Am. Geriatr. Soc.* 53, 695–699. doi: 10.1111/j.1532-5415.2005.53221.x

Paolucci, S. (2013). Role, indications, and controversies of antidepressant therapy in chronic stroke patients. *Eur. J. Phys. Rehabil. Med.* 49, 233–241.

Paolucci, S., Antonucci, G., Gialloreti, L. E., Traballesi, M., Lubich, S., Pratesi, L., et al. (1996). Predicting stroke inpatient rehabilitation outcome: The prominent role of neuropsychological disorders. *Eur. Neurol.* 36, 385–390. doi: 10.1159/000117298

Richard Clark, C., Veltmeyer, M., Hamilton, R., Simms, E., Paul, R., Hermens, D., et al. (2004). Spontaneous alpha peak frequency predicts working memory performance across the age span. *Int. J. Psychophysiol.* 53, 1–9. doi: 10.1016/j.ijpsycho.2003.12.011

Rossini, P. M., Burke, D., Chen, R., Cohen, L. G., Daskalakis, Z., Di Iorio, R., et al. (2015). Non-invasive electrical and magnetic stimulation of the brain, spinal cord, roots and peripheral nerves: Basic principles and procedures for routine clinical and research application. An updated report from an I.F.C.N. Committee. *Clin. Neurophysiol.* 126, 1071–1107. doi: 10.1016/j.clinph.2015.02.001

Sato, Y., Schmitt, O., Ip, Z., Rabiller, G., Omodaka, S., Tominaga, T., et al. (2022). Pathological changes of brain oscillations following ischemic stroke. *J. Cereb. Blood Flow Metab.* 42, 1753–1776. doi: 10.1177/0271678X221105677

Shah, S., Vanclay, F., and Cooper, B. (1989). Improving the sensitivity of the Barthel Index for stroke rehabilitation. *J. Clin. Epidemiol.* 42, 703–709. doi: 10.1016/0895-4356(89)90065-6

Shajahan, P. M., Glabus, M. F., Steele, J. D., Doris, A. B., Anderson, K., Jenkins, J. A., et al. (2002). Left dorso-lateral repetitive transcranial magnetic stimulation affects cortical excitability and functional connectivity, but does not impair cognition in major depression. *Prog. Neuropsychopharmacol. Biol. Psychiatry* 26, 945–954. doi: 10.1016/s0278-5846(02)00210-5

Si, Y., Wu, X., Li, F., Zhang, L., Duan, K., Li, P., et al. (2019). Different decision-making responses occupy different brain networks for information processing: A study based on EEG and TMS. *Cereb. Cortex* 29, 4119–4129. doi: 10.1093/cercor/bhy294

Silva, P. H. R., Spedo, C. T., Barreira, A. A., and Leoni, R. F. (2018). Symbol Digit Modalities Test adaptation for Magnetic Resonance Imaging environment: A systematic review and meta-analysis. *Mult. Scler. Relat. Disord.* 20, 136–143. doi: 10.1016/j.msard.2018.01.014

Tamburro, G., di Fronso, S., Robazza, C., Bertollo, M., and Comani, S. (2020). Modulation of brain functional connectivity and efficiency during an endurance cycling task: A source-level EEG and graph theory approach. *Front. Hum. Neurosci.* 14:243. doi: 10.3389/fnhum.2020.00243

Thut, G., Miniussi, C., and Gross, J. (2012). The functional importance of rhythmic activity in the brain. *Curr. Biol.* 22, R658–R663. doi: 10.1016/j.cub.2012.06.061

Thut, G., Veniero, D., Romei, V., Miniussi, C., Schyns, P., and Gross, J. (2011). Rhythmic TMS causes local entrainment of natural oscillatory signatures. *Curr. Biol.* 21, 1176–1185. doi: 10.1016/j.cub.2011.05.049

Trung, J., Hanganu, A., Jobert, S., Degroot, C., Mejia-Constain, B., Kibreab, M., et al. (2019). Transcranial magnetic stimulation improves cognition over time in Parkinson's disease. *Parkinsonism Relat. Disord.* 66, 3–8. doi: 10.1016/j.parkreldis.2019.07.006

Tsai, P. Y., Lin, W. S., Tsai, K. T., Kuo, C. Y., and Lin, P. H. (2020). High-frequency versus theta burst transcranial magnetic stimulation for the treatment of poststroke cognitive impairment in humans. *J. Psychiatry Neurosci.* 45, 262–270. doi: 10.1503/jpn.190060

Veniero, D., Brignani, D., Thut, G., and Miniussi, C. (2011). Alpha-generation as basic response-signature to transcranial magnetic stimulation

(TMS) targeting the human resting motor cortex: A TMS/EEG co-registration study. *Psychophysiology* 48, 1381–1389. doi: 10.1111/j.1469-8986.2011.01218.x

Viktorisson, A., Andersson, E. M., Lundström, E., and Sunnerhagen, K. S. (2021). Levels of physical activity before and after stroke in relation to early cognitive function. *Sci. Rep.* 11:9078. doi: 10.1038/s41598-021-88606-9

Yu, J., Li, J., and Huang, X. (2012). The Beijing version of the Montreal Cognitive Assessment as a brief screening tool for mild cognitive impairment: A community-based study. *BMC Psychiatry* 12:156. doi: 10.1186/1471-244X-12-156

Zhang, J., Zhong, D., Xiao, X., Yuan, L., Li, Y., Zheng, Y., et al. (2021). Effects of repetitive transcranial magnetic stimulation (rTMS) on aphasia in stroke patients: A systematic review and meta-analysis. *Clin. Rehabil.* 35, 1103–1116. doi: 10.1177/0269215521999554

Zlokovic, B., Gottesman, R., Bernstein, K., Seshadri, S., McKee, A., Snyder, H., et al. (2020). Vascular contributions to cognitive impairment and dementia (VCID): A report from the 2018 national heart, lung, and blood institute and national institute of neurological disorders and stroke workshop. *Alzheimers Dement.* 16, 1714–1733. doi: 10.1002/alz.12157

frontiers | Frontiers in Neuroscience

TYPE Original Research
PUBLISHED 31 March 2023
DOI 10.3389/fnins.2023.1124329



OPEN ACCESS

EDITED BY
Jie Jia,
Fudan University, China

REVIEWED BY
Liam Butler,
Wake Forest University, United States
Shaoyang Cui,
Shenzhen Hospital of Guangzhou University of Chinese Medicine, China

*CORRESPONDENCE
Yundong Shen
✉ yundongshen@fudan.edu.cn
Chi Liu
✉ liuchi1975@163.com

†These authors have contributed equally to this work

SPECIALTY SECTION
This article was submitted to Translational Neuroscience, a section of the journal Frontiers in Neuroscience

RECEIVED 15 December 2022
ACCEPTED 08 March 2023
PUBLISHED 31 March 2023

CITATION
Yu S, Yuan J, Lin H, Xu B, Liu C and Shen Y (2023) A predictive model based on random forest for shoulder-hand syndrome. *Front. Neurosci.* 17:1124329. doi: 10.3389/fnins.2023.1124329



# A predictive model based on random forest for shoulder-hand syndrome

Suli Yu[1†], Jing Yuan[2†], Hua Lin[2†], Bing Xu[2], Chi Liu[3*] and Yundong Shen[1,4*]

[1]Department of Hand and Upper Extremity Surgery, Jing'an District Central Hospital, Fudan University, Shanghai, China, [2]Department of Geriatric Rehabilitation Medicine, Shanghai Fourth Rehabilitation Hospital, Shanghai, China, [3]Department of Geriatrics Center, National Clinical Research Center for Aging and Medicine, Jing'an District Central Hospital of Shanghai, Fudan University, Shanghai, China, [4]Department of Hand Surgery, Huashan Hospital, Fudan University, Shanghai, China

**Objectives:** The shoulder-hand syndrome (SHS) severely impedes the function recovery process of patients after stroke. It is incapable to identify the factors at high risk for its occurrence, and there is no effective treatment. This study intends to apply the random forest (RF) algorithm in ensemble learning to establish a predictive model for the occurrence of SHS after stroke, aiming to identify high-risk SHS in the first-stroke onset population and discuss possible therapeutic methods.

**Methods:** We retrospectively studied all the first-onset stroke patients with one-side hemiplegia, then 36 patients that met the criteria were included. The patients' data concerning a wide spectrum of demographic, clinical, and laboratory data were analyzed. RF algorithms were built to predict the SHS occurrence, and the model's reliability was measured with a confusion matrix and the area under the receiver operating curves (ROC).

**Results:** A binary classification model was trained based on 25 handpicked features. The area under the ROC curve of the prediction model was 0.8 and the out-of-bag accuracy rate was 72.73%. The confusion matrix indicated a sensitivity of 0.8 and a specificity of 0.5, respectively. And the feature importance scored the weights (top 3 from large to small) in the classification were D-dimer, C-reactive protein, and hemoglobin.

**Conclusion:** A reliable predictive model can be established based on post-stroke patients' demographic, clinical, and laboratory data. Combining the results of RF and traditional statistical methods, our model found that D-dimer, CRP, and hemoglobin affected the occurrence of the SHS after stroke in a relatively small sample of data with tightly controlled inclusion criteria.

KEYWORDS

**ensemble learning, random forest, shoulder-hand syndrome, stroke rehabilitation, predictive model**

# Introduction

Complex regional pain syndrome (CRPS) (Harden et al., 2007) are neuropathic pain disorders that generally affect the extremities and can occur after myocardial infarction, cervical spondylosis, craniocerebral trauma, and cerebrovascular disease (Shaparin et al., 2014). CRPS of the paralyzed upper limb after stroke is frequently called shoulder-hand syndrome (SHS), also known as reflex sympathetic dystrophy (RSD), and classified as CRPS type I by the International Association for the Study of Pain.

The etiology of SHS is still unclear (Bussa et al., 2015), and the prevalence varies greatly. Researchers in Korea reported the incidence rate ranged from 2 to 50% (Kim et al., 2020), and the Chinese reported from 12.5 to 74.1% (Zhong and Tang, 2009). SHS usually occurs 1−6 months after a cerebrovascular accident, which happens to be the period with the highest potential for rehabilitation (Kumar et al., 2009) and usually has a significant impact on the patient's life quality and functional recovery. The paralyzed upper limbs frequently appeared painful, and edematous. The symptoms usually started from the hands, then often spread to the fingers and palms, and in severe cases to the lower forearms. Sensory disturbances including burning, stiffness, sweating, cold, or fever occurred along with the nerve distribution and the areas of injury. The pain usually increased with hand joint movements (especially passive movement). If not treated and controlled in time, long-term immobilization and relative hypoxia of tissues would cause atrophy of interosseous muscles and lumbricals, contracture of hand joints, especially metacarpophalangeal capsules, together with fibrosis of exudates causing adhesions, thickening of synovial bursae, and changes of corresponding joint bones, result in irreversible disability (Forouzanfar et al., 2002; Pertoldi and Di Benedetto, 2005; Hartwig et al., 2012; Pervane Vural et al., 2016).

The diagnosis of CRPS is often difficult due to the lack of confirmatory tests, and SHS's diagnosis is not specific and more complex than in other pathological situations. SHS is now generally believed to be associated with incorrect movement patterns in the early stages of stroke patients resulting in shoulder and wrist injuries, impaired upper extremity fluid return, and vasomotor dysfunction following central nervous system injury (Lee et al., 2021). Stroke patients usually have arms hanging to their side for long periods in the recumbent and seated positions. The wrist joint is flexed, the shoulder girdle is retracted and sunken, and the forearm is internally rotated. The flexion and compression of the wrist joint can block a venous return to the upper extremity, resulting in swelling of the wrist and forearm (especially in the fingers and wrist) (Geurts et al., 2000). It is internationally recognized that the increased sympathetic excitability and decreased muscle strength of the affected limb after central nervous system injury cause the muscles to lose their "muscle pump" effect, while the obstruction of a venous return due to motor dysfunction leads to edema and pain in the hemiplegic upper limb (Zorowitz et al., 1996). Currently, no guidelines for the prevention of SHS have been established. Treatments include non-pharmacological therapy, pharmacological therapy, regional anesthesia, neuromodulation, sympathectomy, auxiliary compression facilities (Lin et al., 2020), also rehabilitation exercises. Currently, there is no single treatment to be universally effective. Since it was first introduced 70 years ago, it still is challenging work to make early detection of SHS. Our work aims to establish a predictive model of SHS by machine learning algorithm based on patient clinical information to highlight the risk factors, make early diagnoses, and detect potential intervention targets.

Random forest (RF) is an ensemble learning algorithm to predict a binary outcome (classifier) or a numerical value (regressor). It utilized bootstrap aggregating of both sample and feature bagging to create an uncorrelated forest of decision trees. The method is useful when the samples are relatively small (Breiman, 1996, 2001; Deo, 2015). In RF classification, many classification and regression trees (CARTs) are generated with bootstrap's resampling technique repeatedly and randomly select m samples from the original training sample set of N ($m < N$).

In the process of generating a tree, feature selection is needed for splitting. The splitting principle is to improve the purity as much as possible, which can be measured by indicators such as information gain, gain rate, and Gini index. The bootstrap method is also applied for randomly selected parts of the features to find the one that makes the smallest Gini index, and the optimal solution is found among the selected features and applied to the nodes for splitting (Breiman, 2001; Kuhn and Johnson, 2013; Bzdok et al., 2018; Vabalas et al., 2019).

Random forest makes it easy to evaluate variable importance, or contribution, to the model. There are a few ways to evaluate feature importance. Gini importance and mean decrease in impurity (MDI) are usually used to measure how much the model's accuracy decreases when a given variable is excluded. However, permutation importance, also known as mean decrease accuracy (MDA), is another important measure. MDA identifies the average decrease in accuracy by randomly permutating the feature values in out-of-bag samples (Breiman, 2001; Kuhn and Johnson, 2013; Bzdok et al., 2018; Vabalas et al., 2019). These methods allow us to measure the role of each feature in the classification and thus the importance of the occurrence of the disease.

This study intends to initially explore the application of RF to establish a predictive model and measure the importance of each variation in classification.

# Materials and methods

## Patient selection

This study included all adult patients (aged 18 years and older) who were hospitalized at the rehabilitation department during December 2020 and June 2021 in Shanghai Fourth Rehabilitation Hospital.

We included first-onset stroke patients with unilateral hemiparesis, who were admitted to our rehabilitation department within 1 month after stabilization of neurological symptoms. Exclusion criteria: subjects with more than one stroke episode, patients with a history of surgery on the affected upper limb, combined traumatic brain injury, spinal cord injury, acute myocardial infarction, heart failure, history of tumor, and subjects with severe liver and kidney dysfunction, Subjects with combined immune system disorders, hematologic disorders, subject with fever and pulmonary infections at the time of admission (see **Figure 1**).

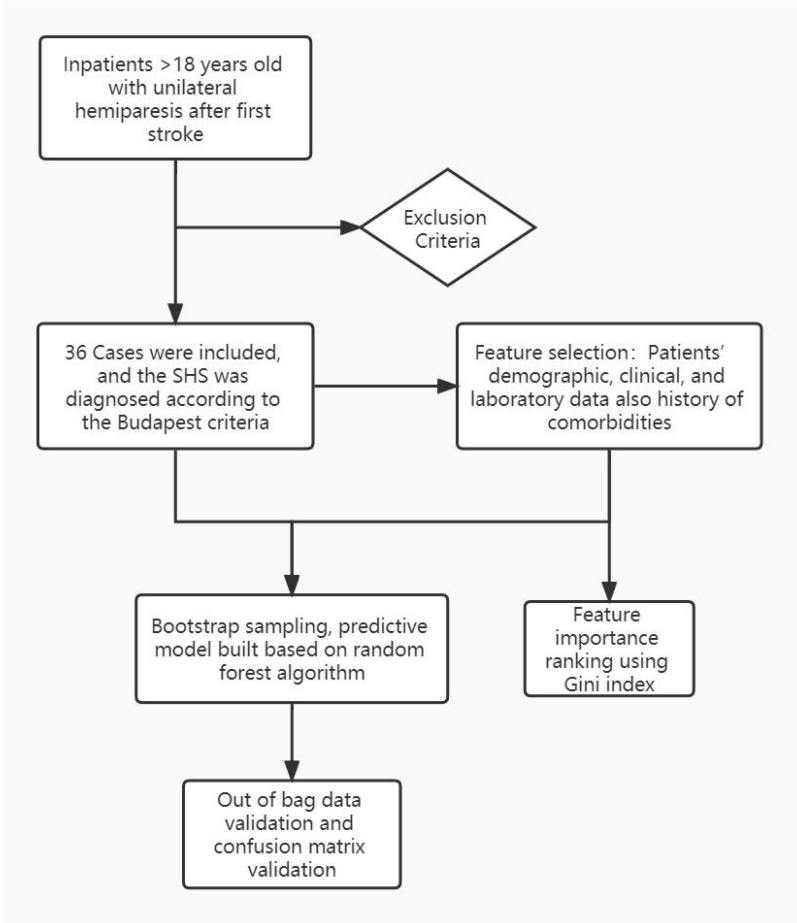


FIGURE 1
The flow chart of the experiment protocol.

Since this study was a predictive model establishment, the laboratory data were collected before the occurrence of the SHS. The site of the stroke was clarified by brain computed tomography or magnetic resonance imaging in all cases. All patients received standardized functional rehabilitation training after admission.

## Ethics approval

This study was approved by the Institutional Review Board of Shanghai Fourth Rehabilitation Hospital with a waiver of informed consent due to the retrospective nature of the study. The data of this study are available from the corresponding author upon reasonable request.

## Assessed variables and feature selection

Patients' demographic, clinical, and laboratory data were used as possible variables as well as the history of the patient's comorbidities. Demographic data included patients' age and sex and laboratory findings consisted of routine examination of blood and biochemistry (Hemoglobin, white blood cell count, platelet count, C-reactive protein, 25-OH vitamin D, D-dimer, creatinine, B-type brain natriuretic peptide, urine microalbumin, homocysteine). Clinical variables included stroke type (infarction, hemorrhage, infarction combined with hemorrhage) and lesion location (cerebral cortex, cerebellum, thalamus, basal ganglia, brainstem).

Post-operative function assessments were not assessed in this study, Due to differences in scale selection and quality control across patients. The outcome was assessed with a follow-up of 6 months of rehabilitation employing the Budapest criteria (**Table 1**)–the mainstream diagnostic tool for CRPS (Pergolizzi et al., 2018).

## Data analysis

Data analysis was performed in python version 3.2.8., using the NumPy, Pandas, scikit-learn, scipy, and matplotlib modules.

Data were summarized by the sample mean and standard deviation (SD) for a continuous variable and by the count for a categorical variable. Demographic characteristics, comorbidities, and laboratory data were compared between two groups using two independent-sample *t*-tests for continuous variables and Fisher's exact tests for categorical variables. Statistically, the significant difference was denoted by a *P*-value of less than 0.05, whereas

TABLE 1 The Budapest criteria: In order to make a clinical diagnosis of CRPS, the following four criteria must be met (Pergolizzi et al., 2018).

| No | Criteria | Categories | | | |
|---|---|---|---|---|---|
| | | Sensory | Vasomotor | Sudomotor/edema | Motor/trophic |
| 1 | Continuing pain, disproportionate to any inciting event | – | – | – | – |
| 2 | Symptoms: must report at least one symptom in three of the four categories shown to the right | Hyperesthesia; Allodynia | Temperature asymmetry; changes in skin color; skin color asymmetry | Edema; sweating changes; sweating asymmetry | Decreased range of motion; motor dysfunction; trophic changes (hair, nails, skin) |
| 3 | Signs: at the time of evaluation, must have at least one sign in two or more of the categories shown to the right | Hyperalgesia (pinprick); Allodynia (light touch or temperature); deep somatic pressure; joint movement | Skin temperature asymmetry (>1°C); changes in skin color; skin color asymmetry | Edema; sweating changes; sweating asymmetry | Decreased range of motion; motor dysfunction (weakness, tremor, dystonia); trophic changes (hair, nails, sin) |
| 4 | No other diagnosis can better explain the patient's signs and symptoms | – | – | – | – |

practical significance was represented by effect sizes. Cohen's d was used to measure effect sizes. In general, a d of 0.2 or smaller is considered to be a small effect size, a d of around 0.5 is considered to be a medium effect size, and a d of 0.8 or larger is considered to be a large effect size.

## Data pre-processing

Empty data were replaced, and the missing value was filled in with the mean to complete the information of all cases. Variables were classified into numeric and categorical variables according to their type.

The categorical variables were:

Gender (male 1, female 2); whether lacunar infarction (yes 1, no 0); brain (lesion involved 1, not involved 0), cerebellum (lesion involved 1, not involved 0), thalamus (lesion involved 1, not involved 0), basal ganglia (lesion involved 1, not involved 0), brain stem (lesion involved 1, not involved 0), stroke type (infarction 1, hemorrhage 2); hemiplegic limbs (left side 1, right side 2); hypertension (d 1, not combined 0), atrial fibrillation (combined 1, not combined 0), diabetes (combined 1, not combined 0).

Numerical variables were: age, white blood cell count, hemoglobin, platelet count, C-reactive protein (CRP), B-type brain natriuretic peptide, D-dimer, 25-OH vitamin D (25-OHD), D dimer Body, creatinine, homocysteine, urine microalbumin.

Use one-hot encoding to convert categorical variables into numeric variables. Perform normalization (scaling) processing for numerical variables. The label prediction was set to 0 (SHS does not occur) and 1 (SHS occurs).

## Random forest algorithm establishment

To predict the occurrence of SHS with imbalanced data recorded (more patients with SHS than without SHS), a classified RF algorithm was trained. Training data were gathered by repeated subsampling (bootstrapping) for inclusion in each tree. Data excluded from the bootstrap subsample (approximately 30% for each tree) were called out-of-bag (OOB). These data were further aggregated into the OOB sample. The number of included decision trees was optimized to achieve the lowest possible error rate, which prevented the over-fitting of the trained model.

Variables were selected using the nested cross-validation and Gini index criterion (a measurement of node purity, the smaller the Gini index, the purer the node, and the more likely the split will take place). The number of trees was selected to minimize the OOB error rate. Node size was optimized using the same criterion.

Predictive power was evaluated on the corresponding OOB data. A confusion matrix was performed to calculate the sensitivity, specificity, and precision. OOB accuracy rate was calculated and receiver operating characteristic (ROC) curves were constructed with corresponding values of area under the curve (AUC) calculated. Values of AUC close to 1 suggest strong predictive capability, whereas values near 0.5 means poor prognostic power.

The RF algorithm had a great quality to measure the relative importance of each feature in the prediction. scikit-learn measured a feature's importance by looking at how much the tree nodes that used that feature reduce impurity across all trees in the forest. The sum of all feature importance scores was equal to one.

Using the bootstrap method sampled 70% size as the training set and the remaining 30% as the test set. Use Python version 3.2.8 to call the Randomforestclassifier module in the scikit-learn library. A total of 99 decision trees were trained under default parameter values (n_estimators = 10, max_depth = None, min_samples_split = 2, random_state = 0). The score function was called to calculate the accuracy of the model on the test set. Confusion_matrix was to calculate the sensitivity, specificity, and precision of the model. The roc_curve function was to draw the ROC curve and obtain the AUC value to evaluate the predictive ability of the model. Feature_importance_ was to obtain the feature importance value and sort it according to its importance.

# Results

## Characteristics of the patients

The inclusion criteria were met by 36 patients (19 men and 13 women). The average age of patients was 59.23 ± 18.27 years. The main recorded comorbidities included arterial hypertension in 31 patients (86.11%), diabetes mellitus (regardless of the type) in 21 patients (58.33%), and atrial fibrillation in 8 patients (22.22%). Left

hemiparesis was present in 16 patients (44.44%). Characteristics of the Patients were summarized in Table 2.

## Prediction of occurrence of post-stroke SHS

To predict whether the occurrence of SHS or not, classified RFs were constructed using 99 trees. The RF prediction model achieved an accuracy rate of 72.73% (0.7272727272727273) on OOB data. The two independent-sample *t*-tests were used for normally distributed and continuous data (see Table 2). The homoscedastic checks (*F*-value) were conducted for all data. The results showed there was a statistically significant difference between the two groups in terms of hemoglobin ($p = 0.048424703$) and D-dimer ($p = 0.042652041$). Then Cohen's d was calculated to measure the effect sizes of the two terms. Cohen's d for hemoglobin was 0.69, and for D-dimer was 0.70, both indicating medium differences between the groups. The occurrence group was prone to lower hemoglobin content and higher D-dimer values. The ranking of the feature importance ordered from largest to smallest was listed in Figure 2. Combining feature importance ranking with *t*-test results, our study indicated that D dimer, CRP, and HB played more important roles in classification and discrimination. The OOB accuracy rate of this model was 72.73%. The confusion matrix analysis (Figure 3) showed a model sensitivity of 0.8, specificity of 0.5, and precision of 0.57142857. The OOB ROC curve of the constructed model had an AUC of 0.8 (Figure 4).

Based on the above 25 characteristics, feature importance showed that the location of the lesion and hemiplegic side had little effect on the classification, indicating its less significant role in predicting the occurrence of SHS. Among the concomitant diseases, concomitant diabetes was more significant than hypertension and atrial fibrillation in predicting the development of SHS despite the low importance ranking score.

# Discussion

Shoulder-hand syndrome is the third most common complication of stroke, after falls and confusion. A previous study found the healthcare utilization cost after diagnosis of SHS is 2.17-fold increased, and at least 8 years after diagnosis such increase persisted (Elsamadicy et al., 2018).

The pathogenesis of SHS is not clear, risk factors cannot be identified, and there are no effective interventions available. Instead of the traditional statistics method, we applied a machine-learning algorithm to build a predictive model and identify high-risk factors for the occurrence of SHS.

Medical dataset may contain noisy information, missing and unbalanced data. When it comes to building disease prediction and diagnostic models, the relevant data may involve many features and complex and non-linear relationships between variable which are often beyond the capacity of traditional statistical data processing.

Random forest is a flexible and easy-to-use machine learning algorithm that hold the advantage of identify the pattern in medical dataset that may not be directly apparent, even without prior knowledge (Hostettler et al., 2018) which made it suitable for the medical dataset.

TABLE 2 Comparison data of demographic and clinical characteristics between the occurrence group and the non-occurring group.

| | Occurrence | Non-occurring | *T*-value | Cohen's d |
|---|---|---|---|---|
| Age | 75.26 ± 10.43 | 73.35 ± 8.38 | 0.551815161 | 0.1 |
| White blood cell | 6.40 ± 1.94 | 7.22 ± 3.26 | 0.373135738 | 0.15 |
| Hemoglobin | 117.89 ± 20.57 | 130.82 ± 16.86 | **0.048424703** | 0.69 |
| Platelet | 209.53 ± 58.81 | 223.29 ± 82.35 | 0.564450443 | 0.19 |
| C-reactive protein | 11.41 ± 21.57 | 13.25 ± 14.86 | 0.77005131 | 0.1 |
| B-type brain natriuretic peptide | 78.77 ± 80.48 | 107.96 ± 169.24 | 0.523183027 | 0.22 |
| D-dimer | 1.80 ± 1.59 | 0.92 ± 0.77 | **0.042652041** | 0.7 |
| 25-OH vitamin D | 30.86 ± 11.95 | 33.06 ± 12.79 | 0.596054774 | 0.18 |
| Homocysteine | 41.68 ± 25.78 | 86.65 ± 211.26 | 0.39585193 | 0.3 |
| Creatinine | 64.72 ± 13.79 | 67.20 ± 28.1 | 0.744649236 | 0.11 |
| Urine microalbumin | 54.16 ± 50.2 | 44.29 ± 43.16 | 0.533938047 | 0.21 |
| | | | Total case ratio | χ |
| Sex male: female | 12: 07 | 11: 06 | 23 (1): 13 (2) | 0.99998918 |
| Stroke type infarction: hemorrhage | 16: 03 | 16: 01 | 32 (1): 4 (2) | 0.925757 |
| Hemiplegic later left: right | 11: 08 | 5: 12 | 16 (1): 20 (2) | 0.56656694 |
| Without hypertension consolidation: non-consolidation | 17: 02 | 14: 03 | 31 (1): 5 (0) | 0.98405107 |
| Without diabetes consolidation: non-consolidation | 7: 12 | 14: 03 | 21 (1): 15 (0) | 0.10544849 |
| Without atrial fibrillation consolidation: non-consolidation | 5: 14 | 3: 14 | 8 (1): 28 (0) | 0.98327996 |

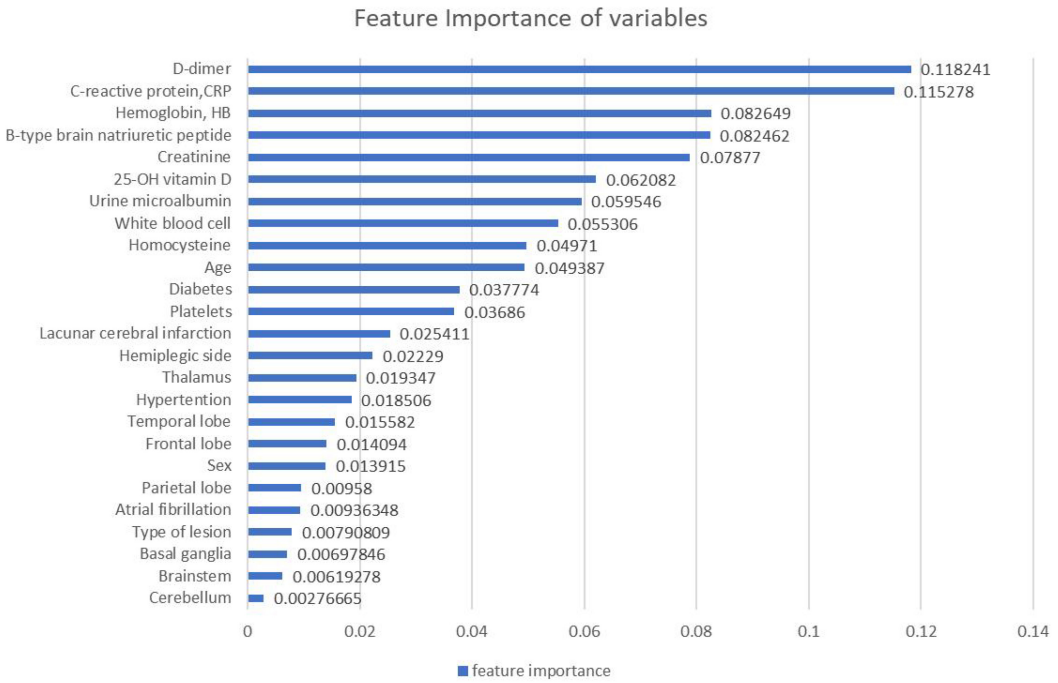


FIGURE 2
Feature importance ranking.

It can process very high dimensional data (many features) and without dimensionality reduction and feature selection. Also it can determine the importance of features and the interaction between different features. These advantages make it particularly suitable for the prediction of diseases with multifactorial involvement (such as SHS) in their pathogenesis, it enable all related or unrelated information during analysis. Also in terms of model building, it is not easy to over-fitting; It can balance the error for unbalanced data sets; If a large part of the features is missing, the accuracy can still be maintained (Vabalas et al., 2019; Liu et al., 2020; Yang et al., 2020).

The onset and severity of SHS appear to be related to the etiology of the stroke (Geurts et al., 2000; Su et al., 2021). Injurious stimuli from stroke lesions can induce inflammatory responses (Shaparin et al., 2014), including classical inflammation (an exaggerated inflammatory response and some chemical mediators around the primary afferent fibers induced peripheral sensitization), neurogenic inflammation (a localized neurogenic inflammation brought edema, vasodilation, and hyperhidrosis, or repeated discharge of the C fibers caused an increased central sensitization), impairment of the autonomic nervous system, and changes of the central nervous system (especially the reorganization of primary somatosensory cortex). Therefore, we included inflammation-related indicators, such as CRP and WBC, and other stroke-related biochemical indicators. Patients' age, hemiplegia side, location of the lesion, etiology of stroke, and comorbidities were also selected into our feature. Feature Selecting for building predictive models is readily available for any medical institution which makes the model practical and generalizable.

It has been suggested that the key to the treatment of SHS is prevention, so some studies have focused on the risk factors for SHS. Potential risk factors had been recognized for SHS like being female, left hemiparesis, spasticity, shoulder subluxation, a lower Brunnstrom stage of the distal upper limb, and an inferior Barthel index (Braus et al., 1994; Sandroni et al., 2003; Ringman et al., 2004; Altas et al., 2020; Su et al., 2021). But no consensus was reached. A population-based study conducted by Sandroni et al. (2003), confirmed female patients had a higher incidence of CRPS compared with male patients, although the mechanisms were not clear so far. And some researchers indicated that patients with left paralysis were more subject to CRPS due to hemineglect more often occurring in a right hemispheric stroke (Braus et al., 1994; Ringman et al., 2004; Altas et al., 2020). Su et al. (2021) conducted a

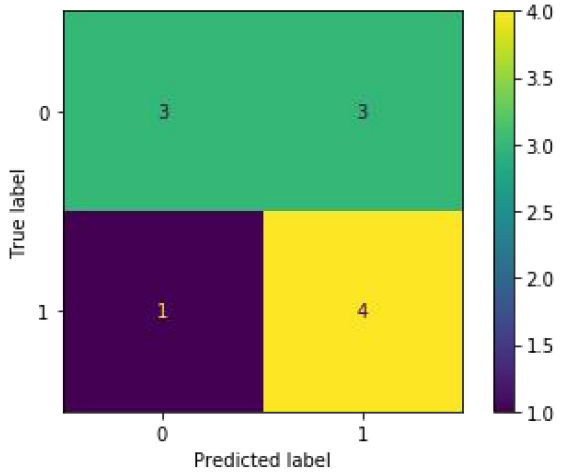


FIGURE 3
Confusion matrix analysis of the test set. (Accuracy: 0.875, sensitivity: 0.8, specificity: 0.5 and precision: 0.57142857).

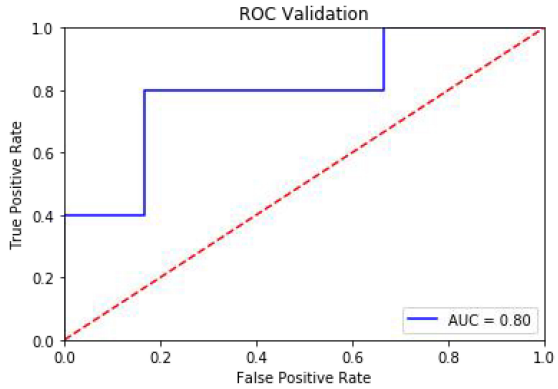


FIGURE 4
The area under the ROC curve evaluates the predictive ability of the model.

meta-analysis comprising 2,225 participants and claimed that age, side of the lesion, etiology of the stroke, the Brunnstrom arm stage, the duration of stroke, and shoulder pain were not found to be associated with SHS. But in *post hoc* analysis they found that women and paralysis of left limbs were found to be more likely to be the feature of SHS.

Our predictive model used feature importance to weigh each feature in classification. It assigned the score of input features based on their significance to predict the output. The more the features were responsible to predict the output, the more their score.

The feature importance of our model assigned a relatively greater value for D-dimer and hemoglobin. Also, statistics analysis found that the SHS group had higher D-dimer levels and lower hemoglobin levels. So a reasonable hypothesis arose whether anticoagulation drugs to decrease the D-dimer and therapies to increase the hemoglobin could be effective precautions or strategies for SHS. Oral corticosteroids were the only recommended drugs for SHS with level 1 evidence of the purpose of anti-inflammatory (Harden et al., 2007). This suggested the important role of anti-inflammatories in the prevention and treatment of SHS. The feature importance ranking assigned CRP a relatively high score in the classification which was not detected in the conventional statistical methods. This result corroborated the reliability and validity of the model to some extent. It also demonstrates the ability of machine learning to far outperform traditional statistical methods in the identification of high-risk factors, even on small sample data.

It is important to note that steroid therapy is somewhat limited in stroke patients (Long and Dagogo-Jack, 2011; Oray et al., 2016). So new approaches are warranted to solve this situation. For the possible implications of D-dimer, hemoglobin in the pathogenesis and treatment of SHS, such as anticoagulant therapy and therapeutic measures to increase hemoglobin levels may prevent or even treat SHS. Confirmation requires larger clinical trials and multiple-center cooperation to validate our preliminary results on a broader sample of numbers and sources.

We also recognize that our model had some limitations due to the small sample for modeling:

1. Our data came from a single medical institution, so our model and findings may not generalize to other populations.

2. The sample size in this study was small, that was why the ROC curve demonstrated a stepped shape. Although it was able to obtain better results with the bootstrap sampling method, it was not sufficient to train a fully valid prediction model and may not provide reliable discrimination of results for out-of-training data. The sample size should be further expanded in future work.

3. Feature selection lacked function assessing indicators. Some researchers indicated that lower function assessment of upper limb like (Barthel index, Brunnstrom stage) may be associated with SHS. The difficulty of our research to incorporate function scale was the lack of uniform quality control. There were inconsistent treatment strategies for functional assessment because patients were seen in different hospitals at the time of stroke onset. Some hospitals had early interventions for functional rehabilitation, while others did not. And there were inconsistencies in the time of assessment, and the functional scores of patients fluctuated widely without good certainty. So we discarded the corresponding functional indicators. Since this study was a preliminary study, we will establish uniform standards for the quality control of functional assessment in the follow-up study.

## Conclusion

The present study demonstrated a ensemble learning method using RF algorithm to predict the occurrence of SHS. Our findings highlighted the predictability of the onset of SHS using common and easily accessible metrics such as the blood biochemistry indicators, site of stroke, etiology, and concurrent diseases. The prediction model had an area under the ROC curve of 0.8, indicating considerable predictive ability. This method has the potential for early diagnosis and identification of high-risk factors with good utility.

## Data availability statement

The original contributions presented in this study are included in the article/**Supplementary material**, further inquiries can be directed to the corresponding authors.

## Ethics statement

The studies involving human participants were reviewed and approved by the Institutional Review Board of Shanghai Fourth Rehabilitation Hospital. The ethics committee waived the requirement of written informed consent for participation.

## Author contributions

SY, JY, and HL: data curation, formal analysis, study design, data collection, and writing–original draft. BX and CL: data collection and data curation. SY, HL, and YS: funding acquisition, supervision, writing–review and editing, and project administration. All authors contributed to the article and approved the submitted version.

## Funding

The project was supported by Medical Research Program of Shanghai Municipal Health Commission Funding (Grant No. 201940055), the Joint Medical Research Program of Shanghai Jing'an District Science and Technology Commission and Health Commission (Grant No. 2020QN07), and National Natural Science Foundation of China (Grant No. 82071406).

## Conflict of interest

The authors declare that the research was conducted in the absence of any commercial or financial relationships that could be construed as a potential conflict of interest.

## Publisher's note

All claims expressed in this article are solely those of the authors and do not necessarily represent those of their affiliated organizations, or those of the publisher, the editors and the reviewers. Any product that may be evaluated in this article, or claim that may be made by its manufacturer, is not guaranteed or endorsed by the publisher.

## Supplementary material

The Supplementary Material for this article can be found online at: https://www.frontiersin.org/articles/10.3389/fnins.2023.1124329/full#supplementary-material

## References

Altas, E. U., Onat, Ş, Konak, H. E., and Polat, C. S. (2020). Post-stroke complex regional pain syndrome and related factors: experiences from a tertiary rehabilitation center. *J. Stroke Cerebrovasc. Dis.* 29:104995. doi: 10.1016/j.jstrokecerebrovasdis.2020.104995

Braus, D. F., Krauss, J. K., and Strobel, J. (1994). The shoulder-hand syndrome after stroke: a prospective clinical trial. *Ann. Neurol.* 36, 728–733. doi: 10.1002/ana.410360507

Breiman, L. (1996). Bagging predictors. *Mach. Learn.* 24, 123–140. doi: 10.1007/BF00058655

Breiman, L. (2001). Random forests. *Mach. Learn.* 45, 5–32. doi: 10.1023/A:1010933404324

Bussa, M., Guttilla, D., Lucia, M., Mascaro, A., and Rinaldi, S. (2015). Complex regional pain syndrome type I: a comprehensive review. *Acta Anaesthesiol. Scand.* 59, 685–697. doi: 10.1111/aas.12489

Bzdok, D., Altman, N., and Krzywinski, M. (2018). Points of significance: statistics versus machine learning. *Nat. Methods* 15, 233–234. doi: 10.1038/nmeth.4642

Deo, R. (2015). Machine learning in medicine. *Circulation* 132, 1920–1930. doi: 10.1161/CIRCULATIONAHA.115.001593

Elsamadicy, A. A., Yang, S., Sergesketter, A. R., Ashraf, B., Charalambous, L., Kemeny, H., et al. (2018). Prevalence and cost analysis of complex regional pain syndrome (CRPS): a role for neuromodulation. *Neuromodul. J. Int. Neuromodul. Soc.* 21, 423–430. doi: 10.1111/ner.12691

Forouzanfar, T., Köke, A., van Kleef, M., and Weber, W. (2002). Treatment of complex regional pain syndrome type I. *Eur. J. Pain* 6, 105–122. doi: 10.1053/eujp.2001.0304

Geurts, A. C. H., Visschers, B., van Limbeek, J., and Ribbers, G. M. (2000). Systematic review of aetiology and treatment of post-stroke hand oedema and shoulder-hand syndrome. *Scand. J. Rehabil. Med.* 32, 4–10. doi: 10.1080/003655000750045668

Harden, R. N., Bruehl, S., Stanton-Hicks, M., and Wilson, P. R. (2007). Proposed new diagnostic criteria for complex regional pain syndrome. *Pain Med.* 8, 326–331. doi: 10.1111/j.1526-4637.2006.00169.x

Hartwig, M., Gelbrich, G., and Griewing, B. (2012). Functional orthosis in shoulder joint subluxation after ischaemic brain stroke to avoid post-hemiplegic shoulder-hand syndrome: a randomized clinical trial. *Clin. Rehabil.* 26, 807–816. doi: 10.1177/0269215511432355

Hostettler, I. C., Muroi, C., Richter, J. K., Schmid, J., Neidert, M., Seule, M., et al. (2018). Decision tree analysis in subarachnoid hemorrhage: prediction of outcome parameters during the course of aneurysmal subarachnoid hemorrhage using decision tree analysis. *J. Neurosurg.* 129, 1499–1510. doi: 10.3171/2017.7.JNS17677

Kim, J. Y., Yoon, S. Y., Kim, J., Jeong, Y. H., and Kim, Y. W. (2020). Neural substrates for poststroke complex regional pain syndrome type I: a retrospective case-control study using voxel-based lesion symptom mapping analysis. *Pain* 161, 1311–1320. doi: 10.1097/j.pain.0000000000001816

Kuhn, M., and Johnson, K. (2013). *Applied predictive modeling*. New York, NY: Springer. doi: 10.1007/978-1-4614-6849-3

Kumar, B., Kalita, J., Kumar, G., and Misra, U. K. (2009). Central poststroke pain: a review of pathophysiology and treatment. *Anesth. Analg.* 108, 1645–1657. doi: 10.1213/ane.0b013e31819d644c

Lee, J. I., Kwon, S. W., Lee, A., Tae, W. S., and Pyun, S. B. (2021). Neuroanatomical correlates of poststroke complex regional pain syndrome: a voxel-based lesion symptom-mapping study. *Sci. Rep.* 11:13093. doi: 10.1038/s41598-021-92564-7

Lin, H., Yu, S., and Yuan, J. (2020). Progress in the study of compression therapy to reduce limb edema. *Chin. J. Phys. Med. Rehabil.* 42, 861–864. doi: 10.3760/cma.j.issn.0254-1424.2020.09.023

Liu, J., Xiong, Y., Zhong, M., Yang, Y., Guo, X., Tan, X., et al. (2020). Predicting long-term outcomes after poor-grade aneurysmal subarachnoid hemorrhage using decision tree modeling. *Neurosurgery* 87, 523–529.

Long, A. N., and Dagogo-Jack, S. (2011). Comorbidities of diabetes and hypertension: mechanisms and approach to target organ protection. *J. Clin. Hypertens.* 13, 244–251. doi: 10.1111/j.1751-7176.2011.00434.x

Oray, M., Abu Samra, K., Ebrahimiadib, N., Meese, H., and Foster, C. S. (2016). Long-term side effects of glucocorticoids. *Expert Opin. Drug Saf.* 15, 457–465. doi: 10.1517/14740338.2016.1140743

Pergolizzi, J., LeQuang, J., Nalamachu, S., Taylor, R., and Bigelsen, R. W. (2018). The Budapest criteria for complex regional pain syndrome: the diagnostic challenge. *Anaesthesiol. Clin. Sci. Res.* 2, 1–10.

Pertoldi, S., and Di Benedetto, P. (2005). Shoulder-hand syndrome after stroke: a complex regional pain syndrome. *Eura Medicophys.* 41, 283–292.

Pervane Vural, S., Nakipoglu Yuzer, G., Sezgin Ozcan, D., Demir Ozbudak, S., and Ozgirgin, N. (2016). Effects of mirror therapy in stroke patients with complex regional pain syndrome type 1: a randomized controlled study. *Arch. Phys. Med. Rehab.* 97, 575–581. doi: 10.1016/j.apmr.2015.12.008

Ringman, J. M., Saver, J. L., Woolson, R. F., Clarke, W. R., and Adams, H. P. (2004). Frequency, risk factors, anatomy, and course of unilateral neglect in an acute stroke cohort. *Neurology* 63:468. doi: 10.1212/01.WNL.0000133011.10689.CE

Sandroni, P., Benrud-Larson, L. M., McClelland, R. L., and Low, P. A. (2003). Complex regional pain syndrome type I: incidence and prevalence in Olmsted county, a population-based study. *Pain* 103, 199–207. doi: 10.1016/S0304-3959(03)00065-4

Shaparin, N., Murakami, M., Kosharskyy, B., and Gritsenko, K. (2014). Complex regional pain syndrome: an update and review of the mechanisms. *Top. Pain Manag.* 30, 1–9.

Su, Y., Guo, Y., Hsieh, P., and Lin, Y. (2021). A meta-analysis and meta-regression of frequency and risk factors for poststroke complex regional pain syndrome. *Medicina* 57:1232. doi: 10.3390/medicina57111232

Vabalas, A., Gowen, E., Poliakoff, E., and Casson, A. J. (2019). Machine learning algorithm validation with a limited sample size. *PLoS One* 14:e0224365. doi: 10.1371/journal.pone.0224365

Yang, L., Wu, H., Jin, X., Zheng, P., Hu, S., Xu, X., et al. (2020). Study of cardiovascular disease prediction model based on random forest in eastern China. *Sci. Rep.* 10:5245. doi: 10.1038/s41598-020-62133-5

Zhong, T., and Tang, X. (2009). Efficacy of exercise therapy combined with block therapy in the treatment of shoulder-hand syndrome after stroke. *J. Pract. Med.* 25, 909–910. doi: 10.3969/j.issn.1006-5725.2009.06.025

Zorowitz, R. D., Hughes, M. B., Idank, D., Ikai, T., and Johnston, M. V. (1996). Shoulder pain and subluxation after stroke: correlation or coincidence? *Am. J. Occup. Ther.* 50, 194–201. doi: 10.5014/ajot.50.3.194

frontiers | Frontiers in Neuroscience

TYPE Review
PUBLISHED 06 April 2023
DOI 10.3389/fnins.2023.1132335



OPEN ACCESS

EDITED BY
Kota Bokuda,
Tokyo Metropolitan Neurological Hospital, Japan

REVIEWED BY
Ryo Morishima,
Tokyo Metropolitan Institute of Medical Science, Japan
Jacqueline Roots,
Queensland University of Technology, Australia

*CORRESPONDENCE
Jie Jia
✉ shannonjj@126.com

SPECIALTY SECTION
This article was submitted to Translational Neuroscience, a section of the journal Frontiers in Neuroscience

RECEIVED 27 December 2022
ACCEPTED 20 March 2023
PUBLISHED 06 April 2023

CITATION
Liu X, Yang Y and Jia J (2023) Respiratory muscle ultrasonography evaluation and its clinical application in stroke patients: A review. *Front. Neurosci.* 17:1132335. doi: 10.3389/fnins.2023.1132335



# Respiratory muscle ultrasonography evaluation and its clinical application in stroke patients: A review

Xiaoman Liu[1], Ying Yang[1] and Jie Jia[2,3,4]*

[1]Department of Rehabilitation Medicine, The People's Hospital of Suzhou New District, Suzhou, China, [2]Department of Rehabilitation Medicine, Fudan University Huashan Hospital, Shanghai, China, [3]National Center for Neurological Disorders, Shanghai, China, [4]National Clinical Research Center for Aging and Medicine, Fudan University Huashan Hospital, Shanghai, China

**Background:** Respiratory muscle ultrasound is a widely available, highly feasible technique that can be used to study the contribution of the individual respiratory muscles related to respiratory dysfunction. Stroke disrupts multiple functions, and the respiratory function is often significantly decreased in stroke patients.

**Method:** A search of the MEDLINE, Web of Science, and PubMed databases was conducted. We identified studies measuring respiratory muscles in healthy and patients by ultrasonography. Two reviewers independently extracted and documented data regarding to the criteria. Data were extracted including participant demographics, ultrasonography evaluation protocol, subject population, reference values, etc.

**Result:** A total of 1954 participants from 39 studies were included. Among them, there were 1,135 participants from 19 studies on diaphragm, 259 participants from 6 studies on extra-diaphragmatic inspiratory muscles, and 560 participants from 14 studies on abdominal expiratory muscles. The ultrasonic evaluation of diaphragm and abdominal expiratory muscle thickness had a relatively typically approach, while, extra-diaphragmatic inspiratory muscles were mainly used in ICU that lack of a consistent paradigm.

**Conclusion:** Diaphragm and expiratory muscle ultrasound has been widely used in the assessment of respiratory muscle function. On the contrary, there is not enough evidence to assess extra-diaphragmatic inspiratory muscles by ultrasound. In addition, the thickness of the diaphragm on the hemiplegic side was lower than that on the non-hemiplegic side in stroke patients. For internal oblique muscle (IO), rectus abdominis muscle (RA), transversus abdominis muscle (TrA), and external oblique muscle (EO), most studies showed that the thickness on the hemiplegic side was lower than that on the non-hemiplegic side.

**Clinical Trial Registration:** The protocol of this review was registered in the PROSPERO database (CRD42022352901).

KEYWORDS

**diaphragm, evaluation, ultrasonography, stroke, respiratory muscle**

# 1. Introduction

The respiratory muscle pump consists of three primary groups controlling ventilation: the primary muscle of inspiration, the accessory inspiratory, and the expiratory muscles (Shi et al., 2021). The primary muscle of inspiration is the diaphragm, a thin dome-shaped muscle positioned between the chest and abdomen. As the most important respiratory muscle, the diaphragm contributes 60–80% of the ventilation needs of the human body. However, the diaphragm is not the only inspiratory muscle involved in ventilation. When the load imposed on the diaphragm increases, the accessory inspiratory muscles, such as the parasternal intercostal muscles, external intercostal muscles, scalene muscles, and sternocleidomastoid muscles, are recruited to assist in inspiration (Tuinman et al., 2020). With further loading, the expiratory muscles are activated in a fixed hierarchy to assist expiration (Shi et al., 2019). The role of expiratory muscle includes reducing end-expiratory lung volume, reducing transpulmonary pressure, and increasing inspiratory muscle volume (Shi et al., 2019). There are also studies (Dres et al., 2020) showing that the muscle fibers of the parasternal intercostal muscles contract during inspiration, which expands the thoracic cavity, thereby increasing the tidal volume. Generally, during tidal ventilation, the diaphragm works in synergy with the scalene and external intercostal muscles to trigger inspiration, as well as with the dilator muscles of the upper airway. In cases of respiratory distress, the sternocleidomastoid muscles and the trapezius are also recruited (Vivier and Mekontso Dessap, 2020).

Ultrasonography can assess the mechanics, thickness, and strength of all the respiratory muscles (Matamis et al., 2013), and it may be possible to provide valuable information in this context to complement clinical examination. Recent studies proved that ultrasound permits the quantitative assessment of the excursion and thickness of the respiratory muscles to quantify their function (Cala et al., 1998; Sferrazza Papa et al., 2016; Yoshida et al., 2019; Bedewi et al., 2021; Kang et al., 2021). Different ultrasonic techniques have been validated through several studies (Adigozali et al., 2016; Tahan et al., 2016; Bedewi et al., 2021). Stroke disrupts multiple functions (Benditt and Boitano, 2013). The respiratory function is often significantly decreased in stroke patients, and the respiratory intensity is only about 50% of the normal population. The respiratory dysfunction can be attributed to the affected respiratory central nervous system and respiratory muscles (Rochester and Mohsenin, 2002; Jandt et al., 2011). In this context, the present review has two objectives. The first is to review the ultrasound assessment of respiratory muscles. The second objective is the clinical application of respiratory muscle ultrasound in stroke patients.

# 2. Methods

## 2.1. Selection of studies

The review was according to the PRISMA 2020 flow diagram (Figure 1 and Supplementary material 3). We intended to identify studies measuring respiratory muscles in healthy and patients by ultrasonography. Based on the suggestions of thoracic ultrasound from European Respiratory Society Statement (Laursen et al., 2021) and previous review on ultrasonography measurement (Sferrazza Papa et al., 2016), we chose studies based on the following criteria: (1) Study subjects were healthy or patients with respiratory muscle disorders for various causes, the subjects included in the part of the clinical application were stroke patients. (2) The ultrasonography evaluation of the respiratory muscle was clearly described with integrated protocol, the ultrasound equipment, experience of the operator, probe frequency selection, subject's measurement position, selection of measuring points/ultrasound probe placement position, respiratory status during measurement, and whether the subject cooperated, and respiratory muscle's values were recorded. (3) All included studies were published in English with full text (English articles that were not published in full text were removed), including original studies and clinical trials.

## 2.2. Data source and search strategy

We searched articles published in the MEDLINE, Web of Science, and PubMed databases with no date restrictions up to 19 November 2022 (Supplementary material 1). The following keywords were used: Respiratory muscle ultrasonography-related words: ultrasonography, ultrasound, echotomography, sonography, echography, diaphragm, respiratory muscles, ventilatory muscles, and intercostal muscles based on title, abstract, and MeSH terms, and trapezius, sternocleidomastoid muscles, scalene muscles, parasternal intercostal muscle, inspiratory muscle, and expiratory muscle based on title and abstract. Stroke-related words were stroke, hemiplegia, cerebrovascular, CVA, apoplexy, vascular, brain, cerebral, intracerebral, hemorrhage, infarct, and ischemia based on title, abstract, and MeSH terms. The search strategy was created based on the PICO strategy: P (patient)—adults (healthy or diseases); I (intervention)—ultrasonography of the respiratory muscles (e.g., diaphragm, extra-diaphragmatic inspiratory muscles, abdominal muscles); C (comparator)—none; O (outcomes)—methodology and reference value.

## 2.3. Literature review and data extraction

Two review authors independently read the titles and abstracts of all literatures searched by the databases. Unified standards were used to extract relevant information from the full text of articles that met the inclusions. Data were extracted including participant demographics, ultrasonography evaluation protocol, subject population, reference values, etc.

# 3. Ultrasonography evaluation of respiratory muscles

## 3.1. Inspiratory muscle

### 3.1.1. Diaphragm

The diaphragm is a dome-shaped, fibromuscular partition between the thoracic and abdominal cavities (Gerscovich et al., 2001) that composed of four components: the transverse septum, pleuroperitoneal folds, esophageal mesentery, and muscular body wall laterally that separates the chest from the abdominal cavity (Sarwal et al., 2013). It is the most important inspiratory muscle and plays a major role in maintaining ventilation (Sferrazza Papa et al., 2016).

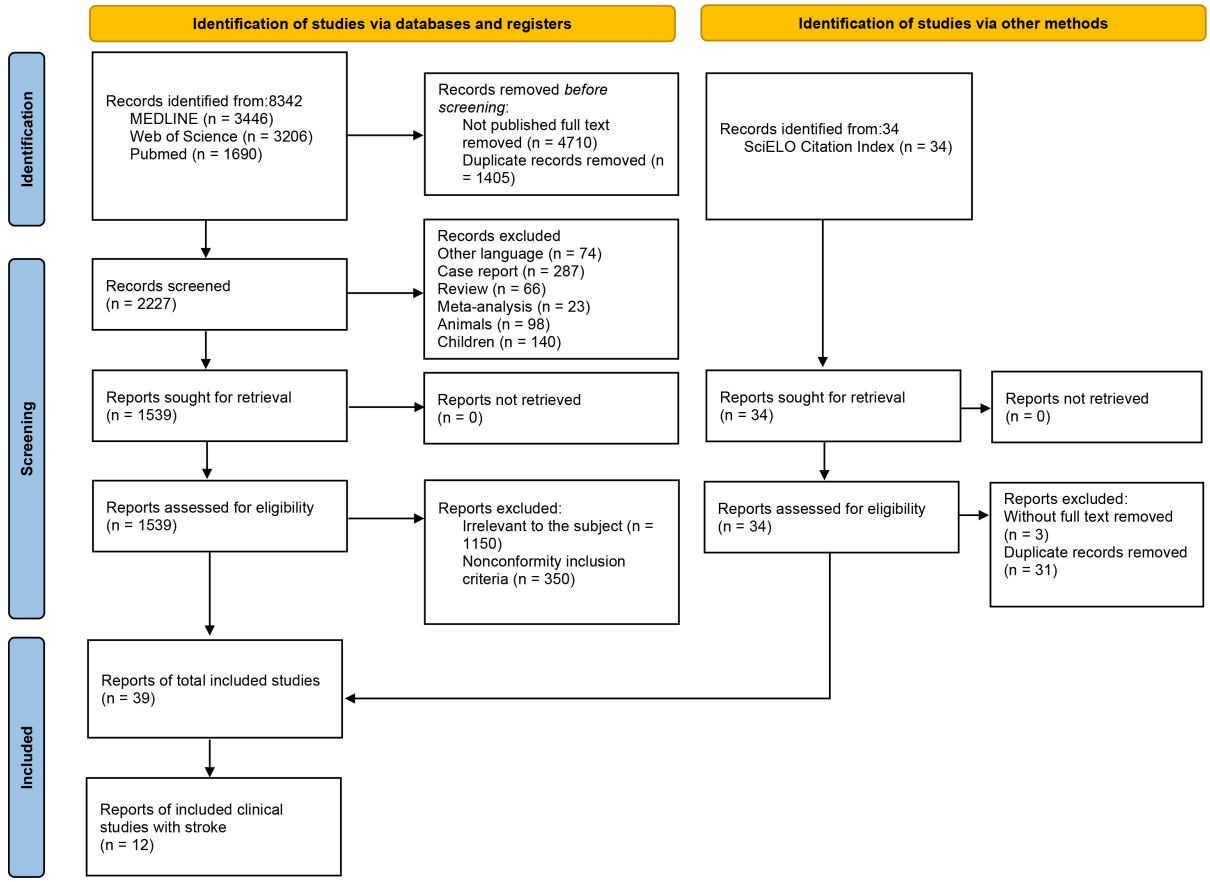


FIGURE 1
Flow diagram of the review.

Diaphragmatic ultrasound has been widely used in healthy individuals (Ueki et al., 1995) and clinical practice (Sferrazza Papa et al., 2016), and a wide range of normal and abnormal values has been reported (Gottesman and McCool, 1997; Boussuges et al., 2009; Sferrazza Papa et al., 2016). In general, there are two major forms of ultrasonographic assessment of the diaphragm: diaphragm excursion and thickness (Supinski et al., 2018).

Diaphragm excursion measurement (Table 1): 2–5 MHz transducer with M-mode ultrasonography is used to measure the diaphragm excursion. The participants are in the supine or standing position during ultrasonic measurement. Usually, the liver is used as a window on the right side, and the diaphragm is examined from the anterior subcostal approach (the right costal margin between the midclavicular and anterior axillary lines). While the spleen is used for the left side, the diaphragm was examined from a subcostal or low intercostal approach (between the anterior axillary and mid-axillary lines). One study has shown that supine position is preferred for the study of diaphragmatic excursion because of less variability in observations (Gerscovich et al., 2001). Visualization of the left diaphragm is more difficult because of the smaller window of the spleen, but can be facilitated by a more coronal approach and by paralleling the ribs (Sarwal et al., 2013). In addition to the common approaches described, several other approaches have been showed in previous studies. Among them, the posterior subcostal approach may not be practical in critically ill or mechanically ventilated patients (Fedullo et al., 1992). However, the subxiphoid approach provides another option for measuring excursion, and it is particularly useful in children (Chavhan et al., 2010). The excursion of diaphragm is usually measured during quiet breathing, deep breathing, or the sniff test.

Diaphragm thickness measurement (Table 1): With the participants in the standing, semi-recumbent, or supine position, 7–13 or 6–15 MHz linear-array transducer with B-mode or M-mode ultrasonography is used to measure the diaphragm thickness at the zone of apposition during inspiration or expiration. The probe is positioned at approximately the anterior axillary line or just cephalad to the lower costal margin at the eighth and ninth intercostal spaces. The diaphragm can be visualized as a three-layered structure consisting of a relatively non-echogenic muscular layer bounded by echogenic membranes of the peritoneum and diaphragmatic pleura with the probe perpendicular to two ribs (Supinski et al., 2018). According to the diaphragm thickness at the end-inspiration and end-expiration, the thickening fraction of the diaphragm (TFdi) can be calculated by the formula. TFdi = (end-inspiratory thickness - end-expiratory thickness)/end-expiratory thickness × 100%. Thickening fraction (TFdi) reflects on tractile activity that can be used to assess muscle function (Wait et al., 1989; Goligher et al., 2015). The ultrasound criteria of diaphragm thickness < 2.0 mm and thickening fraction (TFdi) < 20% was diagnostic of diaphragm paralysis in previous research (Gottesman and McCool, 1997).

TABLE 1 Selected studies providing direct visualization of ultrasonographic assessment of the diaphragm.

| Parameters | Transducer (MHz) | Approach | Position | Condition | Subjects | References |
|---|---|---|---|---|---|---|
| Tdi, TFdi | 10 | At approximately the anterior axillary line, just cephalad to the lower costal margin | Supine | Inspiration (TLC)/end expiration | 49 Healthy, 45 Stroke patients | Kim et al. (2017) |
| Tdi | 7–13 | The eighth or ninth intercostal space, anterior to the anterior axillary line | Supine | End of expiration | 73 male, 77 female | Boon et al. (2013) |
| Tdi, TFdi | 7.5–10 | The eighth and ninth intercostal spaces in the right mid-axillary line | Standing | At FRC | 15 Healthy | Gottesman and McCool (1997) |
| Tdi, TFdi, Excursion | 10–14 | At approximately the anterior axillary line at the 8th and 9th intercostal spaces | Supine | End deep inspiration /end-expiration | 45 Stroke patients | Liu et al. (2022) |
| Tdi | 10 | In the middle of the anterior axillary and mid-axillary line of the 7th intercostal space | Supine | End-inspiration/expiration | 41 Stroke patients | Kılıçoğlu et al. (2022) |
| Tdi | 5–14 | The mid-axillary lines between ribs 8 and 9 on both sides | Supine | Maximum inspiration/ end-expiration | 25 Stroke patients | Cho et al. (2018) |
| Tdi, TFdi, Excursion | 6–13 3–5.5 | At the 8th–9th intercostal space of the right anterior axillary line | Supine | Calm end-expiratory/maximum end-inspiratory | 60 Stroke patients | Cao et al. (2022) |
| Tdi, TFdi, Excursion | 10–15 | The zone of apposition to the rib cage, between the mid-axillary and antero-axillary line | Supine | End-inspiration/end-expiration | 79 Parkinson's disease | Yu et al. (2021) |
| Tdi | 8–13 | At approximately the anterior axillary line, just cephalad to the lower costal margin | Supine | End-expiration or functional residual capacity | 50 COPD Patients | Baria et al. (2014) |
| Tdi, TFdi | 13 | The ninth or tenth intercostal, space near the mid-axillary line | Supine | End-expiratory/peak inspiratory | 66 ventilated patients | Goligher et al. (2015) |
| Tdi | 5–15 | In the right intercostal space, between the antero-axillary and mid-axillary lines | Sitting | At full expiration/ inspiration | 42 ALS Patients | Pinto et al. (2016) |
| Tdi, TFdi | 6–15 | In the anterior axillary line | – | End-expiration/inspiration | 45 MS patients | Şahin et al. (2019) |
| TFdi | 10–15 | The ninth or tenth intercostal, space near the mid-axillary line | Supine | End-expiration/peak inspiration | 122 ventilated patients | Dres et al. (2021) |
| TFdi | 4–10 | Between the mid-axillary and posterior axillary lines | Supine | End-inspiration/end-expiration | 10 COPD patients | Lim et al. (2019) |
| Excursion | 4 | A low intercostal or subcostal approach using the liver or spleen as an acoustic window | Supine | Quiet breathing/deep inspiration/ the sniff test | 23 Healthy | Gerscovich et al. (2001) |
| Excursion | 2.5–3.5 | A low intercostal or subcostal approach using the liver or spleen as an acoustic window | Standing | Quiet breathing/deep inspiration/ the sniff test | 150 men, 60 women | Boussuges et al. (2009) |
| Excursion | – | In the longitudinal semi-coronal plane through a subcostal or intercostal approach | Supine | Spontaneous/deep respiration | 23 Stroke patients | Voyvoda et al. (2012) |
| Excursion | 1–5 | A subcostal approach | Supine | Quiet and deep breathing/ Voluntary sniffing | 10 Stroke patients | Jung et al. (2014) |
| Excursion | 3.5 | The lower intercostal spaces in the anterior axillary lines and the liver | Supine | Quiet/deep breathing | 25 COPD patients | Crimi et al. (2018) |





10.3389/fnins.2023.1132335

### 3.1.2. Extra-diaphragmatic inspiratory muscles

#### 3.1.2.1. Parasternal intercostal muscle and intercostal muscles

Together with the diaphragm, extra-diaphragmatic inspiratory muscles participate in the generation of the tidal volume (Formenti et al., 2020). The intercostal muscles can be directly visualized between the ribs (Laursen et al., 2021) and the European Respiratory Society recommends ultrasound monitoring of the intercostal muscles to assess respiratory function (Laveneziana et al., 2019). The intercostal muscles are composed of three thin layers of muscle fibers occupying each of the intercostal spaces (Formenti et al., 2020). The outer layer is external intercostal; in contrast, the layer is internal intercostal (De Troyer et al., 2005), and the inner layer is the innermost intercostal muscle (Estenne et al., 1985). The intercostal spaces contain two layers of intercostal muscle in their lateral portion but a single layer in their ventral and sometimes in their dorsal portions. Between the sternum and the chondrocostal junctions, the external intercostals are replaced by a fibrous aponeurosis, and this portion of the internal intercostals on the ventral side is conventionally called the Parasternal intercostals (De Troyer et al., 2005). The inspiratory contraction of the Parasternal intercostal muscle involves muscle shortening, acting to elevate the rib cage and expand the lung (Cala et al., 1998). Because their mass remains constant, increases in thickness can be observed using ultrasound imaging during inspiration (Vivier and Mekontso Dessap, 2020). Ultrasound has been used to investigate parasternal intercostal muscles in the easily accessible anterior parasternal region (Cala et al., 1998; Diab et al., 1998). Unlike the parasternal intercostal muscles, in the lateral and in the posterior part of the intercostal space, the internal and external intercostal muscles often overlap, making the ultrasound detection of both muscle layers impossible (Formenti et al., 2020). Therefore, ultrasonography of the intercostal muscles generally measures both the internal and external intercostal muscles. The extra-diaphragmatic respiratory muscles recruitment is a mechanism of compensation that can be activated in presence of diaphragm dysfunction (Dres et al., 2020). The parasternal intercostal muscle, as the main auxiliary inspiratory muscle, has a broad application prospect in mechanically ventilated patients, especially those with diaphragmatic dysfunction. The extra-diaphragmatic respiratory muscles recruitment is a mechanism of compensation that can be activated in presence of diaphragm dysfunction (Dres et al., 2020). The parasternal intercostal muscle, as the main auxiliary inspiratory muscle, has a broad application prospect in mechanically ventilated patients, especially those with diaphragmatic dysfunction.

Parasternal intercostal muscle thickness measurement (Table 2). Parasternal intercostal muscle ultrasound is performed with a 6–14 or 10–15 MHz linear-array transducer positioned in cranio-caudal direction at the second intercostal space, approximately 3–5 cm or 6–8 cm lateral to the sternal edge with a window visualizing between the 2nd and the 3rd rib. The supine position is usually used, and some studies used the participant at 45°. The second parasternal intercostal muscle was identified as a three-layered biconcave structure: two linear hyperechoic membranes running, respectively, from the anterior and posterior aspects of the adjoining ribs, and a medial portion with muscle echotexture. Using B-Mode or M-mode, the thickness of the parasternal intercostal muscle was measured on frozen images at end expiration and at peak inspiration during tidal breathing or total lung capacity. Change in thickness determined the thickening fraction of the parasternal intercostal muscle (TFic) as follows: TFic = (end-inspiration thickness – end-expiratory thickness)/end-expiratory thickness×100% (Dres et al., 2020, 2021). Previous research showed that a value of TFic less than 10%, associated with a TFdi greater than 20% during mechanical ventilation indicates a successful weaning trial (Formenti et al., 2020).

Intercostal muscles thickness measurement (Table 2): Using B-mode ultrasound with 7–12 Hz linear probe to measure contractions of the intercostal muscle. The participants' measurement used the supine position when measuring the anterior intercostal space, while the left side-lying position was used in the right lateral intercostal space and the posterior intercostal space, and the other research chose the sitting position. The measurement of anterior part of the intercostal muscle was the 1st – 6th intercostal spaces and 25–30 mm outside from the right edge of the sternum. The lateral part was the 3rd, 6th, and 9th intercostal space, at the line connecting the axillary anterior border with the anterior superior iliac spine. The posterior part was the 3rd, 6th, and 9th intercostal spaces, and it was 50–60 mm lateral to the thoracic spinous process. To measure the 8th posterior intercostal space, place the ultrasound probe at medial scapula line. Participants were in a supine position and the probe was placed at the level of the mid-axillary line and measurements were made at the 5th and 6th intercostal space (Pietton et al., 2021). One study determined the area of the intercostal muscles at maximal inhalation in one adult person and it was found that measurements at maximal inhalation were more accurate than those taken at maximal exhalation (Diab et al., 1998). Summary of the literature, previous studies have focused on the right intercostal muscles, the structure and contractile function of the bilateral intercostal muscles by ultrasound need to be further studied. Meanwhile, reference values need to be determined.

## 3.2. The scalene muscles, sternocleidomastoid muscles and the trapezius

The human inspiratory muscles in the neck include the scalene and sternomastoid. These muscles have similar respiratory actions on the chest wall and cause cranial displacement of the sternum and ribcage (Hudson et al., 2007). The human scalene are obligatory inspiratory muscles that have a greater mechanical advantage than sternomastoid. Lee et al. (2016) found that stretching of the scalene muscles improved vital capacity. Several studies used computed tomographic scan images to measure the changes in muscle length, muscle mass and size of the sternocleidomastoid muscle (Peche et al., 1996; Legrand et al., 2003).

One study evaluated the reliability of shear-wave elastography (SWE) to assess the anterior and middle scalene muscles in healthy adult subjects. Ultrasound examinations of the scalene muscles were performed by an L18–4 MHz linear-array transducer. The ultrasound transducer was placed just lateral to the thyroid lobe (Bedewi et al., 2021). However, the limitations of this study were the small sample size, and the lack of comparison with pathological tissue. Several studies used B mode linear probe of ultrasonography with frequency of 7–11 or 8.5–10.0 MHz for imaging of the trapezius (Adigozali et al., 2016; Kisilewicz et al., 2020). Subjects were asked to sit on the chair while they were in an upright and relaxed position (Adigozali et al., 2016). In order to measure the thickness and SWE of the trapezius,

TABLE 2 Selected studies providing direct visualization of ultrasonographic assessment of the parasternal intercostal muscle and intercostal muscles.

| Parameters | Transducer (MHz) | Approach | Position | Condition | Subjects | References |
|---|---|---|---|---|---|---|
| Parasternal intercostal muscle | | | | | | |
| Tic, TFic | 10–15 | The level of the 2nd intercostal space, approximately 6–8 cm lateral to the sternal edge with a window visualizing the 2nd/3rd ribs | – | End-expiration/inspiration | 23 Healthy, 54 mechanically ventilated patients | Dres et al. (2020) |
| | 10–15 | 3 cm laterally from the sternum, and oriented along the sagittal plane, between the 2nd and the 3rd ribs | Supine | End-expiratory | 50 mechanically ventilated patients | Paolo et al. (2022) |
| | 6–14 | In the sagittal plane with a window visualizing the 2nd/3rd ribs | at 45° | End-tidal expiration | 32 intubated patients | Formenti et al. (2022) |
| | 6–14 | In the sagittal plane with a window visualizing the 2nd/3rd, 3rd/4th ribs | at 45° | End-tidal inspiration | 20 stable COPD patients | Wallbridge et al. (2018) |
| Intercostal muscle | | | | | | |
| Thickness | 12 | The anterior portion, 1st – 6th intercostal spaces, 25–30 mm outside from the edge of the sternum | Supine | At resting expiratory/maximal inspiratory | 12 healthy men | Yoshida et al. (2019) |
| | 12 | The lateral portion, the 3rd, 6th, and 9th intercostal space, at the line connecting the axillary anterior border with the anterior superior iliac spine | Left side-lying | At resting expiratory/maximal inspiratory | 12 healthy men | Yoshida et al. (2019) |
| | 12 | The posterior portion, the 3rd, 6th, and 9th intercostal spaces, and it was 50–60 mm lateral to the thoracic spinous process | Left side-lying | At resting expiratory/maximal inspiratory | 12 healthy men | Yoshida et al. (2019) |
| | 7–10 | At the 8th posterior right intercostal space at medial right scapula line | Sitting | End of quiet and deep inspiration/expiration | 68 older adults | Rahman et al. (2017) |





10.3389/fnins.2023.1132335

the position of the ultrasound probe was generally chosen the midpoint of the spinous process of 7th cervical vertebra and acromion process of right scapula were determined by palpation. However, due to the peculiarities of anatomy and the limitations of ultrasound technology, there were few ultrasound studies on the scalene, sternocleidomastoid muscles and the trapezius.

## 3.3. Expiratory muscle

The expiratory muscles include the abdominal wall muscles (transversus abdominis muscle (TrA), internal oblique muscle (IO), external oblique muscle (EO), and rectus abdominis muscle (RA)), and some of the rib cage ones (e.g., the internal intercostal muscles and the triangularis sterni muscle) (De Troyer et al., 1998; Wilson et al., 2001; De Troyer et al., 2005; De Troyer and Boriek, 2011). During tidal breathing, the expiratory muscles are largely inactive (Shi et al., 2019), although the transversus abdominis muscle may occasionally show some activity during quiet breathing (De Troyer et al., 1990). Previous study has shown that transversus abdominis has an important role in posture (Belavý et al., 2017). The contraction of the transversus abdominis muscle with the other muscles of the abdominal cavity has also been shown to increase intra-abdominal pressure (Hodges and Gandevia, 2000). Activation of the expiratory muscles during breathing occurs when the load imposed on the inspiratory muscle increases (Shi et al., 2019). In the presence of an imbalance between inspiratory muscle load and capacity, the abdominal wall muscles are recruited during expiration in a fixed hierarchy (Aliverti et al., 1997; Parthasarathy et al., 2007): initially, the transversus abdominis muscle, followed by the internal oblique muscle and the external oblique muscle, and finally the rectus abdominis muscle (Abe et al., 1996; Suzuki et al., 1999). Abdominal ultrasound allows direct visualization of the three layers of the abdominal wall muscles (Misuri et al., 1997; McMeeken et al., 2004; Rankin et al., 2006; Tahan et al., 2016). In healthy subjects, the thickness of individual abdominal wall muscles follows a certain pattern: transversus abdominis < external oblique < internal oblique < rectus abdominis (Tahan et al., 2016).

Expiratory muscle thickness measurement (Table 3): Using 7.5 or 10–15 MHz linear probe in B-mode condition positioned perpendicular to the abdominal wall. Measurements were performed with the subjects in a supine or semi-recumbent position with knees bent and the hips at 45°. To visualize the rectus abdominis muscle, the transducer is positioned in a transverse orientation approximately 2–3 cm above the umbilicus and 2–3 cm lateral from the midline. The external oblique, internal oblique, and transversus abdominis muscles can be identified as three parallel layers, usually at the anterior axillary line, midway between the inferior border of the rib cage and the iliac crest. Several studies measured rectus abdominis at 3 cm or 4 cm lateral to the umbilicus; the external oblique, internal oblique, and transverse abdominis were measured at 2.5 cm anterior to the mid-axillary line and at the midpoint between the inferior rib and iliac crest. The pressure applied to the probe should be kept to a minimum to prevent compression of the abdominal wall as this may alter the shape/thickness of the underlying muscles. Abdominal muscle thickness was performed at the end of a relaxed expiration or at end-inspiration. Thickening fraction of the expiratory abdominal muscles (TFabd) can be calculated as the magnitude of thickness increase during expiration. Change in thickness determined the thickening fraction of the expiratory abdominal muscles (TFadb) as follows: TFadb = (end-expiratory thickness − end-inspiratory thickness)/end-inspiratory thickness × 100% (Tuinman et al., 2020).

## 3.4. Feasibility and reliability of the ultrasound measurements

To be useful, ultrasound measures should be reliable and with good reproducibility, which means that they are stable over time, have minimal variability, and have enough sensitivity to detect clinically important changes (Lexell and Downham, 2005). There were many studies on the feasibility and reliability of the diaphragmatic ultrasound measurements (Baldwin et al., 2011; Goligher et al., 2015). Ultrasonographic technique of diaphragm was previously reported to be reliable, with high intra-class correlation coefficient for intra-rater and inter-rater reliability (Gottesman and McCool, 1997; Boussuges et al., 2009). Diaphragm motion depend on the position of the subject in the study (Sarwal et al., 2013). The supine position is preferred, because there is less overall variability, less side-to-side variability, and greater reproducibility (Gerscovich et al., 2001). Baldwin et al. (2011) also found that ultrasound technique has good reliability in recumbent positions. In addition, the relationship between inspired volume and diaphragmatic motion was found to be linear (Houston et al., 1994).

On the contrary, very few studies have applied ultrasound to evaluate the extra-diaphragmatic inspiratory muscles. Parasternal intercostal muscle ultrasound may be a useful tool in the evaluation of the respiratory muscle in future studies (Tuinman et al., 2020). Dres et al. (2020) have proposed a technique to measure the parasternal intercostal muscle by ultrasonography, while their results need to be confirmed in a larger number of patients (Vivier and Mekontso Dessap, 2020). Intercostal muscle ultrasound offers a repeatable and radiation-free alternative, however requires validation. Wallbridge et al. (2018) found that the inter-rater reliability was not as strong for thickness, particularly in the third intercostal spaces bilaterally. The results of the research demonstrated that real time ultrasonography was a reliable method for measurement of upper trapezius (Adigozali et al., 2016). Other extra-diaphragmatic inspiratory muscles, such as the scalene muscles and sternocleidomastoid muscles, requires further study on their ultrasound approach, reliability, and reproducibility.

The measurement of abdominal wall muscles' thickness was feasible in almost all healthy subjects and patients. A large number of studies evaluated the reproducibility of ultrasound imaging measures of abdominal muscle activity (McMeeken et al., 2004; English et al., 2012). Reliability in the measurement of abdominal muscle thickness was assessed in several studies and their results indicated an excellent inter-and intra-rater reproducibility in measuring the muscle thickness of these muscles (Ota et al., 2012; Shi et al., 2021).

## 3.5. Limitations of respiratory muscle ultrasonography

The operator skills, technical aspects are related to ultrasound physics, and patient characteristics, e.g., probe orientation difficulties, the small muscles, muscle edema, and the pressure of the transducer and manipulator's hand on the wall can all affect measurements

TABLE 3 Selected studies providing direct visualization of ultrasonographic assessment of the expiratory muscles' thickness.

| Parameter | Transducer (MHz) | Approach | Position | Condition | Subjects | References |
|---|---|---|---|---|---|---|
| IO, EO, TrA | 7.5 | The anterior axillary line, midway between the 12th rib and the iliac crest | Supine | End of the expiration | 156, 6 healthy | Misuri et al. (1997) and Tahan et al. (2016) |
| IO, EO, TrA | 8 | 2.5 cm anterior to the axillary line, at the height of the umbilicus | Supine | End of a relaxed expiration | 103 healthy | Ota et al. (2012) |
| IO, EO, TrA | – | The middle line between the sacral crest and the inferior angle of the thoracic cage | Supine | – | 24 healthy | Kang et al. (2021) |
| IO, EO, TrA | 10 | 2.5 cm anterior to the mid-axillary line and at the midpoint between the inferior rib and iliac crest | Supine | End of a relaxed expiration | 39, 23 healthy | Ishida et al. (2014) and Ishida et al. (2015) |
| IO, EO, TrA | 7.5 | The left side of the abdomen | Supine | The thickest muscle at end tidal | 21 healthy | Sugimoto et al. (2018) |
| IO, EO, TrA | 5–13 | The mid-axillary line and the midpoint between the iliac crest and the bottom of the rib cage | Supine | End of normal expiration | 21 women | Abuín-Porras et al. (2020) |
| IO, EO, TrA | 8–12 | 2.5 cm anterior to the mid-axillary line at the midpoint between the inferior rib and the iliac crest | Supine | End of relaxed expiration | 32, 15 stroke patients | Monjo et al. (2018) and Monjo et al. (2022) |
| IO, EO, TrA | 5–12 | At the umbilicus line and horizontally 3 cm medial to the mid-axillary line | Supine | The rest and contraction states | 55 stroke patients | Kim et al. (2020) |
| IO, EO, TrA | 7.5 | Superior to the iliac crest in the transverse plane along the mid-axillary line | Crook-lying | End of expiration | 33 stroke patients | Lee et al. (2018) |
| IO, TrA | 6–12 | Between the 12th rib and iliac crest 25 mm inside | Supine | At the start of expiration | 23 stroke patients | Oh et al. (2016) |
| TrA | 5–13 | At the middle of the 11th costal cartilage and iliac crest, perpendicularly to the mid-axillary line | Supine | At rest (not clear) | 9 stroke patients | Kelli et al. (2020) |
| RA | 7.5 | 2–3 cm above the umbilicus, 2–3 cm from the midline | Supine | At the end of the expiration | 156, 6 healthy | Misuri et al. (1997) and Tahan et al. (2016) |
| RA | 8–10 | 4 cm lateral to the umbilicus | Supine | End of a relaxed expiration | 103, 39, 23 healthy | Ota et al. (2012), Ishida et al. (2014), and Ishida et al. (2015) |
| RA | 8–12 | 3 cm lateral to the umbilicus | Supine | End of relaxed expiration | 32, 15 stroke patients | Monjo et al. (2018) and Monjo et al. (2022) |
| RA | 5–12 | 3 cm lateral to the umbilicus | Supine | The rest and contraction states | 55 stroke patients | Kim et al. (2020) |
| RA | 7.5 | 2–3 cm above the umbilicus | Crook-lying | End of expiration | 33 stroke patients | Lee et al. (2018) |





10.3389/fnins.2023.1132335

(Tuinman et al., 2020; Vivier and Mekontso Dessap, 2020). Furthermore, the spatial axial resolution of the probe plays a critical role. Comparing individual patient results should be done with a degree of caution and only after adequate training (Tuinman et al., 2020).

Previous studies have some methods to reduce variability, such as the same normalized position of the subject and the exact position of the transducer were maintained during the measurement, use the minimum amount of pressure needed to get a clear image while preventing pressure that could alter the shape or thickness of the muscle (Tuinman et al., 2020), the same observer for three different cycles of measurement, and a unified standard for measurement software, etc. (Liu et al., 2022).

### 3.6. Risk of bias

The risk of selection, performance, detection, and reporting bias in the included studies are specified in Table 4.

## 4. Clinical applications of the patients with stroke

### 4.1. Role of diaphragm ultrasound in stroke

The human diaphragm represents one of the muscles that are controlled by an automatic as well as voluntary motor system (Nakayama et al., 2004). It is thought that bilateral hemi-diaphragms are controlled by the contralateral primary motor cortex and, thus, in the presence of paralysis, the diaphragm is also affected on the same side as the paralysis (Aminoff and Sears, 1971; Cohen et al., 1994). The etiology of the paralysis is multiple (Gerscovich et al., 2001). Central nervous system disease, including brain infarction, may impair diaphragmatic motion. Because ultrasonography can distinguish a functioning from a nonfunctioning diaphragm, it can be used to diagnose both unilateral and bilateral diaphragmatic paralysis and to monitor recovery of the paralyzed diaphragm (Gottesman and McCool, 1997; Summerhill et al., 2008). Respiratory exercises could contribute to the well-being of the stroke patients and this contribution could be followed up by diaphragm ultrasound (Kılıçoğlu et al., 2022).

Hemiplegic side of the diaphragm had reduced thickness and motion during voluntary inspiration on the same side of the body paralysis in patients with stroke (Laroche et al., 1988; Kim et al., 2017) and this finding was not seen during quiet breathing (Cohen et al., 1994). Our results of previous study were consistent with (Liu et al., 2022). However, there was controversy about the function of the hemiplegic side and non-hemiplegic side of the diaphragm after stroke. Some researchers showed that the motion of the diaphragm on the hemiplegic side decreases after stroke, and the contralateral showed a larger excursion compensatively (Cohen et al., 1994). However, Houston et al. (1995) found bilaterally decreased volitive diaphragmatic motion in acute cerebral infarction. Recent studies have found that the thickness and motion of the bilateral diaphragm in stroke patients were decreased (Caleffi-Pereira et al., 2018), while diaphragmatic dysfunction was more severe on the hemiplegic side (Catalá-Ripoll et al., 2020). In view of this, we reviewed the diaphragm thickness in hemiplegic patients after stroke at the subacute stage (almost within 1–6 months from the onset) with ultrasound in the literature, as shown in Figure 2. In most of the studies, the thickness of the diaphragm on the hemiplegic side of stroke patients is lower than that on the non-hemiplegic side, no matter at the end of inspiration or end of expiration (Supplementary material 2).

### 4.2. Role of expiratory muscles ultrasound in stroke

The function of hemiplegic expiratory muscles may be affected in stroke patients. It is therefore important to determine the quantitative and qualitative changes in abdominal muscles in stroke survivors. The hemiplegic side has been found to exhibit negative changes in abdominal muscle quantity and quality compared with the non-hemiplegic side or healthy controls (Monjo et al., 2022). One study has shown that the TrA on the hemiplegic side was 16% lower in the stroke patients compared to the matched side in the healthy people (Marsden et al., 2013). However, Kelli et al. (2020) found that bilateral TrA thickness decreased in the hemiplegia patients, suggesting muscle atrophy on both sides of the trunk. Kim et al. (2020) revealed that contractility of RA and EO at the paretic side was significantly lower than at the non-paretic side, while there were no significant difference between non-paretic and paretic sides at rest. Monjo et al. (2018) indicated that changes on the hemiplegic side in stroke survivors might not occur in the abdominal muscles. Regarding the reliability of ultrasound measurements, studies have shown that ultrasound is considered a reliable method for measuring muscle thickness in acute stroke patients (English et al., 2012). We summarized the thickness of abdominal respiratory muscles in hemiplegic patients after stroke in the literature, as shown in Figure 3. In the studies included, the average post-stroke duration of the expiratory muscles-related patients with hemiplegia ranged from months to years. Due to a large duration span, there was a lack of evaluation of possible bias. Consequently, we indicated reference numbers of different studies on the abscissa replaced the average duration of post-stroke in Figure 3. For IO and RA, two of three studies indicated that the thickness of the hemiplegic side of stroke patients was lower than that of the non-hemiplegia side, and one study found the opposite conclusion. For TrA, most studies showed that the thickness on the hemiplegic side was lower than that on the non-hemiplegia side; while for EO, all three studies showed that the thickness on the hemiplegic side was lower than that on the non-hemiplegic side (Supplementary material 2).

## 5. Discussion

It is necessary to assess the muscles of respiratory to measure respiratory function. Respiratory muscle ultrasound is a widely available, highly feasible, non-invasive bedside radiation-free technique that can be easily applied in the clinic. It can provide information about the structure and function of the respiratory muscle. Moreover, ultrasonography can be used to study the contribution of the individual respiratory muscles related to pulmonary dysfunction. At present, diaphragm and expiratory muscle ultrasound has been widely used in the assessment of

TABLE 4 Risk of bias.

| Study | Participant selection | Evaluation protocol | Reference standard | Selective reporting |
|---|---|---|---|---|
| Kim et al. (2017) | ● | ○ | ○ | ○ |
| Boon et al. (2013) | ○ | ○ | ○ | ○ |
| Gottesman and McCool (1997) | ● | ○ | ○ | ● |
| Liu et al. (2022) | ● | ○ | ○ | ○ |
| Kılıçoğlu et al. (2022) | ○ | ○ | ○ | ○ |
| Cho et al. (2018) | ○ | ○ | ○ | ○ |
| Cao et al. (2022) | ○ | ○ | ○ | ○ |
| Yu et al. (2021) | ● | ○ | ○ | ○ |
| Baria et al. (2014) | ● | ○ | ○ | ○ |
| Goligher et al. (2015) | ● | ○ | ○ | ● |
| Pinto et al. (2016) | ● | ○ | ○ | ○ |
| Şahin et al. (2019) | ? | ○ | ○ | ● |
| Dres et al. (2021) | ● | ○ | ○ | ● |
| Lim et al. (2019) | ○ | ○ | ○ | ● |
| Gerscovich et al. (2001) | ● | ○ | ○ | ○ |
| Boussuges et al. (2009) | ● | ○ | ○ | ● |
| Voyvoda et al. (2012) | ● | ? | ○ | ○ |
| Jung et al. (2014) | ● | ○ | ● | ○ |
| Crimi et al. (2018) | ○ | ○ | ○ | ● |
| Dres et al. (2020) | ○ | ○ | ○ | ● |
| Paolo et al. (2022) | ○ | ○ | ○ | ● |
| Formenti et al. (2022) | ● | ○ | ○ | ○ |
| Wallbridge et al. (2018) | ● | ○ | ○ | ● |
| Yoshida et al. (2019) | ● | ○ | ● | ● |
| Rahman et al. (2017) | ○ | ○ | ○ | ● |
| Tahan et al. (2016) | ○ | ○ | ○ | ○ |
| Misuri et al. (1997) | ● | ○ | ○ | ● |
| Ota et al. (2012) | ○ | ○ | ○ | ● |
| Kang et al. (2021) | ● | ? | ○ | ● |
| Ishida et al. (2015) | ● | ○ | ○ | ● |
| Ishida et al. (2014) | ● | ○ | ○ | ● |
| Sugimoto et al. (2018) | ● | ○ | ● | ● |
| Abuín-Porras et al. (2020) | ● | ○ | ○ | ● |
| Monjo et al. (2018) | ● | ○ | ○ | ○ |
| Monjo et al. (2022) | ● | ○ | ○ | ○ |
| Kim et al. (2020) | ○ | ○ | ● | ○ |
| Lee et al. (2018) | ● | ○ | ○ | ○ |
| Oh et al. (2016) | ● | ○ | ● | ● |
| Kelli et al. (2020) | ● | ○ | ● | ○ |

Selection bias, participant selection; Performance bias, evaluation protocol; Detection bias, reference standard; Reporting bias, selective reporting. ○ Low risk; ● High risk; ? Unclear risk.

respiratory muscle function in healthy people, and there have been some studies on its repeatability and reliability. However, its application in diseases and the outlier values need more studies to verify. In addition, there is not enough evidence to use ultrasound measurements to assess extra-diaphragmatic inspiratory muscles, and further studies using standardized

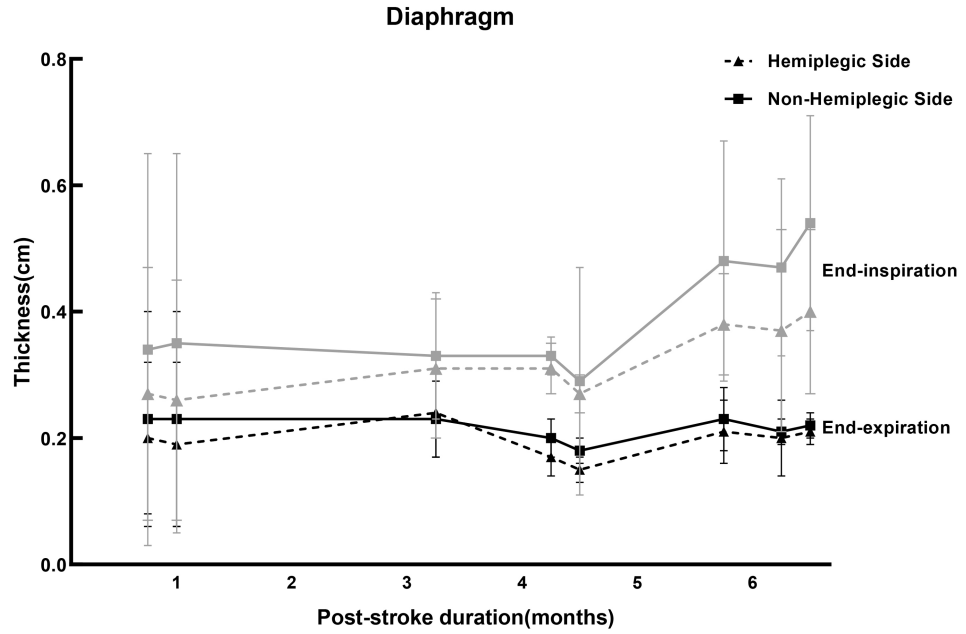


FIGURE 2
Studies for the thickness of the diaphragm ultrasound in stroke patients. The reference values of the diaphragm thickness of the stroke patients at the subacute stage at end-expiration and end-inspiration measured by ultrasound in different studies in Supplementary material 2, presented by the mean±standard deviation. Where the gray curves (solid and dotted lines) represented the diaphragm thickness at the end of inspiration, and the black curves (solid and dotted lines) were the thickness of the diaphragm at the end of expiration. The solid lines were the thickness of the diaphragm on non-hemiplegic side, while the dotted lines were the hemiplegic side. The values on the abscissa represented the average duration of post-stroke (months).

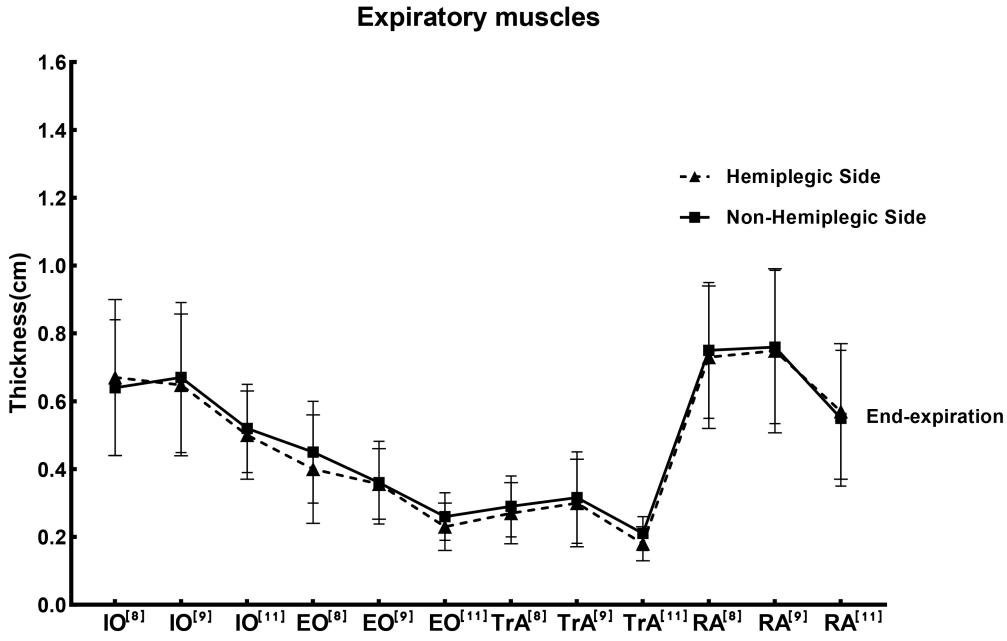


FIGURE 3
Studies for the thickness of the expiratory muscle ultrasound in stroke patients. The reference values of the thickness of expiratory muscle at end-expiration measured by ultrasound in different studies in Supplementary material 2, presented by the mean±standard deviation. Where the solid line was the thickness of the expiratory muscles on non-hemiplegic side, while the dotted line was the hemiplegic side. Labels at the top-right of the abbreviations on the abscissa axis, such as [8],[9],[11], are shown in Supplementary material 2. The abbreviations on the abscissa represented different studies. IO, Internal oblique muscle; EO, External oblique muscle; RA, Rectus abdominis muscle; TrA, Transversus abdominis muscle.

methodology are needed. The impairment of respiratory function is a frequent and serious complication for stroke patients (Kim et al., 2015). Early detection of respiratory dysfunction is important for protecting patients from comorbid pulmonary problems (Kılıçoğlu et al., 2022). By summarizing the function of respiratory muscle on hemiplegic side and non-hemiplegic side

of stroke patients in the studies included, we found that the average thickness of diaphragm on the hemiplegic side of stroke patients was significantly lower than that on the non-hemiplegic side, while the average thickness of abdominal expiratory muscles on the hemiplegic side were mostly lower than that on the non-hemiplegic side. However, there are several limitations in this review. We summarized and described the applications of ultrasonic measurement of respiratory muscle according to different parameters; but there was a lack of evaluation of differences and possible bias. In addition, due to the inclusion of fewer studies, the included stroke patients were not distinguished by age, gender, type of stroke, etc., at the clinical application of this review. Due to the inconsistency of indicators reflecting diaphragmatic contractility in the included studies, diaphragmatic thickness at the end-inspiratory and end-expiratory was used instead of diaphragmatic thickening fraction in Figure 2. Moreover, the average post-stroke duration of the expiratory muscles-related patients with hemiplegia ranged from months to years in the studies included. Future research can analyze and summarize these influencing factors before elaboration.

## Author contributions

XL conceived and designed the review. XL and YY drafted the manuscript, designed the tables, and designed the figures. XL, YY, and JJ modified the language and checked the text. XL and JJ checked and confirmed the information. All authors read and approved the final manuscript.

## Funding

This research was funded by National Key Research and Development Program of the Ministry of Science and Technology of the People's Republic of China, grant numbers 2018YFC2002300 and 2018YFC2002301.

## Conflict of interest

The authors declare that the research was conducted in the absence of any commercial or financial relationships that could be construed as a potential conflict of interest.

## Publisher's note



## Supplementary material

The Supplementary material for this article can be found online at: https://www.frontiersin.org/articles/10.3389/fnins.2023.1132335/full#supplementary-material

## References

Abe, T., Kusuhara, N., Yoshimura, N., Tomita, T., and Easton, P. A. (1996). Differential respiratory activity of four abdominal muscles in humans. *J. Appl. Physiol.* 80, 1379–1389. doi: 10.1152/jappl.1996.80.4.1379

Abuín-Porras, V., Maldonado-Tello, P., de la Cueva-Reguera, M., Rodríguez-Sanz, D., Calvo-Lobo, C., López-López, D., et al. (2020). Comparison of lateral abdominal musculature activation during expiration with an expiratory flow control device versus the abdominal drawing-in maneuver in healthy women: a cross-sectional observational pilot study. *Medicina* 56:84. doi: 10.3390/medicina56020084

Adigozali, H., Shadmehr, A., Ebrahimi, E., Rezasoltani, A., and Naderi, F. (2016). Ultrasonography for the assessment of the upper trapezius properties in healthy females: a reliability study. *Muscles Ligaments Tendons J.* 6, 167–172. doi: 10.11138/mltj/2016.6.1.167

Aliverti, A., Cala, S. J., Duranti, R., Ferrigno, G., Kenyon, C. M., Pedotti, A., et al. (1997). Human respiratory muscle actions and control during exercise. *J. Appl. Physiol.* 83, 1256–1269. doi: 10.1152/jappl.1997.83.4.1256

Aminoff, M. J., and Sears, T. A. (1971). Spinal integration of segmental, cortical and breathing inputs to thoracic respiratory motoneurones. *J. Physiol.* 215, 557–575. doi: 10.1113/jphysiol.1971.sp009485

Baldwin, C. E., Paratz, J. D., and Bersten, A. D. (2011). Diaphragm and peripheral muscle thickness on ultrasound: intra-rater reliability and variability of a methodology using non-standard recumbent positions. *Respirology* 16, 1136–1143. doi: 10.1111/j.1440-1843.2011.02005.x

Baria, M. R., Shahgholi, L., Sorenson, E. J., Harper, C. J., Lim, K. G., Strommen, J. A., et al. (2014). B-mode ultrasound assessment of diaphragm structure and function in patients with COPD. *Chest* 146, 680–685. doi: 10.1378/chest.13-2306

Bedewi, M. A., Alhariqi, B. A., Aldossary, N. M., Gaballah, A. H., and Sandougah, K. J. (2021). Shear wave elastography of the scalene muscles in healthy adults. *Medicine* 100:e26891. doi: 10.1097/MD.0000000000026891

Belavý, D. L., Gast, U., and Felsenberg, D. (2017). Exercise and transversus abdominis muscle atrophy after 60-d bed rest. *Med. Sci. Sports Exerc.* 49, 238–246. doi: 10.1249/MSS.0000000000001096

Benditt, J. O., and Boitano, L. J. (2013). Pulmonary issues in patients with chronic neuromuscular disease. *Am. J. Resp. Crit. Care.* 187, 1046–1055. doi: 10.1164/rccm.201210-1804CI

Boon, A. J., Harper, C. J., Ghahfarokhi, L. S., Strommen, J. A., Watson, J. C., and Sorenson, E. J. (2013). Two-dimensional ultrasound imaging of the diaphragm: quantitative values in normal subjects. *Muscle Nerve* 47, 884–889. doi: 10.1002/mus.23702

Boussuges, A., Gole, Y., and Blanc, P. (2009). Diaphragmatic motion studied by m-mode ultrasonography: methods, reproducibility, and normal values. *Chest* 135, 391–400. doi: 10.1378/chest.08-1541

Cala, S. J., Kenyon, C. M., Lee, A., Watkin, K., Macklem, P. T., and Rochester, D. F. (1998). Respiratory ultrasonography of human parasternal intercostal muscle in vivo. *Ultrasound Med. Biol.* 24, 313–326. doi: 10.1016/s0301-5629(97)00271-8

Caleffi-Pereira, M., Pletsch-Assunção, R., Cardenas, L. Z., Santana, P. V., Ferreira, J. G., Iamonti, V. C., et al. (2018). Unilateral diaphragm paralysis: a dysfunction restricted not just to one hemidiaphragm. *BMC Pulm. Med.* 18:126. doi: 10.1186/s12890-018-0698-1

Cao, H., Chen, X., Ren, X., Chen, Z., Liu, C., Ni, J., et al. (2022). Repetitive transcranial magnetic stimulation combined with respiratory muscle training for pulmonary rehabilitation after ischemic stroke—a randomized, case-control study. *Front. Aging Neurosci.* 14:1006696. doi: 10.3389/fnagi.2022.1006696

Catalá-Ripoll, J. V., Monsalve-Naharro, J. Á., and Hernández-Fernández, F. (2020). Incidence and predictive factors of diaphragmatic dysfunction in acute stroke. *BMC Neurol.* 20:79. doi: 10.1186/s12883-020-01664-w

Chavhan, G. B., Babyn, P. S., Cohen, R. A., and Langer, J. C. (2010). Multimodality imaging of the pediatric diaphragm: anatomy and pathologic conditions. *Radiographics* 30, 1797–1817. doi: 10.1148/rg.307105046

Cho, J. E., Lee, H. J., Kim, M. K., and Lee, W. H. (2018). The improvement in respiratory function by inspiratory muscle training is due to structural muscle changes in patients with stroke: a randomized controlled pilot trial. *Top. Stroke Rehabil.* 25, 37–43. doi: 10.1080/10749357.2017.1383681

Cohen, E., Mier, A., Heywood, P., Murphy, K., Boultbee, J., and Guz, A. (1994). Diaphragmatic movement in hemiplegic patients measured by ultrasonography. *Thorax* 49, 890–895. doi: 10.1136/thx.49.9.890

Crimi, C., Heffler, E., Augelletti, T., Campisi, R., Noto, A., Vancheri, C., et al. (2018). Utility of ultrasound assessment of diaphragmatic function before and after pulmonary

rehabilitation in COPD patients. *Int. J. Chron. Obstruct. Pulmon. Dis.* 13, 3131–3139. doi: 10.2147/COPD.S171134

De Troyer, A., and Boriek, A. M. (2011). Mechanics of the respiratory muscles. *Compr. Physiol.* 1, 1273–1300. doi: 10.1002/cphy.c100009

De Troyer, A., Estenne, M., Ninane, V., Van Gansbeke, D., and Gorini, M. (1990). Transversus abdominis muscle function in humans. *J. Appl. Physiol.* 68, 1010–1016. doi: 10.1152/jappl.1990.68.3.1010

De Troyer, A., Kirkwood, P. A., and Wilson, T. A. (2005). Respiratory action of the intercostal muscles. *Physiol. Rev.* 85, 717–756. doi: 10.1152/physrev.00007.2004

De Troyer, A., Legrand, A., Gevenois, P. A., and Wilson, T. A. (1998). Mechanical advantage of the human parasternal intercostal and triangularis sterni muscles. *J. Physiol.* 513, 915–925. doi: 10.1111/j.1469-7793.1998.915ba.x

Diab, K. M., Shalabi, A., Sevastik, J. A., and Guntner, P. (1998). A method for morphometric study of the intercostal muscles by high-resolution ultrasound. *Eur. Spine J.* 7, 224–228. doi: 10.1007/s005860050061

Dres, M., Dubé, B., Goligher, E., Vorona, S., Demiri, S., Morawiec, E., et al. (2020). Usefulness of parasternal intercostal muscle ultrasound during weaning from mechanical ventilation. *Anesthesiology* 132, 1114–1125. doi: 10.1097/ALN.0000000000003191

Dres, M., Similowski, T., Goligher, E. C., Pham, T., Sergenyuk, L., Telias, I., et al. (2021). Dyspnoea and respiratory muscle ultrasound to predict extubation failure. *Eur. Respir. J.* 58:2100002. doi: 10.1183/13993003.00002-2021

English, C. K., Thoirs, K. A., Fisher, L., McLennan, H., and Bernhardt, J. (2012). Ultrasound is a reliable measure of muscle thickness in acute stroke patients, for some, but not all anatomical sites: a study of the intra-rater reliability of muscle thickness measures in acute stroke patients. *Ultrasound Med. Biol.* 38, 368–376. doi: 10.1016/j.ultrasmedbio.2011.12.012

Estenne, M., Yernault, J. C., and De Troyer, A. (1985). Rib cage and diaphragm-abdomen compliance in humans: effects of age and posture. *J. Appl. Physiol.* 59, 1842–1848. doi: 10.1152/jappl.1985.59.6.1842

Fedullo, A. J., Lerner, R. M., Gibson, J., and Shayne, D. S. (1992). Sonographic measurement of diaphragmatic motion after coronary artery bypass surgery. *Chest* 102, 1683–1686. doi: 10.1378/chest.102.6.1683

Formenti, P., Umbrello, M., Castagna, V., Cenci, S., Bichi, F., Pozzi, T., et al. (2022). Respiratory and peripheral muscular ultrasound characteristics in ICU COVID 19 ARDS patients. *J. Crit. Care* 67, 14–20. doi: 10.1016/j.jcrc.2021.09.007

Formenti, P., Umbrello, M., Dres, M., and Chiumello, D. (2020). Ultrasonographic assessment of parasternal intercostal muscles during mechanical ventilation. *Ann. Intensive Care* 10:120. doi: 10.1186/s13613-020-00735-y

Gerscovich, E. O., Cronan, M., McGahan, J. P., Jain, K., Jones, C. D., and McDonald, C. (2001). Ultrasonographic evaluation of diaphragmatic motion. *J. Ultrasound Med.* 20, 597–604. doi: 10.7863/jum.2001.20.6.597

Goligher, E. C., Laghi, F., Detsky, M. E., Farias, P., Murray, A., Brace, D., et al. (2015). Measuring diaphragm thickness with ultrasound in mechanically ventilated patients: feasibility, reproducibility and validity. *Intens. Care Med.* 41, 642–649. doi: 10.1007/s00134-015-3687-3

Gottesman, E., and McCool, F. D. (1997). Ultrasound evaluation of the paralyzed diaphragm. *Am. J. Resp. Crit. Care.* 155, 1570–1574. doi: 10.1164/ajrccm.155.5.9154859

Hodges, P. W., and Gandevia, S. C. (2000). Changes in intra-abdominal pressure during postural and respiratory activation of the human diaphragm. *J. Appl. Physiol.* 89, 967–976. doi: 10.1152/jappl.2000.89.3.967

Houston, J. G., Angus, R. M., Cowan, M. D., McMillan, N. C., and Thomson, N. C. (1994). Ultrasound assessment of normal hemidiaphragmatic movement: relation to inspiratory volume. *Thorax* 49, 500–503. doi: 10.1136/thx.49.5.500

Houston, J. G., Morris, A. D., Grosset, D. G., Lees, K. R., McMillan, N., and Bone, I. (1995). Ultrasonic evaluation of movement of the diaphragm after acute cerebral infarction. *J. Neurol. Neurosurg. Psychiatry* 58, 738–741. doi: 10.1136/jnnp.58.6.738

Hudson, A. L., Gandevia, S. C., and Butler, J. E. (2007). The effect of lung volume on the co-ordinated recruitment of scalene and sternomastoid muscles in humans. *J. Physiol.* 584, 261–270. doi: 10.1113/jphysiol.2007.137240

Ishida, H., Kobara, K., Osaka, H., Suehiro, T., Ito, T., Kurozumi, C., et al. (2014). Correlation between peak expiratory flow and abdominal muscle thickness. *J. Phys. Ther. Sci.* 26, 1791–1793. doi: 10.1589/jpts.26.1791

Ishida, H., Suehiro, T., Kurozumi, C., Ono, K., and Watanabe, S. (2015). Correlation between abdominal muscle thickness and maximal expiratory pressure. *J. Ultras. Med.* 34, 2001–2005. doi: 10.7863/ultra.14.12006

Jandt, S. R., Da Sil Caballero, R. M., Junior, L. A. F., and Dias, A. S. (2011). Correlation between trunk control, respiratory muscle strength and spirometry in patients with stroke: an observational study. *Physiother. Res. Int.* 16, 218–224. doi: 10.1002/pri.495

Jung, K., Park, J., Hwang, D., Kim, J., and Kim, J. (2014). Ultrasonographic diaphragmatic motion analysis and its correlation with pulmonary function in hemiplegic stroke patients. *Ann. Rehabil. Med.* 38, 29–37. doi: 10.5535/arm.2014.38.1.29

Kang, K. W., Kwon, Y. H., and Son, S. M. (2021). Ultrasound measurement of the transverse abdominis, internal oblique, and external oblique muscles associated with forward head posture and reduced Cranio-vertebral angle. *Med. Sci. Monitor.* 27:e928987. doi: 10.12659/MSM.928987

Kelli, A., Kellis, E., Galanis, N., Dafkou, K., Sahinis, C., and Ellinoudis, A. (2020). Transversus abdominis thickness at rest and exercise in individuals with poststroke hemiparesis. *Sports* 8:86. doi: 10.3390/sports8060086

Kılıçoğlu, M. S., Yurdakul, O. V., Çelik, Y., and Aydın, T. (2022). Investigating the correlation between pulmonary function tests and ultrasonographic diaphragm measurements and the effects of respiratory exercises on these parameters in hemiplegic patients. *Top. Stroke Rehabil.* 29, 218–229. doi: 10.1080/10749357.2021.1911748

Kim, C., Lee, J., Kim, H., and Kim, I. (2015). Effects of the combination of respiratory muscle training and abdominal drawing-in maneuver on respiratory muscle activity in patients with post-stroke hemiplegia: A pilot randomized controlled trial. *Top. Stroke Rehabil.* 22, 262–270. doi: 10.1179/1074935714Z.0000000020

Kim, Y., Kim, J., Nam, H., Kim, H. D., Eom, M. J., Jung, S. H., et al. (2020). Ultrasound imaging of the trunk muscles in acute stroke patients and relations with balance scales. *Ann. Rehabil. Med.* 44, 273–283. doi: 10.5535/arm.19125

Kim, M., Lee, K., Cho, J., and Lee, W. (2017). Diaphragm thickness and inspiratory muscle functions in chronic stroke patients. *Med. Sci. Monitor.* 23, 1247–1253. doi: 10.12659/MSM.900529

Kisilewicz, A., Madeleine, P., Ignasiak, Z., Ciszek, B., Kawczynski, A., and Larsen, R. G. (2020). Eccentric exercise reduces upper trapezius muscle stiffness assessed by shear wave elastography and myotonometry. *Front. Bioeng. Biotechnol.* 8:928. doi: 10.3389/fbioe.2020.00928

Laroche, C. M., Mier, A. K., Moxham, J., and Green, M. (1988). Diaphragm strength in patients with recent hemidiaphragm paralysis. *Thorax* 43, 170–174. doi: 10.1136/thx.43.3.170

Laursen, C. B., Clive, A., Hallifax, R., Pietersen, P. I., Asciak, R., Davidsen, J. R. M., et al. (2021). European respiratory society statement on thoracic ultrasound. *Eur. Respir. J.* 57:2001519. doi: 10.1183/13993003.01519-2020

Laveneziana, P., Albuquerque, A., Aliverti, A., Babb, T., Barreiro, E., Dres, M., et al. (2019). ERS statement on respiratory muscle testing at rest and during exercise. *Eur. Respir. J.* 53:1801214. doi: 10.1183/13993003.01214-2018

Lee, K., Cho, J., Hwang, D., and Lee, W. (2018). Decreased respiratory muscle function is associated with impaired trunk balance among chronic stroke patients: a cross-sectional study. *Tohoku J. Exp. Med.* 245, 79–88. doi: 10.1620/tjem.245.79

Lee, J., Hwang, S., Han, S., and Han, D. (2016). Effects of stretching the scalene muscles on slow vital capacity. *J. Phys. Ther. Sci.* 28, 1825–1828. doi: 10.1589/jpts.28.1825

Legrand, A., Schneider, E., Gevenois, P., and De Troyer, A. (2003). Respiratory effects of the scalene and sternomastoid muscles in humans. *J. Appl. Physiol.* 94, 1467–1472. doi: 10.1152/japplphysiol.00869.2002

Lexell, J. E., and Downham, D. Y. (2005). How to assess the reliability of measurements in rehabilitation [retracted]. *Am. J. Phys. Med. Rehab.* 84, 719–723. doi: 10.1097/01.phm.0000176452.17771.20

Lim, S. Y., Lim, G., Lee, Y. J., Cho, Y. J., Park, J. S., Yoon, H. I., et al. (2019). Ultrasound assessment of diaphragmatic function during acute exacerbation of chronic obstructive pulmonary disease: a pilot study. *Int. J. Chron. Obstruct. Pulmon. Dis.* 14, 2479–2484. doi: 10.2147/COPD.S214716

Liu, X., Qu, Q., Deng, P., Zhao, Y., Liu, C., Fu, C., et al. (2022). Assessment of diaphragm in hemiplegic patients after stroke with ultrasound and its correlation of extremity motor and balance function. *Brain Sci.* 12:882. doi: 10.3390/brainsci12070882

Marsden, J. F., Hough, A., Shum, G., Shaw, S., and Freeman, J. A. (2013). Deep abdominal muscle activity following supratentorial stroke. *J. Electromyogr. Kines.* 23, 985–990. doi: 10.1016/j.jelekin.2013.04.003

Matamis, D., Soilemezi, E., Tsagourias, M., Akoumianaki, E., Dimassi, S., Boroli, F., et al. (2013). Sonographic evaluation of the diaphragm in critically ill patients. Technique and clinical applications. *Intensive Care Med.* 39, 801–810. doi: 10.1007/s00134-013-2823-1

McMeeken, J. M., Beith, I. D., Newham, D. J., Milligan, P., and Critchley, D. J. (2004). The relationship between EMG and change in thickness of transversus abdominis. *Clin. Biomech.* 19, 337–342. doi: 10.1016/j.clinbiomech.2004.01.007

Misuri, G., Colagrande, S., Gorini, M., Iandelli, I., Mancini, M., Duranti, R., et al. (1997). In vivo ultrasound assessment of respiratory function of abdominal muscles in normal subjects. *Eur. Respir. J.* 10, 2861–2867. doi: 10.1183/09031936.97.10122861

Monjo, H., Fukumoto, Y., Asai, T., Ohshima, K., Kubo, H., Tajitsu, H., et al. (2022). Changes in muscle thickness and echo intensity in chronic stroke survivors: a 2-year longitudinal study. *J. Clin. Neurol.* 18, 308–314. doi: 10.3988/jcn.2022.18.3.308

Monjo, H., Fukumoto, Y., Asai, T., and Shuntoh, H. (2018). Muscle thickness and echo intensity of the abdominal and lower extremity muscles in stroke survivors. *J. Clin. Neurol.* 14, 549–554. doi: 10.3988/jcn.2018.14.4.549

Nakayama, T., Fujii, Y., Suzuki, K., Kanazawa, I., and Nakada, T. (2004). The primary motor area for voluntary diaphragmatic motion identified by high field fMRI. *J. Neurol.* 251, 730–735. doi: 10.1007/s00415-004-0413-4

Oh, D., Kim, G., Lee, W., and Shin, M. M. (2016). Effects of inspiratory muscle training on balance ability and abdominal muscle thickness in chronic stroke patients. *J. Phys. Ther. Sci.* 28, 107–111. doi: 10.1589/jpts.28.107

Ota, M., Ikezoe, T., Kaneoka, K., and Ichihashi, N. (2012). Age-related changes in the thickness of the deep and superficial abdominal muscles in women. *Arch. Gerontol. Geriat.* 55, e26–e30. doi: 10.1016/j.archger.2012.03.007

Paolo, F., Valentina, D. G., Silvia, C., Tommaso, P., Elena, C., Martin, D., et al. (2022). The possible predictive value of muscle ultrasound in the diagnosis of ICUAW in long-term critically ill patients. *J. Crit. Care* 71:154104. doi: 10.1016/j.jcrc.2022.154104

Parthasarathy, S., Jubran, A., Laghi, F., and Tobin, M. J. (2007). Sternomastoid, rib cage, and expiratory muscle activity during weaning failure. *J. Appl. Physiol.* 103, 140–147. doi: 10.1152/japplphysiol.00904.2006

Peche, R., Estenne, M., Gevenois, P. A., Brassinne, E., Yernault, J. C., and De Troyer, A. (1996). Sternomastoid muscle size and strength in patients with severe chronic obstructive pulmonary disease. *Am. J. Resp. Crit. Care.* 153, 422–425. doi: 10.1164/ajrccm.153.1.8542153

Pietton, R., David, M., Hisaund, A., Langlais, T., Skalli, W., Vialle, R., et al. (2021). Biomechanical evaluation of intercostal muscles in healthy children and adolescent idiopathic scoliosis: a preliminary study. *Ultrasound Med. Biol.* 47, 51–57. doi: 10.1016/j.ultrasmedbio.2020.09.011

Pinto, S., Alves, P., Pimentel, B., Swash, M., and de Carvalho, M. (2016). Ultrasound for assessment of diaphragm in ALS. *Clin. Neurophysiol.* 127, 892–897. doi: 10.1016/j.clinph.2015.03.024

Rahman, N. N., Singh, D., and Lee, R. Y. (2017). Correlation between thoracolumbar curvatures and respiratory function in older adults. *Clin. Interv. Aging* 12, 523–529. doi: 10.2147/CIA.S110329

Rankin, G., Stokes, M., and Newham, D. J. (2006). Abdominal muscle size and symmetry in normal subjects. *Muscle Nerve* 34, 320–326. doi: 10.1002/mus.20589

Rochester, C. L., and Mohsenin, V. (2002). Respiratory complications of stroke. *Semin. Respir. Crit. Care Med.* 23, 248–260. doi: 10.1055/s-2002-33033

Şahin, H., Doğan, A., and Ekiz, T. (2019). Ultrasonographic evaluation of the diaphragm thickness in patients with multiple sclerosis. *Mult. Scler. Relat. Disord.* 36:101369. doi: 10.1016/j.msard.2019.08.011

Sarwal, A., Walker, F. O., and Cartwright, M. S. (2013). Neuromuscular ultrasound for evaluation of the diaphragm. *Muscle Nerve* 47, 319–329. doi: 10.1002/mus.23671

Sferrazza Papa, G. F., Pellegrino, G. M., Di Marco, F., Imeri, G., Brochard, L., Goligher, E., et al. (2016). A review of the ultrasound assessment of diaphragmatic function in clinical practice. *Respiration* 91, 403–411. doi: 10.1159/000446518

Shi, Z., de Vries, H., de Grooth, H., Jonkman, A. H., Zhang, Y., Haaksma, M., et al. (2021). Changes in respiratory muscle thickness during mechanical ventilation: focus on expiratory muscles. *Anesthesiology* 134, 748–759. doi: 10.1097/ALN.0000000000003736

Shi, Z., Jonkman, A., de Vries, H., Jansen, D., Ottenheijm, C., Girbes, A., et al. (2019). Expiratory muscle dysfunction in critically ill patients: towards improved understanding. *Intens. Care Med.* 45, 1061–1071. doi: 10.1007/s00134-019-05664-4

Sugimoto, T., Yokogawa, M., Miaki, H., Madokoro, S., and Nakagawa, T. (2018). Changes in thickness of the transversus abdominis during the abdominal drawing-in manoeuvre and expiratory muscle training in elderly people. *J. Phys. Ther. Sci.* 30, 119–123. doi: 10.1589/jpts.30.119

Summerhill, E. M., El-Sameed, Y. A., Glidden, T. J., and McCool, F. D. (2008). Monitoring recovery from diaphragm paralysis with ultrasound. *Chest* 133, 737–743. doi: 10.1378/chest.07-2200

Supinski, G. S., Morris, P. E., Dhar, S., and Callahan, L. A. (2018). Diaphragm dysfunction in critical illness. *Chest* 153, 1040–1051. doi: 10.1016/j.chest.2017.08.1157

Suzuki, J., Tanaka, R., Yan, S., Chen, R., Macklem, P. T., and Kayser, B. (1999). Assessment of abdominal muscle contractility, strength, and fatigue. *Am. J. Respir. Crit. Care Med.* 159, 1052–1060. doi: 10.1164/ajrccm.159.4.9803025

Tahan, N., Khademi-Kalantari, K., Mohseni-Bandpei, M. A., Mikaili, S., Baghban, A. A., and Jaberzadeh, S. (2016). Measurement of superficial and deep abdominal muscle thickness: an ultrasonography study. *J. Physiol. Anthropol.* 35:17. doi: 10.1186/s40101-016-0106-6

Tuinman, P. R., Jonkman, A. H., Dres, M., Shi, Z., Goligher, E. C., Goffi, A., et al. (2020). Respiratory muscle ultrasonography: methodology, basic and advanced principles and clinical applications in ICU and ED patients—a narrative review. *Intens. Care Med.* 46, 594–605. doi: 10.1007/s00134-019-05892-8

Ueki, J., De Bruin, P. F., and Pride, N. B. (1995). In vivo assessment of diaphragm contraction by ultrasound in normal subjects. *Thorax* 50, 1157–1161. doi: 10.1136/thx.50.11.1157

Vivier, E., and Mekontso Dessap, A. (2020). Bedside ultrasound for weaning from mechanical ventilation. *Anesthesiology* 132, 947–948. doi: 10.1097/ALN.0000000000003235

Voyvoda, N., Yücel, C., Karatas, G., Oguzulgen, I., and Oktar, S. (2012). An evaluation of diaphragmatic movements in hemiplegic patients. *Brit. J. Radiol.* 85, 411–414. doi: 10.1259/bjr/71968119

Wait, J. L., Nahormek, P. A., Yost, W. T., and Rochester, D. P. (1989). Diaphragmatic thickness-lung volume relationship in vivo. *J. Appl. Physiol.* 67, 1560–1568. doi: 10.1152/jappl.1989.67.4.1560

Wallbridge, P., Parry, S. M., Das, S., Law, C., Hammerschlag, G., Irving, L., et al. (2018). Parasternal intercostal muscle ultrasound in chronic obstructive pulmonary disease correlates with spirometric severity. *Sci. Rep.* 8:15274. doi: 10.1038/s41598-018-33666-7

Wilson, T. A., Legrand, A., Gevenois, P. A., and Troyer, A. (2001). Respiratory effects of the external and internal intercostal muscles in humans. *J. Physiol.* 530, 319–330. doi: 10.1111/j.1469-7793.2001.0319l.x

Yoshida, R., Tomita, K., Kawamura, K., Nozaki, T., Setaka, Y., Monma, M., et al. (2019). Measurement of intercostal muscle thickness with ultrasound imaging during maximal breathing. *J. Phys. Ther. Sci.* 31, 340–343. doi: 10.1589/jpts.31.340

Yu, X., Jiang, H., Zhang, C., Jin, Z., Gao, L., Wang, R., et al. (2021). The role of the diaphragm in postural stability and visceral function in Parkinson's disease. *Front. Aging Neurosci.* 13:785020. doi: 10.3389/fnagi.2021.785020

frontiers | Frontiers in Neuroscience

TYPE Study Protocol
PUBLISHED 27 April 2023
DOI 10.3389/fnins.2023.1180454



OPEN ACCESS

EDITED BY
Jie Jia,
Fudan University, China

REVIEWED BY
Abdulhameed Tomeh,
Universiti Putra Malaysia, Malaysia
Abdul Hanif Khan Yusof Khan,
Putra Malaysia University, Malaysia

*CORRESPONDENCE
Shi-Zhong Wang
✉ 1365866912@qq.com
Xin-Yuan Chen
✉ fychenxinyuan@fjmu.edu.cn
Shi-Rui Gan
✉ ganshirui@fjmu.edu.cn

†These authors have contributed equally to this work and share first authorship

RECEIVED 06 March 2023
ACCEPTED 13 April 2023
PUBLISHED 27 April 2023

CITATION
Liu X, Lin W, Zhang L, Zhang W-L, Cheng X-P, Lian Y-H, Li M-C, Wang S-Z, Chen X-Y and Gan S-R (2023) Effects of cerebellar transcranial alternating current stimulation in cerebellar ataxia: study protocol for a randomised controlled trial.
*Front. Neurosci.* 17:1180454.
doi: 10.3389/fnins.2023.1180454



# Effects of cerebellar transcranial alternating current stimulation in cerebellar ataxia: study protocol for a randomised controlled trial

Xia Liu[1†], Wei Lin[2†], Lin Zhang[3†], Wan-Li Zhang[4], Xiao-Ping Cheng[1], Yan-Hua Lian[5], Meng-Cheng Li[3], Shi-Zhong Wang[1,5*], Xin-Yuan Chen[1,6*] and Shi-Rui Gan[2*]

[1]Department of Rehabilitation Medicine, The First Affiliated Hospital, Fujian Medical University, Fuzhou, China, [2]Department of Neurology and Institute of Neurology, The First Affiliated Hospital, Fujian Medical University, Fuzhou, China, [3]Department of Radiology, The First Affiliated Hospital, Fujian Medical University, Fuzhou, China, [4]College of Mechanical Engineering and Automation, Fuzhou University, Fuzhou, China, [5]The School of Health, Fujian Medical University, Fuzhou, China, [6]National Regional Medical Center, Binhai Campus of the First Affiliated Hospital, Fujian Medical University, Fuzhou, China

**Background:** Cerebellar ataxia (CA) is a movement disorder that can affect balance and gait, limb movement, oculomotor control, and cognition. Multiple system atrophy-cerebellar type (MSA-C) and spinocerebellar ataxia type 3 (SCA3) are the most common forms of CA, for which no effective treatment is currently available. Transcranial alternating current stimulation (tACS) is a non-invasive method of brain stimulation supposed to alter cortical excitability and brain electrical activity, modulating functional connectivity within the brain. The cerebellar tACS can modulate the cerebellar outflow and cerebellum-linked behavior and it is a proven safe technique for humans. Therefore, the aim of this study is to 1) examine whether cerebellar tACS improves ataxia severity and various non-motor symptoms in a homogeneous cohort of CA patients consisting of MSA-C and SCA3, 2) explore the time course of these effects, and 3) assess the safety and tolerance of cerebellar tACS in all participants.

**Methods/design:** This is a 2-week, triple-blind, randomised, sham-controlled study. 164 patients (MSA-C: 84, SCA3: 80) will be recruited and randomly assigned to either active cerebellar tACS or sham cerebellar tACS, in a 1:1 ratio. Patients, investigators, and outcome assessors are unaware of treatment allocation. Cerebellar tACS (40 min, 2 mA, ramp-up and down periods of 10s each) will be delivered over 10 sessions, distributed in two groups of five consecutive days with a two-day break in between. Outcomes are assessed after the tenth stimulation (T1), and after 1month (T2) and 3 months (T3). The primary outcome measure is the difference between the active and sham groups in the proportion of patients with an improvement of 1.5 points in the Scale for the Assessment and Rating of Ataxia (SARA) score after 2weeks of treatment. In addition, effects on a variety of non-motor symptoms, quality of life, and autonomic nerve dysfunctions are assessed via relative scales. Gait imbalance, dysarthria, and finger dexterity are objectively valued via relative tools. Finally, functional magnetic resonance imaging is performed to explore the possible mechanism of treatment effects.

**Discussion:** The results of this study will inform whether repeated sessions of active cerebellar tACS benefit CA patients and whether this form of non-invasive stimulation might be a novel therapeutic approach to consider in a neuro-rehabilitation setting.

**Clinical Trial Registration:** ClinicalTrials.gov, identifier NCT05557786; https://www.clinicaltrials.gov/ct2/show/NCT05557786.

KEYWORDS

spinocerebellar ataxia, multiple system atrophy, transcranial alternating current stimulation, randomised controlled trial, treatment

# Introduction

Cerebellar ataxia (CA) is a major cause of gait imbalance, limb dyskinesia, impaired motor-ocular control, and cognitive impairment (Manto et al., 2020). CA can be divided into sporadic ataxia and inherited ataxia, with the multiple system atrophy of cerebellar type (MSA-C) and spinocerebellar ataxia type 3 (SCA3) as the most common types, respectively (Anheim et al., 2012; Poewe et al., 2022). Although the pathogenic factors of these two types of CA are complex and varied, the common pathological features are injury, atrophy or dysfunction of the cerebellar and/or its afferent/efferent neural pathways (Radmard et al., 2023). At present, except for a few CA with very clear pathogenesis, there is still a lack of effective targeted treatment in clinic (Marmolino and Manto, 2010; Gandini et al., 2020; Beaudin et al., 2022; Correia et al., 2023). Therefore, an in-depth study of the neural mechanism of CA is of great significance for understanding cerebellar motor regulation and developing new therapeutic targets and strategies.

Transcranial alternating current stimulation (tACS) delivers brain stimulation by modulating cortical excitability and spontaneous brain activity in the scalp via a weak electrical current (Cabral-Calderin and Wilke, 2020). In the context of human neuroscience research, cerebellar tACS (CB-tACS) technique was pioneered by Mehta and colleagues (Mehta et al., 2014). This technique facilitates the study of cerebellar oscillations through the interaction of reactive neuronal elements (Wessel et al., 2022), enriches the imaging method of electrophysiology, and affects corticospinal excitability through the thalamic cortical pathway of the cerebellum, helping to explore the oscillatory mechanism triggered by the cerebellum and its associated circuits (Asan and Sahin, 2019; Wessel et al., 2022). A growing number of studies have demonstrated the ability of tACS to modulate different domains of human behavior rhythm and gait (Koganemaru et al., 2020), such as motor learning (Schubert et al., 2021), improving motor skills (Wessel et al., 2020), working memory (Abellaneda-Pérez et al., 2019; Grover et al., 2022), and the processing of emotional stimuli (Hu et al., 2021) and cognition (Del Felice et al., 2019). Furthermore, the safety of CB-tACS has been confirmed in healthy adult studies with only a few subjects reporting scalp burning, mild tingling, phosphorescent sensation, and other transient adverse reactions (Antal et al., 2017; Matsumoto and Ugawa, 2017). More recently, research has also begun to explore its therapeutic potential in various neurological disorders. Although tACS has been suggested as a treatment for different neurological conditions (PD (Del Felice et al., 2019), AD (Benussi et al., 2022), schizophrenia (Ahn et al., 2019), depression (Wang et al., 2022), and insomnia (Hong-Xing et al., 2020)), no evidence was reported yet for the tACS treatment on CA patients.

Based on these abovementioned results, we performed our clinical CB-tACS study. Our aims were 1) investigate whether cerebellar tACS decreases ataxia severity and a variety of non-motor symptoms in a homogeneous cohort of patients of MSA and SCA3 and 2) what is the duration of this beneficial effect.

# Methods

## Ethics and dissemination

This study was carried out according to the Declaration of Helsinki and got the approval of the local ethics committee of The First Affiliated Hospital of Fujian Medical University, Fuzhou, China (MRCTA, ECFAH of FMU [2022]399) on Aug 5, 2022. The contacts of the ethics committee are: 0086–0591-87,981,028, fykyll@163.com, and No.20, Chazhong Road, Fuzhou, Fujian Province, China. Participants need to sign an informed consent form before this study and receive medical care after the study. The research results will be published through articles or conferences. Thus, this study will benefit the treatment of CA patients and hopefully supply an effective non-pharmacological intervention soon.

## Experimental design, randomization, and blinding

This is a single-centre, triple-blind, randomised, sham-controlled intervention trial. The total of 164 recruited participants with CA (MSA: 84, SCA3: 80) will be randomly and equally assigned to the active or sham treatment group. The randomization was created by a computer program in permuted blocks of four and managed by an offsite statistician who does not participate in this study. Every participant gets an unknown-beforehand number from a sealed opaque envelope, which determines the trial he/she will participate in. The envelopes for the two tACS plans (sham and active) have the same characteristics regarding size, color, appearance, weight, and odor, and different plans are numbered by the statistician. All participants were blinded to the specific assignment during the triple-blind treatment period until the end of the follow-up, except for any emergency when the blinding will be stopped. Participants will receive a 2-week intervention, followed by a 4-week follow-up (conducted at the 6th week) and a 12-week follow-up (conducted at the 14th week). The entire process will strictly follow the consolidated standards of reporting trials guidelines (Figure 1)

and standard protocol items: recommendations for interventional trials checklist (Chan et al., 2013a, b).

Termination of the trial will be decided by the principal investigators, according to the following criteria: (1) lack of two consecutive tACS sessions, (2) severe adverse events (AEs), and (3) affected tACS-Assessment by treatment of other diseases. If a patient is lost to follow-up at weeks 6 or 14, the data collected up to that point will still be used in the statistical analysis at T2/T3.

## Study participants

Participants with CA who will receive research at the clinical Observation Cohort study of CA (NCT04010214) in the Department of Neurology, the First Affiliated Hospital of Fujian Medical University from August 2022 to April 2023 by our investigators will be identified for their eligibilities. All eligible participants will get access to the specific treatment plans and they can register directly to attend the trial for randomization. All potential risks will be informed in the consent. The withdrawal reason will be carefully recorded if any participant quits halfway. To maximize trial compliance, potential risks, requirements, the study schedule, and benefits will be fully explained to all recruited participants.

Participants will be instructed to avoid any anti-rehabilitation treatment for CA during the study. All participants will have freedom to quit at any time and choose other medical therapy strategies.

# Eligibility criteria

## Inclusion criteria

- 1 Inclusion Criteria for SCA3 patients:
- 1.1 Detectable clinical symptoms and a confirmed diagnosis for SCA3.
- 1.2 18–80 years old.
- 1.3 Signed informed consent by patients or their family members.
- 1.4 3-30pre-study Scale for the Assessment and Rating of Ataxia (SARA).
- 2.Inclusion Criteria for MSA-C:
- 2.1 30–80 years old;
- 2.2 Clinically diagnose or probable MSA-C according to the latest MSA diagnostic criteria (Wenning et al., 2022);
- 2.3 <4 years MSA-C medical history;
- 2.4 Independent walk (or with assistance);
- 2.5 >3 years life expectancy;
- 2.6 Contraceptive measures for women of childbearing age.
- 3. Exclusion Criteria for both SCA3 and MSA-C:
- 3.1 Patients with medical history of stroke, encephalitis, and epilepsy.
- 3.2 Patients with serious cognitive and behavioral disorders, or mental illness.
- 3.3 Patients with severe medical illness (such as kidney failure, convulsions, stomach ulcers, liver disease) and uncontrolled high blood pressure or diabetes.

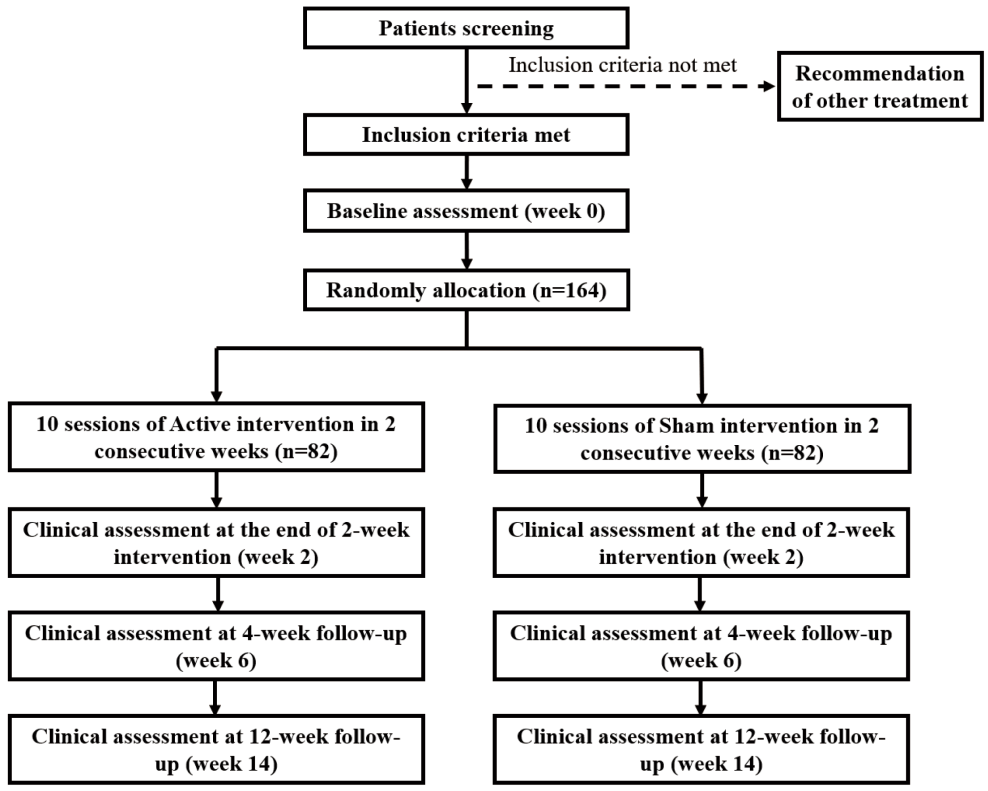


FIGURE 1
Design and flow of participants through the study.

- 3.4 Patients with head injury, neurosurgery, or mental issues within the head.
- 3.5 Patients who took investigational products within 4 weeks prior to this enrollment, or who are pregnant or breastfeeding.
- 3.6 Patients with metallic particles in the eye, medical pumps like implanted cardiac pacemaker or neurostimulators, and surgical clips (above the shoulder line), etc.

## Sample size calculation

Positive effect is supposed to occur in both groups according to previous report (Romano et al., 2015). The primary criterion was a $\geq$ 1.5 points SARA score decrease caused by 2 weeks of treatment. The SARA scores was expected to increase in 25% of placebo patients and 60% of the treated patients. 80% power was tested for 36 patients in each group, with a 35% δ between the groups, by using a bilateral test and 5% $\alpha$. Taking 10% attrition rate in consideration, 40 patients for each group will be needed to reach a minimum total sample size of 72. Based on these calculations, we estimate that 80 SCA3 participants will enroll in the study.

Our sample size was calculated as previously described (Levin et al., 2019). This study is expected to produce $\alpha$ of 0.05 at 80% power for a treatment effect of 50% on the annual progression of the movement examination score on the Unified Multiple System Atrophy Rating Scale (UMSARS); this contains 4 points from the active group and 8 points from the placebo group, which is above the minimal clinically detectable significant level of 3.8 points (Krismer et al., 2016). Therefore, we conducted this study to determine whether active tACS treatment would have a positive effect on MSA-C patients. The target total patients was 84, with an expected attrition rate of 10%.

## TACS intervention

Professional doctors will guide the participants to accept Active tACS (A-tACS) or Sham tACS (S-tACS) intervention under the same conditions during all sessions for 2 weeks. The tACS session was delivered via three 0.9% NaCl soaked surface sponge electrodes (5X7cm) on a current stimulator (Neustim NSS18, Neuracle, Changzhou, China). The return electrode was placed 2 cm below the inion and the two active electrodes were over the bilateral buccinator muscles. After computational modeling of electric field distribution, we chose this tACS particular montage with an extracephalic electrode, which can lead to significant entrainment of brain oscillations (Sadeghihassanabadi et al., 2022). Electrodes are fixed with elastic gauze and coated with conductive gel to reduce contact resistance (<5 kΩ).

An alternating sinusoidal current of 1 mA peak-to-baseline with a frequency of 70 Hz was used to stimulate the A-tACS throughout the whole behavioral treatment session (40 min) based on previous studies (Hong-Xing et al., 2020; Wang et al., 2022). The molecular mechanism of tACS remains unclear (Wessel et al., 2022). Currently, $\gamma$-tACS is most commonly applied into neurodegeneration and psychiatric disorders, γ-band is about 30 ~ 80 Hz, the electrical activity of the brain is mainly involved in cognitive function (Hu et al., 2021; Grover et al., 2022), motor function (Wessel et al., 2020; Giustiniani et al., 2021; Miyaguchi et al., 2022), and abnormal γ activity is commonly seen in various neuropsychiatric diseases. Therefore, gamma waves were selected in our study to explore the efficacy in cerebellar ataxia. For the S-tACS stimulation, the electrode placement was as the same as A-tACS, but the current was gradually decreased 40s after stimulus onset to simulate the experimental stimulus; in this manner, patients were blinded whether they were treated with active or sham tACS.

Participants were asked to sit in a bright and quiet room during all stimulation period, with their eyes open but no speaking and no large movement. Each participant will receive 10 interventions within 2 weeks, once a day from Monday to Friday. To examine differences between simulated perceptions, participants need to answer whether they feel they were treated with real or sham stimulation, and whether they experienced tingling skin sensations or phosphenes/light flickers. Sensations were rated from 0 (no sensation) to 4 (very strong sensations). The treatment type (A-tACS vs. S-tACS) was encoded in the in-house software and was masked for both patients and the researchers. Researchers only needed to enter a patient name and session number to start stimulation, but the technician confirmed whether an active or sham stimulation was delivered after each treatment was done.

## Outcome measures

Considering the wide clinical signs and symptoms of CA, various outcome measures which were validated for CA were selected to determine the improvement degrees of motor and non-motor functions. Measurements will be carried out under supervision, and data will be collected by specialist examiners or trained doctors. All results were obtained at baseline, weeks 2, 6, and 14, respectively (Table 1).

## Primary outcome measurements

The primary outcome for both SCA3 and MSA-C was the difference between the active and placebo groups in the proportion of patients with an improvement of 1.5 points in SARA score after 2 weeks of treatment. SARA (Schmitz-Hübsch et al., 2006) consists of 8 items: sitting, gait, finger chase, stance, speech disturbance, fast alternating hand movements, heel-shin slide, and nose-finger test. Higher score represents worse performance. SARA scoring will be done by experienced but blinded investigators under videotaping.

There was an alternative primary outcome for MSA-C, which was the difference in total UMSARS score between the two groups being treated for 2 weeks. The UMSARS consists of four parts (I, II, III, and IV) (Wenning et al., 2004), in which UMSARS-I and II are usually taken as key endpoints during clinical trials (Palma et al., 2022).

## Secondary outcome measurements

Except for the cardinal symptom of ataxia, there are a variety of complex non-motor symptoms in SCA3 and MSA-C, including

TABLE 1 Schedule of enrolment, interventions, and assessments.

| Week | Screening-2w | Baseline (T0) 0w | Treatment (T1) 2w | Follow-up (T2) 6w | Follow-up (T3) 14w |
|---|---|---|---|---|---|
| Enrolment | | | | | |
| Signed informed consent | | √ | | | |
| Diagnosis | √ | | | | |
| Randomization | | √ | | | |
| Interventions | | | | | |
| Sham intervention group | | √ | √ | | |
| Active intervention group | | √ | √ | | |
| Assessments | | | | | |
| Primary outcome | | | | | |
| SARA | | √ | √ | √ | √ |
| UMSARS (only for MSA-C) | | √ | √ | √ | √ |
| Secondary outcomes | | | | | |
| ICARS | | √ | √ | √ | √ |
| 9HPT | | √ | √ | √ | √ |
| Dysarthria | | √ | √ | √ | √ |
| Fatigue-14 | | √ | √ | √ | √ |
| PSQI | | √ | √ | √ | √ |
| Epworth score | | √ | √ | √ | √ |
| MoCA | | √ | √ | √ | √ |
| MMSE | | √ | √ | √ | √ |
| HAMA | | √ | √ | √ | √ |
| HAMD | | √ | √ | √ | √ |
| EQ-5D-5L/MSA-QoL | | √ | √ | √ | √ |
| SCOPA-Aut(only for MSA-C) | | √ | √ | √ | √ |
| Gait parameters | | √ | √ | √ | √ |
| EEG | | √ | √ | √ | √ |
| fMRI | | √ | √ | √ | √ |
| Temperature, blood pressure, heart rate | √ | | √ | √ | √ |
| Patients' compliance | | √ | √ | √ | √ |
| Blinding assessment | | √ | √ | √ | √ |

cognitive and emotional impairments, fatigue, sleep disorders, and dysfunction of the autonomic nerve. Therefore, in order to comprehensively analyze the treatment effect and its duration, we further studied the variation of a series of motor and non-motor indicators as the secondary outcome measurements at the end of the treatment and at 1 and 3 months after the treatment.

## Assessment of symptom of ataxia

To further investigate the treatment effect in ataxia, we adopted ICARS, which is a widely used scale for the ataxia severity measurement. The ICARS is composed by 19 items from four subscales, including 7 posture and gait disturbances, 7 kinetic functions, 2 speech disorders, and 3 oculomotor disorders. The total 0–100 scores allow for individual subscore's analysis (Trouillas et al., 1997).

## Assessment of non-motor symptoms

To investigate whether the treatment improves the non-motor symptoms, the following scales are used: The Montreal Cognitive Assessment (MoCA) (Nasreddine et al., 2005) and The Mini-Mental State Examination (MMSE) (Folstein et al., 1975) for evaluating cognitive change; Hamilton Anxiety Scale (HAMA) (HAMILTON Hamilton, 1959) and Hamilton Rating Scale for Depression

(HAMD-17) (Lin et al., 2018) for evaluating the changes in the status of anxiety and depression, respectively; The 14-item Fatigue Scale (FS-14) (Chalder et al., 1993) for evaluating symptoms of fatigue; finally, Sleep habits self-assessment (Pittsburgh Sleep Quality Index (PSQI) (Buysse et al., 1989) and Epworth Sleepiness Scale (ESS) (Johns, 1991) are used for investigating the improvement in sleep disturbance.

## Assessment of life ability and quality of life

To explore whether the treatment improves life quality of patients, the EuroQol Five-dimensional questionnaire (EQ-5D) and the Multiple System Atrophy Quality of Life questionnaires (MSA-QoL) are used for the participants of SCA3 and MSA-C, respectively. EQ-5D is an ordinal quality of life scale that can address the problems from mobility, selfcare, usual activities, pain/discomfort, or anxiety/depression (Bolzan et al., 2022). MSA-QoL is a MSA-specific self-report assessment. MSA-QoL and UMSARS have the same motor subscales (Schrag et al., 2007).

## Assessment of dysfunction of autonomic nerve

To explore whether the treatment improves the symptoms of dysfunction of the autonomic nerve in participants of MSA-C, the SCOPA-Aut questionnaire (0–69) is assessed (Visser et al., 2004). The scores of 26 SCOPA-Aut items range from 0 to 69, with higher scores indicating more severe symptoms.

## Assessment of finger dexterity

The 9-Hole Peg Test (9HPT) were performed under limited time to examine the finger dexterity and upper limb coordination as previously described (Feys et al., 2017).

## Assessment of dysarthria

We used the speech sounds to analyze the following parameters through the DIVAS2.5 voice analysis system (Wuyts et al., 2000): (1) Fundamental frequency perturbation (Jitter) and amplitude perturbation (Shimmer) reflect the stability of vocal cord vibration, which is related to the degree of roughness and hoarse sound, (2) Intensity (including maximum intensity (SPLmax)), minimum intensity (SPLmin) and range of intensity (SPLrng), reflects the maximum, minimum and range of sound intensity during phonation, and is related to the closure degree of the glottis, (3) The longest articulation time (MPT) assesses respiratory function and glottic closure, and (4) Dysphonia severity index (DSI) is a comprehensive evaluation parameter of pronunciation.

## Assessment of gait imbalance

To objectively and quantitatively evaluate the improvement of gait after the treatment, we used a gait analysis system, which consists of a gait acquisition system and gait analysis software. The gait acquisition system consists of two smart insoles (20 sensing points) and two nine-axis gyroscopes. The smart insoles are placed in the shoes for the left and right feet, and the gyroscopes are placed on the toes of the left and right feet, respectively.

The subjects wore the gait acquisition system and completed three tasks at designated locations: (1) 3 min-standing with eyes open, (2) 3 min-standing with eyes closed, and (3) walking in the corridor at a normal speed for 20 m. A series of gait parameters are then processed and calculated in gait analysis software: (1) Gait speed (meters walked per second), (2) Step length (distance between left heel and right foot contact point) (in meters), (3) Cadence (steps per minute), (4) Gait cycle (the time from when one heel hits the ground to when the heel hits the ground again) (in seconds), (5) Single support phase (percentage of the gait cycle from the time when one heel hits the ground to the time when the toe leaves the ground on this side), (6) Double support phase (percentage of gait cycle during which one side is single support period and the other side is also single support period), (7) Toe-out angle (the angle between one side of the foot and the walking direction during the walking phase) (in degree), (8) Toe-off angle (the angle when one toe leaves the ground) (in degree), (9) Average value of plantar pressure (in N), (10) Variance of plantar pressure, (11) Variation coefficient of step length (step length average/standard deviation), and (12) Variation coefficient of gait cycle (gait cycle average/standard deviation).

## Assessment of neuroimaging characters

To explore the possible mechanism of the treatment, we performed Resting-state functional magnetic resonance imaging (RS-fMRI), which can reflect neural activity through blood oxygen level-dependent (BOLD) signals and be used to analyze functional changes of the brain. There are three commonly used indicators for RS-fMRI: (1) Amplitude of low frequency (ALFF) indicates the intensity of brain activity in a specific region and (2) ReHo is an indicator for the synchronization of neuronal activity (Zang et al., 2004); Functional connectivity (FC) represents the synchronization of different neurophysiological events with spatial distance (Friston et al., 1993), identifies reliable patterns of covarying brain signals that indicate neural activity.

For the magnetic resonance image acquisition and data preprocessing, all participants used the same neuroimaging process via a Skyra scanner (3.0 Tesla Siemens) with a 20-channel head and neck coil, in which a head holder is set to minimize the head movement. Sagittal anatomical images were obtained using T1-weighted three-dimensional (3D) magnetization prepared rapid gradient echo (MP-RAGE) sequences with the following scan parameters: Repetition time (TR) = 2,300 ms, echo time (TE) = 2.3 ms, reversal time (TI) = 900 ms, flip Angle = 8°, field of view (FOV) = 240 mm × 256 mm, matrix size = 240 × 256, Bandwidth = 200 Hz/Px, slice = 192, voxel size = 1 mm × 1 mm × 1 mm, total acquisition time = 5 min and 12 s. All MRI data were quality-controlled by an experienced radiologist.

The data of resting-state functional Magnetic Resonance Imaging (RS-fMRI) were pre-processed by using MATLAB R2016b-DPARSFA. The image preprocessing process is as follows: (1) The first ten functional images were discarded for signal equilibration, (2) The remaining volumes were co-registered to the individual's corresponding MPRAGE image after the slice-timing correction and spatial realignme, (3) The anatomical images of gray matter, white matter (WM), and cerebrospinal fluid (CSF) were normalized to a

3x3x3mm3 space according to the Montreal Neurological Institute (MNI) standard, (4) The WM-and CSF-extracted average signals and the head movements estimated from the Friston 24-parameter model were used for physiological noise removal by nuisance regression, and (5) Detrend and bandpass filtering (0.01–0.09 Hz).

The amplitude of low frequency (ALFF) value was calculated as described (Kiviniemi et al., 2004). After subtracting the mean, ALFF was divided by the whole-brain voxel bias, followed by the normalization to make a Z-distribution, and the bandpass filtering.

The similarity between a single voxel and its surrounding 27 voxels was analyzed based on Regional homogeneity (ReHo) using Kendall's coefficient of consistency (KCC). The individual ReHo value was divided by the average ReHo value of all groups. And finally, a 6-mm smoothing check was used to smoothen the ReHo brain map spatially (Zang et al., 2004).

The connections between seed points and the whole brain were examined by FC. If there is a statistical relationship between the time series of two regions, it can be assumed that the functional behavior of the two regions is correlated and that they are coupled to each other or are components of the same network. First, a seed region of interest was mapped out, and second, time series was extracted to perform Pearson correlation analysis with other regions; the goal was to examine whether the activity patterns of other brain regions were time-related to the activity patterns observed in the seed region.

## Safety variables

Vital signs will be examined at baseline, week 2, 6, and 14, respectively. All AEs collected will be recorded in the case report form (CRF) and their duration, severity, development, and causal relationship to the tACS will be evaluated. Once serious AEs occur (such as hospitalization, risk of death, significant or persistent disability, or incapacity), their details should be recorded in CRF, reported to the local ethics committee, principal investigators, and the China FDA within 24 h, and tracked until their disappearance or losing clinical significance. In addition, the adverse reactions during the treatments will be recorded by the self-made questionnaire (Wang et al., 2022) consisting of 18 items will be used to evaluate whether each in our study participant has the common tACS-associated AEs, such as adverse reactions.

## Data processing and quality control

To ensure the rigor of this study, the whole process will be carried out strictly according to Guidelines for Good Clinical Practice of the International Conference on Harmonisation (ICH). Data will be collected from baseline, week 2, 6, and 14, respectively (Table 1). All investigators, trial supervisors, and raters involved in the study must be trained before they participate in communicating and instructing participants, assessing, collecting data, and completing the CRF. Double entries of data into the software DeZhentech EDV V1.0 (Dezhen, China) will be finished by two independent investigators, and these electronic data will be stored on a secure university server with regularly back-up and password protection. DeZhentech EDV V1.0 has an authority management mechanism associated with personnel and roles and a strict data audit mechanism to fully protect the security of data utilisation. Double-check will be performed to correct inconsistent entries or typos. The details of the quit participants, including reasons, date, AEs, and duration of the treatment, will be recorded. The final trial dataset, including the intent-to-treat and per-protocol dataset will be analyzed by an independent statistician.

## Statistical analysis

SPSS statistical software (version 26.0, United States) was used for statistical analysis. $p < 0.05$ represents significant difference. All tests are two-sided. Mean and standard deviation will be used for continuous variables, and frequency and percentage will be used to represent categorical variables. Regarding the comparison between groups, the continuous and categorical variables between groups were tested by Mann–Whitney U and the Chi-square test (or Fisher exact test), respectively. The intention-to-treat analysis works for the primary outcome, with worst-case imputation and repeated continuous outcomes represented by a mixed linear model.

# Discussion

The therapeutic effects of a cerebellar tACS in CA patients will be evaluated by our designed trial which is randomised, double-blind, and sham-controlled. We observed that patients with less severe ataxia showed the largest decrease, which is consistent with a previous study (Benussi et al., 2017) and suggests the regulation of motor activity by the volume of viable cerebellar cortex via the cerebello-thalamocortical connections. For this reason, our study will include individuals who were affected by CA mildly to moderately. In this trial, we mainly aim to investigate the effects of cerebellar tACS on CA severity, we also display the defective spectrum in SCA3 patients by using various outcome measures.

TACS is a common non-invasive form of brain stimulation (Antal et al., 2008; Bologna et al., 2019), which transfers low-intensity sinusoidal alternating current to the scalp and regulates its internal nerve oscillation (Elyamany et al., 2021) by forcing the resting membrane potential to a slightly-increased depolarisation or hyperpolarisation (Wu et al., 2021). In the depolarisation state, stochastic resonance occurs (Fertonani and Miniussi, 2017), and it locks the firing time of neurons to the increased stimulation frequency (Del Felice et al., 2019). Therefore, tACS can regulate (but not dominant) the causal relationship between neural activity and behavior (Herrmann et al., 2013).

Compared with the direct current stimulation of tDCS, tACS delivers current in a bidirectional manner (Kim et al., 2021). The advantage of tACS is its ability to manipulate and modulate inherent brain oscillations by inputting sinusoidal, biphasic alternating current (Yavari et al., 2018). In some frequency ranges, tACS treatment can induce endogenous brain oscillations, and when the amplitude of this stimulation increases, it causes the brain to oscillate over a wider frequency range (Ali et al., 2013). The tACS, whose current phases alternate regularly between positive and negative voltages, have been shown to be more effective than tDCS in regulating brain oscillations (Ali et al., 2013). Another advantage of tACS is that it can completely bypass sensory stimuli and induce endogenous oscillations through an external, barely perceptible alternating current, in which the endogenous oscillations are synchronized with the exogenous,

rhythmic stimuli (Herrmann et al., 2013). So we want to bring this potential treatment to CA patients.

Although we obtained some valuable data from this trial and they will provide non-pharmacological interventions to treat ataxia severity with minimal side effects, but this trial also has some limitations. Firstly, the study is performed in a single centre, thus it may not represent the results from other regions (The Han nationality is the majority in China). Secondly, the intervention duration may not be long enough and it is uncertain how many interventions will bring the best effect. Thirdly, still have some to-be-solved questions, including whether (and to what extend) other characteristically differences in patients may influence outcomes (Fava et al., 2017). We will perform further researches to improve the outcomes of this trial in the future.

## Ethics statement

The studies involving human participants were reviewed and approved by MRCTA, ECFAH of FMU [2022]399. The patients/participants provided their written informed consent to participate in this study.

## Author contributions

XL: designed the study and drafted the manuscript. WL, LZ, W-LZ, X-PC, Y-HL, and M-CL: collected the clinical data. S-RG, S-ZW, and X-YC: critically revised the manuscript and contributed the most important intellectual content. All authors have read and approved the final manuscript.

## Funding

This work was supported by The Joint Funds for the Innovation of Science and Technology Fujian Province to X-YC (No. 2021Y9088, Fujian).

## Conflict of interest

The authors declare that the research was conducted in the absence of any commercial or financial relationships that could be construed as a potential conflict of interest.

## Publisher's note

All claims expressed in this article are solely those of the authors and do not necessarily represent those of their affiliated organizations, or those of the publisher, the editors and the reviewers. Any product that may be evaluated in this article, or claim that may be made by its manufacturer, is not guaranteed or endorsed by the publisher.

## References

Abellaneda-Pérez, K., Vaqué-Alcázar, L., Perellón-Alfonso, R., Bargalló, N., Kuo, M. F., Pascual-Leone, A., et al. (2019). Differential tDCS and tACS effects on working memory-related neural activity and resting-state connectivity. *Front. Neurosci.* 13:1440. doi: 10.3389/fnins.2019.01440

Ahn, S., Mellin, J. M., Alagapan, S., Alexander, M. L., Gilmore, J. H., Jarskog, L. F., et al. (2019). Targeting reduced neural oscillations in patients with schizophrenia by transcranial alternating current stimulation. *NeuroImage* 186, 126–136. doi: 10.1016/j.neuroimage.2018.10.056

Ali, M. M., Sellers, K. K., and Fröhlich, F. (2013). Transcranial alternating current stimulation modulates large-scale cortical network activity by network resonance. *J. Neurosci.* 33, 11262–11275. doi: 10.1523/JNEUROSCI.5867-12.2013

Anheim, M., Tranchant, C., and Koenig, M. (2012). The autosomal recessive cerebellar ataxias. *N. Engl. J. Med.* 366, 636–646. doi: 10.1056/NEJMra1006610

Antal, A., Alekseichuk, I., Bikson, M., Brockmöller, J., Brunoni, A. R., Chen, R., et al. (2017). Low intensity transcranial electric stimulation: safety, ethical, legal regulatory and application guidelines. *Clin. Neurophysiol.* 128, 1774–1809. doi: 10.1016/j.clinph.2017.06.001

Antal, A., Boros, K., Poreisz, C., Chaieb, L., Terney, D., and Paulus, W. (2008). Comparatively weak after-effects of transcranial alternating current stimulation (tACS) on cortical excitability in humans. *Brain Stimul.* 1, 97–105. doi: 10.1016/j.brs.2007.10.001

Asan, A. S., and Sahin, M. (2019). Modulation of multiunit spike activity by Transcranial AC stimulation (tACS) in the rat cerebellar cortex. *Annu. Int. Conf. IEEE Eng. Med. Biol. Soc.* 2019, 5192–5195. doi: 10.1109/EMBC.2019.8856830

Beaudin, M., Manto, M., Schmahmann, J. D., Pandolfo, M., and Dupre, N. (2022). Recessive cerebellar and afferent ataxias - clinical challenges and future directions. *Nat. Rev. Neurol.* 18, 257–272. doi: 10.1038/s41582-022-00634-9

Benussi, A., Cantoni, V., Grassi, M., Brechet, L., Michel, C. M., Datta, A., et al. (2022). Increasing brain gamma activity improves episodic memory and restores cholinergic dysfunction in Alzheimer's disease. *Ann. Neurol.* 92, 322–334. doi: 10.1002/ana.26411

Benussi, A., Dell'Era, V., Cotelli, M. S., Turla, M., Casali, C., and Padovani, A. (2017). Long term clinical and neurophysiological effects of cerebellar transcranial direct current stimulation in patients with neurodegenerative ataxia. *Brain Stimul.* 10, 242–250. doi: 10.1016/j.brs.2016.11.001

Bologna, M., Guerra, A., Paparella, G., Colella, D., Borrelli, A., Suppa, A., et al. (2019). Transcranial alternating current stimulation has frequency-dependent effects on motor learning in healthy humans. *Neuroscience* 411, 130–139. doi: 10.1016/j.neuroscience.2019.05.041

Bolzan, G., Leotti, V. B., de Oliveira, C. M., Ecco, G., Cappelli, A. H., Rocha, A. G., et al. (2022). Quality of life since pre-ataxic phases of Spinocerebellar Ataxia type 3/Machado-Joseph disease. *Cerebellum* 21, 297–305. doi: 10.1007/s12311-021-01299-8

Buysse, D. J., Reynolds, C. F. 3rd, Monk, T. H., Berman, S. R., and Kupfer, D. J. (1989). The Pittsburgh sleep quality index: a new instrument for psychiatric practice and research. *Psychiatry Res.* 28, 193–213. doi: 10.1016/0165-1781(89)90047-4

Cabral-Calderin, Y., and Wilke, M. (2020). Probing the link between perception and oscillations: lessons from Transcranial alternating current stimulation. *Neuroscientist* 26, 57–73. doi: 10.1177/1073858419828646

Chalder, T., Berelowitz, G., Pawlikowska, T., Watts, L., Wessely, S., Wright, D., et al. (1993). Development of a fatigue scale. *J. Psychosom. Res.* 37, 147–153. doi: 10.1016/0022-3999(93)90081-P

Chan, A. W., Tetzlaff, J. M., Altman, D. G., Laupacis, A., Gøtzsche, P. C., Krleža-Jerić, K., et al. (2013a). SPIRIT 2013 statement: defining standard protocol items for clinical trials. *Ann. Intern. Med.* 158, 200–207. doi: 10.7326/0003-4819-158-3-201302050-00583

Chan, A. W., Tetzlaff, J. M., Gøtzsche, P. C., Altman, D. G., Mann, H., Berlin, J. A., et al. (2013b). SPIRIT 2013 explanation and elaboration: guidance for protocols of clinical trials. *BMJ* 346:e7586. doi: 10.1136/bmj.e7586

Correia, J. S., Duarte-Silva, S., Salgado, A. J., and Maciel, P. (2023). Cell-based therapeutic strategies for treatment of spinocerebellar ataxias: an update. *Neural Regen. Res.* 18, 1203–1212. doi: 10.4103/1673-5374.355981

Del Felice, A., Castiglia, L., Formaggio, E., Cattelan, M., Scarpa, B., Manganotti, P., et al. (2019). Personalized transcranial alternating current stimulation (tACS) and physical therapy to treat motor and cognitive symptoms in Parkinson's disease: a randomized cross-over trial. *Neuroimage Clin.* 22:101768. doi: 10.1016/j.nicl.2019.101768

Elyamany, O., Leicht, G., Herrmann, C. S., and Mulert, C. (2021). Transcranial alternating current stimulation (tACS): from basic mechanisms towards first applications in psychiatry. *Eur. Arch. Psychiatry Clin. Neurosci.* 271, 135–156. doi: 10.1007/s00406-020-01209-9

Fava, G. A., Guidi, J., Rafanelli, C., and Rickels, K. (2017). The clinical inadequacy of the placebo model and the development of an alternative conceptual framework. *Psychother. Psychosom.* 86, 332–340. doi: 10.1159/000480038

Fertonani, A., and Miniussi, C. (2017). Transcranial electrical stimulation: what we know and do not know about mechanisms [J]. *Neuroscientist* 23, 109–123. doi: 10.1177/1073858416631966

Feys, P., Lamers, I., Francis, G., Benedict, R., Phillips, G., LaRocca, N., et al. (2017). The nine-hole peg test as a manual dexterity performance measure for multiple sclerosis [J]. *Mult. Scler.* 23, 711–720. doi: 10.1177/1352458517690824

Folstein, M. F., Folstein, S. E., and McHugh, P. R. (1975). "Mini-mental state". A practical method for grading the cognitive state of patients for the clinician. *J. Psychiatr. Res.* 12, 189–198. doi: 10.1016/0022-3956(75)90026-6

Friston, K. J., Frith, C. D., Liddle, P. F., and Frackowiak, R. S. J. (1993). Functional connectivity: the principal-component analysis of large (PET) data sets. *J. Cereb. Blood Flow Metab.* 13, 5–14. doi: 10.1038/jcbfm.1993.4

Gandini, J., Manto, M., Bremova-Ertl, T., Feil, K., and Strupp, M. (2020). The neurological update: therapies for cerebellar ataxias in 2020. *J. Neurol.* 267, 1211–1220. doi: 10.1007/s00415-020-09717-3

Giustiniani, A., Tarantino, V., Bracco, M., Bonaventura, R. E., and Oliveri, M. (2021). Functional role of cerebellar gamma frequency in motor sequences learning: a tACS study. *Cerebellum* 20, 913–921. doi: 10.1007/s12311-021-01255-6

Grover, S., Wen, W., Viswanathan, V., Gill, C. T., and Reinhart, R. M. G. (2022). Long-lasting, dissociable improvements in working memory and long-term memory in older adults with repetitive neuromodulation. *Nat. Neurosci.* 25, 1237–1246. doi: 10.1038/s41593-022-01132-3

Hamilton, M. (1959). The assessment of anxiety states by rating. *Br. J. Med. Psychol.* 32, 50–55. doi: 10.1111/j.2044-8341.1959.tb00467.x

Herrmann, C. S., Rach, S., Neuling, T., and Strüber, D. (2013). Transcranial alternating current stimulation: a review of the underlying mechanisms and modulation of cognitive processes. *Front. Hum. Neurosci.* 7:279. doi: 10.3389/fnhum.2013.00279

Hong-Xing, W., Li, W., Wen-Rui, Z., et al. (2020). Effect of Transcranial alternating current stimulation for the treatment of chronic insomnia: a randomized, double-blind, parallel-group, Placebo-Controlled Clinical Trial. *Psychother. Psychosom.* 89, 38–47. doi: 10.1159/000504609

Hu, P., He, Y., Liu, X., Ren, Z., and Liu, S. (2021). Modulating emotion processing using transcranial alternating current stimulation (tACS) - a sham-controlled study in healthy human participants. *Annu. Int. Conf. IEEE Eng. Med. Biol. Soc.* 2021, 6667–6670. doi: 10.1109/EMBC46164.2021.9630564

Johns, M. W. (1991). A new method for measuring daytime sleepiness: the Epworth sleepiness scale. *Sleep* 14, 540–545. doi: 10.1093/sleep/14.6.540

Kim, J., Kim, H., Jeong, H., Roh, D., and Kim, D. H. (2021). tACS as a promising therapeutic option for improving cognitive function in mild cognitive impairment: a direct comparison between tACS and tDCS. *J. Psychiatr. Res.* 141, 248–256. doi: 10.1016/j.jpsychires.2021.07.012

Kiviniemi, V., Kantola, J. H., Jauhiainen, J., and Tervonen, O. (2004). Comparison of methods for detecting nondeterministic BOLD fluctuation in fMRI. *Magn. Reson. Imaging* 22, 197–203. doi: 10.1016/j.mri.2003.09.007

Koganemaru, S., Mikami, Y., Matsuhashi, M., Truong, D. Q., Bikson, M., Kansaku, K., et al. (2020). Cerebellar transcranial alternating current stimulation modulates human gait rhythm [J]. *Neurosci. Res.* 156, 265–270. doi: 10.1016/j.neures.2019.12.003

Krismer, F., Seppi, K., Wenning, G. K., Abler, V., Papapetropoulos, S., and Poewe, W. (2016). Minimally clinically important decline in the parkinsonian variant of multiple system atrophy. *Mov. Disord.* 31, 1577–1581. doi: 10.1002/mds.26743

Levin, J., Maaß, S., Schuberth, M., Giese, A., Oertel, W. H., Poewe, W., et al. (2019). Safety and efficacy of epigallocatechin gallate in multiple system atrophy (PROMESA): a randomised, double-blind, placebo-controlled trial. *Lancet Neurol.* 18, 724–735. doi: 10.1016/S1474-4422(19)30141-3

Lin, J., Wang, X., Dong, F., du, Y., Shen, J., Ding, S., et al. (2018). Validation of the Chinese version of the Hamilton rating scale for depression in adults with epilepsy. *Epilepsy Behav.* 89, 148–152. doi: 10.1016/j.yebeh.2018.10.009

Manto, M., Gandini, J., Feil, K., and Strupp, M. (2020). Cerebellar ataxias: an update. *Curr. Opin. Neurol.* 33, 150–160. doi: 10.1097/WCO.0000000000000774

Marmolino, D., and Manto, M. (2010). Past, present and future therapeutics for cerebellar ataxias. *Curr. Neuropharmacol.* 8, 41–61. doi: 10.2174/157015910790909476

Matsumoto, H., and Ugawa, Y. (2017). Adverse events of tDCS and tACS: a review. *Clin. Neurophysiol. Pract.* 2, 19–25. doi: 10.1016/j.cnp.2016.12.003

Mehta, A. R., Brittain, J. S., and Brown, P. (2014). The selective influence of rhythmic cortical versus cerebellar transcranial stimulation on human physiological tremor. *J. Neurosci.* 34, 7501–7508. doi: 10.1523/JNEUROSCI.0510-14.2014

Miyaguchi, S., Inukai, Y., Mitsumoto, S., Otsuru, N., and Onishi, H. (2022). Gamma-transcranial alternating current stimulation on the cerebellum and supplementary motor area improves bimanual motor skill. *Behav. Brain Res.* 424:113805. doi: 10.1016/j.bbr.2022.113805

Nasreddine, Z. S., Phillips, N. A., Bédirian, V., Whitehead, V., Collin, I., Cummings, J. L., et al. (2005). The Montreal cognitive assessment, MoCA: a brief screening tool for mild cognitive impairment. *J. Am. Geriatr. Soc.* 53, 695–699. doi: 10.1111/j.1532-5415.2005.53221.x

Palma, J. A., Martinez, J., Millar Vernetti, P., Ma, T., Perez, M. A., Zhong, J., et al. (2022). mTOR inhibition with Sirolimus in multiple system atrophy: a randomized, double-blind, placebo-controlled futility trial and 1-year biomarker longitudinal analysis. *Mov. Disord.* 37, 778–789. doi: 10.1002/mds.28923

Poewe, W., Stankovic, I., Halliday, G., Meissner, W. G., Wenning, G. K., Pellecchia, M. T., et al. (2022). Multiple system atrophy. *Nat. Rev. Dis. Primers.* 8:56. doi: 10.1038/s41572-022-00382-6

Radmard, S., Zesiewicz, T. A., and Kuo, S. H. (2023). Evaluation of cerebellar ataxic patients. *Neurol. Clin.* 41, 21–44. doi: 10.1016/j.ncl.2022.05.002

Romano, S., Coarelli, G., Marcotulli, C., Leonardi, L., Piccolo, F., Spadaro, M., et al. (2015). Riluzole in patients with hereditary cerebellar ataxia: a randomised, double-blind, placebo-controlled trial. *Lancet Neurol.* 14, 985–991. doi: 10.1016/S1474-4422(15)00201-X

Sadeghihassanabadi, F., Misselhorn, J., Gerloff, C., and Zittel, S. (2022). Optimizing the montage for cerebellar transcranial alternating current stimulation (tACS): a combined computational and experimental study. *J. Neural Eng.* 19:026060. doi: 10.1088/1741-2552/ac676f

Schmitz-Hübsch, T., du Montcel, S. T., Baliko, L., Berciano, J., Boesch, S., Depondt, C., et al. (2006). Scale for the assessment and rating of ataxia: development of a new clinical scale. *Neurology* 66, 1717–1720. doi: 10.1212/01.wnl.0000219042.60538.92

Schrag, A., Selai, C., Mathias, C., Low, P., Hobart, J., Brady, N., et al. (2007). Measuring health-related quality of life in MSA: the MSA-QoL. *Mov. Disord.* 22, 2332–2338. doi: 10.1002/mds.21649

Schubert, C., Dabbagh, A., Classen, J., Krämer, U. M., and Tzvi, E. (2021). Alpha oscillations modulate premotor-cerebellar connectivity in motor learning: insights from transcranial alternating current stimulation. *NeuroImage* 241:118410. doi: 10.1016/j.neuroimage.2021.118410

Trouillas, P., Takayanagi, T., Hallett, M., Currier, R. D., Subramony, S. H., Wessel, K., et al. (1997). International cooperative Ataxia rating scale for pharmacological assessment of the cerebellar syndrome. The Ataxia neuropharmacology Committee of the World Federation of neurology. *J. Neurol. Sci.* 145, 205–211. doi: 10.1016/s0022-510x(96)00231-6

Visser, M., Marinus, J., Stiggelbout, A. M., and van Hilten, J. J. (2004). Assessment of autonomic dysfunction in Parkinson's disease: the SCOPA-AUT. *Mov. Disord.* 19, 1306–1312. doi: 10.1002/mds.20153

Wang, H., Wang, K., Xue, Q., Peng, M., Yin, L., Gu, X., et al. (2022). Transcranial alternating current stimulation for treating depression: a randomized controlled trial. *Brain* 145, 83–91. doi: 10.1093/brain/awab252

Wenning, G. K., Stankovic, I., Vignatelli, L., Fanciulli, A., Calandra-Buonaura, G., Seppi, K., et al. (2022). The Movement Disorder Society criteria for the diagnosis of multiple system atrophy. *Mov. Disord.* 37, 1131–1148. doi: 10.1002/mds.29005

Wenning, G. K., Tison, F., Seppi, K., Diem, A., Yekhlef, F., Ghorayeb, I., et al. (2004). Development and validation of the unified multiple system atrophy rating scale (UMSARS). *Mov. Disord.* 19, 1391–1402. doi: 10.1002/mds.20255

Wessel, M. J., Draaisma, L. R., de Boer, A., Park, C.-H., Maceira-Elvira, P., Durand-Ruel, M., et al. (2020). Cerebellar transcranial alternating current stimulation in the gamma range applied during the acquisition of a novel motor skill. *Sci. Rep.* 10:11217. doi: 10.1038/s41598-020-68028-9

Wessel, M. J., Draaisma, L. R., and Hummel, F. C. (2022). Mini-review: Transcranial alternating current stimulation and the cerebellum. *Cerebellum* 22, 120–128. doi: 10.1007/s12311-021-01362-4

Wu, L., Liu, T., and Wang, J. (2021). Improving the effect of Transcranial alternating current stimulation (tACS): a systematic review. *Front. Hum. Neurosci.* 15:652393. doi: 10.3389/fnhum.2021.652393

Wuyts, F. L., De Bodt, M. S., Molenberghs, G., Remacle, M., Heylen, L., Millet, B., et al. (2000). The dysphonia severity index: an objective measure of vocal quality based on a multiparameter approach. *J. Speech Lang. Hear. Res.* 43, 796–809. doi: 10.1044/jslhr.4303.796

Yavari, F., Jamil, A., Mosayebi Samani, M., Vidor, L. P., and Nitsche, M. A. (2018). Basic and functional effects of transcranial electrical stimulation (tES)-an introduction. *Neurosci. Biobehav. Rev.* 85, 81–92. doi: 10.1016/j.neubiorev.2017.06.015

Zang, Y., Jiang, T., Lu, Y., He, Y., and Tian, L. (2004). Regional homogeneity approach to fMRI data analysis. *NeuroImage* 22, 394–400. doi: 10.1016/j.neuroimage.2003.12.030

frontiers | Frontiers in Neuroscience

TYPE Systematic Review
PUBLISHED 16 May 2023
DOI 10.3389/fnins.2023.1102311



OPEN ACCESS

EDITED BY
Lin Yao,
Zhejiang University, China

REVIEWED BY
Fang Li,
Capital Medical University, China
Hesheng Liu,
Peking University, China

*CORRESPONDENCE
Hao Zhang
✉ crrczh2020@163.com

†These authors have contributed equally to this work and share first authorship

RECEIVED 24 November 2022
ACCEPTED 25 April 2023
PUBLISHED 16 May 2023

CITATION
Han K, Liu J, Tang Z, Su W, Liu Y, Lu H and Zhang H (2023) Effects of excitatory transcranial magnetic stimulation over the different cerebral hemispheres dorsolateral prefrontal cortex for post-stroke cognitive impairment: a systematic review and meta-analysis. *Front. Neurosci.* 17:1102311. doi: 10.3389/fnins.2023.1102311



# Effects of excitatory transcranial magnetic stimulation over the different cerebral hemispheres dorsolateral prefrontal cortex for post-stroke cognitive impairment: a systematic review and meta-analysis

Kaiyue Han[1,2†], Jiajie Liu[1,2†], Zhiqing Tang[1,2], Wenlong Su[1,2,3], Ying Liu[1,2], Haitao Lu[1,2] and Hao Zhang[1,2,3,4*]

[1]School of Rehabilitation, Capital Medical University, Beijing, China, [2]China Rehabilitation Research Center, Beijing Bo'ai Hospital, Beijing, China, [3]University of Health and Rehabilitation Sciences, Qingdao, China, [4]Cheeloo College of Medicine, Shandong University, Jinan, China

**Background:** Post-stroke cognitive impairment (PSCI) is a significant health concern. Transcranial magnetic stimulation (TMS) is considered a promising rehabilitation therapy for improving cognition, and the effects of excitatory TMS on PSCI have received much attention in recent years. However, the effects of different cerebral hemispheres on excitatory TMS treatment of cognitive impairment have not been studied. This review aimed to study the effects of excitatory TMS over the dorsolateral prefrontal cortex (DLPFC) of different cerebral hemispheres on the cognitive function of patients with PSCI.

**Methods:** Literature published in PubMed, Web of Science, Embase, Cochrane Library, Scopus, and Wiley from inception to September 30, 2022, were searched. Two researchers independently performed literature screening, data extraction, and quality assessment. Furthermore, we conducted a meta-analysis using RevMan software (version 5.4) and rated the strength of evidence using GRADEpro.

**Results:** A total of 19 studies were included in this meta-analysis. The results showed that excitatory TMS over the left hemisphere DLPFC was significantly better in improving global cognition (SMD = 2.26, 95% CI 1.67–2.86, $P < 0.00001$; vs. SMD = 2.53, 95% CI 1.86–3.20, $P < 0.00001$), memory (SMD = 1.29, 95% CI 0.72–1.87, $P < 0.0001$), attention (SMD = 2.32, 95% CI 1.64–3.01, $P < 0.00001$), executive (SMD = 0.64, 95% CI 0.21–1.07, $P = 0.004$), P300 latency (SMD = 2.69, 95% CI 2.13–3.25, $P < 0.00001$), and depression (SMD = 0.95, 95% CI 0.26–1.63, $P = 0.007$) than that of the control group, but the effect on improving activities of daily living (ADL) was unclear ($P = 0.03$ vs. $P = 0.17$). Subgroup analysis further showed that excitatory TMS over the right hemisphere DLPFC was effective in improving the global cognition of PSCI patients ($P < 0.00001$), but the stimulation effect over the ipsilateral hemisphere DLPFC was unclear ($P = 0.11$ vs. $P = 0.003$). Additionally, excitatory TMS over the ipsilateral hemisphere DLPFC showed no statistical difference in improving ADL between the two groups ($P = 0.25$).

**Conclusions:** Compared to other hemispheric sides, excitatory TMS over the left hemisphere DLPFC was a more effective stimulation area, which can significantly improved the global cognitive function, memory, attention, executive, P300

latency, and depression in patients with PSCI. There was no apparent therapeutic effect on improving activities of daily living (ADL). In the future, more randomized controlled trials with large-sample, high quality, and follow-up are necessary to explore a usable protocol further.

**Systematic review registration:** https://www.crd.york.ac.uk/PROSPERO/, identifier: CRD42022369096.

KEYWORDS

**stroke, transcranial magnetic stimulation, dorsolateral prefrontal cortex, cognitive function, meta-analysis**

# 1. Introduction

Stroke, a cerebrovascular disease with high mortality and disability rates, can expose survivors to various dysfunctions. Cognitive impairment is a common post-stroke complication with an incidence of 20–80% (Huang et al., 2022). Notably, post-stroke cognitive impairment (PSCI) refers to a series of syndromes that meet the diagnostic criteria of cognitive dysfunction within 6 months after the clinical event of stroke (Rost et al., 2022), mainly manifested in memory decline, inattention, and executive dysfunction. According to epidemiological data, 17–92% of stroke patients experience cognitive impairment within 3 months after onset (Snyder et al., 2015), severely impacting activities of daily living (ADL) and quality of survival.

Traditional cognitive rehabilitation has primarily improved function through pharmacological therapy or compensatory strategies. Unfortunately, evidence for such effects remains limited and clinical efficacy is poor (Zhao et al., 2021). In recent years, transcranial magnetic stimulation (TMS), a non-invasive neuromodulation technique, is applied to the cerebral cortex with a pulsed magnetic field to induce changes in its local or distal neural activity (Kobayashi and Pascual-Leone, 2003). According to the different modulations of cortical excitability, TMS can be divided into excitatory and inhibitory types (Gilio et al., 2007). Excitatory TMS includes high-frequency rTMS (HF-rTMS) and intermittent theta burst stimulation (iTBS), which can promote neuronal activity (Wang et al., 2018). In contrast, inhibitory TMS includes low-frequency rTMS (LF-rTMS) and continuous theta burst stimulation (cTBS), which can inhibit neuronal activity (Li et al., 2021a).

From literature reviews, most studies performed excitatory TMS treatment over the dorsolateral prefrontal cortex (DLPFC) of patients with PSCI. It is well known that DLPFC is closely related to the process of cognitive control and plays an important role in the recovery of memory, attention, execution, and other cognitive functions after stroke (Chen et al., 2013; Webler et al., 2022). Studies have shown that Excitatory TMS over the DLPFC can affect intracerebral metabolism and increase cortical excitability, altering neuronal activity in the target cortical area and functional connectivity between brain networks to improve cognitive function in patients with PSCI (Wilson et al., 2018; Wu et al., 2021).

DLPFC is a relatively large area (Siebner and Rothwell, 2003), and the application sites of excitatory TMS in the treatment of cognitive impairment are different. Four studies (Ding et al., 2019; Wang et al., 2019, 2021; Cha et al., 2022) applied high-frequency rTMS over the ipsilateral hemisphere DLPFC in patients with PSCI, while Bie and Wang (2011) over the right DLPFC, and all of these studies have reported certain positive effects in improving the cognition of patients. In recent years, we have found that more studies have focused on excitatory TMS treatment over the left hemisphere DLPFC for PSCI patients to improve cognition. However, the difference between the left and right hemispheres is an important effect factor, and there is a lack of research on stimulating DLPFC over different cerebral hemispheres to treat cognitive impairment with TMS. Therefore, the application site of excitatory TMS remains controversial (Yang et al., 2015b). Based on this, the aim of this study was to analyze the effects of excitatory TMS over the DLPFC of different cerebral hemispheres on cognitive function in patients with PSCI.

# 2. Methods

This review was conducted according to the Preferred Reporting Items for Systematic Reviews and Meta-Analyses (PRISMA) (Moher et al., 2015). It was registered in the International Prospective Register of Systematic Reviews (CRD42022369096).

## 2.1. Search strategy

Two investigators independently performed the literature published in PubMed, Web of Science, Embase, Cochrane Library, Scopus, and Wiley from inception to September 30, 2022. Additionally, we manually searched all reference lists of the selected articles and related review articles, and we used the same search terms in Google Scholar to perform additional searches. We used the search terms "transcranial magnetic stimulation," "stroke," and "cognitive function," or their synonyms. The detailed search strategy is provided in Supplementary Table S1.

## 2.2. Selection of studies

Studies were included in this study if they met the following criteria: (1) population: adult patients (≥18 years) diagnosed with stroke and cognitive dysfunction; (2) intervention: HF-rTMS or

iTBS over the DLPFC, with or without conventional rehabilitation; (3) control: sham stimulation or placebo or blank control, with or without conventional rehabilitation; (4) results: measures that evaluated the global cognition or memory or attention or execution; (5) study type: randomized controlled trials (RCTs) or prospective controlled trials (PCTs); (6) language: English and Chinese.

## 2.3. Data collection and extraction

Two researchers (HKY, LJJ) independently screened the literature, extracted information, and cross-checked it. In case of disagreement, a third researcher (TZQ) reviewed until a consensus was reached. For every study, we extracted the following information: the name of the first author, the year of publication, country, dysfunction diagnosis, sample size, patient characteristics (gender, age, onset time of stroke, and education), intervention protocol (site of stimulation, type of TMS, frequency, intensity, and duration), control condition, outcome measures, follow-up, drop-out rate, and PEDro score. We emailed the authors for questionable or incomplete data to clarify or add the missing information. Only data immediately after the intervention were extracted for studies that included post-intervention and follow-up data. If the results were only presented graphically, we used GetData Graph Digitizer 2.20 to extract the required data (Zhang et al., 2017).

## 2.4. Risk of bias and quality assessment

Two reviewers (HKY, LJJ) independently assessed the bias of the included studies according to the Cochrane Handbook for Systematic Reviews of Interventions (Higgins et al., 2011), and disagreements were resolved by discussing with the third reviewer (TZQ). The assessment items included selection bias, performance bias, detection bias, attrition bias, reporting bias, and other biases. Each item was rated as "high," "low," or "unclear."

The PEDro scale (consisting of 11 items) was used to assess the methodological quality of the included studies, and studies with a score of <6 were considered low-quality (Cashin and McAuley, 2020). Furthermore, we used the online GRADEpro to assess the quality of evidence for pooled results in this meta-analysis, including the risk of bias, inconsistency, indirectness, imprecision, and publication bias (Cui et al., 2019).

## 2.5. Statistical analysis

We used RevMan 5.4 to perform the meta-analysis. The Mini-mental state examination (MMSE) and Montreal cognitive assessment (MoCA) were used to assess patients' global cognitive function. The Rivermead behavioral memory test (RBMT) was used to assess memory. The Trail Making Test (TMT), Digit Symbol Test (DST), and Digital Span Test (DS) were used to evaluate attention. The Stroop Color and Word test (SCWT) was used to assess executive function. The Modified Barthel Index (MBI) and independent function measure (FIM) were used to assess the ADL. The event-related potential (ERP) P300 was used to evaluate cognitive deterioration, and Beck's Depression Inventory (BDI) was used to assess depression. Since all data were continuous information and measuring the same outcome using different scales, we selected Standardized Mean Difference (SMD) with 95% confidence intervals (CIs). We used the Cochrane Q statistic to qualitatively determine whether heterogeneity existed among the included studies (test level $\alpha = 0.05$), while the $I^2$ statistic to assess the magnitude of heterogeneity quantitatively. If $P \geq 0.1$ and $I^2 \leq 50\%$, the heterogeneity was considered insignificant, and we selected the fixed-effect (FE) model. Conversely, we selected the random-effect (RE) model and performed a subgroup analysis and sensitivity analysis to identify factors that might cause heterogeneity. Descriptive analysis was used if the source of heterogeneity could not ultimately be determined.

# 3. Results

## 3.1. Study selection

We initially retrieved 2,886 articles from 6 databases, and tools removed 2,118 articles before the screening. The 719 articles that did not meet the criteria were removed after reading the title and abstract, and one article was not retrieved. After that, the remaining 48 articles were read in full text, of which 19 articles had no eligible controls, 6 articles had no relevant outcomes, and 4 articles could not get complete data. Finally, 19 articles were included in this meta-analysis (Kim et al., 2010; Bie and Wang, 2011; Liu et al., 2017, 2020; Zheng et al., 2017, 2020; Yin et al., 2018, 2020; Ding et al., 2019; Luo and Yu, 2019; Wang et al., 2019, 2021; Zhang and Zou, 2019; Li et al., 2020, 2022; Tsai et al., 2020; Zhang et al., 2020, 2022; Cha et al., 2022) (Figure 1).

## 3.2. Study characteristics

A total of 19 studies, 17 randomized controlled studies, and 2 prospective controlled studies were included in this meta-analysis. The mean age range of the subjects was 49.07 ± 9.26 (Zhang et al., 2020) to 66.80 ± 17.20 years (Kim et al., 2010), the mean onset time of stroke was 2.73 ± 1.26 (Zheng et al., 2017) to 33.27 ± 26.40 months (Tsai et al., 2020), and the mean years of education was 7.13 ± 4.05 (Ding et al., 2019) to 14.00 ± 2.80 years (Tsai et al., 2020). Regarding the diagnosis of dysfunction, participants in fourteen, one, two, one, and one studies were diagnosed with post-stroke cognitive impairment (Kim et al., 2010; Yin et al., 2018, 2020; Ding et al., 2019; Luo and Yu, 2019; Wang et al., 2019, 2021; Zhang and Zou, 2019; Li et al., 2020, 2022; Tsai et al., 2020; Zheng et al., 2020; Cha et al., 2022; Zhang et al., 2022), post-stroke mild cognitive impairment (Bie and Wang, 2011), post-stroke vascular cognitive impairment (Zheng et al., 2017; Zhang et al., 2020), post-stroke attention impairment (Liu et al., 2020), and post-stroke executive impairment (Liu et al., 2017), respectively. Regarding the stimulation type, 18 studies used HF-rTMS (Kim et al., 2010; Bie and Wang, 2011; Liu et al., 2017, 2020; Zheng et al., 2017, 2020; Yin et al., 2018, 2020; Ding et al., 2019; Luo and Yu, 2019; Wang et al., 2019, 2021; Zhang and Zou, 2019; Li et al., 2020; Tsai et al., 2020; Zhang et al., 2020, 2022; Cha et al., 2022) and

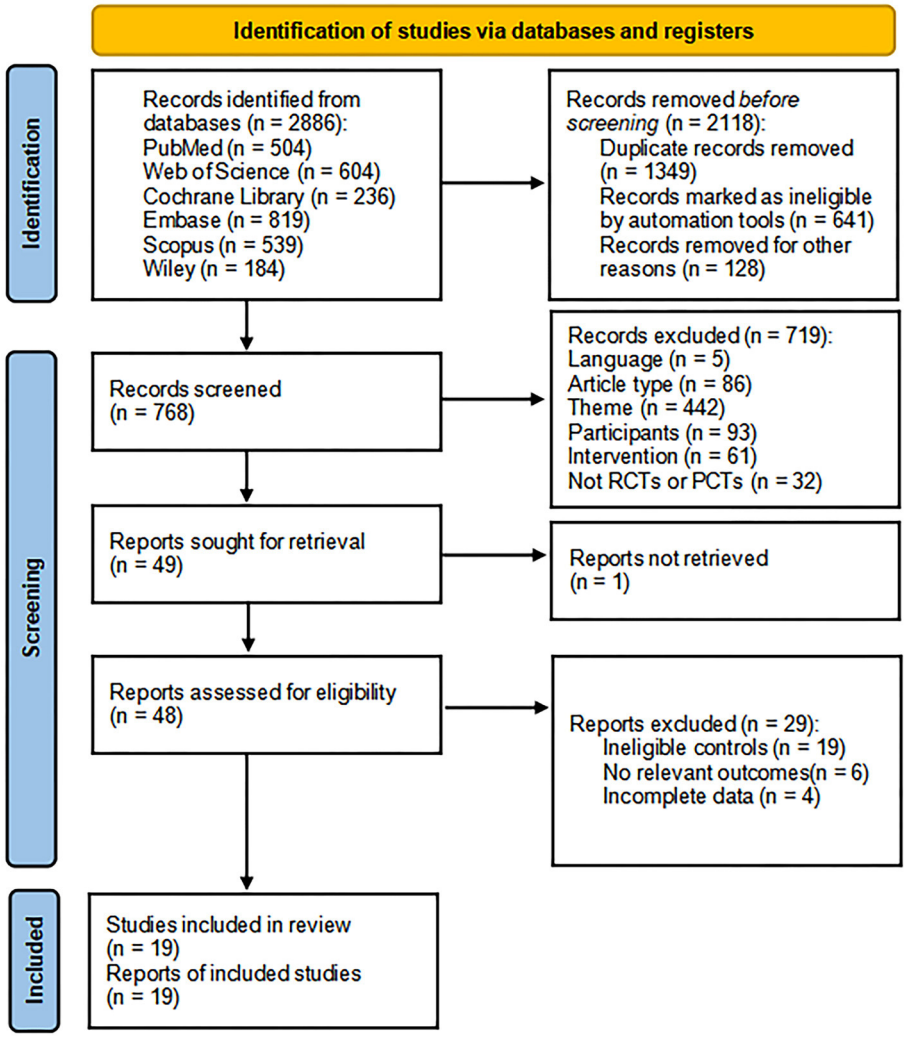


FIGURE 1
PRISMA flowchart of study selection.

2 studies (Tsai et al., 2020; Li et al., 2022) used iTBS. Regarding the stimulation side of the different cerebral hemispheres, fourteen, one, and four studies selected the left DLPFC (Kim et al., 2010; Liu et al., 2017, 2020; Zheng et al., 2017, 2020; Yin et al., 2018, 2020; Luo and Yu, 2019; Zhang and Zou, 2019; Li et al., 2020, 2022; Tsai et al., 2020; Zhang et al., 2020, 2022), right DLPFC (Bie and Wang, 2011), and ipsilateral DLPFC (Ding et al., 2019; Wang et al., 2019, 2021; Cha et al., 2022), respectively. Regarding the stimulation intensity, eleven, two, three, and one studies were set at 80% (Kim et al., 2010; Bie and Wang, 2011; Zheng et al., 2017, 2020; Yin et al., 2018, 2020; Zhang and Zou, 2019; Tsai et al., 2020; Zhang et al., 2020, 2022; Wang et al., 2021), 90% (Liu et al., 2017, 2020), 100% (Li et al., 2020, 2022; Cha et al., 2022), and 110% (Ding et al., 2019) of the resting motor threshold (RMT), respectively. In regards to the stimulation duration, six, two, eight, one, and two studies performed TMS treatment for 2 weeks (Kim et al., 2010; Bie and Wang, 2011; Ding et al., 2019; Tsai et al., 2020; Cha et al., 2022; Li et al., 2022), 3 weeks (Luo and Yu, 2019; Li et al., 2020), 4 weeks (Liu et al., 2017, 2020; Yin et al., 2018, 2020; Wang et al., 2019; Zhang and Zou, 2019; Zheng et al., 2020; Zhang et al., 2022), 6 weeks (Zheng et al., 2017), and 8 weeks (Zhang et al., 2020; Wang et al., 2021), respectively. Furthermore, only three studies performed follow-up assessments (Bie and Wang, 2011; Ding et al., 2019; Cha et al., 2022). The characteristics of the included studies are detailed in Supplementary Table S2.

## 3.3. Risk of bias and quality assessment

Among the 19 studies included in this meta-analysis, 17 studies performed randomization (Kim et al., 2010; Bie and Wang, 2011; Liu et al., 2017, 2020; Zheng et al., 2017, 2020; Yin et al., 2018; Ding et al., 2019; Luo and Yu, 2019; Wang et al., 2019, 2021; Zhang and Zou, 2019; Li et al., 2020, 2022; Tsai et al., 2020; Zhang et al., 2022), 3 studies performed allocation concealment (Liu et al., 2020; Tsai et al., 2020; Li et al., 2022), 12 studies were blinded to participants and personnel (Kim et al., 2010; Bie and Wang, 2011; Liu et al., 2017, 2020; Yin et al., 2018; Luo and Yu, 2019; Zhang and Zou, 2019;

Li et al., 2020, 2022; Tsai et al., 2020; Zheng et al., 2020; Wang et al., 2021), and 11 studies were blinded to assessors (Kim et al., 2010; Liu et al., 2017, 2020; Zheng et al., 2017, 2020; Yin et al., 2018; Luo and Yu, 2019; Zhang and Zou, 2019; Li et al., 2020, 2022; Wang et al., 2021). Additionally, one study reported attrition bias (Zheng et al., 2020) and the other study reported other bias (Wang et al., 2021), respectively, and all studies had no reporting bias (Figure 2).

The PEDro scale demonstrated that 12 studies were of excellent quality (Kim et al., 2010; Liu et al., 2017, 2020; Yin et al., 2018; Ding et al., 2019; Luo and Yu, 2019; Zhang and Zou, 2019; Li et al., 2020, 2022; Tsai et al., 2020; Zheng et al., 2020; Wang et al., 2021) and 7 studies were of good quality (Bie and Wang, 2011; Zheng et al., 2017; Wang et al., 2019; Yin et al., 2020; Zhang et al., 2020, 2022; Cha et al., 2022) in this meta-analysis. For global cognitive function, the GRADE ratings (Zhang et al., 2018) indicated the reliability of excitatory TMS for improving global cognition were both "moderate" using the MMSE and MoCA as outcome measures, respectively (Table 1).

## 3.4. Effects of excitatory TMS over the DLPFC in patients with PSCI

### 3.4.1. Global cognition

Nine studies (Bie and Wang, 2011; Liu et al., 2017, 2020; Zheng et al., 2017; Luo and Yu, 2019; Wang et al., 2019; Li et al., 2020; Zhang et al., 2020; Cha et al., 2022) used the MMSE to assess the efficacy of excitatory TMS on the global cognitive function in patients with PSCI and showed that the experimental group was significantly improved MMSE scores compared to the control group (SMD = 2.48, 95% CI 1.37–3.59, $P < 0.0001$) (Supplementary Figure 1A). Based on the different stimulation sides and due to higher heterogeneity, we performed subgroup and sensitivity analysis. The results showed that excitatory TMS over the left and right hemispheres DLPFC were both superior to the control group in improving the MMSE scores of the experimental group (SMD = 2.26, 95% CI 1.67–2.86, $P < 0.00001$; vs. SMD = 1.72, 95% CI 1.18–2.27, $P < 0.00001$). However, there was no statistical difference over the ipsilateral DLPFC to stimulation between the two groups (SMD = 0.74, 95% CI −0.16 and 1.63, $P = 0.11$) (Figure 3A).

Twelve studies (Zheng et al., 2017, 2020; Yin et al., 2018, 2020; Ding et al., 2019; Luo and Yu, 2019; Wang et al., 2019, 2021; Zhang and Zou, 2019; Li et al., 2020; Zhang et al., 2020, 2022) used MoCA to assess the efficacy of excitatory TMS on global cognitive function in patients with PSCI and showed that the experimental group demonstrated improved MoCA scores than the control group (SMD = 2.64, 95% CI 1.62–3.66, $P < 0.00001$) (Supplementary Figure 1B). Similarly, based on the different stimulation sides and due to the high heterogeneity, we performed subgroup and sensitivity analysis. Our results showed that excitatory TMS over the left and ipsilateral hemispheres DLPFC were both significantly better than that of the control group in improving the MoCA scores of the experimental group (SMD = 2.53, 95% CI 1.86–3.20, $P < 0.00001$; vs. SMD = 0.81, 95% CI 0.28–1.33, $P = 0.003$) (Figure 3B).

### 3.4.2. Memory

Two studies (Yin et al., 2018, 2020), both using RBMT, assessed the efficacy of excitatory TMS over the left hemisphere DLPFC on memory in patients with PSCI. They showed that the experimental group was significantly superior to the control group in improving memory (SMD = 1.29, 95% CI 0.72–1.87, $P < 0.0001$) (Figure 4).

### 3.4.3. Attention

Two studies (Liu et al., 2020; Zhang et al., 2022) assessed the efficacy of excitatory TMS over the left hemisphere DLPFC on attention in patients with PSCI. They showed that attention was significantly improved in the experimental group (SMD = 2.32, 95% CI 1.64–3.01, $P < 0.00001$) (Figure 5). Based on different neuropsychological tests, we performed a subgroup analysis. The changes in TMT-A, DST and DS scores showed that the experimental group were both significantly better than the control group in improving patients' attention intensity and durability, attention conversion, and auditory attention (SMD = 1.89, 95% CI 0.55–3.24, $P = 0.006$; vs. SMD = 3.13, 95% CI 2.35–3.91, $P < 0.00001$; vs. SMD = 2.37, 95% CI 1.81–2.93, $P < 0.00001$).

### 3.4.4. Execution

Two studies (Yin et al., 2018; Zhang et al., 2022) assessed the efficacy of excitatory TMS over the left hemisphere DLPFC on execution in patients with PSCI. Notably, we extracted the time-consuming and correct numbers for completing the Stroop-C section in the included studies to perform subgroup analysis. The results showed that the experimental group was significantly better than the control group in improving the number of corrects (SMD = 0.75, 95% CI 0.24–1.26, $P = 0.004$), but not statistically different in improving the time-consuming (SMD = 1.49, 95% CI −0.72 to 3.70, $P = 0.19$) (Supplementary Figure 2). Subsequently, we performed a sensitivity analysis to reduce heterogeneity, which decreased only after excluding one neuropsychological test, and the overall effect results on executive function remain unchanged (SMD = 0.64, 95% CI 0.21–1.07, $P = 0.004$) (Figure 6).

### 3.4.5. Activities of daily living

Eight studies (Kim et al., 2010; Bie and Wang, 2011; Zheng et al., 2017, 2020; Yin et al., 2018, 2020; Wang et al., 2019; Zhang and Zou, 2019) used MBI to assess the efficacy of excitatory TMS on ADL in patients with PSCI, and the result showed no statistical difference in improving MBI scores between the two groups (SMD = 1.02, 95% CI −0.63 to 2.68, $P = 0.22$) (Supplementary Figure 3). Based on the different stimulation sides and due to the higher heterogeneity, we performed subgroup and sensitivity analysis. We found that studies of stimulation over the right hemisphere DLPFC were an essential factor contributing to the high heterogeneity of the overall effect. Therefore, we pooled the effect after exclusion. Our results showed that excitatory TMS over the left hemisphere DLPFC was better than that of the control group in improving the MBI scores of the experimental group (SMD = 0.72, 95% CI 0.08–1.36, $P = 0.03$). However, there was no statistical difference over the ipsilateral hemisphere DLPFC to stimulation between the two groups (SMD = −0.30, 95% CI −0.81 to 0.21, $P = 0.25$). Furthermore, the pooled

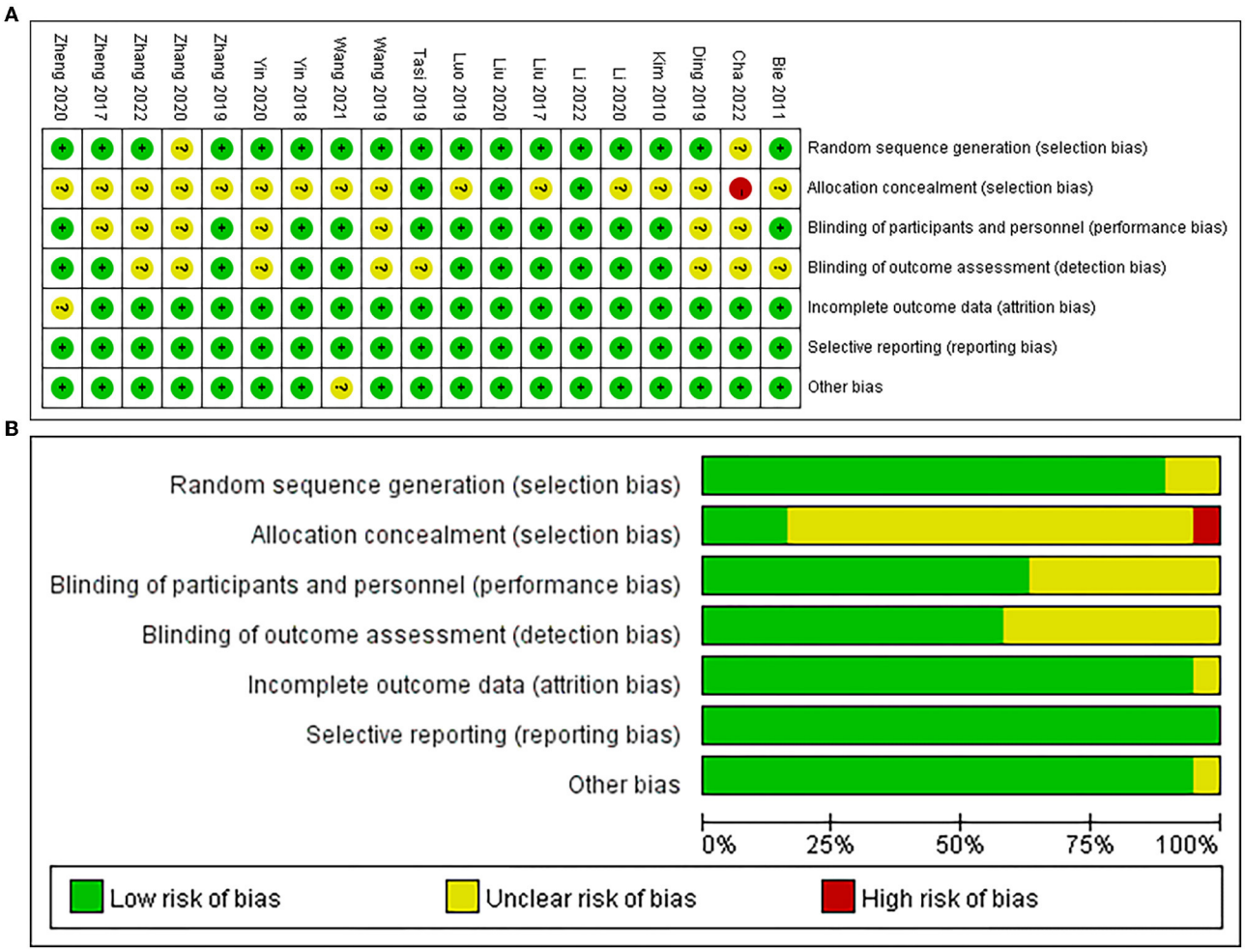


FIGURE 2
Results from the Cochrane risk of bias (ROB) tool. **(A)** ROB graph, **(B)** ROB summary.

TABLE 1 Summary of the GRADEpro.

**Question:** Effects of excitatory transcranial magnetic stimulation (TMS) over the dorsolateral prefrontal cortex (DLPFC) of different cerebral hemispheres in the global cognition for patients with post-stroke cognitive impairment (PSCI).
**Setting:** Hospitals.
**Intervention:** Excitatory TMS on the DLPFC, with or without conventional rehabilitation.
**Comparison:** Sham stimulation or placebo or blank control, with or without conventional rehabilitation.

| Outcome measure | No of studies | No of the participants | Anticipated absolute effects* (95% CI) | certainty of the evidence (GRADE) |
|---|---|---|---|---|
| MMSE | 6 | 247 | SMD 1.93 higher (1.38 lower to 2.47 higher) | ⊕⊕⊕◯ Moderate[a] |
| MoCA | 9 | 387 | SMD 2.32 higher (1.55 lower to 3.10 higher) | ⊕⊕⊕◯ Moderate[b] |

**Certainty of the evidence (GRADE)**
High quality: We are very confident that future research lies close to the estimate of effect.
Moderate quality: We are moderately confident in the effect estimate. Future research is likely to be close to the estimate of the effect, but there is a possibility that it may change the estimate.
Low quality: Our confidence in the effect estimate is limited. Future research may be substantially different from the estimate of the effect and likely to change the estimate.
Very low quality: We are very uncertain about the estimate of effect.

*The risk in the intervention group (and its 95% CI) is based on the assumed risk in the comparison group and the relative effect of the intervention (and its 95% CI).
CI, confidence interval; MMSE, the Mini-Mental State Examination; SMD, standardized mean difference; MoCA, the Montreal Cognitive Assessment.
[a]Most of the RCTs were low quality with an inadequate level of blinding and unclear risk of concealment of allocation.
[b]The statistical test for heterogeneity showed that large variation ($I^2 > 50\%$) existed in point estimates due to the among study differences.

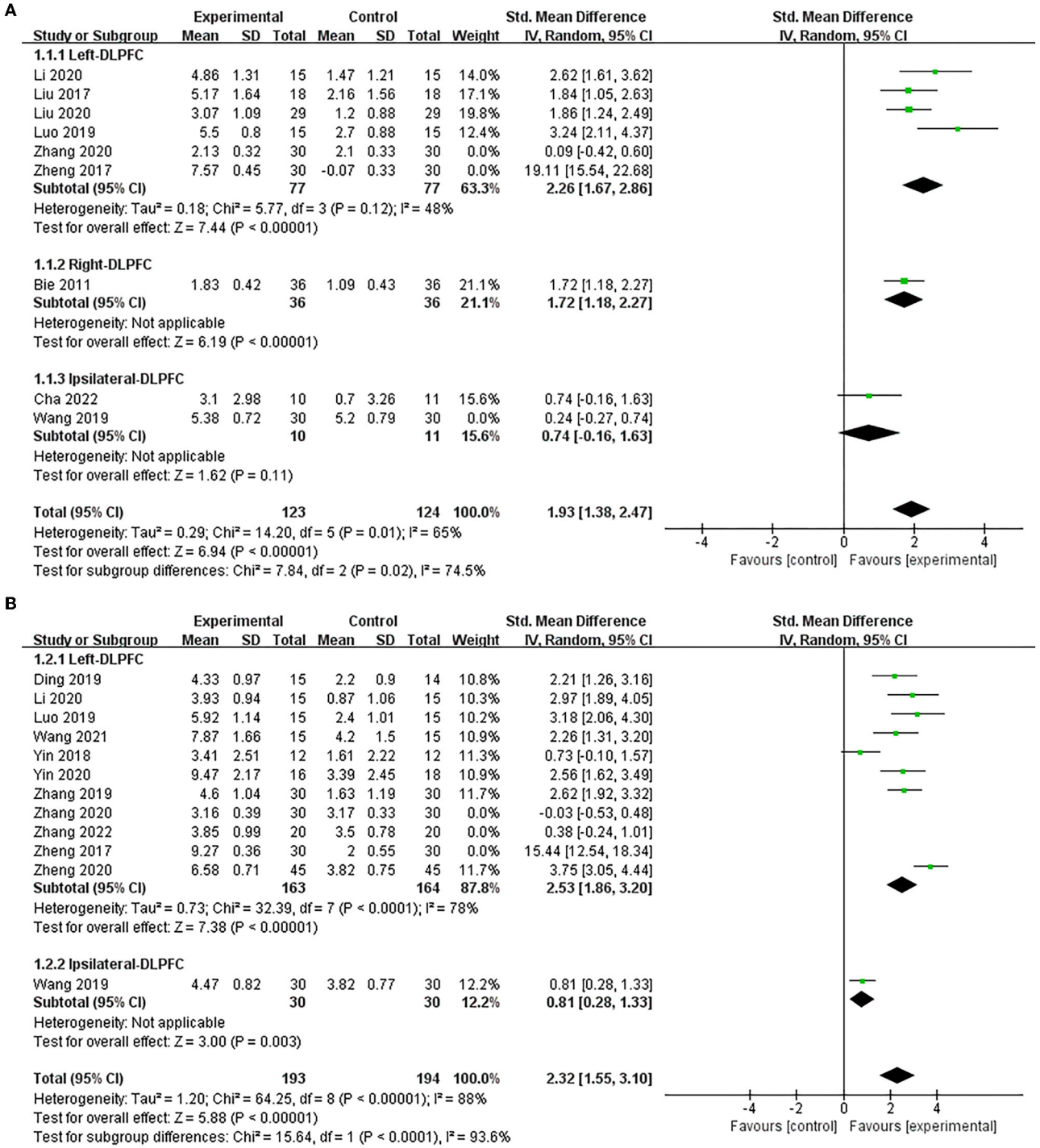


FIGURE 3
Forest plot of the efficacy of excitatory TMS over the DLPFC on global cognition in patients with PSCI compared to the control group (sensitive analysis). **(A)** MMSE, **(B)** MoCA.

overall effect was not changed (SMD = 0.46, 95% CI −0.27 to 1.19, $P = 0.21$) (Figure 7A).

Only two studies (Ding et al., 2019; Liu et al., 2020) used FIM to assess the efficacy of excitatory TMS over the left hemisphere DLPFC on ADL in patients with PSCI. The results also showed no significant difference between the two groups in improving FIM scores (SMD = 1.31, 95% CI −0.57 to 3.20, $P = 0.17$) (Figure 7B).

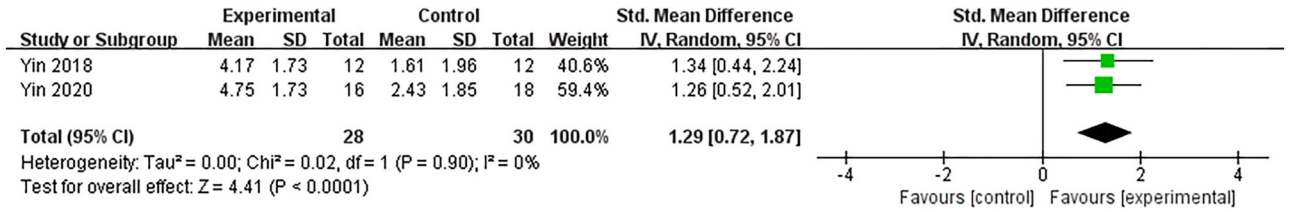


FIGURE 4
Forest plot of the efficacy of excitatory TMS over the left hemisphere DLPFC on memory in patients with PSCI compared to the control group.

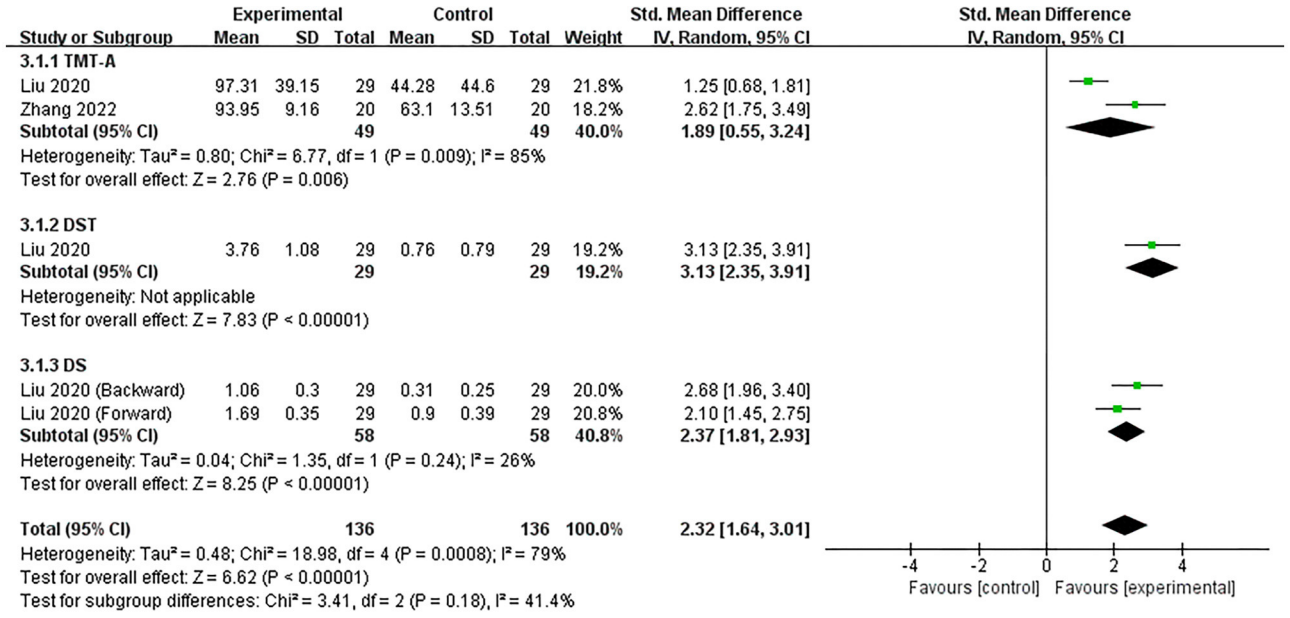


FIGURE 5
Forest plot of the efficacy of excitatory TMS over the left hemisphere DLPFC on attention in patients with PSCI compared to the control group.

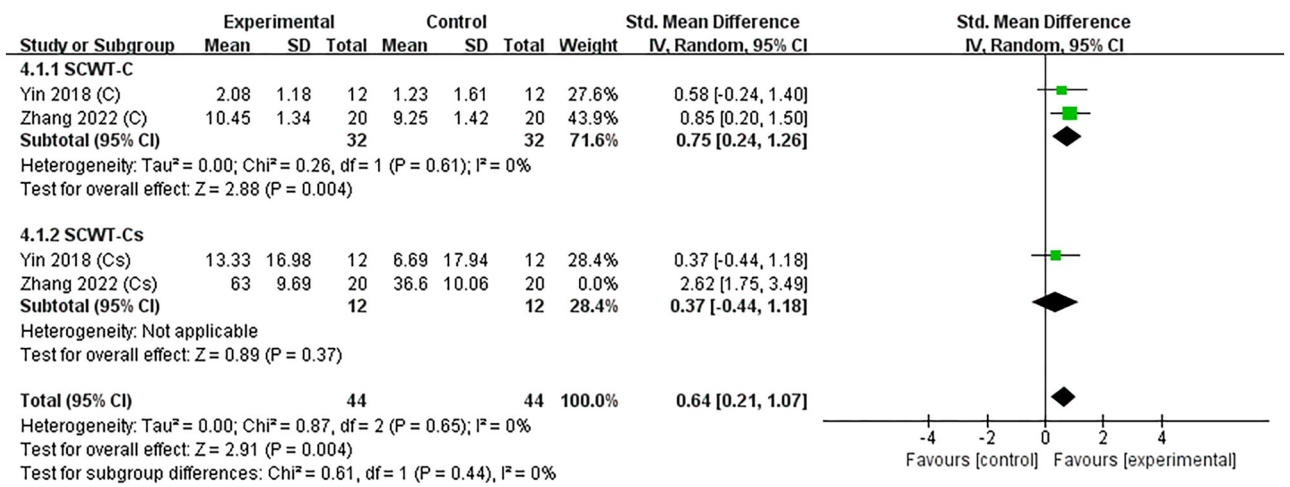


FIGURE 6
Forest plot of the efficacy of excitatory TMS over the left hemisphere DLPFC on execution in patients with PSCI compared to the control group (sensitive analysis).

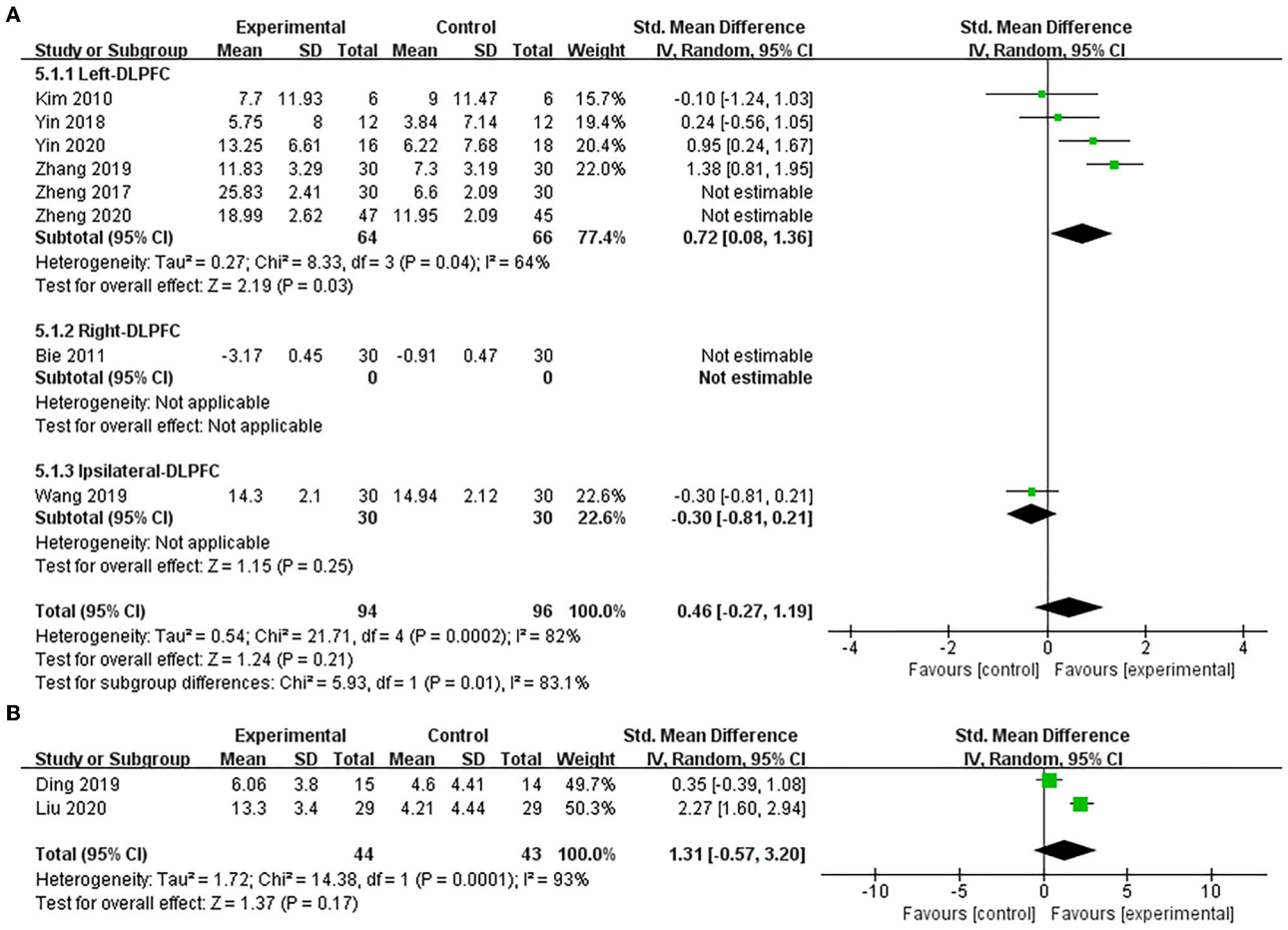


FIGURE 7
Forest plot of the efficacy of excitatory TMS over the DLPFC on ADL in patients with PSCI compared to the control group. **(A)** MBI (sensitive analysis), **(B)** FIM.

### 3.4.6. P300

Four studies (Ding et al., 2019; Zheng et al., 2020; Li et al., 2022; Zhang et al., 2022) used the P300 latency to assess the efficacy of excitatory TMS over the left hemisphere DLPFC on cognition in patients with PSCI. The results showed that with acceptable heterogeneity ($P = 0.10$, $I^2 = 52\%$), the experimental group was much better than the control group in improving P300 latency (SMD = 2.69, 95% CI 2.13–3.25, $P < 0.00001$) (Figure 8). Additionally, two studies (Zheng et al., 2020; Li et al., 2022) used P300 amplitude to assess the efficacy of excitatory TMS. However, we did not perform a meta-analysis because the data were not fully available.

### 3.4.7. Depression

Two studies (Kim et al., 2010; Tsai et al., 2020) used BDI to assess the efficacy of excitatory TMS over the left hemisphere DLPFC on depression in patients with PSCI. They showed that the experimental group was superior to the control group in improving depression (SMD = 0.95, 95% CI 0.26–1.63, $P = 0.007$) (Figure 9).

### 3.4.8. Adverse events

Of the 19 studies included in this meta-analysis, 8 studies did not mention adverse events (Bie and Wang, 2011; Liu et al., 2017; Ding et al., 2019; Luo and Yu, 2019; Yin et al., 2020; Zhang et al., 2020, 2022; Wang et al., 2021), and 5 reported no adverse events (Kim et al., 2010; Zhang and Zou, 2019; Liu et al., 2020; Tsai et al., 2020; Cha et al., 2022). Five studies reported no obvious adverse events, of which three reported transient mild dizziness or headache, but all were tolerable and relieved with rest (Yin et al., 2018; Li et al., 2020; Zheng et al., 2020); one study reported stimulus-related sneezing symptoms (Li et al., 2022); one study reported patients with inattention or sleep disorders (Zheng et al., 2020). Only one reported the occurrence of seizures in patients (Wang et al., 2019). Thus, more extensive randomized controlled trials are needed to further confirm the efficacy and safety of TMS for PSCI in the future.

## 4. Discussion

Unlike previous studies, this is the first meta-analysis to explore the effects of excitatory TMS over the DLPFC in different cerebral

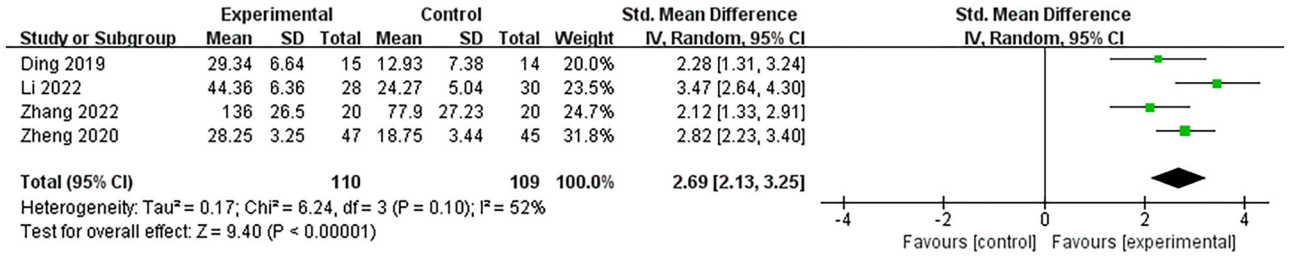


FIGURE 8
Forest plot of the efficacy of excitatory TMS over the left hemisphere DLPFC on P300 latency in patients with PSCI compared to the control group.

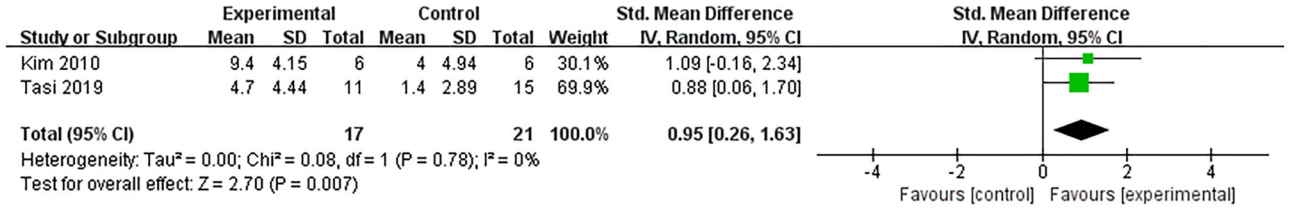


FIGURE 9
Forest plot of the efficacy of excitatory TMS over the left hemisphere DLPFC on depression in patients with PSCI compared to the control group.

hemispheres on cognitive function in patients with PSCI. Our results showed that excitatory TMS over the left hemisphere DLPFC significantly improved global cognitive function, memory, attention, executive, P300 latency, and depression in patients with PSCI. Additionally, it provided an evidence-based rationale for its clinical application.

As a non-invasive, painless, and safe neuromodulation technique, TMS is based on the principle of electromagnetic induction, where a stored energy capacitor rapidly discharges into the stimulation coil to generate a pulsed magnetic field. In doing so, it creates a painless current to stimulate neurons while affecting the neural activity and cortical excitability in the brain (Rossi et al., 2009). Our study focused on excitatory TMS, including HF-rTMS and iTBS. ITBS is an optimized mode of rTMS with the advantages of low stimulation intensity, short cycle, and long benefit (Pinto et al., 2021). Importantly, the results showed that excitatory TMS improved the cognitive function of patients with PSCI. This is consistent with the findings of Selingardi et al. (2019), which showed that excitatory TMS could promote local nerve regeneration, enhance neuroplasticity and intercortical connectivity, and thus improve cognitive function.

The DLPFC, a common target brain region for TMS research and application, involves various cognitive functions such as memory, attention, and execution (Baker et al., 2014; Panikratova et al., 2020). Consistent with the results of our study, Tsai et al. (2020) found that iTBS intervention over the left hemisphere DLPFC improved the global cognition and memory function of stroke patients. On this basis, this study further performed subgroup analysis and, for the first time, explored the efficacy difference of excitatory TMS over the DLPFC in different hemispheres to improve cognitive function, ADL, and depression. The results showed that the left hemispheric DLPFC was a more effective treatment area than excitatory TMS treatment on the ipsilateral and right hemispheres DLPFC. The left hemisphere DLPFC, a key node of the central executive network (CEN) (Bigliassi and Filho, 2022), is closely related to advanced cognitive functions such as working memory, episodic memory, and selective attention. Furthermore, studies have shown that excitatory TMS over the left hemisphere DLPFC can improve cognition in patients by promoting corticospinal excitability (Guse et al., 2010; Li et al., 2020). Motes et al. (2018) also observed by functional magnetic resonance imaging (fMRI) that the improvement in cognitive function was strongly correlated with enhanced neural activity over the left hemisphere DLPFC.

Following a stroke, patients often have changes in brain tissue structure due to insufficient blood and oxygen supply to the brain (D'Souza et al., 2021), gradual degeneration of brain nerves with neuronal loss, and damage to the conduction pathways of neurotransmitters such as acetylcholine, causing impairment in brain cell information transmission, which gradually manifests as cognitive impairment (Girouard and Iadecola, 2006). Our study showed that excitatory TMS over the left hemisphere DLPFC significantly improved memory, attention, executive, and global cognitive function in patients with PSCI. Notably, the improvement of cognitive function can be attributed to multiple factors. First, excitatory TMS can reduce the inhibitory control of pyramidal cells to increase excitatory output (Cirillo et al., 2017), increase cerebral blood flow, improve brain cell metabolism, promote white matter repair and growth, and thereby repair cognitive circuits (Wu et al., 2021). Second, cognitive function is improved by binding DLPFC to the caudate nucleus, promoting the expression of neurotrophic factors and increasing the release of neurotransmitters (Anderkova and Rektorova, 2014; Hoy et al., 2016). Third, the left hemisphere

DLPFC contains the vital cognitive function network (Gomes-Osman et al., 2018), excitatory TMS over the left hemisphere DLPFC can also increase cortical excitability and neuroplasticity by inducing long-term potentiation (LTP) (Wang and Voss, 2015), as well as modulating functional connectivity between brain networks (Yang et al., 2015a). Li et al. (2020) used fMRI to demonstrate that rTMS improved neuroplasticity and changes in neural activity, enhancing the functional connection between the target area and other cognitive processing networks. Furthermore, excitatory TMS can promote hippocampal cells' proliferation and neural regeneration in the dentate gyrus, which is closely related to memory and learning processes (Ueyama et al., 2011).

P300, an objective electrophysiological index, reflects the information processing of working memory and the speedy processing of participating in decision-making (Dejanović et al., 2015). Notably, latency is related to the information processing of the external environment, reflecting the speed at which the brain classifies and recognizes external stimuli and representing the degree of excitement of the central nervous system during information recognition and processing (Rêgo et al., 2012). Our study showed that excitatory TMS over the left hemisphere DLPFC significantly shortened the P300 latency and improved the global cognitive function in patients with PSCI. This is consistent with previous studies (Pinto et al., 2021), where these improvements may be related to the iTBS-mediated enhancement of neurotransmitter dopaminergic and glutamatergic connections (Anderkova and Rektorova, 2014). Our study also found that excitatory TMS had no apparent therapeutic effect in improving ADL, which was inconsistent with the study of Li et al. (2021b). This may be attributed to the heterogeneity of stimulation protocols between studies. Furthermore, in an animal experiment in rats, HF-rTMS and iTBS on the motor cortex effectively promoted neural regeneration and increased cortical excitability (Luo et al., 2017). This study also reported that excitatory TMS over the left hemisphere DLPFC improved depression in patients with PSCI. However, the effectiveness of HF-rTMS and iTBS in treating depression in patients with PSCI remains controversial in previous studies (De Risio et al., 2020; Cash et al., 2021). Therefore, it is necessary to explore excitatory TMS' efficacy further and study its mechanism in future studies.

### 4.1. Limitations

Our study also has some noted limitations. First, we performed subgroup analysis based on the different stimulus areas, but only one study was included in some subgroups. Thus, this may lead to a certain bias in the results. Second, due to the limited number of included studies, we cannot perform subgroup analysis on stroke type and TMS stimulation parameters. Third, our study focuses on the immediate effects after excitatory TMS treatment and lacks studies on the long-term effects.

## 5. Conclusions

Previous literature lacks research on the effect of excitatory TMS over the DLPFC in different hemispheres on the rehabilitation outcome of PSCI patients. This meta-analysis found that compared to other hemispheric sides, excitatory TMS over the left hemisphere DLPFC was a more effective stimulation area, which can significantly improve global cognitive function, memory, attention, executive, P300 latency, and depression in patients with PSCI. However, there was no apparent treatment effect on improving ADL. In the future, more randomized controlled trials with large-sample, high-quality, and follow-up are needed to explore a usable protocol further.

## Data availability statement

The original contributions presented in the study are included in the article/Supplementary material, further inquiries can be directed to the corresponding author.

## Author contributions

KH, JL, ZT, and WS participated in literature search and screening, quality assessment, and data extraction. KH and YL performed data collation and analysis. KH wrote the manuscript. HZ and HL participated in the study design and guidance and reviewed the final manuscript. All authors contributed to the article and approved the submitted version.

## Funding

This work was supported by the National Key Research and Development Program of China (No. 2018YFC2001703), the Special Scientific Research Project for Health Development in the Capital (No. 2020-1-6011), and China Rehabilitation Research Center Project (Nos. 2021ZX-19 and 2020kfdx-010).

## Conflict of interest

The authors declare that the research was conducted in the absence of any commercial or financial relationships that could be construed as a potential conflict of interest.

## Publisher's note



## Supplementary material

The Supplementary Material for this article can be found online at: https://www.frontiersin.org/articles/10.3389/fnins.2023.1102311/full#supplementary-material

# References


Anderkova, L., and Rektorova, I. (2014). Cognitive effects of repetitive transcranial magnetic stimulation in patients with neurodegenerative diseases - clinician's perspective. *J. Neurol. Sci.* 339, 15–25. doi: 10.1016/j.jns.2014.01.037

Baker, J. T., Holmes, A. J., Masters, G. A., Yeo, B. T. T., Krienen, F., Buckner, R. L., et al. (2014). Disruption of cortical association networks in schizophrenia and psychotic bipolar disorder. *JAMA Psychiatry* 71, 109–118. doi: 10.1001/jamapsychiatry.2013.3469

Bie, H., and Wang, X. (2011). Tiaoshen Tongluo acupuncture combined with repetitive transcranial magnetic stimulation treatment. *J. Tradit. Chin. Med.* 52, 335–337.

Bigliassi, M., and Filho, E. (2022). Functional significance of the dorsolateral prefrontal cortex during exhaustive exercise. *Biol. Psychol.* 175, 108442. doi: 10.1016/j.biopsycho.2022.108442

Cash, R. F. H., Cocchi, L., Lv, J., Wu, Y., Fitzgerald, P. B., and Zalesky, A. (2021). Personalized connectivity-guided DLPFC-TMS for depression: advancing computational feasibility, precision and reproducibility. *Hum. Brain Mapp.* 42, 4155–4172. doi: 10.1002/hbm.25330

Cashin, A. G., and McAuley, J. H. (2020). Clinimetrics: physiotherapy evidence database (PEDro) scale. *J. Physiother.* 66, 59. doi: 10.1016/j.jphys.2019.08.005

Cha, B., Kim, J., Kim, J. M., Choi, J.-W., Choi, J., Kim, K., et al. (2022). Therapeutic effect of repetitive transcranial magnetic stimulation for post-stroke vascular cognitive impairment: a prospective pilot study. *Front. Neurol.* 13, 813597. doi: 10.3389/fneur.2022.813597

Chen, A. C., Oathes, D. J., Chang, C., Bradley, T., Zhou, Z. W., Williams, L. M., et al. (2013). Causal interactions between fronto-parietal central executive and default-mode networks in humans. *Proc. Natl. Acad. Sci. U. S. A.* 110, 19944–19949. doi: 10.1073/pnas.1311772110

Cirillo, G., Di Pino, G., Capone, F., Ranieri, F., Florio, L., Todisco, V., et al. (2017). Neurobiological after-effects of non-invasive brain stimulation. *Brain Stimulat.* 10, 1–18. doi: 10.1016/j.brs.2016.11.009

Cui, S., Chen, N., Yang, M., Guo, J., Zhou, M., Zhu, C., et al. (2019). Cerebrolysin for vascular dementia. *Cochrane Database Syst. Rev.* 2019, CD008900. doi: 10.1002/14651858.CD008900.pub3

De Risio, L., Borgi, M., Pettorruso, M., Miuli, A., Ottomana, A. M., Sociali, A., et al. (2020). Recovering from depression with repetitive transcranial magnetic stimulation (rTMS): a systematic review and meta-analysis of preclinical studies. *Transl. Psychiatry* 10, 1–19. doi: 10.1038/s41398-020-01055-2

Dejanović, M., Ivetić, V., Nestorović, V., Erić, M., Stanojević, Z., and Leštarević, S. (2015). The role of P300 event-related potentials in the cognitive recovery after the stroke. *Acta Neurol. Belg.* 115, 589–595. doi: 10.1007/s13760-015-0428-x

Ding, Q., Li, Z., Guo, G., Guan, C., Le, L., Hao, D., et al. (2019). Effects of repetitive transcranial magnetic stimulation with different frequencies on cognitive impairment in stroke patients. *Chin. J. Rehabil.* 34, 513–517. doi: 10.3870/zgkf.2019.010.002

D'Souza, C. E., Greenway, M. R. F., Graff-Radford, J., and Meschia, J. F. (2021). Cognitive impairment in patients with stroke. *Semin. Neurol.* 41, 75–84. doi: 10.1055/s-0040-1722217

Gilio, F., Conte, A., Vanacore, N., Frasca, V., Inghilleri, M., and Berardelli, A. (2007). Excitatory and inhibitory after-effects after repetitive magnetic transcranial stimulation (rTMS) in normal subjects. *Exp. Brain Res.* 176, 588–593. doi: 10.1007/s00221-006-0638-9

Girouard, H., and Iadecola, C. (2006). Neurovascular coupling in the normal brain and in hypertension, stroke, and Alzheimer disease. *J. Appl. Physiol.* 100, 328–335. doi: 10.1152/japplphysiol.00966.2005

Gomes-Osman, J., Indahlastari, A., Fried, P. J., Cabral, D. L. F., Rice, J., Nissim, N. R., et al. (2018). Non-invasive brain stimulation: probing intracortical circuits and improving cognition in the aging brain. *Front. Aging Neurosci.* 10, 177. doi: 10.3389/fnagi.2018.00177

Guse, B., Falkai, P., and Wobrock, T. (2010). Cognitive effects of high-frequency repetitive transcranial magnetic stimulation: a systematic review. *J. Neural Transm. Vienna Austria* 117, 105–122. doi: 10.1007/s00702-009-0333-7

Higgins, J. P. T., Altman, D. G., Gøtzsche, P. C., Jüni, P., Moher, D., Oxman, A. D., et al. (2011). The Cochrane Collaboration's tool for assessing risk of bias in randomised trials. *BMJ* 343, d5928. doi: 10.1136/bmj.d5928

Hoy, K. E., Bailey, N., Michael, M., Fitzgibbon, B., Rogasch, N. C., Saeki, T., et al. (2016). Enhancement of working memory and task-related oscillatory activity following intermittent theta burst stimulation in healthy controls. *Cereb. Cortex N. Y. N* 26, 4563–4573. doi: 10.1093/cercor/bhv193

Huang, Y.-Y., Chen, S.-D., Leng, X.-Y., Kuo, K., Wang, Z.-T., Cui, M., et al. (2022). Post-stroke cognitive impairment: epidemiology, risk factors, and management. *J. Alzheimers Dis.* 86, 983–999. doi: 10.3233/JAD-215644

Kim, B. R., Kim, D.-Y., Chun, M. H., Yi, J. H., and Kwon, J. S. (2010). Effect of repetitive transcranial magnetic stimulation on cognition and mood in stroke patients: a double-blind, sham-controlled trial. *Am. J. Phys. Med. Rehabil.* 89, 362–368. doi: 10.1097/PHM.0b013e3181d8a5b1

Kobayashi, M., and Pascual-Leone, A. (2003). Transcranial magnetic stimulation in neurology. *Lancet Neurol.* 2, 145–156. doi: 10.1016/S1474-4422(03)00321-1

Li, D., Cheng, A., Zhang, Z., Sun, Y., and Liu, Y. (2021a). Effects of low-frequency repetitive transcranial magnetic stimulation combined with cerebellar continuous theta burst stimulation on spasticity and limb dyskinesia in patients with stroke. *BMC Neurol.* 21, 369. doi: 10.1186/s12883-021-02406-2

Li, H., Ma, J., Zhang, J., Shi, W.-Y., Mei, H.-N., and Xing, Y. (2021b). Repetitive transcranial magnetic stimulation (rTMS) modulates thyroid hormones level and cognition in the recovery stage of stroke patients with cognitive dysfunction. *Med. Sci. Monit. Int. Med. J. Exp. Clin. Res.* 27, e931914. doi: 10.12659/MSM.931914

Li, W., Wen, Q., Xie, Y.-H., Hu, A.-L., Wu, Q., and Wang, Y.-X. (2022). Improvement of poststroke cognitive impairment by intermittent theta bursts: a double-blind randomized controlled trial. *Brain Behav.* 12, e2569. doi: 10.1002/brb3.2569

Li, Y., Luo, H., Yu, Q., Yin, L., Li, K., Li, Y., et al. (2020). Cerebral functional manipulation of repetitive transcranial magnetic stimulation in cognitive impairment patients after stroke: an fMRI study. *Front. Neurol.* 11, 977. doi: 10.3389/fneur.2020.00977

Liu, Y., Fang, J., Jiang, R., Hu, N., Pan, C., Ye, Z., et al. (2017). Effects of high frequency repetitive transcranial magnetic stimulation on executive function in patients after stroke. *Chin. J. Neurol.* 50, 745–750. doi: 10.12659/MSM.905636

Liu, Y., Yin, M., Luo, J., Huang, L., Zhang, S., Pan, C., et al. (2020). Effects of transcranial magnetic stimulation on the performance of the activities of daily living and attention function after stroke: a randomized controlled trial. *Clin. Rehabil.* 34, 1465–1473. doi: 10.1177/0269215520946386

Luo, H., and Yu, Q. (2019). Observation of high-frequency repetitive transcranial magnetic stimulation based on resting-state fMRI technique. *Chin. J. Phys. Med. Rehabil.* 04, 279–282. doi: 10.3760/cma.j.issn.0254-1424.2019.04.010

Luo, J., Zheng, H., Zhang, L., Zhang, Q., Li, L., Pei, Z., et al. (2017). High-frequency repetitive transcranial magnetic stimulation (rTMS) improves functional recovery by enhancing neurogenesis and activating BDNF/TrkB signaling in ischemic rats. *Int. J. Mol. Sci.* 18, E455. doi: 10.3390/ijms18020455

Moher, D., Shamseer, L., Clarke, M., Ghersi, D., Liberati, A., Petticrew, M., et al. (2015). Preferred reporting items for systematic review and meta-analysis protocols (PRISMA-P) 2015 statement. *Syst. Rev.* 4, 1. doi: 10.1186/2046-4053-4-1

Motes, M. A., Yezhuvath, U. S., Aslan, S., Spence, J. S., Rypma, B., and Chapman, S. B. (2018). Higher-order cognitive training effects on processing speed-related neural activity: a randomized trial. *Neurobiol. Aging* 62, 72–81. doi: 10.1016/j.neurobiolaging.2017.10.003

Panikratova, Y. R., Vlasova, R. M., Akhutina, T. V., Korneev, A. A., Sinitsyn, V. E., and Pechenkova, E. V. (2020). Functional connectivity of the dorsolateral prefrontal cortex contributes to different components of executive functions. *Int. J. Psychophysiol.* 151, 70–79. doi: 10.1016/j.ijpsycho.2020.02.013

Pinto, N. F. C., Duarte, M., Gonçalves, H., Silva, R., Gama, J., and Pato, M. V. (2021). Theta-burst stimulation is able to impact cognitive processing: a P300 and neuropsychological test study. *Neuropsychobiology* 80, 288–298. doi: 10.1159/000511605

Rêgo, S. R. M., Marcolin, M. A., May, G., and Gjini, K. (2012). Effects of transcranial magnetic stimulation on the cognitive event-related potential p300: a literature review. *Clin. EEG Neurosci.* 43, 285–290. doi: 10.1177/1550059412445657

Rossi, S., Hallett, M., Rossini, P. M., Pascual-Leone, A., and Safety of, T. M. S., Consensus Group (2009). Safety, ethical considerations, and application guidelines for the use of transcranial magnetic stimulation in clinical practice and research. *Clin. Neurophysiol.* 120, 2008–2039. doi: 10.1016/j.clinph.2009.08.016

Rost, N. S., Brodtmann, A., Pase, M. P., van Veluw, S. J., Biffi, A., Duering, M., et al. (2022). Post-stroke cognitive impairment and dementia. *Circ. Res.* 130, 1252–1271. doi: 10.1161/CIRCRESAHA.122.319951

Selingardi, P. M. L., de Lima Rodrigues, A. L., da Silva, V. A., Fernandes, D. T. R. M., Rosí, J., Marcolin, M. A., et al. (2019). Long-term deep-TMS does not negatively affect cognitive functions in stroke and spinal cord injury patients with central neuropathic pain. *BMC Neurol.* 19, 319. doi: 10.1186/s12883-019-1531-z

Siebner, H. R., and Rothwell, J. (2003). Transcranial magnetic stimulation: new insights into representational cortical plasticity. *Exp. Brain Res.* 148, 1–16. doi: 10.1007/s00221-002-1234-2

Snyder, H. M., Corriveau, R. A., Craft, S., Faber, J. E., Greenberg, S. M., Knopman, D., et al. (2015). Vascular contributions to cognitive impairment and dementia including Alzheimer's disease. *Alzheimers Dement. J. Alzheimers Assoc.* 11, 710–717. doi: 10.1016/j.jalz.2014.10.008

Tsai, P.-Y., Lin, W.-S., Tsai, K.-T., Kuo, C.-Y., and Lin, P.-H. (2020). High-frequency versus theta burst transcranial magnetic stimulation for the treatment of poststroke cognitive impairment in humans. *J. Psychiatry Neurosci.* 45, 262–270. doi: 10.1503/jpn.190060

Ueyama, E., Ukai, S., Ogawa, A., Yamamoto, M., Kawaguchi, S., Ishii, R., et al. (2011). Chronic repetitive transcranial magnetic stimulation increases hippocampal neurogenesis in rats. *Psychiatry Clin. Neurosci.* 65, 77–81. doi: 10.1111/j.1440-1819.2010.02170.x

Wang, J., Zheng, C., Cui, X., Xu, T., Zhang, Y., and Xia, W. (2019). Efficacy of repetitive transcranial magnetic stimulation combined with cognitive trainingon stroke patients with cognitive impairment. *Neural. Inj. Funct. Reconstr.* 14, 11–14. doi: 10.16780/j.cnki.sjssgncj.2019.01.003

Wang, J. X., and Voss, J. L. (2015). Long-lasting enhancements of memory and hippocampal-cortical functional connectivity following multiple-day targeted noninvasive stimulation. *Hippocampus* 25, 877–883. doi: 10.1002/hipo.22416

Wang, S., Gong, Z., Chen, W., Wang, M., and Bi, Y. (2021). Effect of different frequency repetitive transcranial magnetic stimulation on cognitive impairment after stroke. *Chin. J. Phys. Med. Rehabil.* 43, 721–723. doi: 10.3760/cma.j.issn.0254-1424.2021.08.012

Wang, W.-C., Wing, E. A., Murphy, D. L. K., Luber, B. M., Lisanby, S. H., Cabeza, R., et al. (2018). Excitatory TMS modulates memory representations. *Cogn. Neurosci.* 9, 151–166. doi: 10.1080/17588928.2018.1512482

Webler, R. D., Fox, J., McTeague, L. M., Burton, P. C., Dowdle, L., Short, E. B., et al. (2022). DLPFC stimulation alters working memory related activations and performance: an interleaved TMS-fMRI study. *Brain Stimulat.* 15, 823–832. doi: 10.1016/j.brs.2022.05.014

Wilson, M. T., Fulcher, B. D., Fung, P. K., Robinson, P. A., Fornito, A., and Rogasch, N. C. (2018). Biophysical modeling of neural plasticity induced by transcranial magnetic stimulation. *Clin. Neurophysiol.* 129, 1230–1241. doi: 10.1016/j.clinph.2018.03.018

Wu, X., Wang, L., Geng, Z., Wei, L., Yan, Y., Xie, C., et al. (2021). Improved cognitive promotion through accelerated magnetic stimulation. *eNeuro* 8, ENEURO.0392-20.2020. doi: 10.1523/ENEURO.0392-20.2020

Yang, H.-Y., Liu, Y., Xie, J.-C., Liu, N.-N., and Tian, X. (2015a). Effects of repetitive transcranial magnetic stimulation on synaptic plasticity and apoptosis in vascular dementia rats. *Behav. Brain Res.* 281, 149–155. doi: 10.1016/j.bbr.2014.12.037

Yang, W., Liu, T.-T., Song, X.-B., Zhang, Y., Li, Z.-H., Cui, Z.-H., et al. (2015b). Comparison of different stimulation parameters of repetitive transcranial magnetic stimulation for unilateral spatial neglect in stroke patients. *J. Neurol. Sci.* 359, 219–225. doi: 10.1016/j.jns.2015.08.1541

Yin, M., Liu, Y., Zhang, L., Zheng, H., Peng, L., Ai, Y., et al. (2020). Effects of rTMS treatment on cognitive impairment and resting-state brain activity in stroke patients: a randomized clinical trial. *Front. Neural Circuits* 14, 563777. doi: 10.3389/fncir.2020.563777

Yin, M., Luo, J., Hu, X., Xian, Q., Huang, L., Zhang, S., et al. (2018). Effects of high frequency repetitive transcranial magnetic stimulation on post-stroke cognitive impairment. *Chin. J. Rehabil. Med.* 33, 763–769. doi: 10.3969/j.issn.1001-1242.2018.07.003

Zhang, F., and Zou, S. (2019). Effects of high frequency repetitive transcranial magnetic stimulation on cognitive function in stroke patients in convalescent stage. *Chin. J. Pract. Nerv. Dis.* 22, 2479–2485. doi: 10.12083/SYSJ.2019.22.404

Zhang, J., Wu, L., Cheng, D., Ren, J., Liu, L., and Li, Y. (2022). The effect of high-frequency repetitive transcranial magnetic stimulation on cognitive function after stroke based on electroencephalogram nonlinear analysis. *J. Chongqing. Med. Univ.* 47, 762–767. doi: 10.13406/j.cnki.cyxb.003059

Zhang, L., Xing, G., Shuai, S., Guo, Z., Chen, H., McClure, M. A., et al. (2017). Low-frequency repetitive transcranial magnetic stimulation for stroke-induced upper limb motor deficit: a meta-analysis. *Neural Plast.* 2017, e2758097. doi: 10.1155/2017/2758097

Zhang, Y., Akl, E. A., and Schünemann, H. J. (2018). Using systematic reviews in guideline development: the GRADE approach. *Res. Synth. Methods.* 10, 312–329. doi: 10.1002/jrsm.1313

Zhang, Y., Mo, L., Nie, Y., and Liu, A. (2020). Application of functional near-infrared spectroscopy in the treatment of mild cognitive impairment after stroke with repeated transcranial magnetic stimulation. *J. Capit. Univ. Med. Sci.* 41, 965–969. doi: 10.3969/j.issn.1006-7795.2020.06.016

Zhao, Q., Wang, X., Wang, T., Dmytriw, A. A., Zhang, X., Yang, K., et al. (2021). Cognitive rehabilitation interventions after stroke: protocol for a systematic review and meta-analysis of randomized controlled trials. *Syst. Rev.* 10, 66. doi: 10.1186/s13643-021-01607-7

Zheng, C., Xia, W., Duan, C., Li, Z., Wang, J., Cui, X., et al. (2020). Repeated transcranial magnetic stimulation combined with Donepezil can improve the cognition of cognitively impaired stroke survivors. *Chin. J. Phys. Med. Rehabil.* 1, 32–33. doi: 10.3760/cma.j.issn.0254-1424.2020.01.008

Zheng, J., Shi, J., Gu, L., Gao, X., Li, Z., Jiao, L., et al. (2017). Therapeutic effects of high frequency repetitive transcranial magnetic stimulation in treating vascular cognitive impairment after stroke but no dementia. *Chin. J. Rehabil.* 32, 488–491. doi: 10.3870/zgkf.2017.06.014

frontiers | Frontiers in Neuroscience

TYPE Original Research
PUBLISHED 23 May 2023
DOI 10.3389/fnins.2023.1134904



OPEN ACCESS

EDITED BY
Jie Jia,
Fudan University, China

REVIEWED BY
Jiang Ma,
Shijiazhuang People's Hospital, China
Chao Ma,
Sun Yat-sen Memorial Hospital, China
Jingpu Zhao,
Shenzhen Second People's Hospital, China

*CORRESPONDENCE
Xun Luo
✉ larryluoxun@163.com
Yongfeng Hong
✉ hy_feng@163.com

†These authors have contributed equally to this work and share first authorship

RECEIVED 31 December 2022
ACCEPTED 10 May 2023
PUBLISHED 23 May 2023

CITATION
Zhang S, Yu Y, Xu P, Shen X, Fang C, Wu X, Qu P, Wu T, Wang QM, Luo X and Hong Y (2023) Mechanical digit sensory stimulation: a randomized control trial on neurological and motor recovery in acute stroke.
*Front. Neurosci.* 17:1134904.
doi: 10.3389/fnins.2023.1134904



# Mechanical digit sensory stimulation: a randomized control trial on neurological and motor recovery in acute stroke

Shuting Zhang[1†], Yang Yu[1†], Panpan Xu[1], Xianshan Shen[1], Chuanqin Fang[2], Xiaosan Wu[2], Ping Qu[2], Tingting Wu[3], Qing Mei Wang[4], Xun Luo[5*] and Yongfeng Hong[1*]

[1]Department of Rehabilitation Medicine, The Second Affiliated Hospital of Anhui Medical University, Hefei, Anhui Province, China, [2]Department of Neurology, The Second Hospital of Anhui Medical University, Hefei, Anhui Province, China, [3]Key Laboratory of Oral Disease Research of Anhui Province, Stomatologic Hospital and College, Anhui Medical University, Hefei, Anhui Province, China, [4]Stroke Biological Recovery Laboratory, Spaulding Rehabilitation Hospital, Harvard Medical School, Boston, MA, United States, [5]School of Medicine, Shenzhen University, Shenzhen, Guangdong Province, China

**Background:** Mechanical digit sensory stimulation (MDSS) is a novel therapy designed to accelerate the recovery of upper limb (including hand) function in patients with hemiplegia following a stroke. The primary goal of this study was to investigate the effect of MDSS on patients with acute ischemic stroke (AIS).

**Methods:** Sixty-one inpatients with AIS were randomly divided into conventional rehabilitation group (RG) and stimulation group (SG), and the latter group received MDSS therapy. A healthy group consisting of 30 healthy adults was also included. The interleukin-17A (IL-17A), vascular endothelial growth factor A (VEGF-A), and tumor necrosis factor-alpha (TNF-α) plasma levels were measured in all subjects. The neurological and motor functions of patients were evaluated using the National Institutes of Health Stroke Scale (NIHSS), Mini-Mental State Examination (MMSE), Fugel-Meyer Assessment (FMA), and Modified Barthel Index (MBI).

**Results:** After 12days of intervention, the IL-17A, TNF-α, and NIHSS levels were significantly decreased, while the VEGF-A, MMSE, FMA, and MBI levels were significantly increased in both disease groups. No significant difference was observed between both disease groups after intervention. The levels of IL-17A and TNF-α were positively correlated with NIHSS but negatively correlated with MMSE, FMA, and MBI. The VEGF-A levels were negatively correlated with NIHSS but positively correlated with MMSE, FMA, and MBI.

**Conclusion:** Both MDSS and conventional rehabilitation significantly reduce the production of IL-17A and TNF-α, increase the VEGF-A levels, and effectively improve cognition and motor function of hemiplegic patients with AIS, and the effects of MDSS and conventional rehabilitation are comparable.

KEYWORDS

**acute ischemic stroke, mechanical digit sensory stimulation, IL-17A, TNF-α, VEGF-A**

# 1. Introduction

Acute ischemic stroke (AIS) is a medical emergency with high morbidity, mortality, and disability rates worldwide, resulting in various degrees of cognitive and motor dysfunction, even after rehabilitation treatment (Tsivgoulis et al., 2016). According to statistics from the World Health Organization, the incidences of cognitive impairment and motor dysfunction of the upper limbs caused by stroke are around 37 and 60% in the sixth month of the disease, respectively (Arba et al., 2018; Dawson et al., 2021).

Mechanical digit sensory stimulation (MDSS), which primarily stimulates pressure sensation, is a novel therapy designed by our team to accelerate the recovery of the upper limb (including hand) function in patients with hemiplegia after stroke. We have developed a digit sensory stimulator (DSS) with a screen that can display the intensity of stimulation in real time. Our previous clinical observation of more than 1 year suggests that DSS is suitable for clinical application and can promote the cognitive and limb motor functions of patients after stroke.

Chandrasekaran et al. found that the sulcal stimulation in the primary somatosensory cortex (S1) could induce sensory perception located in the fingertip better than the gyral stimulation, and the perception caused by the sulcal stimulation was often highly concentrated in a single segment of the finger, especially the distal phalanx including the fingertip (Chandrasekaran et al., 2021). Kattenstroth et al. pointed out that compared with any other part of the body, fingertips and toetips are more sensitive sites with a higher density of nerve endings and somatosensory receptors, and these sites are the most innervated, and stimulation of these two sites can induce the excitement of specific targeted somatosensory cortical areas (Kattenstroth et al., 2018). Appropriate sensory stimulation of the fingers/toes in some patients with central nervous system injury can induce more cerebral cortical excitation and limb movements (Dobkin, 2003; Kattenstroth et al., 2018; Ayoobi et al., 2021). Therefore, the sites of sensory stimulation were concentrated on the hemiplegic finger/toenail beds to achieve good results in this study. In addition, Kattenstroth et al. reported that electrical stimulation of the affected fingertip of patients with subacute stroke for 2 weeks significantly improved their upper limbs' sensory and motor function (Kattenstroth et al., 2018). However, the specific effects of MDSS on hemiplegic patients with AIS remain unclear.

Previous studies have shown that inflammatory response significantly contributes to ischemic brain injury (Bustamante et al., 2016; Nakamura and Shichita, 2019). Interleukin-17A (IL-17A), an essential immune cytokine, aggravates cerebral ischemia in the acute stage of ischemic stroke by upregulating inflammatory mediators and chemokines (Liu et al., 2019). Tumor necrosis factor-alpha (TNF-α) is a pro-inflammatory cytokine involved in neuroinflammation and neuronal damage induced by cerebral ischemia (Lambertsen et al., 2019). It also promotes the release of neurotoxic substances and aggravates ischemic injury (Lambertsen et al., 2012; Bokhari et al., 2014; Chen et al., 2019). Vascular endothelial growth factor A (VEGF-A) is a crucial cytokine responsible for the regulation of angiogenesis, which promotes neurogenesis and nerve function recovery after ischemic stroke (Lucitti et al., 2012; Ma et al., 2012). Taken together, IL-17A, TNF-α, and VEGF-A are closely related to ischemic stroke occurrence and development (Kawabori and Yenari, 2015).

Somatosensory stimulation of the brain of some patients with central nervous system injury through their fingers may affect the metabolism and functional recovery of the brain (Dobkin, 2003; Ayoobi et al., 2021). Previous studies have revealed that ischemic stroke temporarily but significantly increased IL-17A, TNF-α, and VEGF-A levels (Arango-Dávila et al., 2015; Liu et al., 2019; Moon et al., 2021; Xu et al., 2022). Therefore, the purpose of this study was to investigate the effects of MDSS on the plasma levels of cytokines and the cognitive and motor functions of hemiplegic patients with AIS and to explore its noninferiority in terms of rehabilitation outcomes when compared with the conventional therapy.

# 2. Methods

## 2.1. Participants

In this single-center, randomized study, the hemiplegic patients with AIS admitted to the Department of Neurology in the Second Hospital of Anhui Medical University between December 2020 and September 2022 were recruited. A healthy group of some age-and gender-matched healthy adults were also enrolled. This study was approved by the Medical Ethics Committee of the Second Hospital of Anhui Medical University [Approval No. YX2020-030(F1)] and performed in accordance with the Declaration of Helsinki. Written informed consent was obtained from each participant before enrollment.

## 2.2. Inclusion and exclusion criteria

Healthy subjects were recruited from the workers, interns, and ward attendants of Department of Rehabilitation Medicine in the Second Hospital of Anhui Medical University. The inclusion criteria of healthy subjects were as follows: (a) aged between 18 and 80 years; (b) clear consciousness and normal cognition; (c) no history of heart disease, stroke, rheumatic disease, acute gout, tumor, tuberculosis, infection (including viral and bacterial), new fracture, etc. (d) willing to sign informed consent. All healthy subjects were asked to ensure adequate sleep and normal mental state before the experiment, and to avoid smoking and intake of irritating foods, such as alcohol, tea, and coffee.

Patients who met the following criteria were qualified for inclusion: (a) aged between 18 and 80 years; (b) diagnosed with partial anterior circulation infarct (PACI) for the first time with the diagnosis confirmed by magnetic resonance imaging or computerized tomography scan (Novotny et al., 2021); (c) hospitalized within 48 h of ischemic stroke onset with stable vital signs (systolic blood pressure, 90–160 mmHg; diastolic blood pressure, 60–100 mmHg; oxygen saturation, > 92%; resting heart rate, 60–110 beats/min; and body temperature, ≤38°C); (d) clear consciousness and willing and able to cooperate with the assessments and treatments; (e) the strength of all muscles of the upper limb, including shoulder, elbow, wrist, and hand, and the lower limb, including hip, knee, ankle, and foot, on the hemiplegic side was ≤ grade 3 in the manual muscle testing (Ciesla et al., 2011), while that on the unaffected side showed no dysfunction; and (f) self-identified as right-handed and confirmed by his/her family member.

The exclusion criteria for patients were as follows: (a) two or more strokes before the study; (b) other types of AIS other than PACI; (c) evidence of continued deterioration of the condition with unstable vital signs; (d) complications with heart, lung, liver, or renal insufficiency or a malignant tumor; (e) pregnant or lactating; (f) treated with antibiotics for an infection in any site, such as the lung or the urinary tract; and (g) currently participating in other clinical trials.

## 2.3. Mechanical digit sensory stimulation

The DSS device consists of a handle, a spring, an axle, a pressure tip, a card slot, and a screen displaying the pressure (Figure 1). During the MDSS therapy, the operator held the device's handle and placed the pressure tip at the hemiplegic side's fingernail/toenail bed root. Then, the operator relaxed the handle relatively quickly, so the pressure tip could rapidly stimulate the fingernail/toenail bed. If the stimulation intensity was acceptable to the patient, the operator gripped the device's handle to stop stimulation as soon as the extension of the stimulated fingers/toes or the retraction of the stimulated upper/lower limbs was observed. However, if the stimulation intensity exceeded the acceptable range, the operator stopped stimulation immediately, even if finger/toe extension or limb retraction was not observed. The screen on the reverse of the device displayed real-time stimulation intensity in Newtons (N), as shown in Figure 2.

## 2.4. Grouping and treatment

After screening for eligibility by a medical doctor, hemiplegic patients with AIS were randomly assigned to two groups: the stimulation group (SG) that received MDSS therapy with the DSS (Figures 1, 2) and the rehabilitation group (RG) that received conventional rehabilitation without the MDSS.

All patients received comprehensive neurological treatment according to the Guidelines for the Early Management of Patients with Acute Ischemic Stroke (Powers et al., 2019). Patients in the RG received conventional rehabilitation treatment, including body massage, breathing exercises, active movement of the unaffected limb, active/assisted/passive movement of the hemiplegic limbs according to the patient's condition, and neuromuscular electrical stimulation of the upper and lower limbs on the hemiplegic side. In the RG, all treatments were administered once a day, with daily treatment lasting 50–70 min.

Body massage was applied only to the upper and lower limbs of the hemiplegic side. Since all patients were in the acute phase of cerebral infarction, the muscle tone of the upper and lower limbs on the hemiplegia side was low, so we used rapid manual massage with moderate force for the flexor and extensor muscles of the hemiplegic limb, once a day for 10 min. The breathing exercises were carried out by inhaling deep through the nose, pouting and blowing hard through the mouth, mainly to train abdominal breathing. Each set of breathing exercises consisted of 5 repetitions, and 3–5 sets were performed consecutively, with a 30-second break between two sets, a total of 5–10 min, and 3–5

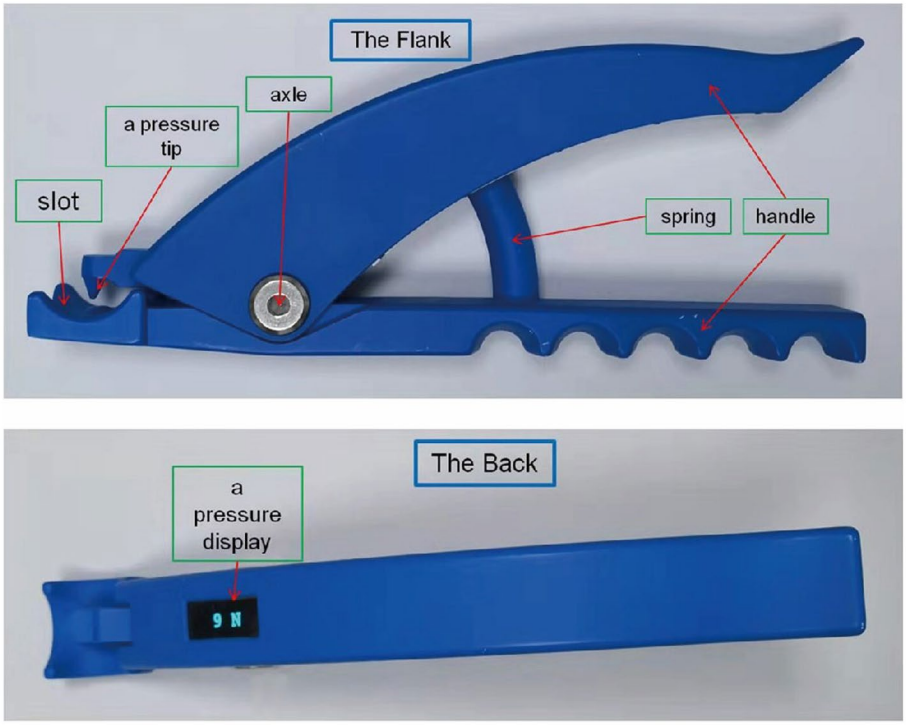


FIGURE 1
Digit sensory stimulator.

FIGURE 2
Implementation of mechanical digit sensory stimulation.

sets per day. Movement patterns of the unaffected and affected limbs were mainly forward flexion and abduction of the upper limb and straight leg raising, overall flexion and extension of the lower limb in the supine position. During the movement of the unaffected limb, the unaffected hand held a bottle of mineral water or a proper weight sandbag was tied around the unaffected wrist/ankle. Active/assisted/passive movements were selected according to the muscle strength of the upper and lower limbs on the hemiplegic side. Each movement of the limb was performed 10 times in a set, with an interval of 30 s between two sets, a total time of 20–30 min per day. We used low-frequency electrical stimulation of the upper and lower limbs on the hemiplegic side, and the specific sites of electrical stimulation were selected according to the residual muscle strength. The biceps brachii and quadriceps femoris were first selected as targets for electrical stimulation. However, if the muscle strengths of the biceps brachii and quadriceps femoris were ≥ grade 2 (manual muscle testing, MMT), their antagonist muscles were electrically stimulated, and the upper and lower limbs were electrically stimulated at the same time, for 15–20 min once daily.

Instead of conventional rehabilitation, patients in the SG received MDSS therapy. The same investigator performed the therapy for all patients in the group. With the patient in a supine position, the investigator stimulated the nail bed root of all five fingers and toes separately on the hemiplegic side using the DSS, from the little finger/toe to the thumb/big toe. The stimulation pressure was between 30 and 50 N, enough to cause active extension of the fingers/toes or retraction of the upper/lower limbs on the hemiplegic side and was tolerable for the patient. The stimulation duration for each finger/toe was 2–3 s, and the interval between two adjacent stimulations was 5–10 s. The total stimulation time of five fingers and five toes was 70–120 s. Based on ethical grounds and in view of the short time required for each stimulation, patients in the SG were treated three times daily, once in the morning, once at noon, and once in the evening to guarantee that all patients have access to effective treatment.

The interventions (conventional rehabilitation in the RG and MDSS therapy in the SG) started from the third day after disease onset and continued for 12 days (until the 14th day after disease onset). The timeline of the interventions is shown in Figure 3.

## 2.5. Safety and acceptability evaluation

All patients were observed for discomfort, seizure, recurrent cerebral hemorrhage or infarction, pulmonary embolism, myocardial infarction, and death during the study. After the first and last stimulation, patients in the SG were asked to self-assess the degree of pain caused by MDSS using the visual analog scale (VAS): 0, no pain; 1–3, mild pain; 4–6, marked pain; and 7–10, intense pain (Sung and Wu, 2018). The acceptance was evaluated by a subjective 4-item questionnaire after 12 days of intervention: (Q1) "Is the therapy with the MDSS motivating?" (0 no, 1 yes), (Q2) "Would you recommend the MDSS to other subjects with stroke?" (0 no, 1 yes), (Q3) "Has the MDSS therapy led to concrete improvements?" (0 no, 1 yes), (Q4) "How comfortable was the therapy with the MDSS for you?" (0 uncomfortable, 10 very comfortable; Ranzani et al., 2020).

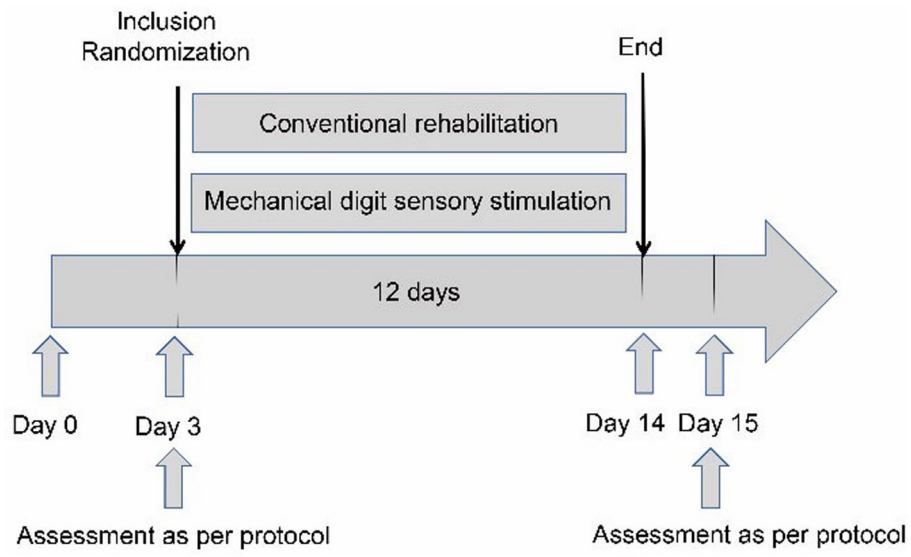


FIGURE 3
Flow chart.

## 2.6. Measurement of plasma cytokines levels

Fasting venous blood (3 ml) was collected in the morning from each subject in the disease groups before intervention (the third day after disease onset) and after 12 consecutive days of intervention (the 15th day after disease onset). The same amount of fasting venous blood was collected from each subject in the healthy group immediately after enrollment. Blood samples were centrifuged at 3,000 rpm for 15 min. Then, the plasma was isolated using a pipette and stored at −80°C until analysis (Tang et al., 2017). The IL-17A, TNF-α, and VEGF-A plasma levels were determined using enzyme-linked immunosorbent assay kits (Shanghai Jianglai Industrial Co., Ltd., Shanghai, China) according to the manufacturer's instructions (Aydin, 2015; Eble, 2018).

## 2.7. Neurological and motor function assessment

The neurological and motor functions of each patient were evaluated using multiple assessment scales before and after intervention. The National Institutes of Health Stroke Scale (NIHSS) was used to evaluate neurological deficits. The total score ranges between 0 and 42, with higher scores indicating more severe nerve damage. The NIHSS is scored as follows: 0–1, normal; 2–4, mild impairment; 5–15, moderate impairment; 16–20, moderate to severe impairment; and ≥21, severe impairment (Lyden, 2017). The Mini-Mental State Examination (MMSE) was used to evaluate cognitive function. It consists of 19 items with a total of 30 points. Higher scores indicate better cognitive function. A score of ≤26 indicates cognitive impairment, while a score of 27–30 is considered within the normal range (Körver et al., 2019). The Fugel-Meyer Assessment (FMA) was used to evaluate the motor function of the upper and lower limbs and has a total score of 100. Higher scores indicate better limb motor function. A score of 0–50 suggests severe limb paralysis, a score of 51–84 indicates significant limb paralysis, a score of 85–95 denotes moderate limb paralysis, and a score of 96–100 represents mild limb paralysis (Fugl-Meyer et al., 1975). The Modified Barthel Index (MBI) was used to assess the ability to complete activities of daily living with a total score of 100. The higher the score, the higher the ability to complete daily living activities. The MBI is scored as follows: 0–20, severe functional impairment; 25–45, serious functional impairment; 50–70, moderate functional impairment; 75–95, mild functional impairment; and 95–100, normal (Taghizadeh et al., 2020). The primary outcome of the study, which was tested for equivalence, was the change in motor impairment at the end of treatment relative to before intervention, assessed by the FMA. The FMA scale was used as the primary outcome measure due to its widespread use in sensorimotor rehabilitation assessment (Ranzani et al., 2020).

## 2.8. Statistical analysis

The sample size was estimated to achieve a power $(1-\beta)$ of 0.8 to detect a 4.66-point difference in FMA (Metzger et al., 2014), with a 2-sided significance level of 0.05. A total of 27 patients in each group were required. Allowing for a 10% loss, 30 patients in each group should be recruited, for a total of 60 patients. The sample size was determined using the G*Power software (version 3.1.9.7). Data were analyzed using the SPSS 25.0 software. The chi-square test compared categorical variables. All quantitative variables were tested for normal distribution using the Shapiro–Wilk test. Normally distributed data were expressed as mean ± standard deviation (SD). The independent sample t-test was used to compare quantitative variables between the two disease groups; The paired sample t-test was used to compare the

data before and after intervention in each group. Pearson correlation analysis was used to determine the correlations of plasma levels of IL-17A, TNF-α, and VEGF-A with the score of each assessment. A value of $p < 0.05$ indicated statistical significance. Equivalence analysis was used to investigate whether the two disease groups showed an equivalent change in terms of the primary outcome measure (Walker and Nowacki, 2011). Equivalence was established if the difference in the FMA score between the two disease groups lay within an equivalence boundary of ±5.2 points, which was reported to be the minimal detectable/clinically important difference for the FMA (Wagner et al., 2008; Ranzani et al., 2020).

## 2.9. Data availability statement

The data associated with the paper are not publicly available but are available from the corresponding author upon reasonable request.

# 3. Results

Sixty-seven subjects with AIS were eligible and consented to participate in the study, 33 of whom were randomly assigned to the RG and 34 to the SG. Six (3 in the RG and 3 in the SG) subjects did not complete the intervention protocol due to early discharge from hospital and dropped out halfway through the study. Only 61 subjects (30 in the RG and 31 in the SG) received corresponding interventions and assessments (Figure 4). No adverse event related to the intervention was observed during the study. A healthy group consisting of 30 age-and gender-matched healthy adults were also enrolled.

## 3.1. Baseline characteristics

The demographics and clinical characteristics of different groups at baseline are summarized in Table 1. Participants were aged between

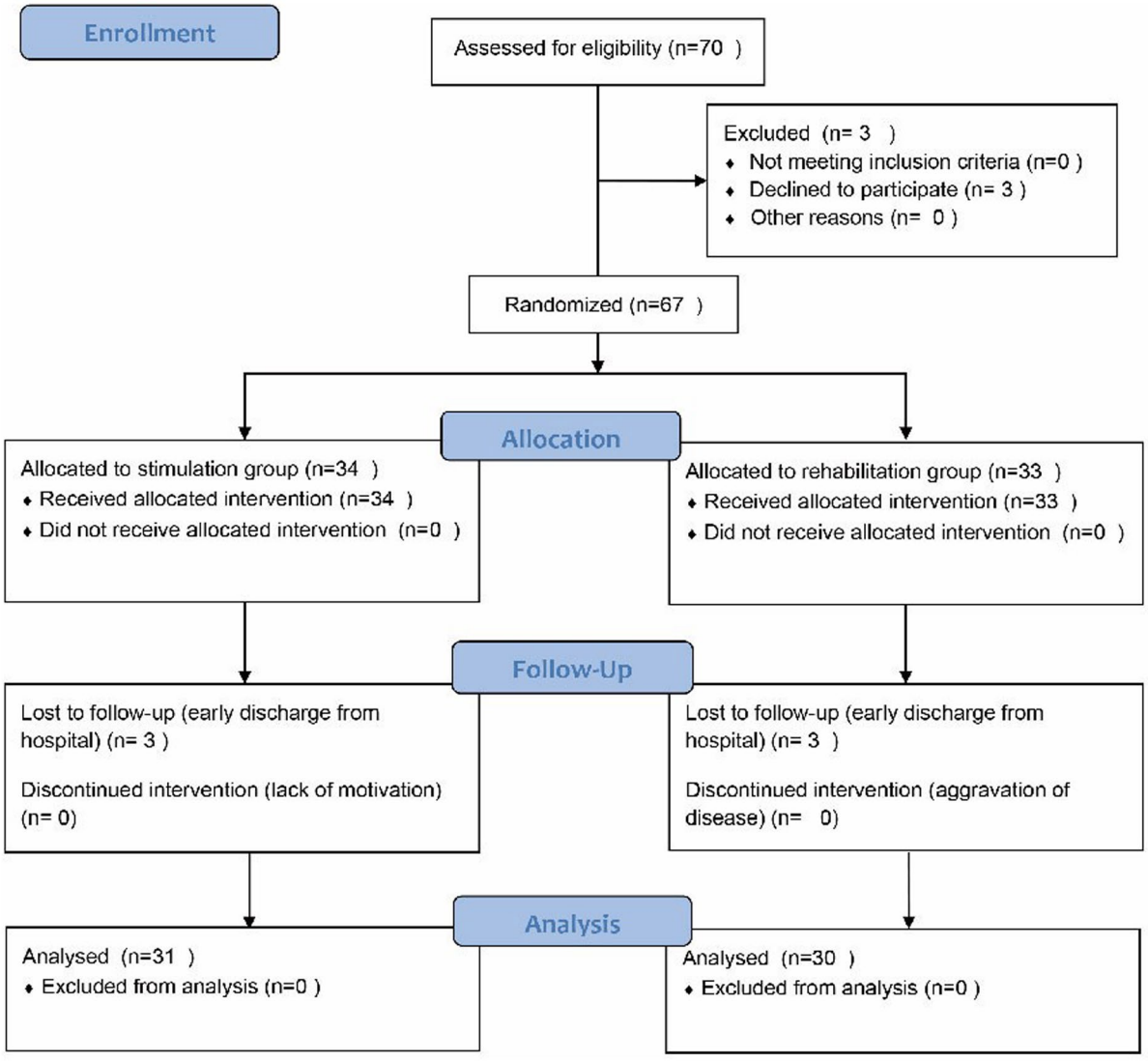


FIGURE 4
Trial profile describing the participants population.

TABLE 1 Baseline characteristics of the randomized study participants.

| Characteristics | Rehabilitation group ($n$=30) | Stimulation group ($n$=31) | Healthy group ($n$=30) | $\chi^2$/F | $p$ |
|---|---|---|---|---|---|
| Age (years) mean (SD) | 68.73 (11.08) | 63.68 (12.60) | 65.03 (6.19) | 1.938 | 0.150 |
| Sex (Male/Female) | 1614 | 22/9 | 16/14 | 2.634 | 0.268 |
| Smoking history (%) | 13 (43.33%) | 17 (54.84%) | 10 (33.33%) | 2.869 | 0.238 |
| Drinking history (%) | 11 (36.67%) | 12 (38.71) | 13 (43.33%) | 0.293 | 0.864 |
| Diabetes (%) | 9 (30%) | 11 (35.49%) | 12 (40%) | 0.660 | 0.719 |
| Obesity (%) | 4 (13.33%) | 10 (32.26%) | 9 (30%) | 3.420 | 0.181 |
| Hypertension (%) | 25 (83.33%) | 25 (80.65%) | 23 (76.67) | 0.426 | 0.808 |
| Intravenous thrombolysis or arterial embolectomy (%) | 6 (20%) | 9 (29.03%) | - | 0.671 | 0.554 |

TABLE 2 Plasma levels of IL-17A, TNF-α, and VEGF-A in different groups (pg/ml).

| Cytokine | Healthy Group mean (SD) | Disease groups before intervention mean (SD) | | | Disease groups after intervention mean (SD) | | |
|---|---|---|---|---|---|---|---|
| | | Rehabilitation group | Stimulation group | $p$ | Rehabilitation group | Stimulation group | $p$ |
| IL-17A | 14.45 (1.63) | 24.76 (6.33)$^{\#}$ | 23.44 (6.14)$^{\#}$ | 0.322 | 18.53 (6.99)*$^{\#}$ | 17.46 (6.52)*$^{\#}$ | 0.538 |
| TNF-α | 31.83 (6.37) | 50.78 (7.37)$^{\#}$ | 46.90 (9.37)$^{\#}$ | 0.056 | 36.38 (11.35)* | 31.00 (10.84)* | 0.063 |
| VEGF-A | 123.30 (9.55) | 142.19 (23.96)$^{\#}$ | 138.40 (28.08)$^{\#}$ | 0.542 | 189.95 (37.84)*$^{\#}$ | 198.83 (29.85)*$^{\#}$ | 0.312 |

Intra-group comparison before and after intervention, *$p < 0.01$; compared with Healthy Group, $^{\#}p < 0.01$.

26 and 80 years. No statistically significant differences were found in gender, age, and history of smoking, drinking, diabetes, obesity, hypertension, intravenous thrombolysis or arterial embolectomy among the three groups ($p > 0.05$).

## 3.2. Plasma levels of IL-17A, TNF-α, and VEGF-A

The IL-17A, TNF-α, and VEGF-A plasma levels in the RG and SG before intervention were significantly higher than those in the healthy group (all $p < 0.01$), but no significant difference was observed between the two disease groups ($p > 0.05$). The IL-17A and TNF-α levels in both disease groups after intervention were significantly decreased, while those of VEGF-A were significantly increased compared with those before intervention (all $p < 0.01$). However, no significant difference in cytokine levels was observed between the RG and SG after intervention ($p > 0.05$). Compared with those in the healthy group, the IL-17A and VEGF-A levels in the RG and SG after intervention were significantly increased ($p < 0.01$), while the TNF-α levels were not significantly different ($p > 0.05$). As shown in Table 2.

## 3.3. Results of assessment scales

The NIHSS, MMSE, FMA, and MBI scores were not significantly different between the RG and SG before intervention ($p > 0.05$). The NIHSS scores were significantly decreased, while the MMSE, FMA, and MBI scores were significantly increased in the two disease groups after intervention (all $p < 0.01$). However, no significant difference in the assessment scales' results after intervention was observed between the two disease groups ($p > 0.05$). As shown in Table 3. According to the equivalence analysis (Figure 5), the change in the FMA score in the SG could be considered as non-inferior to that in the RG. The 90% confidence interval lay within the equivalence boundaries in favor of the MDSS therapy at the end of the study. Before and after intervention, subjects in the SG improved on average by 17.90 FMA points, while those in the RG showed an average increase of 17.47 FMA points. In both disease groups, these changes were above the minimal detectable/clinically important difference (Shelton et al., 2001; Wagner et al., 2008).

## 3.4. Correlation analysis

The levels of IL-17A and TNF-α before and after intervention were positively correlated with the NIHSS scores, but negatively correlated with the MMSE, FMA, and MBI scores ($p < 0.01$); The VEGF-A levels before and after intervention were negatively correlated with the NIHSS scores but positively correlated with the MMSE, FMA, and MBI scores ($p < 0.01$). As shown in Table 4.

## 3.5. Acceptance of MDSS therapy

All patients in the SG had a VAS score of ≤6, and the mean VAS score of this cohort was 1.25 ± 1.06, suggesting that the pain caused by MDSS was mild. Of 31 participants who answered the questionnaire in the SG, 90.32% found the MDSS therapy motivating (Q1), 83.87% would recommend the MDSS therapy program to other persons with stroke (Q2), and 87.10% experienced concrete improvements in their health status at the end of the therapy program (Q3). Participants

TABLE 3 Results of NIHSS, MMSE, FMA, and MBI before and after intervention.

| Scale | Before intervention mean (SD) | | | After intervention mean (SD) | | |
|---|---|---|---|---|---|---|
| | Rehabilitation group | Stimulation group | *p* | Rehabilitation group | Stimulation group | *p* |
| NIHSS | 8.87 (2.79) | 8.26 (3.67) | 0.470 | 4.53 (1.68)* | 4.52 (2.86)* | 0.977 |
| MMSE | 20.40 (3.25) | 21.74 (3.32) | 0.116 | 23.27 (2.57)* | 24.52 (2.84)* | 0.077 |
| FMA | 54.27 (11.93) | 55.61 (10.72) | 0.645 | 71.73 (10.24)* | 73.52 (11.16)* | 0.519 |
| MBI | 36.50 (13.01) | 37.90 (11.75) | 0.660 | 62.50 (9.54)* | 66.61 (13.75)* | 0.181 |

Intra-group comparison before and after intervention. *$p < 0.01$.

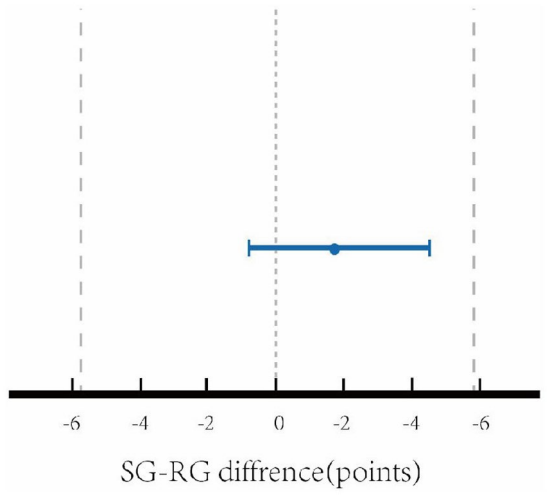


FIGURE 5
Equivalence analysis between stimulation group and rehabilitation group with reference to the FMA change.

rated the MDSS treatment as comfortable with a score of 7.81 ± 1.25 out of 10 (Q4).

## 4. Discussion

This study shows that MDSS is a safe and effective therapy for patients with AIS. Treatment with the DSS decreased inflammatory factors (i.e., IL-17A and TNF-α), increased nerve regeneration factor VEGF-A levels, alleviated neurological impairment, and restored cognitive and limb motor functions. The result of the equivalence analysis comparing the evolution in the FMA demonstrated that the motor recovery in the stimulation group is non-inferior with respect to the control group. The correlation analysis revealed that plasma cytokine levels were correlated with the results of clinical assessment scales.

Previous studies have shown that a time window of neuroplasticity exists in the early post-stroke period, during which the brain's dynamic response to rehabilitation treatment is sensitive and robust (Coleman et al., 2017). There is no consensus on the optimal time to start rehabilitation after stroke. However, increasing evidence has demonstrated that intensive rehabilitation treatment within 24 h after stroke might harm patients, while treatment within the first 2 weeks after stroke will alleviate functional impairment (Li et al., 2017). Early rehabilitation, which starts between 24 and 72 h after stroke, has been shown to reduce the levels of inflammatory cytokines, protect the blood–brain barrier, inhibit apoptosis, promote neurogenesis, and upregulate brain-derived neurotrophic factor levels (Kim et al., 2005; Zhang et al., 2013). Li et al. found that exercise within 6–24 h after stroke increased the plasma levels of inflammatory cytokines, while the same exercise starting from the third day after stroke reduced the production of these cytokines (Li et al., 2017). Consistent with this, Tang et al. treated patients with AIS with di-3-n-butylphthalide from the third to the 14th day after disease onset and observed increased serum levels of VEGF and basic fibroblast growth factor after treatment (Tang et al., 2017). Therefore, in this study, all interventions started from the third day after disease onset.

Neurological changes after stroke are significantly associated with pro-inflammatory and anti-inflammatory cytokines (Yan et al., 2015). The imbalance and balance between these cytokines play a vital role in the processes of nerve injury and repair after stroke (Vila et al., 2000). Lin et al. found that IL-17A is released by γδT cells, peaks on day three after stroke, and aggravates ischemic brain injury (Lin et al., 2016). The TNF-α levels are significantly increased after AIS. This increase may lead to the activation of neutrophils, which enhances white blood cell phagocytosis, promotes the secretion of inflammatory cytokines, and eventually increases vascular permeability and aggravates edema (Camelo et al., 2001; Shi et al., 2017). In addition, VEGF-A stimulates the proliferation and migration of vascular endothelial cells, accelerates new blood vessel formation, and constructs a collateral circulation network that can save the ischemic penumbra (Lucitti et al., 2012). The neuroprotective effect of VEGF-A has also been observed in a rat model of middle cerebral artery embolization (Liang et al., 2020).

In this study, we found that the IL-17A, TNF-α, and VEGF-A plasma levels of patients with AIS on day three after disease onset were significantly higher than those of the healthy group. Both the IL-17A and TNF-α levels were significantly decreased, while the VEGF-A levels were significantly increased in the RG and SG after intervention. These findings were consistent with the studies by Lin et al. (2016), Tang et al. (2017), and Chen and Zhao (2018). Moreover, compared to the results obtained before intervention, the NIHSS scores were significantly decreased, while the scores of MMSE, FMA, and MBI were significantly increased in both groups of AIS patients on the 15th day after disease onset. Similarly, the study by Kattenstroth et al. showed that the rehabilitation including repetitive sensory stimulation was more effective than standard therapy alone in sensorimotor recovery (Kattenstroth et al., 2018). According to previous studies and our experimental results, the primary measures (the FMA scores) of the patient's function in the

TABLE 4 Correlations of cytokine levels with the results of each assessment scale.

| Cytokine | NIHSS (r/*p*) | MMSE (r/*p*) | FMA (r/*p*) | MBI (r/*p*) |
|---|---|---|---|---|
| IL-17A | 0.2664/0.003 | −0.3628/0.0001 | −0.2810/0.0017 | −0.3724/0.0001 |
| TNF-α | 0.3057/0.0006 | −0.4098/0.0001 | −0.3755/0.0001 | −0.4890/0.0001 |
| VEGF-A | −0.4137/0.0001 | 0.3784/0.0001 | 0.4848/0.0001 | 0.5231/0.0001 |

rehabilitation and stimulation groups exceeded the minimal clinically important difference (+5.2 points) after corresponding treatment, indicating not only statistical differences, but also clinical significance (Hsieh et al., 2007; Cervera et al., 2018). The correlation analysis showed that the IL-17A and TNF-α levels were negatively correlated with the MMSE, FMA, and MBI scores ($p < 0.01$), and the VEGF-A level was positively correlated with the MMSE, FMA, and MBI scores ($p < 0.01$). These results suggest that IL-17A and TNF-α may inhibit cognitive and motor recovery, while VEGF-A may alleviate brain injury and accelerate brain function recovery at an early stage following ischemic stroke, which is in line with the results from previous studies (Rreed et al., 2020; Zuo et al., 2022).

Data on the 15th day after disease onset showed that the NIHSS score was significantly decreased, while the MMSE, FMA, and MBI scores were significantly increased in both disease groups after intervention, which was consistent with the findings by Kattenstroth et al. (2018). In addition, the rehabilitation and stimulation groups showed significantly lower levels of IL-17A and TNF-α, which tended to be at normal range, and higher levels of VEGF-A, which deviated even more from normal after intervention. These results suggest that both conventional rehabilitation and MDSS therapy were effective in inhibiting the secretion of pro-inflammatory cytokines (i.e., IL-17A and TNF-α) and promoting the production of nerve regeneration factor VEGF-A, thereby reducing neurological impairment and accelerating cognitive and limb motor function recovery (Zhang et al., 2021; Cha et al., 2022). There was no significant difference in the IL-17A, TNF-α, and VEGF-A levels, or the NIHSS, MMSE, FMA, and MBI results between the rehabilitation and stimulation groups after intervention. Furthermore, the equivalent analysis of FMA changes showed that the motor function recovery of the stimulation group was non-inferior to the rehabilitation group. MDSS is essentially a pressure stimulation that can be considered as a variation of the Rood technique targeting the fingers and toes. The Rood technique is a multi-sensory stimulation therapy developed by Margaret Rood (Nielsen et al., 1986). It emphasizes the use of touch, squeeze, pull, vibration, percussion, and friction to produce different sensory stimulations, and to induce active muscle contraction while inhibiting antagonistic muscle contraction. Meanwhile, the Rood technique can input a variety of sensations into the central nervous system to improve the activity level of central neurons, thereby causing motor, cognitive, and other reactions, and promoting the recovery of neurological function (Bordoloi and Deka, 2019; Bordoloi and Deka, 2020; Chaturvedi and Kalani, 2023). In this study, DSS device was used to induce active retraction movements of the upper and lower limbs in patients with AIS by targeting the roots of the hemiplegic finger/toennail beds to produce tactile pressure sensation, mild pain sensation, and proprioception stimulation, which meet the definition of the Rood technique. Compared to stimulation on other parts of the body, stimulation of the fingertips and toetips, which are the most innervated regions, allows more specific targeting in the somatosensory cortical area (Kattenstroth et al., 2018). MDSS can achieve a good effect because the nerve endings and somatosensory receptors in fingers/toes are remarkably rich and sensitive. Appropriate mechanical stimulation of the fingers/toes on the hemiplegic side of patients with AIS can induce stronger excitement of the cerebral cortex and result in more limb movements, this can lead to a greater increase neuroplasticity and more significantly improvements in cognitive and motor functions compared to stimulation of other body part (Dobkin, 2003; Kattenstroth et al., 2018; Ayoobi et al., 2021). Conventional rehabilitation often requires expensive equipment (e.g., neuromuscular electrical stimulation), which costs a few hundred to tens of thousands of Chinese Yuan and takes 20–30 min per session. The DSS is a less-costly, safe, and user-friendly device and MDSS therapy only takes 70–120 s per session. In addition, our results showed that the VAS scores of all patients after MDSS were ≤6, and the mean VAS score of this cohort was $1.25 \pm 1.06$, indicating that the pain caused by MDSS was within the acceptable range for patients. More importantly, caregivers and family members can implement MDSS using the DSS after simple training, allowing MDSS application both in the ward and at home.

The present study has some limitations. Firstly, the long-term effects of MDSS remain unknown due to the short observation period. Secondly, the effects of MDSS on different subgroups were not explored because the sample size of this study was relatively small. Finally, the researchers were not blinded to grouping. To maintain experimental rigor, it would be necessary to establish a group that does not receive rehabilitation treatment; however, such a group would be considered unethical. Further studies with larger sample sizes, more extended observation periods, and inclusion of patients with unclear consciousness due to AIS need to be performed, and the experiment should be blinded.

## 5. Conclusion

In conclusion, this randomized, controlled trial demonstrates that IL-17A and TNF-α play an inflammatory role in the acute and subacute stages of stroke and aggravate brain injury, while VEGF-A exerts a neuroprotective effect. MDSS inhibits the expressions of IL-17A and TNF-α, induces VEGF-A secretion, decreases the NIHSS score, and increases the MMSE, FMA, and MBI scores in patients with AIS. MDSS and conventional rehabilitation therapy enhance the neurological and motor functions of hemiplegic patients with AIS after 12 days of treatment, and the effectiveness of the two methods is comparable. Compared with conventional rehabilitation, MDSS is simpler, less time-consuming, less costly, and more suitable for hospital, community and home use.

## Data availability statement

The original contributions presented in the study are included in the article/Supplementary material, further inquiries can be directed to the corresponding authors.

## Ethics statement

The studies involving human participants were reviewed and approved by the Medical Ethics Committee of the Second Hospital of Anhui Medical University [Approval No. YX2020-030 (F1)]. The patients/participants provided their written informed consent to participate in this study.

## Author contributions

SZ, YY and PX: patient data collection. SZ: writing the first draft of the manuscript. TW, QW, XL and YH: study design, data analysis, and revising the manuscript. XS and CF: drawing the figures. XW and PQ: implementing rehabilitation treatment. All authors contributed to the article and approved the submitted version.

## Funding

This study was supported by the Scientific Research Fund Project from Anhui Academy of Translational Medicine (No. 2021zhyx-C50) and the Shenzhen Science and Technology Innovation Program (No. JCYJ20180305163652073).

## Acknowledgments

We extend our deepest thanks to the nurses and doctors of the hospital for their help with conducting the study. We also thank Medjaden Inc. for scientific editing of this manuscript.

## Conflict of interest

The authors declare that the research was conducted in the absence of any commercial or financial relationships that could be construed as a potential conflict of interest.

## Publisher's note

All claims expressed in this article are solely those of the authors and do not necessarily represent those of their affiliated organizations, or those of the publisher, the editors and the reviewers. Any product that may be evaluated in this article, or claim that may be made by its manufacturer, is not guaranteed or endorsed by the publisher.

## Supplementary material

The Supplementary material for this article can be found online at: https://www.frontiersin.org/articles/10.3389/fnins.2023.1134904/full#supplementary-material

## References

Arango-Dávila, C. A., Vera, A., Londoño, A. C., Echeverri, A. F., Cañas, F., Cardozo, C. F., et al. (2015). Soluble or soluble/membrane TNF-α inhibitors protect the brain from focal ischemic injury in rats. *Int. J. Neurosci.* 125, 936–940. doi: 10.3109/00207454.2014.980906

Arba, F., Quinn, T. J., Hankey, G. J., Lees, K. R., Wardlaw, J. M., Ali, M., et al. (2018). VISTA collaboration. Enlarged perivascular spaces and cognitive impairment after stroke and transient ischemic attack. *Int. J. Stroke* 13, 47–56. doi: 10.1177/1747493016666091

Aydin, S. (2015). A short history, principles, and types of ELISA, and our laboratory experience with peptide/protein analyses using ELISA. *Peptides* 72, 4–15. doi: 10.1016/j.peptides.2015.04.012

Ayoobi, F., Khalili, P., Azin, H., Shahrokhabadi, S., and Azin, M. (2021). Effects of tactile stimulation on the sensory, motor and cognitive function in people with multiple sclerosis. *Clin. Neurol. Neurosurg.* 205:106643. doi: 10.1016/j.clineuro.2021.106643

Bokhari, F. A., Shakoori, T. A., Butt, A., and Ghafoor, F. (2014). TNF-alpha: a risk factor for ischemic stroke. *J. Ayub Med. Coll. Abbottabad* 26, 111–114.

Bordoloi, K., and Deka, R. S. (2019). Effectiveness of home exercise program with modified rood's approach on muscle strength in post cerebral haemorrhagic individuals of Assam: a randomized trial. *Int. J. Theor. Phys.* 6, 231–239.

Bordoloi, K., and Deka, R. S. (2020). Modified Rood's approach and ability of independent selfcare in haemorrhagic stroke patients of Assam, India. *Int. J. Res. Med. Sci.* 8:1070. doi: 10.18203/2320-6012.ijrms20200783

Bustamante, A., Simats, A., Vilar-Bergua, A., García-Berrocoso, T., and Montaner, J. (2016). Blood/brain biomarkers of inflammation after stroke and their association with outcome: from C-reactive protein to damage-associated molecular patterns. *Neurotherapeutics* 13, 671–684. doi: 10.1007/s13311-016-0470-2

Camelo, S., Lafage, M., Galelli, A., and Lafon, M. (2001). Selective role for the p55 Kd TNF-alpha receptor in immune unresponsiveness induced by an acute viral encephalitis. *J. Neuroimmunol.* 113, 95–108. doi: 10.1016/s0165-5728(00)00427-6

Cervera, M. A., Soekadar, S. R., Ushiba, J., Millán, J., Liu, M., Birbaumer, N., et al. (2018). Brain-computer interfaces for post-stroke motor rehabilitation: a meta-analysis. *Ann. Clin. Transl. Neurol.* 5, 651–663. doi: 10.1002/acn3.544

Cha, B., Kim, J., Kim, J. M., Choi, J. W., Choi, J., Kim, K., et al. (2022). Therapeutic effect of repetitive transcranial magnetic stimulation for post-stroke vascular cognitive impairment: a prospective pilot study. *Front. Neurol.* 13:813597. doi: 10.3389/fneur.2022.813597

Chandrasekaran, S., Bickel, S., Herrero, J. L., Kim, J. W., Markowitz, N., Espinal, E., et al. (2021). Evoking highly focal percepts in the fingertips through targeted stimulation of sulcal regions of the brain for sensory restoration. *Brain Stimul.* 14, 1184–1196. doi: 10.1016/j.brs.2021.07.009

Chaturvedi, P., and Kalani, A. (2023). Motor rehabilitation of aphasic stroke patient: the possibility of Rood's approach. *Neural Regen. Res.* 18:551. doi: 10.4103/1673-5374.346467

Chen, Y., Huang, W., Li, Z., Duan, Y., Liang, Z., Zhou, H., et al. (2019). The effect of acupuncture on the expression of inflammatory factors TNF-α, IL-6,IL-1 and CRP in cerebral infarction: a protocol of systematic review and meta-analysis. *Medicine (Baltimore)* 98:e15408. doi: 10.1097/MD.0000000000015408

Chen, Y., and Zhao, Y. (2018). Curative efficacy of penehyclidine combined with edaravone on acute cerebral infarction and their effects on serum TNF-α and NDS score in rats. *Eur Rev Med Pharmaco.* 22, 223–228. doi: 10.26355/eurrev_201801_14121

Ciesla, N., Dinglas, V., Fan, E., Kho, M., Kuramoto, J., and Needham, D. (2011). Manual muscle testing: a method of measuring extremity muscle strength applied to critically ill patients. *J. Vis. Exp.* 12:2632. doi: 10.3791/2632

Coleman, E. R., Moudgal, R., Lang, K., Hyacinth, H. I., Awosika, O. O., Kissela, B. M., et al. (2017). Early rehabilitation after stroke: a narrative review. *Curr. Atheroscler. Rep.* 19:59. doi: 10.1007/s11883-017-0686-6

Dawson, J., Liu, C. Y., Francisco, G. E., Cramer, S. C., Wolf, S. L., Dixit, A., et al. (2021). Vagus nerve stimulation paired with rehabilitation for upper limb motor function after

ischaemic stroke (VNS-REHAB): a randomised, blinded, pivotal, device trial. *Lancet* 397, 1545–1553. doi: 10.1016/S0140-6736(21)00475-X

Dobkin, B. H. (2003). Do electrically stimulated sensory inputs and movements lead to long-term plasticity and rehabilitation gains? *Curr. Opin. Neurol.* 16, 685–691. doi: 10.1097/01.wco.0000102622.38669.ac

Eble, J. A. (2018). Titration ELISA as a method to determine the dissociation constant of receptor ligand interaction. *J. Vis. Exp.* 132:57334. doi: 10.3791/57334

Fugl-Meyer, A. R., Jääskö, L., Leyman, I., Olsson, S., and Steglind, S. (1975). The post-stroke hemiplegic patient. 1. A method for evaluation of physical performance. *Scand. J. Rehabil. Med.* 7, 13–31.

Hsieh, Y. W., Wang, C. H., Wu, S. C., Chen, P. C., Sheu, C. F., and Hsieh, C. L. (2007). Establishing the minimal clinically important difference of the Barthel index in stroke patients. *Neurorehabil. Neural Repair* 21, 233–238. doi: 10.1177/1545968306294729

Kattenstroth, J. C., Kalisch, T., Sczesny-Kaiser, M., Greulich, W., Tegenthoff, M., and Dinse, H. R. (2018). Daily repetitive sensory stimulation of the paretic hand for the treatment of sensorimotor deficits in patients with subacute stroke: RESET, a randomized, sham-controlled trial. *BMC Neurol.* 18:2. doi: 10.1186/s12883-017-1006-z

Kawabori, M., and Yenari, M. A. (2015). Inflammatory responses in brain ischemia. *Curr. Med. Chem.* 22, 1258–1277. doi: 10.2174/0929867322666150209154036

Kim, M. W., Bang, M. S., Han, T. R., Ko, Y. J., Yoon, B. W., Kim, J. H., et al. (2005). Exercise increased BDNF and trkB in the contralateral hemisphere of the ischemic rat brain. *Brain Res.* 1052, 16–21. doi: 10.1016/j.brainres.05.070

Körver, S., Schraaf, S. A. J., Geurtsen, G. J., Hollak, C. E. M., van Schaik, I. N., and Langeveld, M. (2019). The Mini mental state examination does not accurately screen for objective cognitive impairment in Fabry disease. *JIMD Rep.* 48, 53–59. doi: 10.1002/jmd2.12036

Lambertsen, K. L., Biber, K., and Finsen, B. (2012). Inflammatory cytokines in experimental and human stroke. *J. Cereb. Blood Flow Metab.* 32, 1677–1698. doi: 10.1038/jcbfm.2012.88

Lambertsen, K. L., Finsen, B., and Clausen, B. H. (2019). Post-stroke inflammation-target or tool for therapy? *Acta Neuropathol.* 137, 693–714. doi: 10.1007/s00401-018-1930-z

Li, F., Pendy, J. T. Jr., Ding, J. N., Peng, C., Li, X., Shen, J., et al. (2017). Exercise rehabilitation immediately following ischemic stroke exacerbates inflammatory injury. *Neurol. Res.* 39, 530–537. doi: 10.1080/01616412.2017.1315882

Liang, C., Ni, G. X., Shi, X. L., Jia, L., and Wang, Y. L. (2020). Astragaloside IV regulates the HIF/VEGF/Notch signaling pathway through miRNA-210 to promote angiogenesis after ischemic stroke. *Restor. Neurol. Neurosci.* 38, 271–282. doi: 10.3233/RNN-201001

Lin, Y., Zhang, J. C., Yao, C. Y., Wu, Y., Abdelgawad, A. F., Yao, S. L., et al. (2016). Critical role of astrocytic interleukin-17 A in post-stroke survival and neuronal differentiation of neural precursor cells in adult mice. *Cell Death Dis.* 7:e2273. doi: 10.1038/cddis.2015.284

Liu, T., Han, S., Dai, Q., Zheng, J., Liu, C., Li, S., et al. (2019). IL-17A-mediated excessive autophagy aggravated neuronal ischemic injuries via Src-PP2B-mTOR pathway. *Front. Immunol.* 10:2952. doi: 10.3389/fimmu.2019.02952

Lucitti, J. L., Mackey, J. K., Morrison, J. C., Haigh, J. J., Adams, R. H., and Faber, J. E. (2012). Formation of the collateral circulation is regulated by vascular endothelial growth factor-a and a disintegrin and metalloprotease family members 10 and 17. *Circ. Res.* 111, 1539–1550. doi: 10.1161/CIRCRESAHA.112.279109

Lyden, P. (2017). Using the National Institutes of Health stroke scale: a cautionary tale. *Stroke* 48, 513–519. doi: 10.1161/STROKEAHA.116.015434

Ma, Y., Zechariah, A., Qu, Y., and Hermann, D. M. (2012). Effects of vascular endothelial growth factor in ischemic stroke. *J. Neurosci. Res.* 90, 1873–1882. doi: 10.1002/jnr.23088

Metzger, J.-C., Lambercy, O., Califfi, A., Dinacci, D., Petrillo, C., Rossi, P., et al. (2014). Assessment-driven selection and adaptation of exercise difficulty in robot-assisted therapy: a pilot study with a hand rehabilitation robot. *J. Neuroeng. Rehabil.* 11:154. doi: 10.1186/1743-0003-11-154

Moon, S., Chang, M., Koh, S., and Choi, Y. K. (2021). Repair mechanisms of the neurovascular unit after ischemic stroke with a focus on VEGF. *Int. J. Mol. Sci.* 22:8543. doi: 10.3390/ijms22168543

Nakamura, K., and Shichita, T. (2019). Cellular and molecular mechanisms of sterile inflammation in ischaemic stroke. *J. Biochem.* 165, 459–464. doi: 10.1093/jb/mvz017

Nielsen, A. J., Grady, S., Sussman, C., Henry, M., Feichtmann, C., Dodge, M., et al. (1986). A brushup on Rood's technique. *Phys. Ther.* 66, 579–580. doi: 10.1093/ptj/66.4.579b

Novotny, V., Aarli, S. J., Netland, K. A., Bjerkreim, A. T., Elnan, K. C., Fromm, A., et al. (2021). Clinical manifestation of acute cerebral infarcts in multiple arterial territories. *Brain Behav.* 11:e2296. doi: 10.1002/brb3.2296

Powers, W. J., Rabinstein, A. A., Ackerson, T., Adeoye, O. M., Bambakidis, N. C., Becker, K., et al. (2019). Guidelines for the early management of patients with acute ischemic stroke: 2019 update to the 2018 guidelines for the early Management of Acute Ischemic Stroke: a guideline for healthcare professionals from the American Heart Association/American Stroke Association. *Stroke* 50, e344–e418. doi: 10.1161/STR.0000000000000211

Ranzani, R., Lambercy, O., Metzger, J. C., Califfi, A., Regazzi, S., Dinacci, D., et al. (2020). Neurocognitive robot-assisted rehabilitation of hand function: a randomized control trial on motor recovery in subacute stroke. *J. Neuroeng. Rehabil.* 17:115. doi: 10.1186/s12984-020-00746-7

Rreed, M. D., Yim, Y. S., Wimmer, R. D., Kim, H., Ryu, C., Welch, G. M., et al. (2020). IL-17a promotes sociability in mouse models of neurodevelopmental disorders. *Nature* 577, 249–253. doi: 10.1038/s41586-019-1843-6

Shelton, F. D., Volpe, B. T., and Reding, M. (2001). Motor impairment as a predictor of functional recovery and guide to rehabilitation treatment after stroke. *Neurorehabil. Neural Repair* 15, 229–237. doi: 10.1177/154596830101500311

Shi, X., Yu, W., Liu, L., Liu, W., Zhang, X., Yang, T., et al. (2017). Panax notoginseng saponins administration modulates pro-/anti-inflammatory factor expression and improves neurologic outcome following permanent MCAO in rats. *Metab. Brain Dis.* 32, 221–233. doi: 10.1007/s11011-016-9901-3

Sung, Y. T., and Wu, J. S. (2018). The visual analogue scale for rating, ranking and paired-comparison (VAS-RRP): a new technique for psychological measurement. *Behav. Res. Methods* 50, 1694–1715. doi: 10.3758/s13428-018-1041-8

Taghizadeh, G., Martinez-Martin, P., Meimandi, M., Habibi, S., Jamali, S., Dehmiyani, A., et al. (2020). Barthel index and modified Rankin scale: psychometric properties during medication phases in idiopathic Parkinson disease. *Ann. Phys. Rehabil. Med.* 63, 500–504. doi: 10.1016/j.rehab.2019.08.006

Tang, S. C., Luo, C. J., Zhang, K. H., Li, K., Fan, X. H., Ning, L. P., et al. (2017). Effects of dl-3-n-butylphthalide on serum VEGF and bFGF levels in acute cerebral infarction. *Eur. Rev. Med. Pharmacol. Sci.* 21, 4431–4436.

Tsivgoulis, G., Zand, R., Katsanos, A. H., Turc, G., Nolte, C. H., Jung, S., et al. (2016). Risk of symptomatic intracerebral hemorrhage after intravenous thrombolysis in patients with acute ischemic stroke and high cerebral microbleed burden: a meta-analysis. *JAMA Neurol.* 73, 675–683. doi: 10.1001/jamaneurol.2016.0292

Vila, N., Castillo, J., Davalos, A., and Chamorro, A. (2000). Proinflammatory cytokines and early neurological worsening in ischemic stroke. *Stroke* 31, 2325–2329. doi: 10.1161/01.str.31.10.2325

Wagner, J. M., Rhodes, J. A., and Patten, C. (2008). Reproducibility and minimal detectable change of three-dimensional kinematic analysis of reaching tasks in people with hemiparesis after stroke. *Phys. Ther.* 88, 652–663. doi: 10.2522/ptj.20070255

Walker, E., and Nowacki, A. S. (2011). Understanding equivalence and noninferiority testing. *J. Gen. Intern. Med.* 26, 192–196. doi: 10.1007/s11606-010-1513-8

Xu, P., Zhang, S., Kan, X., Shen, X., Mao, J., Fang, C., et al. (2022). Changes and roles of IL-17A, VEGF-A and TNF-α in patients with cerebral infarction during the acute phase and early stage of recovery. *Clin. Biochem.* 107, 67–72. doi: 10.1016/j.clinbiochem.2022.05.001

Yan, T., Chopp, M., and Chen, J. (2015). Experimental animal models and inflammatory cellular changes in cerebral ischemic and hemorrhagic stroke. *Neurosci. Bull.* 31, 717–734. doi: 10.1007/s12264-015-1567-z

Zhang, X. F., Xiang, S. Y., Lu, J., Li, Y., Zhao, S. J., Jiang, C. W., et al. (2021). Electroacupuncture inhibits IL-17/IL-17R and post-receptor MAPK signaling pathways in a rat model of chronic obstructive pulmonary disease. *Acupunct. Med.* 39, 663–672. doi: 10.1177/0964528421996720

Zhang, Y., Zhang, P., Shen, X., Tian, S., Wu, Y., Zhu, Y., et al. (2013). Early exercise protects the blood-brain barrier from ischemic brain injury via the regulation of MMP-9 and occludin in rats. *Int. J. Mol. Sci.* 14, 11096–11112. doi: 10.3390/ijms140611096

Zuo, C., Ma, J., Pan, Y., Zheng, D., Chen, C., Ruan, N., et al. (2022). Isoflurane and sevoflurane induce cognitive impairment in neonatal rats by inhibiting neural stem cell development through microglial activation, neuroinflammation, and suppression of VEGFR2 signaling pathway. *Neurotox. Res.* 40, 775–790. doi: 10.1007/s12640-022-00511-9

frontiers | Frontiers in Neuroscience

TYPE Brief Research Report
PUBLISHED 25 May 2023
DOI 10.3389/fnins.2023.1116273



OPEN ACCESS

EDITED BY
Jie Jia,
Fudan University, China

REVIEWED BY
Ying Shen,
The First Affiliated Hospital of Nanjing Medical University, China
Stephanie Lefebvre,
University of Bern, Switzerland

*CORRESPONDENCE
Amit Mehndiratta
✉ amit.mehndiratta@keble.oxon.org

RECEIVED 05 December 2022
ACCEPTED 09 May 2023
PUBLISHED 25 May 2023

CITATION
Singh N, Saini M, Kumar N, Padma Srivastava M and Mehndiratta A (2023) Individualized closed-loop TMS synchronized with exoskeleton for modulation of cortical-excitability in patients with stroke: a proof-of-concept study.
*Front. Neurosci.* 17:1116273.
doi: 10.3389/fnins.2023.1116273



# Individualized closed-loop TMS synchronized with exoskeleton for modulation of cortical-excitability in patients with stroke: a proof-of-concept study

Neha Singh[1], Megha Saini[1], Nand Kumar[2], M. V. Padma Srivastava[3] and Amit Mehndiratta[1,4]*

[1]Centre for Biomedical Engineering, Indian Institute of Technology, New Delhi, India, [2]Department of Psychiatry, All India Institute of Medical Sciences (AIIMS), New Delhi, India, [3]Department of Neurology, AIIMS, New Delhi, India, [4]Department of Biomedical Engineering, AIIMS, New Delhi, India

**Background:** Repetitive TMS is used in stroke rehabilitation with predefined passive low and high-frequency stimulation. Brain State-Dependent Stimulation (BSDS)/Activity-Dependent Stimulation (ADS) using bio-signal has been observed to strengthen synaptic connections. Without the personalization of brain-stimulation protocols, we risk a one-size-fits-all approach.

**Methods:** We attempted to close the ADS loop via intrinsic-proprioceptive (via exoskeleton-movement) and extrinsic-visual-feedback to the brain. We developed a patient-specific brain stimulation platform with a two-way feedback system, to synchronize single-pulse TMS with exoskeleton along with adaptive performance visual feedback, in real-time, for a focused neurorehabilitation strategy to voluntarily engage the patient in the brain stimulation process.

**Results:** The novel TMS Synchronized Exoskeleton Feedback (TSEF) platform, controlled by the patient's residual Electromyogram, simultaneously triggered exoskeleton movement and single-pulse TMS, once in 10s, implying 0.1Hz frequency. The TSEF platform was tested for a demonstration on three patients ($n$=3) with different spasticity on the Modified Ashworth Scale (MAS=1, 1+, 2) for one session each. Three patients completed their session in their own timing; patients with (more) spasticity tend to take (more) inter-trial intervals. A proof-of-concept study on two groups—TSEF-group and a physiotherapy control-group was performed for 45min/day for 20-sessions. Dose-matched Physiotherapy was given to control-group. Post 20 sessions, an increase in ipsilesional cortical-excitability was observed; Motor Evoked Potential increased by ~48.5μV at a decreased Resting Motor Threshold by ~15.6%, with improvement in clinical scales relevant to the Fugl-Mayer Wrist/Hand joint (involved in training) by 2.6units, an effect not found in control-group. This strategy could voluntarily engage the patient.

**Conclusion:** A brain stimulation platform with a real-time two-way feedback system was developed to voluntarily engage the patients during the brain stimulation process and a proof-of-concept study on three patients indicates clinical gains with increased cortical excitability, an effect not observed in the control-group; and the encouraging results nudge for further investigations on a larger cohort.

KEYWORDS

stroke, transcranial magnetic stimulation, exoskeleton, closed-loop brain stimulation, neuro-rehabilitation, motor evoked potential, spasticity

## 1. Introduction

Repetitive-Transcranial Magnetic Stimulation (rTMS) is a potential therapeutic modality post-stroke that can facilitate neuroplasticity through the process of restoration of transcallosal interhemispheric inhibition by targeting Long-Term-Potentiation (LTP) and Long-Term-Depression (LTD) through high-frequency stimulation of the ipsilesional and low-frequency stimulation of contralesional-hemisphere, respectively (Hoogendam et al., 2010; Thabit et al., 2010; Edwardson et al., 2013, 2014; Rossini et al., 2015). However, these rTMS frequencies are predefined (such as 1/5/10 Hz) and involve a non-specific, passive-stimulation process where the patient lies in the TMS chair comfortably with the TMS coil on the head. Since, the patient is not voluntarily involved in the brain-stimulation protocol, at times; the patient is not responsive to treatment or might even be asleep during the sessions. The predefined frequencies used are independent of the current brain-state of the patient and do not engage the patient voluntarily or directly in the brain stimulation protocol (Edwardson et al., 2013). The whole passive-stimulation process lacks feedback to the patient, hence, is referred to as an open-loop therapeutic approach. Various factors being the determinant of the therapeutic outcomes apart from brain stimulation parameters (such as phase, frequency, and intensity), its effect is also highly dependent on the current-states of the brain, and without personalization of brain-stimulation protocols, we assume an one-size-fits-all approach (Mitchell et al., 2007; Edwardson et al., 2013).

Unlike these open-loop approaches, Brain-State-Dependent-Stimulation (BSDS) or Activity-Dependent Brain Stimulation (ADS) paradigm is an alternative that employs a closed-loop approach to facilitate focused neuroplasticity. Neuroplastic changes presumably occur in connections between motor cortical neurons firing naturally during the generation of voluntary muscle-contraction and those artificially stimulated by brain stimulation, a mechanism of hebbian plasticity (Gerstner, 2011; Edwardson et al., 2013, 2014). LTP can also be induced by pairing protocols, e.g., associative or hebbian LTP, which allows activity-dependent modification of synaptic-strength by synchronous activation of neurons which is the basis of learning and memory (Martin et al., 2000; Thabit et al., 2010; Edwardson et al., 2013). ADS entails making brain stimulation contingent on voluntary neural/muscle activity and hence, the brain is stimulated depending on its current state using the bio-signal (neural or muscle-activity), as opposed to a fixed frequency in an open-loop approach in rTMS, providing a method of invoking Hebbian mechanism by pairing each episode of motor-activity, and brain stimulation (Edwardson et al., 2013, 2014; Gharabaghi et al., 2014; Kraus et al., 2016; Mrachacz-Kersting et al., 2019).

Different cellular investigations evidenced that the connections between the two neurons are strengthened when the firing of one neuron repeatedly contributes to the firing of another neuron (Bi and Poo, 1998, 2001; Feldman, 2000). A similar effect was demonstrated with stimulation of the median nerve at the wrist paired with TMS, in healthy subjects, which can lead to LTP or LTD-like effects, depending on their relative timing (Jung and Ziemann, 2009). Compelling evidence exists in favor of the ADS paradigm documenting potentiating effects and consistent strengthening of specific connections between neurons in the motor cortex in animals such as primates (Jackson et al., 2006) and rodents-models (Rebesco et al., 2010; Edwardson et al., 2013). Primates' animal studies evidenced that triggering motor cortex stimulation from contralateral muscle-activity produces neuroplasticity effects. Activity-dependent single-pulse TMS on healthy subjects (Bütefisch et al., 2004; Thabit et al., 2010; Edwardson et al., 2014), and even in stroke survivors (Bütefisch et al., 2004; Izumi et al., 2008; Buetefisch et al., 2011) has also been started in the last 2 decades, evidencing induced motor learning (Bütefisch et al., 2004), increased cortical-excitability (Thabit et al., 2010), and subtle evidence of neuroplasticity (Buetefisch et al., 2011). These rare seminal studies indicated the feasibility of Activity-Dependent single-pulse TMS, where motor activity from affected-hand triggers TMS to the lesioned motor cortex. These studies also indicate the importance of ADS in designing protocols to capitalize on the unique physiology resulting in robust neuroplasticity (Edwardson et al., 2013).

These studies used stimulation in strict temporal relation with the movement attempted which showed increased cortical-excitability, demonstrating the ability of Electroencephalogram (EEG)/Electromyogram (EMG) signal stimulating the brain to drive the cortical-plasticity with LTP-like effects (Bütefisch et al., 2004; Thabit et al., 2010; Edwardson et al., 2013, 2014; Schaworonkow et al., 2018). The studies on stroke-survivors (for one or more sessions) are present in which stimulation is used in strict temporal relation with the movement attempted (Izumi et al., 2008; Buetefisch et al., 2011; Walter et al., 2012; Gharabaghi et al., 2014; Kraus et al., 2016; Mrachacz-Kersting et al., 2019; Wu et al., 2019). However, these studies were "ADS" only in terms of using their bio-signal for triggering brain stimulation. Very few studies have attempted to close the loop in ADS "via feedback," a crucial phenomenon in stroke rehabilitation (Buetefisch et al., 2011; Gomez-Rodriguez et al., 2011; Gharabaghi et al., 2014). In addition, out of these studies showing the effect of closed-loop ADS in healthy subjects (Izumi et al., 2008) as well as chronic stroke-population, over one or more sessions, only few studies have evaluated the therapeutic-effectiveness of Activity Dependent TMS on stroke patients (Buetefisch et al., 2011; Revill et al., 2020). Even though ADS studies are documented in literature, its effect with various types of feedback is not explored. Moreover, ADS can encourage impairment oriented functional-plasticity by focusing on the impaired and functionally important muscle such as Extensor Digitorum Communis (EDC), by stimulating its respective cortical-representation, for a focused rehabilitation strategy unlike stimulating Abductor Pollicis Brevis (APB) muscle used commonly (Thabit et al., 2010; Edwardson et al., 2013).

Spasticity and Flexor-Hypertonia (FH), which is one of the most common symptoms of stroke, leads to impaired Activities of daily-living (ADL). If not rehabilitated, may cause deformities, and even contractures and can further hinder any therapeutic intervention. Reducing the spasticity of muscles is the initial step in stroke rehabilitation followed by the ADL-training (Singh et al., 2019a). If a patient with spasticity has to be involved in a therapy that is meant to be voluntary and with movement, therapy should take the spasticity as a critical consideration. Till now, no brain stimulation study has considered the spasticity factor in the intervention protocol or evaluated the therapeutic effectiveness of BSDS focusing on spasticity. Spasticity is an important challenge and rarely discussed obstacle in stroke-rehabilitation literature, which might be pertaining to the challenges involved in dealing with spasticity in patients with stroke.

For making the brain stimulation contingent on voluntary muscle-activity, we designed an Activity-dependent TMS system with a two-way feedback novel protocol individualized for patients with different spasticity. We attempted to close the ADS-loop via feedback to the brain through proprioceptive and visual feedback, to voluntarily involve the patient throughout the process. Our hypothesis was if providing brain stimulation while the motor cortex is engaged in generating movement, providing proprioceptive feedback (via exoskeleton-device; Singh et al., 2019a) to the brain by assisting the voluntary-attempted movement, along with visual performance-feedback, in real-time, could potentially improve post-stroke motor-recovery. For motor training, an exoskeleton device (Singh et al., 2019a) was used which can assist the patient in completing the movement, giving proprioceptive feedback to the brain. Considering the criticality of spasticity and feedback in stroke-rehabilitation, and most importantly individualization of the TMS protocols, our goal was to design and develop a novel customized brain-stimulation platform that can be patient-specific according to their clinical presentation, establish the patient-specific novel protocol, perform demonstration study, and at last carry out the feasibility-study for patients with stroke, WRT control group for 20-sessions and take the subjective-feedback of patients.

# 2. Materials and methods

For an Activity-Dependent TMS system with a feedback approach, the fundamental assumptions of system design are: (i) the patient needs to be directly and actively engaged during the brain stimulation protocol to generate voluntary bio-signal and (ii) TMS must be induced/ triggered by bio-signal generating the voluntary movement. This intention of the voluntary movement (is detected in the bio-signal) was synchronized with TMS, making the process of brain stimulation dependent on the current state of the brain. To entail the patient voluntarily in the therapeutic intervention, an exoskeleton device (Singh et al., 2019a) was used to assist to complete the movement attempted as and when intended by the patient. IRB approved the study (protocol-number-IEC/NP-99/13.03.2015) and a pilot study was registered (ISRCTN95291802). All patients signed the written informed consent. The study was designed in clinical settings and a clear description of the method and the intervention is presented below.

## 2.1. Aim of the study

The aim of this novel customized platform was that once the intention of the movement is detected through bio-signal, it triggers both the TMS-pulse and the exoskeleton device. Hence, we designed a system pairing each episode of voluntary motor activity with TMS, where the motor activity from the affected hand of the patient triggers TMS to the lesioned motor cortex. The goal of this study was to design and develop a platform with a novel protocol and perform a demonstration study along with a feasibility-study wrt control group.

## 2.2. Materials

### 2.2.1. Muscle-selection

The Extensor Digitorum Communis (EDC) muscle of affected-hand was chosen (Figure 1A) as this muscle is often impaired in stroke due to flexor-hypertonia leading to spasticity, also because of its critical involvement in ADL for wrist extension, and easily detectable nature of surface-muscle (Singh et al., 2019a). The disposable gel-based wet Ag/AgCl surface-electrodes were used on the belly-tendon configuration; muscle-contraction causing extension of wrist and extension of third-digit of hand was observed for identification of muscle-belly and electrodes-placement. Electrodes were connected to an EMG amplifier (BIOPAC-MP150, Gentech; Figure 1B).

### 2.2.2. Configuration of EMG threshold

A 20% of Maximum Voluntary Contraction (MVC) of each patient's residual EMG-activity was considered as predefined activation-threshold. This activation threshold was set on the Root-Mean-Square (RMS) of the EMG signal of the affected hand and represented target muscle activation (Figure 1B). The activation threshold of RMS-EMG was used to simultaneously trigger exoskeleton-device and single-pulse TMS, whenever voluntary effort-induced EMG activity crossed the predefined threshold. Configurability of the residual EMG, activation threshold, RMS amplitude, and RMS EMG threshold was customized individually for affected-hand according to the individual's residual EMG activity, with the advantage of making the system patient-specific and ensuring patients with even minimal EMG activity can be involved in the voluntary brain-stimulation protocol.

### 2.2.3. Exoskeleton device

Electromyogram-triggered exoskeleton device was developed for rehabilitation of wrist-joint and fingers-joint (Singh et al., 2019a; Figure 1A) and used to move the affected-hand as-and-when intended in the brain-stimulation protocol. EDC muscle activity was chosen to trigger the exoskeleton device whenever the patient made the voluntary effort to extend the wrist. In the baseline position, the patient is instructed to put effort into wrist extension. The sequence of motion of the exoskeleton device was: wrist at the neutral position, finger-extension (baseline-position, Supplementary material) → wrist-extension and finger-flexion (final-position, Supplementary material) → wrist at neural position and finger-extension (back to the baseline-position). The range of Motion (ROM) of exoskeleton-device are customizable according to the comfort and clinical presentation (spasticity, contractures, and pain) of the patient, pertaining to one of the features of the exoskeleton device, hence, can accommodate a large

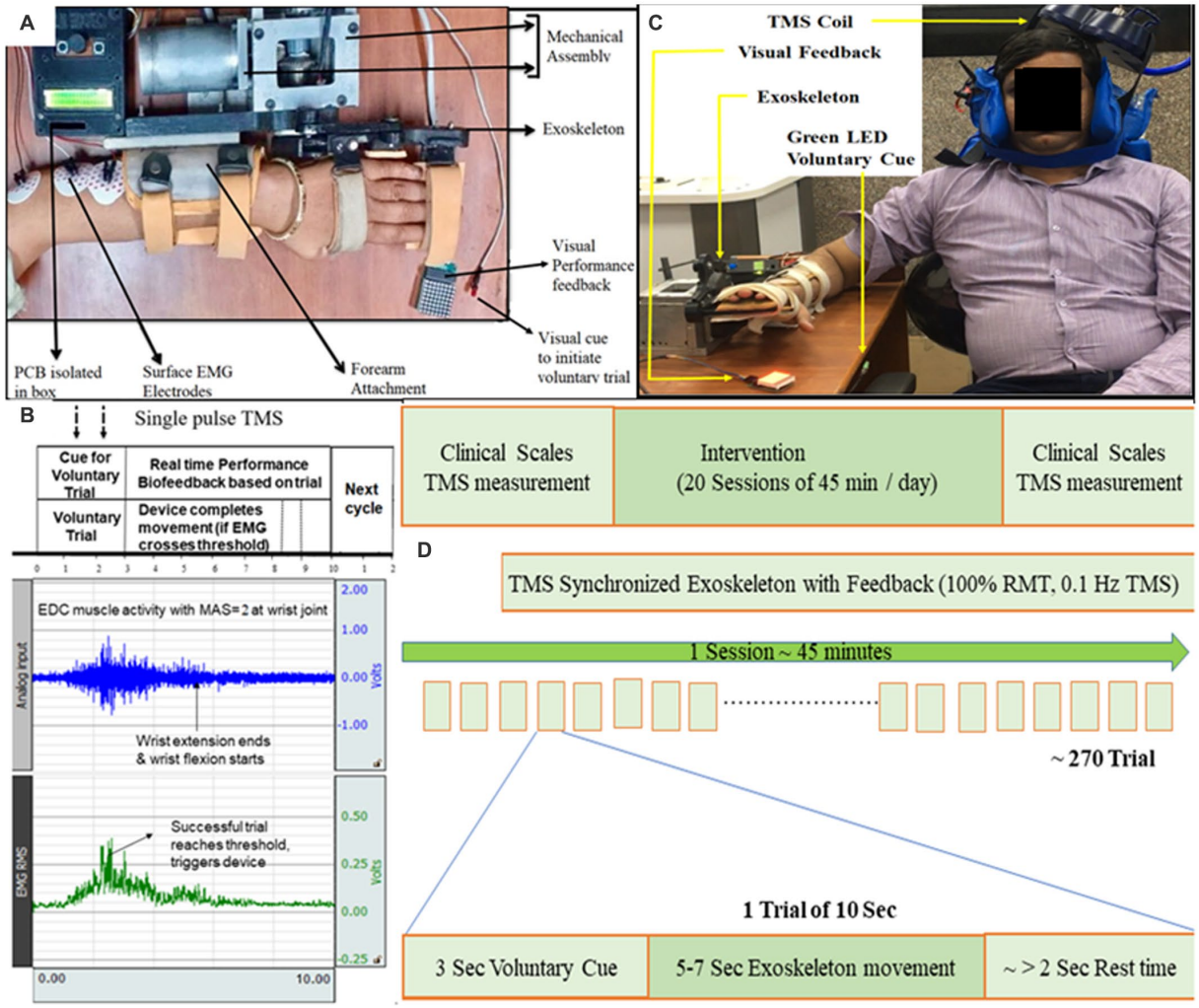


FIGURE 1
**(A)** Exoskeleton mounted on the hand of a representative patient. Baseline position: wrist in neutral position with fingers extension. Final position: wrist extension with fingers flexion. Motion sequence: Baseline to Final to Baseline position. **(B)** Protocol showing EMG activity during a 10-s trial. 10s included a "voluntary cue" for attempting the wrist extension (3s), completing movement (5–7s), and remaining as the "rest-time" (remaining in 10s). Raw EMG signal (blue, sampling frequency of 1,000Hz and gain=2,000) was filtered (Bandpass-filter=20–500Hz, Notch-filter=50Hz), amplified and Root Mean Square (RMS; green) was calculated. The patient's effort detected in EMG simultaneously triggered the exoskeleton device and TMS-pulse; TMS-pulse was delivered within the first half of the EMG burst generated by EDC (within the time of voluntary-trial time) as soon as the predefined activation threshold on RMS-EMG is crossed. If the threshold is not reached by the patient, the 10-s trial starts again. The effort made by the patient (detected in EMG) is directly proportional to the visual feedback (LED Dot Matrix; **C**) Set-up for TMS synchronized with exoskeleton-device, TMS coil being set to TMS hotspot being EDC muscle cortico-representation. **(D)** Study design of TSEF for patients with stroke (*n*=3).

patient population. The exoskeleton device is used for developing a platform for synchronizing TMS with the exoskeleton.

## 2.3. Participants

Patients were enrolled based on inclusion criteria: age 18–70 years, having ischemic/hemorrhagic stroke within 3–24 months, Mini-Mental Scale (MMS) = 24–30; Barthel-Index (BI) = 0–100, and Modified-Ashworth-Scale (MAS) = 1, 1 +, 2. MAS was used to measure spasticity at wrist-joint (Gregson et al., 1999; Takahashi et al., 2008; Sale et al., 2014; Singh et al., 2021). Three patients were enrolled, one patient each on MAS 1, MAS 1+, and MAS 2. Patients with contra-indication to TMS, no detectable Electromyogram (EMG) activity, and any other progressive neurological or cognitive disorders were excluded from the study. All patients signed the written informed consent. All patients were given care according to current clinical standards, as advised by the IRB. Three different persons executed three different aspects, applied the intervention, assessed the clinical data, and analyzed it; blinded to other's observations with patients.

## 2.4. Data collection

All the participants underwent clinical assessment by a trained physiotherapists with more than 5 years of experience; a pre-therapy assessment a day before the initiation of the intervention sessions. The post-therapy assessment was performed

a day after the completion of the intervention. The level of spasticity at the wrist joint measured by the MAS (MAS 0–4), the range of voluntary wrist movement defined in terms of the Passive Range of motion of the wrist (PROM 0–70 degrees) as measured by a goniometer, Barthel Index (0–100), and functional and sensorimotor-control of upper-limb as measured by Fugl-Meyer Scale Upper Limb (FMU/L 0–66) for whole arm, later segregated into its wrist hand (FMW/H) and shoulder elbow (FMS/E) components.

Cortical excitability was measured in terms of Resting Motor-Threshold (RMT) and Motor Evoked Potential (MEP) amplitude using Transcranial Magnetic Stimulation (TMS) over ipsilesional according to the standard protocol (Thair et al., 2017) on cortical representation area of EDC muscle between Cz and C3/C4 of the contralateral primary motor cortex with reference to the Electroencephalogram (EEG) cap. RMT was defined as the minimum intensity of TMS required to elicit an MEP in the target contralateral-muscle in five out of 10 trials, recorded in EMG, over the muscle cortical representation in the primary motor cortex. MEP obtained can be recorded as EMG activity in a target contralateral muscle. MEP encapsulates information relevant to the cortical excitability of the brain providing insights into membrane excitability of neurons, conduction and functional integrity of cortico-spinal tract, and neuromuscular junctions and is of prognostic importance in disease monitoring (Singh et al., 2019b). MEP should be $\geq 50\,\mu v$ peak-to-peak amplitude at the hotspot in five out of 10 consecutive trials. The five MEP signals were then averaged for reporting.

## 2.5. Experimental set-up

The patient sat comfortably in the chair, kept forearm pronated, elbow joint at 90–120° flexion, wrist joint at a neutral position, and fingers at rest. The disposable gel-based wet Ag/AgCl surface electrodes were used in a bipolar configuration in which active electrodes were placed on the muscle belly of EDC with a center-to-center inter-electrode distance of 20 mm and the ground electrode was placed on the lateral epicondyle. Muscle contraction causing extension of the third digit of the hand was observed for identification of muscle belly and electrode placement. Electrodes were connected to the EMG amplifier and with TMS [type-D70 (AC), serial no. 0326, Magstim Rapid$^2$, United Kingdom]. Specific hotspot for the EDC muscle was determined. Single-pulse TMS stimuli at the Resting motor threshold (RMT) were applied with the procedure widely used, using a flat 70 mm figure-of-eight coil placed tangentially with the handle pointing toward the back, 90° to the central sulcus and 45° to the midsagittal line for transsynaptic activation of the corticospinal tract (Rossini et al., 2015). TMS-stimuli were delivered by moving the coil in millimeters in all directions until the hotspot, producing maximum MEP response, was localized. Cortical-excitability once the hotspot was localized, RMT was measured by progressively increasing the Maximum Stimulator Output (MSO) starting from stimulus intensity of 35% in steps of 2–5% until a reliable MEP (>50 μV peak-to-peak) appears (Rothwell et al., 1999). Then, MSO is lowered in steps of 1% until there are five consecutive responses out of 10 trials. Each pulse was given at an interval between each stimulus of >5 s (Rossini et al., 2015).

## 2.6. Experimental protocol

Once the patient with spasticity is comfortable with the exoskeleton device mounted on the affected hand and can voluntarily make an effort for wrist extension, TMS-coil was set on the "hotspot" of EDC-muscle cortical-representation marked during RMT acquisition. Once the MEP was determined at the hotspot, the location of the hotspot was measured (with measuring tape) wrt nasion, inion, pre-auricular point, and Cz. The location of the hotspot was also noted on the 10–20 system EEG cap to maintain the position across the sessions. The stability of the hotspot of EDC muscle throughout the experiment was ensured by marking the area with a permanent marker (Werhahn et al., 1994; Awiszus, 2003; Thair et al., 2017; Singh et al., 2019b). The primary requirement of system hardware is to simultaneously trigger the TMS pulse and the exoskeleton-device, once the intention of the movement is detected in EMG. EMG-acquisition-system connected to the custom-designed hardware having a novel algorithm detects if the predefined activation threshold is crossed. Once the threshold is crossed, it simultaneously actuates the exoskeleton device and sends a Transistor-Transistor Logic (TTL) pulse to the TMS machine for generating a single-pulse TMS, in real-time.

The protocol had each motion trial fixed to 10 s that included a "voluntary-cue" for attempting the wrist extension (3 s), completing movement (5–7 s, depending on the motion parameters chosen based on clinical presentation), and remaining as the "rest-time" (remaining in 10-s; Figures 1B,C). During each 10-s trial, if (only) the voluntary effort is made within the voluntary-cue (3 s) and crosses the predefined EMG-activation-threshold, the controller in real-time simultaneously performs three tasks: (i) triggers single-pulse TMS at the hotspot, (ii) actuates exoskeleton-device (assisting wrist-extension), and (iii) provides performance-biofeedback (Figures 1B,C). A 10-s trial time was given to the patients with spasticity to put effort, completing the movement and relaxing the muscle with spasticity after the movement. 10 s is divided into three sections—3 + ~5 + ~1 s, hence, the first 3 s is a voluntary-trial to detect the EMG (to trigger TMS and Exoskeleton). Another 4–6 s to make movements assisted by the exoskeleton will depend on the clinical presentation of patients (range of motion, speed; Figure 1C). Since the protocol allows the experimenter to choose the motion parameters (range of motion and speed), depending on the patient's clinical presentation (comfortable range of motion, contractures, and pain), each patient completed the movement at a different time, and the remaining few seconds (~1–2 s) will be given as a delay for getting the patient's hand with spasticity relaxed and to maintain the consistency of protocol as 10 s trial. Depending on the individual clinical presentation, if the patient wants to take rest in between the trials due to fatigue, pain, or spasticity, the patient might make a voluntary effort after a gap of 1–2 s between any trials of 10 s each. If (only) the activation threshold is reached by voluntary effort, the controller triggers TMS-pulse and exoskeleton device and if it does not reach the predefined threshold in the first 3 s, trial-cycle is missed and the

system is reset to begin a new trial, starting with visual voluntary-cue via green LED, maintaining the consistency of 10-s in the protocol. TMS-pulse is delivered within first-half of the EMG-burst generated by EDC (within the time of voluntary-trial time; Figure 1C) as soon as the predefined activation threshold on RMS-EMG is crossed, the average time-interval from the crossing of EMG-threshold to delivery of TMS-pulse being less than 50 ms.

As each complete trial (presented in Figure 1D) lasted 10 s (voluntary cue, movement, and rest time) and TMS stimulated the motor cortex once in 10 s by delivering single-pulse TMS, implying 0.1 Hz frequency, as used in literature (Buetefisch et al., 2011; Revill et al., 2020). Single-pulse TMS was applied at 100% Motor-Threshold, generating MEP at every pulse, synchronous with every voluntary wrist extension. If the patient with spasticity has to be voluntarily involved and with movement throughout the session, spasticity should be considered profoundly, i.e., time taken by muscle to initiate the movement, complete the movement, relax after the movement, and prepare for the movement the next trial.

Two types of bio-feedbacks in real-time were provided- intrinsic proprioceptive-biofeedback via exoskeleton-device assisting the movement and extrinsic adaptive visual-performance biofeedback, which was made proportional to RMS EMG amplitude. The visual feedback to the brain is given by the LEDs and the number of glowing LEDs is proportional to the effort by the patient during the assistance of movement (wrist extension) in real-time. Out of four EMG thresholds, other than the (first) activation threshold which triggered TMS-pulse and exoskeleton-device simultaneously, three other RMS EMG thresholds were pre-determined and calibrated as directly proportional to (glowing rows of LEDs) 8*8 dot-matrix and made adaptive after few trials. After the first 20 initial trials (as training), these three thresholds were used to make the EMG-performance biofeedback adaptive, (i.e., the number of times the thresholds were consistently attained/not attained), were used to constantly increase/decrease the visual performance feedback targets during device-motion in each cycle in real-time.

## 3. Results

All patients were able to comprehend and complete the session in time and tolerated sessions well with no complaints.

### 3.1. Demonstrating the activity-dependent TMS system in one session

After written informed consent, three patients ($n = 3$) were enrolled (Table 1) and clinical measures were obtained (Table 2). Each session of TMS synchronized with the exoskeleton-device and feedback (TSEF) platform, had ~270 trials of 10 s corresponding to 45 min and was given to three patients each. Three patients with different spasticity, on Modified-Ashworth-Scale (MAS = 1, 1+, and 2) at wrist-joint, completed their session in their timing (instead of 45-min session)- 50.85, 50.96, and 53.8 min respectively, with an average of 51.87 ± 1.67 min. The patients with (more) spasticity tend to take (more) inter-trial intervals and hence, with the increase in spasticity, the session time also increased. With respect to MAS-1 patients, patients with MAS-2 tend to take more time and had a

TABLE 1 Details of enrolled patients.

| Group | Patient | Sex | Age | Handedness | Stroke | Chronicity | Hypertension | Smoking and alcohol | Diabetic | Family history stroke | Mini mental scale |
|---|---|---|---|---|---|---|---|---|---|---|---|
| TSEF | P1 | M | 31 | Right | R GC bleed | 9 | No | No | No | No | 30 |
| | P2 | M | 53 | Right | L ACA, MCA infarct | 3 | No | No | No | No | 29 |
| | P3 | M | 25 | Right | R MCA infarct | 6 | No | Yes | No | No | 30 |
| Physiotherapy control | P4 | M | 40 | Right | R MCA infarct | 8 | No | No | No | Yes | 30 |
| | P5 | M | 38 | Right | R MCA Lacunar infarct | 9 | No | Yes | Yes | No | 30 |
| | P6 | M | 42 | Right | L Parietal & BG infarct | 8 | No | No | No | Yes | 27 |

GC, gangliocapsular; ACA, anterior cerebral artery; MCA, middle cerebral artery; and BG, basal ganglia.

TABLE 2 Details of patients' pre- and post-sessions measures of clinical scales and cortical-excitability.

| Group | Patient | Chronicity | Age | MAS | | BI | | FMUE | | FMWH | | PROM | | RMT | | MEP | |
|---|---|---|---|---|---|---|---|---|---|---|---|---|---|---|---|---|---|
| | | | | Pre | Post | Pre | Post | Pre | Post | Pre | Post | Pre | Post | Pre | Post | Pre | Post |
| TSEF | P1 | 9 | 31 | 2 | 1.5 | 75 | 90 | 34 | 40 | 8 | 12 | 15 | 30 | 100 | 78 | 0* | 66.3 |
| | P2 | 3 | 53 | 1.5 | 1 | 70 | 90 | 43 | 53 | 10 | 14 | 20 | 50 | 75 | 70 | 112 | 131 |
| | P3 | 6 | 25 | 1 | 0 | 80 | 100 | 34 | 44 | 10 | 13 | 20 | 40 | 100 | 80 | 0* | 60.5 |
| | (Mean ± SD) | 6 ± 3 | 36.3 ± 14.7 | 1.5 ± 0.5 | 0.8 ± 0.7 | 75 ± 5 | 93.3 ± 5.7 | 37 ± 5.2 | 45.6 ± 4.7 | 9.33 ± 1.15 | 13 ± 1 | 18.3 ± 2.8 | 40 ± 10 | 91.6 ± 14.4 | 76 ± 5.2 | 37.5 ± 64.9 | 86 ± 39.2 |
| **Difference (Post-Pre)** | | | | **0.67** | | **18.3** | | **8.6** | | **2.6** | | **21.7** | | **15.6** | | **48.5** | |
| **Relative % Improvement (Post-Pre)/Pre** | | | | **46** | | **24** | | **23** | | **31** | | **118** | | **18** | | **129** | |
| Physiotherapy Control | P4 | 8 | 40 | 2 | 2 | 50 | 55 | 25 | 29 | 11 | 11 | 5 | 15 | 99 | 97 | 60 | 62 |
| | P5 | 9 | 38 | 1.5 | 1.5 | 50 | 60 | 24 | 28 | 10 | 10 | 15 | 30 | 100 | 100 | 0 | 0 |
| | P6 | 8 | 42 | 2 | 2 | 75 | 80 | 18 | 23 | 5 | 6 | 20 | 25 | 65 | 64 | 89 | 98 |
| | (Mean ± SD) | 8.3 ± 0.5 | 40 ± 0.2 | 1.8 ± 0.2 | 1.8 ± 0.2 | 58.3 ± 14.4 | 65 ± 13.2 | 22.3 ± 3.7 | 26.6 ± 3.2 | 8.6 ± 3.2 | 9 ± 2.6 | 13.3 ± 7.6 | 23.3 ± 7.6 | 88 ± 19.9 | 87 ± 19.9 | 49.6 ± 5.3 | 52 ± 49.2 |
| **Difference (Post-Pre)** | | | | **0** | | **6.66** | | **4.3** | | **0.33** | | **10** | | **1** | | **2.33** | |
| **Relative % Improvement (Post-Pre)/Pre** | | | | **0** | | **11.4** | | **19.2** | | **4.6** | | **75** | | **1.1** | | **4.8** | |

MAS (max 4): modified ashworth scale (a measure of spasticity).
BI (max 100): Barthel index (a measure of ADL).
FMUL (max 66): Fugl-Meyer upper limb.
FMWH (max 24): Fugl-Meyer wrist hand.
PROM (max 70): passive range of motion of wrist-joint.
RMT (%): resting motor threshold EDC hotspot.
MEP (μv): motor evoked potential amplitude.
Δ relative % clinical improvement = (Post clinical score—Pre clinical score/Pre clinical score)*100.
*MEP was not obtained even after giving 100% Maximum Stimulator Output due to decreased cortical-excitability after stroke (Chen et al., 2008).
Difference represents (Post Clinical score-Pre Clinical Score).
Bold are the derived parameters from values in Table 2 for easier understanding of readers.





10.3389/fnins.2023.1116273

TABLE 3 Patient's Subjective Feedback given in the TSEF group.

| S.No | Protocol | Patient's feedback |
|---|---|---|
| 1 | Robotic Exoskeleton mounted on hand with the elbow at 90 degrees. | Difficult to maintain the elbow at 90 degrees with a TMS coil on the head. |
| 2 | Robotic exoskeleton on the flat-surfaced table. | The robotic exoskeleton's table should be inclined such that the elbow could be 120 degrees to easily maintain the TMS coil on the head. |
| 3 | Table with the non-adjustable height of 30 in. | The height of the table on which the robotic exoskeleton is placed should be adjustable. |
| 4 | Thumb free during the wrist and finger joint movement. | A strap to hold the thumb should also be included in the exoskeleton. |
| 5 | Visual LED feedback placed on the table. | LED feedback should be in front of us to easily see without moving the eyes sideways as the head is fixed due to the TMS coil. |
| 6 | It was instructed to not use the proximal joints—Elbow, and shoulder and to put full effort into the wrist movement for EMG to be detected from EDC. | Stress on elbow and shoulder causing pain, a few minutes gap would be better. |
| 7 | The protocol had exoskeleton focusing only on wrist and fingers joint. | It should be made multi-joint to involve shoulder and elbow joints training too. It should not be limited to only the wrist and hand. |
| 8 | 45 min of the session with additional 3-min of breaks in between the session. | I will not be able to do this for more than this duration. |
| 9 | The 10 s trial was made voluntary according to the patient. According to their clinical presentation (spasticity, pain, and contractures), they might/might not take a gap in between the trial and start the effort for wrist extension. | Initially, it was fine with six trials/min but after 5–10 min, it is easy if we have a 1–2 s gap between the trials. |

difference of ~3 min (corresponding to ~18 trials of 10 s each) taken in between the trials. Additional 3 min' rest were given to all the patients in between the session as rest.

## 3.2. Proof-of-concept study

After a demonstration of the TSEF protocol on three patients (section 3.1), a Proof-of-concept study was attempted for exploring the differences in clinical gains and cortical-excitability in patients with two groups: TSEF-group ($n = 3$, age = 36.3 ± 14.5, chronicity = 6 ± 3 months same patients as section 3.1) and physiotherapy group ($n = 3$, age = 40 ± 0.2, chronicity = 8.33 ± 0.5 months; serving as control). All six patients were right-handed, male with non-hypertension; five were non-diabetic, and two had a history of stroke in the family (Table 1). Clinical measures were acquired the day before the first-session and the day after the 20th-session (Table 2) along with the subjective-feedback (from TSEF-group, Table 3). In TSEF sessions, patients were motivated by the therapist for putting effort for wrist movement. TSEF sessions were given 45 min/per day for 20-sessions via the coil-holder system. The control-group received the dose-matched physiotherapy of 45 min/day for 20-sessions (details in Supplementary material).

Post 20-sessions, reduction in spasticity of wrist joint on MAS was also observed with one grade each in all three patients, however, control-group showed no change in spasticity post 20-sessions (Table 2). TSEF also showed considerable clinical gains (Barthel Index—mean 18.3, FMUE—mean 8.6 units, and PROM—mean 21.7 units), however, control-group showed minimal increase in clinical-gains (Barthel-Index—mean 6.6 units, FMUE—mean 4.3 units, and PROM—mean 10 units). FM for the upper-limb (FMUE) signifies measurement of sensorimotor functions of the whole arm including shoulder, elbow, wrist, and hand. Evaluating recovery at distal joints (Wrist/Hand) is critical in this study as it is focused on distal joints with exoskeleton training in TSEF sessions (along with stimulation of cortico-representation hotspot of EDC muscle responsible for wrist extension movement). Hence, we segregated FMUE (FM-upper-limb) into proximal-joints FMSE (FM-Shoulder/Elbow) and distal-joints FMWH (FM-Wrist/Hand). Post 20-sessions, in TSEF-group FMWH score was observed to increase in all three patients (P1 by 4 units, P2 by 4 units, and P3 by 3 units), however, control-group showed improvement in only one patient by 1 unit (Table 2).

Pre-therapy, MEP were not obtained in two patients (P1 and P3) in TSEF-group and one patient (P5) in control-group, even after giving 100% Maximum Stimulator Output possibly due to decreased cortical-excitability after stroke (Chen et al., 2008) and for these patients, hotspot was determined for the unaffected hand at unaffected-hemisphere and the corresponding measurements were made for the affected-hemisphere, a standard procedure described in the literature (Chang et al., 2010; de Freitas et al., 2023). After 20 intervention-sessions in TSEF-group, patients demonstrated improvement in cortical-excitability (Table 2) i.e., P1 and P3 showed the appearance of MEP at decreased RMT. The mean MEP increased by ~48.5 μV at a decrease of mean RMT by ~15.6%, however, post 20 physiotherapy-sessions in control-group, the cortical-excitability remained same for all the patients with mean MEP increased by ~2.33 μV at a decrease of mean RMT by ~1% (Table 2).

Subjective feedback (Table 3) by patients showed the experience of TSEF sessions WRT patients' experience. Adjustments in the table's height and angles and arrangement for the thumb were suggested along with a request to make it a multi-joint training device. The patient suggested that due to spasticity, the duration of use could not be longer due to fatigue caused in the hand.

## 4. Discussion

A novel Activity-Dependent TMS with a two-way feedback system and novel protocol, to voluntarily involve the patient throughout the sessions, has been developed and its functioning has been demonstrated along with a feasibility-study (intervention $n = 3$ and controls $n = 3$). We attempted to close the loop between the intrinsic brain state, cortical stimulation, and biofeedback (intrinsic-proprioceptive and extrinsic-visual) to the brain. In every 10-s trial, the EMG-triggered TMS platform uses real-time EDC-muscle EMG to simultaneously (a) trigger impaired EDC muscle cortical representation (by voluntary-activated EDC muscle activity); (b) actuate exoskeleton-device utilizing use-dependent-plasticity and providing intrinsic-proprioceptive-biofeedback via skin-mechanoreceptors, muscle-spindles, joints, etc., by assisting the attempted movement completing the sensorimotor-loop (Gomez-Rodriguez et al., 2011); and (c) provide extrinsic adaptive visual performance-biofeedback, considering the criticality of intrinsic and extrinsic-biofeedback in post-stroke recovery (Gomez-Rodriguez et al., 2011). This strategy potentially synchronizes a group of neurons excited for muscle activity and exoskeleton training with another group of neurons through TMS-pulse leading to the strengthening of synaptic connections between these two groups of neurons, facilitating Hebbian-learning (Gerstner, 2011; Revill et al., 2020). Moreover, neuroplasticity happens in synaptic connections between motor neurons firing voluntarily and neurons activated by stimulation (Edwardson et al., 2013). In non-human primates, motor-cortex activity associated with movement lasts for 250 ms after EMG-onset, therefore, TMS-pulse was applied to the motor cortex within the first half of EMG-bursts, to arrive synchronously with cortical activity in the motor cortex generating wrist-extension (Revill et al., 2020).

Using a functionally important and often affected muscle, i.e., EDC is neuro-anatomically and physiologically justified and was attempted to target impairment-oriented-functional-neuroplasticity, unlike the APB muscle used commonly (Izumi et al., 2008; Hoogendam et al., 2010). Considering the criticality of feedback in stroke rehabilitation, the proprioceptive feedback during exoskeleton assistance is considered an overarching somatosensory-theme, through mechanoreceptors consisting of joint-position sense, kinaesthesia, sense of force, and sense of joint-velocity on stretch-receptor in ligaments and muscle-spindles (Ager et al., 2020). The proprioceptive feedback to the brain is known to modulate the ongoing cortical activity, completing the sensorimotor loop (Darvishi et al., 2017), which we are exploring in this study (during the assistance of wrist extension by exoskeleton-device simultaneous with the MEP at every trial). Post-sessions, the relative % change in all clinical scores was observed in both groups. With TSEF-group, MAS showed a decrease of 46%, with an increased Barthel Index of 24%, FMUE 23%, and PROM 118%, however, in control-group, MAS does not show any change, with increased Barthel Index of 11%, FMUE 19%, and PROM 75%. It is worth noting that in TSEF-group, FMWH, a relevant joint in training, showed a considerable increase of 31% compared to only ~5% increase in control-group (Table 2).

The improvements in cortical-excitability (of EDC-hotspot involved in cortical stimulation) were observed in TSEF-group. Post-sessions, 2/3 of patients showed the appearance of MEP at decreased RMT. In TSEF-group, MEP was increased by 129% at a decrease of RMT by 18%, however, in control-group, the MEP was observed to increase by only ~5% at a decreased RMT of ~1% (Table 2). Increased cortical-excitability with decreased spasticity, along with specifically increased FMWH and passive-ROM indicated functional gains. Patients seemed more confident in ADLs like holding the door knob or having a glass of water while continuously holding the glass. As the functional gain is critically dependent on the motor cortex, improved cortical-excitability (increased MEP at decreased RMT), and clinical gains observed in this might suggest clinically relevant neuroplasticity (Revill et al., 2020). Although, improvement might be pertaining to exoskeleton training alone and needs to be further investigated in the future with larger-cohort, the clinical gains and increase in cortical-excitability are in line with the ADS studies in literature for animals, healthy and stroke patients, indicating the feasibility of patient-specific ADS with feedback to capitalize the unique physiology resulting in robust neural plasticity (Edwardson et al., 2013; Revill et al., 2020). The subjective feedback asserted towards the acceptability of the protocol and precious suggestions and feedback, such as placement of visual feedback, the height of the table where the exoskeleton is placed, about improving the comfort for future protocols and their acceptance and "look forward" approach towards such protocols for other proximal joints as well.

Spasticity is a rarely discussed obstacle in stroke-rehabilitation literature, which might be pertaining to the clinical challenges involved in dealing with spasticity. TSEF sessions showed to decrease the spasticity in each patient, and have the potential to be tailored to each patient with different spasticity. The critical effect of spasticity from MAS 1 to 1+ to 2 was observed in this feasibility-study for the TSEF-group, the inter-trial interval was found to be increased with an increase in spasticity, indicating the importance of individualized patient-specific tailored-protocol with inter-trial interval and "rest-time" within each trial. A similar observation is also indicated by patients' subjective-feedback number-9 (Table 3) which speaks profoundly about the acceptability of the individualized protocol tailored according to the spasticity as the patient can decide the inter-trial interval. If a patient with spasticity has to be involved in a therapy process that is meant to be voluntary and with the movement, therapy should take the spasticity as a critical consideration, i.e., time taken by the muscle to initiate the movement, complete the movement, relax after the movement, and prepare for the movement for the next trial. The rationale behind 0.1 Hz frequency TMS for the proposed customized Hebbian stimulation was that the patient (with spasticity) has to be voluntarily involved throughout the therapy process and cortical stimulation should be synchronized with neural activity (attempt of wrist extension).

The proposed protocol was voluntary-activated with patient-specific inter-trial intervals, to ensure the patient with spasticity makes effort only when comfortable enough, patient was actively and voluntarily involved in the process instead of passively sitting during rTMS-therapy. With the given advantage of the exoskeleton being customizable in terms of motion parameters according to different ranges of clinical presentation (spasticity, contractures, and pain), finger height-support, voluntary-activated, and configurability of residual-EMG of individual-patient, the individualized and voluntary-activated protocol might be able to serve large patient-population. The main limitation of this proof-of-concept study is the small number of patients and the absence of

long-term outcome assessments. Since, all the patient cohort included in this study were found to be young, generalization of results to a larger cohort of the patient population is not possible and warrants further investigation on a larger cohort.

## 5. Conclusion

An individualized TSEF platform having the potential to be tailored to each patient with different spasticity has been developed, and demonstrated and its clinical potential has been evaluated in the feasibility-study. An increase in cortical-excitability and clinical-gains were observed which was not observed in control-group. Being voluntarily involved during the whole brain stimulation protocol might add clinically relevant neuroplasticity.

## Data availability statement

The original contributions presented in the study are included in the article/Supplementary material, further inquiries can be directed to the corresponding author.

## Ethics statement

The studies involving human participants were reviewed and approved by Institute Review Board, All India Institute of Medical Sciences, Delhi, India. The patients/participants provided their written informed consent to participate in this study.

## Author contributions

NS: conceptualization, methodology, data curation, writing—original draft, writing—review and editing. MS: data curation, intellectual feedback about patients, writing—review and editing. NK and MP: writing—review and editing, scientific resources, and supervision. AM: conceptualization, methodology, supervision, scientific resources, and writing— review and editing. All authors contributed to the article and approved the submitted version.

## Funding

This work was supported by SERB-DST, India (YSS/2015/000697) and Abdul Kalam Technology Innovation National Fellowship by Indian National Academy of Engineering (INAE/121/AKF/38).

## Acknowledgments

We sincerely thank the patients who participated in the study.

## Conflict of interest

The authors declare that the research was conducted in the absence of any commercial or financial relationships that could be construed as a potential conflict of interest.

## Publisher's note

All claims expressed in this article are solely those of the authors and do not necessarily represent those of their affiliated organizations, or those of the publisher, the editors and the reviewers. Any product that may be evaluated in this article, or claim that may be made by its manufacturer, is not guaranteed or endorsed by the publisher.

## Supplementary material

The Supplementary material for this article can be found online at: https://www.frontiersin.org/articles/10.3389/fnins.2023.1116273/full#supplementary-material

## References

Ager, A. L., Borms, D., Deschepper, L., Dhooghe, R., Dijkhuis, J., Roy, J. S., et al. (2020). Proprioception: how is it affected by shoulder pain? A systematic review. *J. Hand Ther.* 33, 507–516. doi: 10.1016/j.jht.2019.06.002

Awiszus, F. (2003). Chapter 2 TMS and threshold hunting. *Suppl. Clin. Neurophysiol.* 56, 13–23. doi: 10.1016/S1567-424X(09)70205-3

Bi, G. Q., and Poo, M. M. (1998). Synaptic modifications in cultured hippocampal neurons: dependence on spike timing, synaptic strength, and postsynaptic cell type. *J. Neurosci.* 18, 10464–10472. doi: 10.1523/JNEUROSCI.18-24-10464.1998

Bi, G., and Poo, M. (2001). Synaptic modification by correlated activity: Hebb's postulate revisited. *Annu. Rev. Neurosci.* 24, 139–166. doi: 10.1146/annurev.neuro.24.1.139

Buetefisch, C., Heger, R., Schicks, W., Seitz, R., and Netz, J. (2011). Hebbian-type stimulation during robot-assisted training in patients with stroke. *Neurorehabil. Neural Repair* 25, 645–655. doi: 10.1177/1545968311402507

Bütefisch, C. M., Khurana, V., Kopylev, L., and Cohen, L. G. (2004). Enhancing encoding of a motor memory in the primary motor cortex by cortical stimulation enhancing encoding of a motor memory in the primary motor cortex by cortical stimulation. *J. Neurophysiol.* 91, 2110–2116. doi: 10.1152/jn.01038.2003

Chang, W. H., Kim, Y. H., Bang, O. Y., Kim, S. T., Park, Y. H., and Lee, P. K. W. (2010). Long-term effects of RTMS on motor recovery in patients after subacute stroke. *J. Rehabil. Med.* 42, 758–764. doi: 10.2340/16501977-0590

Chen, R., Cros, D., Curra, A., Di Lazzaro, V., Lefaucheur, J.-P., Magistris, M. R., et al. (2008). The clinical diagnostic utility of transcranial magnetic stimulation: report of an IFCN committee. *Clin. Neurophysiol.* 119, 504–532. doi: 10.1016/j.clinph.2007.10.014

Darvishi, S., Gharabaghi, A., Boulay, C. B., Ridding, M. C., Abbott, D., and Baumert, M. (2017). Proprioceptive feedback facilitates motor imagery-related operant learning of sensorimotor β-band modulation. *Front. Neurosci.* 11:60. doi: 10.3389/fnins.2017.00060

de Freitas, Z. A., Romeiro da Silva, A. C., Baltar Do Rego Maciel, A., Shirahige Gomes Do Nascimento, L., Bezerra Da Silva, A., Piscitelli, D., et al. (2023). Sensory and motor cortical excitability changes induced by rTMS and sensory stimulation in stroke: a randomized clinical trial. *Front. Neurosci.* 16:2349. doi: 10.3389/fnins.2022.985754

Edwardson, M. A., Avery, D. H., and Fetz, E. E. (2014). Volitional muscle activity paired with transcranial magnetic stimulation increases corticospinal excitability. *Front. Neurosci.* 8:442. doi: 10.3389/fnins.2014.00442

Edwardson, M. A., Lucas, T. H., Carey, J. R., and Fetz, E. E. (2013). New modalities of brain stimulation for stroke rehabilitation. *Exp. Brain Res.* 224, 335–358. doi: 10.1007/s00221-012-3315-1

Feldman, D. E. (2000). Timing-based LTP and LTD at vertical inputs to layer II/III pyramidal cells in rat barrel cortex. *Neuron* 27, 45–56. doi: 10.1016/S0896-6273(00)00008-8

Gerstner, W. (2011). "Hebbian learning and plasticity," in *From Neuron to Cognition via Computational Neuroscience*. eds. M. A. Arbib and J. J. Bonaiuto (London: MIT Press Cambridge), 1–25.

Gharabaghi, A., Kraus, D., Leão, M. T., Spüler, M., Walter, A., Bogdan, M., et al. (2014). Coupling brain-machine interfaces with cortical stimulation for brain-state dependent stimulation: enhancing motor cortex excitability for neurorehabilitation. *Front. Hum. Neurosci.* 8:122. doi: 10.3389/fnhum.2014.00122

Gomez-Rodriguez, M., Peters, J., Hill, J., Schölkopf, B., Gharabaghi, A., and Grosse-Wentrup, M. (2011). Closing the sensorimotor loop: haptic feedback facilitates decoding of motor imagery. *J. Neural Eng.* 8:036005. doi: 10.1088/1741-2560/8/3/036005

Gregson, J. M., Leathley, M., Moore, A. P., Sharma, A. K., Smith, T. L., and Watkins, C. L. (1999). Reliability of the tone assessment scale and the modified Ashworth scale as clinical tools for assessing poststroke spasticity. *Arch. Phys. Med. Rehabil.* 80, 1013–1016. doi: 10.1016/S0003-9993(99)90053-9

Hoogendam, J. M., Ramakers, G. M. J., and Di Lazzaro, V. (2010). Physiology of repetitive transcranial magnetic stimulation of the human brain. *Brain Stimul.* 3, 95–118. doi: 10.1016/j.brs.2009.10.005

Izumi, S. I., Kondo, T., and Shindo, K. (2008). Transcranial magnetic stimulation synchronized with maximal movement effort of the hemiplegic hand after stroke: a double-blinded controlled pilot study. *J. Rehabil. Med.* 40, 49–54. doi: 10.2340/16501977-0133

Jackson, A., Mavoori, J., and Fetz, E. E. (2006). Long-term motor cortex plasticity induced by an electronic neural implant. *Nature* 444, 56–60. doi: 10.1038/nature05226

Jung, P., and Ziemann, U. (2009). Homeostatic and nonhomeostatic modulation of learning in human motor cortex. *J. Neurosci.* 29, 5597–5604. doi: 10.1523/JNEUROSCI.0222-09.2009

Kraus, D., Naros, G., Bauer, R., Khademi, F., Leão, M. T., Ziemann, U., et al. (2016). Brain state-dependent transcranial magnetic closed-loop stimulation controlled by sensorimotor desynchronization induces robust increase of corticospinal excitability. *Brain Stimul.* 9, 415–424. doi: 10.1016/j.brs.2016.02.007

Martin, S. J., Grimwood, P. D., and Morris, R. G. M. (2000). Synaptic plasticity and memory: an evaluation of the hypothesis. *Annu. Rev. Neurosci.* 23, 649–711. doi: 10.1146/annurev.neuro.23.1.649

Mitchell, W. K., Baker, M. R., and Baker, S. N. (2007). Muscle responses to transcranial stimulation in man depend on background oscillatory activity. *J. Physiol.* 583, 567–579. doi: 10.1113/jphysiol.2007.134031

Mrachacz-Kersting, N., Stevenson, A. J. T., Jørgensen, H. R. M., Severinsen, K. E., Aliakbaryhosseinabadi, S., Jiang, N., et al. (2019). Brain state-dependent stimulation boosts functional recovery following stroke. *Ann. Neurol.* 85, 84–95. doi: 10.1002/ana.25375

Rebesco, J. M., Stevenson, I. H., Körding, K. P., Solla, S. A., and Miller, L. E. (2010). Rewiring neural interactions by Micro-stimulation. *Front. Syst. Neurosci.* 4:39. doi: 10.3389/fnsys.2010.00039

Revill, K. P., Haut, M. W., Belagaje, S. R., Nahab, F., Drake, D., and Buetefisch, C. M. (2020). Hebbian-type primary motor cortex stimulation: a potential treatment of impaired hand function in chronic stroke patients. *Neurorehabil. Neural Repair* 34, 159–171. doi: 10.1177/1545968319899911

Rossini, P. M., Burke, D., Chen, R., Cohen, L. G., Daskalakis, Z., Di Iorio, R., et al. (2015). Non-invasive electrical and magnetic stimulation of the brain, spinal cord, roots and peripheral nerves: basic principles and procedures for routine clinical and research application: an updated report from an I.F.C.N. Committee. *Clin. Neurophysiol.* 126, 1071–1107. doi: 10.1016/j.clinph.2015.02.001

Rothwell, J. C., Hallett, M., Berardelli, A., Eisen, A., Rossini, P., and Paulus, W. (1999). Magnetic stimulation: motor evoked potentials. The International Federation of Clinical Neurophysiology. *Electroencephalogr. Clin. Neurophysiol.* 52, 97–103.

Sale, P., Mazzoleni, S., Lombardi, V., Galafate, D., Massimiani, M. P., Posteraro, F., et al. (2014). Recovery of hand function with robot-assisted therapy in acute stroke patients: a randomized-controlled trial. *Int. J. Rehabil. Res.* 37, 236–242. doi: 10.1097/MRR.0000000000000059

Schaworonkow, N, Triesch, J, Ziemann, U, and Zrenner, C (2018). EEG-triggered TMS reveals stronger brain state-dependent modulation of motor evoked potentials at weaker stimulation intensities. bioRxiv [Preprint]. doi: 10.1101/251363v1.abstract

Singh, N., Saini, M., Anand, S., Kumar, N., Srivastava, M. V. P., and Mehndiratta, A. (2019a). Robotic exoskeleton for wrist and fingers joint in post-stroke neuro-rehabilitation for low-resource settings. *IEEE Trans. Neural Syst. Rehabil. Eng.* 27, 2369–2377. doi: 10.1109/TNSRE.2019.2943005

Singh, N., Saini, M., Kumar, N., Deepak, K. K., Anand, S., Srivastava, M. V. P., et al. (2019b). Time-frequency analysis of motor-evoked potential in patients with stroke vs healthy subjects: a transcranial magnetic stimulation study. *SN Compr. Clin. Med.* 1, 764–780. doi: 10.1007/s42399-019-00113-1

Singh, N., Saini, M., Kumar, N., Srivastava, M. V. P., and Mehndiratta, A. (2021). Evidence of neuroplasticity with robotic hand exoskeleton for post-stroke rehabilitation: a randomized controlled trial. *J. Neuroeng. Rehabil.* 18:76. doi: 10.1186/s12984-021-00867-7

Takahashi, C. D., Der-Y, Ã. L., Le, V., Motiwala, R. R., and Cramer, S. C. (2008). Robot-based hand motor therapy after stroke. *Brain* 131, 425–437. doi: 10.1093/brain/awm311

Thabit, M. N., Ueki, Y., Koganemaru, S., Fawi, G., Fukuyama, H., and Mima, T. (2010). Movement-related cortical stimulation can induce human motor plasticity. *J. Neurosci.* 30, 11529–11536. doi: 10.1523/JNEUROSCI.1829-10.2010

Thair, H., Holloway, A. L., Newport, R., and Smith, A. D. (2017). Transcranial direct current stimulation (tDCS): a Beginner's guide for design and implementation. *Front. Neurosci.* 11:641. doi: 10.3389/fnins.2017.00641

Walter, A., Murguialday, A. R., Rosenstiel, W., Birbaumer, N., and Bogdan, M. (2012). Coupling BCI and cortical stimulation for brain-state-dependent stimulation: methods for spectral estimation in the presence of stimulation after-effects. *Front. Neural Circuits* 6:87. doi: 10.3389/fncir.2012.00087/abstract

Werhahn, K. J., Fong, J. K. Y., Meyer, B.-U., Priori, A., Rothwell, J. C., Day, B. L., et al. (1994). The effect of magnetic coil orientation on the latency of surface EMG and single motor unit responses in the first dorsal interosseous muscle. *Electroencephalogr. Clin. Neurophysiol. Potent. Sect.* 93, 138–146. doi: 10.1016/0168-5597(94)90077-9

Wu, Y.-K., Saeed, S., Limonta, J. M., Bailey, E., Maher, M. T., and Harel, N. Y. (2019). Proceedings #52: development of surface EMG-triggered closed loop stimulation for individuals with spinal cord injury. *Brain Stimul.* 12, e125–e126. doi: 10.1016/j.brs.2018.12.221

frontiers | Frontiers in Neuroscience

TYPE Clinical Trial
PUBLISHED 15 June 2023
DOI 10.3389/fnins.2023.1088218



OPEN ACCESS

EDITED BY
Danilo Dimitri,
Centro Puzzle, Italy

REVIEWED BY
Stephanie Lefebvre,
University of Bern, Switzerland
Maria Martzoukou,
University of Ioannina, Greece

*CORRESPONDENCE
Jie Jia
✉ shannonjj@126.com
Hongxia Xing
✉ Xhxwh02@163.com

†These authors have contributed equally to this work and share first authorship

RECEIVED 03 November 2022
ACCEPTED 31 May 2023
PUBLISHED 15 June 2023

CITATION
Yan Z, He X, Cheng M, Fan X, Wei D, Xu S, Li C, Li X, Xing H and Jia J (2023) Clinical study of melodic intonation therapy combined with transcranial direct current stimulation for post-stroke aphasia: a single-blind, randomized controlled trial.
*Front. Neurosci.* 17:1088218.
doi: 10.3389/fnins.2023.1088218



# Clinical study of melodic intonation therapy combined with transcranial direct current stimulation for post-stroke aphasia: a single-blind, randomized controlled trial

Zhijie Yan[1,2†], Xinyuan He[1,2†], Mangmang Cheng[1], Xiaoqing Fan[1], Dongshuai Wei[1,2], Shuo Xu[2], Chong Li[2], Xiaofang Li[1], Hongxia Xing[1*] and Jie Jia[1,2,3*]

[1]Department of Rehabilitation Medicine, The Third Affiliated Hospital of Xinxiang Medical University, Xinxiang, China, [2]Department of Rehabilitation Medicine, Huashan Hospital, Fudan University, Shanghai, China, [3]National Clinical Research Center for Aging and Medicine, Huashan Hospital, Fudan University, Shanghai, China

**Background:** Globally, more than 10 million new stroke cases occur annually, of which aphasia accounts for about one-third. Aphasia has become an independent predictor of functional dependence and death for the stroke population. The closed-loop rehabilitation of combining behavioral therapy with central nerve stimulation seems to be the research trend of post-stroke aphasia (PSA) due to its advantages in improving linguistic deficits.

**Objective:** To verify the clinical efficacy of a closed-loop rehabilitation program combining melodic intonation therapy (MIT) with transcranial direct current stimulation (tDCS) for PSA.

**Methods:** This was a single-center, assessor-blinded, randomized controlled clinical trial, which screened 179 patients and included 39 PSA subjects, with the registration number ChiCTR2200056393 in China. Demographic and clinical data were documented. The primary outcome was the Western Aphasia Battery (WAB) used to assess language function, and the secondary outcomes included Montreal Cognitive Assessment (MoCA), Fugl-Meyer Assessment (FMA), and Barthel Index (BI) for evaluating cognition, motor, and activities of daily living, respectively. With the computer-generated randomization sequence, subjects were randomly divided into the conventional group (CG), MIT combined with sham stimulation group (SG), and MIT combined with tDCS group (TG). After the three-week intervention, the functional changes in each group were analyzed by the paired sample *T*-test, and the functional difference between the three groups was analyzed by ANOVA.

**Results:** There was no statistical difference on the baseline. After the intervention, the WAB's aphasia quotient (WAB-AQ), MoCA, FMA, and BI were statistically different in SG and TG, including all the sub-items in WAB and FMA, while only listening comprehension, FMA, and BI were statistically different in CG. The differences of WAB-AQ, MoCA, and FMA were statistically different among the three groups, but BI was not. The *post hoc* test results revealed that the changes of WAB-AQ and MoCA in TG were more significant than the others.

**Conclusion:** MIT combined with tDCS can augment the positive effect on language and cognitive recovery in PSA.

KEYWORDS

stroke, aphasia, tDCS, melodic intonation therapy, closed-loop rehabilitation

# 1. Introduction

Globally, more than 10 million new stroke cases occur annually, of which post-stroke aphasia (PSA) accounts for about one-third (Stefaniak et al., 2020). About 21–40% of stroke patients have persistent language impairment symptoms, which seriously affect the quality of life (Cichon et al., 2021). Research has shown that aphasia is an independent predictor of functional dependence and death after stroke, which has led to aphasia, an acquired language defect, becoming a clinical problem to be solved urgently (Stefaniak et al., 2020). At present, speech-language therapy (SLT) in behavioral science is still the mainstream treatment for aphasia (Fridriksson and Hillis, 2021). High-dose and high-intensity SLT is beneficial to the functional recovery of PSA (Breitenstein et al., 2017), but when SLT is more than 2 h per day, the benefit does not increase significantly (Rehabilitation and Recovery of People with Aphasia after Stroke, 2022). In the context of limited medical resources, treatment strategies need to be reconsidered based on the existing evidence to maximize language recovery and cost-effectiveness.

The closed-loop rehabilitation is a treatment paradigm designed based on the central-peripheral-central concept, which organically combines central nervous system regulation with peripheral therapy to compensate for the limitations of simple peripheral or central intervention. In closed-loop rehabilitation that can activate functional pathways, the central intervention represented by non-invasive brain stimulation (NIBS) can promote the activation of corresponding brain functional areas and enhance neuroplasticity, and peripheral intervention represented by behavioral therapy strengthens positive feedback through continuous input of motor and sensory signals, and some scholars believe that neuroimmunology mechanisms may also be involved (Jia, 2022). Several studies provide clues to closed-loop treatment strategies that boost functional recovery in aphasia (Vines et al., 2011; Wang et al., 2014; Fridriksson et al., 2018a,b; Cichon et al., 2021; Sheppard and Sebastian, 2021). However, the combination of peripheral and central interventions requires more evidence of randomized controlled trials to support its clinical implementation.

Multi-center cross-sectional study shows that there is a positive correlation between upper limb motor function and language function in the stroke population (Xu et al., 2021), which may suggest giving priority to treatment models involving both upper limb movement and language. Melodic Intonation Therapy (MIT) can be applied to aphasia, especially non-fluent aphasia caused by ischemic damage in the left dominant hemisphere (American Academy of Neurology, 1994; Cichon et al., 2021). MIT mainly emphasizes the use of external features of speech, such as intonation, rhythm, stress, etc., to recite polysyllabic words, high-frequency phrases, long sentences, and complex sentences musically, and finally to communicate in a normal rhythm and intonation (Cichon et al., 2021). During the treatment, allow the patient to clap according to the rhythm (Haro-Martinez et al., 2019). Compared with conventional speech therapy, MIT, as a behavioral therapy, has shown its advantages in the functional recovery of spontaneous, comprehension, repetition, naming, communication, and other aspects (Kasdan and Kiran, 2018; Huang et al., 2021; Zhang X. Y. et al., 2021; Zhang X. et al., 2021; Siponkoski et al., 2023). With the onset of PSA, the earlier MIT gets involved, the more significant this advantage will be (van der Meulen et al., 2014, 2016). The researches show that MIT is an intervention that is expected to improve language ability in the long run and is effective for many language families (Cortese et al., 2015; Martzoukou et al., 2021; Zhang X. Y. et al., 2021; Zhang X. et al., 2021).

In addition, NIBS has become an important auxiliary means for the treatment of PSA. There is evidence that NIBS is effective for aphasia symptoms and augments the effect of behavioral therapy through a neural plasticity mechanism (Fridriksson and Hillis, 2021). Transcranial direct current stimulation (tDCS), as a technology in NIBS, has great potential in central regulation (Duncan et al., 2020). The results of the systematic review and meta-analysis show that the most effective intervention of tDCS in improving language function may be to stimulate the inferior frontal gyrus (IFG) of the left dominant hemisphere with the anode (Elsner et al., 2020). Its mechanism is that the tDCS anode depolarizes the neuron cell membrane, thereby enhancing cortical activity (Duncan et al., 2020; Cichon et al., 2021). It is generally believed that tDCS is a therapeutic method with minimal risk and may be one of the most promising therapeutic methods besides language training (Bikson et al., 2016).

To optimize the outcome of rehabilitation, this trial was designed to verify whether tDCS anode stimulation of left IFG combined with MIT can augment the positive effect and provide a more evidence-based basis for aphasia rehabilitation.

# 2. Materials and methods

## 2.1. Trial design and sample size calculation

This was a single-center, assessor-blinded, three-arm, randomized controlled trial, granted by the Ethics Committee of the Third Affiliated Hospital of Xinxiang Medical University (ethical approval no. K2021-040-01), with the registration number ChiCTR220056393 in China. The software of Power Analysis and Sample Size Version 15.0.5 (PASS V15.0.5) was applied to calculate the sample size. The enrolled participants were evenly allocated to three arms in a ratio of 1:1:1. Based on the previous research results, the estimated effect size was 0.58. With the 0.05 two-sided significance level ($\alpha = 0.05$) and an 80% power of the test ($\beta = 0.2$), 13 cases per arm were calculated considering a 15% dropout rate.

## 2.2. Participants

39 PSA from the Third Affiliated Hospital of Xinxiang Medical University were recruited between December 2021 and October 2022.

The inclusion criteria were as follows: (a) right-handedness, (b) Chinese as the first language, (c) first stroke, (d) ischemic lesion of the left hemisphere, (e) course >1 week, (f) aphasia quotient (AQ) of Western Aphasia Battery (WAB) lower than 93.8, (g) non-fluent aphasia demonstrated by the Chinese aphasia fluency characteristics scale score of 9–13, (h) can cooperate to complete all assessments and treatments, and sign informed consent.

The exclusion criteria were as follows: (a) recurrent stroke, (b) history of brain surgery or metal implantation, (c) history of seizures, (d) sensitive scalp, (e) cerebellar and brainstem lesions or severe dysarthria, (f) severe audiovisual impairment, (g) other serious medical diseases or unstable conditions.

## 2.3. Outcome measures

In this study, WAB, as the primary outcome, was used to judge whether it was PSA and the severity. The AQ of WAB (WAB-AQ) was indirectly calculated from the scores of four sub-items of spontaneous, listening comprehension, repetition, and naming obtained through direct testing. For example, the evaluator provided scores of fluency and information content, which were added together to obtain the score of spontaneous speech, according to the scoring standards of WAB after the patient answered the questions. Combined with symptoms, medical history, and imaging data, stroke patients with a WAB-AQ lower than 93.8 points were judged as PSA, and the lower the WAB-AQ, the more severe the aphasia (Kertesz and Poole, 2004; Yan et al., 2022a). The secondary outcome measures included the Montreal Cognitive Assessment (MoCA), Fugl-Meyer Assessment (FMA), and Barthel Index (BI), which were selected to evaluate the cognitive function, motor function, and activities of daily living, respectively (Shah et al., 1989; Gladstone et al., 2002; Nasreddine et al., 2005). It should be pointed out that the evaluation of motor function was divided into FMA Upper Extremity (FMA-UE) and FMA Lower Extremity (FMA-LE) in this trial. The corresponding data were collected at baseline (T0) and week 3 (T1) by uniformly trained evaluators, who were blind.

## 2.4. Intervention

The random sequence was generated by the computer-generated random numbers. The random number was placed in a sealed and opaque envelope and implemented by the independent researcher. All subjects were divided into the conventional group (CG), MIT combined with sham stimulation group (SG), and MIT combined with tDCS group (TG) based on the random numbers.

CG: The speech therapist provided 30 min one-on-one training to the patient once a day, with a total dose of 15 sessions over 3 weeks, including voice induction, monosyllabic and polysyllabic word, and sentence pronunciation, picture naming, picture speaking, etc.

SG: (a) MIT: Each one-on-one training lasted for 30 min, with a total dose equivalent to conventional treatment. The patient was induced to use rhythmic hand tapping to facilitate the reproduction of items. MIT consisted of three levels, from words to phrases to sentences, with gradually increasing difficulty. Patients could not progress to the next difficulty level unless they could complete more than 95% five times in a row. The speech therapist gradually reduced assistance until the patient regained independent verbal expression in an almost normal manner. (b) Sham stimulation: The anode of tDCS acted on the left IFG of the cerebral hemisphere, and the cathode is placed on the right supra-brow frontal region. Each session only lasted for the first 30s and the duration was 15 sessions over 3 weeks.

TG: (a) MIT: same as SG; (b) tDCS: The location of electrodes was the same as SG. The stimulation intensity was 1 mA, lasting for 20 min per day, and the duration of tDCS was 15 sessions over 3 weeks.

The equipment used in this study was an ActivaDose®II portable transcranial direct current stimulator manufactured by ActivaTek Company of the United States.

## 2.5. Statistical analysis

Statistical analyses were conducted using SPSS 25.0 (IBM Corporation, Armonk, NY, United State). The mean values of three groups of continuous numerical variables were compared using one-way ANOVA. Categorical variables were expressed by rate, using Pearson's Chi-square test. In the baseline characteristic analysis of this study, age, years of education, post-stroke duration, NIHSS, WAB, MoCA, FMA, and BI were statistically analyzed by one-way ANOVA, and gender was analyzed by Pearson's Chi-square test. The paired sample T-test was used to statistically analyze the functional changes of each group of subjects before and after the intervention. The functional difference between the three groups of subjects before and after the intervention was statistically analyzed using the method of one-way ANOVA, and the variables with statistical differences among the three groups were further compared with each other using the *post hoc* test. A two-sided $p < 0.05$ was considered to be statistically significant in this study.

# 3. Results

## 3.1. Baseline characteristics

Between December 2021 and October 2022, we assessed 179 patients for eligibility. 39 patients (22%) were enrolled and randomly assigned to CG, SG, and TG according to the ratio of 1:1:1 (Figure 1). The participants had a mean (SD) age of 58.6 (11.1) years, had 11 (3) years of education, and were 5 (9) months from stroke onset. There were 17 (44%) females, and the median NIHSS score before intervention was 15 (IQR 13–19). The three arms before intervention had no statistical difference in demographic and clinical characteristics (Table 1).

## 3.2. Comparison of functional values before and after intervention in each group

In CG, except for WAB-AQ (37.746 ± 37.172, $p = 0.06$) and MoCA (5.08 ± 7.740, $p = 0.190$), FMA (35.00 ± 25.668, $p = 0.008$) and BI (52.69 ± 23.859, $p < 0.001$) were improved after intervention, which

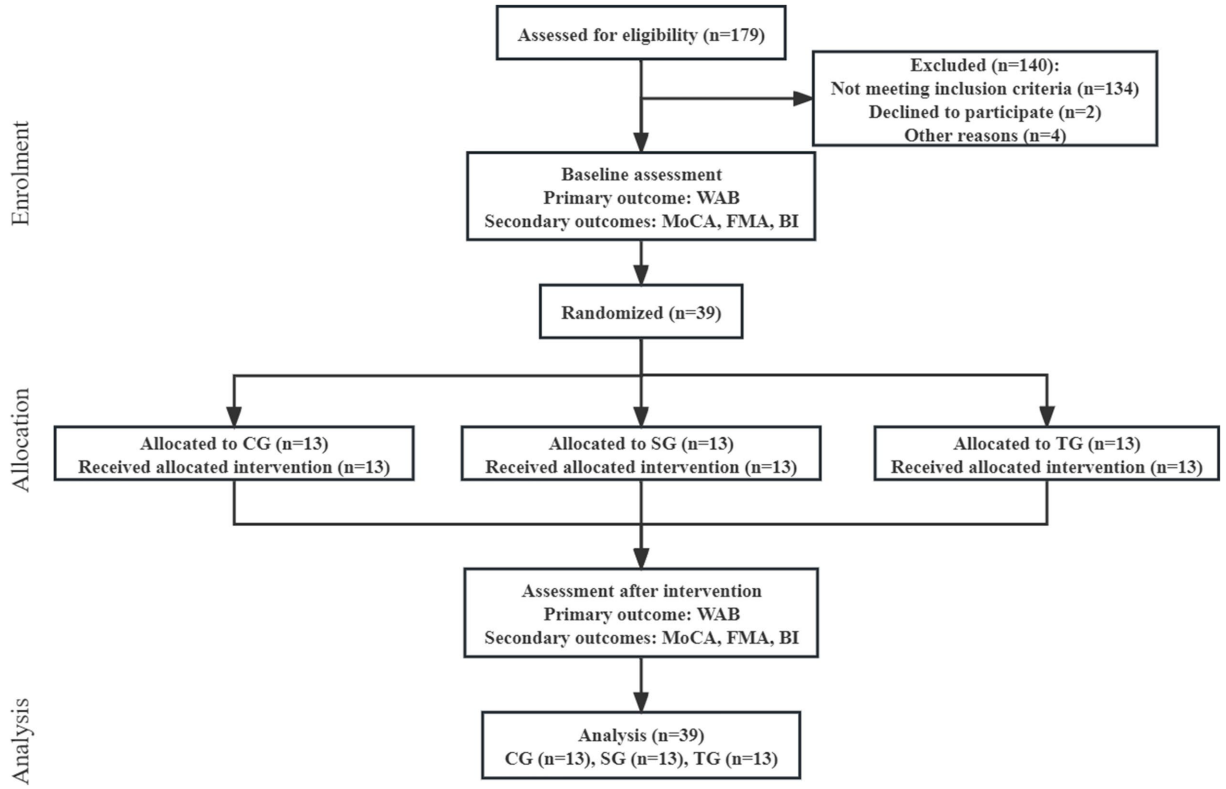


FIGURE 1
Flow diagram. WAB, Western Aphasia Battery; MoCA, Montreal Cognitive Assessment; FMA, Fugl-Meyer Assessment; BI, Barthel Index; CG, conventional group; SG, melodic intonation therapy combined with sham stimulation group; TG, melodic intonation therapy combined with transcranial direct current stimulation.

was statistically significant. The analysis results of sub-items in WAB and FMA showed that there was no statistical difference in other sub-items except listening comprehension ($89.62 \pm 86.358$, $p = 0.017$), FMA-UE ($19.38 \pm 16.556$, $p = 0.019$), and FMA-LE ($15.62 \pm 9.760$, $p = 0.017$). In SG and TG, the functional value changes of WAB-AQ, MoCA, FMA, and BI before and after intervention were statistically significant, including the sub-items of spontaneous, listening comprehension, repetition, naming, FMA-UE, and FMA-LE ($p < 0.05$; Table 2; Figure 2).

## 3.3. Comparison of functional differences among three groups

The difference of WAB-AQ ($p < 0.001$), MoCA ($p = 0.024$), and FMA ($p = 0.044$) before and after the intervention was statistically different among the three groups, but BI ($p = 0.154$) was not. The statistical analysis of sub-items in WAB and FMA showed that there were statistical differences in the functional differences among the three groups in spontaneous ($p = 0.003$), listening comprehension ($p = 0.001$), repetition ($p = 0.005$), naming ($p = 0.005$), and FMA-UE ($p = 0.041$), but FMA-LE ($p = 0.432$) was not (Table 3).

The *post hoc* test results of ANOVA showed that the changes of WAB-AQ and MoCA in TG before and after the intervention were more significant than CG ($p < 0.001$, $p = 0.009$) and SG ($p = 0.01$, $p = 0.042$), and the change of FMA in TG was more significant than CG ($p = 0.013$), but there was no statistical difference between TG and SG ($p = 0.224$; Figure 3). In terms of spontaneous and repetition, there was a significant difference between TG and CG ($p = 0.001$, $p = 0.001$), while there was no significant difference between TG and SG ($p = 0.076$, $p = 0.067$). In terms of comprehension and naming, there were significant differences between TG and CG ($p < 0.001$, $p = 0.002$) and SG ($p = 0.01$, $p = 0.011$). As for FMA-UE, TG showed a more significant improvement than TG ($p = 0.012$), while there were no statistical differences between the other groups.

No serious adverse events occurred during the whole study.

# 4. Discussion

In this trial, tDCS, as a central stimulus, activated the left dominant hemisphere language functional area through anodic stimulation, and MIT, as a peripheral stimulus, strengthened positive feedback through continuous input of signals including motion, vision, and hearing. Together, they formed the complete closed-loop treatment system for aphasia to explore the clinical efficiency of the closed-loop scheme on functional recovery and provide a clinical reference for linguistic rehabilitation. The results of this study revealed that, immediately after the intervention, both SG and TG improved in terms of language function, while CG was not significantly. Although SG and TG had a similar effect on spontaneous and repetition, SG was

TABLE 1 Baseline characteristics.

| | CG (*n* =13) | SG (*n* =13) | TG (*n* =13) | *p* value |
|---|---|---|---|---|
| Age (years) | 56.77 ± 9.791 | 55.46 ± 12.204 | 63.46 ± 10.187 | 0.142[a] |
| Gender | | | | 0.174[b] |
| Female | 6 (46.2) | 3 (23.1) | 8 (61.5) | |
| Male | 7 (53.8) | 10 (76.9) | 5 (38.5) | |
| Education (years) | 9.92 ± 2.842 | 11.54 ± 4.390 | 10.23 ± 2.488 | 0.434[a] |
| Post-stroke duration (days) | 122.38 ± 299.172 | 92.23 ± 122.415 | 241.23 ± 373.781 | 0.381[a] |
| NIHSS | 14.77 ± 7.585 | 15.54 ± 4.521 | 14.23 ± 5.510 | 0.857[a] |
| WAB-AQ | 35.085 ± 37.906 | 30.138 ± 27.582 | 24.915 ± 26.579 | 0.709[a] |
| Spontaneous | 6.38 ± 7.654 | 5.08 ± 6.006 | 3.38 ± 4.610 | 0.475[a] |
| Comprehension | 85.31 ± 86.505 | 84.46 ± 63.763 | 100.08 ± 62.758 | 0.824[a] |
| Repetition | 43.00 ± 45.200 | 37.85 ± 39.179 | 22.85 ± 38.773 | 0.439[a] |
| Naming | 25.92 ± 40.323 | 16.77 ± 24.749 | 17.85 ± 30.506 | 0.737[a] |
| MoCA | 4.62 ± 6.935 | 3.32 ± 6.379 | 3.62 ± 5.268 | 0.844[a] |
| FMA | 31.15 ± 24.283 | 20.62 ± 20.974 | 31.31 ± 24.295 | 0.414[a] |
| FMA-UE | 17.00 ± 15.875 | 9.77 ± 14.143 | 15.69 ± 15.628 | 0.444[a] |
| FMA-LE | 14.15 ± 9.063 | 10.85 ± 8.153 | 15.62 ± 11.012 | 0.431[a] |
| BI | 38.46 ± 23.838 | 33.46 ± 17.957 | 46.92 ± 28.250 | 0.354[a] |

Data are expressed as mean ± SD or number of observations (% of total observation). NIHSS, National Institute of Health Stroke Scale, WAB-AQ, aphasia quotient of Western Aphasia Battery; MoCA, Montreal Cognitive Assessment; FMA, Fugl-Meyer Assessment; FMA-UE, Fugl-Meyer Assessment Upper Extremity; FMA-LE, Fugl-Meyer Assessment Lower Extremity; BI, Barthel Index; CG, conventional group; SG, melodic intonation therapy combined with sham stimulation group; TG, melodic intonation therapy combined with transcranial direct current stimulation.
[a]1-way analysis of variance.
[b]Pearson's Chi-square test.

TABLE 2 Comparison of functional values before and after intervention in each group.

| | CG (*n* =13) | | *p* value | SG (*n* =13) | | *p* value | TG (*n* =13) | | *p* value |
|---|---|---|---|---|---|---|---|---|---|
| | T0 | T1 | | T0 | T1 | | T0 | T1 | |
| WAB-AQ | 35.085 ± 37.906 | 37.746 ± 37.172 | 0.060[a] | 30.138 ± 27.582 | 41.323 ± 23.526 | 0.004[a] | 24.915 ± 26.579 | 49.715 ± 29.183 | <0.001[a] |
| Spontaneous | 6.38 ± 7.654 | 7.23 ± 7.339 | 0.059[a] | 5.08 ± 6.006 | 8.15 ± 4.705 | 0.005[a] | 3.38 ± 4.610 | 8.62 ± 5.938 | <0.001[a] |
| Comprehension | 85.31 ± 86.505 | 89.62 ± 86.358 | 0.017[a] | 84.46 ± 63.763 | 99.85 ± 52.451 | 0.019[a] | 100.08 ± 62.758 | 139.08 ± 50.457 | 0.001[a] |
| Repetition | 43.00 ± 45.200 | 44.23 ± 43.43.924 | 0.400[a] | 37.85 ± 39.179 | 53.00 ± 38.240 | 0.015[a] | 22.85 ± 38.773 | 54.00 ± 41.002 | 0.004[a] |
| Naming | 25.92 ± 40.323 | 27.38 ± 40.582 | 0.288[a] | 16.77 ± 24.749 | 22.15 ± 25.848 | 0.032[a] | 17.85 ± 30.506 | 39.54 ± 34.374 | 0.009[a] |
| MoCA | 4.62 ± 6.936 | 5.08 ± 7.740 | 0.190[a] | 3.23 ± 6.379 | 4.38 ± 6.526 | 0.007[a] | 3.62 ± 5.268 | 7.00 ± 7.439 | 0.016[a] |
| FMA | 31.15 ± 24.283 | 35.00 ± 25.668 | 0.008[a] | 20.62 ± 20.974 | 28.23 ± 22.873 | 0.004[a] | 31.31 ± 24.295 | 42.31 ± 26.033 | <0.001[a] |
| FMA-UE | 17.00 ± 15.875 | 19.38 ± 16.556 | 0.019[a] | 9.77 ± 14.143 | 15.23 ± 15.595 | 0.008[a] | 15.69 ± 15.628 | 23.92 ± 18.301 | 0.001[a] |
| FMA-LE | 14.15 ± 9.063 | 15.62 ± 9.760 | 0.017[a] | 10.85 ± 8.153 | 13.00 ± 8.287 | 0.004[a] | 15.62 ± 11.012 | 18.38 ± 9.483 | 0.011[a] |
| BI | 38.46 ± 23.838 | 52.69 ± 23.859 | <0.001[a] | 33.46 ± 17.957 | 53.46 ± 14.632 | <0.001[a] | 46.92 ± 28.250 | 59.62 ± 24.278 | <0.001[a] |

Data are expressed as mean ± SD. WAB-AQ, aphasia quotient of Western Aphasia Battery; MoCA, Montreal Cognitive Assessment; FMA, Fugl-Meyer Assessment; FMA-UE, Fugl-Meyer Assessment Upper Extremity; FMA-LE, Fugl-Meyer Assessment Lower Extremity; BI, Barthel Index; CG, conventional group; SG, melodic intonation therapy combined with sham stimulation group; TG, melodic intonation therapy combined with transcranial direct current stimulation; T0, baseline; T1, week 3. [a]Paired sample *T*-test.

inferior to TG in comprehension and naming, and the overall efficiency of TG was better than SG.

Language recovery was related to nervous system reorganization (Stefaniak et al., 2020). The review showed that the closed-loop rehabilitation system could augment the positive effect of simple peripheral or central stimulation (Jia, 2022), which was related to a previous study that concluded that peripheral intervention combined with central intervention enhanced synaptic plasticity more strongly than any individual intervention (Fritsch et al., 2010). Based on extensive activation of the cerebral cortex by tDCS, TG, combined with behavioral training, enhanced the plasticity of synapses participating in specific tasks, which would appear in the short term and continue in the long term (Fridriksson and Hillis, 2021). This result provided an effective evidence basis for the clinical application of closed-loop rehabilitation of aphasia. Spontaneous neuroplasticity, which could be affected by therapy, was the norm in the early poststroke period (Dabrowski et al., 2019). Remarkably, the mean post-stroke duration of TG is about 8 months, which was longer than the other two groups in this trial, but the therapeutic efficacy of TG was stronger. It might be another piece of evidence supporting

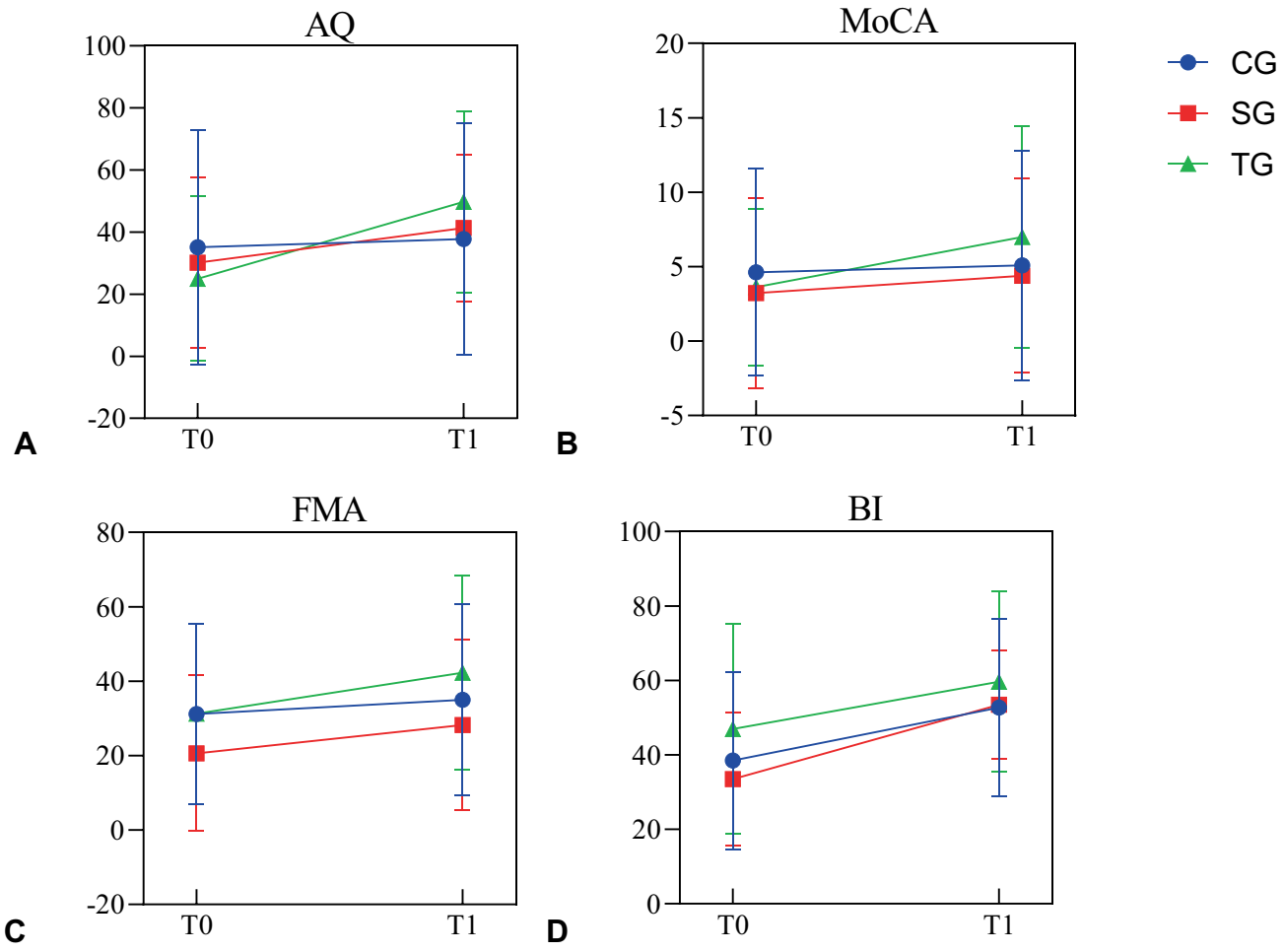


FIGURE 2
The functional values before and after intervention in three groups. **(A)** The values of AQ before and after intervention in three groups. **(B)** The values of MoCA before and after intervention in three groups. **(C)** The values of FMA before and after intervention in three groups. **(D)** The values of BI before and after intervention in three groups. AQ, aphasia quotient; MoCA, Montreal Cognitive Assessment; FMA, Fugl-Meyer Assessment; BI, Barthel Index; CG, conventional group; SG, melodic intonation therapy combined with sham stimulation group; TG, melodic intonation therapy combined with transcranial direct current stimulation; T0, baseline; T1, week 3.

TABLE 3 Comparison of functional differences among three groups.

| | CG (*n* =13) | SG (*n* =13) | TG (*n* =13) | *p* value |
|---|---|---|---|---|
| ΔWAB-AQ | 2.662 ± 4.624 | 11.185 ± 11.304 | 24.800 ± 18.420 | <0.001[a] |
| ΔSpontaneous | 0.85 ± 1.463 | 3.08 ± 3.278 | 5.23 ± 3.767 | 0.003[a] |
| ΔComprehension | 4.31 ± 5.603 | 15.38 ± 20.394 | 39.00 ± 31.815 | 0.001[a] |
| ΔRepetition | 1.23 ± 5.085 | 15.15 ± 19.200 | 31.15 ± 31.704 | 0.005[a] |
| ΔNaming | 1.46 ± 4.737 | 5.38 ± 7.995 | 21.69 ± 25.131 | 0.005[a] |
| ΔMoCA | 0.46 ± 1.198 | 1.15 ± 1.281 | 3.38 ± 4.331 | 0.024[a] |
| ΔFMA | 3.85 ± 4.356 | 7.62 ± 7.859 | 11.00 ± 8.073 | 0.044[a] |
| ΔFMA-UE | 2.38 ± 3.176 | 5.46 ± 6.200 | 8.23 ± 6.870 | 0.041[a] |
| ΔFMA-LE | 1.46 ± 1.898 | 2.15 ± 2.193 | 2.77 ± 3.320 | 0.432[a] |
| ΔBI | 14.23 ± 10.576 | 20.00 ± 10.408 | 12.69 ± 8.567 | 0.154[a] |

Data are expressed as mean ± SD. Δ, subtract the baseline score from the 3-week score; WAB-AQ, aphasia quotient of Western Aphasia Battery; MoCA, Montreal Cognitive Assessment; FMA, Fugl-Meyer Assessment; FMA-UE, Fugl-Meyer Assessment Upper Extremity; FMA-LE, Fugl-Meyer Assessment Lower Extremity; BI, Barthel Index; CG, conventional group; SG, melodic intonation therapy combined with sham stimulation group; TG, melodic intonation therapy combined with transcranial direct current stimulation.[a]1-way analysis of variance.

closed-loop rehabilitation. In the future, it is necessary to continue to carry out stratified research according to the course of the disease. Additionally, although SG was superior to CG, it had limitations in integrally improving communication. 112.5 h of MIT intervention promoted language output but not comprehension (Marchina et al., 2023). Moreover, due to previous studies focusing on behavioral indicators and insufficient imaging evidence, the neurological effect of MIT on aphasia patients was still unclear (Zhang X. Y. et al., 2021; Zhang X. et al., 2021). In this study, there was also a lack of neuroimaging detection, and the potential neural recovery mechanism of closed-loop rehabilitation also needed to be further supplemented.

The results of cognitive function analysis in this study showed that both SG and TG significantly improved after intervention, but CG was not. Moreover, the *post hoc* test supported the result that TG had the most significant effect on promoting cognitive function. The above results had a similar development tendency with the analysis of language function. Cognition is the general term for the process of recognizing and understanding objects, which belongs to the high-level activities of the cerebral cortex and interacts with language function (Norris et al., 2016; Ardila and Rubio-Bruno, 2018). Some studies had shown that the cognitive level of patients with aphasia after stroke was lower than that of non-aphasic patients, and there was a positive correlation between cognition and language (Fonseca et al., 2019; Yan et al., 2022b). These explained the experimental results and provided evidence for cognition-language integration intervention, which might be further explored in future research.

In language processing, language-related gestures might promote language performance (Grechuta et al., 2019). In our study, we found that although motor function improved in all three groups after treatment, SG and TG showed differences from CG in FMA and FMA-UE. In addition, a positive correlation between language and upper limb motor function was also found in the cross-sectional study (Xu et al., 2021). These suggested that the behavioral therapy paradigm in this trial might also facilitate motor function recovery, especially in the upper limbs, which needed to be verified by larger studies in the future.

The reason why the difference of BI was not statistically different among the three groups might be the lack of language components in BI, and the closed-loop rehabilitation program designed in this study mainly aimed at promoting the recovery of language function. In addition, the ability of daily living reflected by BI could be affected by other non-language factors, such as motor function, auxiliary appliance application, functional compensation, etc.

## 5. Conclusion

MIT combined with tDCS or sham stimulation is effective for patients with PSA, but the conventional treatment cannot significantly

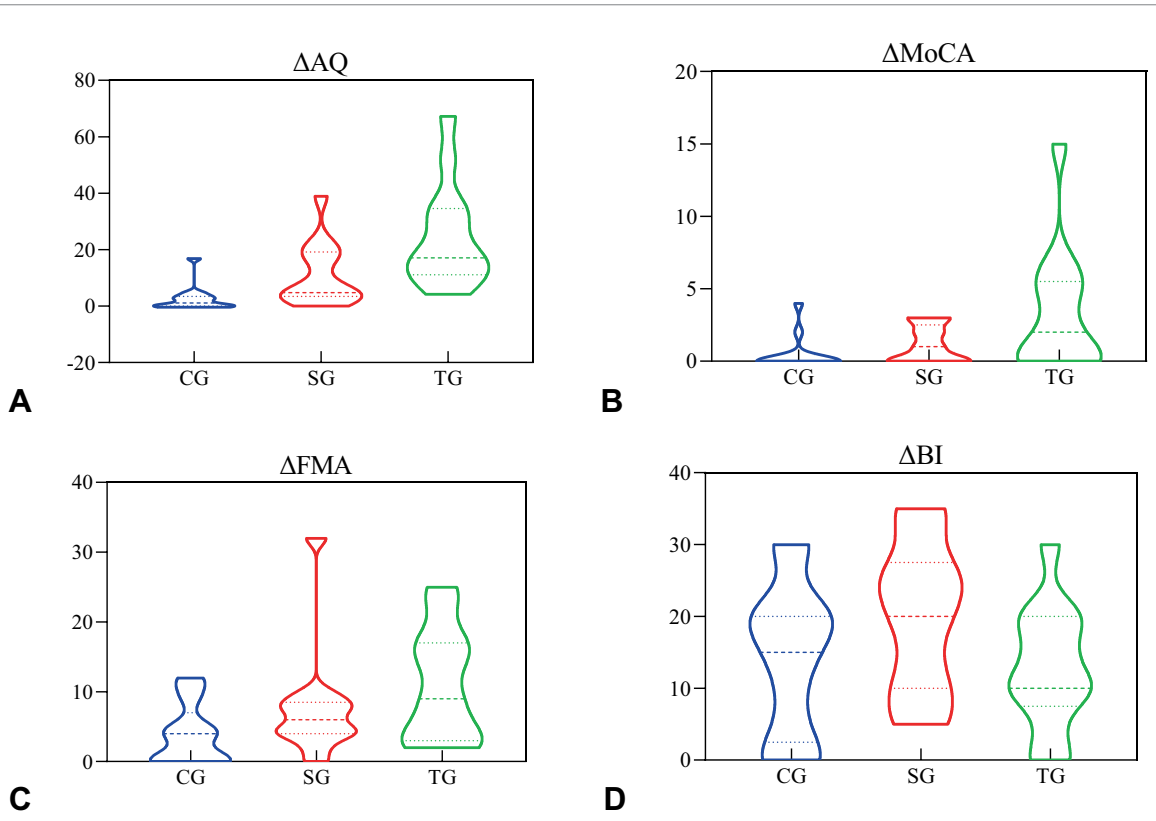


FIGURE 3
The functional difference before and after the intervention. **(A)** The difference of AQ before and after intervention in three groups. **(B)** The difference of MoCA before and after intervention in three groups. **(C)** The difference of FMA before and after intervention in three groups. **(D)** The difference of BI before and after intervention in three groups. Δ, subtract the baseline score from the 3-week score; AQ, aphasia quotient; MoCA, Montreal Cognitive Assessment; FMA, Fugl-Meyer Assessment; BI, Barthel Index; CG, conventional group; SG, melodic intonation therapy combined with sham stimulation group; TG, melodic intonation therapy combined with transcranial direct current stimulation.

improve aphasia in the short term. Compared with sham stimulation, the closed-loop rehabilitation scheme combining MIT and tDCS can augment the positive effect on language and cognitive recovery in PSA and deserves promotion in clinical practice.

## Data availability statement

The original contributions presented in the study are included in the article/supplementary material, further inquiries can be directed to the corresponding authors.

## Ethics statement

The studies involving human participants were reviewed and approved by the Ethics Committee of the Third Affiliated Hospital of Xinxiang Medical University. The patients/participants provided their written informed consent to participate in this study.

## Author contributions

ZY and JJ conceived and designed the analysis and writing – original draft. ZY, XH, MC, XF, and DW collected the data. ZY, XH, MC, XF, DW, SX, CL, XL, HX, and JJ contributed data or analysis tools, writing – review and editing, and discussed the results. ZY and XH performed the analysis. All authors contributed to the article and approved the submitted version.

## Funding

This work was supported by the National Key R&D Program of China (2018YFC2002300), the National Natural Innovation Research Group Project of China (82021002), and the National Natural Major Research Program Integration Project of China (91948302).

## Acknowledgments

Acknowledge the contributions of the Department of Rehabilitation Medicine, the Third Affiliated Hospital of Xinxiang Medical University that aided the efforts of the authors.

## Conflict of interest

The authors declare that the research was conducted in the absence of any commercial or financial relationships that could be construed as a potential conflict of interest.

## Publisher's note



## References

American Academy of Neurology (1994). Assessment: melodic intonation therapy. Report of the Therapeutics and Technology Assessment Subcommittee of the American Academy of Neurology. *Neurology* 44, 566–568.

Ardila, A., and Rubio-Bruno, S. (2018). Aphasia from the inside: the cognitive world of the aphasic patient. *Appl. Neuropsychol. Adult* 25, 434–440. doi: 10.1080/23279095.2017.1323753

Bikson, M., Grossman, P., Thomas, C., Zannou, A. L., Jiang, J., Adnan, T., et al. (2016). Safety of transcranial direct current stimulation: evidence based update 2016. *Brain Stimul.* 9, 641–661. doi: 10.1016/j.brs.2016.06.004

Breitenstein, C., Grewe, T., Floel, A., Ziegler, W., Springer, L., Martus, P., et al. (2017). Intensive speech and language therapy in patients with chronic aphasia after stroke: a randomised, open-label, blinded-endpoint, controlled trial in a health-care setting. *Lancet* 389, 1528–1538. doi: 10.1016/S0140-6736(17)30067-3

Cichon, N., Wlodarczyk, L., Saluk-Bijak, J., Bijak, M., Redlicka, J., Gorniak, L., et al. (2021). Novel advances to post-stroke aphasia pharmacology and rehabilitation. *J. Clin. Med.* 10:3778. doi: 10.3390/jcm10173778

Cortese, M. D., Riganello, F., Arcuri, F., Pignataro, L. M., and Buglione, I. (2015). Rehabilitation of aphasia: application of melodic-rhythmic therapy to Italian language. *Front. Hum. Neurosci.* 9:520. doi: 10.3389/fnhum.2015.00520

Dabrowski, J., Czajka, A., Zielinska-Turek, J., Jaroszynski, J., Furtak-Niczyporuk, M., Mela, A., et al. (2019). Brain functional reserve in the context of neuroplasticity after stroke. *Neural Plast.* 2019:9708905. doi: 10.1155/2019/9708905

Duncan, E. S., Pradeep, A. A., and Small, S. L. (2020). A review of biological interventions in chronic aphasia. *Ann. Indian Acad. Neurol.* 23, S82–S94. doi: 10.4103/aian.AIAN_549_20

Elsner, B., Kugler, J., and Mehrholz, J. (2020). Transcranial direct current stimulation (tDCS) for improving aphasia after stroke: a systematic review with network meta-analysis of randomized controlled trials. *J. Neuroeng. Rehabil.* 17:88. doi: 10.1186/s12984-020-00708-z

Fonseca, J., Raposo, A., and Martins, I. P. (2019). Cognitive functioning in chronic post-stroke aphasia. *Appl. Neuropsychol. Adult* 26, 355–364. doi: 10.1080/23279095.2018.1429442

Fridriksson, J., Elm, J., Stark, B. C., Basilakos, A., Rorden, C., Sen, S., et al. (2018a). BDNF genotype and tDCS interaction in aphasia treatment. *Brain Stimul.* 11, 1276–1281. doi: 10.1016/j.brs.2018.08.009

Fridriksson, J., and Hillis, A. E. (2021). Current approaches to the treatment of post-stroke aphasia. *J Stroke* 23, 183–201. doi: 10.5853/jos.2020.05015

Fridriksson, J., Rorden, C., Elm, J., Sen, S., George, M. S., and Bonilha, L. (2018b). Transcranial direct current stimulation vs sham stimulation to treat aphasia after stroke: a randomized clinical trial. *JAMA Neurol.* 75, 1470–1476. doi: 10.1001/jamaneurol.2018.2287

Fritsch, B., Reis, J., Martinowich, K., Schambra, H. M., Ji, Y., Cohen, L. G., et al. (2010). Direct current stimulation promotes BDNF-dependent synaptic plasticity: potential implications for motor learning. *Neuron* 66, 198–204. doi: 10.1016/j.neuron.2010.03.035

Gladstone, D. J., Danells, C. J., and Black, S. E. (2002). The fugl-meyer assessment of motor recovery after stroke: a critical review of its measurement properties. *Neurorehabil. Neural Repair* 16, 232–240. doi: 10.1177/154596802401105171

Grechuta, K., Rubio, B. B., Espin, M. R., Usabiaga, B. T., Molina, H. B., Mohr, B., et al. (2019). Augmented dyadic therapy boosts recovery of language function in patients with nonfluent aphasia. *Stroke* 50, 1270–1274. doi: 10.1161/STROKEAHA.118.023729

Haro-Martinez, A. M., Lubrini, G., Madero-Jarabo, R., Diez-Tejedor, E., and Fuentes, B. (2019). Melodic intonation therapy in post-stroke nonfluent aphasia: a randomized pilot trial. *Clin. Rehabil.* 33, 44–53. doi: 10.1177/0269215518791004

Huang, Y. A., Wang, Y. H., Hou, W. H., and Kang, Y. N. (2021). Melodic intonation therapy may improve repetition in non-fluent aphasia after stroke. *Psychogeriatrics* 21, 850–851. doi: 10.1111/psyg.12744

Jia, J. (2022). Exploration on neurobiological mechanisms of the central-peripheral-central closed-loop rehabilitation. *Front. Cell. Neurosci.* 16:982881. doi: 10.3389/fncel.2022.982881

Kasdan, A., and Kiran, S. (2018). Please don't stop the music: song completion in patients with aphasia. *J. Commun. Disord.* 75, 72–86. doi: 10.1016/j.jcomdis.2018.06.005

Kertesz, A., and Poole, E. (2004). The aphasia quotient: the taxonomic approach to measurement of aphasic disability. 1974. *Can. J. Neurol. Sci.* 31, 175–184. doi: 10.1017/S0317167100120736

Marchina, S., Norton, A., and Schlaug, G. (2023). Effects of melodic intonation therapy in patients with chronic nonfluent aphasia. *Ann. N. Y. Acad. Sci.* 1519, 173–185. doi: 10.1111/nyas.14927

Martzoukou, M., Nousia, A., Nasios, G., and Tsiouris, S. (2021). Adaptation of melodic intonation therapy to Greek: a clinical study in Broca's aphasia with brain perfusion SPECT validation. *Front. Aging Neurosci.* 13:664581. doi: 10.3389/fnagi.2021.664581

Nasreddine, Z. S., Phillips, N. A., Bedirian, V., Charbonneau, S., Whitehead, V., Collin, I., et al. (2005). The Montreal cognitive assessment, MoCA: a brief screening tool for mild cognitive impairment. *J. Am. Geriatr. Soc.* 53, 695–699. doi: 10.1111/j.1532-5415.2005.53221.x

Norris, D., Clark, M. S., and Shipley, S. (2016). The mental status examination. *Am. Fam. Physician* 94, 635–641.

Rehabilitation and Recovery of People with Aphasia after Stroke (2022). Dosage, intensity, and frequency of language therapy for aphasia: a systematic review-based, individual participant data network meta-analysis. *Stroke* 53, 956–967. doi: 10.1161/STROKEAHA.121.035216

Shah, S., Vanclay, F., and Cooper, B. (1989). Improving the sensitivity of the Barthel index for stroke rehabilitation. *J. Clin. Epidemiol.* 42, 703–709. doi: 10.1016/0895-4356(89)90065-6

Sheppard, S. M., and Sebastian, R. (2021). Diagnosing and managing post-stroke aphasia. *Expert. Rev. Neurother.* 21, 221–234. doi: 10.1080/14737175.2020.1855976

Siponkoski, S. T., Pitkaniemi, A., Laitinen, S., Sarkamo, E. R., Pentikainen, E., Eloranta, H., et al. (2023). Efficacy of a multicomponent singing intervention on communication and psychosocial functioning in chronic aphasia: a randomized controlled crossover trial. *Brain Commun* 5:fcac337. doi: 10.1093/braincomms/fcac337

Stefaniak, J. D., Halai, A. D., and Lambon, R. M. (2020). The neural and neurocomputational bases of recovery from post-stroke aphasia. *Nat. Rev. Neurol.* 16, 43–55. doi: 10.1038/s41582-019-0282-1

Van Der Meulen, I., Van De Sandt-Koenderman, M. W., Heijenbrok, M. H., Visch-Brink, E., and Ribbers, G. M. (2016). Melodic intonation therapy in chronic aphasia: evidence from a pilot randomized controlled trial. *Front. Hum. Neurosci.* 10:533. doi: 10.3389/fnhum.2016.00533

Van Der Meulen, I., Van De Sandt-Koenderman, W. M., Heijenbrok-Kal, M. H., Visch-Brink, E. G., and Ribbers, G. M. (2014). The efficacy and timing of melodic intonation therapy in subacute aphasia. *Neurorehabil. Neural Repair* 28, 536–544. doi: 10.1177/1545968313517753

Vines, B. W., Norton, A. C., and Schlaug, G. (2011). Non-invasive brain stimulation enhances the effects of melodic intonation therapy. *Front. Psychol.* 2:230. doi: 10.3389/fpsyg.2011.00230

Wang, C. P., Hsieh, C. Y., Tsai, P. Y., Wang, C. T., Lin, F. G., and Chan, R. C. (2014). Efficacy of synchronous verbal training during repetitive transcranial magnetic stimulation in patients with chronic aphasia. *Stroke* 45, 3656–3662. doi: 10.1161/STROKEAHA.114.007058

Xu, S., Yan, Z., Pan, Y., Yang, Q., Liu, Z., Gao, J., et al. (2021). Associations between upper extremity motor function and aphasia after stroke: a multicenter cross-sectional study. *Behav. Neurol.* 2021, 1–10. doi: 10.1155/2021/9417173

Yan, Z., Wei, D., Xu, S., Zhang, J., Yang, C., He, X., et al. (2022a). Determining levels of linguistic deficit by applying cluster analysis to the aphasia quotient of Western aphasia battery in post-stroke aphasia. *Sci. Rep.* 12:15108. doi: 10.1038/s41598-022-17997-0

Yan, Z., Xu, S., Wei, D., He, X., Li, C., Zhang, Y., et al. (2022b). Comparison of three cognitive assessment methods in post-stroke aphasia patients. *Front. Psychol.* 13:896095. doi: 10.3389/fpsyg.2022.896095

Zhang, X., Li, J., and Du, Y. (2021). Melodic intonation therapy on non-fluent aphasia after stroke: a systematic review and analysis on clinical trials. *Front. Neurosci.* 15:753356. doi: 10.3389/fnins.2021.753356

Zhang, X. Y., Yu, W. Y., Teng, W. J., Lu, M. Y., Wu, X. L., Yang, Y. Q., et al. (2021). Effectiveness of melodic intonation therapy in Chinese mandarin on non-fluent aphasia in patients after stroke: a randomized control trial. *Front. Neurosci.* 15:648724. doi: 10.3389/fnins.2021.648724

frontiers | Frontiers in Neuroscience

TYPE Review
PUBLISHED 18 July' 2023
DOI 10.3389/fnins.2023.1177283



OPEN ACCESS

EDITED BY
Jie Jia,
Fudan University, China

REVIEWED BY
Ying Shen,
The First Affiliated Hospital of Nanjing Medical University, China
Xun Luo,
Kerry Rehabilitation Medicine Research Institute, China

*CORRESPONDENCE
Pengyue Zhang
✉ zpy19802000@163.com
Zuhong Wang
✉ wangzuhong@sina.com

RECEIVED 01 March 2023
ACCEPTED 28 June 2023
PUBLISHED 18 July' 2023

CITATION
Zhou L, Jin Y, Wu D, Cun Y, Zhang C, Peng Y, Chen N, Yang X, Zhang S, Ning R, Kuang P, Wang Z and Zhang P (2023) Current evidence, clinical applications, and future directions of transcranial magnetic stimulation as a treatment for ischemic stroke.
*Front. Neurosci.* 17:1177283.
doi: 10.3389/fnins.2023.1177283



# Current evidence, clinical applications, and future directions of transcranial magnetic stimulation as a treatment for ischemic stroke

Li Zhou[1], Yaju Jin[1], Danli Wu[1], Yongdan Cun[1], Chengcai Zhang[1], Yicheng Peng[1], Na Chen[1], Xichen Yang[1], Simei Zhang[1], Rong Ning[1], Peng Kuang[1], Zuhong Wang[2]* and Pengyue Zhang[1]*

[1]Key Laboratory of Acupuncture and Massage for Treatment of Encephalopathy, College of Acupuncture, Tuina and Rehabilitation, Yunnan University of Traditional Chinese Medicine, Kunming, China, [2]Kunming Municipal Hospital of Traditional Chinese Medicine, Kunming, Yunnan, China

Transcranial magnetic stimulation (TMS) is a non-invasive brain neurostimulation technique that can be used as one of the adjunctive treatment techniques for neurological recovery after stroke. Animal studies have shown that TMS treatment of rats with middle cerebral artery occlusion (MCAO) model reduced cerebral infarct volume and improved neurological dysfunction in model rats. In addition, clinical case reports have also shown that TMS treatment has positive neuroprotective effects in stroke patients, improving a variety of post-stroke neurological deficits such as motor function, swallowing, cognitive function, speech function, central post-stroke pain, spasticity, and other post-stroke sequelae. However, even though numerous studies have shown a neuroprotective effect of TMS in stroke patients, its possible neuroprotective mechanism is not clear. Therefore, in this review, we describe the potential mechanisms of TMS to improve neurological function in terms of neurogenesis, angiogenesis, anti-inflammation, antioxidant, and anti-apoptosis, and provide insight into the current clinical application of TMS in multiple neurological dysfunctions in stroke. Finally, some of the current challenges faced by TMS are summarized and some suggestions for its future research directions are made.

KEYWORDS

**transcranial magnetic stimulation, ischemic stroke, underlying mechanisms, clinical applications, challenges, literature search and methods**

## Literature search and methods

We retrieved a large amount of literature from Web of Science, Science, SCI-hub, Google Scholar, Pubmed and other databases to search for keywords such as stroke, ischemic stroke, cerebrovascular accident, noninvasive brain stimulation technique (NIBS), transcranial magnetic stimulation (TMS), repetitive transcranial magnetic stimulation, single pulse transcranial magnetic stimulation (spTMS), paired pulsed transcranial magnetic stimulation (ppTMS), theta burst repetitive TMS (TBS), interhemispheric inhibition, cerebral ischemia–reperfusion injury (CIRI), neurotransmitters, excitatory neurotransmitters, glutamate, brain-derived neurotrophic factor (BDNF), $Ca^{2+}$, neurogenesis, blood–brain barrier (BBB), astrocytes,

microglia, oxidative stress injury, apoptosis, upper limb function, lower extremity function, speech, swallowing, cognition, post-stroke depression, spasticity, central post-stroke pain, adverse effects of TMS, and epilepsy, and kicked out studies that reported only protocols, trials that had not yet been completed, and caseloads of less than 8. A total of 136 randomized controlled trials, 23 experimental basic studies, and 5 meta-analyses were finally included (see Figure 1 for details).

## Introduction

Stroke is a cerebrovascular disease of the middle-aged and elderly due to impaired cerebral blood flow circulation leading to tissue damage. With the economic and social development of countries, the occurrence of stroke is becoming younger and younger. Stroke includes two types of stroke: ischemic and hemorrhagic stroke, ischemic stroke accounts for 87% of all strokes and is characterized by high morbidity, disability and mortality, and is the leading cause of disability and death induced by human diseases [NCD Risk Factor Collaboration (NCD-RisC), 2021]. According to stroke epidemiology in 2020, the number of stroke patients worldwide is expected to increase by about 30 million per year, which will place a heavy burden on the global society and economy (The Lancet Neurology, 2021).

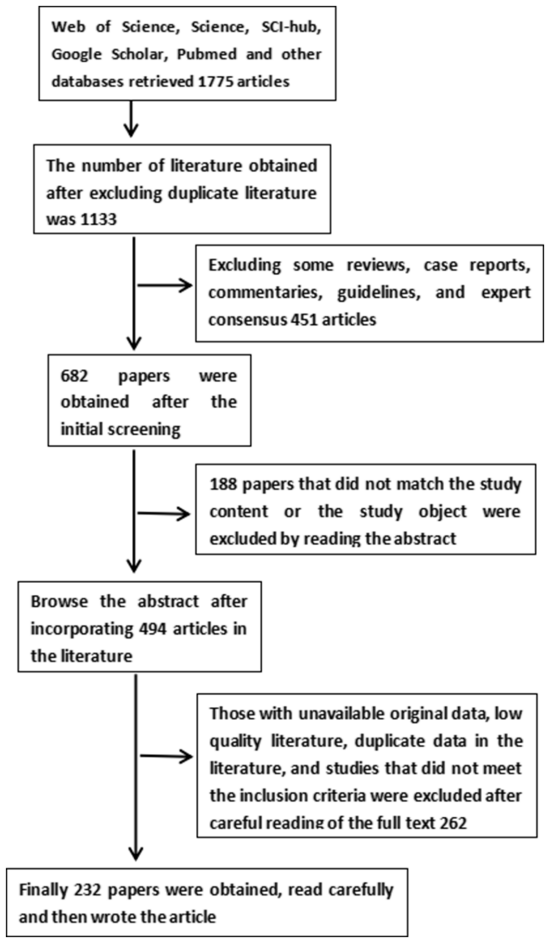


FIGURE 1
Flow chart of literature search.

After ischemic stroke, the key treatment strategy to save damaged brain tissue is to achieve cerebral blood flow recanalization. Commonly used treatments include intravenous thrombolysis (Higashida et al., 2003), endovascular therapy (Chen C. J. et al., 2015) and bridging therapy (Albuquerque, 2014), all of which are reperfusion therapies based on thrombolysis and thrombus retrieval as a clinical tool to mitigate further neurological deterioration in stroke patients by salvaging the semidark zone tissue. However, due to the strict time window for cerebral blood flow reperfusion therapy, only about 15% of stroke patients are able to achieve cerebral blood flow recanalization (Wahlgren et al., 2016). Although the time window for thrombolytic therapy in stroke patients has been extended to 24 h in recent years (Ragoschke-Schumm and Walter, 2018), reperfusion therapy still faces great challenges and risks and may even further aggravate neurological deficits in stroke patients, such as neurological disorders in cognition (Delavaran et al., 2017), speech (Schumacher et al., 2019), swallowing (Sreedharan et al., 2022), and sensorimotor function (D'Imperio et al., 2021). Therefore, with the trend of increasing stroke incidence year by year, it is extremely necessary to propose a new adjuvant therapy to improve neurological dysfunction and enhance activities of daily living in stroke patients.

TMS is a non-invasive neurostimulation technique that is painless, non-invasive and needs to be used while the patient is awake, and consists of two main components: the main unit and the treatment cap or probe (with coils). During treatment, the probe is placed on the cerebral cortex to be stimulated and an electric current is passed through the coil to generate a magnetic field, followed by an induced current that affects the cerebral cortex, thus achieving a transient enhancement or suppression of cortical neuroexcitability (Kobayashi and Pascual-Leone, 2003; Rossini and Rossi, 2007; Kesikburun, 2022). TMS has been reported to have neuroprotective effects in a variety of neurological disorders, such as Alzheimer's disease (Mimura et al., 2021), Parkinson's (Chen and Chen, 2019), multiple sclerosis (Aloizou et al., 2021), depression (Toth et al., 2022), vascular dementia (Nardone et al., 2011), and stroke (Tosun et al., 2017). Some studies have shown that TMS combined with a variety of rehabilitation treatments can significantly reduce neurological dysfunction, improve the ability to perform activities of daily living, and improve the quality of life of stroke patients (Dionísio et al., 2021; Hoonhorst et al., 2021; Zong et al., 2022). This suggests that TMS is a feasible adjunctive treatment for stroke.

There are differences in the site and timing of TMS stimulation for different dysfunctions in stroke. Currently, the commonly used stimulation sites in stroke are primary motor cortex (M1), left dorsolateral prefrontal cortex (DLPFC), superior temporal gyrus, inferior frontal gyrus, and secondary somatosensory cortex (S2) (Lee et al., 2022). In addition, there are brain areas that are used as stimulation sites according to their functional counterparts. Among these stimulation sites, the primary motor cortex is by far the most commonly used stimulation site, presumably because M1 is the central regulatory point for motor control and functional decision making in the body (Lee et al., 2022); second, M1 is a multi-overlapping, multifunctional cortical area involved in multiple functions such as motor, cognitive, speech, and swallowing. Therefore, for stroke, a multifunctional disorder neurological disease, M1 is one of the common stimulation targets irreplaceable for TMS treatment of stroke disease. In addition, the duration of TMS stimulation time varies, and the determination of its treatment time is related to the acute and

chronic stage of the disease, its severity, the patient's tolerance level, and the treatment goal. However, although TMS has been widely used to improve neurological dysfunction after stroke, its potential mechanisms, optimal stimulation modality, site, frequency, and duration to promote neural repair are not clear and need to be further explored. Therefore, this review will summarize the potential mechanisms of TMS to improve post-stroke neurological function, review the relevant clinical applications of TMS in stroke patients, and summarize the current risks and challenges that remain with TMS.

## Classification of transcranial magnetic stimulation

TMS is not only a therapeutic tool for many neurological disorders, but also a common screening or diagnostic tool. When it is applied to the motor cortex of the brain, the target cortical muscles produce corresponding motor evoked potentials (MEP), and the MEP can be recorded in real time with surface electromyography (EMG) to determine the continuity and integrity of motor neural pathways. In addition, the EEG values recorded in combination with EEG are real-time readings of TMS-induced changes in cortical excitability. Thus, TMS can be used as a test tool to record changes in cortical neurological function and brain dynamics. Currently, TMS is often divided into three forms: single-pulse TMS (spTMS) (Henriette et al., 2022), paired-pulse TMS (ppTMS) (Du et al., 2014) and repetitive TMS (rTMS) (Klomjai et al., 2015).

The spTMS is a single-pulse stimulus that occurs every few seconds, and is commonly used to study individual motor thresholds as well as cortical neural excitability (Klomjai et al., 2015; Jarczok et al., 2021). Similarly, ppTMS is the exploration of intracortical circuit excitability (Boulogne et al., 2016) by generating two consecutive pulses of stimulation every few seconds, including both intracortical inhibition (ICI) and intracortical facilitation (ICF) endings, which ultimately lead to different courses of ICI and ICF depending on the intensity of the stimulus before and after the two pulses, and the interval between the two stimuli (Hanajima et al., 2002; Ilić et al., 2002; Mcclintock et al., 2011). The rTMS is a repetitive pulse stimulation of the same frequency and intensity for a certain period of time, and after the cumulative sum of these repetitive pulse stimuli reaches the threshold of evoked neural activity, the stimulated site can briefly produce neural excitatory or inhibitory activity (Vlachos et al., 2012). If rTMS stimulation is repeated several times, then the effects produced can last longer and even form synapses that persist (Kricheldorff et al., 2022).

In addition, rTMS has been extended by simulating the firing pattern of hippocampal neurons with a new type of TMS, in which three pulses at 50 Hz occur at 200 ms intervals, called theta burst repetitive TMS (TBS) (Ferrarelli and Phillips, 2021). Compared with conventional rTMS, TBS can induce longer duration and more intense neural activity with low-intensity, short duration stimulation (Kricheldorff et al., 2022). TBS includes interstitial theta pulse stimulation (iTBS) and continuous theta pulse stimulation (cTBS) (Bai Z. et al., 2022). In general, iTBS increases neuronal excitability and enhances LTP-like effects, while cTBS induces LTD-like effects and suppresses neuronal excitability (Huang et al., 2009). However, not all iTBS and cTBS follow this pattern, as Xue et al. found that cTBS treatment upregulated the release of neurotrophic factors in stroke patients, increased the number of new neurons in the penumbra region, and promoted post-stroke neurogenesis (Zong et al., 2022). The reason for this heterogeneity may be due to the different neuronal populations finally activated by cTBS and iTBS (Volz et al., 2015), as well as the different recruitment of indirect (I) wave in the late corticospinal overhead jerk after stimulation (Di Lazzaro et al., 2008). In addition to TBS, rTMS includes a quadruple pulse stimulation (QPS) with four monophasic pulse stimulation repeated every 5 s (Nakatani-Enomoto et al., 2012), which produces a bidirectional effect when acting on the motor cortex of the brain, i.e., short interval QPS enhances neuroplasticity and long interval QPS inhibits neuroplasticity (Hamada et al., 2008; Ni and Chen, 2008). Although QPS is similar to ppTMS, Masashi et al. found that QPS was more effective than ppTMS in inducing motor cortical neuroplasticity with better persistence and specificity than ppTMS (Hamada et al., 2007).

## Effects of transcranial magnetic stimulation parameters on cortical excitability

Impaired excitability of the motor cortex in the hemisphere of the post-stroke lesion results in limited movement of the hemiplegic side of the limb (Liepert et al., 2000), one of the causes of this impairment is dysregulation of interhemispheric inhibition after stroke (Xu et al., 2019). In a healthy state, both hemispheres regulate each other's cortical excitability via the corpus callosum pathway, so that the bilateral interhemispheric excitability is maintained in balance and no over inhibition occurs (Duque et al., 2005). In contrast, after stroke, interhemispheric inhibition is imbalanced, and cortical excitability in the lesioned hemisphere is reduced by oversuppression of excitability, while cortical excitability in the non-lesioned hemisphere is increased. This leads to a variety of neurological sequelae after stroke and reduces the quality of patient survival (Bütefisch et al., 2008; Wahl et al., 2016; Patel et al., 2019). Therefore, regulation of interhemispheric excitability balance is an indispensable remedy to improve post-stroke neurological dysfunction (Lin et al., 2020; Sharma et al., 2020).

The world's first transcranial magnetic device was developed in 1985 by Barker et al. (1985) as a tool to study changes in excitability of the motor cortex of the brain after stimulation. So how is the target cortical excitability modulated when TMS is used to treat stroke patients? In general, high frequency TMS (HF-TMS) in the lesioned hemisphere increases cortical excitability and low frequency TMS (LF-TMS) in the non-lesioned hemisphere decreases cortical excitability (Iyer et al., 2003; Kim et al., 2004; Chen M. et al., 2015; Nordmann et al., 2015). However, is there a boundary between HF-TMS and LF-TMS? Most studies consider low frequency $\leq$ 1 Hz and high frequency > 1 Hz (Modugno et al., 2003; Filipović et al., 2010; Fried et al., 2017; Tugin et al., 2021); some studies consider high frequency $\geq$ 5–20 Hz (Somaa et al., 2022); and a few other researchers consider high frequency $\geq$ 3 Hz (Kubis, 2016; Tian and Izumi, 2022). Thus, it seems that LF-TMS is relatively stable compared to HF-TMS, which are in the range of 0-1 Hz, and the majority of studies mostly use 1 Hz (Heide et al., 2006; Meng et al., 2020). And some studies have shown that the inhibitory effect of 1 Hz-rTMS on cortical excitability is the most pronounced (Muller et al., 2014). However, LF-rTMS at 0.25 Hz (Muller et al., 2014), 0.1 Hz (Chen et al., 1997), 0.3 Hz (Cincotta et al., 2003), 0.6 Hz (Khedr et al., 2004), and 0.9 Hz have also been used in some studies (Kricheldorff et al., 2022).

The modulation of target cortical excitability by TMS is also influenced by stimulus parameters (Lang et al., 2006; Taylor and Loo, 2007; Jung et al., 2008; De Jesus et al., 2014). Within a certain range, cortical excitability produces stronger and more sustained effects with increasing TMS pulse number (Tang et al., 2019). In other words, the number of pulses is proportional to cortical excitability within a certain limit (Touge et al., 2001; Peinemann et al., 2004), which also varies from individual to individual. Therefore, when patients receive TMS for the first time, they should be pre-stimulated to explore the optimal TMS parameters. In addition to this, cortical excitability is influenced by stimulation intensity and time. The differences caused by stimulus intensity are mainly related to interindividual motor thresholds (MT) (D'amico et al., 2020; Rizzo et al., 2020). Cortical excitability tends to change at the MT intensity node, with stimulus intensities greater than MT increasing MEP amplitude and thus target cortical excitability; conversely, target cortical excitability usually decreases when stimulus intensities are less than MT (Modugno et al., 2001; Fitzgerald et al., 2002). However, who is more dominant in the effect of TMS frequency and intensity on cortical excitability? Or are they of equal status? Heide et al. (2006) found that rTMS at a frequency of 1 Hz and an intensity of 115% of resting motor threshold (RMT) applied to primary motor cortex (M1) for several minutes resulted in reduced cortical excitability (Meng et al., 2020). This suggests that frequency may be more important for the modulation of cortical excitability. However, a study by Gabrielle et al. using HF-rTMS at three low intensities (70, 80 and 90% of active motor threshold (AMT)) found that only stimulus intensities up to 90% AMT promoted target cortical excitability, whereas both 70 and 80% AMT inhibited cortical excitability (Todd et al., 2006). This suggests that it is the modulation of cortical excitability by stimulus intensity that may be more important. In summary, we suggest that frequency and intensity may be equally important for the modulation of cortical excitability, but that the expected effects differ due to inter-individual differences in MT. Of course, these are our speculations and the exact mechanisms are not yet clear. In addition, target cortical excitability is also influenced by the stimulus waveform (Arai et al., 2005), with monophasic pulses having a stronger cortical excitatory effect due to preferential activation of neuronal populations in the same direction compared to biphasic pulses (Arai et al., 2007).

## Potential mechanisms of transcranial magnetic stimulation for stroke

TMS is known to promote the improvement of different neurological functions through different stimulation sites. For example, sites such as M1 (Bai G. et al., 2022), dorsolateral prefrontal cortex (DLPFC; Hara et al., 2021), and parietal cortex (Rushworth and Taylor, 2006) can improve motor, cognitive (Zhang et al., 2022), and speech dysfunctions in stroke patients. However, there is no more comprehensive summary of how TMS facilitates the improvement of neurological function after stroke. Therefore, in the following, we will briefly describe the potential mechanisms of TMS from these aspects.

### Transcranial magnetic stimulation regulates the concentration of excitatory neurotransmitter-glutamate

Neuroexcitotoxicity after ischemic stroke is a key link leading to neuronal death, which can induce a series of pathological cascade reactions that eventually lead neurons to apoptosis or necrosis. Neuroexcitotoxicity is mainly caused by $Ca^{2+}$ overload after cerebral ischemia and hypoxia, massive release of excitatory neurotransmitter glutamate and excessive activation of ionotropic glutamate receptors. Therefore, glutamate receptor inhibitors have been used clinically to block the over-activation of glutamate receptors and thus reduce the damage caused by neuroexcitotoxicity after stroke, but the effect is not very obvious. In recent years, it has been found that TMS can regulate human excitatory neurotransmitter-glutamate levels, which may be one of the potential targets to prevent or mitigate post-stroke excitotoxicity.

TMS can modulate neural activity by regulating glutamate concentrations in the nervous system, e.g., 10 Hz-rTMS significantly downregulates glutamate levels in the striatum (dorsal and NAc; Poh et al., 2019). Similarly, Eugenia et al. demonstrated that rTMS reduces the concentration of neurotransmitters such as glutamate, striatal serine, threonine, sarcosine, and aspartate in the nervous system (Poh et al., 2019). It has also been shown that 0.5-Hz-rTMS leads to significantly higher levels of glutamate in the hippocampus and striatum, but glutamate levels in the hypothalamus are reduced. These results suggest that the regulation of glutamate concentration by rTMS may be influenced by the stimulation site, frequency, and the concentration of glutamate levels in various brain regions, and that its main purpose is to regulate glutamate concentration to a normal range; thus, the mechanism by which rTMS regulates glutamate concentration varies in different brain regions. However, this is our speculation and more studies are needed to verify it (Yue et al., 2009).

In addition, TMS can promote glutamate uptake by neurons and decrease glutamate accumulation between neurons by upregulating glutamate receptor activity or expression. For example, Adeline et al. observed that 1 Hz-rTMS promotes upregulation of glutamate receptor 5 (GluA5) receptor expression (Etiévant et al., 2015). Similar studies have shown that TMS promotes the upregulation of the number and density of α-amino-3-hydroxy-5-methyl-4-isoxazolepropionic acid (AMPA) receptors of glutamate receptor 1 (GluA1; Vlachos et al., 2012; Lenz et al., 2015). Furthermore, in addition to regulating glutamate receptors, glutamate transporter proteins can also regulate extracellular glutamate levels. Therefore, it has been suggested that TMS regulation of glutamate concentration may also be related to the expression of glutamate transporter proteins. A study showed that rTMS promotes upregulation of the expression of genes of glutamate transporter proteins such as EAAT4, GLAST, GLT1, and EAAC24 (Ikeda et al., 2019). This is the first study in which rTMS was observed to regulate the expression of glutamate transporter proteins, providing a potential direction for future studies on the mechanism of rTMS.

### Transcranial magnetic stimulation promotes neurogenesis

Neurogenesis plays a pivotal role in promoting improved neurological function after stroke. Brain-derived neurotrophic factor (BDNF), a member of the neurotrophic factor family, is one of the most important regulators of activity-dependent neuroplasticity (Luo et al., 2017). In healthy states, BDNF is involved in promoting neurogenesis in the central nervous system in addition to nutritional support of nerve cells (Tan et al., 2021). For example, it promotes the formation of dendritic spines (Chaturvedi et al., 2020) and facilitates synaptic long-term potentiation (LTP) (Leal et al., 2014). In addition,

BDNF regulates the balance of excitatory and inhibitory neurotransmitters in the brain (Karantali et al., 2021). In addition, it has been shown that patients with significantly lower serum BDNF levels and increased brain infarct volume after stroke have a worse functional outcome of stroke (Qiao et al., 2017; Duan et al., 2018). It is thus clear that regulation of BDNF expression has an irreplaceable role in promoting post-stroke neurogenesis.

In recent years, TMS has become an integral part of stroke rehabilitation treatment strategies. Ma et al. (2014) found that 110% RMT, 1 Hz-rTMS activated the BDNF/tyrosine kinase receptor B (TrkB) pathway and promoted neuroplasticity; however, as the stimulation intensity increased to 150% RMT, the BDNF/TrkB pathway was inhibited, the number of synapses decreased, the density and thickness thinned, and neurogenesis was suppressed. In addition, Guo et al. (2014) found that TMS significantly upregulated miR-25 expression and promoted the proliferation of neural stem cells (NSCs) in the subventricular zone of stroke patients. It has also been shown that the proliferation and differentiation of newborn neural stem cells to the ischemic lesion area after stroke is regulated by BDNF, and overexpression of BDNF accelerates the recruitment of newborn neural stem cells and their migration to the ischemic brain tissue area (Young et al., 2011; Jansson et al., 2012). In addition to the above possible mechanisms, it has also been shown that iTBS regulates intrasynaptic $Ca^{2+}$ concentration by affecting N-methyl-D-aspartate (NMDA) activity, thereby increasing intrasynaptic transmission efficiency and promoting LTP-like effects (Saudargiene et al., 2015; Diao et al., 2022). It is thus clear that TMS promotes improved neurological function after stroke and is closely related to multiple pathway-mediated neurogenesis.

## Transcranial magnetic stimulation promotes vascular regeneration

Vascular injury and blood–brain barrier (BBB) disruption caused by ischemia after stroke induces brain edema formation, which exacerbates post-stroke neurological dysfunction (Fagan et al., 2005; Rodríguez-Yáñez et al., 2006). Therefore, promoting angiogenesis becomes one of the potential targets to rescue ischemic brain tissue and improve neurological function. Astrocytes are the most abundant neuronal cells in the brain (Yu G. et al., 2021) and have two phenotypes: classical activation (A1) and alternative activation (A2) (Liddelow et al., 2017). In general, both types of astrocytes play important physiological roles both in healthy and injured conditions. A1-type astrocytes promote the release of inflammatory factors to induce inflammatory responses, while A2-type astrocytes increase the release of angiogenesis-related factors such as transforming growth factor-β (TGFβ) and vascular endothelial growth factor (VEGF) to promote angiogenesis (Blackburn et al., 2009; Liddelow and Barres, 2017).Mark et al. found that chronic intracerebroventricular infusion of VEGF significantly promoted vascular collateral circulation formation and increased vascular density (Harrigan et al., 2002). Sun et al. (2003) also found that increasing VEGF levels stimulated vascular regeneration after cerebral ischemia. In summary, promoting upregulation of VEGF levels by promoting the polarization of A1-type astrocytes to A2-type astrocytes and thus promoting vascular regeneration may be one of the molecular mechanisms to improve neural repair after stroke.

In recent years, with the rapid development of TMS, studies on the mechanism of TMS to improve neurological function after stroke have been increasing. One study showed that 10 Hz-rTMS promoted the polarization of A1-type astrocytes to A2-type, thereby reducing infarct volume and promoting neurological recovery in MCAO rats (Hong et al., 2020). Similarly, Zong X. et al. (2020a) reported that rTMS promoted the polarization of A2-type astrocytes, elevated the levels of angiogenesis-related factors TGFβ, VEGF, and hypoxia-inducible factor 1α (HIF-1α), and increased the density and volume of neovascularization in the penumbra region of MCAO rats. The above studies suggest that one of the mechanisms of neuroprotective effects of TMS is the induction of A2-type astrocyte polarization and promotion of vascular regeneration.

## Anti-inflammatory properties of transcranial magnetic stimulation

The immune inflammatory response is rapidly activated after stroke and continues throughout the stroke period. In general, the early inflammatory response contributes to neuroprotection by phagocytosis of dead cell debris or certain harmful toxic substances (Wen et al., 2006), but prolonged inflammatory factor infiltration is detrimental to post-stroke neuronal survival (Qin et al., 2019). Therefore, reducing the inflammatory response and preventing excessive release of inflammatory factors are essential to improve the internal environment for neuronal survival after stroke.

Microglia act as neurological macrophages in the brain and play an important role in maintaining the homeostasis of the intracerebral environment (Ma et al., 2017). There are two phenotypes, classical activated (M1) and alternative activated (M2), which play different roles in response to different stimuli during different pathological stages of ischemic stroke (Hu et al., 2015). M1 microglia release tumor necrosis factor (TNF-α), interleukin 1β (IL-1β), interferon γ (IFN-γ), interleukin 6 (IL-6), inducible nitric oxide synthase (iNOS), matrix metalloproteinase 9 (MMP9), matrix metalloproteinase 3 (MMP3), and other pro-inflammatory mediators, induce BBB permeabilization and accelerate ischemic neuronal death (Kreutzberg, 1996; Yenari et al., 2010). In contrast, M2 microglia release anti-inflammatory and pro-angiogenic mediators such as interleukin 10 (IL-10), TGF-β, and VEGF, which exert neuroprotective effects (Ponomarev et al., 2013; Prinz et al., 2014). Once stroke occurs, M1 and M2 microglia are activated to release both pro-inflammatory and anti-inflammatory mediators, and the resistance of these two mediators determines the fate course of neuronal cells in the ischemic infarct zone (Hu et al., 2012; Zhao et al., 2017). Therefore, regulation of M1/M2 microglia polarization during different stages of stroke may be one of the mechanisms regulating the brain microenvironment and promoting neural repair.

TMS is currently used as a common intervention for stroke rehabilitation. Zhao et al. (2019) found that rTMS significantly reduced IL-1β and TNF-α serum levels in patients. In the MCAO model, the 10 Hz-rTMS experimental group activated more M2 microglia and reduced activation of M1 microglia than the no sham stimulation group (Hong et al., 2022). Immediately after, this study also showed that rTMS significantly increased microglia let-7b-5p levels and inhibited their downstream NF-kB signaling pathway, thereby reducing the size of cerebral infarcts in MCAO rats; in addition, *in vitro* experiments showed that administration of rTMS to microglia increased the concentration of interleukin 10 (IL-10) and decreased the concentration of TNF-α in the culture medium, while knockdown of let-7b -5p reversed these phenomena (Hong et al.,

2022). This study repeatedly verified from *in vivo* and *ex vivo* experiments that rTMS ameliorates neurological dysfunction in MCAO model mice by promoting M2-type microglia polarization, regulating the let-7b-5p/NF-kB signaling pathway, and attenuating the inflammatory response. Similarly, it was shown (Luo et al., 2022) that iTBS significantly reduced IL-1β, interleukin 17A (IL-17A), TNF-α, and IFN-γ concentrations in MCAO mice by inhibiting M1 activation, promoting M2 polarization, and downregulating Toll-like receptor 4 (TLR4)/NF-κB/NLR family Pyrin domain-containing protein 3 (NLRP3) signaling pathway. Elevated IL-10 concentrations reduced neuromotor dysfunction in MCAO mice, whereas removal of microglia after using the inhibitor eliminated the efficacy of iTBS application, which inversely verified that iTBS ameliorated post-stroke neurological dysfunction by regulating the balance of M1/M2 phenotype of microglia.

### Antioxidant properties of transcranial magnetic stimulation

Achieving blood flow recanalization as soon as possible after stroke is a top priority to salvage the ischemic semidark zone. However, cerebral ischemia–reperfusion is prone to cerebral ischemia–reperfusion injury (CIRI) because it has a strict time window (Zhao et al., 2022). Therefore, it is important to explore the underlying mechanisms of CIRI to explore potential targets for stroke therapy. It has been reported that CIRI injury is mainly caused by the reactivation of mitochondrial aerobic respiration after blood flow recanalization, which generates large amounts of reactive oxygen species (ROS) and induces oxidative stress in neuronal cells (Orellana-Urzúa et al., 2020; Yu S. et al., 2021). Therefore, reducing ROS release after stroke and enhancing the antioxidant capacity of the body are key steps to reduce CIRI injury. Studies have shown that TMS promotes functional repair in a variety of neurological diseases in association with its powerful antioxidant effects (Post et al., 1999; Medina-Fernandez et al., 2017). For example, Hui et al. found that rTMS attenuates CIRI injury by activating the nuclear factor E2-related factor 2 (Nrf2) signaling pathway, upregulating the expression of antioxidant proteins such as Nrf2, heme oxygenase 1 (HO-1), and superoxide dismutase 1 (SOD1), and reducing oxidative stress (Liang et al., 2021).

### Anti-apoptotic properties of transcranial magnetic stimulation

The tissue blood supply around the ischemic infarct foci (penumbra zone) in the early post-stroke period is still maintained at 20–40% while retaining some oxygenated metabolic activity (Hou et al., 2019). Therefore, salvaging the penumbra for a certain period of time is essential to reduce the volume of post-stroke cerebral infarction. However, it has been found that within hours or days after cerebral ischemia, the ischemic penumbra in response to ischemic–hypoxic stress induces some neuronal cells toward apoptosis and releases toxic substances that further accelerate neuronal death (Vexler et al., 1997; Radak et al., 2017). Thus, apoptosis, which is activated in the acute phase of stroke, is a major obstacle to the remodeling of neuronal cell structure and function in the ischemic penumbra region after stroke.

A recent study showed that the potential mechanism by which rTMS promotes neurological recovery in MCAO rats is related to the inhibition of premature apoptosis of neuronal cells in the penumbra region (Gao et al., 2010; Yoon et al., 2011). Yamei et al. showed that rTMS upregulated B lymphocytoma-2 gene (Bcl-2) levels and decreased Bcl-2-related X protein (Bax) expression significantly inhibited apoptosis, thereby improving neurological recovery in MCAO rats (Guo et al., 2017). Similarly, a similar study also found that TMS combined with electroacupuncture treatment inhibited post-ischemic neuronal apoptosis by significantly reducing cystein-3 (Caspase-3) levels and increasing Bcl-2 mRNA expression levels (Li et al., 2012). In addition, rTMS can reduce mitochondrial damage, maintain mitochondrial membrane integrity, inhibit the activation of the mitochondria-dependent apoptotic cystatase-9 (Caspase-9)/Caspase-3 signaling pathway, and reduce neuronal death (Sasso et al., 2016; Zong et al., 2020b).

## Clinical application of transcranial magnetic stimulation in stroke diseases

Stroke is one of the leading causes of neurological disability in the world (Saini et al., 2021). Once stroke occurs, a variety of neurological complications follow, leading to severe limitations in patients' activities of daily living (Chohan et al., 2019). Therefore, exploring the application of new technologies in stroke rehabilitation is pivotal to provide more clinical experience in the future treatment of stroke patients; in addition, it will provide a better understanding of the advantages and disadvantages, indications, contraindications, and precautions of this technology and promote better service of this technology to society. In recent years, more and more studies have reported that TMS plays an irreplaceable role in the neurological rehabilitation process of stroke, involving upper and lower limb motor function, speech, swallowing, cognitive function, post-stroke depression, spasticity, and central post-stroke pain (see Table 1 for details). However, the potential mechanisms by which TMS improves the above neurological dysfunctions? and whether the stimulation frequency, intensity, duration and site are consistent are unclear? Therefore, the clinical application of TMS in stroke rehabilitation is briefly described below, and each of these queries will be explored.

## Motor dysfunction

### Upper extremity

Motor dysfunction of the upper extremity after stroke is mainly characterized by reduced movement, limb coordination and dexterity and accounts for 55–75% of all stroke patients (Wolf et al., 2006). Compared with the lower extremity, the recovery of motor function in the upper extremity after stroke progresses relatively slowly and is mainly concentrated in the first 6 months. Due to the weak awareness of rehabilitation in most patients, by the time they start to intervene in rehabilitation, they have already missed the golden time of upper limb function recovery. Therefore, it is crucial to raise the patients' awareness of rehabilitation and to find an effective complementary therapy.

Recently, several randomized controlled trials have shown that rTMS modulates cortical excitability and restores interhemispheric inhibitory balance to improve motor dysfunction after stroke (Kim et al., 2006; Long et al., 2018). A study by Avenanti et al. showed that HF-rTMS significantly increased cortical excitability in the lesioned

TABLE 1 Clinical application of transcranial magnetic stimulation in post-stroke sequelae.

| Type of Research | Stimulation site | Stimulation frequency | Stimulation time | Sample size | Amount of effect | Results | References |
|---|---|---|---|---|---|---|---|
| Clinical Studies | Lesioned hemisphere | 10 Hz | 1 time/day, 5 days/week, 4 weeks in total | 9 | 9 | Improvement in upper limb motor function | Ni et al. (2022) |
| | | 5 Hz | 1 time/day, 6 days/week, 10 times in total | 20 | 18 | | Hosomi et al. (2016) |
| | | 10 Hz | 1 time/day, 20 min/time, 13 days in total | 19 | 19 | Improvement in lower limb walking speed | Kakuda et al. (2013) |
| | | 5 Hz | 1 time/day, 15 min/time, 3 times/week, total 3 weeks | 6 | 6 | | Wang et al. (2019) |
| | | 10 Hz | 1 time/day, 40 min/day for 2 weeks | 15 | 15 | Motor function, muscle strength improvement | Wang et al. (2020) |
| | | 10 Hz | 1 time/day, 20 min/time, 5 times/week, 4 weeks in total | 18 | 16 | Improved cognitive function | Yin et al. (2020) |
| | | 20 Hz | 1 time/day, 20 min/time, 5 times/week for 2 weeks | 10 | 10 | | Cha et al. (2022) |
| | | 50 Hz (iTBS) | 1 time/day, 20 min/time, 5 times/week, total 6 weeks | 22 | 21 | | Chu et al. (2022) |
| | | 10 Hz | 1 time/day, 30 min/time, 5 times/week for 2 weeks | 11 | 11 | Improvement in swallowing function | Park et al. (2017) |
| | | 5 Hz | 1 time/day, 30 min/day for 4 weeks | 15 | 14 | | |
| | | | 1 time/day, 10 min/time, for 2 weeks | 9 | 9 | | Park et al. (2013) |
| | | | 1 time/day, 30 min/time, 5 times/week for 2 weeks | 30 | 23 | | Liu et al. (2022) |
| | | 3 Hz | 1 time/day, 20 min/time, 5 times/week for 2 weeks | 32 | 21 | | Jiao et al. (2022) |
| | | | 1 time/day, 10 min/day, 5 days in total | 14 | 14 | | Khedr et al. (2009) |
| | | 10 Hz | 1 time/day, 10 min/time, 10 times in total | 10 | 10 | Improvement in speech function at 2-month follow-up | Hu et al. (2018) |
| | Undiseased hemisphere | 1 Hz | 1 time/day, 20 min/time, for 2 weeks | 11 | 11 | Improvement in upper limb motor function | Noh et al. (2019) |
| | | | 1 time/day, 10 min/time, 5 times/week for 2 weeks | 23 | 21 | | Pan et al. (2019) |
| | | | 1 time/day, 5 days/week, total 8 weeks | 20 | 15 | | Qin et al. (2023) |
| | | | 1 time/day, 3 days/week, 10 times in total | 10 | 10 | | Barros Galvão et al. (2014) |
| | | | 1 time/day, 5 days/week for 2 weeks | 17 | 14 | | Gottlieb et al. (2021) |
| | | | 1 time/day for 15 days | 21 | 21 | | Long et al. (2018) |
| | | | 1 time/day, 20 min/day for 2 weeks | 9 | 9 | Improvement of fine motor function of the hand | Tosun et al. (2017) |
| | | | 1 time/day, 20 min/day, 5 days/week, total 2 weeks | 20 | 20 | | Aşkın et al. (2017) |
| | | | 1 time/day, 20 min/time, 10 times in total | 9 | 9 | | Tretriluxana et al. (2013) |
| | | | 1 time/day, 30 min/time, 6 times/week for 2 weeks | 20 | 20 | | Yang et al. (2022) |

*(Continued)*

TABLE 1 (Continued)

| Type of Research | Stimulation site | Stimulation frequency | Stimulation time | Sample size | Amount of effect | Results | References |
|---|---|---|---|---|---|---|---|
| | | | 5 times/day for 1 week | 10 | 7 | Lower extremity motor function and spasticity improvement | Rastgoo et al. (2016) |
| | | | 1 time/day, 6 days/week, 4 weeks in total | 30 | 30 | | Li et al. (2021) |
| | | | 1 time/day, 30 min/time, 10 times in total | 14 | 12 | | Wang et al. (2012) |
| | | | 1 time/day, 40 min/day for 2 weeks | 15 | 15 | Motor function, muscle strength improvement | Wang et al. (2020) |
| | | | 1 time/day, 5 days/week, total 8 weeks | 18 | 18 | Improved cognitive function | Yingli et al. (2022) |
| | | | 1 time/day, 5 days/week, 4 weeks in total | 30 | 28 | Language function improvement | Bai G. et al. (2022) |
| | | | 1 time/day, 30 min/time, 5 times/week for 2 weeks | 6 | 6 | | Haghighi et al. (2017) |
| | | | 1 time/day, 10 min/day, 10 times in total | 10 | 10 | | Hu et al. (2018) |
| | | | 1 time/day, 20 min/time, for 15 days | 36 | 31 | | Ren et al. (2019) |
| | | | 1 time/day, 40 min/time, 6 times/week, 10 times in total | 24 | 24 | | Abo et al. (2012) |
| | | | 1 time/day, 30 min/time, 5 times/week, 15 times in total | 13 | 8 | | Waldowski et al. (2012) |
| | Bilateral hemispheres | 10 Hz and 1 Hz | 1 time/day, 5 days/week, 4 weeks in total | 9 | 9 | Improvement in upper limb motor function | Ni et al. (2022) |
| | | | 1 time/day, 40 min/day for 2 weeks | 15 | 15 | Motor function, muscle strength improvement | Wang et al. (2020) |
| | | 5 Hz and 1 Hz | 1 time/day, 30 min/day for 4 weeks | 15 | 15 | Improvement in swallowing function | |

hemisphere, thus promoting improved distal upper limb movements, finger dexterity and coordination in stroke patients (Kim et al., 2006). However, during stimulation of upper limb motor function, one study found that bilateral TMS (high frequency on the lesioned side and low frequency on the unlesioned side) was more beneficial than unilateral TMS in improving upper limb motor function (Long et al., 2018). However, another meta-analysis found that this view was only supported in the acute phase of stroke, whereas in the subacute and chronic phases, TMS on the lesioned and unlesioned side alone achieved better outcomes (Chen et al., 2022). This suggests that promoting cortical excitability in the lesioned hemisphere during the acute and subacute phases of stroke is the main strategy to improve neurological function in the upper limbs of patients, whereas inhibiting cortical excitability in the unlesioned hemisphere and reducing its inhibition of the lesioned hemisphere during the chronic phase is the main mechanism to improve neurological function. In conclusion, the different periods of the disease are also important factors in determining the TMS treatment plan.

In addition, a similar picture exists for different stimulation modalities, e.g., TBS is more beneficial for the recovery of upper limb motor function in the acute phase of stroke, whereas rTMS is more effective in the subacute and chronic phases (Chen et al., 2022). In addition, it is worth noting that rTMS promotes the recovery of fine motor function of the upper limbs in stroke patients by indirectly modulating the excitability of the corticospinal tract in addition to directly modulating the excitability of the cerebral cortex, however, this process is heavily dependent on the integrity of the corticospinal tract (Wu et al., 2023). Therefore, when applying rTMS to improve upper limb motor function after stroke, the integrity of the corticospinal tract can be tested before developing an appropriate rTMS protocol. This process can be referred to the results of the study by Birute et al. For example, low-frequency rTMS is more adapted for stroke patients with high corticospinal tract (CST) integrity; in contrast, high-frequency rTMS showed more significant clinical effects in patients with low CST integrity (Wang et al., 2022).

### Lower extremity

It is well known that both lower extremities play an important role in human motor function, as demonstrated by walking and balance coordination (Paul et al., 2007). After stroke, patients often suffer from lower extremity motor dysfunction, gait abnormalities, and other sequelae that severely reduce patients' family and social participation. TMS is an emerging therapy for stroke treatment that can increase walking speed (Li et al., 2018; Vaz et al., 2019), correct gait symmetry (Wang et al., 2019), reduce lower extremity muscle spasticity (Naghdi et al., 2015; Rastgoo et al., 2016), and increase balance and motor control (Wang et al., 2012; Kang et al., 2020) to improve lower limb function in stroke patients.

A randomized controlled trial showed that rTMS significantly improved walking, motor control, and motor function in stroke patients, a finding further emphasized by late follow-up data (Veldema and Gharabaghi, 2022). This study followed the theory of interhemispheric inhibition, using HF-rTMS to promote reactivation of cortical excitability in the diseased hemisphere and LF-rTMS to reduce cortical excitability in the unlesioned hemisphere and alleviate its overinhibition of the diseased hemisphere, thereby readjusting the bilateral interhemispheric inhibitory balance. In this study, the bilateral rTMS regimen was superior to the unilateral rTMS regimen, i.e., bilateral rTMS > HF-rTMS on the lesioned side > LF-rTMS on the unlesioned side (Veldema and Gharabaghi, 2022). In fact, in most studies, it has been demonstrated that bilateral rTMS regimens are superior to unilateral regimens, which is similar to the fact that in some diseases combined treatment is superior to monotherapy, which is uncontroversial. Then, leaving aside the bilateral rTMS regimen, why HF-rTMS on the lesioned side > LF-rTMS on the unlesioned side? We believe that after brain injury, reduced excitability in the lesioned hemisphere is the main cause of interhemispheric inhibition imbalance, and therefore, reactivation of cortical excitability in the lesioned hemisphere may be the main strategy to restore interhemispheric inhibition balance compared to reducing excitability in the unlesioned hemisphere. However, this dominance is not invariable, and depending on the etiology, location of the lesion, the urgency of the disease, and individual patient differences, some patients show that reducing excitability in the unlesioned hemisphere is more likely to promote interhemispheric inhibitory homeostasis. As found in a meta-analysis, LF-rTMS in the unlesioned hemisphere produced more clinically significant effects than HF-rTMS in the lesioned hemisphere during the chronic phase of stroke (Chen et al., 2022).

In addition, there is some controversy about TMS improving lower limb function in stroke, for example, a meta-analysis showed that both high and low frequency rTMS had a positive effect on the gait speed of stroke patients (Vaz et al., 2019). However, this was not supported by a study by Raffaella et al. who found that 20 Hz HF-rTMS, while significantly improving lower limb motor function in chronic stroke patients, did not increase the patients' walking speed (Chieffo et al., 2014). In addition, Ying et al. found that LF- rTMS (1 Hz) administered in the unlesioned hemisphere did not significantly improve motor and walking function in stroke patients (Huang et al., 2018). However, in another study the opposite result was obtained, that LF-rTMS in the unlesioned hemisphere improved muscle spasticity in patients' lower extremities, thus promoting improved motor function in the lower extremities (Rastgoo et al., 2016), this idea was also supported by the studies of Soofia et al. and Liu et al. (Naghdi et al., 2015; Liu et al., 2021). And this research variability may arise from the fact that walking is a complex process consisting of several parameters such as walking speed and angle, step width, stride width, and step length. And the regulation of these parameters is modulated by multiple neural systems such as cortical, subcortical and spinal integrated networks. As when walking, multiple sites such as primary sensorimotor areas, primary motor areas, supplementary motor areas, basal ganglia and cerebellar earthworms were detected to be activated with increased cerebral blood flow (Veldema and Gharabaghi, 2022). This suggests that TMS improves lower extremity motor function in patients not only by the TMS protocol, but also by the different stimulation sites and the interactions between brain regions. Therefore, future studies are needed to create more and more beneficial evidence for the various differences arising from TMS application and further advance TMS.

## Cognitive impairment

One study reported that one third of stroke patients have varying degrees of cognitive impairment, referred to as post-stroke cognitive impairment (PSCI), and PSCI can rapidly develop into dementia in a short period of time, which will seriously reduce the quality of life of patients (Li Y. et al., 2020). Therefore, active rehabilitation measures to prevent PSCI from developing into dementia are extremely important to improve the quality of life and social participation of stroke patients.

Studies have shown, TMS may improve cognitive function in patients with PSCI through anti-inflammation and increased cerebral blood flow (Cha et al., 2022). For example, Takatoshi et al. showed that 10 Hz-rTMS promotes improved memory, attention and executive function in PSCI patients by increasing blood perfusion in ischemic brain regions (Hara et al., 2017). The dorsolateral prefrontal cortex (DLPFC) is often used as a stimulation site for TMS to improve PSCI and plays an important role in modulating higher cognitive functions such as memory, attention, and executive functions (Bressler and Menon, 2010). Yin et al. (2020) showed that left DLPFC HF-rTMS significantly improved executive function in PSCI patients. Similarly, according to the theory of interhemispheric inhibitory balance, right-sided DLPFC LF-rTMS also promotes improved cognitive and memory functions in patients with PSCI (Lu et al., 2015; Yingli et al., 2022). Furthermore, a meta-analysis showed that rTMS improved PSCI better when stimulated for longer than 4 weeks and at a stimulation intensity in the range of 80–110% MT (Yin et al., 2020; Wang et al., 2022). However, in addition to rTMS, iTBS is one of the commonly used stimulation modalities to improve PSCI, and left-sided DLPFC iTBS significantly promotes improvements in cognitive functions such as executive function and semantic comprehension in patients with PSCI compared to sham stimulation (Chu et al., 2022; Li et al., 2022).

## Swallowing disorders

More than 65% of new stroke patients each year have dysphagia (Martino et al., 2005). Although dysphagia is a self-resolving complication in most cases, 11–50% of patients will have permanent dysphagia without intervention (Kumar et al., 2010). Therefore, it is necessary to prevent dysphagia from becoming a permanent sequel with external means.

Studies have shown that TMS treatment applied in the M1 brain region can promote the improvement of swallowing function after stroke (Du et al., 2016). However, M1 area covers multiple neurological functions, and how to precisely locate the functional area of M1 swallowing becomes a major obstacle. Until Li S. et al. (2020) used functional MRI (fMRI)-guided TMS in the motor cortex of the brain to excite surface electromyography of the labial orbicularis muscle and detected motor evoked potentials (MEPs) in the submandibular complex (SMC) muscle as a way to locate MSC targets in the M1 swallowing functional area. This study provides a more precise target stimulation site for TMS to improve post-stroke swallowing dysfunction. However, as the process is an individualized one, it may target different individuals with slightly different MSC target locations. Therefore, repositioning of SMC targets for different individuals is necessary for effective improvement of post-stroke swallowing function.

Guided by fMRI, TMS can more accurately and effectively promote improvement in swallowing function, especially HF-TMS (Du et al., 2016; Liao et al., 2017). Xiang et al. showed that HF-rTMS improved dysphagia in stroke for a longer duration and with more significant effects than LF-rTMS (Liao et al., 2017). It is also noteworthy that LF-rTMS (1 Hz) only improved appetite in stroke patients compared to conventional swallowing function treatment, while it did not seem to have a significant effect on the recovery of swallowing function (Ünlüer et al., 2019). Furthermore, Cheng et al. (2015) showed that swallowing function was significantly improved in chronic stroke patients after 3,000 magnetic pulses of 5 Hz-rTMS applied to the tongue motor area of the diseased hemisphere for 2 weeks of continuous treatment. However, in another study, similar results were not obtained with the same stimulation parameters, and no improvement in swallowing function was observed in stroke patients at 2, 6, or even 12 months follow-up after the end of treatment (Cheng et al., 2017). This is in contrast to the findings of Cheng et al. (2015). These two refuting studies suggest that the clinical efficacy of TMS may vary even within the same disease depending on the severity of the disease, individual differences between patients, or other external factors, and therefore, exploring the optimal clinical efficacy of TMS still requires a long time to figure out.

Similarly, a randomized controlled trial observed that the recovery of swallowing function was significantly better in the bilateral stimulation group (simultaneous application of rTMS treatment to the lesioned and unlesioned side of the hyoid muscle) compared to the unilateral stimulation group (500 10 Hz-rTMS pulses applied to the lesioned side of the hyoid muscle for 2 weeks; Park et al., 2017). This finding was supported by a study by Momosaki et al. (2014). However, in another meta-analysis, no significant difference in swallowing function was found between subgroups with different stimulation sites (lesioned hemisphere, unlesioned hemisphere, or bilateral hemisphere) ($p = 0.53$; Wen et al., 2022). We believe that this phenomenon may be due to partial case error and that perhaps the meta-analysis is more convincing compared to the control trial and could continue to be illustrated by continuing to increase the sample size.

## Aphasia

Post-stroke aphasia (PSA) is a common acquired language disorder in patients with acute or subacute stroke, which can lead to varying degrees of impairment in four areas of listening, reading, and writing (Hara and Abo, 2021). In the long term, this will lead to loss of self-confidence in life and may induce post-stroke depression in severe cases (Hilari et al., 2010). Therefore, early treatment of patients with PSA is a key step in preventing post-stroke depression.

TMS has been used since 2005 for the treatment of aphasia in patients with chronic stroke (Gholami et al., 2022). Compared with conventional speech therapy, TMS significantly promotes improvements in naming, comprehension, repetition, and writing in PSA patients (Yao et al., 2020). In general, TMS treatment protocols vary among PSA patients with different language dysfunctions. For example, LF-rTMS is more beneficial for the improvement of function in spontaneous speech and auditory comprehension in PSA patients (Hu et al., 2018). In addition, the site of stimulation is a major factor in TMS parameters that affects clinical efficacy. The superior temporal gyrus is the main lesioned brain region in sensory aphasia (also known as Wernicke's aphasia), where severe impairment in spoken language comprehension is the main clinical manifestation; therefore, the superior temporal gyrus is preferentially chosen as the stimulation site when the patient is Wernicke's aphasic (Ren et al., 2019). Similarly, another typical aphasia, motor aphasia (also known as Broca's aphasia), has a lesion in the inferior frontal gyrus, and when this area is stimulated, the patient's spontaneous speech and repetition components are significantly improved (Ren et al., 2019). This shows that it is perfectly feasible to select the site of TMS stimulation according to the lesioned brain areas of different aphasia types. However, although the lesioned brain area can be used as a stimulation site for PSA patients, it is not clear whether this site is the best stimulation site for TMS, and there are no relevant studies to prove this idea. Therefore, future studies can try to compare different stimulation sites for the same aphasia type to observe the treatment effect of both groups and verify whether the lesioned brain area is the best stimulation site for PSA patients.

## Post-stroke depression

Post-stroke depression (PSD) is the most common neuropsychiatric sequelae in stroke patients, with approximately one-third of new patients experiencing PSD each year (Shen et al., 2017). Currently, antidepressants are the most common treatment for PSD, but the clinical time to effect of pharmacological treatment is long and only some patients improve significantly after pharmacological treatment. Therefore, the search for a treatment other than medication is promising for promoting improvement in PSD. And as early as 2008, it was demonstrated that rTMS treatment in the dorsolateral prefrontal cortex to promote improvement in PSD is safe and effective with few side effects (Duan et al., 2023). Therefore, rTMS is undoubtedly a safe and reliable alternative for those patients with PSD for whom psychotherapy is ineffective or for whom pharmacological treatment has serious side effects.

The traditional rTMS regimen of 5 days of treatment per week for 4–6 weeks has been reported to have significant positive effects in patients with chronic major depression (Duan et al., 2023). However, the duration of this rTMS regimen is relatively long, and is it possible to achieve the same effect while reducing the duration of treatment in a clinical setting for certain patients with poor compliance or who cannot adhere to daily rTMS sessions? Jessica et al. found that

accelerated rTMS (20 Hz, 110% RMT, 5 sessions per day for 4 days) significantly reduced PSD and sustained a positive effect at 3-month follow-up (Frey et al., 2020). In addition, this study showed that accelerated rTMS is also safe and feasible in patients with subacute PSD, with no risk of inducing epilepsy yet (Frey et al., 2020). However, because the study had only six cases, the number was small and a larger sample size is needed for validation. Based on this study, we can tentatively conclude that accelerated rTMS is indeed more effective than conventional rTMS in the acute subacute phase of PSD; this may be because in the early phase of stroke recovery, the body recovers neurologically faster, and therefore, seizing the opportunity for high-intensity intervention during that time is also a safe and feasible treatment option. This is similar to the fact that the first 6 months after stroke is a critical period for patients to recover upper limb function, and if that time window is not seized, the possibility of upper limb function recovery may be missed; because for most stroke patients, upper limb function is slow to recover, and if rehabilitation is not done well in the first 6 months, it is possible that later rehabilitation will have minimal effect on their neurological function improvement. However, is there a critical period for recovery of different neurological functions or are they all consistent? This is a key point that should be addressed. If we are clear about the critical period for each type of neurological recovery, we may be able to promote the recovery of neurological functions more effectively, even without unnecessary sequelae due to time problems.

## Spasticity

The early intervention of rehabilitative exercise training is the cornerstone of the future social reintegration of stroke patients. However, post-stroke spasticity (PSS), a complication that can seriously affect the recovery process, is a major disorder that severely affects motor training and is characterized by a speed-dependent increase in reflex tone. In general, not all stroke patients experience hypertonia as a clinical manifestation. About 30–80% of stroke patients are experiencing or are about to suffer from spasticity, which can cause pain, contracture, deformity, or even stiffness and immobility in the joints if not taken promptly (Wei et al., 2022).

Although numerous clinical studies have demonstrated that TMS significantly reduces post-stroke limb spasticity, a small number of studies have not yielded similar results, and they suggest that the reasons for this heterogeneity may be multifaceted, such as stimulation parameters, stimulation site, type of coil, and the severity and acute and chronic phase of stroke patients can affect the effect of TMS in reducing muscle spasticity in patients (Xia et al., 2022). Different types of coils have different degrees of influence in improving the spasticity state, with the figure-of-eight coil featuring higher focal stimulation having a significant effect in reducing spasticity symptoms compared to the H-type coil (Li et al., 2021). Second, the therapeutic effect of spasticity also varies depending on the different stimulation sites of TMS. In addition to the cerebral motor cortex, the cerebellum plays an important role in motor control and regulation of muscle tone stabilization. It was found that cerebellar cTBS can reduce muscle spasticity in stroke patients by regulating corticospinal excitability through the cerebellar-dentate thalamus-cortex pathway (Li et al., 2021). Therefore, cerebellar cTBS may be one of the more promising stimulation modalities among the methods to reduce muscle spasticity in the future development of TMS to reduce spasticity. However, it has been found that lesions in a common functional region connected to the bilateral nucleus accumbens and pallidum on the side of the lesion may be a potentially critical region contributing to PSS (Qin et al., 2022), so could this region be used as a TMS target to directly improve PSS? As we know, this region is located in the striatal area under the cortical overlay, which is a higher subcortical center that regulates a variety of complex neural functions such as motor, sensory and memory. As TMS is a non-invasive neurostimulation technique, if we want TMS to target the common area of bilateral nucleus accumbens and pallidum, we can only indirectly stimulate to this area through the cerebral cortex, so how can we exclude the influence of the cerebral cortex and the interaction between these two areas? It is also possible that this is one of the reasons why this region has not been used as a TMS target.

## Central post-stroke pain

Central post-stroke pain (CPSP) is one of the common neuropathic pain sequelae after cerebral ischemic injury, often manifesting as sensory hypersensitivity or sensory abnormalities at the site corresponding to the vascular lesion, which is easily confused with stroke-induced shoulder subluxation pain and muscle spasticity pain, resulting in patients who may miss the best early symptomatic treatment period and seriously reduce their quality of life. Currently, CPSP is mainly treated with pharmacological agents, such as anticonvulsants, which have good effects on improving the symptoms of CPSP (Bo et al., 2022), but when it comes to intractable CPSP, the drugs may only play the role of placebo and do not provide a good solution to the patient's CPSP troubles. A recent study found that rTMS in the cerebral motor cortex had a significant effect on relieving recalcitrant CPSP (Malfitano et al., 2021), but the duration varied, which may be related to the site of ischemia, the period of disease progression, the site of stimulation, and individual patient differences. Therefore, there is a need to explore the therapeutic parameters related to the improvement of CPSP by TMS.

In addition, most studies suggest that the possible cause of CPSP is central de-inhibition or central imbalance due to ischemia (Ri, 2022), then restoration of abnormal cortical excitability by TMS may be one of the potential mechanisms for the relief of recalcitrant CPSP. As found in the study, 10 Hz HF-rTMS had significant analgesic effects in CPSP patients in all periods, and M1 HF-rTMS had better analgesic effects than M1 LF-rTMS (Leung et al., 2020; Malfitano et al., 2021). This suggests that in patients with CPSP, increasing cortical excitability in the lesioned hemisphere is far more effective than inhibiting cortical excitability in the unlesioned hemisphere, after all, the imbalance in the regulation of downstream somatosensory pathways due to reduced cortical excitability in the lesioned hemisphere is the most direct cause of CPSP. Therefore, restoration of cortical excitability in the lesioned hemisphere of CPSP patients is one of the potential mechanisms for the analgesic effect of rTMS. In addition, one study found that rTMS significantly relieved CPSP was associated with changes in serum BDNF levels, and an increase in BDNF levels reduced pain in CPSP patients (Zhao et al., 2021). In addition, rTMS increases the functional link between somatosensory pathways, which in turn has an analgesic effect (Kadono et al., 2021). The above studies suggest that the analgesic effect of rTMS in CPSP

patients may be related to the modulation of neuroplasticity in the lesioned hemisphere and cortical excitability during the recovery period.

## Challenges and prospects

Although TMS is a commonly used stroke treatment today, there are some safety risks associated with the action of TMS in humans. For example, in a meta-analysis trial, 13 patients out of 273 subjects experienced adverse events such as headache, dizziness, rhinorrhea, syncope, and seizures (Qiao et al., 2022). Among them, epilepsy is the most serious sequelae of TMS and is currently the most controversial point for scientists to question TMS.

The TMS safety guidelines suggest that the occurrence of epilepsy is influenced by a variety of external and internal factors (Walton et al., 2021). External factors generally include errors present in TMS equipment, errors in the operation of medical personnel, and the adjustment of TMS-related parameters. In general, TMS devices need to be checked for their hardware devices when they are first used to prevent the occurrence of adverse reactions such as epilepsy due to inaccuracies in the devices (Bae et al., 2007). Secondly, the occurrence of adverse reactions is also related to TMS type, frequency, intensity, time, and coil shape. TMS protocols with high frequencies, intensities >120% MT, and short pulse intervals are more likely to induce epilepsy (Tendler et al., 2018; Rossi et al., 2021). However, what is the range of high frequencies? A study showed that TMS at 15 Hz, 120% MT, and 0.75 s pulse interval induced epilepsy (Tendler et al., 2018). Does that suggest that HF-TMS at 15 Hz or greater than 15 Hz necessarily leads to epileptogenesis? The answer does not seem to be the case, as a subset of clinical studies with TMS frequencies above 15 Hz or even up to 20 Hz did not induce epilepsy or other adverse effects (Chieffo et al., 2014). This suggests that TMS is not always accompanied by the occurrence of adverse reactions and that inter-individual differences between patients are a factor in its incidence. Second, coil type also affects the incidence of epilepsy, with the incidence of digital-8 coils inducing epilepsy at 3/1000 or less than 1%(Oberman et al., 2011). The incidence of digital-8 coils inducing epilepsy has also been reported to be in the range of 0.08/1000, while H-type coils affect epilepsy in the range of 0.12–0.43/1000 (Stultz et al., 2020). In this comparison, it seems that the figure-of-8 coil is a little safer, but TMS adverse effects are influenced by more factors, and we are not sure whether the interference of other factors has been discharged when the figure-of-8 and H coils were compared. Therefore, the conclusion still lacks some credibility. In addition, internal factors mainly refer to the variability of TMS for different individuals, including aspects such as history of disease and history of taking medications. Patients with a history of brain injury, epilepsy, and those who have taken antidepressants (Kreuzer et al., 2013) or antiepileptic drugs (Dobek et al., 2015) have been reported to be prone to epilepsy.

TMS-induced epilepsy is influenced by numerous factors; therefore, when a patient is first treated with TMS, the patient should be pre-evaluated for acceptability of TMS treatment and potential triggers for adverse reactions before developing a safe and reliable individualized TMS protocol for the patient. This includes the optimal parameters for TMS, the most suitable stimulation site, and precautions to be taken during the treatment. However, it is worth noting that the optimal parameters are not necessarily within the safe range, and in some patients the optimal parameters exceed the safe range of TMS without inducing an adverse event. Therefore, is it necessary to choose the optimal TMS parameters in such cases in a big but, or to choose the safe parameters of TMS for insurance purposes remains a clinical problem? In addition, some patients experience adverse reactions within the safe range. In summary, the triggering factors of TMS adverse reactions may also be influenced by other factors that have not yet been identified; therefore, further exploration of the triggering factors of TMS adverse reactions and prevention of side effects such as seizures in patients is still a direction of urgent research. In addition, although there are many animal experiments on TMS, few trials have been conducted to validate it in humans, which is undoubtedly a major obstacle to the development process of TMS.

# Conclusion

To date, there is a large body of clinical evidence supporting the value of TMS in improving post-stroke neurological deficits (upper and lower extremity motor, cognition, swallowing, speech, mood, spasticity, post-stroke neuropathic pain). Although the exact mechanism by which TMS improves post-stroke neurological deficits is inconclusive, the current status of TMS is at a critical period of translation of its value for clinical application. At this stage, it is necessary to document in detail the clinical efficacy, precautions, and adverse events of TMS for stroke, and to optimize and adjust the optimal stimulation parameters for TMS. However, TMS uses different stimulation parameters depending on the type of stroke, disease urgency, duration of disease, and post-stroke neurological sequelae, and perhaps even the timing of TMS intervention, which makes the optimal treatment protocol for various post-stroke sequelae difficult to find. Therefore, the optimal treatment protocol for TMS needs to be further explored with a large number and variety of stroke cases, a difficult process that requires small adjustments to various stimulation parameters and observation of efficacy. This process may be interrupted at any time due to patient non-cooperation, poor tolerance, financial constraints, and difficulties in follow-up, making it difficult to explore the optimal treatment protocol for stroke neurological deficits. Secondly, although there is a lot of basic research on TMS, the brains of experimental animals are relatively small compared to the human brain, and the TMS probe is about the same size as the probe used in the human brain in clinical practice, so can the TMS probe in animal studies be positioned as accurately as in the human brain? There is no evidence to support this yet. It is also one of the reasons why some researchers question the results of basic TMS studies. Therefore, the development of TMS probes that are more suitable for the head size of experimental animals is important to explore the potential molecular mechanisms of TMS treatment more precisely in the future.

# Author contributions

PZ and ZW developed the idea and revised the manuscript. LZ prepared and revised the manuscript. YJ, DW, YC, CZ, YP, NC, XY,

SZ, RN, and PK reviewed the literature. All authors have read and approved the final manuscript.

## Funding

This study was supported by the National Natural Science Foundation of China (81960731 and 81860878), Yunnan Province biological medicine major special project (202102AA100016), Joint Special Project of Traditional Chinese Medicine in Science and Technology Department of Yunnan Province (2019FF002(-008), 202001AZ0700 01-002 and 030), Yunnan Province University Innovation Team Projects (2019YGC04), Yunnan province project Education Fund (2022Y372).

## Conflict of interest

The authors declare that the research was conducted in the absence of any commercial or financial relationships that could be construed as a potential conflict of interest.

## Publisher's note



## References

Abo, M., Kakuda, W., Watanabe, M., Morooka, A., Kawakami, K., and Senoo, A. (2012). Effectiveness of low-frequency rTMS and intensive speech therapy in poststroke patients with aphasia: a pilot study based on evaluation by fMRI in relation to type of aphasia. *Eur. Neurol.* 68, 199–208. doi: 10.1159/000338773

Albuquerque, F. C. (2014). Bridging treatment and stroke. *World Neurosurg.* 82, e413–e414. doi: 10.1016/j.wneu.2013.02.086

Aloizou, A. M., Pateraki, G., Anargyros, K., Siokas, V., Bakirtzis, C., Liampas, I., et al. (2021). Transcranial magnetic stimulation (TMS) and repetitive TMS in multiple sclerosis. *Rev. Neurosci.* 32, 723–736. doi: 10.1515/revneuro-2020-0140

Arai, N., Okabe, S., Furubayashi, T., Mochizuki, H., Iwata, N. K., Hanajima, R., et al. (2007). Differences in after-effect between monophasic and biphasic high-frequency rTMS of the human motor cortex. *Clin. Neurophysiol.* 118, 2227–2233. doi: 10.1016/j.clinph.2007.07.006

Arai, N., Okabe, S., Furubayashi, T., Terao, Y., Yuasa, K., and Ugawa, Y. (2005). Comparison between short train, monophasic and biphasic repetitive transcranial magnetic stimulation (rTMS) of the human motor cortex. *Clin. Neurophysiol.* 116, 605–613. doi: 10.1016/j.clinph.2004.09.020

Aşkın, A., Tosun, A., and Demirdal, Ü. S. (2017). Effects of low-frequency repetitive transcranial magnetic stimulation on upper extremity motor recovery and functional outcomes in chronic stroke patients: a randomized controlled trial. *Somatosens. Mot. Res.* 34, 102–107. doi: 10.1080/08990220.2017.1316254

Bae, E. H., Schrader, L. M., Machii, K., Alonso-Alonso, M., Riviello, J. J. Jr., Pascual-Leone, A., et al. (2007). Safety and tolerability of repetitive transcranial magnetic stimulation in patients with epilepsy: a review of the literature. *Epilepsy Behav.* 10, 521–528. doi: 10.1016/j.yebeh.2007.03.004

Bai, G., Jiang, L., Huan, S., Meng, P., Wang, Y., Pan, X., et al. (2022). Study on low-frequency repetitive transcranial magnetic stimulation improves speech function and mechanism in patients with non-fluent aphasia after stroke. *Front. Aging Neurosci.* 14:883542. doi: 10.3389/fnagi.2022.883542

Bai, Z., Zhang, J., and Fong, K. N. K. (2022). Effects of transcranial magnetic stimulation in modulating cortical excitability in patients with stroke: a systematic review and meta-analysis. *J. Neuroeng. Rehabil.* 19:24. doi: 10.1186/s12984-022-00999-4

Barker, A. T., Jalinous, R., and Freeston, I. L. (1985). Non-invasive magnetic stimulation of human motor cortex. *Lancet* 1, 1106–1107. doi: 10.1016/s0140-6736(85)92413-4

Barros Galvão, S. C., Costa Dos Santos, R. B., dos Santos, P. B., Cabral, M. E., Monte-Silva, K., et al. (2014). Efficacy of coupling repetitive transcranial magnetic stimulation and physical therapy to reduce upper-limb spasticity in patients with stroke: a randomized controlled trial. *Arch. Phys. Med. Rehabil.* 95, 222–229. doi: 10.1016/j.apmr.2013.10.023

Blackburn, D., Sargsyan, S., Monk, P. N., and Shaw, P. J. (2009). Astrocyte function and role in motor neuron disease: a future therapeutic target? *Glia* 57, 1251–1264. doi: 10.1002/glia.20848

Bo, Z., Jian, Y., Yan, L., Gangfeng, G., Xiaojing, L., Xiaolan, L., et al. (2022). Pharmacotherapies for central Post-stroke pain: a systematic review and network meta-analysis. *Oxidative Med. Cell. Longev.* 2022, 1–10. doi: 10.1155/2022/3511385

Boulogne, S., Andre-Obadia, N., Kimiskidis, V. K., Ryvlin, P., and Rheims, S. (2016). Cortico-cortical and motor evoked potentials to single and paired-pulse stimuli: an exploratory transcranial magnetic and intracranial electric brain stimulation study. *Hum. Brain Mapp.* 37, 3767–3778. doi: 10.1002/hbm.23274

Bressler, S. L., and Menon, V. (2010). Large-scale brain networks in cognition: emerging methods and principles. *Trends Cogn. Sci.* 14, 277–290. doi: 10.1016/j.tics.2010.04.004

Bütefisch, C. M., Weβling, M., Netz, J., Seitz, R. J., and Hömberg, V. (2008). Relationship between interhemispheric inhibition and motor cortex excitability in subacute stroke patients. *Neurorehabil. Neural Repair* 22, 4–21. doi: 10.1177/1545968307301769

Cha, B., Kim, J., Kim, J. M., Yin, L., Li, K., Li, Y., et al. (2022). Therapeutic effect of repetitive transcranial magnetic stimulation for Post-stroke vascular cognitive impairment: a prospective pilot study. *Front. Neurol.* 13:813597. doi: 10.3389/fneur.2022.813597

Chaturvedi, P., Singh, A. K., Tiwari, V., and Thacker, A. K. (2020). Brain-derived neurotrophic factor levels in acute stroke and its clinical implications. *Brain Circ.* 6, 185–190. doi: 10.4103/bc.bc_23_20

Chen, K. S., and Chen, R. (2019). Invasive and noninvasive brain stimulation in Parkinson's disease: clinical effects and future perspectives. *Clin. Pharmacol. Ther.* 106, 763–775. doi: 10.1002/cpt.1542

Chen, R., Classen, J., Gerloff, C., Celnik, P., Wassermann, E. M., Hallett, M., et al. (1997). Depression of motor cortex excitability by low-frequency transcranial magnetic stimulation. *Neurology* 48, 1398–1403. doi: 10.1212/WNL.48.5.1398

Chen, M., Deng, H., Schmidt, R. L., and Kimberley, T. J. (2015). Low-frequency repetitive transcranial magnetic stimulation targeted to premotor cortex followed by primary motor cortex modulates excitability differently than premotor cortex or primary motor cortex stimulation alone. *Neuromodulation* 18, 678–685. doi: 10.1111/ner.12337

Chen, C. J., Ding, D., Starke, R. M., Mehndiratta, P., Crowley, R. W., Liu, K. C., et al. (2015). Endovascular vs medical management of acute ischemic stroke. *Neurology* 85, 1980–1990. doi: 10.1212/WNL.0000000000002176

Chen, G., Lin, T., Wu, M., Cai, G., Ding, Q., Xu, J., et al. (2022). Effects of repetitive transcranial magnetic stimulation on upper-limb and finger function in stroke patients: a systematic review and meta-analysis of randomized controlled trials. *Front. Neurol.* 13:940467. doi: 10.3389/fneur.2022.940467

Cheng, I. K., Chan, K. M., Wong, C. S., and Cheung, R. T. F. (2015). Preliminary evidence of the effects of high-frequency repetitive transcranial magnetic stimulation (rTMS) on swallowing functions in post-stroke individuals with chronic dysphagia. *Int. J. Lang. Commun. Disord.* 50, 389–396. doi: 10.1111/1460-6984.12144

Cheng, I. K. Y., Chan, K. M. K., Wong, C. S., Li, L., Chiu, K., Cheung, R., et al. (2017). Neuronavigated high-frequency repetitive transcranial magnetic stimulation for chronic post-stroke dysphagia: a randomized controlled study. *J. Rehabil. Med.* 49, 475–481. doi: 10.2340/16501977-2235

Chieffo, R., de Prezzo, S., Houdayer, E., Nuara, A., di Maggio, G., Coppi, E., et al. (2014). Deep repetitive transcranial magnetic stimulation with H-coil on lower limb motor function in chronic stroke: a pilot study. *Arch. Phys. Med. Rehabil.* 95, 1141–1147. doi: 10.1016/j.apmr.2014.02.019

Chohan, S. A., Venkatesh, P. K., and How, C. H. (2019). Long-term complications of stroke and secondary prevention: an overview for primary care physicians. *Singap. Med. J.* 60, 616–620. doi: 10.11622/smedj.2019158

Chu, M., Zhang, Y., Chen, J., Chen, W., Hong, Z., Zhang, Y., et al. (2022). Efficacy of intermittent theta-burst stimulation and transcranial direct current stimulation in treatment of Post-stroke cognitive impairment. *J. Integr. Neurosci.* 21:130. doi: 10.31083/j.jin2105130

Cincotta, M., Borgheresi, A., Gambetti, C., Balestrieri, F., Rossi, L., Zaccara, G., et al. (2003). Suprathreshold 0.3 Hz repetitive TMS prolongs the cortical silent period: potential implications for therapeutic trials in epilepsy. *Clin. Neurophysiol.* 114, 1827–1833. doi: 10.1016/S1388-2457(03)00181-0

D'amico, J. M., Dongés, S. C., and Taylor, J. L. (2020). High-intensity, low-frequency repetitive transcranial magnetic stimulation enhances excitability of the

human corticospinal pathway. *J. Neurophysiol.* 123, 1969–1978. doi: 10.1152/jn.00607.2019

de Jesus, D. R., Favalli, G. P. S., Hoppenbrouwers, S. S., Barr, M. S., Chen, R., Fitzgerald, P. B., et al. (2014). Determining optimal rTMS parameters through changes in cortical inhibition. *Clin. Neurophysiol.* 125, 755–762. doi: 10.1016/j.clinph.2013.09.011

Delavaran, H., Jönsson, A. C., Lövkvist, H., Iwarsson, S., Elmståhl, S., Norrving, B., et al. (2017). Cognitive function in stroke survivors: a 10-year follow-up study. *Acta Neurol. Scand.* 136, 187–194. doi: 10.1111/ane.12709

di Lazzaro, V., Pilato, F., Dileone, M., Profice, P., Oliviero, A., Mazzone, P., et al. (2008). The physiological basis of the effects of intermittent theta burst stimulation of the human motor cortex. *J. Physiol.* 586, 3871–3879. doi: 10.1113/jphysiol.2008.152736

Diao, X., Lu, Q., Qiao, L., Gong, Y., Lu, X., Feng, M., et al. (2022). Cortical inhibition state-dependent iTBS induced neural plasticity. *Front. Neurosci.* 16:788538. doi: 10.3389/fnins.2022.788538

D'Imperio, D., Romeo, Z., Maistrello, L., Durgoni, E., Pietà, C. D., De Grazia, M. D. F., et al. (2021). Sensorimotor, attentional, and neuroanatomical predictors of upper limb motor deficits and rehabilitation outcome after stroke. *Neural. Plast.* 2021:8845685. doi: 10.1155/2021/8845685

Dionísio, A., Gouveia, R., Castelhano, J., Duarte, I. C., Santo, G. C., Sargento-Freitas, J., et al. (2021). The role of continuous theta burst TMS in the neurorehabilitation of subacute stroke patients: a placebo-controlled study. *Front. Neurol.* 12:749798. doi: 10.3389/fneur.2021.749798

Dobek, C. E., Blumberger, D. M., Downar, J., and Daskalakis, Z. J. (2015). Risk of seizures in transcranial magnetic stimulation: a clinical review to inform consent process focused on bupropion. *Neuropsychiatr. Dis. Treat.* 11, 2975–2987. doi: 10.2147/NDT.S91126

Du, X., Summerfelt, A., Chiappelli, J., Holcomb, H. H., and Hong, L. E. (2014). Individualized brain inhibition and excitation profile in response to paired-pulse TMS. *J. Mot. Behav.* 46, 39–48. doi: 10.1080/00222895.2013.850401

du, J., Yang, F., Liu, L., Hu, J., Cai, B., Liu, W., et al. (2016). Repetitive transcranial magnetic stimulation for rehabilitation of poststroke dysphagia: a randomized, double-blind clinical trial. *Clin. Neurophysiol.* 127, 1907–1913. doi: 10.1016/j.clinph.2015.11.045

Duan, H., Yan, X., Meng, S., Qiu, L., Zhang, J., Yang, C., et al. (2023). Effectiveness evaluation of repetitive transcranial magnetic stimulation therapy combined with mindfulness-based stress reduction for people with Post-stroke depression: a randomized controlled trial. *Int. J. Environ. Res. Public Health* 20:930. doi: 10.3390/ijerph20020930

Duan, X., Yao, G., Liu, Z., Cui, R., and Yang, W. (2018). Mechanisms of transcranial magnetic stimulation treating on Post-stroke depression. *Front. Hum. Neurosci.* 12:215. doi: 10.3389/fnhum.2018.00215

Duque, J., Hummel, F., Celnik, P., Murase, N., Mazzocchio, R., and Cohen, L. G. (2005). Transcallosal inhibition in chronic subcortical stroke. *NeuroImage* 28, 940–946. doi: 10.1016/j.neuroimage.2005.06.033

Etiévant, A., Manta, S., Latapy, C., Magno, L. A. V., Fecteau, S., and Beaulieu, J.-M. (2015). Repetitive transcranial magnetic stimulation induces long-lasting changes in protein expression and histone acetylation. *Sci. Rep.* 5:16873. doi: 10.1038/srep16873

Fagan, S. C., Hess, D. C., Machado, L. S., Hohnadel, E. J., Pollock, D. M., and Ergul, A. (2005). Tactics for vascular protection after acute ischemic stroke. *Pharmacotherapy* 25, 387–395. doi: 10.1592/phco.25.3.387.61592

Ferrarelli, F., and Phillips, M. L. (2021). Examining and modulating neural circuits in psychiatric disorders with transcranial magnetic stimulation and electroencephalography: present practices and future developments. *Am. J. Psychiatry* 178, 400–413. doi: 10.1176/appi.ajp.2020.20071050

Filipović, S. R., Rothwell, J. C., and Bhatia, K. (2010). Slow (1 Hz) repetitive transcranial magnetic stimulation (rTMS) induces a sustained change in cortical excitability in patients with Parkinson's disease. *Clin. Neurophysiol.* 121, 1129–1137. doi: 10.1016/j.clinph.2010.01.031

Fitzgerald, P. B., Brown, T. L., Daskalakis, Z. J., Chen, R., and Kulkarni, J. (2002). Intensity-dependent effects of 1 Hz rTMS on human corticospinal excitability. *Clin. Neurophysiol.* 113, 1136–1141. doi: 10.1016/S1388-2457(02)00145-1

Frey, J., Najib, U., Lilly, C., and Adcock, A. (2020). Novel TMS for stroke and depression (NoTSAD): accelerated repetitive transcranial magnetic stimulation as a safe and effective treatment for Post-stroke depression. *Front. Neurol.* 11:788. doi: 10.3389/fneur.2020.00788

Fried, P. J., Jannati, A., Davila-Pérez, P., and Pascual-Leone, A. (2017). Reproducibility of single-pulse, paired-pulse, and intermittent theta-burst TMS measures in healthy aging, Type-2 diabetes, and Alzheimer's disease. *Front. Aging Neurosci.* 9:263. doi: 10.3389/fnagi.2017.00263

Gao, F., Wang, S., Guo, Y., Wang, J., Lou, M., Wu, J., et al. (2010). Protective effects of repetitive transcranial magnetic stimulation in a rat model of transient cerebral ischaemia: a microPET study. *Eur. J. Nucl. Med. Mol. Imaging* 37, 954–961. doi: 10.1007/s00259-009-1342-3

Gholami, M., Pourbaghi, N., and Taghvatalab, S. (2022). Evaluation of rTMS in patients with poststroke aphasia: a systematic review and focused meta-analysis. *Neurol. Sci.* 43, 4685–4694. doi: 10.1007/s10072-022-06092-x

Gottlieb, A., Boltzmann, M., Schmidt, S. B., Gutenbrunner, C., Krauss, J. K., Stangel, M., et al. (2021). Treatment of upper limb spasticity with inhibitory repetitive transcranial magnetic stimulation: a randomized placebo-controlled trial. *NeuroRehabilitation* 49, 425–434. doi: 10.3233/NRE-210088

Guo, F., Han, X., Zhang, J., Zhao, X., Lou, J., Chen, H., et al. (2014). Repetitive transcranial magnetic stimulation promotes neural stem cell proliferation via the regulation of MiR-25 in a rat model of focal cerebral ischemia. *PLoS One* 9:e109267. doi: 10.1371/journal.pone.0109267

Guo, F., Lou, J., Han, X., Deng, Y., and Huang, X. (2017). Repetitive transcranial magnetic stimulation ameliorates cognitive impairment by enhancing neurogenesis and suppressing apoptosis in the hippocampus in rats with ischemic stroke. *Front. Physiol.* 8:559. doi: 10.3389/fphys.2017.00559

Haghighi, M., Mazdeh, M., and Ranjbar, N. (2017). Further evidence of the positive influence of repetitive transcranial magnetic stimulation on speech and language in patients with aphasia after stroke: results from a double-blind intervention with sham condition. *Neuropsychobiology* 75, 185–192. doi: 10.1159/000486144

Hamada, M., Hanajima, R., Terao, Y., Arai, N., Furubayashi, T., Inomata-Terada, S., et al. (2007). Quadro-pulse stimulation is more effective than paired-pulse stimulation for plasticity induction of the human motor cortex. *Clin. Neurophysiol.* 118, 2672–2682. doi: 10.1016/j.clinph.2007.09.062

Hamada, M., Terao, Y., Hanajima, R., Shirota, Y., Nakatani-Enomoto, S., Furubayashi, T., et al. (2008). Bidirectional long-term motor cortical plasticity and metaplasticity induced by quadripulse transcranial magnetic stimulation. *J. Physiol.* 586, 3927–3947. doi: 10.1113/jphysiol.2008.152793

Hanajima, R., Ugawa, Y., Terao, Y., Enomoto, H., Shiio, Y., Mochizuki, H., et al. (2002). Mechanisms of intracortical I-wave facilitation elicited with paired-pulse magnetic stimulation in humans. *J. Physiol.* 538, 253–261. doi: 10.1113/jphysiol.2001.013094

Hara, T., and Abo, M. (2021). New treatment strategy using repetitive transcranial magnetic stimulation for Post-stroke aphasia. *Diagnostics (Basel)* 11:1853. doi: 10.3390/diagnostics11101853

Hara, T., Abo, M., Sasaki, N., Yamada, N., Niimi, M., Kenmoku, M., et al. (2017). Improvement of higher brain dysfunction after brain injury by repetitive transcranial magnetic stimulation and intensive rehabilitation therapy: case report. *Neuroreport* 28, 800–807. doi: 10.1097/WNR.0000000000000830

Hara, T., Shanmugalingam, A., McIntyre, A., and Burhan, A. M. (2021). The effect of non-invasive brain stimulation (NIBS) on attention and memory function in stroke rehabilitation patients: a systematic review and meta-analysis. *Diagnostics* 11:227. doi: 10.3390/diagnostics11020227

Harrigan, M. R., Ennis, S. R., Masada, T., and Keep, R. F. (2002). Intraventricular infusion of vascular endothelial growth factor promotes cerebral angiogenesis with minimal brain edema. *Neurosurgery* 50, 589–598. doi: 10.1097/00006123-200203000-00030

Heide, G., Witte, O. W., and Ziemann, U. (2006). Physiology of modulation of motor cortex excitability by low-frequency suprathreshold repetitive transcranial magnetic stimulation. *Exp. Brain Res.* 171, 26–34. doi: 10.1007/s00221-005-0262-0

Henriette, B., Marianne, N., Rønne, P. J., Glavin, K. M., Wesenberg, K. T., Thorgaard, S. S., et al. (2022). Test-retest reliability and agreement of single pulse transcranial magnetic stimulation (TMS) for measuring activity in motor cortex in patients with acute ischemic stroke. *J Exp Neurosci* 17:263310552211450. doi: 10.1177/26331055221145002

Higashida, R. T., Furlan, A. J., Roberts, H., Tomsick, T., Connors, B., Barr, J., et al. (2003). Trial design and reporting standards for intra-arterial cerebral thrombolysis for acute ischemic stroke. *Stroke* 34, e109–e137. doi: 10.1161/01.STR.0000082721.62796.09

Hilari, K., Northcott, S., Roy, P., Marshall, J., Wiggins, R. D., Chataway, J., et al. (2010). Psychological distress after stroke and aphasia: the first six months. *Clin. Rehabil.* 24, 181–190. doi: 10.1177/0269215509346090

Hong, Y., Liu, Q., Peng, M., Bai, M., Li, J., Sun, R., et al. (2020). High-frequency repetitive transcranial magnetic stimulation improves functional recovery by inhibiting neurotoxic polarization of astrocytes in ischemic rats. *J. Neuroinflammation* 17:150. doi: 10.1186/s12974-020-01747-y

Hong, Y., Lyu, J., Zhu, L., Wang, X., Peng, M., Chen, X., et al. (2022). High-frequency repetitive transcranial magnetic stimulation (rTMS) protects against ischemic stroke by inhibiting M1 microglia polarization through let-7b-5p/HMGA2/NF-κB signaling pathway. *BMC Neurosci.* 23:49. doi: 10.1186/s12868-022-00735-7

Hoonhorst, M. H. J., Nijland, R. H. M., Emmelot, C. H., Kollen, B. J., and Kwakkel, G. (2021). TMS-induced central motor conduction time at the non-infarcted hemisphere is associated with spontaneous motor recovery of the paretic upper limb after severe stroke. *Brain Sci.* 11:648. doi: 10.3390/brainsci11050648

Hosomi, K., Morris, S., Sakamoto, T., Taguchi, J., Maruo, T., Kageyama, Y., et al. (2016). Daily repetitive transcranial magnetic stimulation for poststroke upper limb paresis in the subacute period. *J. Stroke Cerebrovasc. Dis.* 25, 1655–1664. doi: 10.1016/j.jstrokecerebrovasdis.2016.02.024

Hou, K., Xu, D., Li, F., Chen, S., and Li, Y. (2019). The progress of neuronal autophagy in cerebral ischemia stroke: mechanisms, roles and research methods. *J. Neurol. Sci.* 400, 72–82. doi: 10.1016/j.jns.2019.03.015

Hu, X., Leak, R. K., Shi, Y., Suenaga, J., Gao, Y., Zheng, P., et al. (2015). Microglial and macrophage polarization—new prospects for brain repair. *Nat. Rev. Neurol.* 11, 56–64. doi: 10.1038/nrneurol.2014.207

Hu, X., Li, P., Guo, Y., Wang, H., Leak, R. K., Chen, S., et al. (2012). Microglia/macrophage polarization dynamics reveal novel mechanism of injury expansion after focal cerebral ischemia. *Stroke* 43, 3063–3070. doi: 10.1161/STROKEAHA.112.659656

Hu, X. Y., Zhang, T., Rajah, G. B., Stone, C., Liu, L. X., He, J. J., et al. (2018). Effects of different frequencies of repetitive transcranial magnetic stimulation in stroke patients with non-fluent aphasia: a randomized, sham-controlled study. *Neurol. Res.* 40, 459–465. doi: 10.1080/01616412.2018.1453980

Huang, Y. Z., Lin, L. F., Chang, K. H., Hu, C. J., Liou, T. H., and Lin, Y. N. (2018). Priming with 1-Hz repetitive transcranial magnetic stimulation over Contralesional leg motor cortex does not increase the rate of regaining ambulation within 3 months of stroke: a randomized controlled trial. *Am. J. Phys. Med. Rehabil.* 97, 339–345. doi: 10.1097/PHM.0000000000000850

Huang, Y. Z., Rothwell, J. C., Lu, C. S., Wang, J. J., Weng, Y. H., Lai, S. C., et al. (2009). The effect of continuous theta burst stimulation over premotor cortex on circuits in primary motor cortex and spinal cord. *Clin. Neurophysiol.* 120, 796–801. doi: 10.1016/j.clinph.2009.01.003

Ikeda, T., Kobayashi, S., and Morimoto, C. (2019). Effects of repetitive transcranial magnetic stimulation on ER stress-related genes and glutamate, γ-aminobutyric acid and glycine transporter genes in mouse brain. *Biochem. Biophys. Rep.* 17, 10–16. doi: 10.1016/j.bbrep.2018.10.015

Ilić, T. V., Meintzschel, F., Cleff, U., Ruge, D., Kessler, K. R., and Ziemann, U. (2002). Short-interval paired-pulse inhibition and facilitation of human motor cortex: the dimension of stimulus intensity. *J. Physiol.* 545, 153–167. doi: 10.1113/jphysiol.2002.030122

Iyer, M. B., Schleper, N., and Wassermann, E. M. (2003). Priming stimulation enhances the depressant effect of low-frequency repetitive transcranial magnetic stimulation. *J. Neurosci.* 23, 10867–10872. doi: 10.1523/JNEUROSCI.23-34-10867.2003

Jansson, L. C., Louhivuori, L., Wigren, H. K., Nordström, T., Louhivuori, V., Castrén, M. L., et al. (2012). Brain-derived neurotrophic factor increases the motility of a particular N-methyl-D-aspartate/GABA-responsive subset of neural progenitor cells. *Neuroscience* 224, 223–234. doi: 10.1016/j.neuroscience.2012.08.038

Jarczok, T. A., Roebruck, F., Pokorny, L., Biermann, L., Roessner, V., Klein, C., et al. (2021). Single-pulse TMS to the Temporo-occipital and dorsolateral prefrontal cortex evokes lateralized Long latency EEG responses at the stimulation site. *Front. Neurosci.* 15:616667. doi: 10.3389/fnins.2021.616667

Jiao, Y., Li, G., and Dai, Y. (2022). Clinical effect of repetitive transcranial magnetic stimulation on dysphagia due to stroke. *Neurol. Sci.* 43, 3139–3144. doi: 10.1007/s10072-021-05799-7

Jung, S. H., Shin, J. E., Jeong, Y. S., and Shin, H. I. (2008). Changes in motor cortical excitability induced by high-frequency repetitive transcranial magnetic stimulation of different stimulation durations. *Clin. Neurophysiol.* 119, 71–79. doi: 10.1016/j.clinph.2007.09.124

Kadono, Y., Koguchi, K., Okada, K. I., Hosomi, K., Hiraishi, M., Ueguchi, T., et al. (2021). Repetitive transcranial magnetic stimulation restores altered functional connectivity of central poststroke pain model monkeys. *Sci. Rep.* 11:6126. doi: 10.1038/s41598-021-85409-w

Kakuda, W., Abo, M., Watanabe, S., Momosaki, R., Hashimoto, G., Nakayama, Y., et al. (2013). High-frequency rTMS applied over bilateral leg motor areas combined with mobility training for gait disturbance after stroke: a preliminary study. *Brain Inj.* 27, 1080–1086. doi: 10.3109/02699052.2013.794973

Kang, N., Lee, R. D., Lee, J. H., and Hwang, M. H. (2020). Functional balance and postural control improvements in patients with stroke after noninvasive brain stimulation: a meta-analysis. *Arch. Phys. Med. Rehabil.* 101, 141–153. doi: 10.1016/j.apmr.2019.09.003

Karantali, E., Kazis, D., Papavasileiou, V., Prevezianou, A., Chatzikonstantinou, S., Petridis, F., et al. (2021). Serum BDNF levels in acute stroke: A systematic review and meta-analysis. *Medicina (Kaunas)* 57:297. doi: 10.3390/medicina57030297

Kesikburun, S. (2022). Non-invasive brain stimulation in rehabilitation. *Turk J. Phys. Med. Rehabil.* 68, 1–8. doi: 10.5606/tftrd.2022.10608

Khedr, E. M., Abo-Elfetoh, N., and Rothwell, J. C. (2009). Treatment of post-stroke dysphagia with repetitive transcranial magnetic stimulation. *Acta Neurol. Scand.* 119, 155–161. doi: 10.1111/j.1600-0404.2008.01093.x

Khedr, E. M., Gilio, F., and Rothwell, J. (2004). Effects of low frequency and low intensity repetitive paired pulse stimulation of the primary motor cortex. *Clin. Neurophysiol.* 115, 1259–1263. doi: 10.1016/j.clinph.2003.08.025

Kim, Y. H., Park, J. W., Ko, M. H., Jang, S. H., and Lee, P. K. W. (2004). Facilitative effect of high frequency subthreshold repetitive transcranial magnetic stimulation on complex sequential motor learning in humans. *Neurosci. Lett.* 367, 181–185. doi: 10.1016/j.neulet.2004.05.113

Kim, Y. H., You, S. H., Ko, M. H., Park, J. W., Lee, K. H., Jang, S. H., et al. (2006). Repetitive transcranial magnetic stimulation-induced corticomotor excitability and associated motor skill acquisition in chronic stroke. *Stroke* 37, 1471–1476. doi: 10.1161/01.STR.0000221233.55497.51

Klomjai, W., Katz, R., and Lackmy-Vallée, A. (2015). Basic principles of transcranial magnetic stimulation (TMS) and repetitive TMS (rTMS). *Ann. Phys. Rehabil. Med.* 58, 208–213. doi: 10.1016/j.rehab.2015.05.005

Kobayashi, M., and Pascual-Leone, A. (2003). Transcranial magnetic stimulation in neurology. *Lancet Neurol.* 2, 145–156. doi: 10.1016/S1474-4422(03)00321-1

Kreutzberg, G. W. (1996). Microglia: a sensor for pathological events in the CNS. *Trends Neurosci.* 19, 312–318. doi: 10.1016/0166-2236(96)10049-7

Kreuzer, P. M., Landgrebe, M., Frank, E., and Langguth, B. (2013). Repetitive transcranial magnetic stimulation for the treatment of chronic tinnitus after traumatic brain injury: a case study. *J. Head Trauma Rehabil.* 28, 386–389. doi: 10.1097/HTR.0b013e318254736e

Kricheldorff, J., Göke, K., Kiebs, M., Kasten, F. H., Herrmann, C. S., Witt, K., et al. (2022). Evidence of neuroplastic changes after transcranial magnetic, electric, and deep brain stimulation. *Brain Sci.* 12:929. doi: 10.3390/brainsci12070929

Kubis, N. (2016). Non-invasive brain stimulation to enhance Post-stroke recovery. *Front. Neural. Circuits* 10:56. doi: 10.3389/fncir.2016.00056

Kumar, S., Selim, M. H., and Caplan, L. R. (2010). Medical complications after stroke. *Lancet Neurol.* 9, 105–118. doi: 10.1016/S1474-4422(09)70266-2

Lang, N., Harms, J., Weyh, T., Lemon, R. N., Paulus, W., Rothwell, J. C., et al. (2006). Stimulus intensity and coil characteristics influence the efficacy of rTMS to suppress cortical excitability. *Clin. Neurophysiol.* 117, 2292–2301. doi: 10.1016/j.clinph.2006.05.030

Leal, G., Comprido, D., and Duarte, C. B. (2014). BDNF-induced local protein synthesis and synaptic plasticity. *Neuropharmacology* 76, 639–656. doi: 10.1016/j.neuropharm.2013.04.005

Lee, C., Kim, Y., and Kaang, B. K. (2022). The primary motor cortex: The hub of motor learning in rodents. *Neuroscience* 485, 163–170. doi: 10.1016/j.neuroscience.2022.01.009

Lenz, M., Platschek, S., Priesemann, V., Becker, D., Willems, L. M., Ziemann, U., et al. (2015). Repetitive magnetic stimulation induces plasticity of excitatory postsynapses on proximal dendrites of cultured mouse CA1 pyramidal neurons. *Brain Struct. Funct.* 220, 3323–3337. doi: 10.1007/s00429-014-0859-9

Leung, A., Shirvalkar, P., Chen, R., Kuluva, J., Vaninetti, M., Bermudes, R., et al. (2020). Transcranial magnetic stimulation for pain, headache, and comorbid depression: INS-NANS expert consensus panel review and recommendation. *Neuromodulation* 23, 267–290. doi: 10.1111/ner.13094

Li, D., Cheng, A., Zhang, Z., Sun, Y., and Liu, Y. (2021). Effects of low-frequency repetitive transcranial magnetic stimulation combined with cerebellar continuous theta burst stimulation on spasticity and limb dyskinesia in patients with stroke. *BMC Neurol.* 21:369. doi: 10.1186/s12883-021-02406-2

Li, S., Eshghi, M., Khan, S., Tian, Q., Joutsa, J., Ou, Y., et al. (2020). Localizing central swallowing functions by combining non-invasive brain stimulation with neuroimaging. *Brain Stimul.* 13, 1207–1210. doi: 10.1016/j.brs.2020.06.003

Li, Y., Fan, J., Yang, J., He, C., and Li, S. (2018). Effects of repetitive transcranial magnetic stimulation on walking and balance function after stroke: a systematic review and meta-analysis. *Am. J. Phys. Med. Rehabil.* 97, 773–781. doi: 10.1097/PHM.0000000000000948

Li, Y., Luo, H., Yu, Q., Yin, L., Li, K., Li, Y., et al. (2020). Cerebral functional manipulation of repetitive transcranial magnetic stimulation in cognitive impairment patients after stroke: an fMRI study. *Front. Neurol.* 11:977. doi: 10.3389/fneur.2020.00977

Li, M., Peng, J., Song, Y., Liang, H., Mei, Y., and Fang, Y. (2012). Electro-acupuncture combined with transcranial magnetic stimulation improves learning and memory function of rats with cerebral infarction by inhibiting neuron cell apoptosis. *J. Huazhong Univ. Sci. Technolog. Med. Sci.* 32, 746–749. doi: 10.1007/s11596-012-1028-0

Li, W., Wen, Q., Xie, Y. H., Hu, A. L., Wu, Q., and Wang, Y. X. (2022). Improvement of poststroke cognitive impairment by intermittent theta bursts: a double-blind randomized controlled trial. *Brain Behav.* 12:e2569. doi: 10.1002/brb3.2569

Liang, H., Xu, C., Hu, S., Wen, G., Lin, J., Liu, T., et al. (2021). Repetitive transcranial magnetic stimulation improves neuropathy and oxidative stress levels in rats with experimental cerebral infarction through the Nrf2 Signaling pathway. *Evid. Compl. Alternat. Med.* 2021, 1–8. doi: 10.1155/2021/3908677

Liao, X., Xing, G., Guo, Z., Jin, Y., Tang, Q., He, B., et al. (2017). Repetitive transcranial magnetic stimulation as an alternative therapy for dysphagia after stroke: a systematic review and meta-analysis. *Clin. Rehabil.* 31, 289–298. doi: 10.1177/0269215516644771

Liddelow, S. A., and Barres, B. A. (2017). Reactive astrocytes: production, function, and therapeutic potential. *Immunity* 46, 957–967. doi: 10.1016/j.immuni.2017.06.006

Liddelow, S. A., Guttenplan, K. A., Clarke, L. E., Bennett, F. C., Bohlen, C. J., Schirmer, L., et al. (2017). Neurotoxic reactive astrocytes are induced by activated microglia. *Nature* 541, 481–487. doi: 10.1038/nature21029

Liepert, J., Hamzei, F., and Weiller, C. (2000). Motor cortex disinhibition of the unaffected hemisphere after acute stroke. *Muscle Nerve* 23, 1761–1763. doi: 10.1002/1097-4598(200011)23:11<1761::AID-MUS14>3.0.CO;2-M

Lin, Y. L., Potter-Baker, K. A., Cunningham, D. A., Li, M., Sankarasubramanian, V., Lee, J., et al. (2020). Stratifying chronic stroke patients based on the influence of contralesional motor cortices: an inter-hemispheric inhibition study. *Clin. Neurophysiol.* 131, 2516–2525. doi: 10.1016/j.clinph.2020.06.016

Liu, Y., Li, H., Zhang, J., Zhao, Q. Q., Mei, H. N., and Ma, J. (2021). A meta-analysis: whether repetitive transcranial magnetic stimulation improves dysfunction caused by stroke with lower limb spasticity. *Evid. Based Complement. Alternat. Med.* 2021, 1–10. doi: 10.1155/2021/7219293

Liu, H., Peng, Y., Liu, Z., Wen, X., Li, F., Zhong, L., et al. (2022). Hemodynamic signal changes and swallowing improvement of repetitive transcranial magnetic stimulation on stroke patients with dysphagia: a randomized controlled study. *Front. Neurol.* 13:918974. doi: 10.3389/fneur.2022.918974

Long, H., Wang, H., Zhao, C., Duan, Q., Feng, F., Hui, N., et al. (2018). Effects of combining high- and low-frequency repetitive transcranial magnetic stimulation on upper limb hemiparesis in the early phase of stroke. *Restor. Neurol. Neurosci.* 36, 21–30. doi: 10.3233/RNN-170733

Lu, H., Zhang, T., Wen, M., and Sun, L. (2015). Impact of repetitive transcranial magnetic stimulation on post-stroke dysmnesia and the role of BDNF Val66Met SNP. *Med. Sci. Monit.* 21, 761–768. doi: 10.12659/MSM.892337

Luo, L., Liu, M., Fan, Y., Zhang, J., Liu, L., Li, Y., et al. (2022). Intermittent theta-burst stimulation improves motor function by inhibiting neuronal pyroptosis and regulating microglial polarization via TLR4/NFκB/NLRP3 signaling pathway in cerebral ischemic mice. *J. Neuroinflammation* 19:141. doi: 10.1186/s12974-022-02501-2

Luo, J., Zheng, H., Zhang, L., Zhang, Q., Li, L., Pei, Z., et al. (2017). High-frequency repetitive transcranial magnetic stimulation (rTMS) improves functional recovery by enhancing neurogenesis and activating BDNF/TrkB Signaling in ischemic rats. *Int. J. Mol. Sci.* 18:455. doi: 10.3390/ijms18020455

Ma, Y., Wang, J., Wang, Y., and Yang, G. Y. (2017). The biphasic function of microglia in ischemic stroke. *Prog. Neurobiol.* 157, 247–272. doi: 10.1016/j.pneurobio.2016.01.005

Ma, J., Zhang, Z., Kang, L., Geng, D., Wang, Y., Wang, M., et al. (2014). Repetitive transcranial magnetic stimulation (rTMS) influences spatial cognition and modulates hippocampal structural synaptic plasticity in aging mice. *Exp. Gerontol.* 58, 256–268. doi: 10.1016/j.exger.2014.08.011

Malfitano, C., Rossetti, A., Scarano, S., Malloggi, C., and Tesio, L. (2021). Efficacy of repetitive transcranial magnetic stimulation for acute central Post-stroke pain: a case study. *Front. Neurol.* 12:742567. doi: 10.3389/fneur.2021.742567

Martino, R., Foley, N., Bhogal, S., Diamant, N., Speechley, M., and Teasell, R. (2005). Dysphagia after stroke: incidence, diagnosis, and pulmonary complications. *Stroke* 36, 2756–2763. doi: 10.1161/01.STR.0000190056.76543.eb

McClintock, S. M., Freitas, C., Oberman, L., Lisanby, S. H., and Pascual-Leone, A. (2011). Transcranial magnetic stimulation: a neuroscientific probe of cortical function in schizophrenia. *Biol. Psychiatry* 70, 19–27. doi: 10.1016/j.biopsych.2011.02.031

Medina-Fernandez, F. J., Escribano, B. M., Agüera, E., Aguilar-Luque, M., Feijoo, M., Luque, E., et al. (2017). Effects of transcranial magnetic stimulation on oxidative stress in experimental autoimmune encephalomyelitis. *Free Radic. Res.* 51, 460–469. doi: 10.1080/10715762.2017.1324955

Meng, Y., Zhang, D., Hai, H., Zhao, Y. Y., and Ma, Y. W. (2020). Efficacy of coupling intermittent theta-burst stimulation and 1Hz repetitive transcranial magnetic stimulation to enhance upper limb motor recovery in subacute stroke patients: a randomized controlled trial. *Restor. Neurol. Neurosci.* 38, 109–118. doi: 10.3233/RNN-190953

Mimura, Y., Nishida, H., Nakajima, S., Tsugawa, S., Morita, S., Yoshida, K., et al. (2021). Neurophysiological biomarkers using transcranial magnetic stimulation in Alzheimer's disease and mild cognitive impairment: a systematic review and meta-analysis. *Neurosci. Biobehav. Rev.* 121, 47–59. doi: 10.1016/j.neubiorev.2020.12.003

Modugno, N., Currà, A., Conte, A., Inghilleri, M., Fofi, L., Agostino, R., et al. (2003). Depressed intracortical inhibition after long trains of subthreshold repetitive magnetic stimuli at low frequency. *Clin. Neurophysiol.* 114, 2416–2422. doi: 10.1016/S1388-2457(03)00262-1

Modugno, N., Nakamura, Y., MacKinnon, C., Filipovic, S., Bestmann, S., Berardelli, A., et al. (2001). Motor cortex excitability following short trains of repetitive magnetic stimuli. *Exp. Brain Res.* 140, 453–459. doi: 10.1007/s002210100843

Momosaki, R., Abo, M., and Kakuda, W. (2014). Bilateral repetitive transcranial magnetic stimulation combined with intensive swallowing rehabilitation for chronic stroke dysphagia: a case series study. *Case Rep. Neurol.* 6, 60–67. doi: 10.1159/000360936

Muller, P. A., Dhamne, S. C., Vahabzadeh-Hagh, A. M., Pascual-Leone, A., Jensen, F. E., and Rotenberg, A. (2014). Suppression of motor cortical excitability in anesthetized rats by low frequency repetitive transcranial magnetic stimulation. *PLoS One* 9:e91065. doi: 10.1371/journal.pone.0091065

Naghdi, S., Ansari, N. N., Rastgoo, M., Forogh, B., Jalaie, S., and Olyaei, G. (2015). A pilot study on the effects of low frequency repetitive transcranial magnetic stimulation on lower extremity spasticity and motor neuron excitability in patients after stroke. *J. Bodyw. Mov. Ther.* 19, 616–623. doi: 10.1016/j.jbmt.2014.10.001

Nakatani-Enomoto, S., Hanajima, R., Hamada, M., Terao, Y., Matsumoto, H., Shirota, Y., et al. (2012). Bidirectional modulation of sensory cortical excitability by quadripulse transcranial magnetic stimulation (QPS) in humans. *Clin. Neurophysiol.* 123, 1415–1421. doi: 10.1016/j.clinph.2011.11.037

Nardone, R., De Blasi, P., Seidl, M., Höller, Y., Caleri, F., Tezzon, F., et al. (2011). Cognitive function and cholinergic transmission in patients with subcortical vascular dementia and microbleeds: a TMS study. *J. Neural Transm. (Vienna)* 118, 1349–1358. doi: 10.1007/s00702-011-0650-5

NCD Risk Factor Collaboration (NCD-RisC) (2021). Worldwide trends in hypertension prevalence and progress in treatment and control from 1990 to 2019: a pooled analysis of 1201 population-representative studies with 104 million participants. *Lancet* 398, 957–980. doi: 10.1016/S0140-6736(21)01330-1

Ni, Z., and Chen, R. (2008). Repetitive transcranial magnetic stimulation: faster or longer is not necessarily more. *J. Physiol.* 586, 3733–3734. doi: 10.1113/jphysiol.2008.159301

Ni, J., Jiang, W., Gong, X., Fan, Y., Qiu, H., Dou, J., et al. (2022). Effect of rTMS intervention on upper limb motor function after stroke: a study based on fNIRS. *Front. Aging Neurosci.* 14:1077218. doi: 10.3389/fnagi.2022.1077218

Noh, J. S., Lim, J. H., Choi, T. W., Jang, S. G., and Pyun, S.-B. (2019). Effects and safety of combined rTMS and action observation for recovery of function in the upper extremities in stroke patients: a randomized controlled trial. *Restor. Neurol. Neurosci.* 37, 219–230. doi: 10.3233/RNN-180883

Nordmann, G., Azorina, V., Langguth, B., and Schecklmann, M. (2015). A systematic review of non-motor rTMS induced motor cortex plasticity. *Front. Hum. Neurosci.* 9:416. doi: 10.3389/fnhum.2015.00416

Oberman, L., Edwards, D., Eldaief, M., and Pascual-Leone, A. (2011). Safety of theta burst transcranial magnetic stimulation: a systematic review of the literature. *J. Clin. Neurophysiol.* 28, 67–74. doi: 10.1097/WNP.0b013e318205135f

Orellana-Urzúa, S., Rojas, I., Líbano, L., and Rodrigo, R. (2020). Pathophysiology of ischemic stroke: role of oxidative stress. *Curr. Pharm. Des.* 26, 4246–4260. doi: 10.2174/1381612826666200708133912

Pan, W., Wang, P., Song, X., Sun, X., and Xie, Q. (2019). The effects of combined low frequency repetitive transcranial magnetic stimulation and motor imagery on upper extremity motor recovery following stroke. *Front. Neurol.* 10:96. doi: 10.3389/fneur.2019.00096

Park, E., Kim, M. S., Chang, W. H., Oh, S. M., Kim, Y. K., Lee, A., et al. (2017). Effects of bilateral repetitive transcranial magnetic stimulation on post-stroke dysphagia. *Brain Stimul.* 10, 75–82. doi: 10.1016/j.brs.2016.08.005

Park, J. W., Oh, J. C., Lee, J. W., Yeo, J.-S., and Ryu, K. H. (2013). The effect of 5Hz high-frequency rTMS over contralesional pharyngeal motor cortex in post-stroke oropharyngeal dysphagia: a randomized controlled study. *Neurogastroenterol. Motil.* 25, 324–e250. doi: 10.1111/nmo.12063

Patel, J., Fluet, G., Qiu, Q., Yarossi, M., Merians, A., Tunik, E., et al. (2019). Intensive virtual reality and robotic based upper limb training compared to usual care, and associated cortical reorganization, in the acute and early sub-acute periods post-stroke: a feasibility study. *J. Neuroeng. Rehabil.* 16:92. doi: 10.1186/s12984-019-0563-3

Paul, S. L., Srikanth, V. K., and Thrift, A. G. (2007). The large and growing burden of stroke. *Curr. Drug Targets* 8, 786–793. doi: 10.2174/138945007781077418

Peinemann, A., Reimer, B., Löer, C., Quartarone, A., Münchau, A., Conrad, B., et al. (2004). Long-lasting increase in corticospinal excitability after 1800 pulses of subthreshold 5 Hz repetitive TMS to the primary motor cortex. *Clin. Neurophysiol.* 115, 1519–1526. doi: 10.1016/j.clinph.2004.02.005

Poh, E. Z., Hahne, D., Moretti, J., Harvey, A. R., Clarke, M. W., and Rodger, J. (2019). Simultaneous quantification of dopamine, serotonin, their metabolites and amino acids by LC-MS/MS in mouse brain following repetitive transcranial magnetic stimulation. *Neurochem. Int.* 131:104546. doi: 10.1016/j.neuint.2019.104546

Ponomarev, E. D., Veremeyko, T., and Weiner, H. L. (2013). MicroRNAs are universal regulators of differentiation, activation, and polarization of microglia and macrophages in normal and diseased CNS. *Glia* 61, 91–103. doi: 10.1002/glia.22363

Post, A., Müller, M. B., Engelmann, M., and Keck, M. E. (1999). Repetitive transcranial magnetic stimulation in rats: evidence for a neuroprotective effect in vitro and in vivo. *Eur. J. Neurosci.* 11, 3247–3254. doi: 10.1046/j.1460-9568.1999.00747.x

Prinz, M., Tay, T. L., Wolf, Y., and Jung, S. (2014). Microglia: unique and common features with other tissue macrophages. *Acta Neuropathol.* 128, 319–331. doi: 10.1007/s00401-014-1267-1

Qiao, H. J., Li, Z. Z., Wang, L. M., Sun, W., Yu, J.-C., and Wang, B. (2017). Association of lower serum brain-derived neurotrophic factor levels with larger infarct volumes in acute ischemic stroke. *J. Neuroimmunol.* 307, 69–73. doi: 10.1016/j.jneuroim.2017.04.002

Qiao, J., Ye, Q. P., Wu, Z. M., Dai, Y., and Dou, Z. L. (2022). The effect and optimal parameters of repetitive transcranial magnetic stimulation on poststroke dysphagia: a meta-analysis of randomized controlled trials. *Front. Neurosci.* 16:845737. doi: 10.3389/fnins.2022.845737

Qin, Y., Liu, X., Zhang, Y., Wu, J., and Wang, X. (2023). Effects of transcranial combined with peripheral repetitive magnetic stimulation on limb spasticity and resting-state brain activity in stroke patients. *Front. Hum. Neurosci.* 17:992424. doi: 10.3389/fnhum.2023.992424

Qin, Y., Qiu, S., Liu, X., Xu, S., Wang, X., et al. (2022). Lesions causing post-stroke spasticity localize to a common brain network. *Front. Aging Neurosci.* 14:1011812. doi: 10.3389/fnagi.2022.1011812

Qin, C., Zhou, L. Q., Ma, X. T., Hu, Z.-W., Yang, S., Chen, M., et al. (2019). Dual functions of microglia in ischemic stroke. *Neurosci. Bull.* 35, 921–933. doi: 10.1007/s12264-019-00388-3

Radak, D., Katsiki, N., Resanovic, I., Jovanovic, A., Sudar-Milovanovic, E., Zafirovic, S., et al. (2017). Apoptosis and acute brain ischemia in ischemic stroke. *Curr. Vasc. Pharmacol.* 15, 115–122. doi: 10.2174/1570161115666161104095522

Ragoschke-Schumm, A., and Walter, S. (2018). DAWN and DEFUSE-3 trials: is time still important? *Radiologe* 58, 20–23. doi: 10.1007/s00117-018-0406-4

Rastgoo, M., Naghdi, S., Nakhostin Ansari, N., Olyaei, G., Jalaei, S., Forogh, B., et al. (2016). Effects of repetitive transcranial magnetic stimulation on lower extremity spasticity and motor function in stroke patients. *Disabil. Rehabil.* 38, 1918–1926. doi: 10.3109/09638288.2015.1107780

Ren, C., Zhang, G., Xu, X., Hao, J., Fang, H., Chen, P., et al. (2019). The effect of rTMS over the different targets on language recovery in stroke patients with global aphasia: a randomized sham-controlled study. *Biomed. Res. Int.* 2019, 1–7. doi: 10.1155/2019/4589056

Ri, S. (2022). The Management of Poststroke Thalamic Pain: update in clinical practice. *Diagnostics (Basel)* 12:1439. doi: 10.3390/diagnostics12061439

Rizzo, V., Mastroeni, C., Maggio, R., Terranova, C., Girlanda, P., Siebner, H. R., et al. (2020). Low-intensity repetitive paired associative stimulation targeting the motor hand area at theta frequency causes a lasting reduction in corticospinal excitability. *Clin. Neurophysiol.* 131, 2402–2409. doi: 10.1016/j.clinph.2020.06.033

Rodríguez-Yáñez, M., Castellanos, M., Blanco, M., Mosquera, E., and Castillo, J. (2006). Vascular protection in brain ischemia. *Cerebrovasc. Dis.* 21, 21–29. doi: 10.1159/000091700

Rossi, S., Antal, A., Bestmann, S., Bikson, M., Brewer, C., Brockmöller, J., et al. (2021). Safety and recommendations for TMS use in healthy subjects and patient populations, with updates on training, ethical and regulatory issues: expert guidelines. *Clin. Neurophysiol.* 132, 269–306. doi: 10.1016/j.clinph.2020.10.003

Rossini, P. M., and Rossi, S. (2007). Transcranial magnetic stimulation: diagnostic, therapeutic, and research potential. *Neurology* 68, 484–488. doi: 10.1212/01.wnl.0000250268.13789.b2

Rushworth, M. F., and Taylor, P. C. (2006). TMS in the parietal cortex: updating representations for attention and action. *Neuropsychologia* 44, 2700–2716. doi: 10.1016/j.neuropsychologia.2005.12.007

Saini, V., Guada, L., and Yavagal, D. R. (2021). Global epidemiology of stroke and access to acute ischemic stroke interventions. *Neurology* 97, S6–s16. doi: 10.1212/WNL.0000000000012781

Sasso, V., Bisicchia, E., Latini, L., Ghiglieri, V., Cacace, F., Carola, V., et al. (2016). Repetitive transcranial magnetic stimulation reduces remote apoptotic cell death and inflammation after focal brain injury. *J. Neuroinflamm.* 13:150. doi: 10.1186/s12974-016-0616-5

Saudargiene, A., Cobb, S., and Graham, B. P. (2015). A computational study on plasticity during theta cycles at Schaffer collateral synapses on CA1 pyramidal cells in the hippocampus. *Hippocampus* 25, 208–218. doi: 10.1002/hipo.22365

Schumacher, R., Halai, A. D., and Lambon Ralph, M. A. (2019). Assessing and mapping language, attention and executive multidimensional deficits in stroke aphasia. *Brain* 142, 3202–3216. doi: 10.1093/brain/awz258

Sharma, H., Vishnu, V. Y., Kumar, N., Sreenivas, V., Rajeswari, M. R., Bhatia, R., et al. (2020). Efficacy of low-frequency repetitive transcranial magnetic stimulation in ischemic stroke: a double-blind randomized controlled trial. *Archives of Rehabilitation Research and Clinical Translation* 2:100039. doi: 10.1016/j.arrct.2020.100039

Shen, X., Liu, M., Cheng, Y., Jia, C., Pan, X. Y., Gou, Q. Y., et al. (2017). Repetitive transcranial magnetic stimulation for the treatment of post-stroke depression: a systematic review and meta-analysis of randomized controlled clinical trials. *J. Affect. Disord.* 211, 65–74. doi: 10.1016/j.jad.2016.12.058

Somaa, F. A., De Graaf, T. A., and Sack, A. T. (2022). Transcranial magnetic stimulation in the treatment of neurological diseases. *Front. Neurol.* 13:793253. doi: 10.3389/fneur.2022.793253

Sreedharan, S. E., Sayed, J. V., Vipina, V. P., Mohan, P. M., Jissa, V. T., Sylaja, P. N., et al. (2022). Dysphagia continues to impact recovery at one year after stroke-an observational study. *J. Stroke Cerebrovasc. Dis.* 31:106545. doi: 10.1016/j.jstrokecerebrovasdis.2022.106545

Stultz, D. J., Osburn, S., Burns, T., Pawlowska-Wajswol, S., Walton, R., et al. (2020). Transcranial magnetic stimulation (TMS) safety with respect to seizures: a literature review. *Neuropsychiatr. Dis. Treat.* 16, 2989–3000. doi: 10.2147/NDT.S276635

Sun, Y., Jin, K., Xie, L., Childs, J., Mao, X. O., Logvinova, A., et al. (2003). VEGF-induced neuroprotection, neurogenesis, and angiogenesis after focal cerebral ischemia. *J. Clin. Invest.* 111, 1843–1851. doi: 10.1172/JCI200317977

Tan, X. D., Liu, B., Jiang, Y., Yu, H., and Li, C. (2021). Gadd45b mediates environmental enrichment-induced neurogenesis in the SVZ of rats following ischemia stroke via BDNF. *Neurosci. Lett.* 745:135616. doi: 10.1016/j.neulet.2020.135616

Tang, Z. M., Xuan, C. Y., Li, X., Dou, Z.-L., Lan, Y.-J., and Wen, H.-M. (2019). Effect of different pulse numbers of transcranial magnetic stimulation on motor cortex excitability: single-blind, randomized cross-over design. *CNS Neurosci. Ther.* 25, 1277–1281. doi: 10.1111/cns.13248

Taylor, J. L., and Loo, C. K. (2007). Stimulus waveform influences the efficacy of repetitive transcranial magnetic stimulation. *J. Affect. Disord.* 97, 271–276. doi: 10.1016/j.jad.2006.06.027

Tendler, A., Roth, Y., and Zangen, A. (2018). Rate of inadvertently induced seizures with deep repetitive transcranial magnetic stimulation. *Brain Stimul.* 11, 1410–1414. doi: 10.1016/j.brs.2018.09.001

The Lancet Neurology (2021). A social dimension for brain health: the mounting pressure. *Lancet Neurol.* 20:773. doi: 10.1016/S1474-4422(21)00295-7

Tian, D., and Izumi, S. I. (2022). Interhemispheric facilitatory effect of high-frequency rTMS: perspective from intracortical facilitation and inhibition. *Brain Sci.* 12:970. doi: 10.3390/brainsci12080970

Todd, G., Flavel, S. C., and Ridding, M. C. (2006). Low-intensity repetitive transcranial magnetic stimulation decreases motor cortical excitability in humans. *J. Appl. Physiol. (1985)* 101, 500–505. doi: 10.1152/japplphysiol.01399.2005

Tosun, A., Türe, S., Askin, A., Yardimci, E. U., Demirdal, S. U., Incesu, T. K., et al. (2017). Effects of low-frequency repetitive transcranial magnetic stimulation and neuromuscular electrical stimulation on upper extremity motor recovery in the early period after stroke: a preliminary study. *Top. Stroke Rehabil.* 24, 361–367. doi: 10.1080/10749357.2017.1305644

Toth, C., King Johnson, M. L., Heinzerling, A., and Trapp, N. (2022). Response to TMS treatment for depression associated with higher levels of psychological well-being. *J. Psychiatr. Res.* 150, 142–146. doi: 10.1016/j.jpsychires.2022.03.030

Touge, T., Gerschlager, W., Brown, P., and Rothwell, J. C. (2001). Are the after-effects of low-frequency rTMS on motor cortex excitability due to changes in the efficacy of cortical synapses? *Clin. Neurophysiol.* 112, 2138–2145. doi: 10.1016/S1388-2457(01)00651-4

Tretriluxana, J., Kantak, S., Tretriluxana, S., Wu, A. D., and Fisher, B. E. (2013). Low frequency repetitive transcranial magnetic stimulation to the non-lesioned hemisphere improves paretic arm reach-to-grasp performance after chronic stroke. *Disabil. Rehabil. Assist. Technol.* 8, 121–124. doi: 10.3109/17483107.2012.737136

Tugin, S., Souza, V. H., Nazarova, M. A., Novikov, P. A., Tervo, A. E., Nieminen, J. O., et al. (2021). Effect of stimulus orientation and intensity on short-interval intracortical inhibition (SICI) and facilitation (SICF): a multi-channel transcranial magnetic stimulation study. *PLoS One* 16:e0257554. doi: 10.1371/journal.pone.0257554

Ünlüer, N., Temuçin, Ç. M., Demir, N., Arslan, S. S., and Karaduman, A. A. (2019). Effects of low-frequency repetitive transcranial magnetic stimulation on swallowing function and quality of life of Post-stroke patients. *Dysphagia* 34, 360–371. doi: 10.1007/s00455-018-09965-6

Vaz, P. G., Salazar, A., Stein, C., Marchese, R. R., Lukrafka, J. L., Plentz, R. D. M., et al. (2019). Noninvasive brain stimulation combined with other therapies improves gait speed after stroke: a systematic review and meta-analysis. *Top. Stroke Rehabil.* 26, 201–213. doi: 10.1080/10749357.2019.1565696

Veldema, J., and Gharabaghi, A. (2022). Non-invasive brain stimulation for improving gait, balance, and lower limbs motor function in stroke. *J. Neuroeng. Rehabil.* 19:84. doi: 10.1186/s12984-022-01062-y

Vexler, Z. S., Roberts, T. P., Bollen, A. W., Derugin, N., Arieff, A. I., et al. (1997). Transient cerebral ischemia. Association of apoptosis induction with hypoperfusion. *J. Clin. Invest.* 99, 1453–1459. doi: 10.1172/JCI119304

Vlachos, A., Müller-Dahlhaus, F., Rosskopp, J., Lenz, M., Ziemann, U., and Deller, T. (2012). Repetitive magnetic stimulation induces functional and structural plasticity of excitatory postsynapses in mouse organotypic hippocampal slice cultures. *J. Neurosci.* 32, 17514–17523. doi: 10.1523/JNEUROSCI.0409-12.2012

Volz, L. J., Hamada, M., Rothwell, J. C., and Grefkes, C. (2015). What makes the muscle twitch: motor system connectivity and TMS-induced activity. *Cereb. Cortex* 25, 2346–2353. doi: 10.1093/cercor/bhu032

Wahl, M., Lauterbach-Soon, B., Hattingen, E., Hübers, A., and Ziemann, U. (2016). Callosal anatomical and effective connectivity between primary motor cortices predicts visually cued bimanual temporal coordination performance. *Brain Struct. Funct.* 221, 3427–3443. doi: 10.1007/s00429-015-1110-z

Wahlgren, N., Moreira, T., Michel, P., Steiner, T., Jansen, O., Cognard, C., et al. (2016). Mechanical thrombectomy in acute ischemic stroke: consensus statement by ESO-Karolinska stroke update 2014/2015, supported by ESO, ESMINT, ESNR and EAN. *Int. J. Stroke* 11, 134–147. doi: 10.1177/1747493015609778

Waldowski, K., Seniów, J., Leśniak, M., Iwański, S., and Członkowska, A. (2012). Effect of low-frequency repetitive transcranial magnetic stimulation on naming abilities in early-stroke aphasic patients: a prospective, randomized, double-blind sham-controlled study. *ScientificWorldJournal* 2012:518568. doi: 10.1100/2012/518568

Walton, D., Spencer, D. C., Nevitt, S. J., and Michael, B. D. (2021). Transcranial magnetic stimulation for the treatment of epilepsy. *Cochrane Database Syst. Rev.* 4:Cd011025. doi: 10.1002/14651858.CD011025.pub3

Wang, R. Y., Tseng, H. Y., Liao, K. K., Wang, C. J., Lai, K. L., and Yang, Y. R. (2012). rTMS combined with task-oriented training to improve symmetry of interhemispheric corticomotor excitability and gait performance after stroke: a randomized trial. *Neurorehabil. Neural Repair* 26, 222–230. doi: 10.1177/1545968311423265

Wang, R. Y., Wang, F. Y., and Huang, S. F. (2019). High-frequency repetitive transcranial magnetic stimulation enhanced treadmill training effects on gait performance in individuals with chronic stroke: a double-blinded randomized controlled pilot trial. *Gait Posture* 68, 382–387. doi: 10.1016/j.gaitpost.2018.12.023

Wang, Y., Xu, N., Wang, R., and Zai, W. (2022). Systematic review and network meta-analysis of effects of noninvasive brain stimulation on post-stroke cognitive impairment. *Front. Neurosci.* 16:1082383. doi: 10.3389/fnins.2022.1082383

Wang, Q., Zhang, D., Zhao, Y. Y., Hai, H., and Ma, Y. W. (2020). Effects of high-frequency repetitive transcranial magnetic stimulation over the contralesional motor cortex on motor recovery in severe hemiplegic stroke: a randomized clinical trial. *Brain Stimul.* 13, 979–986. doi: 10.1016/j.brs.2020.03.020

Wang, L., Zhu, Q. X., Zhong, M. H., Zhou, R.-Z., Liu, X.-Q., Tang, N.-S., et al. (2022). Effects of corticospinal tract integrity on upper limb motor function recovery in stroke patients treated with repetitive transcranial magnetic stimulation. *J. Integr. Neurosci.* 21:50. doi: 10.31083/j.jin2102050

Wei, X., Xia, N., Li, Y. A., Gu, M., Zhang, T., Gao, W., et al. (2022). Immediate and short-term effects of continuous theta burst transcranial magnetic stimulation over contralesional premotor area on post-stroke spasticity in patients with severe hemiplegia: study protocol for a randomized controlled trial. *Front. Neurol.* 13:895580. doi: 10.3389/fneur.2022.895580

Wen, X., Liu, Z., Zhong, L., Peng, Y., Wang, J., Liu, H., et al. (2022). The effectiveness of repetitive transcranial magnetic stimulation for Post-stroke dysphagia: a systematic review and meta-analysis. *Front. Hum. Neurosci.* 16:841781. doi: 10.3389/fnhum.2022.841781

Wen, Y. D., Zhang, H. L., and Qin, Z. H. (2006). Inflammatory mechanism in ischemic neuronal injury. *Neurosci. Bull.* 22, 171–182.

Wolf, S. L., Winstein, C. J., Miller, J. P., Taub, E., Uswatte, G., Morris, D., et al. (2006). Effect of constraint-induced movement therapy on upper extremity function 3 to 9 months after stroke: the EXCITE randomized clinical trial. *JAMA* 296, 2095–2104. doi: 10.1001/jama.296.17.2095

Wu, X., Wang, R., Wu, Q., Liao, C., Zhang, J., Jiao, H., et al. (2023). The effects of combined high-frequency repetitive transcranial magnetic stimulation and cervical nerve root magnetic stimulation on upper extremity motor recovery following stroke. *Front. Neurosci.* 17:1100464. doi: 10.3389/fnins.2023.1100464

Xia, Y., Xu, Y., Li, Y., Lu, Y., and Wang, Z. (2022). Comparative efficacy of different repetitive transcranial magnetic stimulation protocols for stroke: a network meta-analysis. *Front. Neurol.* 13:918786. doi: 10.3389/fneur.2022.918786

Xu, J., Branscheidt, M., Schambra, H., Steiner, L., Widmer, M., Diedrichsen, J., et al. (2019). Rethinking interhemispheric imbalance as a target for stroke neurorehabilitation. *Ann. Neurol.* 85, 502–513. doi: 10.1002/ana.25452

Yang, Z., Qiao, L., He, J., Zhao, X., and Zhang, M. (2022). Effects of repetitive transcranial magnetic stimulation combined with functional electrical stimulation on hand function of stroke: a randomized controlled trial. *NeuroRehabilitation* 51, 283–289. doi: 10.3233/NRE-220074

Yao, L., Zhao, H., Shen, C., Liu, F., Qiu, L., and Fu, L. (2020). Low-frequency repetitive transcranial magnetic stimulation in patients with poststroke aphasia: systematic review and meta-analysis of its effect upon communication. *J. Speech Lang. Hear. Res.* 63, 3801–3815. doi: 10.1044/2020_JSLHR-19-00077

Yenari, M. A., Kauppinen, T. M., and Swanson, R. A. (2010). Microglial activation in stroke: therapeutic targets. *Neurotherapeutics* 7, 378–391. doi: 10.1016/j.nurt.2010.07.005

Yin, M., Liu, Y., Zhang, L., Zheng, H., Peng, L., Ai, Y., et al. (2020). Effects of rTMS treatment on cognitive impairment and resting-state brain activity in stroke patients: a randomized clinical trial. *Front. Neural. Circuits* 14:563777. doi: 10.3389/fncir.2020.563777

Yingli, B., Zunke, G., Wei, C., and Shiyan, W. (2022). Cerebral activity manipulation of low-frequency repetitive transcranial magnetic stimulation in post-stroke patients with cognitive impairment. *Front. Neurol.* 13:951209. doi: 10.3389/fneur.2022.951209

Yoon, K. J., Lee, Y. T., and Han, T. R. (2011). Mechanism of functional recovery after repetitive transcranial magnetic stimulation (rTMS) in the subacute cerebral ischemic rat model: neural plasticity or anti-apoptosis? *Exp. Brain Res.* 214, 549–556. doi: 10.1007/s00221-011-2853-2

Young, C. C., Brooks, K. J., Buchan, A. M., and Szele, F. G. (2011). Cellular and molecular determinants of stroke-induced changes in subventricular zone cell migration. *Antioxid. Redox Signal.* 14, 1877–1888. doi: 10.1089/ars.2010.3435

Yu, S., Zhai, J., Yu, J., Yang, Q., and Yang, J. (2021). miR-98-5p protects against cerebral ischemia/reperfusion injury through anti-apoptosis and anti-oxidative stress in mice. *J. Biochem.* 169, 195–206. doi: 10.1093/jb/mvaa099

Yu, G., Zhang, Y., and Ning, B. (2021). Reactive astrocytes in central nervous system injury: subgroup and potential therapy. *Front. Cell. Neurosci.* 15:792764. doi: 10.3389/fncel.2021.792764

Yue, L., Xiao-Lin, H., and Tao, S. (2009). The effects of chronic repetitive transcranial magnetic stimulation on glutamate and gamma-aminobutyric acid in rat brain. *Brain Res.* 1260, 94–99. doi: 10.1016/j.brainres.2009.01.009

Zhang, T., Sui, Y., Lu, Q., Xu, X., Zhu, Y., Dai, W., et al. (2022). Effects of rTMS treatment on global cognitive function in Alzheimer's disease: a systematic review and meta-analysis. *Front. Aging Neurosci.* 14:984708. doi: 10.3389/fnagi.2022.984708

Zhao, X., He, Y., Zhang, Y., Wan, H., Wan, H., and Yang, J. (2022). Inhibition of oxidative stress: an important molecular mechanism of Chinese herbal medicine (Astragalus membranaceus, *Carthamus tinctorius* L., radix salvia Miltiorrhizae, etc.) in the treatment of ischemic stroke by regulating the antioxidant system. *Oxidative Med. Cell. Longev.* 2022, 1–10. doi: 10.1155/2022/1425369

Zhao, X., Li, Y., Tian, Q., Zhu, B., and Zhao, Z. (2019). Repetitive transcranial magnetic stimulation increases serum brain-derived neurotrophic factor and decreases interleukin-1β and tumor necrosis factor-α in elderly patients with refractory depression. *J. Int. Med. Res.* 47, 1848–1855. doi: 10.1177/0300060518817417

Zhao, S. C., Ma, L. S., Chu, Z. H., Xu, H., Wu, W. Q., and Liu, F. (2017). Regulation of microglial activation in stroke. *Acta Pharmacol. Sin.* 38, 445–458. doi: 10.1038/aps.2016.162

Zhao, C. G., Sun, W., Ju, F., Jiang, S., Wang, H., Sun, X. L., et al. (2021). Analgesic effects of navigated repetitive transcranial magnetic stimulation in patients with acute central poststroke pain. *Pain Ther.* 10, 1085–1100. doi: 10.1007/s40122-021-00261-0

Zong, X., Dong, Y., Li, Y., Yang, L., Li, Y., Yang, B., et al. (2020a). Beneficial effects of theta-burst transcranial magnetic stimulation on stroke injury via improving neuronal microenvironment and mitochondrial integrity. *Transl. Stroke Res.* 11, 450–467. doi: 10.1007/s12975-019-00731-w

Zong, X., Gu, J., Zhou, S., Ding, D., Hu, Y., Tucker, L., et al. (2022). Continuous theta-burst stimulation enhances and sustains neurogenesis following ischemic stroke. *Theranostics* 12, 5710–5726. doi: 10.7150/thno.71832

Zong, X., Li, Y., Liu, C., Qi, W., Han, D., Tucker, L., et al. (2020b). Theta-burst transcranial magnetic stimulation promotes stroke recovery by vascular protection and neovascularization. *Theranostics* 10, 12090–12110. doi: 10.7150/thno.51573

frontiers | Frontiers in Neuroscience

TYPE Original Research
PUBLISHED 19 July 2023
DOI 10.3389/fnins.2023.1202705



OPEN ACCESS

EDITED BY
Jingchun Guo,
Fudan University, China

REVIEWED BY
Ningbo Yu,
Nankai University, China
Paola Pinti,
Birkbeck University of London, United Kingdom
Jessica Gemignani,
Università di Padova, Italy

*CORRESPONDENCE
Michele Lacerenza
✉ lacerenza@pionirs.com

RECEIVED 09 April 2023
ACCEPTED 16 June 2023
PUBLISHED 19 July 2023

CITATION
Lacerenza M, Frabasile L, Buttafava M, Spinelli L, Bassani E, Micheloni F, Amendola C, Torricelli A and Contini D (2023) Motor cortex hemodynamic response to goal-oriented and non-goal-oriented tasks in healthy subjects. *Front. Neurosci.* 17:1202705. doi: 10.3389/fnins.2023.1202705



# Motor cortex hemodynamic response to goal-oriented and non-goal-oriented tasks in healthy subjects

Michele Lacerenza[1,2]*, Lorenzo Frabasile[1], Mauro Buttafava[2], Lorenzo Spinelli[3], Elisa Bassani[4,5], Francesco Micheloni[5], Caterina Amendola[1], Alessandro Torricelli[1,3] and Davide Contini[1]

[1]Dipartimento di Fisica, Politecnico di Milano, Milano, Italy, [2]PIONIRS s.r.l., Milano, Italy, [3]Istituto di Fotonica e Nanotecnologie, Consiglio Nazionale delle Ricerche, Milano, Italy, [4]Scuola Universitaria Professionale della Svizzera Italiana, Manno, Switzerland, [5]Centro Studi Riabilitazione Neurologica, Neuropsicologia e Neuropsicoterapia, Milano, Italy

**Background:** Motor disorders are one of the world's major scourges, and neuromotor rehabilitation is paramount for prevention and monitoring plans. In this scenario, exercises and motor tasks to be performed by patients are crucial to follow and assess treatments' progression and efficacy. Nowadays, in clinical environments, quantitative assessment of motor cortex activities during task execution is rare, due to the bulkiness of instrumentation and the need for immobility during measurements [e.g., functional magnetic resonance imaging (MRI)]. Functional near-infrared spectroscopy (fNIRS) can contribute to a better understanding of how neuromotor processes work by measuring motor cortex activity non-invasively in freely moving subjects.

**Aim:** Exploit fNIRS to measure functional activation of the motor cortex area during arm-raising actions.

**Design:** All subjects performed three different upper limbs motor tasks: arm raising (non-goal-oriented), arm raising and grasping (goal oriented), and assisted arm raising (passive task). Each task was repeated ten times. The block design for each task was divided into 5 seconds of baseline, 5 seconds of activity, and 15 seconds of recovery.

**Population:** Sixteen healthy subjects (11 males and 5 females) with an average (+/– standard deviation) of 37.9 (+/– 13.0) years old.

**Methods:** Cerebral hemodynamic responses have been recorded in two locations, motor cortex (activation area) and prefrontal cortex (control location) exploiting commercial time-domain fNIRS devices. Haemodynamic signals were analyzed, separating the brain cortex hemodynamic response from extracerebral hemodynamic variations.

**Results:** The hemodynamic response was recorded in the cortical motor area for goal-oriented and not-goaloriented tasks, while no response was noticed in the control location (prefrontal cortex position).

**Conclusions:** This study provides a basis for canonical upper limb motor cortex activations that can be potentially compared to pathological cerebral responses in patients. It also highlights the potential use of TD-fNIRS to study goal-oriented versus non-goaloriented motor tasks. Impact: the findings of this study may have implications for clinical rehabilitation by providing a better understanding of the neural mechanisms underlying goal-oriented versus non-goal-oriented motor tasks. This may lead to more effective rehabilitation strategies for individuals with

motor disorders and a more effective diagnosis of motor dysfunction supported by objective and quantitative neurophysiological readings.

KEYWORDS

motor disorders, functional near infrared spectroscopy, supplementary motor area, neuromotor rehabilitation, cerebral hemodynamic response function, non-goal-directed movements, goal-directed movement, motor cortex

## Introduction

Motor neuron diseases are a group of neurodegenerative disorders related to upper and lower motor neuron degradation that strongly affect the global population. The study by Logroscino et al. (2018) shows a high incidence of neuromotor diseases reaching around 5% prevalence in the 50 years old world population and overtaking 20% incidence for individuals older than 70. This study also shows a higher incidence in the male population compared to the female one.

It is of primary importance to tackle an early diagnosis and implement prevention and monitoring plans, considering such prevalence of functional neurological disorder, its disabling consequences, and its costly handling. After being marginalized in the late 20th century, there has been renewed interest in this field in the last decade (Perez et al., 2021) for both diagnosis and treatments in patients with motor functional disorders, including also functional limb weakness. The resurgence of interest in this field encouraged us to enter this sector to help catalyze diagnostic and therapeutic improvements.

In the neuro-motor rehabilitation field, the selection of exercises and motor tasks to be performed by the patients is of paramount importance. It has been studied in previous literature the effect of goal-oriented (or goal-directed) exercises in motor learning mechanisms. Goal-oriented tasks require the subject to perform a specific movement with the intention of achieving a certain result, while non-goal-oriented tasks require the subject to simply perform a movement without any specific outcome in mind. In contrast with interventions that focus on changing body functions with simple motion tasks, goal-oriented training with activity-based approach to therapy proved to give meaningful advantages (Mastos et al., 2007; Wevers et al., 2009).

During goal-oriented tasks, the pre-motor cortex and the parietal cortex, which are associated with attention, planning, and execution of the movement, tend to be more active (Rizzolatti et al., 1987, 2014). Additionally, brain regions associated with feedback, such as the anterior cingulate cortex and the supplementary motor area (SMA) (Diedrichsen et al., 2006; Yamagata et al., 2012) tend to be highly involved during goal-oriented tasks, allowing for adjustments to be made based on the outcome of the movement.

Non-goal-oriented tasks instead, tend to activate brain regions associated with movement execution and sensory processing, such as the primary motor cortex and the supplementary motor area. These regions are responsible for the planning and execution of the movement itself, rather than the goal that the movement is trying to achieve. Brain regions associated with attention and feedback are typically less active during non-goal-oriented tasks, as the focus is on the movement itself rather than on its outcome.

Goal-oriented therapy has emerged as a promising approach to neurorehabilitation that emphasizes the setting of specific, achievable goals in order to guide and tailor rehabilitation interventions. Goal-oriented movements appear to produce a better reaching performance than the same movements performed without a specific goal (Wu et al., 2000) and can improve patient motivation and engagement in rehabilitation, which can further improve outcomes. In the study of Nathan et al. (2012), to understand neural correlates of upper extremity task executions (functional vs. non-functional) and their influence on neuromotor control strategies, it is found that neuromotor strategy for functional goal-oriented movements is different from rhythmic movements such as finger tapping or non-functional movements, and this difference can be quantified and mapped using functional magnetic resonance imaging (fMRI). These results support the concept of using goal-oriented tasks in rehabilitation and therapy for restoration of a function, that is task and context specific. Importantly, by tailoring rehabilitation interventions to specific goals and capacities of the patient, goal-oriented therapy can lead to more efficient and effective neurorehabilitation.

Despite these interesting and meaningful results, most of the motor learning studies performed in humans presented in literature, lack of a quantitative assessment of the actual involvement of the motor cortex real-time during the task execution. This is mainly due to the techniques used to assess brain activations, often based on fMRI, electroencephalography (EEG) and positron emission tomography (PET), which are highly limited by their bulkiness, cost and sensitivity to motion artifacts. Being able to quantify the motor cortex involvement in motor exercises in goal-oriented tasks compared to non-goal-oriented tasks would strengthen the hypothesis of higher effectiveness of goal-oriented ones in motor rehabilitation, confirming the results of previous studies based on less objective evaluations such as goal attainment scaling.

The scientific community envisages functional near-infrared spectroscopy (fNIRS) technology as a promising tool for providing easy and non-invasive access to cerebral hemodynamics, which can be paramount in the process of diagnosing and monitoring motor dysfunctions strongly related to neuro-functional processes (Leff et al., 2011). fNIRS is a non-invasive neuroimaging technique that measures changes in the concentration of oxygenated ($O_2Hb$) and deoxygenated (HHb) hemoglobin in the brain by means of infrared light which penetrate the skull reaching the brain cortex. It is used to study brain functions in both research and clinical settings.

Time-domain (TD)-fNIRS (Lange and Tachtsidis, 2019), which exploits laser pulses instead of continuous wave light, outperforms standard fNIRS approach (Ortega-Martinez et al., 2023) and can unlock the possibility of quantitatively measuring the hemodynamic response, thanks to the discrimination between cerebral and extra-cerebral signals, potentially offering the ability to assess progress of patient conditions with physiological indexes (i.e., features of the hemodynamic response function, HRF) when treated with specific therapies or rehabilitation programs.

TD-fNIRS has been already used to measure functional motor cortex activation in various motor task exercises (Re et al., 2013; Muthalib et al., 2015; Lacerenza et al., 2021), also comparing results with other techniques such as EEG and fMRI (Visani et al., 2015). As examples, the study conducted by Muthalib et al. (2015) explores the potential of TD-NIRS as a neuroimaging tool to observe distinctive patterns of neural activity associated with external stimuli, such as sensory inputs, compared to voluntary actions; research conducted by Lacerenza et al. (2021) investigates how hemodynamic activation linked to similar motor actions can be differentiated based on hemodynamic activity patterns. No previous TD-NIRS studies have been found investigating differences in motor cortex activation related to goal-oriented and non goal oriented tasks. Compared to previous works performed with fMRI in humans on this topic (Nathan et al., 2012), in which the hemodynamic response was reported as the average activation intensity resulting form multiple task executions in a defined period (e.g., 30 s), this study aims to recover the actual temporal hemodynamic response due to the functional activation, including both oxygenated and deoxygenated hemoglobin concentrations during tasks execution (<10 s time period).

In this work, the investigation has been focused on studying differences in brain activations during goal-oriented motor tasks versus non-goal-oriented motor tasks via TD-fNIRS on healthy subjects. Volunteers' brain hemodynamics was recorded in real-time from two locations: prefrontal cortex and motor cortex, with two synchronized TD-fNIRS devices (NIRSBOX, PIONIRS s.r.l., Milano, Italy) and different upper limbs motor tasks have been studied. The protocol was divided into three tasks: arm raising (active movement not goal-oriented), arm raising combined with grasping of a small object (active, goal-oriented movement), and helped arm raising (passive movement).

The possibility of having quantitative information on the brain activation (not affected by extra cerebral hemodynamic variations) will enable to retrieve reliable brain hemodynamic responses from these three motor tasks in healthy subjects. This will help in setting the basis of canonical upper limb motor cortex activations that will be potentially compared to pathological cerebral responses in future patients.

# Methods

## Subjects

In this study, 16 healthy volunteers, have been enrolled (11 males and 5 females) with an average (±standard deviation) of 37.9 (±13.0) years old. All subjects included in these measurements cooperated voluntarily and previously provided written informed consent to the procedures of the study, which was conducted according to the guidelines of the Declaration of Helsinki and approved by the Ethics Committee of Politecnico di Milano.

## Protocol

Protocol design and probe positioning were selected based on previous literature. To be able to record data from the motor cortex and the prefrontal cortex (as control location, where no significant brain activation is expected) two NIRSBOX devices (Lacerenza et al., 2022) (PIONIRS s.r.l., Milano, Italy) have been used. These instruments exploit two low-power (<5 mW) laser sources with wavelengths 685 nm and 830 nm; they acquire data at 1 Hz sampling frequency, transmitting to a laptop PC through USB connection and are synchronized together using hardware logic signals, to ensure true real-time acquisitions. The first unit was used to measure the region related to motor activation (C3 position following EEG10/20 system mapping, covering primary motor cortex and supplementary motor areas), while the second one was placed on the prefrontal region, Fp2 location (control channel). A schematic of the probe locations is reported in Figure 1A. Measurements have been performed in typical laboratory settings at Politecnico di Milano, a free area of at least six meters squared was left around the subjects to allow for unrestricted movement in space. Three left-handed subjects were present in the population under study and have been included in the analysis: in this case probe positions were C4 and Fp1, being motor task performed with the dominant arm. Unlike previous measurements and common fNIRS publications (in which subjects with dense or dark head hair are often excluded) in this work, we employed a dedicated optical probe design (PIONIRS s.r.l., Milano, Italy) which has allowed to recruit volunteers regardless of their scalp and hair characteristics. Source detector distance in this probe was 3 cm, with one injection and one detection channel. Retractable, spring-loaded optical fiber terminations were employed, impinging vertically on the head surface and facilitating direct contact with the skin without applying excessive pressure thus avoiding uncomfortable wearing by the subject. A picture of this probe is reported in Figure 1B. Probes have been secured with black elastic bandages around the head of the volunteers, without covering eyes and ears. For the simultaneous acquisition on the prefrontal cortex, a standard flat probe with horizontal-placed fiber cables has been used (B5 probe, PIONIRS S.r.l.) (PIONIRS S.r.l, 2023). Source/detection separation distance was 3 cm also for Fp2 acquisitions.

For each task, the subject's arm moved (actively or passively) from the resting position, longitudinally to the body, up to the height of the eyes, keeping the elbow straight and returning to the resting position. Each block consisted of 5 s of baseline, 5 s of task and 15 s of rest, repeated 10 times. The synchronization of the tasks was performed using audio commands. In the arm raising task (AR, not goal-oriented) the subject was asked to lift his arm autonomously and lower it down in a maximum time range of 5 s. The arm raising and grasping task (ARG, goal-oriented) consisted in raising the arm to the same height of the previous exercise and grasping a small and lightweight object (20 × 50 × 10 mm). During the following repetition, the subject must reposition back the object in the original location. In the final task, helped arm raising (HAR) task, an operator was raising the subject's arm to the height of the subject's eye, making the subject performing a "passive" exercise, without any voluntary action by the subject. During this experiment the operator was holding the subject's wrist for the full exercise period (baseline, task, and rest) to avoid any possible confounding effect due to the involvement of the motor cortex or SMA. If the operator perceived the subject making any active movements throughout the task, voice feedback was supplied to the subject asking to relax all arm muscles and allow the operator to solely lead the subject's arm. A schematic of the three exercise performed during the protocol is reported in Figure 2.

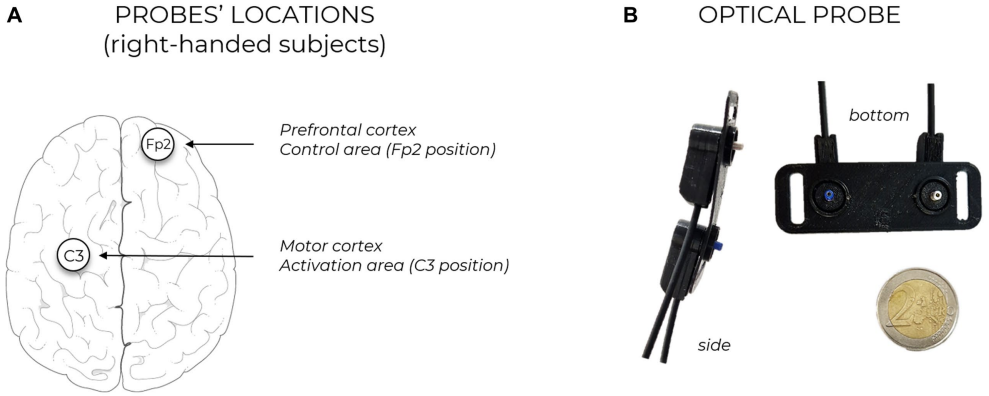


FIGURE 1
**(A)** Sketch of probe locations, in case of right-handed subject. The positioning of the probes is performed following EEG10/20 system mapping, injection and detection points are equidistant form the selected location. Each probe is connected to one TD-fNIRS device. The two devices are synchronized together for parallel and bilateral brain hemodynamic acquisition. **(B)** Pictures of the custom developed optical probe.

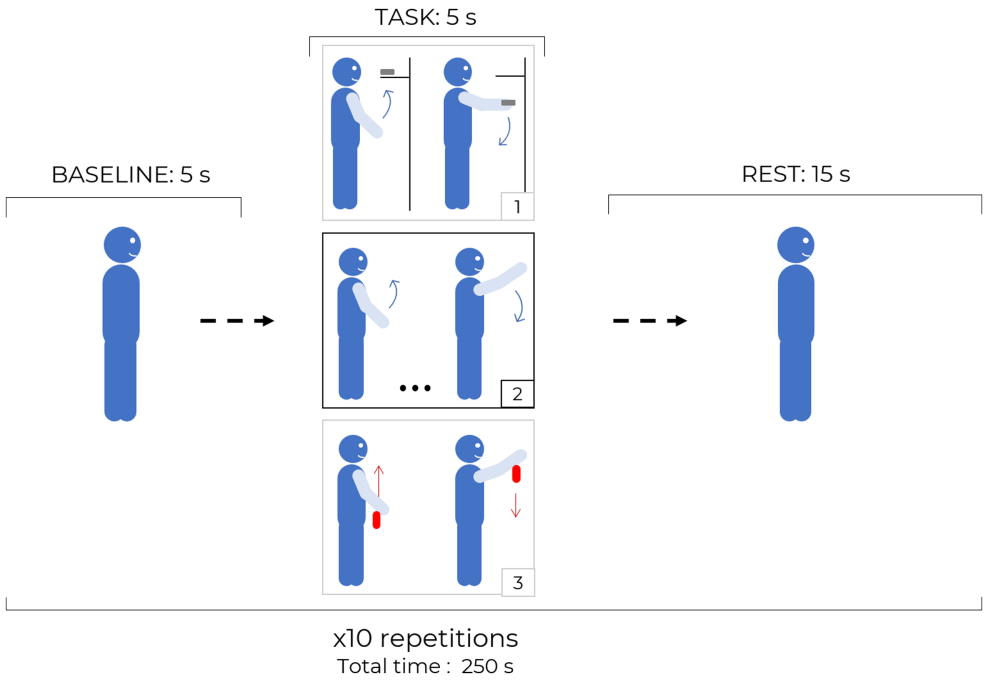


FIGURE 2
Protocol structure: each block is composed by 5 s baseline, 5 s task and 15 s rest periods and it is repeated 10 times for the same task. The three different tasks are sketched in the black and gray squares: 1. ARG, 2. AR, 3. HAR, red arrows indicate passive movements while blue arrows indicate active and independent motion of the subject.

## Data analysis

TD-fNIRS data were acquired as distribution of time-of-flight (DTOFs) of the photons backscattered from the probed tissue. Absolute optical coefficients have been retrieved by exploiting the convolved paths method (Zucchelli et al., 2013), which can reject superficial perturbations enhancing the contrast created by deeper layers' variations. By computing the information about the absorption coefficient at different depths and different wavelengths it is possible to retrieve the absolute concentration of oxygenated and deoxygenated hemoglobin. By repeating this at every sampling time it is possible to calculate the hemodynamic response function (HRF).

The HRF used to fit our data is therefore composed by the sum of three gamma functions ($\Gamma$) with different signs, and different peak delays (Eq. 1) to possibly include the several different processes involved in the neurovascular coupling mechanism (e.g., feed-forward effect, fee-back effect, initial dip) (Iadecola, 2017; Kamran et al., 2018). The shape of the HRF depends on the following adaptive parameters: amplitude ($A$) and peak delay of the positive gamma function from the beginning of the task ($\tau_p$); peak delays of the negative gamma

functions ($\tau_d$ and $\tau_e$) and their relative amplitudes $B$ and $C$ (ranging from 0 to 1) with respect to the amplitude of the positive gamma function (main peak). $A$, $B$, and $C$ values have opposite signs in case of deoxy-HR (negative HRF). By convolving the curve resulting from the linear combination of the three gamma functions ($h$) with a boxcar function ($N$) as long as the length of the performed task, we obtain the initial guess of the HR: $f(t)$ (Eq. 2). The same boxcar function ($N$) has been used for each motor task and in both measuring locations.

$$h(t) = A\left(\frac{t^{\tau_e+\tau_p}\, e^{-t}}{\Gamma(\tau_e+\tau_p+1)} - B\frac{t^{\tau_e+\tau_p+\tau_d}\, e^{-t}}{\Gamma(\tau_e+\tau_p+\tau_d+1)} - C\frac{t^{\tau_e}\, e^{-t}}{\Gamma(\tau_e+1)}\right) \quad (1)$$

$$f(t) = h(\tau_p, t) * N \quad (2)$$

The initial HRF will then be fitted through the Levenberg–Marquardt algorithm to minimize the mean square error between the theoretical HRF and the measured data. The fitted parameters are: $A$, $B$, $C$, $\tau_p$, $\tau_d$, and $\tau_e$. Boundaries and initial guesses for the fitting process are summarized in Table 1. Note that since the "initial dip" ($B$) and the "undershoot" ($C$) amplitudes are relative to the main peak amplitude ($A$), their values range from 0 to 1. Their, their initial guesses were set to 0.5. The fitting results were examined using Pearson's correlation coefficient ($R$) to determine the quality of the fitting procedure: $R<0.3$ translates in weak correlation, $0.3<R<0.7$ in moderate correlation and $R>0.7$ in high correlation.

Average results obtained from the HRF fitting procedure over the entire population have been analysed individually, to look for significant differences between average values within the three different tasks. For each comparison, a paired two-sample, two-tailed $t$-test has been exploited. The null hypothesis was formulated assuming that there is no significant difference between values being compared. Additionally, the Kolmogorov–Smirnov (KS) test of normality with KS $p$-value >0.05 was used to make sure that the samples under study did not differ significantly from a normal distribution.

The two measuring channels (pre-frontal cortex and motor cortex) have been treated independently. Since no significant activations have been recorded in the prefrontal cortex (control channel), statistical analysis on the hemodynamic responses have been focused on the motor cortex channel only. To address the issue of multiple comparisons due to the multiple $t$-tests performed on the same population performing different tasks, a correction for multiple comparisons was applied using the Bonferroni method, lowering the potential occurrence of false positives. Considering the comparisons within three distinct tasks, a total of three comparisons were considered in the analysis. This correction resulted in an adjusted significance threshold of alpha = 0.017, reducing the likelihood of Type 1 errors (false positives). Therefore, to determine statistical significance, differences with $p$-values below the threshold $p = 0.017$ were deemed statistically significant.

TABLE 1 Boundaries (Max and Min) values for the fitted parameters and their initial guess value.

| | $A$ (μM) | $\tau_e$ (s) | $\tau_p$ (s) | $\tau_d$ (s) |
|---|---|---|---|---|
| Min | 0 ($O_2$Hb)<br>−5 (HHb) | 1 | 4 | 7 |
| Max | 5 ($O_2$Hb)<br>−0 (HHb) | 6 | 14 | 19 |
| Initial guess | 1 ($O_2$Hb)<br>−1 (HHb) | 5 | 7 | 12 |

## Results

Averaged results across all 16 subjects and task repetitions are presented in Figure 3, for the prefrontal cortex (Fp2/1 position) and in Figure 4 for the motor cortex area (C3/4 position). For every exercise, results are shown in terms of hemodynamic variations from baseline values. Both figures report results relative to the upper layer, extra cerebral contribution (first row), and the lower layer, relative to the cerebral cortex (second row). Each column, from left to right, is relative to one exercise: arm raising (AR) arm raising and grasping (ARG) and helped harm raising (HAR). The adaptive HRF model used was the three-gamma-functions model, suitable to fit the initial dip of the $O_2$Hb and the initial raising peak of the HHb. Only the results relative to the lower layers of the brain cortex have been fitted with the HRF model.

As expected, no significant task-related hemodynamic activations (i.e., increase in oxy-and simultaneous decrease in deoxy-hemoglobin concentrations during the task period) were noticed in the prefrontal cortex position neither in deeper cerebral layers nor in extracerebral regions, as shown in Figure 3. On the other hand, substantial brain activation was clearly visible in deeper layers of the primary motor cortex and SMA in both AR and ARG tasks, as shown in Figure 4. In these tasks, the hemodynamic response is characterized by an increase of the oxy-hemoglobin concentration and a concomitant decrease of the deoxy-hemoglobin. No systemic superficial hemodynamic variations have been noticed on average in the motor cortex area. Both oxygenated and deoxygenated hemoglobin variations during the goal-oriented task (ARG) are substantially more intense than the variations of the not goal-oriented task (AR): as a matter of fact, absolute peaks values are doubled for both hemoglobin concentrations in the ARG case.

The adaptive HRF model has been applied both on oxy-and deoxy-hemoglobin readings on every subject and every task, after averaging the five repetitions. With the aim of finding a standardized procedure to quantify the average brain activation for the three different tasks the output parameters of the fitting procedures have been averaged across all subjects and the relative differences have been studied. A deeper analysis of the HRF fitted parameters regarding the motor cortex (lower layers) area is here shown (Tables 2, 3).

From Table 2 it is possible to appreciate the average values of the fitted parameters and in which cases their variations can be considered as statistically significant between different tasks. Standard errors relative to the average values are summarized in Table 3. The significance of the test has been performed exploiting the two-tailed paired two-sample $t$-test, supposing equal variances of the two populations and correcting for multiple comparison trough the Bonferroni method. $t$-test resulting in $p$-values <0.017 have been considered significant and the null hypothesis (no difference between variables under test) can therefore be rejected. Oxy-HR (oxygenated hemoglobin hemodynamic response) activations show significantly higher intensity in case of the ARG exercises compared to both AR and HAR. No significant differences have been found between the

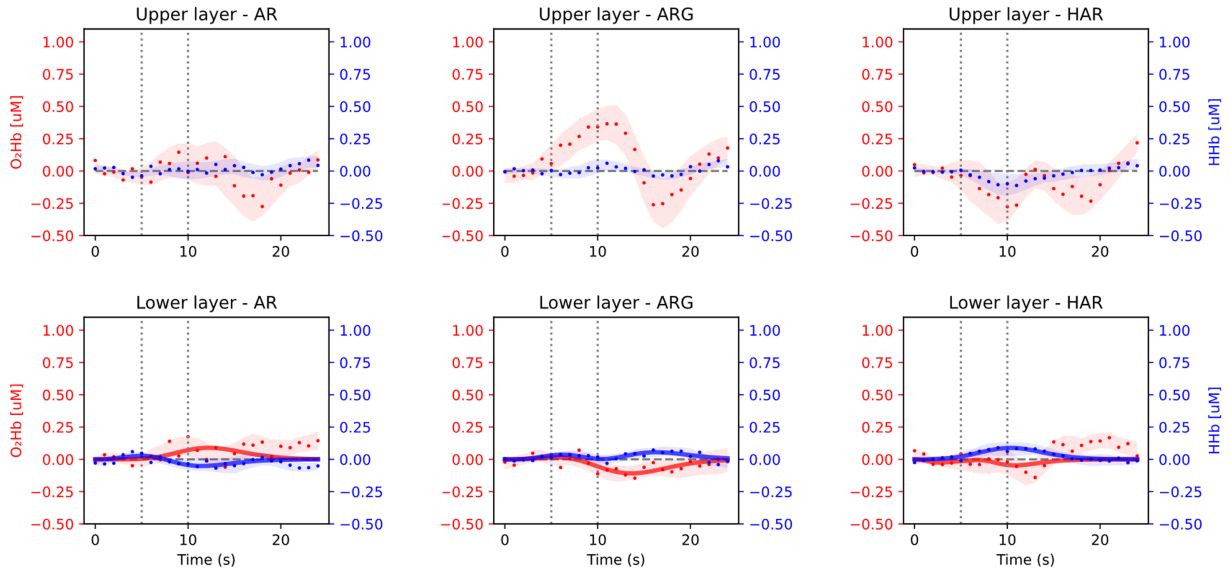


FIGURE 3
Average results from the prefrontal cortex acquisition during the three motor tasks: arm raising (AR), arm raising and grasping (ARG), and helped arm raising (HAR). Shaded areas represent the standard error calculated across all subjects. Upper row shows results from the extra-cerebral layers and lower row from cerebral cortex.

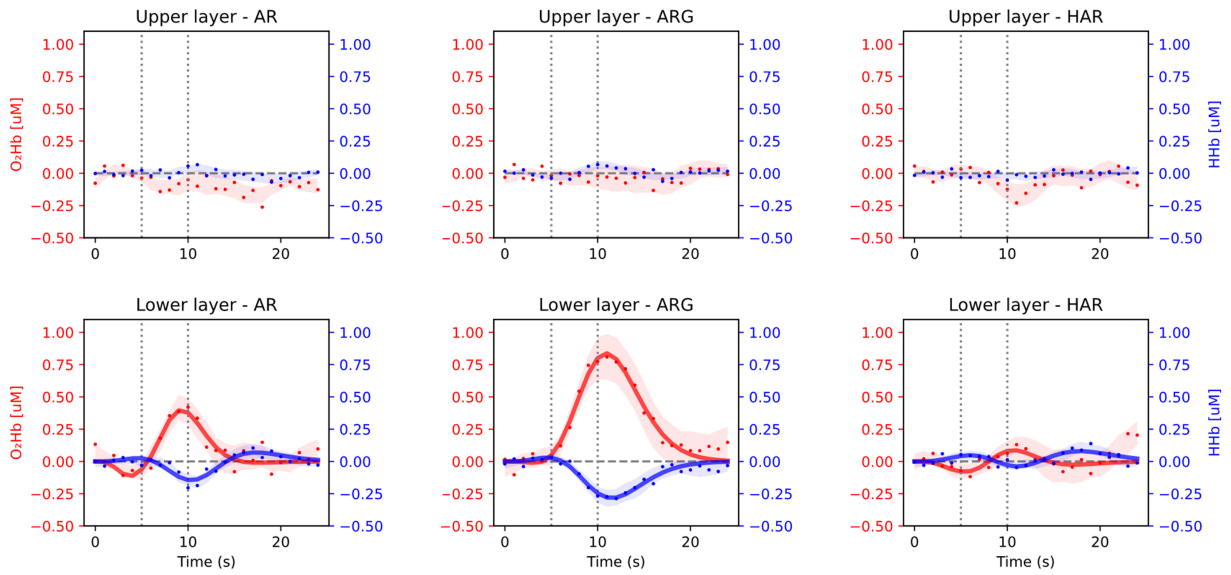


FIGURE 4
Average results from the motor cortex position during the three motor tasks: arm raising (AR), arm raising and grasping (ARG), and helped arm raising (HAR). Shaded areas represent the standard error calculated across all subjects. Upper row shows results from the extra-cerebral layers and lower row from cerebral cortex.

activation intensity of AR and HAR oxy-hemoglobin responses; this might be due to higher standard deviation characterizing these two values. In the AR task the activation peak of the oxygenated hemoglobin showed to occur significantly before if compared to the ARG and the HAR task. Additionally, the amplitude ratio of the undershoot of the oxy-HR activation (*B*) showed to be greater in the HAR exercise compared to the ARG one.

The significant differences found across different exercises in the deoxy-HR fitted parameters are related to the amplitude of the activation peak, the initial dip, main peak and also the undershoot, while no significant differences have been found within peaks' delay. In particular, the amplitude of the peak (*A*) is significantly more pronounced, (larger negative value) in case of AR exercise compared to the HAR one, similarly amplitudes *B* and *C* are greater in HAR with respect to ARG deoxy-HR.

Finally, comparing oxy-and deoxy-HR responses, it has been noticed that the delay of the main activation peak ($\tau_p$) is significantly greater in the HHb compared to the $O_2Hb$ only in case of the AR task.

TABLE 2 Average values of the fitted parameters of the HR, relative to oxygenated and deoxygenated hemoglobin concentrations over all subjects and all tasks. B and C values are unitless since they are fractions of A. Squared brackets signs indicates the couple of values which showed significant difference from each other ($p<0.017$) based on the two-tailed paired t-test and corrected for multiple comparisons (Bonferroni method), p-value is reported in the text boxes next to the bracket sign. For A parameter, differences between oxy and deoxy values are always significant ($p<0.0001$) but are not signed for a clearer presentation. R is average Pearson correlation coefficient between the measurement and the fitted HR.

| | Task | $A$ (μM) | $\tau_p$ (s) | $B$ | $\tau_d$ (s) | $C$ | $\tau_e$ (s) | $R$ |
|---|---|---|---|---|---|---|---|---|
| $O_2Hb$ | AR | 0.5 [0.0003] | 2.6 [0.0001] | 0.5 [0.006] | 2.8 | 0.6 | 4.6 | 0.7 |
| | ARG | 1.1 [0.003] | 4.2 [0.008] | 0.4 | 3.5 | 0.2 | 4.4 | 0.8 |
| | HAR | 0.4 | 4.1 | 0.7 | 2.8 | 0.6 | 4.5 | 0.5 |
| HHb | AR | -0.3 [0.015] | 4.0 | 0.8 | 2.4 | 0.5 | 4.8 | 0.5 |
| | ARG | -0.4 | 4.5 | 0.5 [0.014] | 2.6 | 0.3 [0.004] | 5.0 | 0.6 |
| | HAR | -0.2 | 3.6 | 1.0 | 3.4 | 0.7 | 4.6 | 0.4 |

TABLE 3 Standard error of the values reported in Table 2.

| | Task | $A$ (μM) | $\tau_p$(s) | $B$ | $\tau_d$(s) | $C$ | $\tau_e$(s) | $R$ |
|---|---|---|---|---|---|---|---|---|
| $O_2Hb$ | AR | 0.09 | 0.37 | 0.09 | 0.70 | 0.15 | 0.17 | 0.10 |
| | ARG | 0.17 | 0.22 | 0.13 | 0.78 | 0.22 | 0.07 | 0.06 |
| | HAR | 0.07 | 0.35 | 0.15 | 0.73 | 0.20 | 0.17 | 0.08 |
| HHb | AR | 0.03 | 0.35 | 0.13 | 0.65 | 0.12 | 0.24 | 0.10 |
| | ARG | 0.07 | 0.25 | 0.09 | 0.76 | 0.08 | 0.09 | 0.09 |
| | HAR | 0.03 | 0.32 | 0.13 | 0.70 | 0.14 | 0.27 | 0.09 |

No significant (inter-hemoglobin) differences have been found on other HR parameters.

## Discussion

Specific brain cortex areas can activate due to external stimulus or voluntary actions. Brain activation related to a particular task performed by a subject will be defined as "functional" brain activation. During the stimulus, a functional cerebral hemodynamic response typically involves a rise in oxygenated hemoglobin concentration with a concurrent reduction (generally with a lower intensity) in deoxygenated hemoglobin concentration, followed by a relaxation trend toward the original values. The cerebral hemodynamic response in the brain cortex area, where neuronal activation occurs, is driven by the neurovascular coupling that connects neuron and vascular functions. Relying upon the most accredited theories, this mechanism is regulated by two main phenomena: a feed-forward effect, and a feed-back effect (Kamran et al., 2018).

These two effects will eventually translate into the neurovascular response that we record via TD-fNIRS. Scientists working with the blood oxygen level-dependent (BOLD) signal from functional magnetic resonance imaging (fMRI) have established models to characterize such hemodynamic responses (Boynton et al., 1996; Handwerker et al., 2004). Recent publications presented an adaptive HRF model which can be used to fit also fNIRS acquisitions (initially retrieved by CW-fNIRS measurements only), as presented by Uga et al. (2014). The HRF in the mentioned work is composed by the linear combination of two gamma functions, having opposite signs and fixed delay between their peak positions.

It has also been reported that HRF can show different characteristics in different brain regions (Jasdzewski et al., 2003; Kamran et al., 2015). Furthermore, it is well-known that the hemodynamic signal has inter-subject variability as well as inter-trial variations. A modification of the previous model can be proposed by adding one third gamma function having negative sign, in the timeframe between the beginning of the task and the peak of the first gamma function [an example is presented in (Kamran et al., 2018)]. This additional variable allows to account for a faster process of the cerebral hemodynamic response, often called "initial dip" (Kamran et al., 2018), which is most probably related to the feed-forward mechanism of the neurovascular coupling. This approach is not new in the fNIRS world but, to our knowledge, it is the first time it has been applied to TD-fNIRS data. From the results presented in the previous section, on average, the fitting of the hemodynamic measurement with the adaptive HRF model here proposed, showed moderate $R>0.3$ to strong $R>0.7$ correlation (Table 2 reporting average values and $p$-values form the $t$-test and Table 3 reporting their standard errors). Only three subjects showed an average correlation ($R$) over the three tasks lower than 0.3 related only to the deoxy-HR fit. All subjects showed more than 0.3 average correlation, and more than half of the population showed average correlation (over hemoglobins and tasks) greater than 0.7.

In Table 2, the stronger activation seen in the ARG task can be explained by more intense planning of the movement and higher complexity of the overall task. From Figure 4, we also notice that, on average, the peak of the activation of the ARG task is delayed with respect to the AR task for both HHb and $O_2Hb$ (significant only in case of oxy-HR $p$-value = 0.0001, Table 2), this could be potentially related to the more complex planning and execution of the task, requiring more time to be processed. On the other hand, in the helped arm

raising (assisted) task, we did not notice any substantial activation in the motor cortex. Given the passive nature of the exercise (in its optimal execution, where the subject does not plan/perform any movement) no brain activation is expected to occur. Only slight activations were seen on a few subjects, with very low intensity, mainly related to oxygenated hemoglobin variation. It is important to notice that fitting parameters outputs resulting from AR and in particular HAR tasks are highly variable, mainly due to a lower signal to noise ratio of the activations compared to ARG. Since some individuals' HR processes are hard to be detect, average results related to the first and last peak of the HR are of lower significance. It is therefore useful to weight the relevance of the fitted parameters of a specific HRF on its main peak amplitude (*A*).

Considering this study's limitations, it is important to acknowledge that the small number of channels employed (i.e., measurement locations) may result in a partial understanding of the overall hemodynamics of the cerebral cortex. Specifically, utilizing only two measurement locations enabled to capture hemodynamic variations solely from the prefrontal cortex and the motor cortex, while other regions of the cerebral cortex might be potentially involved in the execution of the tasks. Furthermore, the statistical analysis employed in this study is preliminary and tailored to suit the exploratory nature of this pilot investigation. To enhance significance and reliability of the presented findings, future studies should involve a larger cohort of patients.

From the literature it can be seen that most of the available studies in which similar tasks have been investigated are based on continuous wave (CW) fNIRS (Kashou et al., 2016; Jang et al., 2017). Concerning the simple arm-raising exercise, a similar task was found in literature, presented by Jang et al. (2017). In that work, 10 subjects were asked to perform three repetitions of bilateral arm raising while seated on a chair, 10 repetitions for a total task time of 20 s. The protocol included periods of 20 s of baseline before the task and 20 s of recovery after the task (rest period). A 49-channel CW-NIRS device was used, and the motor cortex was the region of interest during the analysis. The study highlighted a significant activation of the supplementary motor area and primary motor cortex zones. However, the reported conclusions only consider the values of changes in oxygenated hemoglobin and total hemoglobin (the latter can be considered a partial index of the regional blood flow) without including deoxygenated hemoglobin information. This weakens the reliability of the exposed results by not providing a comprehensive hemodynamic perspective of the functional response, but it does assist us in better identifying the brain area that will be most engaged in the specified motor task.

In the case of goal-oriented task (arm raising and grasping), no previous studies were found that proposed similar protocols, but it is possible to estimate the extent of the related brain activation by combining information from arm raising and grasping exercises. Grasping tasks are often studied individually and different objects might be selected to be grasped. From the work of Kashou et al. (2016) we foresee that the motor cortex activation related to a grasping task will have a comparable behavior to a finger-tapping exercise. Given the higher complexity of the overall movement, we expect the goal-oriented activation to be more intense with respect to the non-goal-oriented one. Healthy subjects brain activation related to finger-tapping task have already been explored by the authors with the same TD-fNIRS device exploited in this study (Lacerenza et al., 2020).

Since in previous literature no studies have been found comparing passive motor task (e.g., helped arm raising) with active motor task (e.g., standard arm raising task), in this work, the helped arm raising task was added to the protocol to explore the possible cerebral and extracerebral hemodynamic triggered by a passive action. Given that, the motor cortex area will not be actively involved, no significant motor cortex activation was expected in healthy subjects.

The evaluation of brain activation during assessment phase and training phase is of high interest in the neurorehabilitation field. The work by Maier et al. (2019) unifies the neuroscientific literature relevant to the recovery process and rehabilitation practice in order to provide a synthesis of the principles that constitute an effective neurorehabilitation approach. The authors investigate on how to implement the knowledge of these principles and formalize rehabilitative protocols that truly modify the neural substrate and promote skills not only in stroke patients but also in other neurodegenerative diseases such as Parkinson's disease. One of the most important principle is the goal-oriented therapy. As in the article of Maier et al. this work confirms the importance in brain activity of goal-oriented tasks compared to non-goal-oriented ones.

The supplementary motor area, which was considered in this study is involved in important clinical conditions. This area has come under increasing scrutiny from cognitive neuroscientists, motor physiologists and clinicians given its crucial role in linking cognition to action (Nachev et al., 2008). The work by Jacobs et al. (2009) shows that the supplementary motor area contributes to the timing of the anticipatory postural adjustment and that participants with Parkinson's disease exhibit impaired timing of their anticipatory postural adjustments, in part, due to progressive dysfunction of circuits associated with the supplementary motor area. TD-fNIRS devices could investigate the activation of this crucial area during the execution of even more complex functional movements, such as direction changes in gait, which are really complex and difficult for patients with Parkinson's disease (Park et al., 2020).

The investigation using TD-fNIRS could also be fundamental to study and implement other neurorehabilitation principles, such as practice characterized by a particular task. Practice for a task requires that the conditions for performing a task (neuro-muscular synergies) are selective and specific for that same task both in terms of sensorimotor performance and contextual factors. Specialized training facilitates motor learning even during the retention phase, and reduces inhibition of the non-affected hemisphere on the affected one and the relationship between them (Maier et al., 2019). The work from Walsh et al. (2008) using fMRI and Structural Equation Modelling (SEM) to compare unimanual and bimanual movements shows that the dominant hemisphere appears to initiate activity responsible for bimanual movement, and that the networks involved in producing unimanual movements are distinct from the networks involved in contralateral unimanual movements. These findings provide a better understanding of cortical motor physiology in both healthy individuals and those with neurological damage.

Due to their portability, ease of use, and capability to track in real time the hemodynamic activity of key cerebral regions, TD-fNIRS devices may be used to monitor brain activity during functional movement, functional bimanual exercises, or in ongoing movement.

TD-fNIRS has already been used to record prefrontal region activity during cognitive activities. As the prefrontal cortex is crucial in processing the cognitive, emotional, and behavioural information required for normal functioning in daily life, interest in this topic has grown. Dysexecutive disorders that may occur following damage to the prefrontal cortex can include difficulties in planning and organization, working memory, mental flexibility, impulse control, and emotional regulation (Jones and Graff-Radford, 2021). These disorders can negatively affect the individual's ability to perform work activities and to interact effectively with others in a social environment. For example, difficulties in planning and organization can make difficult for an individual to perform complex work tasks or manage his daily life (Diamond and Ling, 2019). Because executive function networks encompass several circuits of cortico-subcortical brain regions and cerebellar sites, the exploitation of TD-fNIRS is promising also in cognitive rehabilitation environments to assess and enhance brain activation (trough tailored exercises) in specific areas associated with executive function.

## Conclusion

Brain activations from 16 healthy subjects have been successfully recorded during upper limb motor exercises, exploiting compact commercial TD-fNIRS devices, without any restriction on subject enrollment due to hair/scalp characteristics. Quantitative oxygenated and deoxygenated hemoglobin regional concentrations have been recorded, probing extracerebral and cerebral tissues, and in two different brain locations simultaneously. Goal-oriented, not goal-oriented and passive tasks have been explored and consistent results have been retrieved across subjects. Thanks to the employed HRF model, it was possible to quantitatively compare shape, amplitude and timing of the motor cortex HRs in the different tasks. The active arm raising and grasping task (ARG) resulted in a significantly stronger activation compared to the active arm raising task (AR), while, on average, the passive arm raising task did not produce any substantial activation in the brain cortex. The valuable results here reported are representative of upper limb motor activations in healthy subjects, forming an explorative dataset to be compared in the future with brain activations in pathological conditions.

This study based on measurements on heathy subjects, supports that the use of TD-fNIRS in the field of neurorehabilitation has the potential to monitor motor learning in individuals with neuromuscular impairments by providing a quantitative and non-invasive method for measuring changes in brain during motor exercises. This can be used to design rehabilitation programs that target specific brain regions, potentially optimizing motor learning and following progress over time.

## Data availability statement

The raw data supporting the conclusions of this article will be made available by the authors, without undue reservation.

## Ethics statement

The studies involving human participants were reviewed and approved by ethics commitee of Politecnico di Milano Milano, Italy. The patients/participants provided their written informed consent to participate in this study.

## Author contributions

All authors contributed to the article and approved the submitted version.

## Funding

This work has received funding from the European Union's Horizon 2020 research and innovation programme under grant agreements No.101016087 (VASCOVID).

## Acknowledgments

We sincerely thank the subjects involved in this study for their enthusiastic participation.

## Conflict of interest

ML, MB, DC, and AT are co-founders of PIONIRS s.r.l., Italy.

The remaining authors declare that the research was conducted in the absence of any commercial or financial relationships that could be construed as a potential conflict of interest.

## Publisher's note



## References

Boynton, G. M., Engel, S. A., Glover, G. H., and Heeger, D. J. (1996). Linear systems analysis of functional magnetic resonance imaging in human V1. *J. Neurosci.* 16, 4207–4221. doi: 10.1523/jneurosci.16-13-04207.1996

Diamond, A., and Ling, D. S. (2019). Aerobic-exercise and resistance-training interventions have been among the least effective ways to improve executive functions of any method tried thus far. *Dev. Cogn. Neurosci.* 37:100572. doi: 10.1016/j.dcn.2018.05.001

Diedrichsen, J., Grafton, S., Albert, N., Hazeltine, E., and Ivry, R. B. (2006). Goal-selection and movement-related conflict during bimanual reaching movements. *Cereb. Cortex* 16, 1729–1738. doi: 10.1093/cercor/bhj108

Handwerker, D. A., Ollinger, J. M., and D'Esposito, M. (2004). Variation of BOLD hemodynamic responses across subjects and brain regions and their effects on statistical analyses. *NeuroImage* 21, 1639–1651. doi: 10.1016/j.neuroimage.2003.11.029

Iadecola, C. (2017). The neurovascular unit coming of age: a journey through neurovascular coupling in health and disease. *Neuron* 96, 17–42. doi: 10.1016/j.neuron.2017.07.030

Jacobs, J. V., Lou, J. S., Kraakevik, J. A., and Horak, F. B. (2009). The supplementary motor area contributes to the timing of the anticipatory postural adjustment during step initiation in participants with and without Parkinson's disease. *Neuroscience* 164, 877–885. doi: 10.1016/j.neuroscience.2009.08.002

Jang, S. H., Seo, J. P., Lee, S. H., Jin, S. H., and Yeo, S. S. (2017). The cortical activation pattern during bilateral arm raising movements. *Neural Regen. Res.* 12, 317–320. doi: 10.4103/1673-5374.200817

Jasdzewski, G., Strangman, G., Wagner, J., Kwong, K. K., Poldrack, R. A., and Boas, D. A. (2003). Differences in the hemodynamic response to event-related motor and visual paradigms as measured by near-infrared spectroscopy. *NeuroImage* 20, 479–488. doi: 10.1016/S1053-8119(03)00311-2

Jones, D. T., and Graff-Radford, J. (2021). Executive dysfunction and the prefrontal cortex. *Contin. Lifelong Learn. Neurol.* 27:1586. doi: 10.1212/CON.0000000000001009

Kamran, M. A., Jeong, M. Y., and Mannan, M. M. N. (2015). Optimal hemodynamic response model for functional near-infrared spectroscopy. *Front. Behav. Neurosci.* 9, 1–11. doi: 10.3389/fnbeh.2015.00151

Kamran, M. A., Naeem Mannan, M. M., and Jeong, M. Y. (2018). Initial-dip existence and estimation in relation to DPF and data drift. *Front. Neuroinform.* 12, 1–13. doi: 10.3389/fninf.2018.00096

Kashou, N. H., Giacherio, B. M., Nahhas, R. W., and Jadcherla, S. R. (2016). Hand-grasping and finger tapping induced similar functional near-infrared spectroscopy cortical responses. *Neurophotonics* 3:025006. doi: 10.1117/1.nph.3.2.025006

Lacerenza, M., Buttafava, M., Renna, M., Mora, A. D., Spinelli, L., Zappa, F., et al. (2020). Wearable and wireless time-domain near-infrared spectroscopy system for brainand muscle hemodynamic monitoring. *Biomed. Opt. Express* 11, 5934–5949. doi: 10.1364/boe.403327

Lacerenza, M., Spinelli, L., Buttafava, M., Dalla Mora, A., Zappa, F., Pifferi, A., et al. (2021). Monitoring the motor cortex hemodynamic response function in freely moving walking subjects: a time-domain fNIRS pilot study. *Neurophotonics* 8:015006. doi: 10.1117/1.nph.8.1.015006

Lacerenza, M., et al., Performance and reproducibility assessment across multiple time-domain near-infrared spectroscopy device replicas, Proc. SPIE 11951, Design and Quality for Biomedical Technologies XV, 1195108, (2022)

Lange, F., and Tachtsidis, I. (2019). Clinical brain monitoring with time domain NIRS: a review and future perspectives. *Appl. Sci.* 9:1612. doi: 10.3390/app9081612

Leff, D. R., Orihuela-Espina, F., Elwell, C. E., Athanasiou, T., Delpy, D. T., Darzi, A. W., et al. (2011). Assessment of the cerebral cortex during motor task behaviours in adults: a systematic review of functional near infrared spectroscopy (fNIRS) studies. *NeuroImage* 54, 2922–2936. doi: 10.1016/J.NEUROIMAGE.2010.10.058

Logroscino, G., Piccininni, M., Marin, B., Nichols, E., Abd-Allah, F., Abdelalim, A., et al. (2018). Global, regional, and national burden of motor neuron diseases 1990–2016: a systematic analysis for the global burden of disease study 2016. *Lancet Neurol.* 17, 1083–1097. doi: 10.1016/S1474-4422(18)30404-6

Maier, M., Ballester, B. R., and Verschure, P. F. M. J. (2019). Principles of neurorehabilitation after stroke based on motor learning and brain plasticity mechanisms. *Front. Syst. Neurosci.* 13:74. doi: 10.3389/fnsys.2019.00074

Mastos, M., Miller, K., Elliasson, A. C., and Imms, C. (2007). Goal-directed training: linking theories of treatment to clinical practice for improved functional activities in daily life. *Clin. Rehabil.* 21, 47–55. doi: 10.1177/0269215506073494

Muthalib, M., Re, R., Zucchelli, L., Perrey, S., Contini, D., Caffini, M., et al. (2015). Effects of increasing neuromuscular electrical stimulation current intensity on cortical sensorimotor network activation: a time domain fNIRS study. *PLoS One* 10:e0131951. doi: 10.1371/JOURNAL.PONE.0131951

Nachev, P., Kennard, C., and Husain, M. (2008). Functional role of the supplementary and pre-supplementary motor areas. *Nat. Rev. Neurosci.* 9:856. doi: 10.1038/nrn2478

Nathan, D. E., Prost, R. W., Guastello, S. J., Jeutter And, D. C., and Reynolds, N. C. (2012). Investigating the neural correlates of goal-oriented upper extremity movements. *Neuro Rehabilitation* 31:421. doi: 10.3233/NRE-2012-00812

Ortega-Martinez, A., Rogers, D. J., Anderson, J., Farzam, P., Gao, Y., Zimmermann, B., et al. (2023). How much do time-domain functional near-infrared spectroscopy (fNIRS) moments improve estimation of brain activity over traditional fNIRS? *Neurophotonics* 10:013504. doi: 10.1117/1.NPH.10.1.013504

Park, H., Youm, C., Lee, M., Noh, B., and Cheon, S. M. (2020). Turning characteristics of the more-affected side in parkinson's disease patients with freezing of gait. *Sensors* 20:3098. doi: 10.3390/s20113098

Perez, D. L., Edwards, M. J., Nielsen, G., Kozlowska, K., Hallett, M., and Curt Lafrance, W. (2021). Decade of progress in motor functional neurological disorder: continuing the momentum. *J. Neurol. Neurosurg. Psychiatry* 92:jnnp-2020-323953. doi: 10.1136/jnnp-2020-323953

PIONIRS S.r.l., (2023). Accessories of the NIRSBOX device, Available at: https://www.pionirs.com/wp/probes/, (Accessed May 27, 2023).

Re, R., Contini, D., Turola, M., Spinelli, L., Zucchelli, L., Caffini, M., et al. (2013). Multi-channel medical device for time domain functional near infrared spectroscopy based on wavelength space multiplexing. *Biomed. Opt. Express* 4, 2231–2246. doi: 10.1364/boe.4.002231

Rizzolatti, G., Cattaneo, L., Fabbri-Destro, M., and Rozzi, S. (2014). Cortical mechanisms underlying the organization of goal-directed actions and mirror neuron-based action understanding. *Physiol. Rev.* 94, 655–706. doi: 10.1152/physrev.00009.2013

Rizzolatti, G., Gentilucci, M., Fogassi, L., Luppino, G., Matelli, M., and Ponzoni-Maggi, S. (1987). Neurons related to goal-directed motor acts in inferior area 6 of the macaque monkey. *Exp. Brain Res.* 67, 220–224. doi: 10.1007/BF00269468

Uga, M., Dan, I., Sano, T., Dan, H., and Watanabe, E. (2014). Optimizing the general linear model for functional near-infrared spectroscopy: an adaptive hemodynamic response function approach. *Neurophotonics* 1:015004. doi: 10.1117/1.nph.1.1.015004

Visani, E., Canafoglia, L., Gilioli, I., Sebastiano, D. R., Contarino, V. E., Duran, D., et al. (2015). Hemodynamic and EEG time-courses during unilateral hand movement in patients with cortical myoclonus. An EEG-fMRI and EEG-TD-fNIRS study. *Brain Topogr.* 28, 915–925. doi: 10.1007/S10548-014-0402-6

Walsh, R. R., Small, S. L., Chen, E. E., and Solodkin, A. (2008). Network activation during bimanual movements in humans. *NeuroImage* 43, 540–553. doi: 10.1016/j.neuroimage.2008.07.019

Wevers, L., van de Port, I., Vermue, M., Mead, G., and Kwakkel, G. (2009). Effects of task-oriented circuit class training on walking competency after stroke: a systematic review. *Stroke* 40:2450. doi: 10.1161/STROKEAHA.108.541946

Wu, C., Trombly, C. A., Lin, K., and Tickle-Degnen, L. (2000). A kinematic study of contextual effects on reaching performance in persons with and without stroke: influences of object availability. *Arch. Phys. Med. Rehabil.* 81, 95–101. doi: 10.1016/S0003-9993(00)90228-4

Yamagata, T., Nakayama, Y., Tanji, J., and Hoshi, E. (2012). Distinct information representation and processing for goal-directed behavior in the dorsolateral and ventrolateral prefrontal cortex and the dorsal premotor cortex. *J. Neurosci.* 32, 12934–12949. doi: 10.1523/JNEUROSCI.2398-12.2012

Zucchelli, L., Contini, D., Re, R., Torricelli, A., and Spinelli, L. (2013). Method for the discrimination of superficial and deep absorption variations by time domain fNIRS. *Biomed. Opt. Express* 4, 2893–2910. doi: 10.1364/boe.4.002893

frontiers | Frontiers in Neuroscience

TYPE Original Research
PUBLISHED 08 August 2023
DOI 10.3389/fnins.2023.1084813



OPEN ACCESS

EDITED BY
Jingchun Guo,
Fudan University, China

REVIEWED BY
Layne Dylla,
University of Colorado Anschutz Medical Campus, United States
Zheng Jiang,
Fujian University of Traditional Chinese Medicine, China
U. K. Misra,
Sanjay Gandhi Post Graduate Institute of Medical Sciences (SGPGI), India

*CORRESPONDENCE
Anren Zhang
anren0124@tongji.edu.cn
Zhonghua Lin
doctor_lzh71@163.com
Xiaohua Ke
kxh22@tongji.edu.cn

†These authors have contributed equally to this work

RECEIVED 31 October 2022
ACCEPTED 18 July 2023
PUBLISHED 08 August 2023

CITATION
Huang D, Yang Y, Song W, Jiang C, Zhang Y, Zhang A, Lin Z and Ke X (2023) Untargeted metabonomic analysis of a cerebral stroke model in rats: a study based on UPLC–MS/MS. *Front. Neurosci.* 17:1084813. doi: 10.3389/fnins.2023.1084813



# Untargeted metabonomic analysis of a cerebral stroke model in rats: a study based on UPLC–MS/MS

Dunbing Huang[1†], Yihan Yang[2†], Wei Song[1†], Cai Jiang[3,4,5,6,7], Yuhao Zhang[8], Anren Zhang[1*], Zhonghua Lin[3,4,5,6,7*] and Xiaohua Ke[1*]

[1]Department of Rehabilitation Medicine, Shanghai Fourth People's Hospital, School of Medicine, Tongji University, Shanghai, China, [2]College of Rehabilitation Medicine, Fujian University of Traditional Chinese Medicine, Fuzhou, China, [3]Shengli Clinical Medical College of Fujian Medical University, Fuzhou, China, [4]Second Rehabilitation Department, Fujian Provincial Hospital, Fuzhou, China, [5]Fujian Provincial Center for Geriatrics, Fujian Provincial Hospital, Fuzhou, China, [6]Fujian Key Laboratory of Geriatrics Diseases, Fujian Provincial Hospital, Fuzhou, China, [7]Department of Complementary Medicine, University of Johannesburg, Johannesburg, South Africa, [8]Department of Rehabilitation Medicine, Nanjing Lishui District Hospital of Traditional Chinese medicine, Nanjing, China

**Introduction:** Brain tissue damage caused by ischemic stroke can trigger changes in the body's metabolic response, and understanding the changes in the metabolic response of the gut after stroke can contribute to research on poststroke brain function recovery. Despite the increase in international research on poststroke metabolic mechanisms and the availability of powerful research tools in recent years, there is still an urgent need for poststroke metabolic studies. Metabolomic examination of feces from a cerebral ischemia–reperfusion rat model can provide new insights into poststroke metabolism and identify key metabolic pathways, which will help reveal diagnostic and therapeutic targets as well as inspire pathophysiological studies after stroke.

**Methods:** We randomly divided 16 healthy adult pathogen-free male Sprague–Dawley (SD) rats into the normal group and the study group, which received middle cerebral artery occlusion/reperfusion (MCAO/R). Ultra-performance liquid chromatography–tandem mass spectrometry (UPLCMS/MS) was used to determine the identities and concentrations of metabolites across all groups, and filtered high-quality data were analyzed for differential screening and differential metabolite functional analysis.

**Results:** After 1 and 14 days of modeling, compared to the normal group, rats in the study group showed significant neurological deficits ($p < 0.001$) and significantly increased infarct volume (day 1: $p < 0.001$; day 14: $p = 0.001$). Mass spectra identified 1,044 and 635 differential metabolites in rat feces in positive and negative ion modes, respectively, which differed significantly between the normal and study groups. The metabolites with increased levels identified in the study group were involved in tryptophan metabolism ($p = 0.036678$, $p < 0.05$), arachidonic acid metabolism ($p = 0.15695$), cysteine and methionine metabolism ($p = 0.24705$), and pyrimidine metabolism ($p = 0.3413$), whereas the metabolites with decreased levels were involved in arginine and proline metabolism ($p = 0.15695$) and starch and sucrose metabolism ($p = 0.52256$).

**Discussion:** We determined that UPLC–MS/MS could be employed for untargeted metabolomics research. Moreover, tryptophan metabolic pathways may have been disordered in the study group. Alterations in the tryptophan metabolome may provide additional theoretical and data support for elucidating stroke pathogenesis and selecting pathways for intervention.

KEYWORDS

**untargeted metabolomics, ischemic stroke, rats, tryptophan metabolism, metabolism**

# 1. Introduction

Ischemic stroke is a clinical syndrome characterized by rapid onset of focal or global brain deficits lasting more than 24 h (Shen et al., 2023). Ischemic stroke condition manifests as motor, sensory, cognitive and speech dysfunction (Winstein et al., 2016) and places a heavy burden on the economy and society due to its high morbidity, mortality and disability rates (Bai et al., 2017). Stroke-induced brain damage is caused by a complex series of neuropathological events, mainly including oxidative stress, excitotoxicity, apoptosis and neuroinflammation (Kunz et al., 2010; Radenovic et al., 2020). The associated pathophysiological responses further leads to changes in the patient's metabolism and alterations in metabolites.

The gut-brain axis (GBA) is a two-way communication network between the gastrointestinal tract and the central nervous system. After stroke, the GBA communicates from the brain to the gut (top-down signaling) and plays a regulatory role at several levels, directly or indirectly. Stroke impairs intestinal function, affecting intestinal motility (Singh et al., 2016; Jiang et al., 2021), subsequently altering intestinal flora (Chen et al., 2019; Lee et al., 2020), resulting in changes in flora metabolism and ultimately metabolites such as feces (Winek et al., 2016; Jiang et al., 2021; Huang et al., 2022). Therefore, the corresponding metabolic changes in the gut microbes are thought to be one of the hallmarks of stroke pathogenesis (Benakis et al., 2016; Zhu et al., 2021). In turn, gut microbiota dysbiosis appears to communicate with the brain through the microbial gut-brain axis (bottom-up signaling), thereby exacerbating the deleterious effects of stroke (Benakis et al., 2016; Singh et al., 2016). Studies have shown that short-chain fatty acids and indole derivatives produced by gut microbes, among others, can influence brain function by influencing energy metabolism, inflammation and neurotransmitter changes in the brain, making them functional preservers of the brain (Winek et al., 2016; Roth et al., 2021; Huang et al., 2022) (2, 27,714,645). Therefore, a growing amount of research supports the notion that gut microbes are significant regulators of GBA and drivers of amino acid metabolism (De Vadder et al., 2014; Fröhlich et al., 2016). Eventually, metabolites related to host–microbe interactions have become new targets for testing (Mu et al., 2016).

Metabolomics is one of the most widely used applications for tracking metabolites (Ma et al., 2012). This approach allows researchers to identify and screen for biomarkers. It also allows the study of typological and quantitative changes in endogenous metabolites, as well as their intrinsic relationship and broad patterns of change with physiological and pathological phenotypes following perturbations. Furthermore, by focusing on host–microbe interactions, metabolomics can identify metabolites (qualitatively and quantitatively) associated with these interactions and ultimately reveal the metabolic mechanisms underlying disease pathogenesis.Thus, metabolomics is uniquely positioned to help identify biomarkers specific to disease mechanisms (Bujak et al., 2016; Johnson et al., 2016). One of the research approaches in metabolomics is nontargeted metabolomics, which is used to analyze as many metabolites as possible without prior knowledge of these metabolites (Dunn et al., 2012). Metabolomics is also increasingly used in the course of clinical research in stroke because of its potential role in the discovery of biomarkers for the early diagnosis of ischemic stroke and the development of new therapeutic targets (Kimberly et al., 2013; Jové et al., 2014; Sidorov et al., 2019; Montaner et al., 2020).

The ultra-performance liquid chromatography (UPLC) employed in this study is the most widely used technique for metabolomics analysis with ultrahigh efficiency, ultrahigh separation, ultrahigh sensitivity and low consumption, and this method dominates the field of metabolomics (Barri and Dragsted, 2013; Yin et al., 2016; Ma et al., 2017). When coupled with mass spectrometry measures, such as quadrupole time of flight (Q-TOF), ESI (QQQ) or MS/MS (Q-Trap), UPLC offers significant advantages in qualitative as well as quantitative analysis. Su et al. (2016) investigated the protective effect of a Raf kinase inhibitor protein against stroke using ultra-high performance liquid chromatography-quadrupole time-of-flight mass spectrometry (UHPLC-Q-TOFMS), which provides a better understanding of the molecular mechanisms of ischemic stroke and a strong foundation for the development of new therapeutic targets for the treatment of ischemic stroke. In contrast, Liu et al. (2017) used liquid chromatography–mass spectrometry and gas chromatography–mass spectrometry to identify a set of five metabolites to differentiate acute ischemic stroke patients from healthy subjects.

Previous literature has typically focused on the analysis of serum from patients or animals with cerebral ischemia, and there is a relative paucity of studies on feces produced by the body after stroke. However, using feces as a sample to study the association between poststroke metabolism and the GBA after stroke has advantages over the methods described above. For example, fecal samples are non-invasive and easy to collect, and it is easier for researchers to collect large numbers or multiple samples over time to study changes in metabolite levels over time, providing a more complete picture of metabolic activity in the gut of stroke patients. Secondly, due to the protective environment of the gut, fecal metabolites tend to be stable and can be stored for longer periods of time without degradation, improving the stability and accuracy of results and facilitating retrospective analysis (Smith et al., 2020; Erben et al., 2021). Most importantly, fecal metabolites directly reflect the metabolic activity of the gut microbiome, facilitating direct interpretation of the link between GBA and stroke pathogenesis (Zierer et al., 2018; Xu et al., 2019). Not only that, Zhao et al. (2022) analysed feces, urine and plasma from ischaemic stroke patients and healthy groups using a combination of non-targeted metabolomics and macrogenomics, and found that fecal metabolites provided the richest metabolic information and showed the strongest correlation with the gut microbiome, helping to study the interaction between gut microbiota and metabolites to understand the disease. And there have been many studies using feces as a sample for metabolomics research. For example, Cheema and Pluznick (2019) used untargeted metabolomics to analyse fecal samples to study changes in fecal metabolites of angiotensin II in conventional and germ-free mice. Lupo et al. (2021) used non-targeted metabolomics to analyse stool samples from patients with chronic fatigue syndrome/myalgic encephalomyelitis (CFS/ME) and healthy controls to study the metabolic differences between the two that underlie CFS/ME. Pathogenesis provides insights. Jiang et al. (2021) used untargeted metabolomics to study fecal samples to identify potential post-stroke depression-associated gut microbes and their functional metabolites in rats.

In the present study, we used Sprague–Dawley (SD) rats as subjects through middle cerebral artery occlusion to model cerebral ischemia–reperfusion. UPLC–MS/MS provided us with a method for metabolomic analysis of feces. Further, the purpose of our study was to investigate potential markers in rat feces after ischemic stroke by UPLC-MS/MS, to obtain basic data on changes in markers after

ischemic stroke, and ultimately to elucidate the potential link between alterations in metabolic function and stroke. Ultimately, this information will improve our knowledge of stroke disease and help us to identify poststroke biomarkers and relevant targets for stroke therapy.

# 2. Materials and methods

## 2.1. Animals and grouping

Healthy adult male SD rats (300 ± 20 g), Shanghai Laboratory Animals Ltd. provided them for the study (No. SYXK 2020–0002). Rats were housed in a flat area with regulated environmental conditions, including noise levels within 60 dB, temperature between 21 and 25°C, humidity between 40 and 60%, and 12 h of light/12 h of darkness per day(light hours: 7:00–19:00). One week was allowed for rats to acclimatize to the standardized laboratory conditions. All rats were allowed to drink water (autoclaved) and food (60Co-irradiated sterilized breeding chow, No. 2019060676, Beijing Huafukang Biotechnology Co., Ltd.), *ad libitum*, and bedding was changed every other day (60Co irradiated corn cobs, Biotechnology Co., Ltd.) and cages (No. IsoRat900N, Tecniplast Group) every other day. All experimental methods were performed in accordance with guidelines for the care and use of laboratory animals in biomedical research (Jones-bolin, 2012).

The random number table method was used to randomly divide the rats into two groups ($n = 8$/group): (1) the normal group, where the rats were kept without any treatment and under the same conditions; (2) the study group, the rat's middle cerebral artery was occluded/reperfused byinserting an intracanalized monofilament in the left internal carotid artery of the rat.

## 2.2. Establishment of the study group model

The study group used the Longa method to establish the MCAO/R model (Longa et al., 1989). After 12 h of preoperative fasting, during which time water was freely available, the rats were immobilized in the supine position and anesthetized with 3% isoflurane in 30% $O_2$ and 67% $N_2$. The skin in the middle of the rats' necks was prepared and disinfected with alcohol iodine, and a longitudinal neck incision was made along the midline. The left common carotid artery, external carotid artery and internal carotid artery were all directly exposed and isolated after the internal and external sternocleidomastoid muscles were separated. Thereafter, the occipital artery and superior thyroid artery were isolated and cauterized to prevent bleeding with a preheated electrocautery device. The pterygopalatine artery, a branch of the internal carotid artery, was ligated; a lasso was made at the distal end of the external carotid artery. The common and internal carotid arteries were then clamped, and the vessel distal to the external carotid artery was cut between the two knots with a microscopic spinning instrument. The external carotid artery was gently pulled so that it was in the same line as the internal carotid artery, and a marked monofilament (Bosterembolus, Boster Biotechnology Co., Ltd., Wuhan, China)was gently pushed through the incision in the direction of the external carotid artery until resistance was minimized(approximately 18 mm). Finally, the monofilament was secured by ligating the proximal external carotid, and the arterial clips of the common and internal carotid arteries were removed. The monofilament was slowly withdrawn after 90 min of ischemia, and the incision was then sutured and postoperatively disinfected with iodine. Until the rats recovered from the anesthetic, their body temperature was maintained at 37 ± 1°C with an electric blanket during the procedure.

## 2.3. Evaluation of the study group

### 2.3.1. Scoring of neurological deficits

The neurological deficits were assessed according to the Long five-point scale and were scored as follows (Longa et al., 1989): 0, no signs; 1, the rat was unable to fully extend the forelimb; 2, the rat was paralyzed in one limb and had tail-chasing; 3, the rat could not stand or roll; 4, no spontaneous movement and had impaired consciousness. Scores of 1 to 3 indicated successful modeling. The normal group and the study group were evaluated for neurological symptoms 2 h and 14 days following modeling (see Supplementary Figure S1).

### 2.3.2. Measurement of cerebral infarct volumes

MRI T2-weighted imaging data were obtained using a 9.4 T MRI Bruker Avance-console and a 35 mm orthogonal volume coil (Pharmascan, microMRI, Bruker Medizintechnik, Germany) to determine the nature of infarction in rats. Scans were performed on each group of rats within 24 h of ischemic stroke. Briefly, isoflurane/$O_2$ (3% for induction and 2% for maintenance) was used to anesthetize rats. The rats were maintained in a stable physiological condition by placing them flat on a rodent bed covered with a warm water bath mat. A physiological detector (SurgiVet V3395TPR, Smiths Medical Inc., St Paul, MN) continuously monitored vital signs (temperature, respiration and heart rate).

T2-weighted imaging (T2WI) was acquired using a relaxation enhanced (RARE) sequence with the following parameters: field of view (FOV) = 32 × 32 mm, repetition time (TR) = 2,500 ms, echo time (TE) = 33 ms, average number of averages (averages) = 4, number of layers (slices) = 21, layer thickness (slice thickness) bandwidth = 326,087 Hz, matrix size = 256 × 256, echo spacing (ESP) = 10,000 ms, refocusing angle = 180°, excitation angle = 90°, echo column length (echo train length, ETL) = 8, and k-zero = 3. ITK-SNAP[1] software was used to segment the images of the cerebral infarct region, and the MATLAB 2013b[2] program was used to calculate the infarct volumes for each subject. The volume of the infarct was obtained as follows: brain infarct volume = number of pixel points in the brain infarct region× spatial resolution of the pixel points.

## 2.4. LC–MS/MS analysis

### 2.4.1. Fecal sample collection

Fourteen days after establishment of the study group, fecal samples were collected in the normal and the study group after a 12 h

1 http://www.itksnap.org/pmwiki/pmwiki.php
2 https://www.mathworks.com

TABLE 1 Chromatographic gradient elution program.

| Time(min) | A% | B% |
|---|---|---|
| 0 | 98 | 2 |
| 1.5 | 98 | 2 |
| 12 | 0 | 100 |
| 14 | 0 | 100 |
| 14.1 | 98 | 2 |
| 17.0 | 98 | 2 |

TABLE 2 Comparison of longa scores between rat groups.

| Group | *n* | 1d | 14 d |
|---|---|---|---|
| normal group | 8 | 0 | 0 |
| Study group | 8 | 2.50 ± 0.54 | 1.38 ± 0.27 |
| Z | | −3.651 | −3.664 |
| *P* | | <0.001 | <0.001 |

fast. Feces were collected by stress defecation, placed in sterile EP tubes and immediately frozen in liquid nitrogen for 10 min and stored at −80°C until use.

### 2.4.2. Sample preparation

First, an EP tube was filled with 100 μL of the sample, and 400 μL of 80% precooled methanol in water was added and mixed thoroughly by vortex shaking. The mixture was then placed in an ice bath for 5 min and centrifuged at 15,000 × g for 20 min at 4°C. The supernatant was collected and analyzed by liquid chromatography–mass spectrometry (LC–MS; Barri and Dragsted, 2013). The final sample was lyophilized, resolubilized using an equal volume of cosolvent (methanol:acetonitrile = 1:1), vortexed and centrifuged at 15,000 × g for 20 min at 4°C.Mass spectrometry water was used to dilute an amount of supernatant twice, and the diluted sample was assessed using the machine.

### 2.4.3. Metabolite detection

On a Vanquish (Thermo Fisher Scientific) ultra-performance liquid chromatograph, the target compounds were separated and chromatographed using a Hypesil Gold column (100 × 2.1 mm, 1.9 μm, Thermo Fisher, United States). Liquid chromatography was performed with mobile phase A containing 5 mM ammonium acetate and 0.1% formic acid (pH = 9.0) and methanol-based mobile phase B. With an injection volume of 1 μL and a flow rate of 0.20 mL/min, the column temperature was set at 40°C. The chromatographic gradient elution program was set up as shown in Table 1; under the control software (Xcalibur, Thermo), the Thermo Q Exactive HFX mass spectrometer was able to acquire primary and secondary mass spectrometry data. The following specific parameters were established: The MS/MS secondary scans are data-dependent scans; capillary temperature is 320°C, sheath gas flow rate is 40 Arb, aux gas flow rate is 10 Arb, spray voltage is 3.2 kV, and polarity is positive and negative.

### 2.4.4. Data extraction and multivariate analysis

For peak detection and alignment, sample data were extracted using Compound Discover (CD) software (version V3.1, Thermo Fisher, Germany). Internal standard normalization was used in the examination of the data, and the final data set, including peak number information, sample name and normalized peak area was then imported into SIMCA software (V16.0.2, Sartorius Stedim Data Analytics AB, Umea, Sweden) for principal component analysis (PCA) of fecal metabolites (Wiklund et al., 2008) and orthogonal partial minimum analysis (OPM). Pattern recognition analysis was performed by orthogonal projections to latent structures-discriminant analysis (OPLS-DA). Metabolites with a variable importance in the projection (VIP) greater than 1 and $p < 0.05$ were considered differential metabolites (Saccenti and Hoefsloot, 2014). Potential biomarkers were found using the Kyoto Encyclopedia of Genes and Genomes (KEGG) database[3] and the Human Metabolome Database (HMDB).[4] In addition, pathway enrichment analysis was performed using many databases, including PubChem[5] and MetaboAnalyst.[6]

## 2.5. Statistical analysis

Excel 2019 for Windows (Microsoft Corporation, San Francisco, CA, United States) was used to generate the database, and IBM SPSS version 24.0 statistical software (SPSS Inc., Chicago, IL, United States) was utilized for all statistical analyses. The normality of the distributions of continuous variables was tested, with normally distributed continuous variables expressed as the mean ± standard deviation (SD); the means of continuous normally distributed variables were compared by independent samples Student's *t* test. Nonnormal variable medians were compared using nonparametric testing. Differences were considered statistically significant if $p < 0.05$.

# 3. Results

## 3.1. Neurological deficit scores and imaging evaluation in model rats with cerebral ischemia stroke

The rats in both groups were scored for neurological deficits at each time point, and the results are present in Table 2. At each time point, the rats in the normal group did not show any neurological deficits, whereas the study group showed different degrees of neurological deficits at 1 and 14 days of ischemic stroke. A statistically significant ($p < 0.001$) difference in scores was noted compared to the normal group. The infarcts of the rats were assessed at 1 and 14 days after ischemic stoke injury using T2WI structural images at the specific infarct locations shown in Figure 1, including brain regions such as the hippocampus, internal olfactory cortex, motor cortex, sensory cortex, dorsal thalamus and striatum. As shown in Table 3, the infarct volume increased more significantly in the study group of rats at different time points 1 day and 14 days after modeling (1 day,

3 http://www.genome.jp/kegg/
4 https://www.hmdb.ca/
5 https://www.ncbi.nlm.nih.gov/pccompound
6 http://www.metaboanalyst.ca/

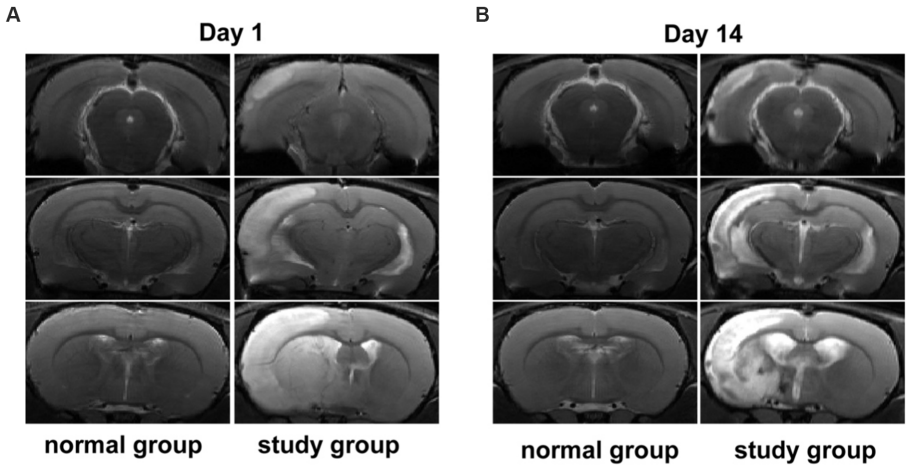


FIGURE 1
**(A,B)** Show the signal changes in the normal group and the study group at day 1 and day 14 after brain infarction.

TABLE 3 Comparison of the percentage of cerebral infarct volume in each group of rats.

| Group | *n* | 1d | 14 d |
|---|---|---|---|
| Normal group | 8 | 0 | 0 |
| Study group | 8 | 20.90 ± 4.50 | 13.85 ± 3.65 |
| t | | 13.131 | 10.724 |
| *P* | | <0.001 | 0.001 |

$p < 0.001$; 14 day: $p = 0.001$). In conclusion, these results provide evidence that the rat model used in this study was stable.

## 3.2. Nontargeted metabolomics results

### 3.2.1. Quality control results

The stability of the assay can be judged by the difference in response peak heights of the internal standards between the quality control samples. The extracted ion current (EIC) plots for all samples are shown in Figures 2A,B. The results indicate that the response intensities and retention periods of the peaks basically overlap, revealing that the variation caused by instrument error is minimal throughout the process. The response peak heights of all samples almost overlap, and the peak heights, peak areas and retention times are approximately the same, indicating good stability of the instrument data acquisition.

### 3.2.2. Results of multivariate statistical analysis of fecal metabolomics

PCA is an unsupervised statistical method that uses an orthogonal transformation to turn a set of observed potentially correlated variables into linearly uncorrelated variables (i.e., principal components), whereas OPLS-DA is a supervised statistical method that allows for repeated analysis of samples between groups, allowing for more reliable group differences in metabolites. The PCA score plot (Figures 3A,B) shows that all samples fell within the 95% confidence interval (Hotelling's T-squared ellipse) and that the normal and model groups were separated in both positive and negative ion modes, indicating that the differences between the two groups' metabolites are displayed.

To assess intergroup differences in fecal metabolites between the normal and studyrat groups, OPLS-DA modeling analysis was performed using SIMCA 16.0.2 software, and model quality was tested using a 7-fold cross-validation test. In both positive and negative ion identification modes, scatter plots of the initial OPLS-DA model scores showed between-group differences between the normal model and studyrat fecal metabolome groups (Figures 4A,D). The $R^2Y$ (to assess the interpretability of the categorical variable Y) and $Q^2$ (to assess the predictability of the model) values were recorded for each of the 200 permutation tests performed on the model (Figures 4B,E). This finding indicates that there is no overfitting in the initial OPLS-DA model, the two models established are more in line with the actual situation of the sample data, and the original model can reasonably explain the differences between the two sample groups. Therefore, the model has good adaptability and predictability. On this basis, volcano plots were used to display the metabolites that were significantly different between the normal group and the model group (Figures 4C,F).

### 3.2.3. Biomarker screening and pathway enrichment analysis

The compounds identified by the positive and negative ion patterns were deredundantly integrated and screened for differential metabolites. According to the above rules, this study's cardinality criterion was a *p* value of less than 0.05 for Student's t test, whereas the OPLS-DA model's first principal component's VIP was more than 1 to screen for differentially expressed metabolites in the two groups. The model and normal groups identified 1,044 differential metabolites in the positive ion model and 635 in the negative ion model. Due to the high-throughput nature of the Q-Exactive (QE) metabolome data, a large number of distinct metabolites were detected in this study, so only differential metabolites with a cardinality criterion of $p < 0.05$ and

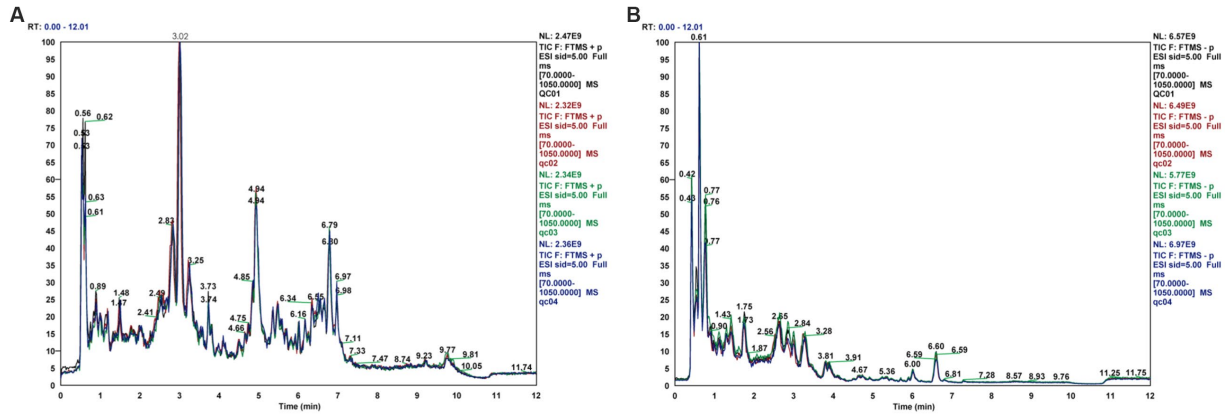


FIGURE 2
Total ion current diagram for rat fecal samples in positive and negative ion modes, **(A)** Total ion current diagram (ESI+), **(B)** Total ion current diagram (ESI-).

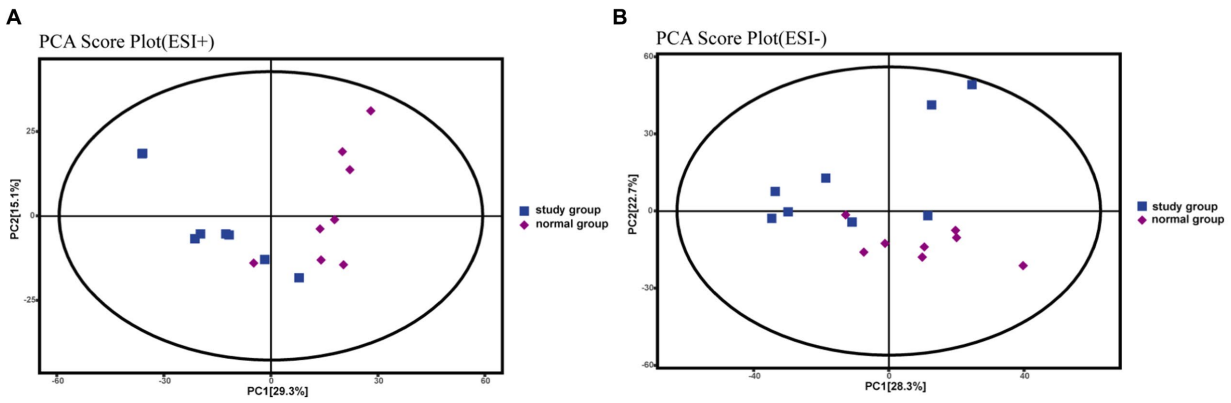


FIGURE 3
PCA score plots for rat fecal metabolomics, **(A)** PCA Score Plot (ESI+), **(B)** PCA Score Plot (ESI-).

a VIP ≥ 2 are listed in this study. Table 4 provides a summary of the basic characteristics of these differential metabolites.

The KEGG IDs of the differential metabolites were then uploaded to MetaboAnalyst for visual analysis and KEGG pathway analysis. The differential abundance score in the KEGG pathway difference abundance analysis is an analysis method based on the metabolic changes in the pathway, which can intuitively display the up- and downregulation of the metabolic pathway and the metabolic type (Figures 5A,C). According to the results, tryptophan metabolism, arginine and proline metabolism, arachidonic acid metabolism, starch and cross metabolism, cysteine and metabolism, and pyrimidine metabolism, are all closely associated with cerebral ischemic stroke injury. Among them, the metabolic pathways upregulated after cerebral ischemia/reperfusion injury included tryptophan metabolism, arachidonic acid metabolism, cysteine and methyl metabolism, and pyrimidine metabolism, and the metabolic pathways downregulated were arginine and proline metabolism and starch and cross metabolism. Through exhaustive analysis of the differential metabolite pathways (including enrichment analysis and topology analysis), we found the key pathway with the highest correlation with the difference in metabolites (Table 5; Figures 5B,D).The difference in metabolites between the normal group rats and the study group rats was mainly related to the tryptophan metabolic pathway, according to the data.

## 4. Discussion

The development of stroke significantly alters the synthesis and molecular metabolism of body substances, and bidirectional communication between the brain and peripheral organs is important in patients after stroke (Iadecola and Anrather, 2011). Gut microbial colonization plays a significant role in the development of the host gut immune response (Gensollen et al., 2016). In contrast, differential metabolites in the pre- and poststroke rat gut reflect pathophysiological processes, such as energy deficit, inflammation, neurotoxicity, oxidative stress, neuroexcitation and injury, and are biochemical indicators that can be used to evaluate physiological and pathological processes (Zhang et al., 2021). Therefore, quantitative metabolomic analysis of pre- and poststroke metabolic changes in rats can increase the understanding of disease pathogenesis and improve the development of treatment protocols. We replicated the MCAO/R

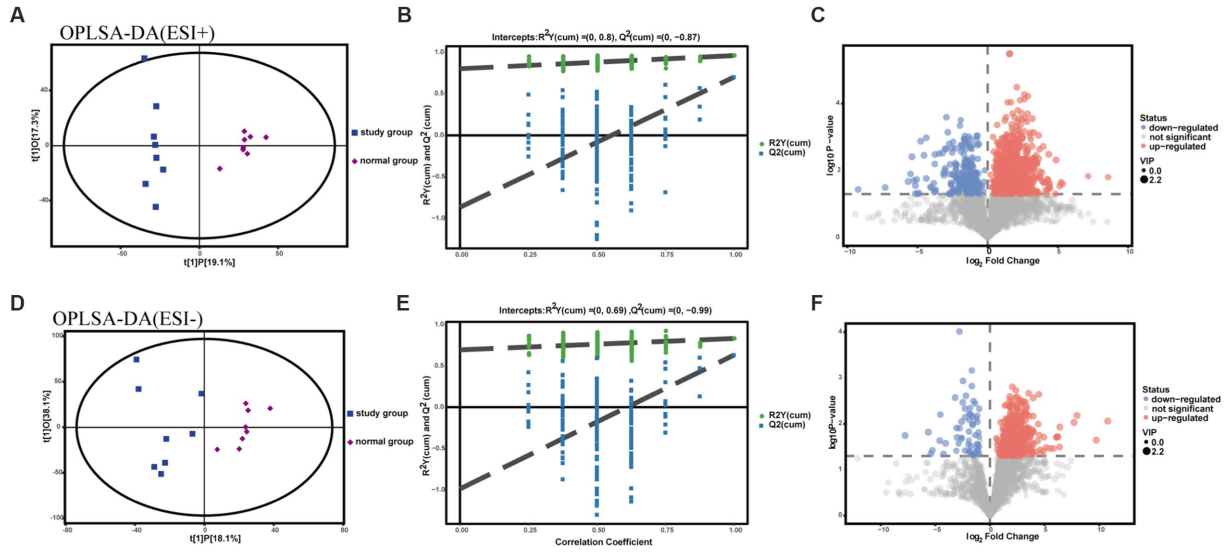


FIGURE 4
OPLS-DA plot, substitution test plot and volcano plot for metabolomic analysis of rat feces. **(A-C)** ESI+ model. **(D-F)** ESI- model.

TABLE 4 Identification of two groups of differential metabolites.

| ID | MS2 name | Mass(m/z) | R.T.(min) | VIP | *p* | Change trend |
|---|---|---|---|---|---|---|
| 308 | Niazicinin A | 370.14868975987 | 427.005 | 2.045006567 | 0.00324 | ↑ |
| 837 | N-Methyl-1-deoxynojirimycin | 178.107096619874 | 121.976 | 2.018372203 | 0.019344 | ↓ |
| 115 | Isogenistein 7-glucoside | 433.11163285909 | 116.655 | 2.022836 | 0.001486 | ↓ |
| *20* | Creatinine | 114.066252904115 | 179.566 | 2.020235 | 0.018372 | ↓ |
| *292* | 5′-Methylthioadenosine | 296.081080810132 | 382.4415 | 2.006154 | 0.004204 | ↑ |

model using the Longa method and found that the MCAO/R rats not only had significant neurological deficits but also a significant increase in infarct volume in the brain after 1 and 14 days of modeling using neurological deficit scores and T2WI structural images. This provides further evidence of the stability of the MCAO\R model used in this study. Afterwards, we used UPLC–MS/MS metabolomics to perform a comprehensive study of metabolites in the feces of rats in an ischemic stroke model to provide an overall picture of metabolite changes. According to the PCA plots, 1,044 and 635 differential metabolites connected to stroke were identified in rat feces in positive and negative ion mode, respectively, separating the study group from the normal group in terms of potential biomarkers. Then, KEGG pathway analysis was performed using MetaboAnalyst, which revealed the presence of poststroke metabolites in rats. Stroke in rats causes abnormalities in the metabolism of a variety of substances, including tryptophan, arachidonic acid, cysteine and methionine, pyrimidine, arginine and proline, starch, and sucrose, suggesting that ischemic brain injury leads to metabolic disorders in the above six metabolic pathways in rats. Specifically, tryptophan metabolism was the most affected.

As mentioned earlier, brain injury due to ischemic stroke is accompanied by neuropathological events, such as oxidative stress and neuroinflammation. In contrast, arachidonic acid is a precursor of proinflammatory mediators and has a crucial role in the development of inflammation. Arachidonic acid is metabolized by the lipoxygenase, cyclooxygenase and cytochrome P450 epoxygenase pathways to produce a variety of active metabolic small molecules, which have a role in regulating the intensity and duration of the inflammatory response and are key regulators of oxidative stress and inflammation (Medzhitov, 2008; Alhouayek and Muccioli, 2014; Zhang et al., 2020). Methionine is crucial for the brain during and after hypoxia and is also a powerful antioxidant, as the sulfhydryl groups contained in methionine scavenge free radicals and have some antioxidant capacity. Thus, methionine plays a crucial role in limiting the level of reactive oxygen radicals, both directly and indirectly (Flores et al., 2013). In addition, methionine and its related derivatives protect the brain from the damaging effects of hypoxia (Burgess et al., 2020). Methionine is involved not only in one-carbon unit metabolism and methylation reactions but also in the synthesis and repair of various DNA strands and in the expression of genes, the regulation and stabilization of protein function and the processing of ribonucleic acids (Goulart et al., 2019), thereby enhancing pyrimidine metabolism. Methionine metabolism produces cysteine, which synthesizes glutathione, a key antioxidant molecule involved in protein translation (Elango, 2020). Therefore, the upregulation of cysteine and methionine metabolic pathways

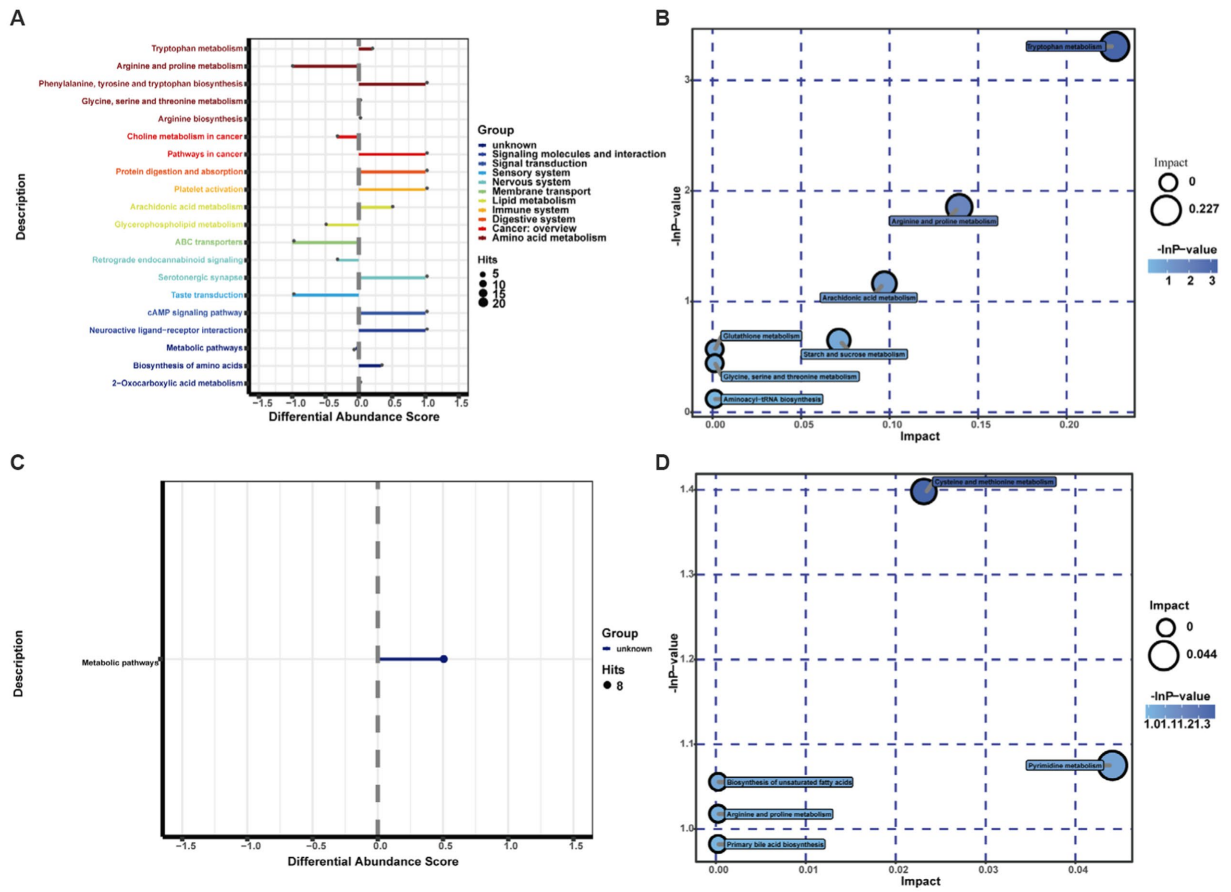


FIGURE 5
Differential pathway scores and metabolic pathway enrichment analysis bubble diagrams for the study group and normal group in positive and negative ion mode: the different colors of the pathways in **(A,C)** indicate the different metabolic classifications to which the pathways belong; the line segments indicate the up- and downregulation of the pathways; positive values of the line segments indicate the overall upregulation of the pathways; conversely, negative values of the line segments indicate the overall downregulation of the pathways; the size of the line endpoints indicates the amount of material annotated in the pathway. Each bubble in **(B,D)** represents a metabolic pathway. The horizontal coordinate of the bubble and the size of the bubble indicate the influence factor of the pathway in the topological analysis; the larger the size, the larger the influence factor. The vertical coordinate of the bubble and the color of the bubble indicate the *p* value [negative natural logarithm, i.e., -ln(p)] of the enrichment analysis. The darker the color, the smaller the *P* value, and the more significant the enrichment.

is the main complementary pathway providing raw material for glutathione synthesis in mammals, enhancing antioxidant action *in vivo*. In turn, arginine, similar to many antioxidants, enhances the body's antioxidant capacity and improves systemic immune function (Mm et al., 2014). Nitric oxide (NO) produced by arginine metabolism has an important role in cardiovascular regulation. NO regulates blood flow, relaxes blood vessels and inhibits platelet aggregation, which facilitates recovery from stroke-related dysfunction (Conti et al., 2013). Arginine is a precursor to proline and creatine, as well as the amino acid with the largest nitrogen-donating capacity (Ge et al., 2020). The metabolism of proline produces electrons and reactive oxygen species, which cause a number of downstream effects, such as blocking the cell cycle, autophagy and apoptosis (Selen et al., 2015). Finally, when the onset of acute cerebral ischemia is followed by the inhibition of oxidative phosphorylation during rapid oxygen dissipation in brain tissue, a dramatic reduction in brain tissue ATP levels within only a few seconds leads to energy metabolic failure and apoptotic necrosis of neurons, allowing for the downregulation of starch and sucrose metabolism, which subsequently affects the body's energy metabolism (Heiss, 2012). Furthermore, mitochondrial DNA encodes genes related to ATP synthesis, and downregulation of their expression results in a decrease in ATP production (Ji et al., 2018). Finally, tryptophan is an inhibitor of gluconeogenesis (Barik, 2020). The above multiple causes contribute to the downregulation of starch and sucrose metabolism.

In contrast, tryptophan and its metabolites are essential for the maintenance of neurological function, immunity and homeostasis *in vivo*, in addition to being the building blocks of protein synthesis. Tryptophan metabolites are implicated in the pathological processes of a variety of diseases, including immune responses, and exert different biological effects in the regulation of many diseases (Comai et al., 2019). Tryptophan metabolism is involved in the regulation of the GBA, and the gut flora can mediate the regulation of the kynurenine pathway by tryptophan

TABLE 5 Results of integrated enrichment analysis of biomarkers using MetaboAnalyst.

| | Pathway name | Total | Hits | Raw *p* | -ln(p) | Impact |
|---|---|---|---|---|---|---|
| 1 | Tryptophan metabolism | 41 | 4 | 0.036678 | 3.3056 | 0.22718 |
| 2 | Arginine and proline metabolism | 44 | 3 | 0.15695 | 1.8518 | 0.13934 |
| 3 | Arachidonic acid metabolism | 36 | 2 | 0.31307 | 1.1613 | 0.09707 |
| 4 | Starch and sucrose metabolism | 23 | 1 | 0.52256 | 0.64902 | 0.07135 |
| 5 | Cysteine and methionine metabolism | 28 | 1 | 0.24705 | 1.3981 | 0.02313 |
| 6 | Pyrimidine metabolism | 41 | 1 | 0.3413 | 1.075 | 0.04412 |

through direct and indirect mechanisms (Kennedy et al., 2017). Tryptophan metabolites, including 5-hydroxytryptophan, kynurenine, tryptamine and indole compounds, have profound effects on the interactions between the gut microbiota and the GBA (Clarke et al., 2012; Rothhammer et al., 2016).

Tryptophan metabolism can be broadly divided into three pathways: (1) the kynurenine pathway, (2) the 5-hydroxytryptamine pathway, and (3) Indole pathway for gut flora (Tomberlin et al., 2016; Wang et al., 2017). Over 95% of total tryptophan in the host is oxidized to kynurenine via the kynurenine pathway (Cervenka et al., 2017). It is believed that the kynurenine pathway plays a crucial role in the regulation of neurotransmission and immune function. In its pathway production, increased inflammation or oxidative stress can activate the activity of rate-limiting enzymes associated with induction (Jiang et al., 2018). Meanwhile, microbial regulation of the kynurenine pathway is similarly regulated by inflammatory mediators and is immunoreactive (Kennedy et al., 2017). The kynurenine pathway is present in many tissues (mainly the liver, brain and gut) (Fernstrom, 2016). In addition, intestinal flora can directly utilize tryptophan, with 4–6% of tryptophan being metabolized by intestinal flora (Wang et al., 2019). Poststroke inflammation induces upregulation of the kynurenine pathway of tryptophan oxidation, leading to neuroprotection (kynurenine acid) and neurotoxic metabolites (quinolinic acid). Wang et al. (2017) used a metabolomics approach to examine the serum metabolic profile between acute ischemic stroke patients and controls and observed reduced tryptophan levels, again demonstrating enhanced tryptophan metabolism. Brouns et al. (2010) found that poststroke inflammation induced upregulation of the kynurenine pathway of tryptophan oxidation by measuring plasma tryptophan and its metabolite concentrations at admission, 24 h, 72 h and day 7 in 149 stroke patients, and has a neuroprotective effect on the organism. Therefore,tryptophan metabolism via the kynurenine pathway is associated with immunity and inflammation and that blocking the associated pathway may prevent inflammatory responses after stroke. Most central nervous system (CNS) kynurenine is of peripheral origin, and once in the CNS, it can also be involved in subsequent metabolism (Gheorghe et al., 2019). The kynurenine pathway produces kynurenine, which is further metabolized by two different pathways: neuroprotective quinolinic acid and kynurenine (Cervenka et al., 2017). These metabolites from the kynurenine pathway, known as "kynurenines," not only act as mediators of inflammation but also cross the blood–brain barrier to reach the central nervous system. Kynurenines are therefore regarded as neuromodulators in numerous physiological and pathological processes of brain and gastrointestinal dysfunction (Kennedy et al., 2017). Not only that, studies have shown that the kynurenine pathway is more active in acute stroke patients. Darlington et al. (2007) demonstrated that acute stroke patients rapidly activate the kynurenine pathway. In contrast, blocking the kynurenine pathway was found to reduce infarct volume in animal models (Cozzi et al., 1999) 0.5-Hydroxytryptamine, also known as serotonin, and tryptophan, the only precursor of serotonin, are important for neurotransmission. Serotonin not only regulates the immune activity of the body but also serves as a critical neurotransmitter in the GBA (Agus et al., 2018) and is involved in a wide range of human physiological functions by activating specific serotonin receptors (Israelyan and Margolis, 2018). However, central serotonin accounts for only a small fraction of the body's total serotonin. Over 90% of serotonin is located in the gastrointestinal tract (Fouquet et al., 2019). Melatonin is mainly produced by the catabolism of serotonin and is a free radical scavenger that has strong antioxidant and anti-inflammatory effects (Gunata et al., 2019; Zhao et al., 2019). The article by Lian et al. (2023) found that inducing melatonin production by the gut microbiota could promote gut homeostasis, improve gut barrier function, and ultimately reduce brain and gut damage, thereby preventing ischaemic stroke.

Finally, tryptophan can be metabolized into a variety of metabolizable indole derivatives, which are mainly produced by gut microbes and are part of the kynurenine pathway. As these indole metabolites are ligands for aromatic hydrocarbon receptors, they are considered to be important components of the immune response (Alexeev et al., 2018). Not only that, but these metabolites play an important role in maintaining gut homeostasis and systemic immunity, and may also influence disease development and progression (Su et al., 2022; Ye et al., 2022). Importantly, studies have shown that related indole derivatives can significantly reduce cellular oxidative stress, inflammation and neuronal apoptosis (Yin et al., 2023). Wei et al. (2021) found that indole derivatives produced by gut microbes can enhance neurogenesis in mice by promoting the differentiation of neural progenitor cells into neurons via aryl hydrocarbon receptors. Indole treatment also increased neurite outgrowth and synaptogenesis in mice.

## 5. Conclusion

In this study, we demonstrated that metabolomics is an experimental approach to explore metabolic pathways in poststroke rats after stroke and that differences in fecal metabolites in rats 14 days after stroke are

most evident in the disruption of tryptophan metabolism. Therefore, future interventions to study the treatment of stroke could target the tryptophan pathway in the gut microbiome or promote the beneficial products of tryptophan metabolism as one of the targets of intervention.

## 6. Limitation

We need to study metabolic changes in the brain tissue of stroke rats in the future to further demonstrate the role of metabolism, such as tryptophan, in the development of stroke. Studies have shown known sex differences in tryptophan metabolism in healthy adults or rats, with females having higher tryptophan metabolism or tryptophan utilization than males (Leskanicova et al., 2020; Cai et al., 2021; Pais et al., 2023), which may limit the translation of our study. Finally, we will invest in further studies in the future to determine whether tryptophan metabolism in female rats versus patients in the clinical setting has the same results as noted in this study.

## Data availability statement

The original data presented in the study is included in the article/supplementary material, further inquiries can be directed to the corresponding authors.

## Ethics statement

The animal study was reviewed and approved by Ethics Committee of Fujian University of Fujian University of Traditional Chinese Medicine.

## Author contributions

AZ and ZL conceived and designed the research. DH and YZ conducted the experiments. YY and WS collected the data. CJ analyzed the data. XK and YY wrote the manuscript. All authors contributed to the article and approved the submitted version.

## Funding

This work was supported by the Research Start-Up Special Foundation of Shanghai Fourth People's Hospital Affiliated to Tongji University (Grant No. sykyqd02001) and Discipline Booster Program of Shanghai Fourth People's Hospital Affiliated to Tongji University (Grant No. sy-xkzt-2022-1004).

## Conflict of interest

The authors declare that the research was conducted in the absence of any commercial or financial relationships that could be construed as a potential conflict of interest.

The reviewer ZJ declared a shared affiliation with the author(s) XK to the handling editor at the time of review.

## Publisher's note



## Supplementary material

The Supplementary material for this article can be found online at: https://www.frontiersin.org/articles/10.3389/fnins.2023.1084813/full#supplementary-material

## References

Agus, A., Planchais, J., and Sokol, H. (2018). Gut microbiota regulation of tryptophan metabolism in health and disease. *Cell Host Microbe* 23, 716–724. doi: 10.1016/j.chom.2018.05.003

Alexeev, E. E., Lanis, J. M., Kao, D. J., Campbell, E. L., Kelly, C. J., Battista, K. D., et al. (2018). Microbiota-derived indole metabolites promote human and murine intestinal homeostasis through regulation of Interleukin-10 receptor. *Am. J. Pathol.* 188, 1183–1194. doi: 10.1016/j.ajpath.2018.01.011

Alhouayek, M., and Muccioli, G. G. (2014). COX-2-derived endocannabinoid metabolites as novel inflammatory mediators. *Trends Pharmacol. Sci.* 35, 284–292. doi: 10.1016/j.tips.2014.03.001

Bai, P. B., Yan, Z., Hao, Y., Zhang, P. Z., Li, P. G., Dekker, P. J., et al. (2017). A randomised controlled multimodal intervention trial in patients with ischaemic stroke in Shandong China. *Lancet* 390:S13. doi: 10.1016/S0140-6736(17)33151-3

Barik, S. (2020). The uniqueness of tryptophan in biology: properties, metabolism, interactions, and localization in proteins. *Int. J. Mol. Sci.* 21:8776. doi: 10.3390/ijms21228776

Barri, T., and Dragsted, L. O. (2013). UPLC-ESI-QTOF / MS and multivariate data analysis for blood plasma and serum metabolomics: effect of experimental artefacts and anticoagulant. *Anal. Chim. Acta* 768, 118–128. doi: 10.1016/j.aca.2013.01.015

Benakis, C., Brea, D., Caballero, S., Faraco, G., Moore, J., Murphy, M., et al. (2016). Commensal microbiota affects ischemic stroke outcome by regulating intestinal γδ T cells. *Nat. Med.* 22, 516–523. doi: 10.1038/nm.4068

Brouns, R., Verkerk, R., Aerts, T., Surgeloose, D.De, Wauters, A., Scharpé, S., et al. (2010). The role of tryptophan catabolism along the kynurenine pathway in acute ischemic stroke. *Neurochem. Res.* 35, 1315–1322. doi: 10.1007/s11064-010-0187-2

Bujak, R., Daghir-wojtkowiak, E., Kaliszan, R., and Markuszewski, M. J. (2016). PLS-based and regularization-based methods for the selection of relevant variables in non-targeted metabolomics data. *Front. Mol. Biosci.* 3:35. doi: 10.3389/fmolb.2016.00035

Burgess, K., Bennett, C., Mosnier, H., Kwatra, N., Bethel, F., and Jadavji, N. M. (2020). The antioxidant role of one-carbon metabolism on stroke. *Antioxidants (Basel)* 9:1141. doi: 10.3390/antiox9111141

Cai, Y., Kim, D. J., Takahashi, T., Broadhurst, D. I., Yan, H., Ma, S., et al. (2021). Kynurenic acid may underlie sex-specific immune responses to COVID-19. *Sci. Signal.* 14:eabf8483. doi: 10.1126/scisignal.abf8483

Cervenka, I., Agudelo, L., and Ruas, J. (2017). Kynurenines: Tryptophan's metabolites in exercise, inflammation, and mental health. *Science* 80:eaaf9794. doi: 10.1126/science.aaf9794

Cheema, M. U., and Pluznick, J. L. (2019). Gut microbiota plays a central role to modulate the plasma and Fecal metabolomes in response to angiotensin II. *Hypertension* 74, 184–193. doi: 10.1161/HYPERTENSIONAHA.119.13155

Chen, R., Xu, Y., Wu, P., Zhou, H., Lasanajak, Y., Fang, Y., et al. (2019). Transplantation of fecal microbiota rich in short chain fatty acids and butyric acid treat cerebral ischemic stroke by regulating gut microbiota. *Pharmacol. Res.* 148:104403. doi: 10.1016/j.phrs.2019.104403

Clarke, G., Grenham, S., Scully, P., Fitzgerald, P., Moloney, R. D., Shanahan, F., et al. (2012). The microbiome-gut-brain axis during early life regulates the hippocampal serotonergic system in a sex-dependent manner. *Mol. Psychiatry* 18, 666–673. doi: 10.1038/mp.2012.77

Comai, S., Bertazzo, A., Brughera, M., and Crotti, S. (2019). Tryptophan in health and disease. *Adv. Clin. Chem.* 95, 165–218. doi: 10.1016/bs.acc.2019.08.005

Conti, V., Russomanno, G., Corbi, G., Izzo, V., Vecchione, C., and Filippelli, A. (2013). Adrenoreceptors and nitric oxide in the cardiovascular system. *Front. Physiol.* 4:321. doi: 10.3389/fphys.2013.00321

Cozzi, A., Carpenedo, R., and Moroni, F. (1999). Kynurenine hydroxylase inhibitors reduce ischemic brain damage: studies with (m-Nitrobenzoyl) -alanine (mNBA) and (Ro 61-8048) in models of focal or global brain ischemia. *J. Cereb. Blood Flow Metab.* 19, 771–777. doi: 10.1097/00004647-199907000-00007

Darlington, L. G., Mackay, G. M., Forrest, C. M., Stoy, N., George, C., and Stone, T. W. (2007). Altered kynurenine metabolism correlates with infarct volume in stroke. *Eur. J. Neurosci.* 26, 2211–2221. doi: 10.1111/j.1460-9568.2007.05838.x

De Vadder, F., Kovatcheva-datchary, P., Goncalves, D., Vinera, J., Zitoun, C., and Mithieux, G. (2014). Microbiota-generated metabolites promote metabolic benefits via gut-brain neural circuits. *Cells* 156, 84–96. doi: 10.1016/j.cell.2013.12.016

Dunn, W., Wilson, I., Nicholls, A., and Broadhurst, D. (2012). The importance of experimental design and QC samples in large-scale and MS-driven untargeted metabolomic studies of humans. *Bioanalysis* 4, 2249–2264. doi: 10.4155/bio.12.204

Elango, R. (2020). Methionine nutrition and metabolism: insights from animal studies to inform human nutrition. *J. Nutr.* 150(Suppl, 2518S–2523S. doi: 10.1093/jn/nxaa155

Erben, V., Poschet, G., Schrotz-King, P., and Brenner, H. (2021). Evaluation of different stool extraction methods for metabolomics measurements in human fecal samples. *BMJ Nutr Prev Heal.* 4, 374–384. doi: 10.1136/bmjnph-2020-000202

Fernstrom, J. D. (2016). A perspective on the safety of supplemental tryptophan based on its metabolic fates. *J. Nutr.* 146, 2601S–2608S. doi: 10.3945/jn.115.228643

Flores, P., Zanusso, M., Tatiane, C., Nata, S., and Alethe, J. S. (2013). Methionine and methionine sulfoxide alter parameters of oxidative stress in the liver of young rats: in vitro and in vivo studies. *Mol. Cell. Biochem.* 384, 21–28. doi: 10.1007/s11010-013-1777-5

Fouquet, A. G., Coman, T., and Francine, C. (2019). Serotonin, hematopoiesis and stem cells. *Pharmacol. Res.* 140, 67–74. doi: 10.1016/j.phrs.2018.08.005

Fröhlich, E. E., Farzi, A., Mayerhofer, R., Reichmann, F., Wagner, B., Zinser, E., et al. (2016). Cognitive impairment by antibiotic-induced gut Dysbiosis: analysis of gut microbiota-brain communication. *Brain Behav. Immun.* 56, 140–155. doi: 10.1016/j.bbi.2016.02.020

Ge, S., Zhang, Q., Tian, Y., Hao, L., Duan, J., and Zhang, B. (2020). Cell metabolic profiling of colorectal cancer via 1H NMR. *Clin. Chim. Acta* 510, 291–297. doi: 10.1016/j.cca.2020.07.039

Gensollen, T., Iyer, S. S., Kasper, D. L., and Blumberg, R. S. (2016). How colonization by microbiota in early life shapes the immune system. *Science* 352, 539–545. doi: 10.1126/science.aad9378

Gheorghe, C. E., Martin, J. A., Manriquez, F. V., Dinan, T. G., Cryan, J. F., and Clarke, G. (2019). Focus on the essentials: tryptophan metabolism and the microbiome-gut-brain axis. *Curr. Opin. Pharmacol.* 48, 137–145. doi: 10.1016/j.coph.2019.08.004

Goulart, V. A. M., Sena, M. M., Mendes, T. O., Menezes, H. C., Cardeal, Z. L., Paiva, M. J. N., et al. (2019). Amino acid biosignature in plasma among ischemic stroke subtypes. *Biomed. Res. Int.* 2019:8480468. doi: 10.1155/2019/8480468

Gunata, M., Parlakpinar, H., and Acet, H. A. (2019). Melatonin: a review of its potential functions and effects on neurological diseases. *Rev. Neurol.* 176, 148–165. doi: 10.1016/j.neurol.2019.07.025

Heiss, W. (2012). The ischemic penumbra: how does tissue injury evolve? *Ann. N. Y. Acad. Sci.* 1268, 26–34. doi: 10.1111/j.1749-6632.2012.06668.x

Huang, Q., Di, L., Yu, F., Feng, X., Liu, Z., Wei, M., et al. (2022). Alterations in the gut microbiome with hemorrhagic transformation in experimental stroke. *CNS Neurosci. Ther.* 28, 77–91. doi: 10.1111/cns.13736

Iadecola, C., and Anrather, J. (2011). Stroke research at a crossroad: asking the brain for directions. *Nat. Neurosci.* 14, 1363–1368. doi: 10.1038/nn.2953

Israelyan, N., and Margolis, K. G. (2018). Serotonin as a link between the gut-brain-microbiome Axis in autism Spectrum disorders. *Pharmacol. Res.* 132, 1–6. doi: 10.1016/j.phrs.2018.03.020

Ji, F., Zhao, C., Wang, B., Tang, Y., Miao, Z., and Wang, Y. (2018). The role of 5-hydroxymethylcytosine in mitochondria after ischemic stroke. *J. Neurosci. Res.* 96, 1717–1726. doi: 10.1002/jnr.24274

Jiang, W., Gong, L., Liu, F., Ren, Y., and Mu, J. (2021). Alteration of gut microbiome and correlated lipid metabolism in post-stroke depression. *Front. Cell. Infect. Microbiol.* 11:663967. doi: 10.3389/fcimb.2021.663967

Jiang, X., Xu, L., Tang, L., Liu, F., Chen, Z., Zhang, J., et al. (2018). Role of the indoleamine-2, 3-dioxygenase / kynurenine pathway of tryptophan metabolism in behavioral alterations in a hepatic encephalopathy rat model. *J. Neuroinflammation* 15:3. doi: 10.1186/s12974-017-1037-9

Johnson, C. H., Ivanisevic, J., and Siuzdak, G. (2016). Metabolomics: beyond biomarkers and towards mechanisms. *Nat. Rev. Mol. Cell Biol.* 17, 451–459. doi: 10.1038/nrm.2016.25

Jones-bolin, S. (2012). Guidelines for the care and use of laboratory animals in biomedical. *Curr Protoc Pharmacol* 1:pha04bs59. doi: 10.1002/0471141755.pha04bs59

Jové, M., Mauri-Capdevila, G., Suárez, I., Cambray, S., Sanahuja, J., Quílez, A., et al. (2014). Metabolomics predicts stroke recurrence after transient ischemic attack. *Neurology* 84, 36–45. doi: 10.1212/WNL.0000000000001093

Kennedy, P. J., Cryan, J. F., Dinan, T. G., and Clarke, G. (2017). Neuropharmacology kynurenine pathway metabolism and the microbiota-gut-brain axis. *Neuropharmacology* 112, 399–412. doi: 10.1016/j.neuropharm.2016.07.002

Kimberly, W. T., Wang, Y., Pham, L., Furie, K. L., and Gerszten, R. E. (2013). Metabolite profiling identifies a branched chain amino acid signature in acute Cardioembolic stroke. *Stroke* 44, 1389–1395. doi: 10.1161/STROKEAHA.111.000397

Kunz, A., Dirnagl, U., and Mergenthaler, P. (2010). Acute pathophysiological processes after ischaemic and traumatic brain injury. *Best Pr. Res Clin Anaesthesiol* 24, 495–509. doi: 10.1016/j.bpa.2010.10.001

Lee, J., D'Aigle, J., Atadja, L., Quaicoe, V., Honarpisheh, P., Ganesh, B. P., et al. (2020). Gut microbiota-derived short-chain fatty acids promote Poststroke recovery in aged mice. *Circ. Res.* 127, 453–465. doi: 10.1161/CIRCRESAHA.119.316448

Leskanicova, A., Chovancova, O., Babincak, M., Verboova, L., Benetinova, Z., Macekova, D., et al. (2020). Sexual dimorphism in energy metabolism of Wistar rats using data analysis. *Molecules* 25:2353. doi: 10.3390/molecules25102353

Lian, Z., Xu, Y., Wang, C., Chen, Y., Yuan, L., Liu, Z., et al. (2023). Gut microbiota-derived melatonin from Puerariae Lobatae radix-resistant starch supplementation attenuates ischemic stroke injury via a positive microbial co-occurrence pattern. *Pharmacol. Res.* 190:106714. doi: 10.1016/j.phrs.2023.106714

Liu, P., Li, R., Antonov, A. A., Wang, L., Li, W., Hua, Y., et al. (2017). Discovery of metabolite biomarkers for acute ischemic stroke progression. *J. Proteome Res.* 16, 773–779. doi: 10.1021/acs.jproteome.6b00779

Longa, E. Z., Weinstein, P. R., Carlson, S., and C. R., (1989). Reversible middle cerebral artery occlusion without craniectomy in rats. *Stroke* 20, 84–91. doi: 10.1161/01.STR.20.1.84

Lupo, G. F. D., Rocchetti, G., Lucini, L., Lorusso, L., Manara, E., Bertelli, M., et al. (2021). Potential role of microbiome in chronic fatigue syndrome/Myalgic Encephalomyelits (CFS/ME). *Sci. Rep.* 11:7043. doi: 10.1038/s41598-021-86425-6

Ma, N., Liu, X., Kong, X., Qin, Z., Li, S., Jiao, Z., et al. (2017). UPLC-Q-TOF/MS-based urine and plasma metabonomics study on the ameliorative effects of aspirin eugenol ester in hyperlipidemia rats. *Toxicol. Appl. Pharmacol.* 332, 40–51. doi: 10.1016/j.taap.2017.07.013

Ma, Y., Zhang, P., Wang, F., Liu, W., and Yang, J. (2012). An integrated proteomics and metabolomics approach for defining Oncofetal biomarkers in the colorectal cancer. *Ann. Surg.* 255, 720–730. doi: 10.1097/SLA.0b013e31824a9a8b

Medzhitov, R. (2008). Origin and physiological roles of inflammation. *Nature* 454, 428–435. doi: 10.1038/nature07201

Mm, K. K., Shu, X., Mm, J. Z., and Mm, T. Y. (2014). Effect of L-arginine on immune function: a meta-analysis. *Asia Pac. J. Clin. Nutr.* 23, 351–359. doi: 10.6133/apjcn.2014.23.3.09

Montaner, J., Makris, K., Jickling, G. C., Debette, S., and Sanchez, J. (2020). Multilevel omics for the discovery of biomarkers and therapeutic targets for stroke. *Nat. Rev. Neurol.* 16, 247–264. doi: 10.1038/s41582-020-0350-6

Mu, C., Yang, Y., and Zhu, W. (2016). Gut microbiota: the brain peacekeeper. *Front. Microbiol.* 17:345. doi: 10.3389/fmicb.2016.00345

Pais, M. L., Martins, J., Castelo-Branco, M., and Gonçalves, J. (2023). Sex differences in tryptophan metabolism: a systematic review focused on neuropsychiatric disorders. *Int. J. Mol. Sci.* 24:6010. doi: 10.3390/ijms24066010

Radenovic, L., Nenadic, M., Kozioł, M. U., Januszewski, S., Czuczwar, J., Andjus, P. R., et al. (2020). Heterogeneity in brain distribution of activated microglia and astrocytes in a rat ischemic model of Alzheimer's disease after 2 years of survival. *Aging (Albany NY)* 12, 12251–12267. doi: 10.18632/aging.103411

Roth, W., Zadeh, K., Vekariya, R., Ge, Y., and Mohamadzadeh, M. (2021). Tryptophan metabolism and gut-brain homeostasis. *Int. J. Mol. Sci.* 22:2973. doi: 10.3390/ijms22062973

Rothhammer, V., Mascanfroni, I. D., Bunse, L., Takenaka, M. C., Kenison, J. E., Mayo, L., et al. (2016). Type I interferons and microbial metabolites of tryptophan modulate astrocyte activity and central nervous system inflammation via the aryl hydrocarbon receptor. *Nat. Med.* 22, 586–597. doi: 10.1038/nm.4106

Saccenti, E., and Hoefsloot, H. C. J. (2014). Reflections on univariate and multivariate analysis of metabolomics data. *Metabolomics* 10, 361–374. doi: 10.1007/s11306-013-0598-6

Selen, E. S., Bolandnazar, Z., Tonelli, M., Daniel, E., Haviland, J. A., Porter, W. P., et al. (2015). NMR metabolomics show evidence for mitochondrial oxidative stress in a

mouse model of polycystic ovary syndrome. *J. Proteome Res.* 14, 3284–3291. doi: 10.1021/acs.jproteome.5b00307

Shen, J., Guo, H., Liu, S., Jin, W., Zhang, Z. W., Zhang, Y., et al. (2023). Aberrant branched-chain amino acid accumulation along the microbiota–gut–brain axis: crucial targets affecting the occurrence and treatment of ischaemic stroke. *Br. J. Pharmacol.* 180, 347–368. doi: 10.1111/bph.15965

Sidorov, E., Sanghera, D. K., and Vanamala, K. P. (2019). Biomarker for ischemic stroke using metabolome: a clinician perspective. *J Stroke* 21, 31–41. doi: 10.5853/jos.2018.03454

Singh, V., Roth, S., Llovera, G., Sadler, R., Garzetti, D., Stecher, B., et al. (2016). Microbiota Dysbiosis controls the Neuroinflammatory response after stroke. *J. Neurosci.* 36, 7428–7440. doi: 10.1523/JNEUROSCI.1114-16.2016

Smith, L., Villaret-cazadamont, J., Claus, S. P., Canlet, C., Guillou, H., Cabaton, N. J., et al. (2020). Important considerations for sample collection in metabolomics studies with a special focus on applications to liver functions. *Meta* 10:104. doi: 10.3390/metabo10030104

Su, X., Gao, Y., and Yang, R. (2022). Gut microbiota-derived tryptophan metabolites maintain gut and systemic homeostasis. *Cells* 11:2296. doi: 10.3390/cells11152296

Su, L., Zhao, H., Zhang, X., Lou, Z., and Dong, X. (2016). UHPLC-Q-TOF-MS based serum metabonomics revealed the metabolic perturbations of ischemic stroke and the protective effect of RKIP in rat models. *Mol. BioSyst.* 12, 1831–1841. doi: 10.1039/C6MB00137H

Tomberlin, J., Crippen, T., Wu, G., and AS, G., TK, W., and RM, K., (2016). Indole: an evolutionarily conserved influencer of behavior across kingdoms. *BioEssays* 39:203. doi: 10.1002/bies.201600203

Wang, G., Huang, S., Wang, Y., Cai, S., Yu, H., Liu, H., et al. (2019). Bridging intestinal immunity and gut microbiota by metabolites. *Cell. Mol. Life Sci.* 76, 3917–3937. doi: 10.1007/s00018-019-03190-6

Wang, D., Kong, J., Wu, J., Wang, X., and Lai, M. (2017). GC-MS-based metabolomics identifies an amino acid signature of acute ischemic stroke. *Neurosci. Lett.* 642, 7–13. doi: 10.1016/j.neulet.2017.01.039

Wei, G. Z., Martin, K. A., Xing, P. Y., Agrawal, R., Whiley, L., Wood, T. K., et al. (2021). Tryptophan-metabolizing gut microbes regulate adult neurogenesis via the aryl hydrocarbon receptor. *Proc. Natl. Acad. Sci. U. S. A.* 118:e2021091118. doi: 10.1073/pnas.2021091118

Wiklund, S., Johansson, E., Sjo, L., Shockcor, J. P., Gottfries, J., Moritz, T., et al. (2008). Visualization of GC / TOF-MS-based metabolomics data for identification of biochemically interesting compounds using OPLS class models. *Anal. Chem.* 80, 115–122. doi: 10.1021/ac0713510

Winek, K., Dirnagl, U., and Meisel, A. (2016). The gut microbiome as therapeutic target in central nervous system diseases: implications for stroke. *Neurotherapeutics* 13, 762–774. doi: 10.1007/s13311-016-0475-x

Winstein, C. J., Stein, J., Arena, R., Bates, B., Cherney, L. R., Cramer, S. C., et al. (2016). Guidelines for adult stroke rehabilitation and recovery: a guideline for healthcare professionals from the American Heart Association/American Stroke Association. *Stroke* 47, e98–e169. doi: 10.1161/STR.0000000000000098

Xu, J., Zhang, Q., Zheng, J., Yuan, B., and Feng, Y. (2019). Trends in analytical chemistry mass spectrometry-based fecal metabolome analysis. *Trends Anal. Chem.* 112, 161–174. doi: 10.1016/j.trac.2018.12.027

Ye, X., Li, H., Anjum, K., Zhong, X., Miao, S., Zheng, G., et al. (2022). Dual role of indoles derived from intestinal microbiota on human health. *Front. Immunol.* 13:903526. doi: 10.3389/fimmu.2022.903526

Yin, J., Xie, J., Guo, X., Ju, L., Li, Y., and Zhang, Y. (2016). Plasma metabolic profiling analysis of cyclophosphamide-induced cardiotoxicity using metabolomics coupled with UPLC / Q-TOF-MS and ROC curve. J Chromatogr B anal. *Technol Biomed Life Sci* 1033–1034, 428–435. doi: 10.1016/j.jchromb.2016.08.042

Yin, J., Zhang, Y., Liu, X., Li, W., Hu, Y., Zhang, B., et al. (2023). Gut microbiota-derived indole derivatives alleviate neurodegeneration in aging through activating GPR30/AMPK/SIRT1 pathway. *Mol. Nutr. Food Res.* 67:e2200739. doi: 10.1002/mnfr.202200739

Zhang, C., He, M., Ni, L., He, K., Su, K., Deng, Y., et al. (2020). The role of arachidonic acid metabolism in myocardial ischemia – reperfusion injury. *Cell Biochem. Biophys.* 78, 255–265. doi: 10.1007/s12013-020-00928-z

Zhang, J., Su, X., Qi, A., Liu, L., Zhang, L., Zhong, Y., et al. (2021). Metabolomic profiling of fatty acid biomarkers for intracerebral hemorrhage stroke. *Talanta* 222:121679. doi: 10.1016/j.talanta.2020.121679

Zhao, L., Wang, C., Peng, S., Zhu, X., Zhang, Z., Zhao, Y., et al. (2022). Pivotal interplays between fecal metabolome and gut microbiome reveal functional signatures in cerebral ischemic stroke. *J. Transl. Med.* 20:459. doi: 10.1186/s12967-022-03669-0

Zhao, D., Yu, Y., Shen, Y., Liu, Q., Zhao, Z., and Sharma, R. (2019). Melatonin synthesis and function: evolutionary history in animals and plants. *Front. Endocrinol.* 10:249. doi: 10.3389/fendo.2019.00249

Zhu, W., Romano, K. A., Li, L., Hajjar, A. M., Didonato, J. A., Hazen, S. L., et al. (2021). Gut microbes impact stroke severity via the trimethylamine N-oxide pathway. *Cell Host Microbe* 29, 1199–1208. doi: 10.1016/j.chom.2021.05.002

Zierer, J., Jackson, M. A., Kastenmüller, G., Mangino, M., Telenti, A., Mohney, R. P., et al. (2018). The fecal metabolome as a functional readout of the gut microbiome. *Nat. Genet.* 50, 790–795. doi: 10.1038/s41588-018-0135-7

frontiers | Frontiers in Neuroscience

TYPE Original Research
PUBLISHED 19 September 2023
DOI 10.3389/fnins.2023.1144480



OPEN ACCESS

EDITED BY
Lin Yao,
Zhejiang University, China

REVIEWED BY
Francesco Asci,
Mediterranean Neurological Institute Neuromed (IRCCS), Italy
Francesco Di Lorenzo,
Santa Lucia Foundation (IRCCS), Italy

*CORRESPONDENCE
Jiyi Huang
✉ hjy0602@163.com
Jie Zhang
✉ jiezhang@xmu.edu.cn

†These authors have contributed equally to this work

RECEIVED 14 January 2023
ACCEPTED 07 July 2023
PUBLISHED 19 September 2023

CITATION
Chen S, He X, Wei X, Huang J and Zhang J (2023) After-effects of repetitive transcranial magnetic stimulation with parameter dependence on long-term potentiation-like plasticity and object recognition memory in rats. *Front. Neurosci.* 17:1144480. doi: 10.3389/fnins.2023.1144480



# After-effects of repetitive transcranial magnetic stimulation with parameter dependence on long-term potentiation-like plasticity and object recognition memory in rats

Shanjia Chen[1,2†], Xiaokuo He[3,4,5†], XinChen Wei[5], Jiyi Huang[1,3*] and Jie Zhang[2*]

[1]The First Affiliated Hospital of Xiamen University, Xiamen, China, [2]Laboratory Neuropathology, Institute Medicine College, Xiamen University, Xiamen, China, [3]Fifth Hospital of Xiamen, Xiamen, China, [4]Xiangyang Central Hospital, Affiliated Hospital of Hubei University of Arts and Science, Xiangyang, Hubei, China, [5]The Graduate School of Fujian Medical University, Fuzhou, Fujian, China

**Objective:** To investigate the after-effects of 25-Hz repetitive transcranial magnetic stimulation (rTMS) at 60, 100, and 120% resting motor threshold (rMT) on long-term potentiation (LTP) in the rat hippocampus, to clarify the intensity dependence of rTMS, and to determine whether it simultaneously affects learning and memory ability.

**Methods:** Five rats were randomly selected from 70 male Wistar rats, and evoked rMT potentials were recorded in response to magnetic stimulation. The remaining 65 rats were randomly assigned to five groups ($n = 13$), including sham rTMS, 1 Hz 100% rMT, and 25 Hz rTMS groups with 3 subgroups of 60% rMT, 100% rMT, and 120% rMT. Five rats in each group were anesthetized and induced by a priming TMS-test design for population spike (PS) response of the perforant path-dentate gyrus in the hippocampus; the remaining eight rats in each group were evaluated for object recognition memory in the novel object recognition (NOR) task after the different rTMS protocols.

**Results:** Forty-five percent (approximately 1.03 T) of the magnetic stimulator output was confirmed as rMT in the biceps femoris muscle. The PS ratio was ranked as follows: 25 Hz 100% rMT (267.78 ± 25.71%) > sham rTMS (182 ± 9.4%) >1 Hz 100% rMT (102.69 ± 6.64%) > 25 Hz 120% rMT (98 ± 11.3%) > 25 Hz 60% rMT (36 ± 8.5%). Significant differences were observed between the groups, except for the difference between the 25 Hz 120% rMT and the 1 Hz 100% rMT groups ($p = 0.446$). LTP was successfully induced over the 60-min recording period only in the sham rTMS and 25 Hz 100% rMT groups. Moreover, these two groups spent more time exploring a novel object than a familiar object during the NOR task ($p < 0.001$), suggesting long-term recognition memory retention. In the between-group analysis of the discrimination index, the following ranking was observed: 25 Hz 100% rMT (0.812 ± 0.158) > sham rTMS (0.653 ± 0.111) > 25 Hz 120% rMT (0.583 ± 0.216) >1 Hz 100% rMT (0.581 ± 0.145) > 25 Hz 60% rMT (0.532 ± 0.220).

**Conclusion:** The after-effect of 25-Hz rTMS was dependent on stimulus intensity and provided an inverted (V-shaped) bidirectional modulation on hippocampal plasticity that involved two forms of metaplasticity. Furthermore, the effects on

the recognition memory ability were positively correlated with those on LTP induction in the hippocampus *in vivo*.

KEYWORDS

**repetitive transcranial magnetic stimulation, intensity dependence, long-term potentiation, rat hippocampus, learning and memory, novel object recognition**

# 1. Introduction

Transcranial magnetic stimulation (TMS), a non-invasive transcranial brain stimulation technique, has emerged as a promising treatment for affective disorders in humans, such as depression and hypomnesia (Muellbacher et al., 2000; Wang et al., 2018). High frequencies (>5 Hz) that facilitate cortical excitability and low frequencies (≤1 Hz) that inhibit it have been applied in clinical treatment (Maeda et al., 2000; Muellbacher et al., 2000). TMS applied at 5 Hz modulated hippocampal excitation with greater encoding-retrieval similarity effects on memory representations compared with 1 Hz TMS (Wang et al., 2018). A meta-analysis demonstrated that repetitive TMS (rTMS), especially at high frequency and stimulation intensity between 80 and 120% of resting motor threshold (rMT), can improve memory function by varying degrees in patients with mild cognitive impairment when it is applied over the dorsolateral prefrontal cortex, which has strong neural connections with the hippocampus (Zhang et al., 2021). However, another meta-analysis indicated the overall effect of rTMS was negligible and statistically nonsignificant on cognitive improvement including attention and working memory (He et al., 2022). It has been reported that the effect of rTMS varies considerably in terms of stimulation intensity. Previous studies that applied rTMS consisting of up to 20 stimuli at 5, 10, or 20 Hz found frequency-dependent inhibition of motor cortical excitability at an intensity equal to the rMT, whereas cortical inhibition gradually changed to excitation at the rMT superthreshold (Modugno et al., 2001), indicating that intensity and frequency parameters were crucial to determining the after-effect of the stimulus on synaptic efficacy. Moreover, the stimulus intensity in short trains reportedly had a greater after-effect on cortical excitability than the frequency (Gilio et al., 2007). However, few studies have examined how the after-effects of rTMS on the induction of neuronal plasticity and memory are influenced by the intensity of stimulation. Understanding the mechanism that underlies this effect is crucial for clinical efficacy, and many of the details are still unknown.

Long-term potentiation (LTP) is the long-lasting increase in synaptic efficacy resulting from high-frequency stimulation of afferent fibers (Nugent et al., 2008). LTP in the hippocampus is considered a reliable model of synaptic plasticity related to the learning and memory (Cohen et al., 1999; Cooke and Bliss, 2006). The rTMS protocol was adopted to assist in rehabilitation training for the cognitive improvement (Chou et al., 2020). Neurons stabilize their synaptic transmission and adapt their intrinsic excitability in response to their prior history of synaptic or cellular activity; this process is known as the homeostatic plasticity (Delvendahl and Muller, 2019). High frequency rTMS intervention has been proved to have advantages of some efficacy and high safety for the treatment of psychobehavioral abnormalities and cognitive decline in Alzheimer's Disease patients (Koch et al., 2018; Jiang et al., 2022). How the after-effects of the rTMS protocol for inducing hippocampal excitability are influenced by the intensity of the stimulation is not fully understood.

To clarify this issue, the present study employed a priming-test design (Karabanov et al., 2015; Muller-Dahlhaus and Ziemann, 2015), which involved a "priming" rTMS protocol that triggers a homeostatic response, followed by a "test" intermittent theta-burst stimulation (iTBS) protocol that captures the homeostatic response. iTBS is particularly effective for promoting hippocampal LTP function because this stimulation rhythm should resonate with the endogenous theta-nested-gamma activity prominent in the hippocampus (Hermiller et al., 2020). Moreover, to verify whether the hippocampal LTP induced by rTMS at different intensities (60, 100, 120% rMT) simultaneously influenced learning and memory ability, a novel object recognition (NOR) test was performed (Kang et al., 2021). We hypothesized that a priming rTMS below the rMT threshold may inhibit the response to subsequent LTP-inducing iTBS, whereas a priming rTMS above the rMT threshold may increase this response instead. In addition, we tested the hypothesis that hippocampal LTP induction was associated with an effect on learning and memory ability. This study was conducted to provide some preliminary guidance for the selection of appropriate rTMS intensity for the enhancement of hippocampal LTP and to contribute some evidence supporting the use of rTMS as a treatment of memory loss in a clinical setting.

# 2. Materials and methods

## 2.1. Ethical approval

This study was approved by the Institutional Animal Care and Use Committee of the Faculty of Medicine, Xiamen University, China (approval no. SYXK(min)-2018–0009).

## 2.2. Animals and experimental protocols

Seventy male Wistar rats weighing approximately 230 ± 10 g (approximately 6 weeks old) were obtained from the National Animal Center, Guangzhou, ZhongShan University, China. The quality certificate number for the experimental animals was 44,008,500,008,720. All the animals were fed with suitable food provided by the animal feeding center, housed at a density of four individuals per cage in a temperature-controlled room (constant 23°C ± 1°C), and maintained at a light–dark cycle of 12:12 h (lights on at 6:00 AM).

One week after arrival, five rats were selected using the random number table method, and the evoked rMT potentials in the biceps femoris muscle were recorded by magnetic stimulation. The remaining 65 rats were randomly assigned to control (sham rTMS, $n = 13$), low-frequency rTMS stimulation (1 Hz 100% rMT, $n = 13$), and high-frequency rTMS stimulation ($n = 39$) groups; the high-frequency group was divided into three subgroups: low intensity (25 Hz 60% rMT, $n = 13$), medium intensity (25 Hz 100% rMT, $n = 13$), and high intensity (25 Hz 120% rMT, $n = 13$) groups. Five rats were anesthetized in each of the five groups, and TMS was used to measure the population spike (PS) response of the perforant path-dentate gyrus (PP-DG) in the hippocampus. The remaining eight rats in each group were subjected to the NOR task to evaluate memory performance. The tests and rTMS treatment was performed in the animal experimental center from 14:00 to 21:00. If one of the subjects died or failed to complete the experimental protocol, additional animals were incorporated into the corresponding experimental group.

## 2.3. Testing apparatus

The transcranial magnetic stimulator used in the experiment (Magstim, Rapid2, UK) is a conventional, air-cooled device, with an eight-shaped coil (inner diameter 40 mm, outer diameter 90 mm) and a maximum output strength of 2.3 T.

### 2.3.1. Electrophysiological testing equipment

Motor evoked potential (MEP) and PS were recorded using an electromyography machine (MedelecSynergy, Oxford Instruments, UK). A double-arm stereoscopic brain locator and flexible spindle craniotomy drill (Stoelting 51603, USA) were employed. Concentric bipolar electrodes were manufactured by A-M Systems (Carlsborg, WA, USA). An extracellular amplifier was applied to a single-channel recording with a filtering range of 0.1–10,000 Hz and a gain of 10 K (A-M Systems 1700, Sequim, WA, USA). The equipment comprised an analog-to-digital converter (Axon Digidata 1,440, Molecular Devices, USA), stimulation isolator (ISO-Flex, Israel), data logging and analysis software (Axon pClamp 10, Molecular Devices, USA), and urethane (ethyl carbamate, lot No. E21262, Jinyu Chemical Co., LTD., China).

### 2.3.2. Behavioral testing equipment

The NOR task was carried out in an open box (80 cm × 80 cm × 80 cm), which was composed of black non-reflective plastic plates with an overhead camera (SONY, HDR-CX405). Soda cans with similar shapes and different colors were used as identifiers A or B.

## 2.4. A priming-test design protocol

### 2.4.1. rMT measurement

Since determining the motor threshold in each individual rat is a stressful and invasive procedure, the five rats with the same age (approximately 6 weeks old) and weight (230 ± 10 g) were anesthetized intraperitoneally with 20% urethane (0.6 ml/100 g) and secured on a stereotaxic brain apparatus (Stoelting 51603, USA) to determine the rMT and exclude the possibility of any brain damage in the formal experiment. The height of the auricular and incisor rods was adjusted such that the anterior fontanelle and herringbone were in the same horizontal plane. EMG signals were recorded bilaterally using microelectrodes inserted in the biceps femoris muscle and connected to an electromyography system *via* a 6-pin male connector. A standard EMG pad was also connected to the tail to serve as the ground electrode. The "figure eight" coil was placed horizontally on the vertex of the rat's head, with the center aligned with the midpoint between the rat's ears. Using 60% TMS output intensity, the coil was gradually moved to determine the best "hotspot," which was based on a stable MEP waveform recorded in the contralateral biceps femoris muscle. Output intensity was adjusted until the MEP peak did not increase, and this value was defined as the maximum MEP. Stimulation output was gradually reduced to 43–51% (average 45.6% ± 5.73%), and an MEP with amplitude ≥50 μV could be obtained three out of five times on the contralateral side at the maximum output intensity. In our study, 45% (approximately 1.03 T) of the magnetic stimulator output was confirmed as rMT, which ensures a relatively appropriate and reliable rMT intervention in each group.

### 2.4.2. Priming rTMS protocol followed by a test iTBS

The present study employed a priming-test design consisting of a "priming" rTMS protocol and a subsequent "test" protocol to investigate the intensity-dependent after-effects of 25-Hz repetitive TMS (rTMS) on LTP in the rat hippocampus. Our previous experiments showed that the stimulation of 100% rMT at 25 Hz for 5 s, with a 30-s intertrain interval, can affect the hippocampal field potential and the amplitude of LTP induced by the subsequent iTBS stimulation. Moreover, Ogiue-Ikeda et al. (2003) investigated the intensity-dependent effect of 25 Hz rTMS on LTP in the rat hippocampus, and Cao et al. (2022) found that 25 Hz rTMS could improve cognitive function of Alzheimer's disease (AD) model mice. Hence, the stimulation frequency of 25 Hz was selected in the present study. The high-frequency rTMS groups received intensity stimulation at 25 Hz for 5 s, which consisted of five 1-s trains of 25 pulses with a 30-s intertrain interval. An intensity of 60–130% rMT was previously used for high-frequency rTMS (Ayache et al., 2012); thus, we defined three subgroups corresponding to three different levels: low intensity (60% rMT), medium intensity (100% rMT), and high intensity (120% rMT).

In general, low-frequency rTMS induces inhibition of synaptic efficiency. Therefore, the low-frequency rTMS group received continuous stimulation of 1 Hz at 100% intensity of rMT for 2 min (Gersner et al., 2011). It was beneficial to keep the amount of stimulus and time frame similar to that in the high-frequency stimulation groups. This method is beneficial for fixing the duration of stimuli while comparing different frequencies and intensities. The control group received sham TMS, which involved exposure to the same noise produced during the simulated stimulus but was treated with a sham coil without real stimulation.

Next, a "test" intermittent theta-burst stimulation (iTBS) protocol was employed to capture the homeostatic response, which consisted of six trains with 10-s intervals between each train containing six bursts at 5 Hz, and each burst containing three pulses at 400 Hz (Kouvaros and Papatheodoropoulos, 2016; Ostrovskaya et al., 2020). The "test" iTBS protocol was administered after the end of priming rTMS in each group.

## 2.5. Experimental schedule

### 2.5.1. Experiment 1: detection of the population spike and LTP in the hippocampal PP-DG *in vivo*

#### 2.5.1.1. Placement of recording electrode

Five rats in each group were anesthetized with 20% urethane and placed in a stereotaxic apparatus. After routine disinfection, the skin and subcutaneous tissue of the rat's head were cut open to expose the skull surface. The soft tissue on the skull surface was detached using hydrogen peroxide to completely expose the bregma and the herringbone seam. The brain stereo-position method was used as described by Bruel-Jungerman et al. (2006). A bipolar, 125-mm concentric stimulating electrode was placed in the PP (coordinates: 7.5 mm posterior to bregma, 4.2 mm lateral to the midline, depth of 3.5 mm). A glass micropipette recording electrode was lowered into the DG of the dorsal hippocampus (coordinates: 3.5 mm posterior to bregma, 2.0 mm lateral to the midline) until the maximal PS response was observed (depth: 3–4 mm) (Levkovitz et al., 1999).

#### 2.5.1.2. PS of PP-DG *in vivo*

The optimal recording position for the PP-DG stimulus used the paired-pulse parameters to identify whether PS response was derived from the PP-DG in the hippocampus (McNaughton and Barnes, 1977). The stimulation intensity was adjusted (0–0.7 mA, 0.05-mA interval) to 100 μs of the biphasic pulse at an interval of 30 s for 10 min to record the input–output curve. The standard stimulus intensity of the test stimuli was sufficient to evoke approximately 50% of the maximum response of the PS amplitude. The characteristic response of hippocampal dentate gyrus (DG) granule cells to perforant path stimulation consists of a positive-going EPSP with a superimposed negative-going field PS. The PS amplitude was measured by averaging the distance from the negative to the positive peak. The baseline PS amplitude ($PS_0$) represents the initial state of synaptic excitability (Niu et al., 2009), which was averaged from five successive PS responses with a 30-s interval between each stimulus pair for 20 min.

#### 2.5.1.3. After-effects of the rTMS protocol on the LTP plasticity

A priming-test design, a "priming" rTMS protocol and "test" iTBS protocol, was employed to clarify the after-effects of the rTMS protocol for inducing hippocampal excitability. The rat's head was fixed by hand, the center of the coil was aligned to the rat's herringbone seam, and the handle was directed outwards in the direction of the longitudinal axis. The PS amplitude after different rTMS ($PS_1$) and PS amplitude after iTBS ($PS_2$) were recorded continuously for 30 min and 60 min (Figure 1A), with up to ten PS recordings taken at 30-s intervals for 5 min. The maximum and minimum PS were removed, and the mean PS amplitude during 5 min was averaged from five successive PS responses.

LTP was used to detect the synaptic plasticity response in the hippocampus. It was induced after stable baseline recording using iTBS, which was at 80% intensity of rMT stimulation and consisted of six trains with 10-s intervals between each train, containing six bursts at 5 Hz, and each burst containing three pulses at 400 Hz (Kouvaros and Papatheodoropoulos, 2016; Ostrovskaya et al., 2020).

### 2.5.2. Experiment 2: the effects of the rTMS protocol on NOR task

A priming-test design, a "priming" rTMS protocol and "test" NOR task, was adopted to explore the effects of the rTMS protocol on object recognition. The NOR task was designed by Ennaceur et al.

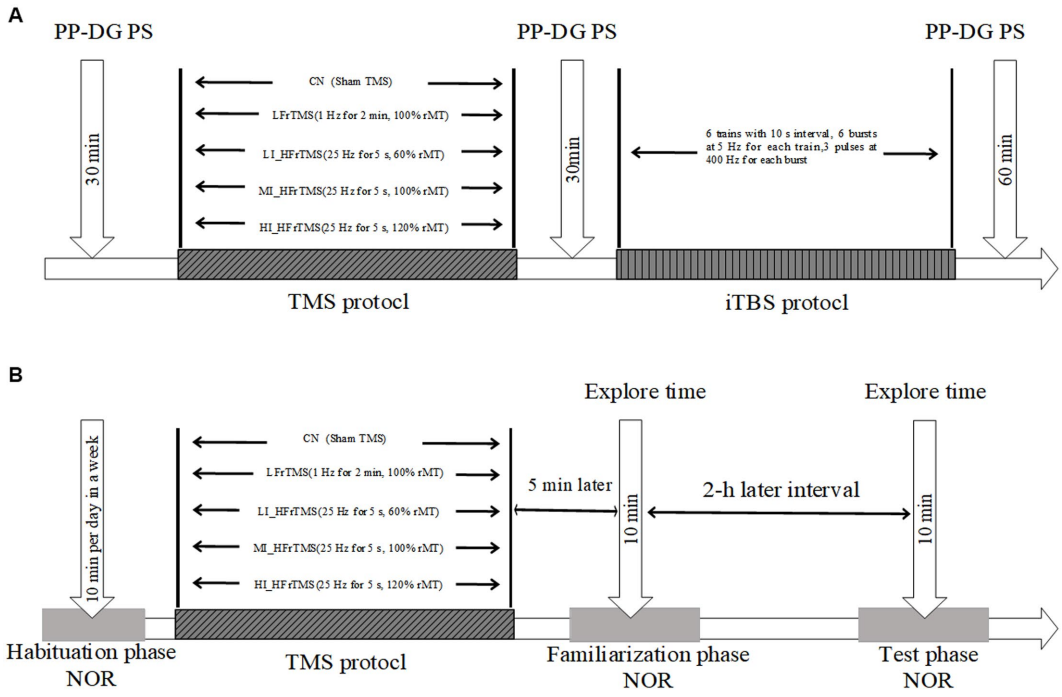


FIGURE 1
**(A–B)** Experimental time-flow diagram. NOR, novel object recognition.

in 1988 (Ennaceur and Delacour, 1988). Briefly, the NOR procedure consists of three phases: habituation, familiarization, and testing. The first week included the habituation phase: each animal was allowed to freely explore the open-field box without any object for 10 min. On the eighth day (familiarization phase), the subject was placed into the open-field arena facing away from two objects and allowed to explore them for 10 min. The exploration time was measured for each of the objects. After a delay of 2 h, the actual testing phase took place: each subject was allowed to explore two different objects (one of them identical to those presented during the familiarization phase, and the other one a novel object) for 10 min. The time spent exploring the novel and familiar objects was recorded by videotaping (Figure 1B).

The behavioral test was conducted in a quiet environment. Soda cans of different colors were chosen as stimuli owing to their appropriate height and weight, which prevented the subjects from climbing up on them or moving them (Pereira et al., 2014). The rats had never been exposed to these particular objects prior to the NOR task. Objects A or B could be randomly replaced during the familiarization phase, and their position could be randomly changed during the test phase (Figure 2). The box and the objects were cleaned with 75% ethanol after each test to eliminate potential odor cues. Exploration behavior was defined as the time spent sniffing with the nose or whiskers at a distance of less than 2 cm in front of the object or with the front paws touching the object. Turning around or sitting near the object was not considered exploration time. Subjects were excluded from the analyses if they failed to spend at least 1 s exploring each object during the test phase (Sanderson et al., 2011).

## 2.6. Statistical analysis

The LTP amplitudes, representing the capacity for synaptic plasticity in the hippocampus, were calculated using the ratio of the mean PS amplitudes (Niu et al., 2009) for 60 min post-TBS ($PS_2$) compared with the pre-tetanus baseline ($PS_0$) and expressed as mean ± standard error of mean %. LTP induction was defined as a sustained amplitude response for more than 60 min that reached levels of 130% of the normalized baseline values (Mulder et al., 1997). The time spent exploring each of the two identical objects was designated as (a1) and (a2), and the total time (e1) spent exploring both objects during the familiarization phase was therefore e1 = a1 + a2. Side preferences were tested by comparing a1 and a2 within each group during the familiarization phase. The time spent exploring the familiar (A) and the novel object (B) during the test phase was used to calculate the total time exploring both objects during this phase (e2). Differences between the groups based on the total time spent exploring both objects during the familiarization and the testing phase were evaluated by estimating an index of habituation (h1) using the following formula: h1 = e1-e2. The preference for the novel object was calculated as a discrimination index, which was the ratio of the time spent exploring the novel object divided by the total time spent exploring during the testing phase (i.e., iB = novel/[novel + familiar] = B/e2) (Sanderson et al., 2011). Within-group comparisons were performed using paired Student's t-test. Between-group comparisons were performed by one-way analysis of variance and post-hoc comparisons. Statistical significance was set at a value of $p$ of <0.05. All statistical analyses were performed using SPSS 25.0 (IBM, Armonk, NY, USA).

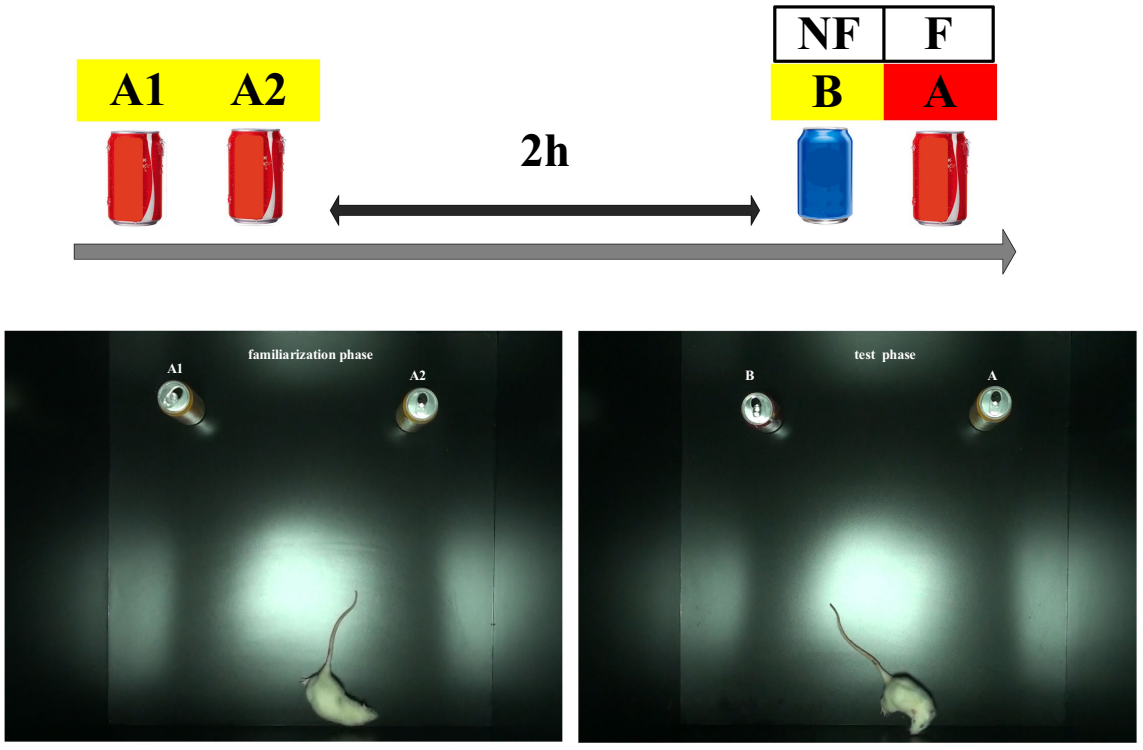


FIGURE 2
Novel object recognition test pattern diagrams.

# 3. Results

## 3.1. Experiment 1: effect of the rTMS protocol on iTBS-induced LTP in the hippocampal PP-DG

In the control group, in which sham rTMS was induced, the ratio of PS2 amplitude normalized to baseline PS1, namely the PS ratio, was 182% ± 9.4% at 60 min following TBS. The PS ratio was ranked as 25 Hz 100% rMT (267.78% ± 25.71%) > sham rTMS (182 ± 9.4%) > 1 Hz 100% rMT (102.69% ± 6.64%) > 25 Hz 120% rMT (98% ± 11.3%) > 25 Hz 60% rMT (36% ± 8.5%). Significant differences were observed among the groups [$F(4,20) = 201.5$, $p < 0.001$]. No significant difference was found between 25 Hz 120% rMT and 1 Hz 100% rMT ($p = 0.446$); other pairwise comparisons were statistically significant ($p < 0.001$). Only the sham rTMS group and 25 Hz 100% rMT group showed significant enhancement of the amplitude ratio by more than 130% of the baseline following 60 min of iTBS completion, demonstrating successful induction and maintenance of LTP during the 60-min recording period (see Figure 3).

## 3.2. Experiment 2: effect of the rTMS protocol on object recognition

During the familiarization phase, no significant side preference was noted in the sham rTMS ($t = -1.967$, $p = 0.097$), 1 Hz 100% rMT ($t = -2.268$, $p = 0.073$), 25 Hz 60% rMT ($t = -1.107$, $p = 0.33$), 25 Hz 100% rMT ($t = -0.043$, $p = 0.967$), or 25 Hz 120% rMT ($t = 0.507$, $p = 0.627$) groups. The time spent exploring the identical objects was comparable within each group ($p > 0.05$).

During the testing phase, the within-group analysis showed that more time was spent exploring the novel object than the familiar object in the sham rTMS ($t = -3.441$, $p = 0.014$) and 25 Hz 100% rMT ($t = -6.009$, $p = 0.001$) groups. In other words, the subjects spent less time exploring the familiar object than the novel object during the testing phase, indicating that rats in the sham rTMS and 25 Hz 100% rMT groups still retained long-term recognition memory for the familiar object 2 h after having been first exposed to it. No significant difference in exploration time between the familiar and novel object was observed in the 1 Hz 100% rMT ($t = -1.544$, $p = 0.073$), 25 Hz 60% rMT ($t = -1.493$, $p = 0.21$), and 25 Hz 120% rMT ($t = -0.831$, $p = 0.433$) groups during the test phase, revealing an impairment in recognition memory (see Figure 4).

In terms of differences in the total exploration time between the familiarization and the testing phase, no significant differences in the habituation index were observed [$F(4,29) = 0.534$, $p = 0.712$]. The total time spent exploring the objects used as stimuli did not decrease from the familiarization phase to the test phase, suggesting that the rats were equally familiar with their surroundings in both phases and that their physical strength and motivation to explore were not affected by the experimental setup.

The discrimination index between the groups were significantly different [$F(4,29) = 2.817$, $p = 0.043$]. The discrimination index was ranked as 25 Hz 100% rMT (0.812 ± 0.158) > sham rTMS (0.653 ± 0.111) > 25 Hz 120% rMT (0.583 ± 0.216) > 1 Hz 100% rMT (0.581 ± 0.145) > 25 Hz 60% rMT (0.532 ± 0.220). In the between-group analysis, there were significant differences between the 25 Hz 100% rMT and the 25 Hz 120% rMT ($p = 0.015$), 25 Hz 60% rMT ($p = 0.006$), and 1 Hz 100% rMT groups ($p = 0.03$). There was no difference between sham rTMS and 25 Hz 100% rMT rats ($p = 0.092$). Only the exposure to 25 Hz 100% rMT could significantly enhance memory retention of the familiar object in our experimental subjects (see Figure 5). Furthermore, the discrimination index during the NOR testing phase was calculated as the ratio of the time spent exploring the novel object divided by the total time spent exploring and was found to have a moderate positive correlation ($r = 0.457$, $p = 0.006$), with PS ratio representing the capacity for synaptic plasticity in the hippocampus. Additionally, it was observed that rTMS-induced after-effects on both neurophysiologic and behavioral parameters had a similar trend, suggesting that the intensity-dependent effects of rTMS on LTP induction in the hippocampus were reflected in the performance of the behavioral task (see Figure 6).

# 4. Discussion

We investigated the after-effects of several rTMS intensities on hippocampal plasticity. Our results revealed that 25 Hz rTMS at 100%

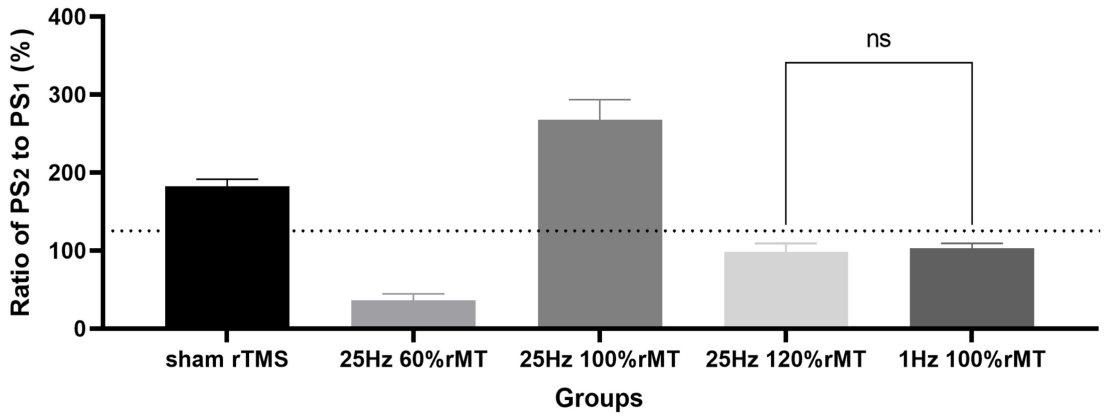


FIGURE 3
Effects of different repetitive transcranial magnetic stimulation protocols on long-term potentiation generation. "ns" represents "no significance" and the horizontal dashed line represents the level of 130% ratio.

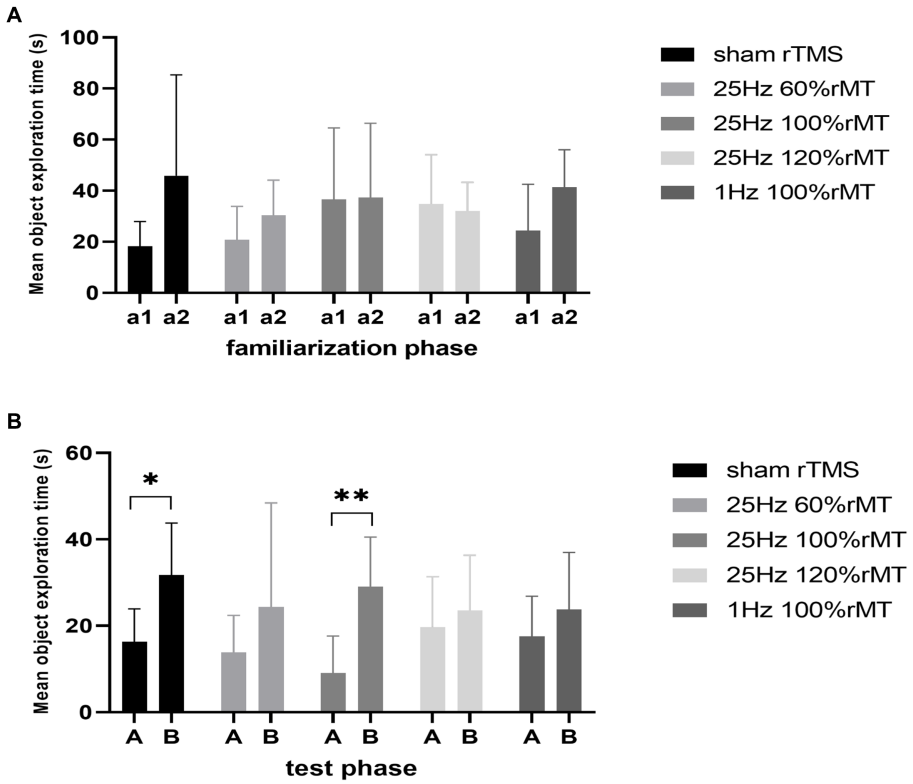


FIGURE 4
Effect of transcranial magnetic stimulation protocols on time spent in exploring objects. **(A)** a1 and a2 represent familiar objects on the left and right sides, respectively. **(B)** A and B represented familiar and novel objects, respectively. *$p < 0.05$, **$p < 0.01$.

rMT facilitated iTBS-induced LTP-like plasticity, whereas both 60% rMT and 120% rMT inhibited hippocampal excitability. This was consistent with the inhibitory effect of 1 Hz 100% rMT on the capacity of iTBS-induced LTP. Second, the PS ratio results from the electrophysiological examination were consistent with those of the discrimination index from the NOR test. Thus, we demonstrate here for the first time that high-frequency (25 Hz) rTMS can exert inverted (V-shaped) bidirectional modulation effects on hippocampal plasticity. High-frequency rTMS had a non-linear and intensity-dependent effect on hippocampal plasticity, involving the two forms of the metaplasticity mechanism. Furthermore, the after-effect of high-frequency rTMS with different intensity parameters on the memory recognition ability was positively correlated with those on LTP induction in the hippocampus *in vivo*.

## 4.1. After-effects of rTMS on induced LTP-like plasticity

Numerous studies have demonstrated that rTMS promote cortical excitation according to increasing stimulus intensity. For example, Huang and Rothwell found that MEPs were enhanced after 50 Hz rTMS over the human motor cortex at 70% or 80% active motor threshold (aMT), but not at 50% aMT (Huang and Rothwell, 2004). 3 Hz TMS at 75, 100, and 125% rMT was applied to the primary motor cortex non-linearly with increasing MEP amplitude to healthy volunteers; the rise in the MEP amplitude rate was greater for rMT above 100% (Fox et al., 2006). Both 2 Hz and 6 Hz stimulation at 70% aMT had no effect and that at 80% aMT reduced the magnitude of the MEPs; however, 90% aMT contributed to significant MEP facilitation in some participants and motor cortical excitability inhibition in others (Todd et al., 2006). However, our findings revealed that the application of a high-frequency (25 Hz) rTMS was characterized by an inverted (V-shaped) bidirectional modulation effect on hippocampal plasticity. This resulted in a greater PS ratio (LTP induction) in the 100% rMT (267.78 ± 25.71%) group than those from the 60% rMT (36 ± 8.5%) and 120% rMT (98 ± 11.3%) groups. In contrast with the findings of Todd et al. (2006), in which high-frequency stimulation (at intensities above 90% aMT) partly favored excitatory effects and those below 90% aMT had completely inhibitory effects, we found that high-frequency stimulation at 60% rMT was associated with inhibitory effects. Moreover, we found that high intensity of rTMS was not always associated with excitation: 100% rMT was facilitatory, but 120% rMT had inhibitory effects. Furthermore, we discovered the PS ratio to be greater in the 1 Hz 100% rMT (102.69 ± 6.64%) group than those in the 25 Hz 60 and 120% rMT groups, although this was not sufficient to induce LTP plasticity. Hippocampal excitability is therefore seemingly inconsistent with what has been described in the cortex, where low-frequency rTMS (<1 Hz) decreases and higher-frequency rTMS (>5 Hz) increases cortical excitability.

Hence, our viewpoint stresses that the modulation of rTMS on LTP in the rat hippocampus is based on the appropriate stimulus intensity but is not necessarily proportional to the intensity or the frequency of the excitation. Ogiue-Ikeda et al. (2003) had previously

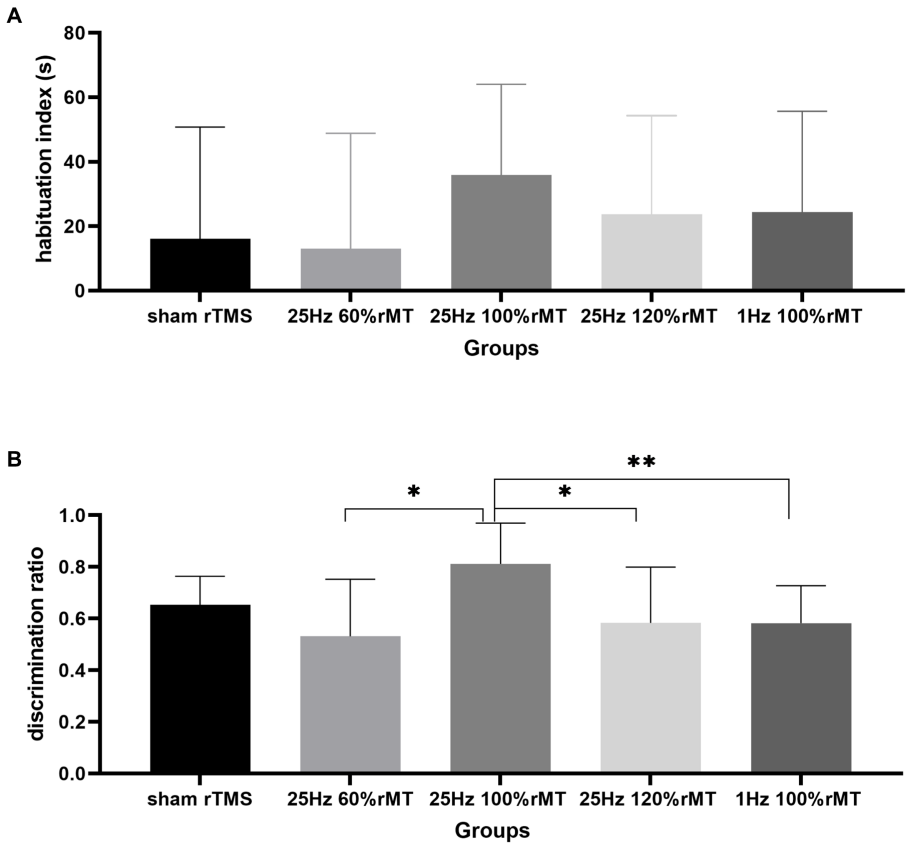


FIGURE 5
Effect of transcranial magnetic stimulation protocols on the habituation index and discrimination index in exploring objects. **(A)** The habituation index represents the desire to explore objects. **(B)** The discrimination index represents the recognition memory of the familiar object. *$p < 0.05$, **$p < 0.01$.

found that LTP in the rat hippocampus was enhanced at 0.75-T intensity (rTMS parameters: 10 1-s trains of 25 pulses with a 1-s intertrain interval) but suppressed by 1.25-T intensity, with no change observed at 0.5-T and 1.0-T. The overall conclusion that can be drawn from both studies is that high-frequency rTMS does not induce a linear increase in LTP with the increase in output intensity but is instead characterized by a V-shaped bidirectional modulation of LTP plasticity.

## 4.2. Association between LTP and memory recognition

NOR memory is hippocampus-dependent (Zhang et al., 2021). The behavioral results related to the NOR test were consistent with the neurophysiology results in this study. Recognition memory was reflected by the discrimination indexes of each experimental group. In Figure 5, the discrimination index ranking according to the rTMS level was as follows: 25 Hz 100% rMT > sham rTMS >25 Hz 120% rMT > 1 Hz 100% rMT > 25 Hz 60% rMT. In Figure 3, the ranking for the LTP ratios was, in turn, 25 Hz 100% rMT > sham rTMS >1 Hz 100% rMT > 25 Hz 120% rMT > 25 Hz 60% rMT. No between-group differences were observed between the 1 Hz 100% rMT and 25 Hz 120% rMT groups. As depicted in Figure 6, the aftereffects of rTMS on neurophysiological and behavioral parameters exhibited a similar trend, indicating that the intensity-dependent effects of rTMS on hippocampal LTP are reflected in the recognition memory performance of the NOR task.

Hippocampal LTP has been considered to represent a synaptic model of memory, associated with some specific forms of behavioral learning (Bliss and Collingridge, 1993). Numerous studies have demonstrated the association of LTP with learning and memory in animals. The earliest landmark studies from 1979 which applied a multi-session high-frequency stimulation protocol to induce LTP *in vivo* in the rat DG, found that aged individuals exhibited lower LTP magnitudes along with slower spatial memory acquisition and accelerated forgetfulness. Furthermore, the LTP magnitude correlated with the task performance in both young and aged rats (Barnes, 1979; Barnes and McNaughton, 1985). Since then, the correlation between the LTP characteristics and memory performance has been widely explored. Rat exposure to environmental levels of lead resulted in learning and memory impairment closely associated with a decrease in LTP induction ability (Lasley et al., 1993; Gilbert et al., 1996). The amplitude of LTP induction was significantly higher in rats with better learning ability than in controls (Wang et al., 2007). Some studies found that Wistar rats with stable LTP during recordings of 180 min following TBS showed increased novel object exploration time, suggesting that LTP maintenance is associated with long-term memory retention (Guimaraes et al., 2018). Proechimys rats showed increased LTP induction but not maintenance, with the potentiation decaying over

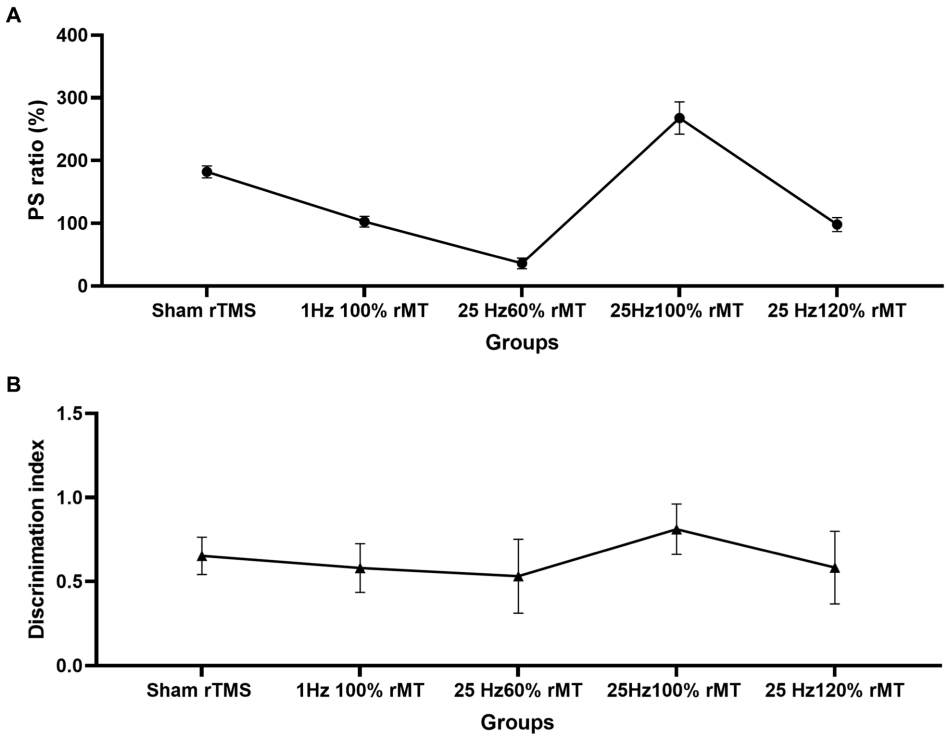


FIGURE 6
Effect of transcranial magnetic stimulation protocols on the neurophysiologic and behavioral parameters. **(A)** Intensity-dependent effects of rTMS on LTP induction in the hippocampus. **(B)** Intensity-dependent effects of rTMS on the discrimination index of the novel object in the NOR task.

time and reaching basal levels 90 min after TBS. These rats spent a similar amount of time exploring familiar and novel objects, suggesting long-lasting memory impairment in addition to the LTP decay (Guimaraes et al., 2018). In the present study, we found sham rTMS and 25 Hz 100% rMT induced higher LTP (>130% of baseline) for 60 min following iTBS, and the subjects retained the memory of familiar objects for a longer period, which supports the LTP-memory hypothesis that enhanced and suppressed LTP correlated with better and impaired learning and memory capacity, respectively (Dringenberg, 2020).

Similarly, the association between LTP and memory recognition was found in the *in vivo* demonstration of synaptic impairment in AD patients. Positron emission tomography of synaptic vesicle glycoprotein 2A has revealed a widespread synaptic loss in the brains of AD patients, demonstrating that alteration of the LTP mechanism is associated with memory impairment (Francesco and Koch, 2021). The investigation of rTMS stimulation parameters in rats has important implications for improving synaptic function. For instance, 25 Hz 100% rMT facilitated LTP induction and maintenance, which may be an effective therapeutic approach to counteract cognitive impairment in pathology. Therefore, it is necessary to identify potential therapeutic targets by investigating detailed rTMS stimulation parameters, including frequency and density, in future human research.

## 4.3. Intensity dependence of the rTMS after-effect on LTP and memory

rTMS protocols vary greatly in the frequency and intensity of stimulation. Overall, studies suggest a facilitatory effect of high-frequency rTMS (i.e., ≥5 Hz) and an inhibitory effect of low-frequency rTMS (≤1 Hz) (Chen et al., 1997; Fitzgerald et al., 2006). We observed that the modulatory effect of high-frequency (25 Hz) rTMS on iTBS-induced LTP-like plasticity was bidirectional, being facilitatory in the case of 25 Hz 100% rMT, and inhibitory in cases of 25 Hz 60 and 120% rMT. On the other hand, 1 Hz 100%, 25 Hz 60, and 120% rMT inhibited LTP induction and aggravated memory impairment in the hippocampal PP-DG, whereas 25 Hz 100% rMT promoted LTP plasticity and enhanced the object recognition ability in our subjects.

Metaplasticity is a higher-order form of synaptic plasticity referring to the synaptic activity that primes the ability to induce subsequent synaptic LTP- or long-term depression (LTD)-like plasticity (Karabanov et al., 2015). According to the Bienenstock, Cooper and Munro (BCM) theory (Jedlicka, 2002), the change in the excitability of synapses would inevitably affect the threshold of synaptic plasticity, which is specifically manifested in two different regulation modes. The greater improvement of memory observed in response to the 25 Hz 100% rMT protocol in the present study was consistent with the results of a previous study in which high-frequency rTMS modulated corticomotor inhibition and enhanced the effect of treadmill training in the motor learning (Yang et al., 2013). Form plasticity of gating mechanisms (Ziemann and Siebner, 2008) may be suitable for the interpretation of excitatory priming rTMS and may increase the response to subsequent iTBS-induced LTP-like plasticity, which may provide an effective means to induce transient disinhibition or depolarization and boost recognition memory. Furthermore, gating is another mechanism of metaplasticity wherein the priming intervention does not have a homeostatic effect on the subsequent

stimulus/training (Karabanov et al., 2015). Similarly, we observed no significant increased effect of 25 Hz 60% rMT on LTP-like plasticity response to subsequent facilitatory iTBS, with memory recognition impairment. This could be attributed to a strong inhibitory effect resulting from high-frequency and low-intensity TMS pulses (Arai et al., 2009). Thus, inhibitory priming rTMS would inhibit the response to subsequent facilitatory iTBS (Todd et al., 2009).

Interestingly, the fact that 25 Hz 120% rMT had an inhibitory effect on iTBS-induced LTP-like plasticity was unexpected. Also, we observed that the in 25 Hz 120% rMT group the discrimination index was low in the NOR task, indicating impaired recognition memory. It has been well-established that synaptic modifications can be reversed by subsequent stimuli, as demonstrated by the reversal of hippocampal LTP in rats upon entry into a novel environment (Zhou and Poo, 2004). We speculated the phenomenon is consistent with the compensatory change in homeostatic plasticity theory, which suggests that facilitatory priming TMS may weaken or reverse the effect of subsequent facilitatory test/intervention measures. This has also been described in another study that demonstrated a reversal in the homeostatic excitability effect using the same consecutively applied non-invasive transcranial brain stimulation protocol (Muller et al., 2007). The previous fundamental studies revealed that the form of homeostatic plasticity emphasized maintaining stabilized neural activity in a meaningful physiological range (Karabanov et al., 2015) to avoid LTP saturation (Moser et al., 1998). Hence, the increase in LTP amplitude was limited, and memory retention declined based on the LTP that correlated with common neural memory mechanisms in the hippocampus, which often required the activation of N-methyl D-aspartate receptors and their intracellular signaling (Roman et al., 1999). Considered a reference of moderate LTP amplitude induced by only iTBS in sham rTMS, increased LTP was induced if primed by 25 Hz 100% rMT but LTP decreased if primed by 25 Hz 60 and 120% rMT, and even 1 Hz 100% rMT. However, the reason for the LTP amplitude of 25 Hz 120% rMT showing no difference from that of 1 Hz 100% rMT, all of which surpassed the 25 Hz 60%, remains unclear.

In summary, the results of this study indicate that the priming protocol characteristics (i.e., intensity and frequency) are critically important for the induction of metaplasticity. We speculate that metaplasticity ensures a safe threshold zone. In cases in which gating plasticity plays a positive regulatory role in excitatory priming rTMS, it would facilitate the response to the subsequent protocol. If the ceiling or floor for homeostatic plasticity is exceeded, the metaplasticity would then provide negative feedback on the inhibitory or facilitatory priming rTMS, weakening or reversing the effect of the subsequent inhibitory or facilitatory protocol to guarantee normal synaptic activity.

### 4.4. Limitations

First, only the intensities of 60, 100, and 120% rMT were used in this study to investigate the effect of 25-Hz high-frequency rTMS stimulus. An intensity range of 60–130% rMT is the most commonly used parameter for high-frequency rTMS in a previous report (Ayache et al., 2012); however, due to time and expense constraints, 60, 100, and 120% rMT were selected as they are clinical commonly used parameters. Fixed parameters of rTMS stimulation frequency and intensity and varying stimulation time also have been tested and will be described in other articles. Second, the study design did not allow us to explore which specific mechanism was involved in the effect we describe. The use of specific antagonists or knockout models for saturating/occluding LTP might provide additional insight into the molecular mechanisms underlying the impaired learning and task acquisition reported. In addition, the exploration index correlated with the amplitude of LTP induction, but there was no significant difference between each of the experimental groups and the group receiving sham TMS. This could be because we only selected a 2-h interval for the NOR test. Ennaceur and Delacour (1988) and Ennaceur and Meliani (1992) found that dose-dependent changes in piracetam-induced changes in memory ability only became evident after longer intervals. Rogel-Salazar et al. (2013) observed that the recognition indexes in rats that had received transcranial focal stimulation were different according to the delay in the evaluation of short- and long-term memory. Thus, we cannot exclude the possibility that the difference between the experimental groups could have been significant if the interval between the familiarization and the testing phases had been extended. Although limited by its design, this trial may contribute another perspective on the application of rTMS for the treatment of memory impairment.

Furthermore, it is important to note that direct stimulation of the hippocampus is not possible in humans, unlike in animal models. However, the cerebellum and dorsolateral prefrontal cortex (DLPFC) have been identified as potential brain areas that are interconnected with the hippocampus, especially in patients with AD (Di Lorenzo et al., 2020; Yao et al., 2022). In addition, the stimulus sequence of the rTMS parameter on plasticity was related to spike-timing-dependent plasticity (STDP) in patients investigating the connections between the cortico-cortical cortex. In particular, STDP was altered in AD patients and this might represent a critical event in memory impairment (Di Lorenzo et al., 2018). Therefore, future animal model studies about the after-effect of rTMS parameters on LTP and memory should be conducted on the same regions that are stimulated in humans. This could help facilitate the development of new potential therapeutic strategies to modulate neural activity in patients with cognitive impairment.

## Data availability statement

The original contributions presented in the study are included in the article/Supplementary materials, further inquiries can be directed to the corresponding authors.

## Ethics statement

The animal study was reviewed and approved by the Institutional Animal Care and Use Committee of the Faculty of Medicine, Xiamen University, China (approval no. SYXK(min)-2018-0009).

## Author contributions

SC and XH conducted the study and including data collection. XW participated in data collection as a member. SC conducted data

analysis, prepared the manuscript, and prepared the manuscript draft with important intellectual input from XH, JH, and JZ. JH and JZ designed the study. All authors contributed to the article and approved the submitted version.

## Funding

This research was funded by the Ministry of Science and Technology of Fujian (Grant numbers: 2020D025 and 2020CXB052) to XH, and the Youth Innovation Project from the Ministry of Science and Technology of Fujian (grant number: 2022D010) to SC.

## Acknowledgments

We thank the First Affiliated Hospital of Xiamen University (Xiang'an Branch) for providing the site and equipment for this study and Professor Xiaokuo He for technical guidance.

## Conflict of interest

The authors declare that the research was conducted in the absence of any commercial or financial relationships that could be construed as a potential conflict of interest.

## Publisher's note

All claims expressed in this article are solely those of the authors and do not necessarily represent those of their affiliated organizations, or those of the publisher, the editors and the reviewers. Any product that may be evaluated in this article, or claim that may be made by its manufacturer, is not guaranteed or endorsed by the publisher.

## Supplementary material

The Supplementary material for this article can be found online at: https://www.frontiersin.org/articles/10.3389/fnins.2023.1144480/full#supplementary-material

## References

Arai, N., Furubayashi, T., Inomata-Terada, S., Okabe, S., Kobayashi-Iwata, N., Hanajima, R., et al. (2009). Effects of a high-frequency, low-intensity, biphasic conditioning train of TMS pulses on the human motor cortex. *Neurosci. Lett.* 462, 188–192. doi: 10.1016/j.neulet.2009.06.062

Ayache, S. S., Farhat, W. H., Zouari, H. G., Hosseini, H., Mylius, V., and Lefaucheur, J. P. (2012). Stroke rehabilitation using noninvasive cortical stimulation: motor deficit. *Expert. Rev. Neurother.* 12, 949–972. doi: 10.1586/ern.12.83

Barnes, C. A. (1979). Memory deficits associated with senescence: a neurophysiological and behavioral study in the rat. *J. Comp. Physiol. Psychol.* 93, 74–104. doi: 10.1037/h0077579

Barnes, C. A., and McNaughton, B. L. (1985). An age comparison of the rates of acquisition and forgetting of spatial information in relation to long-term enhancement of hippocampal synapses. *Behav. Neurosci.* 99, 1040–1048. doi: 10.1037//0735-7044.99.6.1040

Bliss, T. V., and Collingridge, G. L. (1993). A synaptic model of memory: long-term potentiation in the hippocampus. *Nature* 361, 31–39. doi: 10.1038/361031a0

Bruel-Jungerman, E., Davis, S., Rampon, C., and Laroche, S. (2006). Long-term potentiation enhances neurogenesis in the adult dentate gyrus. *J. Neurosci.* 26, 5888–5893. doi: 10.1523/JNEUROSCI.0782-06.2006

Cao, H., Zuo, C., Gu, Z., Huang, Y., Yang, Y., Zhu, L., et al. (2022). High frequency repetitive transcranial magnetic stimulation alleviates cognitive deficits in 3xTg-AD mice by modulating the PI3K/Akt/GLT-1 axis. *Redox Biol.* 54:102354. doi: 10.1016/j.redox.2022.102354

Chen, R., Classen, J., Gerloff, C., Celnik, P., Wassermann, E. M., Hallett, M., et al. (1997). Depression of motor cortex excitability by low-frequency transcranial magnetic stimulation. *Neurology* 48, 1398–1403. doi: 10.1212/wnl.48.5.1398

Chou, Y. H., Ton, T. V., and Sundman, M. (2020). A systematic review and meta-analysis of rTMS effects on cognitive enhancement in mild cognitive impairment and Alzheimer's disease. *Neurobiol. Aging* 86, 1–10. doi: 10.1016/j.neurobiolaging.2019.08.020

Cohen, L. G., Ziemann, U., and Chen, R. (1999). Mechanisms, functional relevance and modulation of plasticity in the human central nervous system. *Electroencephalogr. Clin. Neurophysiol. Suppl.* 51, 174–182.

Cooke, S. F., and Bliss, T. V. (2006). Plasticity in the human central nervous system. *Brain* 129, 1659–1673. doi: 10.1093/brain/awl082

Delvendahl, I., and Muller, M. (2019). Homeostatic plasticity- a presynaptic perspective. *Curr. Opin. Neurobiol.* 54, 155–162. doi: 10.1016/j.conb.2018.10.003

Di Lorenzo, F., Bonni, S., Picazio, S., Motta, C., Caltagirone, C., Martorana, A., et al. (2020). Effects of cerebellar theta burst stimulation on contralateral motor cortex excitability in patients with Alzheimer's disease. *Brain Topogr.* 33, 613–617. doi: 10.1007/s10548-020-00781-6

Di Lorenzo, F., Ponzo, V., Motta, C., Bonni, S., Picazio, S., Caltagirone, C., et al. (2018). Impaired spike timing dependent cortico-cortical plasticity in Alzheimer's disease patients. *J. Alzheimers Dis.* 66, 983–991. doi: 10.3233/JAD-180503

Dringenberg, H. C. (2020). The history of long-term potentiation as a memory mechanism: controversies, confirmation, and some lessons to remember. *Hippocampus* 30, 987–1012. doi: 10.1002/hipo.23213

Ennaceur, A., and Delacour, J. (1988). A new one-trial test for neurobiological studies of memory in rats. 1: behavioral data. *Behav. Brain Res.* 31, 47–59. doi: 10.1016/0166-4328(88)90157-x

Ennaceur, A., and Meliani, K. (1992). A new one-trial test for neurobiological studies of memory in rats. III. Spatial vs. non-spatial working memory. *Behav. Brain Res.* 51, 83–92. doi: 10.1016/s0166-4328(05)80315-8

Fitzgerald, P. B., Fountain, S., and Daskalakis, Z. J. (2006). A comprehensive review of the effects of rTMS on motor cortical excitability and inhibition. *Clin. Neurophysiol.* 117, 2584–2596. doi: 10.1016/j.clinph.2006.06.712

Fox, P. T., Narayana, S., Tandon, N., Fox, S. P., Sandoval, H., Kochunov, P., et al. (2006). Intensity modulation of TMS-induced cortical excitation: primary motor cortex. *Hum. Brain Mapp.* 27, 478–487. doi: 10.1002/hbm.20192

Francesco, D. L., and Koch, G. (2021). Synaptic impairment: the new battlefield of Alzheimer's disease. *Alzheimers Dement.* 17, 314–315. doi: 10.1002/alz.12189

Gersner, R., Kravetz, E., Feil, J., Pell, G., and Zangen, A. (2011). Long-term effects of repetitive transcranial magnetic stimulation on markers for neuroplasticity: differential outcomes in anesthetized and awake animals. *J. Neurosci.* 31, 7521–7526. doi: 10.1523/JNEUROSCI.6751-10.2011

Gilbert, M. E., Mack, C. M., and Lasley, S. M. (1996). Chronic developmental lead exposure increases the threshold for long-term potentiation in rat dentate gyrus in vivo. *Brain Res.* 736, 118–124. doi: 10.1016/0006-8993(96)00665-8

Gilio, F., Conte, A., Vanacore, N., Frasca, V., Inghilleri, M., and Berardelli, A. (2007). Excitatory and inhibitory after-effects after repetitive magnetic transcranial stimulation (rTMS) in normal subjects. *Exp. Brain Res.* 176, 588–593. doi: 10.1007/s00221-006-0638-9

Guimaraes, M. M., Reyes-Garcia, S. Z., Marques-Carneiro, J. E., Lopes-Silva, L. B., Andersen, M. L., Cavalheiro, E. A., et al. (2018). Long-term potentiation decay and poor long-lasting memory process in the wild rodents proechimys from Brazil's amazon rainforest. *Front. Behav. Neurosci.* 12:2. doi: 10.3389/fnbeh.2018.00002

He, P. K., Wang, L. M., Chen, J. N., Zhang, Y. H., Gao, Y. Y., Xu, Q. H., et al. (2022). Repetitive transcranial magnetic stimulation (rTMS) fails to improve cognition in patients with Parkinson's disease: a meta-analysis of randomized controlled trials. *Int. J. Neurosci.* 132, 269–282. doi: 10.1080/00207454.2020.1809394

Hermiller, M. S., Chen, Y. F., Parrish, T. B., and Voss, J. L. (2020). Evidence for immediate enhancement of hippocampal memory encoding by network-targeted theta-burst stimulation during concurrent fMRI. *J. Neurosci.* 40, 7155–7168. doi: 10.1523/JNEUROSCI.0486-20.2020

Huang, Y. Z., and Rothwell, J. C. (2004). The effect of short-duration bursts of high-frequency, low-intensity transcranial magnetic stimulation on the human motor cortex. *Clin. Neurophysiol.* 115, 1069–1075. doi: 10.1016/j.clinph.2003.12.026

Jedlicka, P. (2002). Synaptic plasticity, metaplasticity and BCM theory. *Bratisl. Lek. Listy* 103, 137–143.

Jiang, W., Wu, Z., Wen, L., Sun, L., Zhou, M., Jiang, X., et al. (2022). The efficacy of high- or low-frequency transcranial magnetic stimulation in Alzheimer's disease patients with behavioral and psychological symptoms of dementia. *Adv. Ther.* 39, 286–295. doi: 10.1007/s12325-021-01964-8

Kang, X., Li, C., Xie, Y., He, L. L., Xiao, F., Zhan, K. B., et al. (2021). Hippocampal ornithine decarboxylase/spermidine pathway mediates H2S-alleviated cognitive impairment in diabetic rats: involving enhancement of hippocampal autophagic flux. *J. Adv. Res.* 27, 31–40. doi: 10.1016/j.jare.2020.06.007

Karabanov, A., Ziemann, U., Hamada, M., George, M. S., Quartarone, A., Classen, J., et al. (2015). Consensus paper: probing homeostatic plasticity of human cortex with non-invasive transcranial brain stimulation. *Brain Stimul.* 8, 442–454. doi: 10.1016/j.brs.2015.01.404

Koch, G., Bonni, S., Pellicciari, M. C., Casula, E. P., Mancini, M., Esposito, R., et al. (2018). Transcranial magnetic stimulation of the precuneus enhances memory and neural activity in prodromal Alzheimer's disease. *NeuroImage* 169, 302–311. doi: 10.1016/j.neuroimage.2017.12.048

Kouvaros, S., and Papatheodoropoulos, C. (2016). Theta burst stimulation-induced LTP: differences and similarities between the dorsal and ventral CA1 hippocampal synapses. *Hippocampus* 26, 1542–1559. doi: 10.1002/hipo.22655

Lasley, S. M., Polan-Curtain, J., and Armstrong, D. L. (1993). Chronic exposure to environmental levels of lead impairs in vivo induction of long-term potentiation in rat hippocampal dentate. *Brain Res.* 614, 347–351. doi: 10.1016/0006-8993(93)91054-v

Levkovitz, Y., Marx, J., Grisaru, N., and Segal, M. (1999). Long-term effects of transcranial magnetic stimulation on hippocampal reactivity to afferent stimulation. *J. Neurosci.* 19, 3198–3203. doi: 10.1523/JNEUROSCI.19-08-03198.1999

Maeda, F., Keenan, J. P., Tormos, J. M., Topka, H., and Pascual-Leone, A. (2000). Modulation of corticospinal excitability by repetitive transcranial magnetic stimulation. *Clin. Neurophysiol.* 111, 800–805. doi: 10.1016/s1388-2457(99)00323-5

McNaughton, B. L., and Barnes, C. A. (1977). Physiological identification and analysis of dentate granule cell responses to stimulation of the medial and lateral perforant pathways in the rat. *J. Comp. Neurol.* 175, 439–453. doi: 10.1002/cne.901750404

Modugno, N., Nakamura, Y., MacKinnon, C. D., Filipovic, S. R., Bestmann, S., Berardelli, A., et al. (2001). Motor cortex excitability following short trains of repetitive magnetic stimuli. *Exp. Brain Res.* 140, 453–459. doi: 10.1007/s002210100843

Moser, E. I., Krobert, K. A., Moser, M. B., and Morris, R. G. (1998). Impaired spatial learning after saturation of long-term potentiation. *Science* 281, 2038–2042. doi: 10.1126/science.281.5385.2038

Muellbacher, W., Ziemann, U., Boroojerdi, B., and Hallett, M. (2000). Effects of low-frequency transcranial magnetic stimulation on motor excitability and basic motor behavior. *Clin. Neurophysiol.* 111, 1002–1007. doi: 10.1016/s1388-2457(00)00284-4

Mulder, A. B., Arts, M. P., and Lopes, D. S. F. (1997). Short- and long-term plasticity of the hippocampus to nucleus accumbens and prefrontal cortex pathways in the rat, in vivo. *Eur. J. Neurosci.* 9, 1603–1611. doi: 10.1111/j.1460-9568.1997.tb01518.x

Muller, J. F., Orekhov, Y., Liu, Y., and Ziemann, U. (2007). Homeostatic plasticity in human motor cortex demonstrated by two consecutive sessions of paired associative stimulation. *Eur. J. Neurosci.* 25, 3461–3468. doi: 10.1111/j.1460-9568.2007.05603.x

Muller-Dahlhaus, F., and Ziemann, U. (2015). Metaplasticity in human cortex. *Neuroscientist* 21, 185–202. doi: 10.1177/1073858414526645

Niu, L., Cao, B., Zhu, H., Mei, B., Wang, M., Yang, Y., et al. (2009). Impaired in vivo synaptic plasticity in dentate gyrus and spatial memory in juvenile rats induced by prenatal morphine exposure. *Hippocampus* 19, 649–657. doi: 10.1002/hipo.20540

Nugent, F. S., Hwong, A. R., Udaka, Y., and Kauer, J. A. (2008). High-frequency afferent stimulation induces long-term potentiation of field potentials in the ventral tegmental area. *Neuropsychopharmacology* 33, 1704–1712. doi: 10.1038/sj.npp.1301561

Ogiue-Ikeda, M., Kawato, S., and Ueno, S. (2003). The effect of repetitive transcranial magnetic stimulation on long-term potentiation in rat hippocampus depends on stimulus intensity. *Brain Res.* 993, 222–226. doi: 10.1016/j.brainres.2003.09.009

Ostrovskaya, O. I., Cao, G., Eroglu, C., and Harris, K. M. (2020). Developmental onset of enduring long-term potentiation in mouse hippocampus. *Hippocampus* 30, 1298–1312. doi: 10.1002/hipo.23257

Pereira, L. M., Bastos, C. P., de Souza, J. M., Ribeiro, F. M., and Pereira, G. S. (2014). Estradiol enhances object recognition memory in Swiss female mice by activating hippocampal estrogen receptor alpha. *Neurobiol. Learn. Mem.* 114, 1–09. doi: 10.1016/j.nlm.2014.04.001

Rogel-Salazar, G., Luna-Munguía, H., Stevens, K. E., and Besio, W. G. (2013). Transcranial focal electrical stimulation via tripolar concentric ring electrodes does not modify the short- and long-term memory formation in rats evaluated in the novel object recognition test. *Epilepsy Behav.* 27, 154–158. doi: 10.1016/j.yebeh.2013.01.006

Roman, F. S., Truchet, B., Marchetti, E., Chaillan, F. A., and Soumireu-Mourat, B. (1999). Correlations between electrophysiological observations of synaptic plasticity modifications and behavioral performance in mammals. *Prog. Neurobiol.* 58, 61–87. doi: 10.1016/s0301-0082(98)00076-8

Sanderson, D. J., Hindley, E., Smeaton, E., Denny, N., Taylor, A., Barkus, C., et al. (2011). Deletion of the GluA1 AMPA receptor subunit impairs recency-dependent object recognition memory. *Learn. Mem.* 18, 181–190. doi: 10.1101/lm.2083411

Todd, G., Flavel, S. C., and Ridding, M. C. (2006). Low-intensity repetitive transcranial magnetic stimulation decreases motor cortical excitability in humans. *J. Appl. Physiol.* 101, 500–505. doi: 10.1152/japplphysiol.01399.2005

Todd, G., Flavel, S. C., and Ridding, M. C. (2009). Priming theta-burst repetitive transcranial magnetic stimulation with low- and high-frequency stimulation. *Exp. Brain Res.* 195, 307–315. doi: 10.1007/s00221-009-1791-8

Wang, M., Chen, W. H., Zhu, D. M., She, J. Q., and Ruan, D. Y. (2007). Effects of carbachol on lead-induced impairment of the long-term potentiation/depotentiation in rat dentate gyrus in vivo. *Food Chem. Toxicol.* 45, 412–418. doi: 10.1016/j.fct.2006.08.025

Wang, W. C., Wing, E. A., Murphy, D., Luber, B. M., Lisanby, S. H., Cabeza, R., et al. (2018). Excitatory TMS modulates memory representations. *Cogn. Neurosci.* 9, 151–166. doi: 10.1080/17588928.2018.1512482

Wang, L., Yang, J., Wang, F., Zhou, P., Wang, K., and Ming, D. (2018). Modulation of low-frequency pulsed magnetic field on hippocampal neural oscillation in depression rats. *Annu. Int. Conf. IEEE Eng. Med. Biol. Soc.* 2018, 259–262. doi: 10.1109/EMBC.2018.8512192

Yang, Y. R., Tseng, C. Y., Chiou, S. Y., Liao, K. K., Cheng, S. J., Lai, K. L., et al. (2013). Combination of rTMS and treadmill training modulates corticomotor inhibition and improves walking in Parkinson disease: a randomized trial. *Neurorehabil. Neural Repair* 27, 79–86. doi: 10.1177/1545968312451915

Yao, Q., Tang, F., Wang, Y., Yan, Y., Dong, L., Wang, T., et al. (2022). Effect of cerebellum stimulation on cognitive recovery in patients with Alzheimer disease: a randomized clinical trial. *Brain Stimul.* 15, 910–920. doi: 10.1016/j.brs.2022.06.004

Zhang, X., Lan, X., Chen, C., Ren, H., and Guo, Y. (2021). Effects of repetitive transcranial magnetic stimulation in patients with mild cognitive impairment: a meta-analysis of randomized controlled trials. *Front. Hum. Neurosci.* 15:723715. doi: 10.3389/fnhum.2021.723715

Zhang, L. Q., Zhang, W., Li, T., Yang, T., Yuan, X., Zhou, Y., et al. (2021). GLP-1R activation ameliorated novel-object recognition memory dysfunction via regulating hippocampal AMPK/NF-kappaB pathway in neuropathic pain mice. *Neurobiol. Learn. Mem.* 182:107463. doi: 10.1016/j.nlm.2021.107463

Zhou, Q., and Poo, M. M. (2004). Reversal and consolidation of activity-induced synaptic modifications. *Trends Neurosci.* 27, 378–383. doi: 10.1016/j.tins.2004.05.006

Ziemann, U., and Siebner, H. R. (2008). Modifying motor learning through gating and homeostatic metaplasticity. *Brain Stimul.* 1, 60–66. doi: 10.1016/j.brs.2007.08.003

frontiers | Frontiers in Neuroscience

TYPE Original Research
PUBLISHED 26 October 2023
DOI 10.3389/fnins.2023.1198222



OPEN ACCESS

EDITED BY
Jie Jia,
Fudan University, China

REVIEWED BY
Alessandro Botta,
San Martino Hospital (IRCCS), Italy
Jingying Wang,
University of Florida, United States

*CORRESPONDENCE
Michael Vesia
✉ mvesia@umich.edu

RECEIVED 31 March 2023
ACCEPTED 05 October 2023
PUBLISHED 26 October 2023

CITATION
Goldenkoff ER, Deluisi JA, Destiny DP, Lee TG, Michon KJ, Brissenden JA, Taylor SF, Polk TA and Vesia M (2023) The behavioral and neural effects of parietal theta burst stimulation on the grasp network are stronger during a grasping task than at rest.
*Front. Neurosci.* 17:1198222.
doi: 10.3389/fnins.2023.1198222



# The behavioral and neural effects of parietal theta burst stimulation on the grasp network are stronger during a grasping task than at rest

Elana R. Goldenkoff[1], Joseph A. Deluisi[1], Danielle P. Destiny[2], Taraz G. Lee[2], Katherine J. Michon[2], James A. Brissenden[2], Stephan F. Taylor[3], Thad A. Polk[2] and Michael Vesia[1]*

[1]School of Kinesiology, University of Michigan, Ann Arbor, MI, United States, [2]Department of Psychology, University of Michigan, Ann Arbor, MI, United States, [3]Department of Psychiatry, University of Michigan, Ann Arbor, MI, United States

Repetitive transcranial magnetic stimulation (TMS) is widely used in neuroscience and clinical settings to modulate human cortical activity. The effects of TMS on neural activity depend on the excitability of specific neural populations at the time of stimulation. Accordingly, the brain state at the time of stimulation may influence the persistent effects of repetitive TMS on distal brain activity and associated behaviors. We applied intermittent theta burst stimulation (iTBS) to a region in the posterior parietal cortex (PPC) associated with grasp control to evaluate the interaction between stimulation and brain state. Across two experiments, we demonstrate the immediate responses of motor cortex activity and motor performance to state-dependent parietal stimulation. We randomly assigned 72 healthy adult participants to one of three TMS intervention groups, followed by electrophysiological measures with TMS and behavioral measures. Participants in the first group received iTBS to PPC while performing a grasping task concurrently. Participants in the second group received iTBS to PPC while in a task-free, resting state. A third group of participants received iTBS to a parietal region outside the cortical grasping network while performing a grasping task concurrently. We compared changes in motor cortical excitability and motor performance in the three stimulation groups within an hour of each intervention. We found that parietal stimulation during a behavioral manipulation that activates the cortical grasping network increased downstream motor cortical excitability and improved motor performance relative to stimulation during rest. We conclude that constraining the brain state with a behavioral task during brain stimulation has the potential to optimize plasticity induction in cortical circuit mechanisms that mediate movement processes.

KEYWORDS

**transcranial magnetic stimulation, state-dependency, manual dexterity, functional connectivity, plasticity, theta burst stimulation, posterior parietal cortex, motor cortex**

## Highlights

- Controlling the brain state during TMS with a grasping task improves motor performance.
- Brain-state-dependent parietal TMS induces immediate changes in the motor cortex.
- Brain-state-dependent TMS can enhance the impact of neuromodulation on motor function.

# Introduction

Goal-directed hand actions, such as grasping for objects, are integral to human behavior. Performing such behaviors activates a widespread network of cortical areas, including the prefrontal cortex, premotor cortex, and posterior parietal cortex (PPC; Grafton, 2010; Davare et al., 2011; Turella and Lingnau, 2014; Fattori et al., 2015; Gallivan and Culham, 2015). The primary motor cortex (M1) plays an essential role in motor control and is part of a more extensive parietal–frontal network involved in many aspects of movement planning and decision-making (Kalaska et al., 1997; Andersen and Cui, 2009; Cisek and Kalaska, 2010; Crawford et al., 2011; Vesia and Crawford, 2012). Neural inputs from PPC to motor areas in the frontal lobe are generally thought to mediate motor commands for hand movements (Grafton, 2010; Turella and Lingnau, 2014; Fattori et al., 2015; Gallivan et al., 2018). Current evidence from functional cortico-cortical connectivity measures derived from dual-site transcranial magnetic stimulation (dsTMS) indicates that inputs from PPC exert a facilitatory influence on motor output during the preparation and execution of hand-movement planning, suggesting a functional parietal-motor connection that controls hand muscles (Koch et al., 2007, 2008, 2010; Koch and Rothwell, 2009; Davare et al., 2010; Ziluk et al., 2010; Vesia and Davare, 2011; Karabanov et al., 2013; Vesia et al., 2013, 2017; Koch, 2020). The plasticity of M1 associated with voluntary movements and motor-skill learning also appears to be influenced by distributed activity in functionally related brain areas in the motor network (Sanes and Donoghue, 2000; Hardwick et al., 2013; Buch et al., 2017). However, it is unclear if other brain areas, such as PPC, can modulate this motor plasticity.

Repetitive transcranial magnetic stimulation (rTMS) can induce plastic changes in the brain (Hallett, 2007). For instance, intermittent theta burst stimulation (iTBS), a form of rTMS, can produce durable increases in motor cortical excitability for a period that outlasts the stimulation when applied to M1 (Huang et al., 2005; Suppa et al., 2016). The mechanisms of these changes are caused by processes analogous to long-term potentiation (LTP) that are also seen with skill learning (Capocchi et al., 1992; Bear and Malenka, 1994; Berardelli et al., 1998). This stimulation can directly modify neural activity at the locus of stimulation, as well as the activity of interconnected and functionally coupled brain areas (Siebner et al., 2009b). These persistent effects on neural activity are primarily thought to be constrained within the functional network of the targeted region (Fox et al., 2012). Therefore, it is unsurprising that rTMS can be particularly effective for treatment-induced behavior improvements when applied to functional brain networks (Raffin and Siebner, 2014; Silasi and Murphy, 2014; Fox, 2018; Horn and Fox, 2020). Yet, the persisting effects of rTMS on enduring motor cortical excitability and behavioral outcomes are highly variable and poorly understood (Ziemann and Siebner, 2015).

The variability of rTMS-induced effects on brain and behavior responses can be partly explained by variations in ongoing activity levels of functionally specific neural populations and pathways at the time of stimulation (Silvanto et al., 2008; Romei et al., 2016; Bergmann, 2018). For example, recordings in the visual cortex indicate that the post-stimulation response depends on pre-stimulation activity levels (Pasley et al., 2009). Similarly, pairing rTMS with visual stimuli has shown a direction-selective plasticity induction in the visual system that biases subsequent behavioral responses for a particular motion direction (Chiappini et al., 2018). Therefore, the functional context of neural activity during stimulation appears necessary for targeting brain networks associated with specific functions.

Although we and others have shown that the PPC and associated parietal–frontal circuits of the motor planning network are essential for skilled grasp control (Davare et al., 2010, 2011; Grafton, 2010; Vesia and Crawford, 2012; Turella and Lingnau, 2014; Fattori et al., 2015; Gallivan and Culham, 2015; Vesia et al., 2017), the notion that the functional context of brain activity during PPC stimulation can modulate interactions with functionally connected motor regions to alter plasticity associated with motor control has not been directly tested. We utilized a novel approach that combines an object-driven grasp task, which selectively activates the motor control network, with iTBS to PPC. In the pilot study (Experiment 1), we investigated the immediate effects of state-dependent stimulation on electrophysiological and behavioral responses. Experiment 2 replicated the findings from the pilot study with a larger sample size and additional stimulation sessions. We predicted that applying parietal iTBS while constraining the brain state via a grasping task will be more likely to increase motor cortical excitability than an application of the same stimulation protocol during rest. We also predicted that motor performance improvement would be greater after parietal iTBS during grasp performance compared to parietal iTBS at rest.

# Materials and methods

## Participants

We conducted two experiments involving 72 healthy, right-handed participants (Oldfield, 1971). In Experiment 1 (pilot study), we studied 24 adult participants (13 females and 11 males aged between 18 and 30). For our second experiment, we recruited 48 participants (32 females and 16 males, 18–50 years) and assigned 16 participants to each group. The sample size was determined based on prior research (Fiori et al., 2018), considering a motor performance effect size of 0.11, a desired power of 0.8, a significance level ($\alpha$) of 0.05, and an estimated dropout rate of 10%. All participants provided written informed consent and underwent a TMS Adult Safety Screen to assess the potential risk of adverse reactions to TMS (Keel et al., 2001; Rossi et al., 2011). The Institutional Review Board at the University of Michigan (IRB#: HUM00157197 and HUM00186637) approved experimental procedures in accordance with the Declaration of Helsinki.

## Electromyographic recordings

Electromyography (EMG) activity of the right hand was recorded from the first dorsal interosseous and abductor pollicis brevis muscles using surface electrodes (Ag-AgCl, 9-mm diameter). The active electrode was placed over the muscle belly, and the reference electrode over the metacarpophalangeal joint of the finger. Signals were amplified (×1000), band pass filtered (20 Hz–2.5 kHz; Intronix Technologies Corporation, Model 2024F), digitized at 5 kHz using a Micro 1,401 data acquisition interface controlled by Signal Software

version 7 (Cambridge Electronic Design Ltd.), and stored on a computer for off-line analysis.

## Transcranial magnetic stimulation

Monophasic pulses were delivered from two separate Magstim model 200$^2$ stimulators (Magstim) through a D70$^2$ (loop diameter, 70 mm) or D50 Alpha B.I. (loop diameter, 50 mm) figure-8 coil. First, motor-evoked potentials (MEPs) in the targeted relaxed right-hand muscle were elicited by delivering single-pulse TMS (spTMS) over the hand area of the left primary motor cortex (M1). The TMS coil was placed tangential to the scalp and at a 45° angle from the midsagittal line. The placement of the TMS coil was adjusted to the location where TMS produced the largest MEP from the targeted right-hand muscles. Next, the TMS coil's position was marked and registered using a standard MRI template with a frameless stereotactic neuronavigation system (Brainsight 2, Rogue Research Inc.). The resting motor threshold (RMT) was determined by the minimum stimulator output needed to obtain MEP amplitudes of at least 50 μV in five of ten TMS pulses with the D50 Alpha B.I. coil when the muscle was completely relaxed (Rossini et al., 1994, 2015; Groppa et al., 2012). The intensity of the D70$^2$ coil was adjusted to induce MEP amplitudes of about 1 mV in at least five out of ten trials in the relaxed targeted right-hand muscle.

## Stimulation target identification

We used a function-based search-grid dsTMS technique to establish individualized left PPC locations for Experiment 1. This method uses a "hunting procedure" to target personalized functional interactions in the cortical grasping network. First, the left parietal stimulation target was selected as the P3 (left PPC) electrode position on the 10–20 electroencephalogram (EEG) coordinate system (Herwig et al., 2004; Okamoto et al., 2004) using commercially available 10–20 EEG stretch caps (g.GAMMAcap, g.tec Medical Engineering) in each participant. The P3 electrode location has been previously shown to target the inferior parietal lobule (Vesia et al., 2006, 2008, 2010, 2015). A square, 3 × 3 search grid, with positions separated by 1 cm, centered on the P3 target, was created using Brainsight (Figure 1A). A dsTMS approach with two coils was then used to identify participant-specific stimulation locations in the left PPC where parietal stimulation effectively exerts grasp-specific facilitation on M1 during an object-directed grasp task. This dsTMS technique provides a means for assessing how the behavioral context modulates the strength of interaction between PPC and M1 when the grasp-task demand recruits the parietal-motor circuit (Koch and Rothwell, 2009; Vesia and Davare, 2011; Vesia et al., 2013, 2017; Bestmann et al., 2015; Lafleur et al., 2016; Hallett et al., 2017; Goldenkoff et al., 2020). Specifically, we adopted a paradigm used previously by our group to activate the PPC-M1 circuit early in the motor plan for grasp movements (Vesia et al., 2013, 2017). Participants made one of two object-directed grasp movements to a target object with the right hand (Figure 1B). The target object was a small cylinder (2.5 cm diameter, 6.5 cm height) fixed atop a larger cylinder (7 cm diameter, 6.5 cm height), located 30 cm in front and 10 cm to the right of the starting hand position. Participants maintained visual fixation on two central LEDs in the midline for 2 s. Participants were instructed to grasp: (1) the top cylinder with a precision grip when the top LED flashed or (2) the bottom cylinder with a whole-hand grasp when the bottom LED flashed. To probe causal connectivity between the PPC and M1 in the left hemisphere, a conditioning stimulus (CS) over each PPC target in the grid was applied before delivering a test stimulus (TS) to ipsilateral M1 during reaction time (i.e., action plan phase) of the object-directed grasp such that the MEP recordings were collected before actual movement initiation (Vesia et al., 2017). TS intensity was adjusted to induce MEP amplitudes of about 1 mV. CS preceded TS by an interstimulus interval (ISI) of 5 ms at a stimulation intensity of 90% RMT (Koch et al., 2008; Vesia et al., 2013, 2017). Approximately ten TS and CS-TS were administered randomly at each grid position. The optimal scalp position for coil placement over the left PPC was defined as the point on the grid where CS elicited the largest MEP exceeding 1.2 mV from the contralateral hand muscle of the right (response) hand in three of five consecutive trials (Oliver et al., 2009; Karabanov et al., 2013). Brainsight was used to accurately place both coils throughout the localization of the parietal stimulation target. The stimulation location for the control condition was set at the Pz electrode position, which is not part of the parietal-motor circuit responsible for grasping. The parietal rTMS location on the grid was recorded and reported in Figure 2A.

In our second experiment, the site for PPC stimulation and the cortical control stimulation locations were identified using structural MRI data on each participant. MRI data were acquired using a 3 T GE scanner (MR 750) with a 32-channel head coil. T1-weighted structural images were obtained for anatomical localization. To locate the individualized left parietal stimulation target, we generated a region of interest mask based on the superior medial parietal regions 'L_LIPv, L_7PC' using the MNI projection of the HCP-MMP1 atlas (Glasser et al., 2016). We chose a point within the anatomical mask that overlapped the center of a gyrus. We identified a target in the left visual cortex for the control stimulation group based on anatomical criteria. Notably, the visual cortical region is outside the grasping network. We determined the cortical location reached by the stimulation in each participant by projecting the coil location on the scalp onto their individual MRI using Brainsight. The resulting coordinates were reported in MNI space (Figure 2B). To visualize the data, SimNIBS 4.0 was used to estimate the TMS-induced electric fields (Thielscher et al., 2015; Figure 2C).

## Theta burst stimulation

Intermittent theta burst stimulation (iTBS) to the left cortical targets was administered using a MagPro X100 with MagOption (MagVenture Inc.) and a statically cooled figure-8 coil (MCF-B70). iTBS consisted of three pulses at a frequency of 50 Hz every 200 ms for 2 s and repeated every 10 s for a total of 190 s (600 pulses; Huang et al., 2005). The conventional approach for individualizing iTBS intensity is based on the motor threshold response, which uses an intensity of 80% of the active motor threshold (AMT; Huang et al., 2005). AMT was defined as the lowest intensity required for eliciting MEP of 200 μV in five of ten consecutive trials during a 20% maximum voluntary contraction of the muscle in the right hand with the MCF-B70 coil using biphasic pulses (Huang et al., 2005). We assessed AMT for each participant to compare our stimulation intensity with

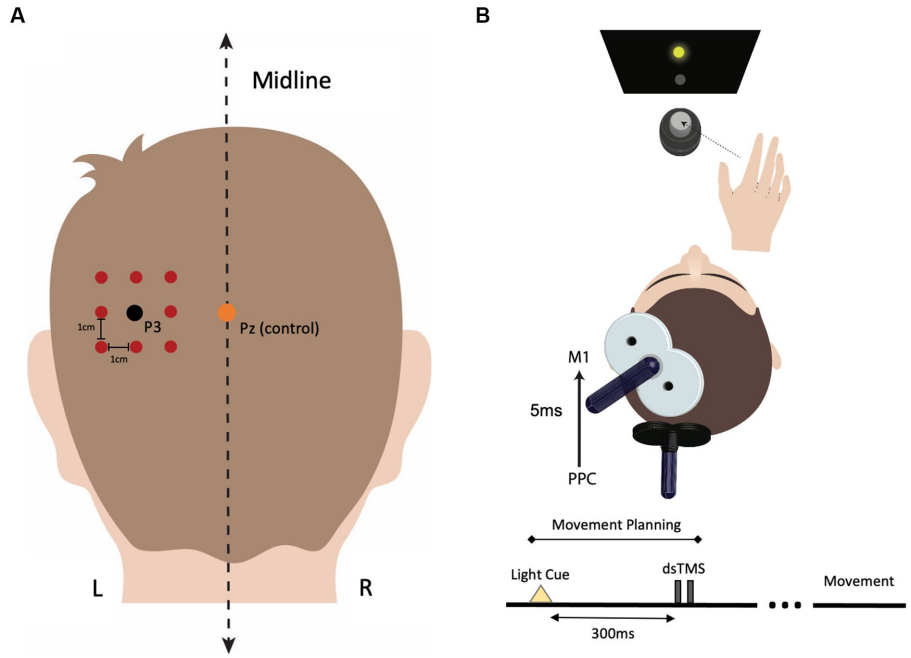


FIGURE 1
Procedure for identifying individualized left parietal stimulation locations. **(A)** The P3 electrode location was marked for each participant using the 10–20 EEG system. A 3 × 3 square search grid, with each point separated by 1 cm, was centered around P3 using Brainsight stereotactic software. The Pz electrode position was used as the stimulation location for the control condition. **(B)** During the functional localization protocol, each grid location over the parietal cortex was assessed for its maximum facilitatory effect on the primary motor cortex (M1). To identify the participant-specific location in PPC where stimulation induced the greatest facilitation in motor-evoked potential (MEP) amplitude, a dual-site, paired-pulse TMS (dsTMS) paradigm was employed using two coils. During dsTMS, participants performed an object-directed grasp task, and dsTMS was applied 300 ms after the movement cue (LED flash) occurred, coinciding with the planning phase of movement. Electromyography (EMG) was used to measure changes in MEP amplitude during the planning phase of the movement. The conditioning pulse intensity over PPC was 90% of the resting motor threshold (RMT), and the test pulse intensity over M1 was adjusted to induce an MEP of ~1 mV in the target hand muscle. The interstimulus interval (ISI) between the conditioning and test pulse was set at 5 ms. Approximately ten dsTMS pairs were delivered at each search grid location, and the location that induced the largest MEP response in three of five consecutive trials was selected as the PPC rTMS location.

previous studies that utilized the conventional approach and ensure that our stimulation intensity adhered to safety guidelines (Oberman et al., 2011; Rossi et al., 2021).

The pilot study (Experiment 1) delivered iTBS at a fixed percentage of maximum stimulator output (% MSO) of 40% to decrease the inter-individual difference in stimulation-induced effects (Vesia et al., 2010). This methodological adjustment is based on evidence demonstrating that motor threshold does not adequately characterize the underlying physiology of non-motor areas of the brain (Stewart et al., 2001; Stokes et al., 2005; Khammash et al., 2020). For Experiment 2, we administered iTBS using a personalized stimulation intensity based on the individual participant's functional neuroanatomy. This personalized approach adjusted AMT according to the distances between the scalp and the underlying cortex (for details, see Stokes et al., 2005). The stimulation intensity was then set at 80% of the adjusted AMT for each participant ($iTBS_{PPC+Grasp}$: 37.4 ± 3.2; $iTBS_{PPC+Rest}$: 36.7 ± 2.7; $iTBS_{Control+Grasp}$: 37.4 ± 3.2).

## Assessment of motor cortical excitability

Long-term potentiation-like plasticity in M1 was assessed by quantifying the changes in the level of motor cortical excitability with the different stimulation protocols (Chen and Udupa, 2009). A fixed percentage of maximum stimulator output was used to elicit MEPs of about 1 mV peak-to-peak amplitude using spTMS with the D70$^2$ coil before iTBS to PPC. Twenty-four MEPs were recorded at every assessment time point before and after (Experiment 1: 0, 15, 30, 45, and 60 min; Experiment 2: 30 and 60 min) each intervention with the 1 mV TMS intensity determined before each intervention. Stimuli were applied every 5 s.

## Assessment of motor performance

Motor performance was assessed by examining changes in the speed to complete a widely used nine-hole pegboard manual dexterity test. The pegboard task requires dexterous control of complex movements such as multi-digit grasping and manipulating small objects (Mathiowetz et al., 1985; Grice et al., 2003; Bunday and Perez, 2012; Fiori et al., 2018). Performance of the pegboard task engages parietal–frontal brain areas in the cortical grasping network subserving sensorimotor functions (Davare et al., 2011; Bunday and Perez, 2012; Fiori et al., 2018). Participants were seated in front of a table with the start position of the right hand positioned 10 cm from the pegboard apparatus. Behavioral performance on the pegboard task was evaluated by measuring the time to complete the task using a stopwatch every time before and after (30 and 60 min) the intervention.

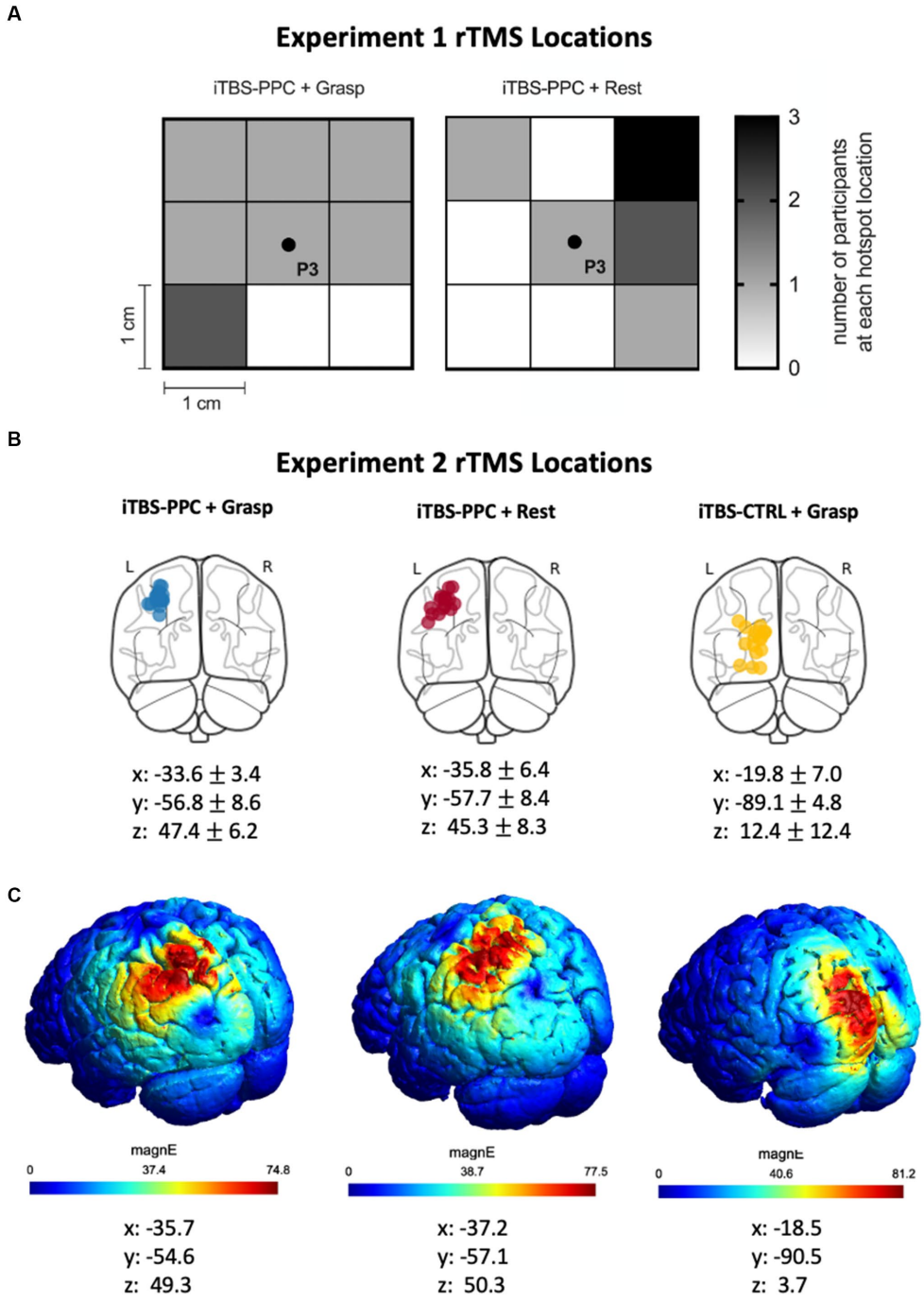


FIGURE 2
**(A)** Heat map indicating the search grid spot that was selected for the participants in the iTBS-PPC + Grasp and iTBS-PPC + Rest groups in Experiment 1. **(B)** In Experiment 2, structural fMRI was used to identify individualized left parietal stimulation locations for both iTBS-PPC + Grasp and iTBS-PPC + Rest groups. For the iTBS-CTRL + Grasp group, a non-correlated region was selected as the stimulation location. The stimulation locations for each participant are indicated on a standard brain, and MNI coordinates (mean ± SD) are shown for each group. **(C)** The electric field induced by transcranial magnetic stimulation (TMS) for one participant from each group is shown.

A choice-reaction visuomotor task (CRT) was used as a control task to assess visuomotor function because it does not involve dexterous shaping and manipulating objects by the hand as required by the pegboard task (Fiori et al., 2018). Therefore, CRT is thought to be less associated with the PPC-to-M1 neural pathway. Participants were seated in front of a monitor and viewed stimuli (central number cue: '1' or '2') from 30 cm. Participants were instructed to respond by pressing the '1' or '2' key on the keyboard with the right index or middle finger. Participants were instructed to perform the task as quickly and as accurately as possible. Participants performed 40 trials at every time point before and after (30 and 60 min) the intervention. Visual stimuli were presented, and the mean reaction time (RT) of hand responses was recorded using PsychoPy (version 2021.2.3; Peirce et al., 2019). RT was defined as the interval between the visual number

cue and the correct key button response. Before each experimental session, participants were familiarized with the pegboard and CRT tasks during a short training period with an instructional video[1] followed by a practice block.

## Experimental design

Our study randomly assigned participants to one of three rTMS intervention groups, followed by electrophysiological measures with TMS and behavioral measures (Figure 3A). Participants in the first group received iTBS to the PPC while concurrently performing a grasping task ($iTBS_{PPC+Grasp}$). Participants in the second group received iTBS to the PPC while in an unconstrained, resting state ($iTBS_{PPC+Rest}$). Contrasting these groups allowed us to elucidate the effects of targeted TMS enhancement of parietal–frontal grasping network and motor function and the interaction between parietal iTBS and behavioral state. To test the functional specificity of stimulation to the PPC, a third group of participants received iTBS to a cortical region outside of the grasping network while concurrently performing a grasping task ($iTBS_{Control+Grasp}$).

In Experiment 1 (pilot study), 24 participants received a single session of iTBS aimed at either the PPC or Pz electrode position (Figure 3B). In the second experiment, 48 participants underwent four consecutive daily sessions of iTBS, targeting either the PPC or the cortical control site. Each assessment session tested for the effects of each iTBS protocol on motor cortical excitability (e.g., MEPs) and behavioral performance (e.g., pegboard task and CRT). To measure changes in MEP amplitude, spTMS was applied to M1 at a fixed intensity that produced an MEP of 1 mV. In Experiment 1, we measured MEP amplitudes at baseline and every 15 min for an hour after the iTBS intervention (0, 15, 30, 45, and 60 min). In the second experiment, we measured MEP amplitudes immediately before and after (30 and 60 min) the fourth iTBS session (Figure 3C). Brainsight was used to place the D702 coil over M1 throughout the experiment accurately. Both experiments assessed manual dexterity and CRT before and after the iTBS intervention (30 and 60 min).

## Statistical analysis

Separate one-way analyses of variance (ANOVA) were used to confirm that the three groups ($iTBS_{PPC+Grasp.}$, $iTBS_{PPC+Rest}$, $iTBS_{Control+Grasp}$) did not differ in age or motor cortical excitability at baseline. MEP amplitudes were measured peak-to-peak for maximum and minimum values in the time window between 10 and 50 ms after spTMS (Carson et al., 2004; Fujiyama et al., 2016; Vesia et al., 2018). Changes in motor cortical excitability across Time and Intervention group were tested by fitting a linear mixed-effects model. The transformed MEP amplitude was used as the dependent variable, with the Intervention group and Time as fixed effects and subject as a random effect. Before including the data in the model, outlier MEP amplitudes that deviated by more than 3 units from the absolute median were removed for each subject. In total, 3.5% of all MEPs were excluded in Experiment 1, and 4.2% were excluded in Experiment 2 (Leys et al., 2013). MEP amplitudes were further transformed to account for their non-normal distribution. In Experiment 1, a power transformation of $x^{-0.16}$ was used, while in Experiment 2, a power transformation of $x^{0.017}$ was applied. The model was then tested using type II Wald F tests with Kenward–Roger degrees of freedom correction.

Changes in motor performance were quantified by expressing mean time as a symmetric percentage change from the baseline of the time to complete the pegboard task and mean reaction time on the CRT for each participant. For the pegboard task, symmetric percentages were subjected to an order norm transformation to meet normality assumptions. Then, a linear mixed-effects model was fitted with transformed symmetric percent change as the dependent variable, Intervention group ($iTBS_{PPC+Grasp.}$, $iTBS_{PPC+Rest}$, $iTBS_{Control+Grasp}$), and Time (30, 60 min) as fixed effects, and subject as a random effect. Similarly, for reaction time, values were log-transformed for normality. A linear mixed-effects model was fitted with transformed reaction time as the dependent variable, Intervention group and Time as fixed effects, and subject as a random effect. After fitting each model, type II Wald F tests with Kenward–Roger degrees of freedom correction were used to test for differences.

In addition, Games-Howell *post hoc* *t*-tests were performed on pairwise comparisons of groups to account for unequal variances between groups and control for multiple comparisons' Type I error rate (Games and Howell, 1976). Analyses were performed using IBM SPSS Statistics Version 26.0 (IBM Corp., Armonk, NY, United States) and R (R Core Team, Vienna, Austria, 2022). Data are given as mean ± standard error of the mean (SEM). The threshold for statistical significance was set at $p \leq 0.05$. Where appropriate, partial $\eta$ squared ($\eta_p^2$) values were computed as a measure of effect size. Cutoffs for effect sizes of ≥0.01, ≥0.06, and ≥0.14 are considered small, medium, and large, respectively (Cohen, 1992).

# Results

All participants tolerated the experimental procedures. As shown in Table 1, we found no significant difference between the three groups in age or measures of motor cortical excitability at baseline (Figure 4).

## Effects of the brain state during parietal stimulation on downstream motor cortical excitability

To test the hypothesis that manipulating the behavioral state during stimulation to PPC would affect motor plasticity associated with motor control, we compared changes in the excitability of the motor cortex by measuring the size of TMS-induced MEPs in the three stimulation groups.

### Experiment 1

There were significant main effects of the Intervention group ($F_{2,21} = 4.17$, $p = 0.029$, $\eta_p^2 = 0.28$) and Time ($F_{5,3192.2} = 3.33$, $p = 0.005$, $\eta_p^2 = 0.005$) and a significant Time × Intervention group interaction ($F_{10,3192.2} = 5.66$, $p < 0.001$, $\eta_p^2 = 0.02$) on the MEP amplitudes; Figure 5A). *Post hoc* analyses revealed that MEP amplitudes for the

1 www.nihtoolbox.org

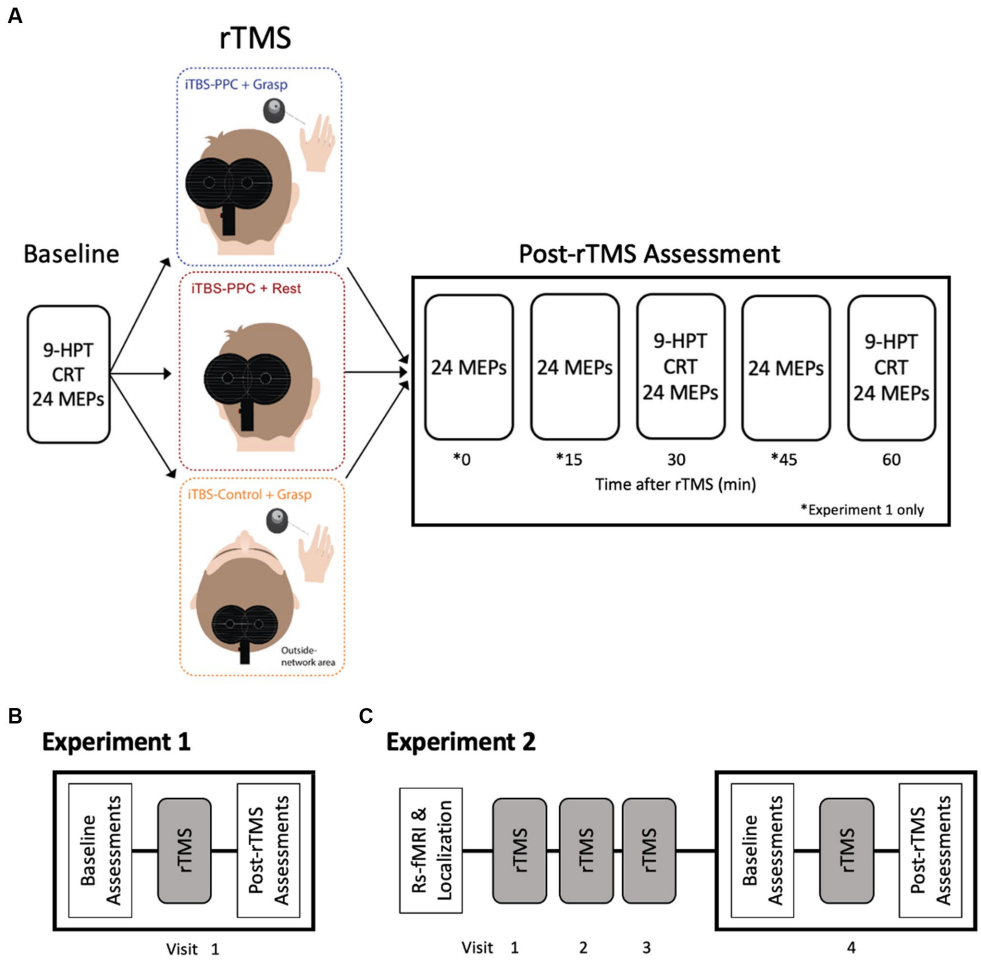


FIGURE 3
Experimental Design. **(A)** Participants were randomly assigned to one of three rTMS intervention groups. Electrophysiological and behavioral measurements were taken before (Baseline) and for an hour after the stimulation intervention. Motor-evoked potential amplitudes were measured at baseline and every 15 min for an hour after the iTBS intervention (0, 15, 30, 45, and 60 min) in Experiment 1 and after 30 and 60 min in Experiment 2. Both experiments measured behavioral performance on a nine-pegboard task (9-HPT) and choice reaction task (CRT) before and after the intervention (30 and 60 min). **(B)** In Experiment 1, participants underwent a single session of stimulation. **(C)** In Experiment 2, participants underwent a structural fMRI scan to determine the parietal stimulation location. Participants received three consecutive daily sessions of rTMS. On Visit 4, participants underwent assessments before (Baseline) and after rTMS, similar to Experiment 1.

$iTBS_{PPC+Grasp}$ group were significantly different from baseline MEPs at 30 min ($p < 0.0001$), and the difference in amplitudes from immediate post-stimulation to 30 min was also significant ($p = 0.002$). For the $iTBS_{PPC+Rest}$ group, MEP amplitudes were significantly different from baseline immediately after stimulation ($p < 0.0001$), at 30 min ($p = 0.03$), and 45 min ($p = 0.03$). Further *post hoc* analyses demonstrated that there were significant differences in MEP amplitude for the $iTBS_{PPC+Grasp}$ group at every time point following baseline compared to both the $iTBS_{PPC+Rest}$ and $iTBS_{Control+Grasp}$ groups (all comparisons $p < 0.0001$, except between $iTBS_{PPC+Grasp}$ and $iTBS_{Control+Grasp}$ immediately post-stimulation, where $p < 0.001$. There were no significant differences in MEP amplitudes between $iTBS_{PPC+Rest}$ and $iTBS_{Control+Grasp}$ at any time point.

Closer inspection of the individualized normalized data showed highly consistent increases in the percentage change of MEP amplitudes across participants at 30 min and 60 min post-stimulation for the $iTBS_{PPC+Grasp}$ group (MEP change (%) increased for 7 out of 8 participants at 30 min; sign test $p = 0.07$; MEP change (%) increased for 6 out of 8 participants at 60 min; sign test $p = 0.29$; Figures 5B,C). Conversely, neither $iTBS_{PPC+Rest}$ (MEP change (%) increased for 1 out of 8 participants at 30 min; sign test $p = 0.07$; MEP change (%) increased for 3 out of 8 participants at 60 min; sign test $p = 0.73$) nor $iTBS_{Control+Grasp}$ (MEP change (%) increased for 2 out of 8 participants at both 30 min and 60 min; sign test $p = 0.29$) affected the magnitude of change in the MEP at these time points.

## Experiment 2

In line with the pilot experiment's findings, Experiment 2 revealed significant main effects of the Intervention group ($F_{2,44} = 5.64$, $p = 0.007$, $\eta_p^2 = 0.2$) and Time ($F_{2,3188.3} = 26.91$, $p < 0.0001$, $\eta_p^2 = 0.02$) and a significant Time × Intervention group interaction ($F_{4,3188.3} = 22.95$, $p < 0.0001$, $\eta_p^2 = 0.03$) on MEP amplitudes (Figure 5D). *Post hoc* tests indicated significant differences in MEP amplitudes for the $iTBS_{PPC+Grasp}$ group from baseline at 30 and 60 min post-stimulation ($p < 0.0001$). MEP amplitudes for $iTBS_{PPC+Rest}$ significantly differed between baseline and 60 min post-stimulation

TABLE 1 Group values for age and stimulator intensities.

| Experiment 1 | | | | |
|---|---|---|---|---|
| | iTBS-PPC + Grasp | iTBS-PPC + Rest | iTBS-Control + Grasp | Statistical comparison |
| Age (years) | 24.0 ± 3.4 | 21.5 ± 2.1 | 24.5 ± 3.3 | $F(2,21) = 2.31$ $p = 0.12$ |
| AMT (% MSO) (MagPro MCF-B70 coil) | 41.6 ± 8.0 | 41.7 ± 8.0 | 39.1 ± 6.7 | $F(2,19) = 0.29$ $p = 0.76$ |
| RMT (% MSO) (Magstim D50 B.I coil) | 45.6 ± 8.6 | 46.9 ± 12.1 | 44 ± 9.3 | $F(2,21) = 0.16$ $p = 0.85$ |
| $SI_{1\,mV}$ (% MSO) (Magstim D70$^2$ coil) | 44.5 ± 6.7 | 47 ± 9.7 | 44.8 ± 9.7 | $F(2,21) = 0.19$ $p = 0.82$ |

| Experiment 2 | | | | |
|---|---|---|---|---|
| | iTBS-PPC + Grasp | iTBS-PPC + Rest | iTBS-Control + Grasp | Statistical comparison |
| Age (years) | 26.4 ± 8.6 | 26.8 ± 8.3 | 27.8 ± 8.3 | $F(2,45) = 0.10$ $p = 0.90$ |
| AMT (% MSO) (MagPro MCF-B70 coil) | 39.5 ± 5.4 | 37.9 ± 3.9 | 40.4 ± 6.2 | $F(2,40) = 0.82$ $p = 0.45$ |
| RMT (% MSO) (Magstim D50 B.I coil) | 43.1 ± 5.6 | 44.5 ± 9.6 | 50 ± 10.9 | $F(2,45) = 2.67$ $p = 0.08$ |
| $SI_{1\,mV}$ (% MSO) (Magstim D70$^2$ coil) | 46.1 ± 7.3 | 47 ± 9.1 | 51.3 ± 11.7 | $F(2,45) = 1.36$ $p = 0.27$ |

Data are presented as mean ± SD. Transcranial magnetic stimulation (TMS) intensity (expressed as a percentage of the maximum stimulator output, % of MSO) of active motor threshold (AMT) and resting motor threshold (RMT). $SI_{1\,mV}$ refers to the percentage of MSO required to produce a ~ 1 mV motor-evoked potential (MEP). Separate one-way analyses of variance (ANOVA) were used to confirm that the three groups did not differ in age or motor cortical excitability at baseline.

($p = 0.002$) and between 30 and 60 min post-stimulation ($p = 0.03$), but not between baseline and 30 min post-stimulation. Conversely, no significant differences in MEP amplitudes were observed between any time points for the $iTBS_{Control + Grasp}$ group. Further *post hoc* tests revealed no significant differences in MEP amplitudes among groups at baseline. However, at both 30 and 60 min post-stimulation, the $iTBS_{PPC + Grasp}$ group showed significantly different MEP amplitudes compared to both $iTBS_{PPC + Rest}$ and $iTBS_{Control + Grasp}$ ($p < 0.0001$). At 60 min post-stimulation, the MEP amplitudes between the $iTBS_{PPC + Rest}$ and $iTBS_{Control + Grasp}$ groups also were significantly different ($p < 0.0001$).

The individualized normalized data showed consistent increases in the percentage change of MEP amplitudes from baseline across participants at 30 min and 60 min post-stimulation for the $iTBS_{PPC + Grasp}$ group (MEP change (%) increased for 15 out of 16 participants at 30 min; sign test $p < 0.0005$; MEP change (%) increased for 16 out of 16 participants at 60 min; sign test $p < 0.0001$; Figures 5E,F). Conversely, neither $iTBS_{PPC + Rest}$ (MEP change (%) increased for 10 out of 16 participants at 30 min; sign test $p = 0.45$; MEP change (%) increased for 12 out of 16 participants at 60 min; sign test $p = 0.08$) nor $iTBS_{Control + Grasp}$ (MEP change (%) increased for 6 out of 16 participants at 30 min; sign test $p = 0.45$; and MEP change (%) increased for 7 out of 16 participants at 60 min; sign test $p = 0.8$) affected the magnitude of change in the MEP at these time points.

Together, these results indicate that the influence of PPC stimulation on motor cortical excitability depended on both the behavioral task being performed and the time at which the assessment was administered. Furthermore, this result reinforces that increased motor cortical excitability resulted from stimulation targeting a specific parietal-motor pathway. Critically, it is apparent that inducing functional activation in the cortical grasping network through a causal behavioral manipulation during parietal stimulation reliably alters downstream motor plasticity.

## The effects of brain state during parietal stimulation on motor performance

### Experiment 1

We examined the participants' motor performance on a pegboard test after (30 and 60 min) each rTMS intervention. There was a significant main effect of the Intervention group ($F_{2,21} = 11.54$, $p < 0.001$, $\eta_p^2 = 0.52$), no main effect of Time ($F_{2,42} = 1.68$, $p = 0.20$, $\eta_p^2 = 0.07$), and a significant interaction between Time and Intervention group ($F_{4,42} = 7.31$, $p < 0.001$, $\eta_p^2 = 0.41$), on the symmetric percentage change from baseline of mean time to complete the pegboard task (Figure 6A). *Post hoc* analyses showed that motor performance significantly improved at each time of measurement for the $iTBS_{PPC + Grasp}$ group compared to the $TBS_{Control + Grasp}$ (30 min, $p = 0.004$; 60 min: $p = 0.002$) and at the 60 min for the $iTBS_{PPC + Rest}$ group ($p = 0.003$). The time to complete the pegboard task decreased for the $iTBS_{PPC + Grasp}$ group, as shown by *post hoc* analyses indicating a significant symmetric percentage change from baseline in motor performance at 30 min ($p = 0.03$) and 60 min ($p < 0.001$). Notably, there was no significant difference in the symmetric percentage from baseline in motor performance at each time point for the $iTBS_{PPC + Rest}$ or the $iTBS_{Control + Grasp}$ groups (all comparisons $p \geq 0.15$).

Improvements in the percentage change from baseline in the time taken to complete the pegboard task were highly consistent across participants in the $iTBS_{PPC + Grasp}$ group (7 out of 8 participants' motor performance improved at 30 min; sign test $p = 0.07$; 8 out of 8 participants motor performance improved at 60 min; sign test

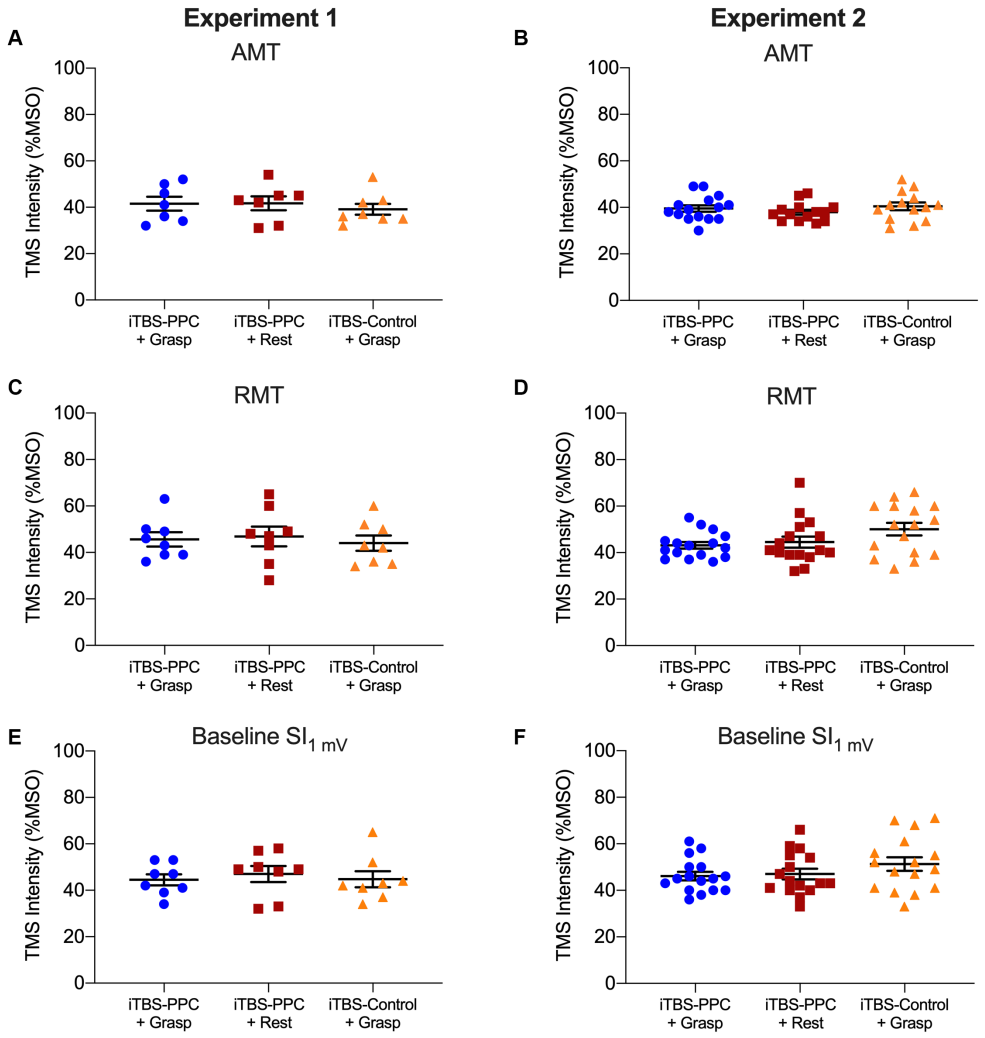


FIGURE 4
Column scatter plots showing the **(A-B)** transcranial magnetic stimulation (TMS) intensity (expressed as a percentage of the maximum stimulator output, MSO) of active motor threshold (AMT), **(C-D)** TMS intensity of resting motor threshold (RMT), and **(E-F)** TMS intensity eliciting 1 mV MEPs at baseline, for each participant for the $iTBS_{PPC+Grasp}$ group (blue circles) and $iTBS_{PPC+Rest}$ group (red squares) and $iTBS_{Control+Grasp}$ group (orange triangles) for each experiment. No differences were found between groups (for statistics, see Table 1).

$p = 0.008$) but not in the $iTBS_{PPC+Rest}$ group (4 out of 8 participants motor performance improved at 30 min; sign test $p = 1.27$; 3 out of 8 participants motor performance improved at 60 min; sign test $p = 0.73$) or the $iTBS_{Control+Grasp}$ group (2 out of 8 participants motor performance improved at 30 min; sign test $p = 0.29$; 3 out of 8 participants motor performance improved at 60 min; sign test $p = 0.73$; Figures 6B,C).

## Experiment 2

The improvements in manual dexterity observed in Experiment 1 were replicated in Experiment 2. We found significant main effects of both Intervention group ($F_{2,45} = 20.98$, $p < 0.001$, $\eta_p^2 = 0.48$) and Time ($F_{2,90} = 3.87$, $p = 0.02$, $\eta_p^2 = 0.08$), as well as a significant Time × Intervention group interaction ($F_{4,90} = 7.61$, $p < 0.001$, $\eta_p^2 = 0.25$) on the symmetric percentage change in the time to complete the pegboard task from baseline (Figure 6D). *Post hoc* tests confirmed that the $iTBS_{PPC+Grasp}$ group showed significant differences from the other intervention groups, and their performance improved over time. Specifically, the $iTBS_{PPC+Grasp}$ group showed significantly different symmetric percentage changes in performance at both 30 and 60 min post-stimulation when compared to either of the other groups ($iTBS_{PPC+Rest}$, 30 min: $p = 0.01$, 60 min: $p = 0.002$; $iTBS_{Control+Grasp}$, 30 min: $p < 0.001$; 60 min: $p < 0.001$). Similar to the findings in Experiment 1, only the $iTBS_{PPC+Grasp}$ group displayed improvements in performance over time, with their symmetric percentage change in time to complete the pegboard task being significantly different from baseline at both 30 and 60 min ($p < 0.001$). In contrast, neither of the other groups showed significant differences at either time (all comparisons $p > 0.07$).

Improvements in the percentage change from baseline in the time taken to complete the pegboard task were highly consistent across participants in the $iTBS_{PPC+Grasp}$ group (15 out of 16 participants' motor performance improved at both 30 and 60 min; sign test $p < 0.0005$) but not in the $iTBS_{PPC+Rest}$ group (10 out of 16 participants motor performance improved at 30 min; sign test $p = 0.45$; 8 out of 16

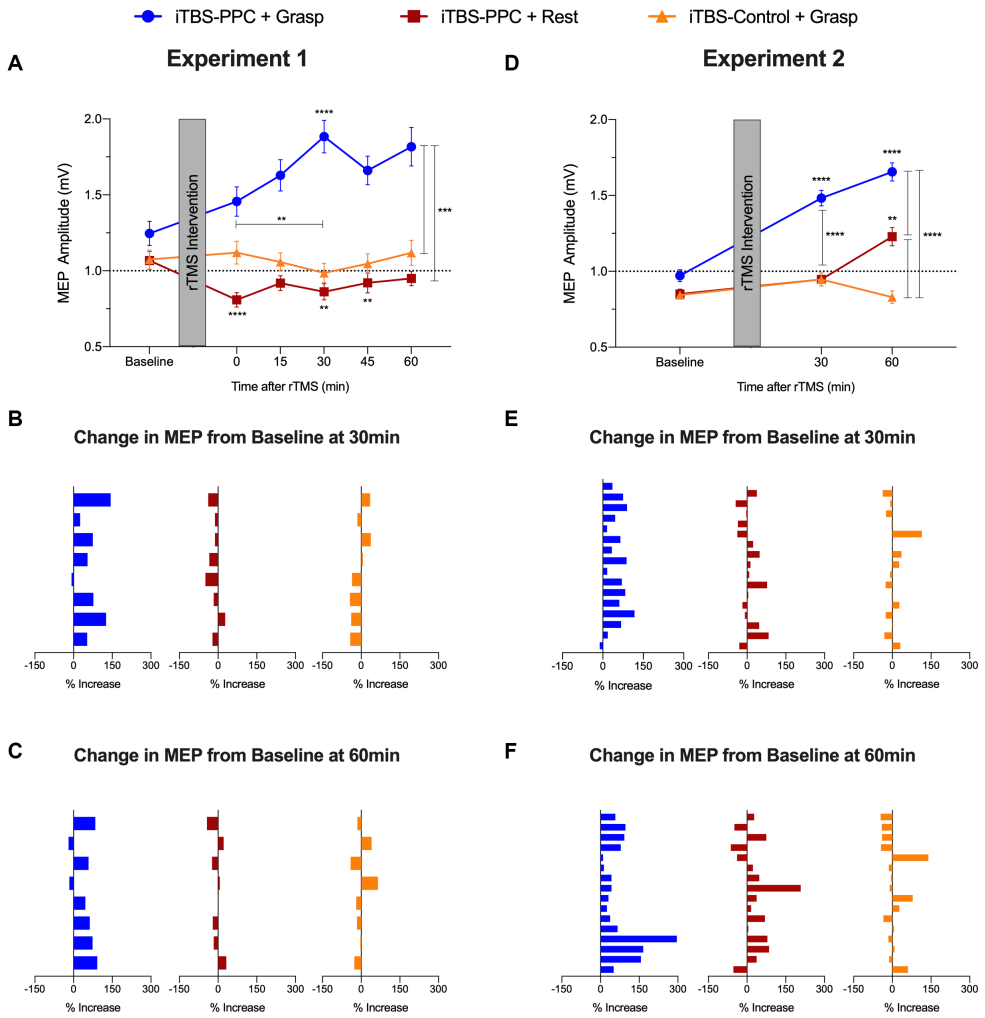


FIGURE 5
Group averaged motor evoked potential (MEP) amplitude (mV) for **(A)** Experiment 1 and **(D)** Experiment 2. Percentage change from baseline of MEP amplitude for each participant **(B)** 30 min and **(C)** 60 min post-stimulation in Experiment 1. Percentage change from baseline of MEP amplitude for each participant **(E)** 30 min and **(F)** 60 min post-stimulation in Experiment 2. Error bars denote the standard error of the mean (SEM). Asterisks indicate significant *post hoc* comparisons, *$p \leq 0.05$, **$p \leq 0.01$, ***$p \leq 0.001$, ****$p \leq 0.0001$.

participants motor performance improved at 60 min; sign test $p = 1.2$) or the $iTBS_{Control+Grasp}$ group (5 out of 16 participants motor performance improved at 30 min; sign test $p = 0.21$; 7 out of 16 participants motor performance improved at 60 min; sign test $p = 0.8$; Figures 6E,F). Thus, motor improvement occurred reliably only when the functional state of the grasp network was engaged with a motor task during the administration of parietal stimulation, not for either control condition. These results underscore the consistent benefits of state-dependent parietal stimulation on manual dexterity across both experiments.

To assess the specificity of the effects of stimulation on motor performance, we compared reaction times for a control visuomotor CRT task that does not involve dexterous hand shaping and object manipulation in both experiments. Across both experiments, no significant differences in visuomotor performance were found across intervention groups or time. In the pilot experiment, after fitting and testing a linear mixed-effect model, there were no main effects of Time ($F_{2,42} = 1.42$, $p = 0.25$, $\eta_p^2 = 0.06$) or Intervention group ($F_{2,21} = 0.03$, $p = 0.97$, $\eta_p^2 < 0.001$), and no significant interaction ($F_{4,42} = 0.60$, $p = 0.67$, $\eta_p^2 = 0.05$; Figure 7A). Similarly, in the second experiment (Figure 7B), there was no significant main effect of Time ($F_{2,90} = 2.64$, $p = 0.07$, $\eta_p^2 = 0.06$), Intervention group ($F_{2,45} = 1.60$, $p = 0.21$, $\eta_p^2 = 0.07$), or interaction ($F_{4,90} = 0.81$, $p = 0.52$, $\eta_p^2 = 0.03$). These findings are consistent with the hypothesis that the effect of parietal stimulation on motor performance is specific to planning and execution states for object-directed grasps rather than a general attention or performance benefit. Motor improvement was selective for skilled object-directed grasps and occurred reliably only when the targeted cortical motor planning network was engaged with a motor behavior at the time of parietal stimulation.

## Discussion

The current study describes brain and behavior responses to intermittent theta burst stimulation to PPC applied during two

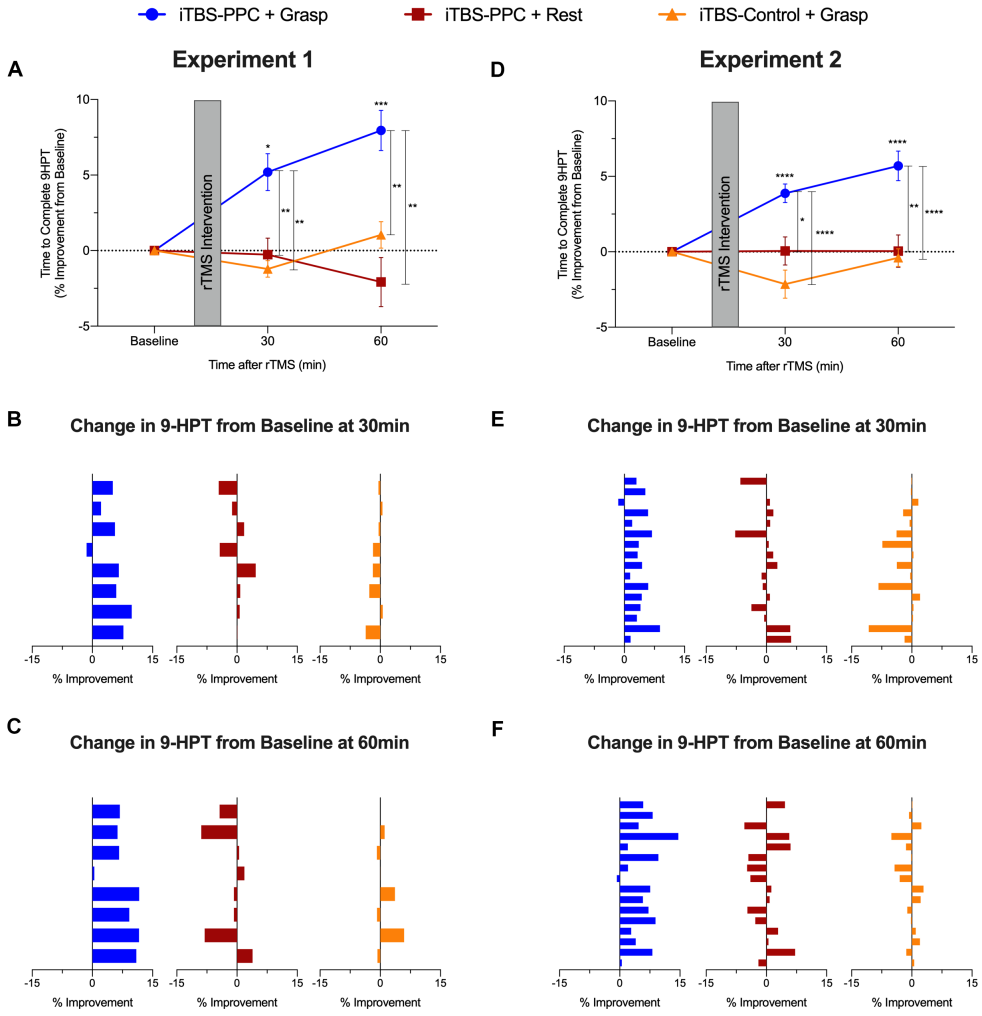


FIGURE 6
Group averaged percentage change from baseline to complete the nine-hole pegboard manual dexterity test (9-HPT) for **(A)** Experiment 1 and (**D**) Experiment 2. Positive values indicate a performance improvement. Mean percentage change from baseline to complete 9-HPT for each participant **(B)** 30 min and **(C)** 60 min post-stimulation in Experiment 1. Mean percentage change from baseline to complete 9-HPT for each participant **(E)** 30 min and **(F)** 60 min post-stimulation in Experiment 2. Error bars denote the standard error of the mean (SEM). Asterisks indicate significant *post hoc* comparisons, *$p \leq 0.05$, **$p \leq 0.01$, ***$p \leq 0.001$, ****$p \leq 0.0001$.

distinct endogenous states of neural activity in the motor system (i.e., brain state at rest versus during action planning and execution). Delivering iTBS to PPC when the cortical grasp network is engaged with a motor task increases the downstream excitability of an interconnected M1 region responsible for fine-motor action and concomitantly improves skilled motor performance for up to an hour. These findings demonstrate that the effects of parietal network-targeted stimulation are brain-state dependent and can influence motor plasticity beyond the stimulated region with high specificity to improve skilled motor control of hand actions immediately after stimulation.

It has been commonly found that there is a large degree of variability in brain activity and behavioral responses following rTMS (Ridding and Rothwell, 2007; Nicolo et al., 2015; Ziemann and Siebner, 2015; Corp et al., 2020; Ozdemir et al., 2020, 2021). For motor control, most work has examined the neural effects of rTMS on a brain at rest (Siebner et al., 2009a; Bergmann et al., 2016). However, recent work has proposed that this variability can be partially explained by state-dependent effects, in which the stimulation response depends on the ongoing level of brain activity during stimulation (Silvanto et al., 2008; Pasley et al., 2009; Romei et al., 2016; Bergmann, 2018; Bradley et al., 2022). In our study, we show that the direction of change in excitability is influenced by the physiological state of the targeted parietal-motor grasp network during stimulation. Our results suggest that PPC's facilitatory influence during grasping may cause recurrent excitation, leading to long-term potentiation-like changes in cortical excitability when stimulated. In contrast, stimulating during periods of PPC-mediated inhibition, such as during rest, may reduce neural activation, resulting in less potentiation. This explanation aligns with studies indicating that the ongoing activity level at the time of stimulation influences corticospinal excitability (Bestmann et al., 2008a; Bestmann and Krakauer, 2015; Zrenner et al., 2018; Naros et al., 2019; Schaworonkow et al., 2019) and is consistent with recent cortico-cortical TMS findings showing remote excitability effects of

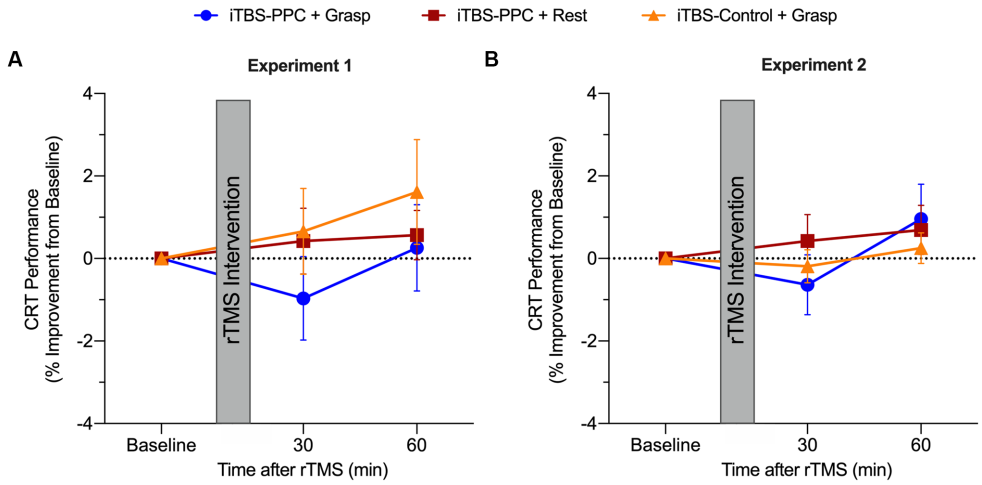


FIGURE 7
Group averaged percentage change from baseline for the choice-reaction visuomotor task (CRT) for 30 and 60 min post-stimulation for **(A)** Experiment 1 and **(B)** Experiment 2. Positive values indicate a performance improvement. Error bars denote the standard error of the mean (SEM).

the parietal cortex on motor cortex reverse in direction with the motor state (Koch et al., 2008; Vesia et al., 2013, 2017).

The current findings also align with TMS's neural and behavioral effects when manipulating sensory, attentional, and cognitive states. Recent findings also have demonstrated that co-administration of low frequency rTMS to the motor cortex with motor training can enhance motor plasticity and improve motor skills in both damaged and intact brains (Bütefisch et al., 2004; Thabit et al., 2010; Buetefisch et al., 2011, 2015; Revill et al., 2020). In addition, cognitive manipulations that direct attention to the hand during rTMS have been shown to produce larger increases in motor cortical excitability (Stefan, 2004; Conte et al., 2007). Other approaches have been used to modulate brain excitability before TMS by selectively preconditioning a specific neuronal population using either stimulation (Siebner, 2004; Ni et al., 2014; Opie et al., 2019) or behavioral adaptation (Silvanto et al., 2007) protocols. For instance, perceptual adaptation has been shown to augment the TMS-induced neural representation of observed motor behavior (Silvanto and Cattaneo, 2014). Our current results extend these prior findings on state-dependent motor responses to rTMS to provide novel physiological evidence that engaging the parietal–frontal network for goal-directed hand movements during parietal stimulation can affect cortical motor output for up to an hour.

The state dependency of neuronal responses to rTMS also can be found in interconnected brain areas (Siebner et al., 2009b). Indeed, it is well established that the effects of stimulation propagate beyond the stimulation site to impact functionally specific brain networks (Siebner et al., 2009a; Fox et al., 2012; Beynel et al., 2020; Lynch et al., 2022). Importantly, the effects of stimulation on brain networks can be influenced by the activation state of interconnected regions within the functional network (Ruff et al., 2006, 2008; Blankenburg et al., 2008, 2010; Moisa et al., 2012). It is possible that the ongoing activity and inherent excitability of neurons can influence the spread of neural excitation within the targeted area and to other regions in the brain. As a result, synchronizing neural firing patterns with stimulation can strengthen connections between neurons and facilitate state-specific changes in the brain (Siebner et al., 2022). For example, activating the motor system with a behavioral task, such as the performance of an isometric hand grip during premotor cortex stimulation, influences contralateral cortex activity (Bestmann et al., 2008b). Cortico-cortical interactions that can be probed with two TMS coils over two connected brain areas have shown dynamic changes in excitability when individuals plan actions (Koch and Rothwell, 2009; Lafleur et al., 2016; Hallett et al., 2017; Goldenkoff et al., 2020; Malderen et al., 2022). Furthermore, our previous dsTMS experiments show that PPC regions involved in encoding hand movements exert an inhibitory influence on motor output at rest. Interestingly, this net inhibitory drive at rest in PPC is facilitated during the preparation of a grasping movement (Vesia et al., 2013, 2017). We, therefore, reasoned that capitalizing on the physiological state of the brain using multi-focal TMS methods can selectively target active neurons when delivering stimulation to the parietal location to enhance the specificity of excitation to the connected motor regions. This approach may increase the excitability of specific neural pathways associated with movement by modulating the connections between pre- and post-synaptic neuronal activities through Hebbian mechanisms (Hebb, 1949; Markram et al., 2011), inducing LTP-like changes in synaptic strength (Suppa et al., 2016). In the current study, intermittent theta burst stimulation may have induced long-lasting changes in cortical excitability by modulating calcium influx via the post-synaptic membrane, resulting in LTP-like effects on cortical synapses (Huang et al., 2011; Suppa et al., 2016). The underlying mechanisms of the brain-state-dependent TMS effects on motor function observed in our data may be activity-dependent plasticity, whereby control over the cortical state with a voluntary movement during stimulation boosts the response in the activated brain network (Siebner et al., 2009b); *cf.* (Paulus and Rothwell, 2016). The current results add to prior research demonstrating that theta burst stimulation to premotor (Huang et al., 2018) and PPC (Premji et al., 2011) regions can impact downstream cortical motor plasticity. Altogether, these findings demonstrate that the effect of stimulation on downstream motor cortical excitability depends on the current state of excitation of the connected brain region being stimulated within the functional network.

The present findings also demonstrate that this state-dependent modulatory effect can improve behavior immediately after stimulation.

For example, we found that theta burst stimulation to the grasping network selectively improves skilled motor performance when the network is active relative to when it is at rest. This result is consistent with previous work in the visual domain, indicating robust state-dependent effects when pairing stimulation with neural activity functionally tuned to visual motion stimuli (Chiappini et al., 2018). One possible mechanism of the immediate state-dependent effect is that selective neural representations and pathways underlying the perceptual and behavioral processes are more susceptible to stimulation (Silvanto et al., 2008; Pasley et al., 2009; Romei et al., 2016; Bradley et al., 2022). Future neuroimaging work is necessary to characterize the neural basis of this neural response, particularly at mesoscale brain circuits that subserve voluntary motor control.

The convergence of the current neurophysiological and behavioral findings strongly suggests that variability in neural activity levels at the time of stimulation contributes to the variability of the responses to rTMS in the motor system. In the current study, the group-averaged data showed that applying theta burst stimulation during a constrained high-activity state through a causal behavioral manipulation improves motor function immediately after stimulation rather than using the same pulse train during spontaneous neural activity discharge while participants are at rest. A closer inspection of individual results clearly shows two distinct patterns diverging based on the functional context of neural activity during stimulation. The group that received brain-state-dependent parietal stimulation showed significant and consistent increases in both excitability and performance in all participants. In contrast, the effects of stimulation on motor plasticity and motor performance changes varied in magnitude and direction across individuals within the control conditions. This implies that variations in resting-state brain activity may influence individual differences in TMS responses and can be reduced by task manipulations (Silvanto et al., 2008; Silvanto and Pascual-Leone, 2008; Siebner et al., 2009b, 2022; Romei et al., 2016; Bergmann, 2018). This relationship may explain, in part, the considerable individual variation in brain and behavior responses within healthy and patient population studies reported in brain stimulation research. Such state-dependent TMS methods can identify novel neural paths to modify the output of the motor cortex and possibly translate into therapeutic approaches that underpin hand control for neurological disorders with aberrant plasticity. Notably, motor impairments after stroke often can be explained by abnormalities in parietal–frontal circuits subserving the integration of sensory input with motor commands, thus demonstrating network-level dysfunction of neural interactions for sensorimotor control (Grefkes and Fink, 2011; Guggisberg et al., 2019). Most therapeutic stimulation has focused on frontal motor circuits (Morishita and Hummel, 2017), encompassing the primary motor cortices, premotor cortices, and supplementary motor areas. Here, we focused on interactions between PPC, a higher-order area significantly involved in action-related processes, and frontal motor areas (Andersen and Cui, 2009). Even though these network effects are relevant to therapeutic response (Fox et al., 2014; Horn and Fox, 2020), few studies have focused modulatory stimulation on the PPC component, an important 'brain hub' (Grefkes and Fink, 2011, 2014; Grefkes and Ward, 2014) of a well-characterized parietal–frontal grasping network (Grafton, 2010; Davare et al., 2011; Vesia and Crawford, 2012; Turella and Lingnau, 2014). This is important because higher levels of functional connectivity in parietal–frontal circuits in the motor system have been related to more favorable motor outcomes after stroke (Schulz et al., 2015, 2016). Given that the current results provide evidence for parietal contributions to motor function, we propose that targeting higher motor areas such as PPC with rTMS, primarily when functionally engaged with other interconnected frontal cortical regions, might be a better alternative for stroke patients with greater sensorimotor impairments (Plow et al., 2014, 2016). Further research is needed to determine the relevance of the proposed rTMS approach in clinical settings.

The current study has some limitations worth noting. First, the number of female participants in Experiment 2 was greater than males. Recent work has highlighted the influence of sex on the brain and behavior responses to TMS (Hanlon and McCalley, 2022). This may relate to various biological metrics, such as the distance between the scalp and cortex, gray matter density, and estradiol and progesterone levels. Still, sex is unlikely to account for the current results because it would be counterbalanced across the intervention groups. In addition, we personalized stimulation intensity based on each participant's neuroanatomy to minimize variance in cortical target site intensities (Stokes et al., 2005). It is also important to consider that the current study did not implement a sham control. We, therefore, cannot rule out the TMS-induced placebo effects on brain and behavioral outcomes (Boucher et al., 2021). We would expect, however, variance in brain and behavior responses in all intervention groups. Yet, our results showed clear and consistent effects of brain-state-dependent parietal TMS on motor excitability and manual dexterity, with notable differences between intervention groups. Future research could benefit from including sham TMS to better differentiate the effects of time on motor function.

In summary, our findings demonstrate that brain-state-dependent stimulation of a higher-order node in the cortical grasping network can alter motor cortical excitability beyond the stimulation site, leading to improved motor control of hand movements for up to an hour. Whether these changes in brain and behavior persist beyond the one-hour period we tested remains to be seen. Similarly, because multiple consecutive days of stimulation can produce long-lasting cumulative effects (Wang and Voss, 2015; Freedberg et al., 2019a,b), future studies should investigate the duration and magnitude of state-dependent changes on motor function caused by multiple-day stimulation, which could be particularly relevant to a clinical cohort. As our data indicate, rTMS results could be more consistent by controlling the behavioral state at the time of stimulation to induce network-specific plasticity in the motor system. It may prove useful to employ this methodological approach to optimize targeted neuromodulation strategies with practiced movements for treating a wide range of neurological disorders marked by movement dysfunction, such as stroke and Parkinson's disease.

## Data availability statement

The raw data supporting the conclusions of this article will be made available by the authors, without undue reservation.

## Ethics statement

The studies involving humans were approved by the University of Michigan IRB. The studies were conducted in accordance with the

local legislation and institutional requirements. The participants provided their written informed consent to participate in this study.

## Author contributions

EG: conceptualization, methodology, formal analysis, writing – original draft, writing – review and editing, visualization. JD: formal analysis, writing – review and editing. DD: investigation, methodology, formal analysis, writing – original draft, writing – review and editing, visualization, project administration. TL: methodology, writing – review and editing, supervision. KM: investigation, methodology, formal analysis, project administration, writing – review and editing. JB: methodology, formal analysis, writing – review and editing. ST: methodology, writing – review and editing. TP: methodology, writing – review and editing. MV: conceptualization, investigation, methodology, resources, writing – review and editing, supervision, funding acquisition. All authors contributed to the article and approved the submitted version.

## Funding

The work was supported by R21NS118055 and S10OD026738 from the National Institutes of Health, the University of Michigan School of Kinesiology Pilot Research Grant, and Mcubed seed-funding from the University of Michigan Office of Research (UMOR). EG was supported by National Science Foundation Graduate Research Fellowship Program (NSF GRFP). A Rackham Merit Fellowship from the University of Michigan supported JD.

## Acknowledgments

We are grateful to Megan Gordon, Tess Davis, Julianna King, Jordan Raschi, Varun Karmaravel, Maxine Kugelmas, and Ashley Rettmann for their assistance in data collection and analysis.

## Conflict of interest

The authors declare that the research was conducted in the absence of any commercial or financial relationships that could be construed as a potential conflict of interest.

## Publisher's note



## References

Andersen, R. A., and Cui, H. (2009). Intention, action planning, and decision making in parietal-frontal circuits. *Neuron* 63, 568–583. doi: 10.1016/j.neuron.2009.08.028

Bear, M. F., and Malenka, R. C. (1994). Synaptic plasticity: LTP and LTD. *Curr. Opin. Neurobiol.* 4, 389–399. doi: 10.1016/0959-4388(94)90101-5

Berardelli, A., Inghilleri, M., Rothwell, J. C., Romeo, S., Currà, A., Gilio, F., et al. (1998). Facilitation of muscle evoked responses after repetitive cortical stimulation in man. *Exp. Brain Res.* 122, 79–84. doi: 10.1007/s002210050493

Bergmann, T. O. (2018). Brain state-dependent brain stimulation. *Front Psychol* 9, 10–14. doi: 10.3389/fpsyg.2018.02108

Bergmann, T. O., Karabanov, A., Hartwigsen, G., Thielscher, A., and Siebner, H. R. (2016). Combining non-invasive transcranial brain stimulation with neuroimaging and electrophysiology: current approaches and future perspectives. *NeuroImage* 140, 4–19. doi: 10.1016/j.neuroimage.2016.02.012

Bestmann, S., Berker, A. O., and Bonaiuto, J. (2015). Understanding the behavioural consequences of noninvasive brain stimulation. *Trends Cogn Sci (Regul Ed)* 19, 13–20. doi: 10.1016/j.tics.2014.10.003

Bestmann, S., Harrison, L. M., Blankenburg, F., Mars, R. B., Haggard, P., Friston, K. J., et al. (2008a). Influence of uncertainty and surprise on human corticospinal excitability during preparation for action. *Curr. Biol.* 18, 775–780. doi: 10.1016/j.cub.2008.04.051

Bestmann, S., and Krakauer, J. W. (2015). The uses and interpretations of the motor-evoked potential for understanding behaviour. *Exp. Brain Res.* 233, 679–689. doi: 10.1007/s00221-014-4183-7

Bestmann, S., Swayne, O., Blankenburg, F., Ruff, C. C., Haggard, P., Weiskopf, N., et al. (2008b). Dorsal premotor cortex exerts state-dependent causal influences on activity in contralateral primary motor and dorsal premotor cortex. *Cereb. Cortex* 18, 1281–1291. doi: 10.1093/cercor/bhm159

Beynel, L., Powers, J. P., and Appelbaum, L. G. (2020). Effects of repetitive transcranial magnetic stimulation on resting-state connectivity: a systematic review. *NeuroImage* 211:116596. doi: 10.1016/j.neuroimage.2020.116596

Blankenburg, F., Ruff, C. C., Bestmann, S., Bjoertomt, O., Eshel, N., Josephs, O., et al. (2008). Interhemispheric effect of parietal TMS on somatosensory response confirmed directly with concurrent TMS-fMRI. *J. Neurosci.* 28, 13202–13208. doi: 10.1523/jneurosci.3043-08.2008

Blankenburg, F., Ruff, C. C., Bestmann, S., Bjoertomt, O., Josephs, O., Deichmann, R., et al. (2010). Studying the role of human parietal cortex in visuospatial attention with concurrent TMS-fMRI. *Cereb. Cortex* 20, 2702–2711. doi: 10.1093/cercor/bhq015

Boucher, P. O., Ozdemir, R. A., Momi, D., Burke, M. J., Jannati, A., Fried, P. J., et al. (2021). Sham-derived effects and the minimal reliability of theta burst stimulation. *Sci. Rep.* 11:21170. doi: 10.1038/s41598-021-98751-w

Bradley, C., Nydam, A. S., Dux, P. E., and Mattingley, J. B. (2022). State-dependent effects of neural stimulation on brain function and cognition. *Nat. Rev. Neurosci.* 23, 459–475. doi: 10.1038/s41583-022-00598-1

Buch, E. R., Liew, S.-L., and Cohen, L. G. (2017). Plasticity of sensorimotor networks. *Neuroscientist* 23, 185–196. doi: 10.1177/1073858416638641

Buetefisch, C., Heger, R., Schicks, W., Seitz, R., and Netz, J. (2011). Hebbian-type stimulation during robot-assisted training in patients with stroke. *Neurorehabil. Neural Repair* 25, 645–655. doi: 10.1177/1545968311402507

Buetefisch, C. M., Howard, C., Korb, C., Haut, M. W., Shuster, L., Pergami, P., et al. (2015). Conditions for enhancing the encoding of an elementary motor memory by rTMS. *Clin. Neurophysiol.* 126, 581–593. doi: 10.1016/j.clinph.2014.07.006

Bunday, K. L., and Perez, M. A. (2012). Motor recovery after spinal cord injury enhanced by strengthening corticospinal synaptic transmission. *Curr. Biol.* 22, 2355–2361. doi: 10.1016/j.cub.2012.10.046

Bütefisch, C. M., Khurana, V., Kopylev, L., and Cohen, L. G. (2004). Enhancing encoding of a motor memory in the primary motor cortex by cortical stimulation. *J. Neurophysiol.* 91, 2110–2116. doi: 10.1152/jn.01038.2003

Capocchi, G., Zampolini, M., and Larson, J. (1992). Theta burst stimulation is optimal for induction of LTP at both apical and basal dendritic synapses on hippocampal CA1 neurons. *Brain Res.* 591, 332–336. doi: 10.1016/0006-8993(92)91715-q

Carson, R. G., Riek, S., Mackey, D. C., Meichenbaum, D. P., Willms, K., Forner, M., et al. (2004). Excitability changes in human forearm corticospinal projections and spinal reflex pathways during rhythmic voluntary movement of the opposite limb. *J. Physiol. Lond.* 560, 929–940. doi: 10.1113/jphysiol.2004.069088

Chen, R., and Udupa, K. (2009). Measurement and modulation of plasticity of the motor system in humans using transcranial magnetic stimulation. *Mot. Control.* 13, 442–453. doi: 10.1123/mcj.13.4.442

Chiappini, E., Silvanto, J., Hibbard, P. B., Avenanti, A., and Romei, V. (2018). Strengthening functionally specific neural pathways with transcranial brain stimulation. *Curr. Biol.* 28, R735–R736. doi: 10.1016/j.cub.2018.05.083

Cisek, P., and Kalaska, J. F. (2010). Neural mechanisms for interacting with a world full of action choices. *Annu. Rev. Neurosci.* 33, 269–298. doi: 10.1146/annurev.neuro.051508.135409

Cohen, J. (1992). A power primer. *Psychol. Bull.* 112, 155–159. doi: 10.1037/0033-2909.112.1.155

Conte, A., Gilio, F., Iezzi, E., Frasca, V., Inghilleri, M., and Berardelli, A. (2007). Attention influences the excitability of cortical motor areas in healthy humans. *Exp. Brain Res.* 182, 109–117. doi: 10.1007/s00221-007-0975-3

Corp, D. T., Bereznicki, H. G. K., Clark, G. M., Youssef, G. J., Fried, P. J., Jannati, A., et al. (2020). Large-scale analysis of interindividual variability in theta-burst stimulation data: results from the 'Big TMS data Collaboration'. *Brain Stimul.* 13, 1476–1488. doi: 10.1016/j.brs.2020.07.018

Crawford, J. D., Henriques, D. Y. P., and Medendorp, W. P. (2011). Three-dimensional transformations for goal-directed action. *Annu. Rev. Neurosci.* 34, 309–331. doi: 10.1146/annurev-neuro-061010-113749

Davare, M., Kraskov, A., Rothwell, J. C., and Lemon, R. N. (2011). Interactions between areas of the cortical grasping network. *Curr. Opin. Neurobiol.* 21, 565–570. doi: 10.1016/j.conb.2011.05.021

Davare, M., Rothwell, J. C., and Lemon, R. N. (2010). Causal connectivity between the human anterior intraparietal area and premotor cortex during grasp. *Curr. Biol.* 20, 176–181. doi: 10.1016/j.cub.2009.11.063

Fattori, P., Breveglieri, R., Bosco, A., Gamberini, M., and Galletti, C. (2015). Vision for Prehension in the medial parietal cortex. *Cereb. Cortex* bhv302:bhv302. doi: 10.1093/cercor/bhv302

Fiori, F., Chiappini, E., and Avenanti, A. (2018). Enhanced action performance following TMS manipulation of associative plasticity in ventral premotor-motor pathway. *NeuroImage* 183, 847–858. doi: 10.1016/j.neuroimage.2018.09.002

Fox, M. D. (2018). Mapping symptoms to brain networks with the human connectome. *N. Engl. J. Med.* 379, 2237–2245. doi: 10.1056/nejmra1706158

Fox, M. D., Buckner, R. L., Liu, H., Chakravarty, M. M., Lozano, A. M., and Pascual-Leone, A. (2014). Resting-state networks link invasive and noninvasive brain stimulation across diverse psychiatric and neurological diseases. *Proc. Natl. Acad. Sci. U. S. A.* 111, E4367–E4375. doi: 10.1073/pnas.1405003111

Fox, M. D., Halko, M. A., Eldaief, M. C., and Pascual-Leone, A. (2012). Measuring and manipulating brain connectivity with resting state functional connectivity magnetic resonance imaging (fcMRI) and transcranial magnetic stimulation (TMS). *NeuroImage* 62, 2232–2243. doi: 10.1016/j.neuroimage.2012.03.035

Freedberg, M., Reeves, J. A., Toader, A. C., Hermiller, M. S., Kim, E., Haubenberger, D., et al. (2019a). Optimizing hippocampal-cortical network modulation via repetitive transcranial magnetic stimulation: a dose-finding study using the continual reassessment method. *Neuromodulation* 23, 366–372. doi: 10.1111/ner.13052

Freedberg, M., Reeves, J. A., Toader, A. C., Hermiller, M. S., Voss, J. L., and Wassermann, E. M. (2019b). Persistent enhancement of hippocampal network connectivity by parietal rTMS is reproducible. *eNeuro* 6. doi: 10.1523/eneuro.0129-19.2019

Fujiyama, H., Soom, J. V., Rens, G., Gooijers, J., Leunissen, I., Levin, O., et al. (2016). Age-related changes in frontal network structural and functional connectivity in relation to bimanual movement control. *J. Neurosci.* 36, 1808–1822. doi: 10.1523/jneurosci.3355-15.2016

Gallivan, J. P., Chapman, C. S., Wolpert, D. M., and Flanagan, J. R. (2018). Decision-making in sensorimotor control. *Nat. Rev. Neurosci.* 19, 519–534. doi: 10.1038/s41583-018-0045-9

Gallivan, J. P., and Culham, J. C. (2015). Neural coding within human brain areas involved in actions. *Curr. Opin. Neurobiol.* 33, 141–149. doi: 10.1016/j.conb.2015.03.012

Games, P. A., and Howell, J. F. (1976). Pairwise multiple comparison procedures with unequal N's and/or variances: a Monte Carlo study. *J. Educ. Stat.* 1:113. doi: 10.2307/1164979

Glasser, M. F., Coalson, T. S., Robinson, E. C., Hacker, C. D., Harwell, J., Yacoub, E., et al. (2016). A multi-modal parcellation of human cerebral cortex. *Nature* 536, 171–178. doi: 10.1038/nature18933

Goldenkoff, E. R., Mashni, A., Michon, K. J., Lavis, H., and Vesia, M. (2020). Measuring and manipulating functionally specific neural pathways in the human motor system with transcranial magnetic stimulation. *J Vis Exp*, 1–13. doi: 10.3791/60706

Grafton, S. T. (2010). The cognitive neuroscience of prehension: recent developments. *Exp. Brain Res.* 204, 475–491. doi: 10.1007/s00221-010-2315-2

Grefkes, C., and Fink, G. R. (2011). Reorganization of cerebral networks after stroke: new insights from neuroimaging with connectivity approaches. *Brain* 134, 1264–1276. doi: 10.1093/brain/awr033

Grefkes, C., and Fink, G. R. (2014). Connectivity-based approaches in stroke and recovery of function. *Lancet Neurol.* 13, 206–216. doi: 10.1016/s1474-4422(13)70264-3

Grefkes, C., and Ward, N. S. (2014). Cortical reorganization after stroke: how much and how functional? *Neuroscientist* 20, 56–70. doi: 10.1177/1073858413491147

Grice, K. O., Vogel, K. A., Le, V., Mitchell, A., Muniz, S., and Vollmer, M. A. (2003). Adult norms for a commercially available nine hole peg test for finger dexterity. *Am. J. Occup. Ther.* 57, 570–573. doi: 10.5014/ajot.57.5.570

Groppa, S., Oliviero, A., Eisen, A., Quartarone, A., Cohen, L. G., Mall, V., et al. (2012). A practical guide to diagnostic transcranial magnetic stimulation: report of an IFCN committee. *Clin. Neurophysiol.* 123, 858–882. doi: 10.1016/j.clinph.2012.01.010

Guggisberg, A. G., Koch, P. J., Hummel, F. C., and Buetefisch, C. M. (2019). Brain networks and their relevance for stroke rehabilitation. *Clin. Neurophysiol.* 130, 1098–1124. doi: 10.1016/j.clinph.2019.04.004

Hallett, M. (2007). Transcranial magnetic stimulation: a primer. *Neuron* 55, 187–199. doi: 10.1016/j.neuron.2007.06.026

Hallett, M., Iorio, R. D., Rossini, P. M., Park, J. E., Chen, R., Celnik, P., et al. (2017). Contribution of transcranial magnetic stimulation to assessment of brain connectivity and networks. *Clin. Neurophysiol.* 128, 2125–2139. doi: 10.1016/j.clinph.2017.08.007

Hanlon, C. A., and McCalley, D. M. (2022). Sex/gender as a factor that influences transcranial magnetic stimulation treatment outcome: three potential biological explanations. *Front. Psych.* 13:869070. doi: 10.3389/fpsyt.2022.869070

Hardwick, R. M., Rottschy, C., Miall, R. C., and Eickhoff, S. B. (2013). A quantitative meta-analysis and review of motor learning in the human brain. *NeuroImage* 67, 283–297. doi: 10.1016/j.neuroimage.2012.11.020

Hebb, D. O. (1949). The Organization of Behavior: A Neurophysiological Approach. *1st Edn*. (Psychology Press). Available at: http://scholar.google.comjavascript:void (Accessed May 1, 2002).

Herwig, U., Satrapi, P., and Schönfeldt-Lecuona, C. (2004). Using the international 10-20 EEG system for positioning of transcranial magnetic stimulation. *Brain Topogr.* 16, 95–99. doi: 10.1023/B:BRAT.0000006333.93597.9d

Horn, A., and Fox, M. D. (2020). Opportunities of connectomic neuromodulation. *NeuroImage* 221:117180. doi: 10.1016/j.neuroimage.2020.117180

Huang, Y.-Z., Chen, R.-S., Fong, P.-Y., Rothwell, J. C., Chuang, W.-L., Weng, Y.-H., et al. (2018). Inter-cortical modulation from premotor to motor plasticity. *J. Physiol. Lond.* 596, 4207–4217. doi: 10.1113/jp276276

Huang, Y.-Z., Edwards, M. J., Rounis, E., Bhatia, K. P., and Rothwell, J. C. (2005). Theta burst stimulation of the human motor cortex. *Neuron* 45, 201–206. doi: 10.1016/j.neuron.2004.12.033

Huang, Y.-Z., Rothwell, J. C., Chen, R.-S., Lu, C.-S., and Chuang, W.-L. (2011). The theoretical model of theta burst form of repetitive transcranial magnetic stimulation. *Clin. Neurophysiol.* 122, 1011–1018. doi: 10.1016/j.clinph.2010.08.016

Kalaska, J. F., Scott, S. H., Cisek, P., and Sergio, L. E. (1997). Cortical control of reaching movements. *Curr. Opin. Neurobiol.* 7, 849–859. doi: 10.1016/S0959-4388(97)80146-8

Karabanov, A. N., Chao, C.-C., Paine, R., and Hallett, M. (2013). Mapping different intra-hemispheric parietal-motor networks using twin coil TMS. *Brain Stimul.* 6, 384–389. doi: 10.1016/j.brs.2012.08.002

Keel, J. C., Smith, M. J., and Wassermann, E. M. (2001). A safety screening questionnaire for transcranial magnetic stimulation. *Clin. Neurophysiol.* 112:720. doi: 10.1016/S1388-2457(00)00518-6

Khammash, D., Simmonite, M., Polk, T. A., Taylor, S. F., and Meehan, S. K. (2020). Probing short-latency cortical inhibition in the visual cortex with transcranial magnetic stimulation: a reliability study. *Brain Stimul.* 12, 702–704. doi: 10.1016/j.brs.2019.01.013

Koch, G. (2020). Cortico-cortical connectivity: the road from basic neurophysiological interactions to therapeutic applications. *Exp. Brain Res.* 238, 1677–1684. doi: 10.1007/s00221-020-05844-5

Koch, G., Cercignani, M., Pecchioli, C., Versace, V., Oliveri, M., Caltagirone, C., et al. (2010). In vivo definition of parieto-motor connections involved in planning of grasping movements. *NeuroImage* 51, 300–312. doi: 10.1016/j.neuroimage.2010.02.022

Koch, G., Olmo, M. F. D., Cheeran, B., Ruge, D., Schippling, S., Caltagirone, C., et al. (2007). Focal stimulation of the posterior parietal cortex increases the excitability of the ipsilateral motor cortex. *J. Neurosci.* 27, 6815–6822. doi: 10.1523/jneurosci.0598-07.2007

Koch, G., Olmo, M. F. D., Olmo, M. F. D., Cheeran, B., Schippling, S., Caltagirone, C., et al. (2008). Functional interplay between posterior parietal and ipsilateral motor cortex revealed by twin-coil transcranial magnetic stimulation during reach planning toward contralateral space. *J. Neurosci.* 28, 5944–5953. doi: 10.1523/jneurosci.0957-08.2008

Koch, G., and Rothwell, J. C. (2009). TMS investigations into the task-dependent functional interplay between human posterior parietal and motor cortex. *Behav. Brain Res.* 202, 147–152. doi: 10.1016/j.bbr.2009.03.023

Lafleur, L.-P., Tremblay, S., Whittingstall, K., and Lepage, J.-F. (2016). Assessment of effective connectivity and plasticity with dual-coil transcranial magnetic stimulation. *Brain Stimul.* 9, 347–355. doi: 10.1016/j.brs.2016.02.010

Leys, C., Ley, C., Klein, O., Bernard, P., and Licata, L. (2013). Detecting outliers: do not use standard deviation around the mean, use absolute deviation around the median. *J. Exp. Soc. Psychol.* 49, 764–766. doi: 10.1016/j.jesp.2013.03.013

Lynch, C. J., Elbau, I. G., Ng, T. H., Wolk, D., Zhu, S., Ayaz, A., et al. (2022). Automated optimization of TMS coil placement for personalized functional network engagement. *Neuron* 110, 3263–3277.e4. doi: 10.1016/j.neuron.2022.08.012

Malderen, S. V., Hehl, M., Verstraelen, S., Swinnen, S. P., and Cuypers, K. (2022). Dual-site TMS as a tool to probe effective interactions within the motor network: a review. *Rev. Neurosci.* 34, 129–221. doi: 10.1515/revneuro-2022-0020

Markram, H., Gerstner, W., and Sjöström, P. J. (2011). A history of spike-timing-dependent plasticity. *Front. Synaptic Neurosci.* 3:4. doi: 10.3389/fnsyn.2011.00004

Mathiowetz, V., Volland, G., Kashman, N., and Weber, K. (1985). Adult norms for the box and block test of manual dexterity. *Am. J. Occup. Ther.* 39, 386–391. doi: 10.5014/ajot.39.6.386

Moisa, M., Siebner, H. R., Pohmann, R., and Thielscher, A. (2012). Uncovering a context-specific connectional fingerprint of human dorsal premotor cortex. *J. Neurosci.* 32, 7244–7252. doi: 10.1523/jneurosci.2757-11.2012

Morishita, T., and Hummel, F. C. (2017). Non-invasive brain stimulation (NIBS) in motor recovery after stroke: concepts to increase efficacy. *Curr. Behav. Neurosci. Rep.* 4, 280–289. doi: 10.1007/s40473-017-0121-x

Naros, G., Lehnertz, T., Leão, M. T., Ziemann, U., and Gharabaghi, A. (2019). Brain state-dependent gain modulation of corticospinal output in the active motor system. *Cereb. Cortex* 30, 371–381. doi: 10.1093/cercor/bhz093

Ni, Z., Gunraj, C., Kailey, P., Cash, R. F. H., and Chen, R. (2014). Heterosynaptic modulation of motor cortical plasticity in human. *J. Neurosci.* 34, 7314–7321. doi: 10.1523/jneurosci.4714-13.2014

Nicolo, P., Ptak, R., and Guggisberg, A. G. (2015). Variability of behavioural responses to transcranial magnetic stimulation: origins and predictors. *Neuropsychologia* 74, 137–144. doi: 10.1016/j.neuropsychologia.2015.01.033

Oberman, L., Edwards, D., and Eldaief, M. (2011). Safety of theta burst transcranial magnetic stimulation: a systematic review of the literature. *J. Clin. Neurophysiol.* 28, 67–74. doi: 10.1097/wnp.0b013e318205135f

Okamoto, M., Dan, H., Sakamoto, K., Takeo, K., Shimizu, K., Kohno, S., et al. (2004). Three-dimensional probabilistic anatomical cranio-cerebral correlation via the international 10-20 system oriented for transcranial functional brain mapping. *NeuroImage* 21, 99–111. doi: 10.1016/j.neuroimage.2003.08.026

Oldfield, R. C. (1971). The assessment and analysis of handedness: the Edinburgh inventory. *Neuropsychologia* 9, 97–113. doi: 10.1016/0028-3932(71)90067-4

Oliver, R., Bjoertomt, O., Driver, J., Greenwood, R., and Rothwell, J. (2009). Novel "hunting" method using transcranial magnetic stimulation over parietal cortex disrupts visuospatial sensitivity in relation to motor thresholds. *Neuropsychologia* 47, 3152–3161. doi: 10.1016/j.neuropsychologia.2009.07.017

Opie, G. M., Vosnakis, E., Ridding, M. C., Ziemann, U., and Semmler, J. G. (2019). Priming theta burst stimulation enhances motor cortex plasticity in young but not old adults. *Brain Stimul.* 10, 298–304. doi: 10.1016/j.brs.2017.01.003

Ozdemir, R. A., Boucher, P., Fried, P. J., Momi, D., Jannati, A., Pascual-Leone, A., et al. (2021). Reproducibility of cortical response modulation induced by intermittent and continuous theta-burst stimulation of the human motor cortex. *Brain Stimul.* 14, 949–964. doi: 10.1016/j.brs.2021.05.013

Ozdemir, R. A., Tadayon, E., Boucher, P., Momi, D., Karakhanyan, K. A., Fox, M. D., et al. (2020). Individualized perturbation of the human connectome reveals reproducible biomarkers of network dynamics relevant to cognition. *Proc. Natl. Acad. Sci. U. S. A.* 117, 8115–8125. doi: 10.1073/pnas.1911240117

Pasley, B. N., Allen, E. A., and Freeman, R. D. (2009). State-dependent variability of neuronal responses to transcranial magnetic stimulation of the visual cortex. *Neuron* 62, 291–303. doi: 10.1016/j.neuron.2009.03.012

Paulus, W., and Rothwell, J. C. (2016). Membrane resistance and shunting inhibition: where biophysics meets state-dependent human neurophysiology. *J. Physiol.* 594, 2719–2728. doi: 10.1113/jp271452

Peirce, J., Gray, J. R., Simpson, S., MacAskill, M., Höchenberger, R., Sogo, H., et al. (2019). PsychoPy2: experiments in behavior made easy. *Behav. Res. Methods* 51, 195–203. doi: 10.3758/s13428-018-01193-y

Plow, E. B., Cunningham, D. A., Varnerin, N., and Machado, A. (2014). Rethinking stimulation of the brain in stroke rehabilitation: why higher motor areas might be better alternatives for patients with greater impairments. *Neuroscientist* 21, 225–240. doi: 10.1177/1073858414537381

Plow, E. B., Sankarasubramanian, V., Cunningham, D. A., Potter-Baker, K., Varnerin, N., Cohen, L. G., et al. (2016). Models to tailor brain stimulation therapies in stroke. *Neural Plast.* 2016, 1–17. doi: 10.1155/2016/4071620

Premji, A., Rai, N., and Nelson, A. (2011). Area 5 influences excitability within the primary motor cortex in humans. *PLoS One* 6:e20023. doi: 10.1371/journal.pone.0020023

Raffin, E., and Siebner, H. R. (2014). Transcranial brain stimulation to promote functional recovery after stroke. *Curr. Opin. Neurol.* 27, 54–60. doi: 10.1097/wco.0000000000000059

Revill, K. P., Haut, M. W., Belagaje, S. R., Nahab, F., Drake, D., and Buetefisch, C. M. (2020). Hebbian-type primary motor cortex stimulation: a potential treatment of impaired hand function in chronic stroke patients. *Neurorehabil. Neural Repair* 34, 159–171. doi: 10.1177/1545968319899911

Ridding, M. C., and Rothwell, J. C. (2007). Is there a future for therapeutic use of transcranial magnetic stimulation? *Nat. Rev. Neurosci.* 8, 559–567. doi: 10.1038/nrn2169

Romei, V., Thut, G., and Silvanto, J. (2016). Information-based approaches of noninvasive transcranial brain stimulation. *Trends Neurosci.* 39, 782–795. doi: 10.1016/j.tins.2016.09.001

Rossi, S., Antal, A., Bestmann, S., Bikson, M., Brewer, C., Brockmöller, J., et al. (2021). Safety and recommendations for TMS use in healthy subjects and patient populations, with updates on training, ethical and regulatory issues: expert guidelines. *Clin. Neurophysiol.* 132, 269–306. doi: 10.1016/j.clinph.2020.10.003

Rossi, S., Hallett, M., Rossini, P. M., and Pascual-Leone, A. (2011). Screening questionnaire before TMS: an update. *Clin. Neurophysiol.* 122:1686. doi: 10.1016/j.clinph.2010.12.037

Rossini, P. M., Barker, A. T., Berardelli, A., Caramia, M. D., Caruso, G., Cracco, R. Q., et al. (1994). Non-invasive electrical and magnetic stimulation of the brain, spinal cord and roots: basic principles and procedures for routine clinical application. Report of an IFCN committee. *Electroencephalogr. Clin. Neurophysiol.* 91, 79–92. doi: 10.1016/0013-4694(94)90029-9

Rossini, P. M., Burke, D., Chen, R., Cohen, L. G., Daskalakis, Z., Iorio, R. D., et al. (2015). Non-invasive electrical and magnetic stimulation of the brain, spinal cord, roots and peripheral nerves: basic principles and procedures for routine clinical and research application. An updated report from an I.F.C.N. Committee. *Clin. Neurophysiol.* 126, 1071–1107. doi: 10.1016/j.clinph.2015.02.001

Ruff, C. C., Bestmann, S., Blankenburg, F., Bjoertomt, O., Josephs, O., Weiskopf, N., et al. (2008). Distinct causal influences of parietal versus frontal areas on human visual cortex: evidence from concurrent TMS-fMRI. *Cereb. Cortex* 18, 817–827. doi: 10.1093/cercor/bhm128

Ruff, C. C., Blankenburg, F., Bjoertomt, O., Bestmann, S., Freeman, E., Haynes, J.-D., et al. (2006). Concurrent TMS-fMRI and psychophysics reveal frontal influences on human retinotopic visual cortex. *Curr. Biol.* 16, 1479–1488. doi: 10.1016/j.cub.2006.06.057

Sanes, J. N., and Donoghue, J. P. (2000). Plasticity and primary motor cortex. *Annu. Rev. Neurosci.* 23, 393–415. doi: 10.1146/annurev.neuro.23.1.393

Schaworonkow, N., Triesch, J., Ziemann, U., and Zrenner, C. (2019). EEG-triggered TMS reveals stronger brain state-dependent modulation of motor evoked potentials at weaker stimulation intensities. *Brain Stimul.* 12, 110–118. doi: 10.1016/j.brs.2018.09.009

Schulz, R., Buchholz, A., Frey, B. M., Bönstrup, M., Cheng, B., Thomalla, G., et al. (2016). Enhanced effective connectivity between primary motor cortex and intraparietal sulcus in well-recovered stroke patients. *Stroke* 47, 482–489. doi: 10.1161/strokeaha.115.011641

Schulz, R., Koch, P., Zimerman, M., Wessel, M., Bönstrup, M., Thomalla, G., et al. (2015). Parietofrontal motor pathways and their association with motor function after stroke. *Brain* 138, 1949–1960. doi: 10.1093/brain/awv100

Siebner, H. R. (2004). Preconditioning of low-frequency repetitive transcranial magnetic stimulation with transcranial direct current stimulation: evidence for homeostatic plasticity in the human motor cortex. *J. Neurosci.* 24, 3379–3385. doi: 10.1523/jneurosci.5316-03.2004

Siebner, H. R., Bergmann, T. O., Bestmann, S., Massimini, M., Johansen-Berg, H., Mochizuki, H., et al. (2009a). Consensus paper: combining transcranial stimulation with neuroimaging. *Brain Stimul.* 2, 58–80. doi: 10.1016/j.brs.2008.11.002

Siebner, H. R., Funke, K., Aberra, A. S., Antal, A., Bestmann, S., Chen, R., et al. (2022). Transcranial magnetic stimulation of the brain: what is stimulated? – a consensus and critical position paper. *Clin. Neurophysiol.* 140, 59–97. doi: 10.1016/j.clinph.2022.04.022

Siebner, H. R., Hartwigsen, G., Kassuba, T., and Rothwell, J. C. (2009b). How does transcranial magnetic stimulation modify neuronal activity in the brain? Implications for studies of cognition. *Cortex* 45, 1035–1042. doi: 10.1016/j.cortex.2009.02.007

Silasi, G., and Murphy, T. H. (2014). Stroke and the connectome: how connectivity guides therapeutic intervention. *Neuron* 83, 1354–1368. doi: 10.1016/j.neuron.2014.08.052

Silvanto, J., and Cattaneo, Z. (2014). "State-dependent transcranial magnetic stimulation (TMS) protocols" in *Transcranial Magnetic Stimulation* eds. A. Rotenberg, J. Horvath and A. Pascual-Leone (New York, NY: Humana Press), 89, 153–176. Available at: https://link.springer.com/protocol/10.1007/978-1-4939-0879-0_9#citeas

Silvanto, J., Muggleton, N. G., Cowey, A., and Walsh, V. (2007). Neural activation state determines behavioral susceptibility to modified theta burst transcranial magnetic stimulation. *Eur. J. Neurosci.* 26, 523–528. doi: 10.1111/j.1460-9568.2007.05682.x

Silvanto, J., Muggleton, N., and Walsh, V. (2008). State-dependency in brain stimulation studies of perception and cognition. *Trends Cogn. Sci.* 12, 447–454. doi: 10.1016/j.tics.2008.09.004

Silvanto, J., and Pascual-Leone, A. (2008). State-dependency of transcranial magnetic stimulation. *Brain Topogr.* 21, 1–10. doi: 10.1007/s10548-008-0067-0

Stefan, K. (2004). Modulation of associative human motor cortical plasticity by attention. *J. Neurophysiol.* 92, 66–72. doi: 10.1152/jn.00383.2003

Stewart, L. M., Walsh, V., and Rothwell, J. C. (2001). Motor and phosphene thresholds: a transcranial magnetic stimulation correlation study. *Neuropsychologia* 39, 415–419. doi: 10.1016/S0028-3932(00)00130-5

Stokes, M. G., Chambers, C. D., Gould, I. C., Henderson, T. R., Janko, N. E., Allen, N. B., et al. (2005). Simple metric for scaling motor threshold based on scalp-cortex distance: application to studies using transcranial magnetic stimulation. *J. Neurophysiol.* 94, 4520–4527. doi: 10.1152/jn.00067.2005

Suppa, A., Huang, Y. Z., Funke, K., Ridding, M. C., Cheeran, B., Lazzaro, V. D., et al. (2016). Ten years of Theta burst stimulation in humans: established knowledge, unknowns and prospects. *Brain Stimul.* 9, 323–335. doi: 10.1016/j.brs.2016.01.006

Thabit, M. N., Ueki, Y., Koganemaru, S., Fawi, G., Fukuyama, H., and Mima, T. (2010). Movement-related cortical stimulation can induce human motor plasticity. *J. Neurosci.* 30, 11529–11536. doi: 10.1523/jneurosci.1829-10.2010

Thielscher, A., Antunes, A., and Saturnino, G. B. (2015). Field modeling for transcranial magnetic stimulation: a useful tool to understand the physiological effects of TMS?**all authors contributed equally to the work. 2015 37th. *Annu. Int. Conf. IEEE Eng. Med. Biol. Soc.* 2015, 222–225. doi: 10.1109/embc.2015.7318340

Turella, L., and Lingnau, A. (2014). Neural correlates of grasping. *Front. Hum. Neurosci.* 8:686. doi: 10.3389/fnhum.2014.00686

Vesia, M., Barnett-Cowan, M., Elahi, B., Jegatheeswaran, G., Isayama, R., Neva, J. L., et al. (2017). Human dorsomedial parieto-motor circuit specifies grasp during the planning of goal-directed hand actions. *Cortex* 92, 175–186. doi: 10.1016/j.cortex.2017.04.007

Vesia, M., Bolton, D. A., Mochizuki, G., and Staines, W. R. (2013). Human parietal and primary motor cortical interactions are selectively modulated during the transport and grip formation of goal-directed hand actions. *Neuropsychologia* 51, 410–417. doi: 10.1016/j.neuropsychologia.2012.11.022

Vesia, M., and Crawford, J. D. (2012). Specialization of reach function in human posterior parietal cortex. *Exp. Brain Res.* 221, 1–18. doi: 10.1007/s00221-012-3158-9

Vesia, M., Culham, J. C., Jegatheeswaran, G., Isayama, R., Le, A., Davare, M., et al. (2018). Functional interaction between human dorsal premotor cortex and the ipsilateral primary motor cortex for grasp plans. *Neuroreport* 29, 1355–1359. doi: 10.1097/wnr.0000000000001117

Vesia, M., and Davare, M. (2011). Decoding action intentions in Parietofrontal circuits. *J. Neurosci.* 31, 16491–16493. doi: 10.1523/jneurosci.4408-11.2011

Vesia, M., Monteon, J. A., Sergio, L. E., and Crawford, J. D. (2006). Hemispheric asymmetry in memory-guided pointing during single-pulse transcranial magnetic stimulation of human parietal cortex. *J. Neurophysiol.* 96, 3016–3027. doi: 10.1152/jn.00411.2006

Vesia, M., Niemeier, M., Black, S. E., and Staines, W. R. (2015). The time course for visual extinction after a "virtual" lesion of right posterior parietal cortex. *Brain Cogn.* 98, 27–34. doi: 10.1016/j.bandc.2015.05.003

Vesia, M., Prime, S. L., Yan, X., Sergio, L. E., and Crawford, J. D. (2010). Specificity of human parietal saccade and reach regions during transcranial magnetic stimulation. *J. Neurosci.* 30, 13053–13065. doi: 10.1523/jneurosci.1644-10.2010

Vesia, M., Yan, X., Henriques, D. Y., Sergio, L. E., and Crawford, J. D. (2008). Transcranial magnetic stimulation over human dorsal-lateral posterior parietal cortex disrupts integration of hand position signals into the reach plan. *J. Neurophysiol.* 100, 2005–2014. doi: 10.1152/jn.90519.2008

Wang, J. X., and Voss, J. L. (2015). Long-lasting enhancements of memory and hippocampal-cortical functional connectivity following multiple-day targeted noninvasive stimulation. *Hippocampus* 25, 877–883. doi: 10.1002/hipo.22416

Ziemann, U., and Siebner, H. R. (2015). Inter-subject and inter- session variability of plasticity induction by non-invasive brain stimulation: boon or bane? *Brain Stimul.* 8, 662–663. doi: 10.1016/j.brs.2015.01.409

Ziluk, A., Premji, A., and Nelson, A. J. (2010). Functional connectivity from area 5 to primary motor cortex via paired-pulse transcranial magnetic stimulation. *Neurosci. Lett.* 484, 81–85. doi: 10.1016/j.neulet.2010.08.025

Zrenner, C., Desideri, D., Belardinelli, P., and Ziemann, U. (2018). Real-time EEG-defined excitability states determine efficacy of TMS-induced plasticity in human motor cortex. *Brain Stimul.* 11, 374–389. doi: 10.1016/j.brs.2017.11.016

# Frontiers in Neuroscience

**Provides a holistic understanding of brain function from genes to behavior**

Part of the most cited neuroscience journal series which explores the brain - from the new eras of causation and anatomical neurosciences to neuroeconomics and neuroenergetics.

---

## Discover the latest Research Topics

See more →

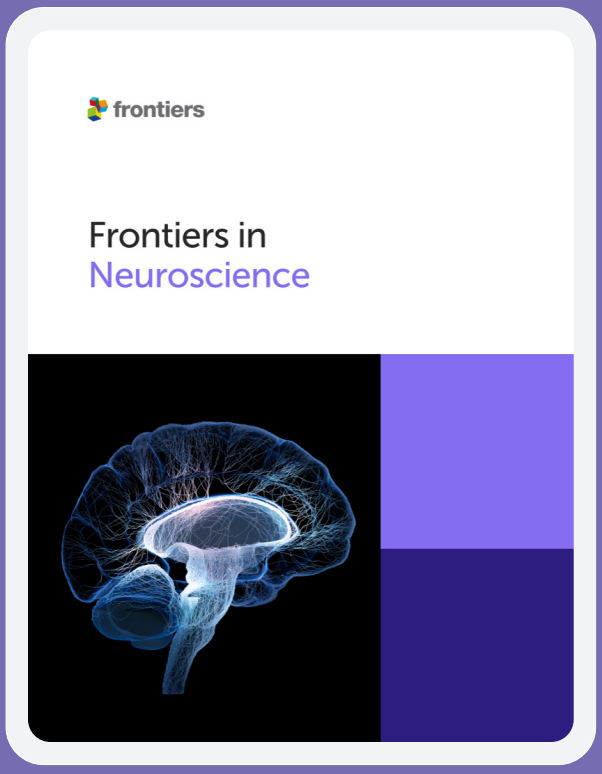


**Frontiers**

Avenue du Tribunal-Fédéral 34
1005 Lausanne, Switzerland
frontiersin.org

**Contact us**

+41 (0)21 510 17 00
frontiersin.org/about/contact